Mt. Zirkel Wilderness Area
Reasonable Attribution Study of Visibility Impairment

Volume II: Results of Data Analysis and Modeling
Final Report

July 1, 1996

PREPARED BY:

Dr. John G. Watson[1] – Principal Investigator
Dr. Donald Blumenthal[2] – Co-Principal Investigator
Dr. Judith Chow[1]
Ms. Catherine Cahill[1]
Dr. L. Willard Richards[2]
Dr. David Dietrich[3]
Mr. Ralph Morris[4]
Dr. James Houck[5]
Mr. Ronald J. Dickson[6]
Mr. Stephen Andersen[7]

PREPARED FOR:

Technical Steering Committee
c/o Colorado Department of Public Health and Environment
Air Pollution Control Division
Denver, CO

ADDITIONAL CONTRIBUTORS AND AFFILIATIONS

1. DESERT RESEARCH INSTITUTE
   - Dr. Douglas H. Lowenthal
   - Dr. Norman F. Robinson
   - Dr. Frank Divita, Jr.
   - Dr. John Gillies
   - Mr. David Schorran

2. SONOMA TECHNOLOGY, INC.
   - Mr. Charles Lindsey
   - Mr. Tim Dye
   - Dr. Naresh Kumar
   - Mr. Tony Ye
   - Mr. Lyle Chinken
   - Mr. Jeff Prouty

3. AIR RESOURCE SPECIALISTS, INC.
   - Mr. Donald Cobb
   - Mr. D. Scott Cismoski
   - Mr. John Molenar
   - Mr. Donald Mussard
   - Ms. Kristi Savig

4. ENVIRON
   - Mr. Chris Emery
   - Dr. Mark Yocke

5. APPLIED GEOTECHNOLOGY INC.
   - Mr. Roger Bighouse

6. RADIAN CORPORATION
   - Ms. Barbara J. Morrison
   - Mr. R. Edward James

7. SECOR INTERNATIONAL INC.
   - Mr. Chris Johnson

8. NATIONAL OCEANIC AND ATMOSPHERIC ADMINISTRATION
   - Mr. James Wilczak

TABLE OF CONTENTS

TABLE OF CONTENTS (continued)

TABLE OF CONTENTS (continued)

TABLE OF CONTENTS (continued)

LIST OF TABLES

LIST OF TABLES (continued)

LIST OF TABLES (continued)

LIST OF TABLES (continued)

LIST OF TABLES (continued)

LIST OF TABLES (continued)

LIST OF TABLES (continued)

LIST OF FIGURES

LIST OF FIGURES (continued)

LIST OF FIGURES (continued)

LIST OF FIGURES (continued)

LIST OF FIGURES (continued)

LIST OF FIGURES (continued)

LIST OF FIGURES (continued)

LIST OF FIGURES (continued)

ABSTRACT

The Mt. Zirkel Visibility Study (MZVS) acquired meteorological, air quality, and visibility measurements in northwestern Colorado from December 1994 through November 1995 to determine the frequency and intensity of visibility impairment in the Mt. Zirkel Wilderness Area (MZWA) in northwestern Colorado. Using several state-of-the-art models and data interpretation methods, the MZVS concluded that visibility in the Wilderness was as good as, or better than, that found in other National Parks and Wilderness areas. There were, however, some occasions where visibility was perceptibly impaired, usually during the summer and fall. The major constituents of non-weather-related light extinction exceeding 20 Mm^{-1} were clean-air scattering and scattering and absorption by small ammonium sulfate and carbon particles.

Contributions from ammonium nitrate and suspended dust were small. Fires and vehicle exhaust, and probably particles formed from organic gases, were the major contributors to carbon concentrations. Much of these contributions originated from areas outside northwestern Colorado, primarily from sources west of the Continental Divide, as evidenced by wind flow patterns, emissions inventories, and simultaneous aerosol measurements near and away from the MZWA. Ammonium sulfate contributions to extinction in the MZWA were most often due to a mixture of sulfur dioxide emissions across a multi-state region that converted to particulate sulfur over multi-day residence times.

Plumes from the Hayden and Craig coal-fired generating stations in the Yampa Valley frequently arrived at the MZWA, as evidenced by short-duration pulses of sulfur dioxide measured near the southern boundary, but these arrivals were not accompanied by perceptible changes in light extinction most of the time. When plumes passed through clouds or fog, however, and when visibility was not obscured by weather, Yampa Valley generating stations caused perceptible changes in light extinction, due to increases in light scattering from ammonium sulfate, on several occasions. Yampa Valley generating station contributions were always accompanied by contributions from other sources, including regional ammonium sulfate, and were often of short duration (a few hours). Plume modeling estimated that the Hayden station's contributions to extinction in the Wilderness were generally two to three times contributions from the Yampa Project (Craig Units 1 and 2). Liquid water content in the atmosphere and in suspended particles enhanced the conversion of SO_2 and oxides of nitrogen to sulfate and nitrate, and it caused these soluble particles to attain sizes that scattered light more efficiently at relative humidities exceeding 80%. Large quantities of liquid water were usually available during, as well as before and after, frequent storms in the region. These storms often obscured visibility owing to the presence of rain, fogs, and clouds.

EXECUTIVE SUMMARY

This executive summary presents the Mt. Zirkel Visibility Study (MZVS) objectives, describes the measurement program, presents a conceptual model of visibility impairment, and summarizes major MZVS findings relevant to the objectives.

S.1 MT. ZIRKEL VISIBILITY STUDY (MZVS) OVERVIEW AND TECHNICAL OBJECTIVES

The Mt. Zirkel Wilderness Area (MZWA) in the Routt National Forest of northwestern Colorado is one of 156 Class I areas in the United States in which visibility is protected. Current regulations, promulgated by U.S. EPA in 1980, address visibility impairment in such areas that is "reasonably attributable" to an existing industrial source or a group of sources (these are often called "plume blight" regulations).

In 1993, the U.S. Forest Service (USFS) certified that occasions existed during which visibility was significantly impaired in the MZWA. The Colorado Department of Public Health and Environment's Air Pollution Control Division determined that existing information was insufficient to reasonably attribute observed visibility impairment to specific sources. As a result, the Mt. Zirkel Visibility Study (MZVS) was commissioned to obtain more information. Potential contributors include sources in the Yampa Valley, which is west of the MZWA and contains the Hayden and Craig coal-fired generating stations, and more distant emitters in Colorado, southern Wyoming, western Utah, and outlying areas.

The purpose of the MZVS was to determine, using scientifically sound principles and established methods and procedures: 1) the extent of visibility impairment, if any, within the MZWA; 2) whether the cause of, or contribution to, any visibility impairment within the MZWA may be reasonably attributed to emissions from any source or group of sources; and 3) the relative contribution of emissions from each source or group of sources to visibility impairment. Specific technical objectives of the MZVS were to:

1. Obtain a documented data set of specified precision, accuracy, and validity that supports modeling and data analysis efforts.

2. Document the frequency, intensity, and character of haze in the MZWA, within the Yampa Valley, and outside of the Yampa Valley and relate these to meteorological conditions.

3. Quantify the contributions from scattering by gases, absorption by gases, scattering by particles, and absorption by particles to different levels of light extinction in the MZWA.

4. Quantify contributions from particulate chemical components to light extinction.

5. Describe the behavior of generating station plumes in the Yampa Valley.

6. Estimate contributions to light extinction in the Wilderness from different emissions sources within and outside of the Yampa Valley.

7. Reconcile results from different modeling and data analysis methods and assign confidence levels to source contribution estimates.

Measurements to address these objectives were made during a one-year period, starting in December 1994. Measurements were made in a "core" study area that included source, receptor, and background measurement sites. Additional data were collected from existing data sources throughout a larger area.

The measurement program included an annual monitoring network, intensive studies during the winter, summer, and fall, and selected emissions measurements. The annual monitoring network was designed to obtain data on the frequency and intensity of the haze in the MZWA and the Yampa Valley, as well in the surrounding upwind background areas. It also documented the behavior of the plumes from the Hayden and Craig generating stations in the Yampa Valley and the surface and upper-air meteorology associated with haze events. The annual measurements included photographic and time lapse video measurements of appropriate views, including the MZWA and the Hayden and Craig stations, and continuous measurements of visibility related parameters (e.g., light scattering) and surface and upper-air meteorology.

During intensive study periods the annual network was supplemented with additional measurements to determine the causes of the haze. These measurements included increased densities of aerosol concentration and chemistry measurements throughout the study region. In the summer and fall intensive periods, continuous measurements of sulfur dioxide (SO_2) and fine-particle light scattering at three wavelengths were made next to the southern boundary of the Wilderness, and ozone was measured at an elevated site in the region.

Selected emissions measurements were made at appropriate times during the year to develop chemical profiles of nearby emissions sources. A regional emissions inventory was acquired and modified for modeling purposes.

Modeling and analysis efforts focused on the core study area, but took into account emissions and transport from the larger study area. Both source and receptor models were applied for source apportionment during selected episodes. Chemical abundances, including isotopic content, were measured in representative emissions sources including the generating station effluents. These same chemical species were analyzed in aerosol samples taken during intensive monitoring periods near the Wilderness, within the Yampa Valley, and outside the Valley to determine contributions from primary emissions.

Plume modeling and trajectory analyses of Yampa Valley generating station emissions were performed for the study year to estimate SO_2 concentrations in the MZWA and their frequency of occurrence. An aerosol evolution model was applied for different

plume aging periods to place upper and lower limits on the amount of SO_2 that is likely to be converted to particulate sulfate under the meteorological conditions associated with haze events.

A conceptual model of the causes of visibility impairment in the MZWA is presented below. It derives from specific results and conclusions of the study which are summarized in the sections that follow.

S.2 CONCEPTUAL MODEL OF VISIBILITY IMPAIRMENT

The following elements describe the prevalent causes of visibility impairment within the Mt. Zirkel Wilderness Area and the contribution of the Hayden generating station and Craig Units 1 and 2 (Yampa Project) to this impairment.

- Light extinction in the MZWA is among the lowest measured in U.S. Class I areas. Winter is the clearest season and summer the haziest. The average light extinction in the MZWA, including scattering by particle-free air, is approximately half that in the Grand Canyon. Most hazes in the MZVS study area are regional, with light extinction comparable at locations that are separated by more than 150 km. Contributions from nearby sources are measurable and perceptible on occasion, and are superimposed on the contributions from a mixture of source emissions from within and outside the region.

- Haze in the Yampa Valley typically appears uniform visually, vertically, and horizontally. Surface layers are sometimes perceptible, especially during morning when a surface temperature inversion is present. Elevated layers are noticeable when noncontinuous emissions such as fires occur or when generating stations malfunction. Although appearing visually uniform, light extinction in the Yampa Valley is often much higher than that measured in the Wilderness and surrounding areas.

- Prescribed burns and wildfires cause visible plumes within and outside of the Yampa Valley. The most visible plumes within the Yampa Valley are those from the Hayden and Craig coal-fired generating stations. The most noticeable of these are steam emissions from cooling towers that rapidly evaporate upon dilution with ambient air. Primary particles that are not captured by the electrostatic precipitators are the main cause of visible emissions from stacks. These primary particle plumes become more visible when precipitators malfunction. The majority of pollutant emissions from generating stations consist of SO_2 and nitric oxide that can be detected instrumentally but not visually.

- Emissions from motor vehicles and residential burning can accumulate at night and during the morning near the floor of the Yampa Valley, to be mixed above the surface when the morning sun heats the surface layer. The time and nature of this coupling determines how these pollutants are transported to the Wilderness.

- The major and most frequent contributors to light extinction in the MZWA are particle-free air (Rayleigh scattering), motor vehicle exhaust and secondary organics (formed from heavy gaseous hydrocarbons), vegetative burning, and regional secondary ammonium sulfate. These contributors are for the most part of regional origins, resulting from a mixture of emissions from source areas that are hundreds of kilometers distant from the MZWA. Liquid water is a major component of particles that cause extinction when relative humidities exceed 80%. The visibility-reducing effects of water-soluble particles such as ammonium sulfate and ammonium nitrate are enhanced when humidities exceed 80%.

- SO_2 and oxides of nitrogen (NO_x), along with ammonia (NH_3), can change into particulate ammonium sulfate and ammonium nitrate that contribute to light extinction. These transformation rates are highly variable, but they can be expected to be slow in clear air and rapid when plumes encounter fogs or clouds.

- Significant, though not major, contributions to light extinction in the MZWA from local power generating stations occur occasionally. These contributions are always superimposed on contributions to extinction from other sources. In the absence of relative humidities larger than 80% (an indicator for passage of plumes through fog or clouds), the Yampa Valley generating station plumes seldom cause perceptible increases in light scattering in the Wilderness, although they regularly arrive in the Wilderness. After passage through fogs or clouds, sufficient transformation of SO_2 to sulfate can take place in generating station plumes to cause perceptible changes in light scattering in the Wilderness.

- Yampa Valley generating station plumes are usually confined below 400 m (1,300 ft) above ground level and flow to the west (down the Valley) at night and in the early morning. In midday, they mix aloft and couple with the upper level winds, which typically transport the plumes to the east, toward the southern end of the Wilderness. The generating station plumes tend to arrive in the Wilderness in pulses with typical durations of less than one to a few hours at any location.

- The largest perceptible effects of the Yampa Valley generating stations on visibility in the Wilderness occur when the emissions accumulate in fogs or low clouds in the early morning or interact with higher clouds after mixing aloft and are subsequently transported to the Wilderness in the afternoon. Pulses of haze attributable to generating station emissions can be seen from the Wilderness on some occasions under these conditions. When they arrive under these conditions, the hazes appear well mixed vertically, rather than as a layer or plume.

- Under nonroutine operating conditions, primary particle emissions from the Yampa Valley generating station stacks can cause perceptible, layered hazes with durations of several hours. These are not due to SO_2 emissions. On one occasion in 1995, a clearly-defined, coherent plume from the Hayden generating station could be seen in a west-facing video view from a camera on Storm Peak (which is south of the Wilderness boundary). The plume was moving toward Storm Peak at

nearly the same elevation as the camera. The extent to which the plume reached or rose over the Continental Divide could not be determined because it could not be seen in views to the north. However, it is clear that the potential existed for the plume to reach the Storm Peak area. This was the only occasion when a clearly-defined, coherent generating station plume was documented coming close to the Wilderness.

- High relative humidity and SO_2 concentrations greater than about 1-2 ppb indicate when generating station emissions might cause visible effects. Model results and measured relative humidity at the southern Wilderness boundary suggest that the plumes arrive in the Wilderness at these concentrations during conditions when relative humidity is larger than 80% on approximately 3% - 8% of the daylight hours during the year. For 1995, the highest incidence (10% - 16%) of these conditions was in May (which was the wettest May on record) and the lowest (0.5% - 2%) in August. During many of these hours, views may be obscured by weather.

- Plumes from the Hayden and Craig stations arrive in the Wilderness together most of the time. Model results suggest that concentrations of Hayden station SO_2 emissions arriving in the Wilderness are three to four times higher than concentrations from the Craig station emissions. This difference is caused by larger dispersion and dilution of Craig station emissions, due to its greater distance from the Wilderness boundary, and SO_2 emission rates during the periods studied that were approximately half the emissions from the Hayden station. On rare occasions, however, for some portions of the Wilderness, the emissions from the two generating stations can arrive separately, and Craig emissions can cause more light extinction than Hayden emissions.

- For the largest documented impact of the Yampa Valley generating stations on visibility in the Wilderness during the study, light scattering peaked at about 60 Mm^{-1} at the southern Wilderness boundary. The relative contribution to six-hour average extinction estimated by a plume chemistry model for the Yampa Valley generating stations for this occasion was 46%. The modeled source contributions were, respectively: particle-free air: 15%; fires, 6%; non-Yampa-Valley sources, 31%; Hayden, 32%; Craig Units 1 & 2, 12%; Craig Unit 3, 2%; and other Yampa Valley sources, 4%. Receptor modeling results differed from the plume model. Receptor model apportionments for this episode were: particle-free air, 17%; fires, 15%; vehicle exhaust, 13%; regional ammonium sulfate, 33%; ammonium nitrate, 7%; and Yampa Valley generating stations, 14%.

- Yampa Valley generating stations have their largest effects on extinction over periods of one or two hours. The same event noted above also included the highest one-hour relative contribution to extinction estimated for Hayden and Craig Units 1 and 2 (the Yampa Project) along any modeled sight path. This contribution was 27% of total extinction, with 21% due to Hayden station and 6% to the Yampa Project. This is equivalent to a 38% increase in the light extinction

that would have occurred without the generating station emissions. The average modeled extinction was 26 Mm^{-1} along the sight path compared to about ~60 Mm^{-1} modeled and measured at the southern Wilderness boundary. The equivalent deciview changes along the same sight path due to Hayden and Yampa Project were 2.39 dv and 0.67 dv, respectively. The sight-path extinction and generating-station percentages were lower than for the southern boundary. This is probably because the southern boundary site is often near the location of the maximum extinction, while the sight paths cover a larger area. Contrast calculations for the above sight path indicate that the total generating station contribution to extinction might be perceptible if images with and without the contribution were viewed side-by-side in a split screen image. It is likely that the Hayden contribution would be perceptible on its own. It is not certain that the Yampa Project contribution would be perceptible.

- The highest deciview contribution of the Yampa Project occurred for a view with an extinction of 16.5 Mm^{-1} and extinction contributions of 0.33 Mm^{-1} (2% of the extinction or 0.2 dv) from the Hayden station and 1.8 Mm^{-1} (11% or 1.16 dv) from the Yampa Project. For the short sight paths within the Wilderness, it is not likely that changes in extinction of these magnitudes would be perceptible.

- For all episodes and views modeled, the greatest changes in the apparent contrasts of ridges against the horizon sky caused by omitting the effects of both the Hayden station and Yampa Project emissions was 0.066 units. The greatest changes in contrast transmittances for features on the surfaces of the targets was 0.092. For Hayden alone, the comparable greatest changes for contrast and contrast transmittance were 0.039 and 0.063, respectively. For Yampa Project alone, the comparable greatest changes for contrast and contrast transmittance were 0.027 and 0.032, respectively.

- These calculated contrast changes are large enough to be perceived if they were displayed in a split-screen image, but it is not known if they are large enough to be perceived by an observer in the MZWA comparing observations made at different times. Of more than 3,000 cases of days/hours/sight-paths modeled, several dozens of cases for Hayden exceeded 2% contrast, while only 10 cases (2 days) exceeded this value for the Yampa Project.

- The views discussed above were for endpoints within the Wilderness. Other views that extended outside the Wilderness were examined; however, by agreement of the sponsors, the effect of removing generating station emissions was only calculated for those portions of sight paths within the boundaries of the Wilderness (or between endpoints that were within the Wilderness). Due to the small proportions of the long sight paths that were within the Wilderness, these sight paths are less sensitive to the removal of generating station emissions than sight paths with both endpoints in the Wilderness. Also by agreement of the study sponsors, estimates of the contributions of the generating stations were focused on

the contributions of Hayden and the Yampa Project, omitting the contribution of Craig Unit 3.

S.3 STUDY FINDINGS

MZVS findings are keyed to sections of the MZVS final report and its appendices to facilitate further investigation of specific topics. Though these findings are specific for the 1995 MZVS period, and the specific magnitudes and frequencies apply only to that year, they are expected to be generally valid for prior and subsequent years providing there are no major changes in emissions and meteorology between those years. Some of the findings listed in this section have already been highlighted as elements of the conceptual model.

S.3.1 MEASUREMENTS

- The measurement network was adequate to detect occurrences of visibility impairment and to assess their causes. (All Sections)

- The major types of visibility impairment were encountered – including regional haze from transport of secondary aerosol, fire emissions, and other particulate matter; local haze from fires, local ground-level emissions, and secondary sulfates from generating station emissions; and surface and elevated haze layers from fires and generating station primary emissions. (Sections 4 & 5)

- The measurement year and the intensive operating periods were reasonably representative of the conditions encountered in other years, except that May was exceptionally stormy. No more than 6% of the days during the study showed major deviations from long-term averages for temperatures, cloud-cover, or rainfall. However, May was the wettest on record for the upper Yampa Valley. (Section 2.2)

- The observables measured were sufficient to detect the presence or absence of major source contributions, including continental dust, vehicle exhaust, vegetative burning, and primary and secondary coal-fired generating station emissions. (Section 6.5)

S.3.2 FREQUENCY, CHARACTER, AND INTENSITY OF HAZE

- Light extinction in the MZWA was among the lowest measured in U.S. Class I areas. Winter is the clearest season and summer the haziest. In winter, the median light extinction at Buffalo Pass (next to the southern boundary of the Wilderness) for days not affected by weather was 11 Mm^{-1}, only 30% above that of clean air. In summer, the median was 16 Mm^{-1}. For comparison, these values are about half those measured at the Grand Canyon. (Section 3.1, Table 3.1.1)

- High mountain views were obscured by weather for either all morning or all afternoon periods on about 25% to 50% of winter and spring days, about 5% of summer days, and 10% to 20% of fall days. (Section 3.2, Figure 3.2.1)

- Haze in the Yampa Valley typically appeared uniform visually, vertically, and horizontally. Surface layers were sometimes perceptible, especially during morning. Layers were noticeable when noncontinuous emissions occurred, especially fires. Although appearing visually uniform, light extinction in the Yampa Valley was often much higher than that measured in the Wilderness and surrounding areas. (Sections 3.1, 3.2, 3.4, 3.5)

- Most hazes were regional, with light extinction comparable at locations separated by more than 150 km. On some days, however, contributions to extinction from nearby sources were measurable and perceptible, and these contributions were superimposed on the contributions from a mixture of emissions from within and outside the region. (Section 3.1, Table 3.1.1, Figure 3.1.1)

S.3.3 COMPONENTS OF LIGHT EXTINCTION

- Clean-air scattering was a large or major component of light extinction in the Wilderness for the most daylight hours not affected by weather. (Section 3.1, Table 3.1.1; Section 3.5, Figures 3.5.1 and 3.5.2)

- Particle light absorption (caused primarily by soot) constituted less than 20% of extinction for most cases, but contributed nearly 50% of extinction during some events. Except during the spring, particle light absorption at Buffalo Pass was almost always less than 15% of total extinction. In spring, it was about 25% of total extinction. In winter and spring at Gilpin Creek (a lower-elevation, more-northerly site next to the Wilderness), light absorption was often one-third of total extinction but much less in other seasons. The high level at Gilpin Creek may be due to local wood or vegetative burning in the Elk River Valley below the site. (Section 3.5, Section 4.3)

- With the exception of the Gilpin Creek site in winter and spring, fine-particle light scattering was the major contributor to extinction that exceeded 20 Mm^{-1}. Coarse particle scattering in the Wilderness was negligible, as evidenced by comparable light scattering measurements from nephelometers with and without $PM_{2.5}$ inlets. (Section 3.5)

S.3.4 CHEMICAL COMPONENTS OF LIGHT EXTINCTION

- When light extinction exceeded 20 Mm^{-1}, organic carbon, and ammonium sulfate each commonly contributed more than 10% of extinction, and together often exceeded 50% of extinction, at all measurement locations for those six-hour and twelve-hour $PM_{2.5}$ samples submitted to chemical analysis. The proportions of their contributions varied from case to case. (Section 4.3, Table 4.3.8)

- $PM_{2.5}$ ammonium nitrate contributed less than 10% of extinction for almost all samples that were chemically analyzed at all sites. Ammonium nitrate was estimated to contribute more than 10% of six-hour average extinction on only two occasions at Buffalo Pass. (Section 4.3, Table 4.3.8)

- Extinction from $PM_{2.5}$ dust seldom contributed more than 10% of extinction. Nine out of 64 aerosol samples at Buffalo Pass showed $PM_{2.5}$ dust contributions that slightly exceeded 10% of extinction, substantially higher and more frequent than dust contributions at other sites in the MZVS. Frequent heavy-duty truck traffic along the unpaved road near the Buffalo Pass site, to facilitate nearby reservoir construction, may, have affected dust contributions, and probably do not appreciably affect extinction along sight paths. (Section 4.3, Table 4.3.8)

- Elemental carbon was a significant contributor in some events (especially at Gilpin Creek), but it was seldom a majority component of extinction. (Section 4.3, Table 4.3.8)

- Liquid water was a large component of particles that caused extinction when relative humidities exceeded 80%. The visibility-reducing effects of water-soluble particles such as ammonium sulfate and ammonium nitrate were enhanced at these humidities because they absorbed water and acted as nucleation sites for the formation of droplets. The conversion of gaseous SO_2 and oxides of nitrogen was also enhanced when they were absorbed in water drops. (Appendix B.4; Sections 4.3, 6.6, and 6.9)

- Average sulfate concentrations ranged from 0.81 $\mu g/m^3$ at the Buffalo Pass site to 1.09 $\mu g/m^3$ at the Hayden VOR site. Maximum sulfate concentrations ranged from 1.8 $\mu g/m^3$ at Juniper Mountain to 4.5 $\mu g/m^3$ at Hayden Waste Water, with maxima of 2.1 $\mu g/m^3$ at Buffalo Pass and 1.9 $\mu g/m^3$ at Gilpin Creek. Though Buffalo Pass did not experience the highest sulfate concentrations in the network, it did experience higher contributions of sulfate to extinction because it recorded the highest relative humidities. The highest sulfate contributions to extinction often occurred when sulfate concentrations were below average, but relative humidity exceeded 95% and large nephelometer readings showed Buffalo Pass to be enveloped in a cloud or fog. (Section 4.2, Table 4.2.1; Section 4.3, Tables 4.3.1 to 4.3.6)

S.3.5 YAMPA VALLEY PLUME BEHAVIOR

- In the absence of overriding synoptic influences, Yampa Valley generating station plumes were usually confined below about 400 m (1,300 ft) above ground level and drained down the Valley at night and in the early morning. In midday, they mixed aloft and coupled with the upper level winds, that typically transported the plumes toward the southern end of the Wilderness. (Sections 5.1, 5.2.3, 5.4.6)

- Both measurements and everyday plume modeling showed that SO_2 arrived at Buffalo Pass in pulses with typical durations of less than one to a few hours. SO_2 is a colorless gas that causes negligible light extinction. SO_2 pulses rarely lasted more than six hours, and SO_2 concentrations were negligible (i.e., below 0.2 ppbv) between pulses. The calculated magnitude and frequency of SO_2 pulses was in qualitative agreement with the measurements. The agreement between the timing of the modeled and measured pulses was often good and sometimes excellent. (Section 5.4)

- Cumulative frequency distributions of SO_2 concentrations calculated by everyday plume modeling showed them to be largest at the southern end of the MZWA, near Buffalo Pass. SO_2 levels decreased uniformly with distance north in the MZWA. Detailed modeling with multiple source emissions showed the same results. This is consistent with the prevailing daytime winds. Receptor sites near the southern end of MZWA provide an upper limit for the concentrations of emissions from Yampa Valley generating stations in the MZWA. (Section 5.2.1, Figure 5.2.6; Section 5.4.6)

- The highest modeled SO_2 concentrations were at Mad Creek, a low-elevation receptor site in a canyon in the southwest corner of the MZWA. The distance to Yampa Valley generating stations is at a minimum in this corner of the MZWA. (Section 5.4.6)

- Model results indicated that the emissions from the Hayden and Craig stations arrived in the MZWA together most of the time. Emissions from only one of these stations rarely arrived at the Wilderness in significant amounts without being accompanied by emissions from the other station. (Section 5.4.7)

- Trajectory analyses for episodes indicated that Yampa Valley generating station emissions can be transported directly to Buffalo Pass in midday in 2 to 5 hours, but emissions that are emitted into the early morning drainage flows could take 6 to 11 hours to arrive. Craig station emissions typically took 1 to 2 hours longer in transit than Hayden station emissions. (Section 5.2)

- The modeled percentage contribution of each generating station unit to SO_2 concentrations in the MZWA was approximately the same for all locations in the MZWA, both for all hours and for only hours with SO_2 concentrations greater than 2 ppbv. The approximate percentage contributions were: Hayden Unit 1, 40 to 45%; Hayden Unit 2, 35 to 40%; Craig Unit 1, 6 to 8%; Craig Unit 2, 7 to 9%; and Craig Unit 3, 3 to 4%. (Section 5.4.1, Table 5.4.1)

- The calculated plume rise for Hayden Unit 2 was greater than for Unit 1, causing more dilution before the emissions reach ground level. (Section 5.4)

- In the absence of relative humidities greater than 80% (a possible surrogate for passage through fog or clouds), the Yampa Valley generating station plumes

rarely cause perceptible increases in light scattering in the Wilderness. (Sections 6.4, 6.5, 6.6)

- After passage through fogs or clouds, sufficient transformation of SO_2 to sulfate can take place to cause perceptible changes in light scattering in the Wilderness. On at least two days (09/18/95 and 08/23/95), increases in haze of one to a few hours duration that coincided with the arrival of SO_2 attributed to the Yampa Valley generating stations were noticeable on video views of the Wilderness and detectable by the nephelometers at Buffalo Pass. (Sections 5.6, 6.4, 6.5, 6.6)

- The largest perceptible effects of the Yampa Valley generating stations on visibility in the Wilderness (including the two events noted above) occurred when the emissions accumulated in fogs or low clouds in the early morning or were mixed into higher clouds after mixing aloft and were subsequently transported to the Wilderness in the afternoon. The interaction of the emissions with fogs or clouds allowed wet conversion of SO_2 to sulfate. (Sections 5.6, 6.6)

- Various analyses suggest that high relative humidity and SO_2 concentrations greater than about 1-2 ppb may be a reasonable surrogate for conditions when generating station emissions might have visible effects. Trajectory model results for each study day and measured relative humidity at Buffalo Pass suggest that the plumes arrived in the Wilderness at these concentrations during conditions when relative humidity was greater than 80% on 3% - 8% of the daylight hours during the year, with the highest incidence (10% - 16%) in May (which was the wettest May on record) and the lowest (0.5% - 2%) in August. During many of these hours, views would have been obscured by weather. (Sections 6.6, 5.4)

- The Buffalo Pass site near the southern Wilderness boundary measured among the highest concentrations of generating station emissions found in the Wilderness. Everyday model results also suggest that the highest concentrations of generating station emissions should be found int he southern portion of the Wilderness. The Buffalo Pass site should be representative of high-altitude sites in the southern portion of the Wilderness. (Section 5.4)

- The addition of ammonia to the Hayden plumes has a negligible effect on transformation rates or the formation of ammonium nitrate. (Sections 6.4, 6.9).

- Under nonroutine operating conditions, primary particle emissions from generating station stacks caused perceptible, layered hazes with durations of several hours. These were not due to SO_2 emissions. For example on 01/03/95, a clearly defined, coherent plume from the Hayden station could be seen in a west-facing video view from a camera on Storm Peak (which is south of Buffalo Pass). The plume moved toward Storm Peak at nearly the same elevation as the camera. The extent to which the plume reached or rose over the Continental Divide could not be determined because it could not be seen in views to the north. However, it is clear that the potential existed for the plume to reach the Storm Peak area. This

was the only time the time-lapse videos showed that a layered haze or well-defined plume attributed to one of the Yampa Valley generating stations reached the vicinity of the Wilderness Area. (Sections 5.3, 5.5)

- Haze events associated with the formation of secondary particles (sulfate and associated water) that could be detected in the time-lapse videos showed a haze that was mixed to the ground and did not have apparent edges or top. Therefore, haze pulses identified from nephelometer measurements of light scattering at elevated locations were considered to be uniform haze rather than layered haze. (Sections 3.2, 5.5, and 6.8)

- Chemical compositions of primary particle emissions were sufficient to separate coal-fired generating stations from other contributors, but not from each other. Abundances of sulfur-32 and sulfur-34 measured in source samples were sufficient to distinguish coal-fired power station, motor vehicle exhaust, and geothermal hot springs from one another. The abundance of these isotopes in coal-fired generating station emissions were too variable, and too similar to those in background air, to improve the resolution between Yampa Valley generating station and regional sulfate contributions. (Section 6.3,6.5, Appendix B.3)

- Craig Unit 3 emissions contain no selenium, and its profile is too similar to geological material to be distinguished from that contributor. (Section 6.3)

S.3.6 SOURCE CONTRIBUTIONS TO LIGHT EXTINCTION

- For primary particles in the $PM_{2.5}$ size fraction, a multi-state (major parts of Colorado, Wyoming, and Utah) emissions inventory showed that motor vehicles accounted for ~46% of primary $PM_{2.5}$, with summer emissions distributed among vehicle exhaust, paved road dust, and unpaved road dust. Another 21% of $PM_{2.5}$ in the summer was emitted from natural dust sources, while 11% was emitted from agricultural tilling. During the winter months, residential wood and coal combustion were significant $PM_{2.5}$ sources, constituting 11% of the emissions. (Section 6.2)

- Residential coal combustion and hot springs were minor contributors to ammonium sulfate. Emissions surveys showed them to constitute less than 1% of sulfur emissions in northwestern Colorado and a multi-state region. Coal combustion, mostly in power generation stations, was the largest sulfur emitter in the Yampa Valley and in a multi-state region. Yampa Valley SO_2 emissions were estimated to be ~6% of all SO_2 emissions in the multi-state region. (Section 6.2)

- Sulfur-32 and sulfur-34 isotopic abundances in emissions from Yampa Valley coal-fired generating stations, motor vehicle exhaust, and geothermal hot springs differed sufficiently to allow contributions to sulfur from any two of these sources to be distinguished from each other. Isotopic abundances in sulfur emissions from Yampa coal-fired generators and sulfur in background air were too similar, within

measured variability, to allow their separation into separate categories. This is possibly due to the dominance of coal-burning as the major SO_2 emitter in the region. (Sections 6.3, 6.5)

- Motor vehicle exhaust and fires (residential, wildfires, and prescribed burning) were the major contributors to the highest organic carbon concentrations. Secondary organic carbon could not be separately resolved and is most probably apportioned as vehicle exhaust by receptor models. (Section 6.5, Appendix D)

- A plume chemistry model was applied to four periods of interest corresponding to 28 days, including five visibility episodes in four modeled periods. Other data analyses and receptor modeling of source contributions to extinction were also applied to data from these periods. Calculations of contrast and the deciview haze index along selected Wilderness sight paths were made for the same days. These periods included several events of elevated light extinction in the Wilderness. Some of these events occurred during dry conditions (08/08/95, 10/19/95) and others occurred under high humidity (08/23/95, 09/18/95, 09/19/95, 10/12/95). Buffalo Pass SO_2 concentrations of about 2 ppb or more were predicted by the everyday modeling and the plume chemistry model, and were measured for all of these events except 10/12/95 and 10/19/95. For 10/12/95, a value of about 2 ppb was estimated by the plume model, but only about 0.5 ppb was measured. These days were examined to assess the source contributions to extinction in the Wilderness. They include the days of the highest estimated generating station contributions to extinction during the summer and fall. (Sections 5.6, 6.5, 6.6, 6.7, 6.8)

- For the dry periods of 08/08/95 and 10/19/95, data analyses, plume modeling, and receptor modeling agree that the Yampa Valley generating stations were negligible contributors to extinction in the Wilderness. These events were dominated by fires, motor vehicle emissions or secondary organic aerosol, and secondary sulfate transported from outside the local region. For example, receptor modeling indicates that for the 08/08/95 afternoon sample at Buffalo Pass (with measured light extinction of 36 ± 6 Mm^{-1}), $23 \pm 7\%$ of the extinction derived from clean-air scattering, $20 \pm 1\%$ was contributed by fires, $29 \pm 29\%$ came from motor vehicle exhaust or secondary organics (note the large uncertainty estimate), $0.6 \pm 0.3\%$ was attributable to local coal-fired generating stations; $13 \pm 2\%$ was from regional ammonium sulfate, $1.7 \pm 0.8\%$ was from secondary ammonium nitrate; and $13 \pm 1\%$ was from suspended dust. The suspended dust contribution was real, but was probably very local and did not affect concentrations along long sight paths. (Sections 5.6, 6.5, 6.7; Table 6.5.6)

- For 08/23/95, trajectory analyses, correlation between SO_2 and particle scattering (b_{sp}), and video images indicated a possible significant contribution to extinction at Buffalo Pass from the Yampa Valley generating stations. Regional background conditions, high values of aerosol light absorption, and the chemistry of the filter samples, however, indicated that geological material, regional sulfate, fires, and

motor vehicles or secondary organics were the dominant contributors to extinction for the six-hour afternoon period. The plume model substantially underestimated the extinction because it did not adequately account for regional transport. The receptor model attributed only 3.5 ± 1.7% of the 37 ± 7 Mm^{-1} measured extinction to the Yampa Valley generating stations. It should be noted, however, that the models were applied for six-hour samples and will underestimate the contribution of the generating stations to extinction for shorter time periods. From the high correlation between SO_2 and b_{sp} seen for this event, it is likely that the generating station contribution to extinction was higher than estimated by the models, but for a short portion of the six-hour averaging interval. A corresponding correlation between light absorption and b_{sp} indicates that other sources than the generating stations also contributed to the event. (Sections 2, 5.6, 6.5, 6.6, 6.7)

- The afternoons of 09/18/95 and 09/19/95 were the times of the largest documented contributions of Yampa Valley generating stations to light extinction in the Wilderness. For these afternoons, light scattering at Buffalo Pass peaked at about 60 Mm^{-1} and 25 Mm^{-1}, respectively, and the plume-model extinction estimates (for a six-hour period) agreed with the peak values. (Sections 5.6, 6.6, 6.7, and 6.8)

- For 09/18/95 and 09/19/95, the percentage contributions to afternoon six-hour-average extinction estimated by the plume chemistry model for the Yampa Valley generating stations were 46% for 09/18/95 and 26% for 09/19/95. The modeled component contributions for these days were, respectively: clean air, 15% and 44%; fires, 6% & 4%; non-Yampa-Valley sources, 31% and 19%; Hayden, 32% and 20%; Craig Units 1 and 2; 12% and 5%; Craig Unit 3, 2% and 1%; and other Yampa Valley sources, 4% and 6%. The receptor model found the following contributions, respectively: clean air, 17 ± 4% and 38 ± 10%; fires, 15 ± 1% and 17 ± 1%; vehicle exhaust and secondary organics, 13 ± 20% and 24 ± 25%; suspended dust, 2 ± 0.4%; background ammonium sulfate, 33 ± 7% and 10 ± 4%; secondary ammonium nitrate, 7 ± 2% and 2 ± 1%; and Yampa Valley generating stations, 14 ± 7% and 7 ± 3%. (Sections 6.5, 6.7)

- For the afternoons of 09/18/95 and 09/19/95, receptor modeling results differed from plume model results. Observations of the magnitude of the changes in b_{sp} coincident with changes in SO_2 from 1200 to 1500 MST on 09/18/95 and from 1400 through 1600 MST on 09/19/95 were closer to the six-hour average plume model results than to the corresponding receptor model results. The plume model may more closely represent the peak light extinction values seen for these days. (Sections 5.6, 6.5, 6.6, Appendix D, Figure 5.6.2)

- The contributions to extinction of Hayden and Craig Units 1 and 2 (the Yampa Project) were calculated using the plume chemistry model for a variety of sight paths. The changes in light extinction and contrast that would occur along the sight paths from eliminating those emissions from the Hayden station and Yampa Project that were within the Wilderness boundaries were modeled. The highest

one-hour percentage contribution estimated for these generating units along any modeled sight path on any day was 27% of total extinction (b_{ext}) on 09/18/95, with 21% due to Hayden station and 6% to the Yampa Project. This is equivalent to a 38% increase in the extinction that would have occurred without the generating station emissions. For this sight path (from Mt. Ethel to the Continental Divide Trail), the average modeled b_{ext} was 26 Mm^{-1}, compared to about 60 Mm^{-1} at Buffalo Pass. The equivalent deciview changes along the same sight path due to the Hayden station and Yampa Project were 2.39 dv and 0.67 dv, respectively. Sight-path extinction and generating-station percentages would be lower than for Buffalo Pass, because the Buffalo Pass site is generally near the location of the maximum extinction, while the sight paths cover a larger area. (Sections 6.7 and 6.8; Tables 6.6.5b, 6.7.9, 6.8.4, and 6.8.5)

- Contrast calculations for 09/18/95 for the above sight path indicated that the total generating station contribution to extinction might be perceptible if images with and without the contribution were viewed side-by-side. (Section 6.8)

- Changes in b_{ext}, measured and modeled, correspond with observed and perceptible changes in contrasts. The OPTEC nephelometer at Buffalo Pass measured a change of total scattering of approximately 36 Mm^{-1} from 1100 to 1300 MST during the 09/18/95 event, accompanied by a 2.1 ppb increase in SO_2. This light scattering change is much larger than the 7.3 Mm^{-1} maximum change along a sight path due to Hayden and Yampa Project emissions calculated by the plume chemistry model. It is also large compared to commonly-discussed perception thresholds. In addition, an obvious haze pulse was perceptible in the time-lapse videos taken from Storm Peak during this event. Given the relative contributions of Hayden station and the Yampa Project to this event, it is likely that the Hayden station contribution would have been perceptible in the absence of the Yampa Project contribution. It cannot be determined that the Yampa Project contribution would have been perceptible on its own. (Section 6.8.4)

- For the 10/12/95 event, the afternoon extinction at Buffalo Pass estimated by the plume model was about 21 Mm^{-1}. This is similar to the extinction measured at the site in midday while clouds were not present. Most of this extinction was attributed to clean-air scattering and a mixture of regional sources. Receptor modeling estimated the significant and large contributors to be clean-air scattering, suspended dust, motor vehicle or secondary organics, fires, and regional sulfate. The Yampa Valley generating station contributions were estimated to be about 14% by the plume model and less than 1% by the receptor model. For the same day, the average extinction calculated by the plume model for the sight paths varied from 12 to 16.5 Mm^{-1}. (Section 6.8.7)

- 10/12/95 is of interest because the maximum deciview change due to the Yampa Project was estimated to occur on that day. On most days, the contribution of Hayden station was about three times that of the Yampa Project. On this day, 9% of the 14% at Buffalo Pass was attributed to Hayden station and 5% to Yampa

Project by the plume chemistry model. For the Mt. Ethel to the Continental Divide Trail View, a b_{ext} of 16.5 Mm^{-1} was estimated with about 13**%** of this attributed to Hayden station and the Yampa Project. For this view, the contribution of the Yampa Project was estimated by the plume model to exceed that of Hayden station. Unit 2 at Hayden station had been shut down for maintenance from 10/07/95 through 10/11/95, just prior to this event. The 13**%** was attributed as 0.33 Mm^{-1} or 2% to Hayden station and 1.8 Mm^{-1} or 11% to the Yampa Project, or alternatively, 0.2 dv to Hayden station and 1.16 dv to the Yampa Project. For this view, the Yampa Project contribution exceeded 1 dv. This value has been discussed as a change that can be noticed by casual observers. This applies, however, for views over distances close to the visual range of the objects observed. For short views such as those within the Wilderness, it is unlikely that the above 1.8 Mm^{-1} b_{ext} change corresponding to the 1.16 dv change would be perceptible by most observers. (Sections 6.5, 6.7, and 6.8; Tables 6.5.7, 6.7.7b, and 6.8.6)

- For the periods modeled above, there were large differences in the calculated apparent contrast and contrast transmittance for different sight paths in the MZWA. These differences were primarily caused by differences in the brightness of the target, which depend on its reflectance and orientation to the sun. For most sight paths, diurnal changes in illumination caused changes in the calculated apparent contrast and contrast transmittance that were far greater than any changes due to changes in the emissions. (Section 6.8)

- Values of the deciview haze index changed by as much as 3.2 units when the effects of the emissions of both the Hayden station and the Yampa Project were omitted. When only the effects of the Hayden station emissions were omitted, the largest change in dv was 2.4 units, and the largest change from omitting the effects Yampa Project emissions was 1.16 units. A one-unit change in dv corresponds to a 10% change in b_{ext}. (Section 6.8)

- For all episodes and views modeled, the largest change in apparent contrast of ridges against the horizon sky caused by omitting the effects of both the Hayden station and Yampa Project emissions was 0.066 units. The largest change in contrast transmittance for features on the surfaces of the targets was 0.092. For Hayden station alone, the comparable largest changes for contrast and contrast transmittance were 0.039 and 0.068, respectively. For the Yampa Project alone, the comparable largest changes for contrast and contrast transmittance were 0.027 and 0.032, respectively. (Section 6.8)

- These calculated contrast changes are large enough to be perceived if they were displayed in a split-screen image, but it is not known if they are large enough to be perceived by an observer in the MZWA comparing observations made at different times. Of more than 3,000 cases of days/hours/sight-paths modeled, several dozens of cases for Hayden station exceeded 2% contrast, while only 10 cases (2 days) exceeded this value for the Yampa Project. (Section 6.8)

- The maximum values of the calculated changes in contrast and contrast transmittance due to changes in generating station emissions were very nearly the same for clear skies and for completely overcast skies. (Section 6.8)

- Yampa Valley generating station contributions are always superimposed on contributions to extinction from other sources. For more than 90% of the daylight hours, their contribution to visibility impairment in the Wilderness was probably negligible. However, during the August-October period, when fine-particle light scattering was measured, approximately twelve events were identified with measurable increases in light scattering accompanying SO_2 pulses. Haze pulses were observed in the time-lapse videos during two of these events (08/23/95 and 09/18/95). In both, the light extinction increased from ~20 to ~60 Mm^{-1} over a few hours. In the remaining cases, the camera views were obscured by weather or changes in haze could not be distinguished in the videos. For the two events noted, the Yampa Valley generating stations plumes passed through clouds or fog, and ammonium sulfate was a large contributor to the extinction. (Sections 5.4, 5.6, 6.5, 6.6, 6.7)

- Increasing ammonia does not effectively increase ammonium nitrate concentrations to significant levels. An aerosol evolution and equilibrium model demonstrated that doubling ammonia concentrations increased particulate nitrate concentrations only when liquid water contents were low. This increase was offset by the small amounts of particle nitrate contained in the smaller amounts of liquid water, with the result that, on average, the increase in particle nitrate was less than 0.1 $\mu g/m^3$. (Section 6.9, Table 6.9.1)

- Increases in particulate nitrate did not exceed 0.1 $\mu g/m^3$ with decreases in sulfate concentrations. Reducing sulfate concentrations frees up ammonia for potential reaction with nitric acid to form particulate ammonium nitrate, but sulfate reductions also reduce the liquid water available for reactions. These phenomena counteract each other. (Section 6.9, Table 6.9.1)

S.3.7 LIMITATIONS OF MODEL RESULTS

- Aside from local generating station emissions that were directly measured, emission rate estimates were only qualitatively accurate in space and time, and may differ from reality by up to an order of magnitude for specific visibility events. This is especially true of fires that are episodic and may have regional, as well as local, influence. (Section 6.2).

- Chemical-specific extinction efficiencies were very sensitive to changes in particle size for the distributions with modes <0.3 μm found during the MZVS. They were also inaccurate for very high humidities (>95%), but views were often obscured by weather under these conditions. (Section 4.1)

- Chemical Mass Balance modeling did not distinguish between separate generating station contributions. Both dry- and wet-aged profiles provided adequate fits to the data. The profile used to apportion contributions from Yampa Valley generating stations was selected for a sample based on evidence of plume processing by fogs and clouds, even though a profile that did not undergo such processing would explain the measurements equally well. Lacking measurement of specific organic compounds, the motor vehicle source contributions probably explain secondary organic aerosol contributions as well as those from directly emitted exhaust. Uncertainties for motor vehicle contributions were high, often exceeding the source contribution estimate. (Section 6.5).

- Since modeled hourly SO_2 concentrations from the Hayden and Craig generating stations showed reasonable agreement with the measured SO_2 concentrations, everyday plume modeling results should be reliable for drawing conclusions related to the frequency of occurrence and locations of SO_2 emissions from the two generating stations and their relative contributions to SO_2. (Section 5.4)

- CALMET/CALPUFF plume chemistry modeling often underestimated measured $PM_{2.5}$ and extinction. This is probably due to source contributions from outside the emissions domain, inaccurate emissions estimates for intermittent sources during episodes, and inadequate mechanisms for determining aqueous-phase conversions of SO_2 to sulfate, that are the cause of most events with perceptible visibility impairments. (Sections 6.4, 6.7)

- Results obtained from CALMET/CALPUFF, CMB, and continuous measurements are qualitatively comparable in terms of timing and magnitude of nearby generating station contributions, but they show substantial quantitative differences. Results are most comparable for dry situations when local generating station contributions to ammonium sulfate were low. They were in greatest disagreement for those cases where transformations in fogs and clouds occurred. (Sections 5.4, 6.5, 6.7)

- Most relations used in the contrast calculations were accurate, but the diffuse skylight flux and horizon sky radiance were calculated from simplified relations of uncertain accuracy. The effect of these simplifications on the calculated contrasts has not been determined. (Section 6.8)

1.0 INTRODUCTION

This section provides an opening overview of the report. The purpose of the study is defined, and the technical objectives are outlined. The technical approach to achieving each of these objectives is briefly summarized. Also included is a guide to the organization of this report as well as of other materials used in conducting the study but not contained in the report. In addition, terms used in the study are defined.

1.1 Study Purpose and Technical Objectives

The Mt. Zirkel Wilderness Area (MZWA) in the Routt National Forest of northwestern Colorado is one of 156 Class I areas in the United States in which visibility is protected. In Class I areas, such as national parks and wilderness areas, industrial activities are not permitted and emissions from new sources outside the Class I boundaries must cause no adverse impact. Current regulations, promulgated by U.S. EPA in 1980, address visibility impairment that is "reasonably attributable" to an existing industrial source or a group of sources (these are often called "plume blight" regulations). Uniform, regional hazes caused by a multitude of sources located near and far from Class I areas are considered under the 1990 Clean Air Act Amendments and are to be treated by visibility transport commissions (VTC). A VTC exists for the Grand Canyon National Park, but no VTC has been established to evaluate regional haze in northwestern Colorado.

Ely *et al.* (1993) assembled available technical information on visibility, air quality, and meteorology in and near the MZWA, including color slides, meteorological data, and emission inventories. The designated land manager for the MZWA, the U.S. Forest Service (USFS), used this information to certify that occasions existed during which visibility was significantly impaired and named the Craig and Hayden coal-fired power generating stations as possible sources. The State of Colorado determined that information was insufficient to reasonably attribute observed visibility impairment to specific sources, and the Mt. Zirkel Visibility Study (MZVS) was commissioned to obtain this information. Potential contributors include sources in the Yampa Valley, which is west of the MZWA and contains the Craig and Hayden generating stations and the Steamboat Springs, Hayden, and Craig population centers, and more distant emitters in Colorado, southern Wyoming, western Utah, and outlying areas.

The purpose of the MZVS (Blumenthal *et al.*, 1995; Watson *et al.*, 1995) is to determine, using scientifically sound principles and established methods and procedures: 1) the extent of visibility impairment, if any, within the MZWA; 2) whether the cause of or contribution to any visibility impairment within the MZWA may be reasonably attributed to emissions from any source or group of sources; and 3) the relative contribution of emissions from each source or group of sources to visibility impairment. Specific technical objectives of the MZVS are to:

1. Obtain a documented data set of specified precision, accuracy, and validity that supports modeling and data analysis efforts.

2. Document the frequency, intensity, and character of haze in the Mt. Zirkel Wilderness, within the Yampa Valley, and outside of the Yampa Valley and relate these to meteorological conditions.

3. Quantify the contributions from scattering by gases, absorption by gases, scattering by particles, and absorption by particles to different levels of light extinction in the Mt. Zirkel Wilderness.

4. Quantify contributions from particulate chemical components to light extinction.

5. Describe the behavior of generating station plumes in the Yampa Valley.

6. Estimate contributions to light extinction in the Wilderness from different emission sources within and outside of the Yampa Valley.

7. Reconcile results from different modeling and data analysis methods, and assign confidence levels to source contribution estimates.

1.2 Technical Approach

There is no single, foolproof method for attaining these objectives. Emission rates, air flow in complex terrain, and chemical transformations of emitted pollutants in the atmosphere are complicated phenomena that are not entirely understood. Even with complete understanding of the processes involved, it is not technically or economically feasible to obtain measurements that fully describe all of the relevant atmospheric variables in space and time.

The MZVS program plan (Watson *et al.*, 1995) examined several previous visibility and particulate source apportionment studies, as well as existing information from the study area. The plan specified measurements, data analyses, and modeling methods that address each of the first six technical objectives. Several different data analysis and modeling methods were identified for each objective, and each of these methods was to be evaluated with respect to its applicability in the study area, completeness and uncertainty of available data, and its relevance to each study objective.

Measurements were taken as part of the MZVS, as well as acquired from existing meteorological, air quality, and visibility monitoring networks. To attain the first technical objective, these measurements were organized into a consistent and documented data base and subjected to several tests to determine their validity, precision, and accuracy. Validation tests are applied to determine which data can be used for other objectives and the uncertainties that they impart to data analysis and modeling. The following measurements were submitted to several comparison and validation tests: nephelometer measurements for light scattering; aethelometer measurements for light absorption; radar profiler and radioacoustic sounding system (RASS) measurements of upper air winds and temperature; meteorological tower measurements of winds, temperatures, and relative humidities; filter-based measurements of aerosol and precursor gas composition; and continuous measurements

of sulfur dioxide. All but the following measurement methods had been applied in prior quantitative source apportionment studies: 1) high time-resolution (every 15 minute) particle sulfur concentrations at levels below 0.1 $\mu g/m^3$; and 2) isotopic abundances of S^{32} and S^{34} in potential primary source emissions as well as in secondary particle sulfate measured at receptors. These methods had high risk of failure, but very high value for attaining the source apportionment objective if they succeeded. The climatology of the 12/01/94 through 11/30/95 study period was examined to determine the extent to which conditions found during that year can be extrapolated to earlier and later years.

The second technical objective of documenting the frequency, intensity, and character of the haze was addressed by visually examining photographs and videos as well as instrumental light scattering measurements. Frequencies of visual and instrumental haze occurrences were compiled for each measurement location. These were compared with each other and with simultaneous light scattering and extinction measurements from other Class I areas. Visual records and relative humidity measurements allow weather-related excursions in light extinction to be separated from haze caused by air pollution. Comparisons of simultaneous visibility measures near the Mt. Zirkel Wilderness, in the Yampa Valley, and outside the Yampa Valley allowed effects of regional and local emissions on visible haze to be discerned. From these analyses, several haze events were identified for more detailed examination to attain subsequent objectives.

The third technical objective of estimating the relative contributions of scattering and absorption was attained by summing the contributions from clean air (Rayleigh) scattering determined from atmospheric temperature and pressure, fine particle scattering determined by nephelometry, and fine particle absorption determined by densitometry measurements of particle deposits on Teflon-membrane filters. Nitrogen dioxide, the major contributor to absorption by gases, has been shown to be a minor contributor even in urban areas where concentrations are high, and its contribution to light extinction is assumed to be negligible in the study area.

The fourth technical objective of attributing light extinction to chemical components was addressed by estimating extinction efficiencies for each of the major aerosol components measured on daytime filter samples of six- and twelve-hour duration. These estimates make use of multi-wavelength nephelometer measurements to infer particle size distributions, relationships between particle size and relative humidity established in this and other studies to estimate particle growth from liquid water absorption, and the Elastic Light Scattering Interactive Efficiencies (ELSIE) (Sloane *et al.*, 1991; Lowenthal *et al.*, 1995) light scattering model to determine the change in extinction associated with changes in chemical concentrations.

The fifth technical objective of documenting generating station plume behavior was addressed by drawing examples from the time-lapse videos of the plumes during daylight hours, estimating transport and mixing within the Yampa Valley from vertically stratified meteorological measurements, identifying variations in generating station emissions of primary particles and sulfur dioxide, applying the CALMET/CALPUFF dispersion model to daily emissions and meteorological measurements for the entire study period, and examining

continuous sulfur dioxide, light scattering, and light absorption measurements near the Wilderness boundary.

The sixth objective of source apportionment presented the greatest challenge to this study. The attainment of the second technical objective identified cases representing different emissions, transport, and aerosol transformation situations. Both primary particles, those directly emitted from sources, and secondary particles, those formed from directly-emitted gases, were believed to be major components of suspended particles that cause light extinction (Watson *et al.*, 1995). Both Yampa Valley and more distant emitters were suspected of contributing the suspended particle concentrations. Emissions, especially intermittent emitters such as fires, were tabulated for the Yampa Valley and a larger domain that included large parts of Colorado, Wyoming, and Utah. Examples of emissions from coal-fired generating stations, vehicle exhaust, residential coal and wood combustion, geothermal springs, wildfires, and suspended dust were acquired and chemically characterized. Source characterizations included measurements of isotopic abundances in sulfur as well as elemental, ionic, carbonaceous, and sulfur dioxide abundances.

An aerosol evolution model (Robinson and Whitbeck, 1985) was applied to the generating station profiles to determine how the abundances of sulfur dioxide, sulfate, and elements might change with time under dry and moist conditions. The Chemical Mass Balance receptor model (Watson *et al.*, 1990) was used with these "aged" and unaged profiles to estimate source contributions for the all of the six- and twelve-hour average aerosol samples that were chemically characterized. Short-term (an hour or two) increments in light scattering and absorption near the Wilderness were determined to estimate maximum impacts from plumes originating in the Yampa Valley, especially when light scattering excursions corresponded to short-term excursions in continuous light absorption and sulfur dioxide. The CALMET/CALPUFF (U.S. EPA, 1995a, 1995b) wind field and air quality models were applied, using emission rates and meteorological data from the MZVS, to independently estimate source contributions from Yampa Valley and regional sources during five multi-day visibility episodes that illustrated different types of events. Nonlinearities associated with emissions changes were examined for perception by calculating changes in contrast along sight paths associated with views from the Wilderness, and by equilibrium modeling of ammonium nitrate concentrations when sulfate, ammonia, and nitric acid precursors are reduced (Kim *et al.*, 1993a, 1993b).

The final technical objective of reconciliation was approached by combining information from each of the previous analyses. Several episodes were selected for detailed analysis, especially ones in which different combinations of source contributions were observed. A conceptual model was formed that explained these episodes, and the ability of each of the simulation models to simulate these episodes was critically examined. The best estimates of each source contribution were selected, with objective and subjective estimates of the uncertainties of these contributions.

1.3 Guide to MZVS Project Documents

This report and its executive summary present the results of the MZVS, the methodology followed to achieve those results, and the rationale for the study conclusions. This section summarizes the technical objectives and the approach to attain them. Section 2 describes the measurement network, with reference to the program plan (Watson *et al.*, 1995) which contains details about the measurement methods, site selection, data analysis and modeling plans, and the data base. Subsequent sections treat each technical objective, following the approach outlined in Section 1.2. Section 3 determines the frequency, character, and intensity of hazes and justifies the selection of visibility episodes that are submitted to further study. Section 3 also quantifies the contributions from clean air scattering, particle scattering, and particle absorption for aerosol measurement periods. Section 4 estimates the contributions from different chemical constituents in suspended particles to those extinction components. The behavior of Yampa Valley plumes and the characteristics of the episodes selected for analysis are discussed in Section 5. Section 6 addresses the source apportionment objectives. Results of the previous sections are summarized and reconciled in Section 7 to support the conclusions in the executive summary. Appendices contain details about data quality and management, data analysis and modeling methods, and presentations of detailed modeling results

Many data volumes, task reports, and plots were generated as part of the MZVS. These are too voluminous to be presented as part of the final report, though they are identified by reference in the body of this report and its appendices, with their detailed citations in Section 9. Copies of these reports are maintained as part of the centralized data base at the Desert Research Institute (DRI). Digital data files, available via Internet in xBase format, constitute the bulk of the MZVS data base. In addition, the data base contains: 1) model input and output files; 2) modeling software; 3) detailed time-lapse videos in VHS format; 4) 35-mm photographs in CD format; 4) a summary time-lapse video with examples of views and visibility events in VHS format; and 5) animation of everyday plume modeling results in CD format.

The digital data base has been organized so that all data are in common units, for common time periods, and with common data validation flags and missing value codes. Traceability files were compiled that allow conversions and validation changes to be traced to the data as originally received from the provider.

1.4 Definitions

Though every attempt is made to be precise and quantitative in terms of statements and conclusions made in this report, it is necessary to use descriptive terms that may have different meanings to different people. Several commonly used, but imprecise terms, are defined for the MZVS as follows:

In references to relative amounts, such as contributions of chemical species to mass concentration, source contributions to light extinction, and components of light extinction, “negligible” means <1%, “minor” means 1% to 10%, “significant” means 10% to 25%,

"large" means 25% to 50%, and "major" means >50%. These terms are defined solely for use in this report, and are not based on any legal definitions used in the federal Clean Air Act or in Colorado's visibility regulations.

In references to frequencies of occurrence, the period of occurrence will be specified (year, season, intensive monitoring period). "Never" means 0% of the time, "rarely" means >0% to 1% of the time, "seldom" means 1% to 10% of the time, "often" means 10% to 25% of the time, "commonly" means 25% to 50% of the time, "most of the time" means >50% of the time, and "always" means 100% of the time. These terms are defined solely for use in this report, and are not based on any legal definitions used in the federal Clean Air Act or in Colorado's visibility regulations.

The term "plume" refers to ducted and nonducted bodies of pollutants in air that are detectable by visual observation or by instrumentation. Plumes do not necessarily originate in well-defined point sources, nor can they necessarily be detected by the naked eye. In particular, the presence of Yampa Valley generating station plumes are often detected in the MZVS near the Wilderness by "pulses" of elevated sulfur dioxide concentrations detected by the continuous sulfur dioxide measurements. These pulses are typically separated by sulfur dioxide readings equal to the instrument baseline. Some sulfur dioxide pulses were accompanied by pulses of elevated light scattering, but many pulses were not accompanied by measurable changes in light scattering.

2.0 MEASUREMENTS

Watson *et al.* (1995) reviewed existing information about the study area and evaluated different measurement methods that would supply the information needed for data analysis and modeling. This section summarizes the measurements taken in terms of their locations, their ability to represent prior or future years, their measurement periods and durations, and their accuracy, precision, and validity. Detailed information related to measurement evaluation, including results of quality audits, is compiled in Appendix A.

2.1 Measurement Domain and Sites

Table 2.1.1 summarizes the measurement systems installed and operated as part of the Mt. Zirkel Visibility Study. Entries in this table show which organization was responsible for each measurement, and the footnotes provide details on the measurement periods and averaging times. The locations at which these measurements were taken are shown in Figure 2.1.1, which also corresponds to the domain selected for mesoscale modeling. The size of this domain was defined so that emissions from within the Yampa Valley could be tracked by dispersion models. Figure 2.1.1 shows the major populated areas, as well as the locations of the Craig and Hayden coal-fired generating stations, within the study domain.

Table 2.1.1 Measurements in the Mt. Zirkel Visibility Study

Six instrumented sites were established to characterize the local and regional nature of light extinction and aerosol concentrations inside and outside the Mt. Zirkel Wilderness area.

- Buffalo Pass, CO: The Buffalo Pass site was intended to represent visibility and aerosol concentrations in the Wilderness, especially at high elevations (>3200 m above mean sea level [MSL]) and at its southern extreme that is closest to Yampa Valley emissions sources. Buffalo Pass was the most highly instrumented of all the monitoring sites. The site is located just south of Buffalo Pass Road at a radio relay station, less than 2 km from the southern boundary of the Wilderness and to the west of and slightly lower than the Continental Divide. The site is in a large clearing surrounded by pine trees, approximately 200 m from the access road to the Fish Creek reservoir. Owing to construction at the reservoir, there was some heavy truck traffic on this road during the summer and fall, but otherwise there were no local sources in the vicinity. A long-term record of light scattering and 24-hour average aerosol measurements is being acquired at this site as part of the IMPROVE monitoring network (Eldred *et al.*, 1994). This provides an opportunity for comparison of visibility measures with those found in and near other Class I areas of the United States. Data analysis shows that this site frequently encountered short-term (one to three hours) excursions of light absorption and sulfur dioxide concentrations, indicative of the arrival of nearby Yampa Valley source emissions.

- Gilpin Creek, CO: The Gilpin Creek site was intended to quantify the spatial differences in visibility and aerosol concentrations that result from being further

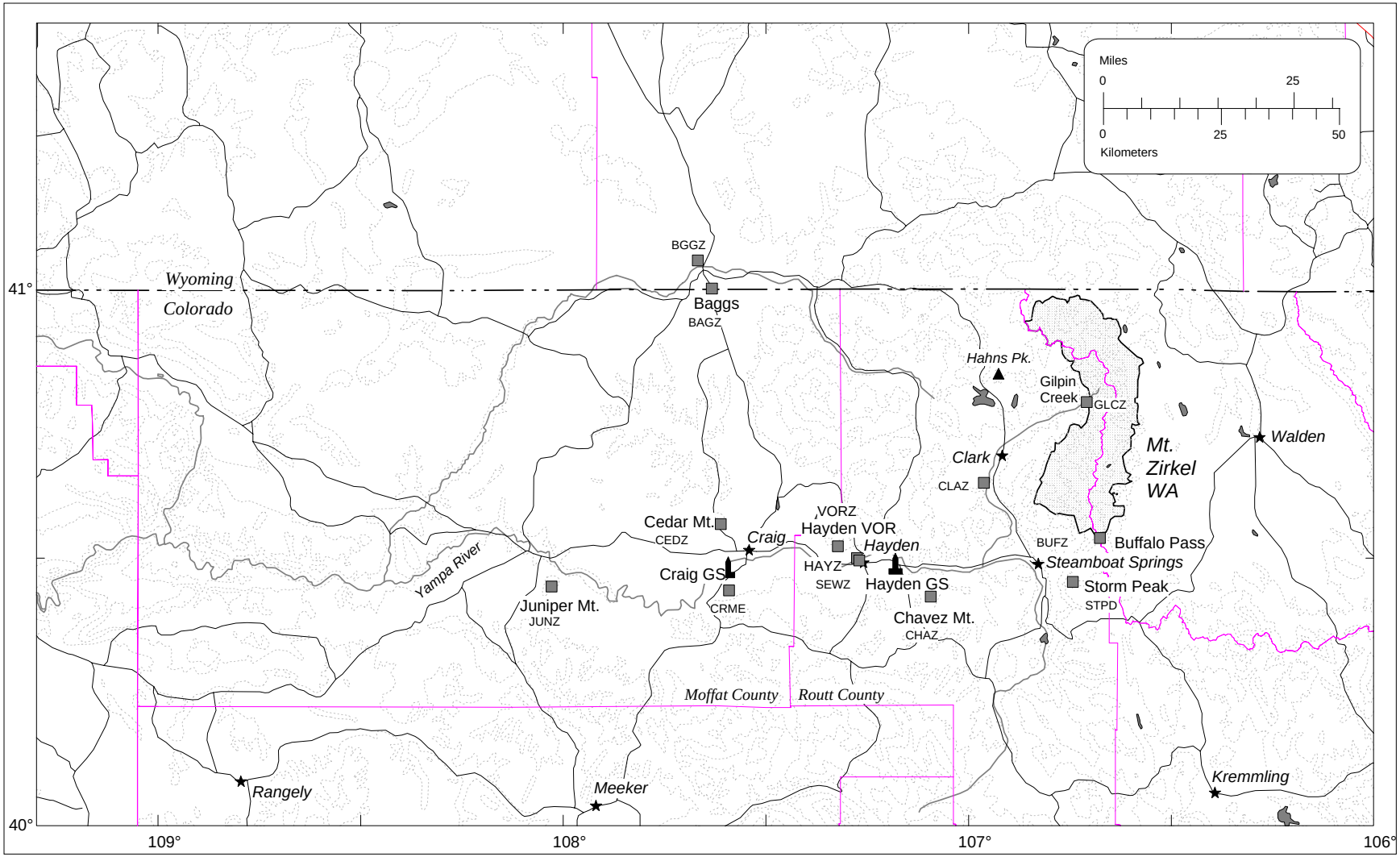

Figure 2.1.1. Mt. Zirkel Visibility Study measurement locations in the mesoscale modeling domain.

north in the Wilderness and at a lower elevation (<2900 m above MSL) than the Buffalo Pass site. The site is approximately 3 km by foot trail from Slovonia at the end of Forest Road 400. It is located just outside of the western Wilderness boundary and is in a small clearing surrounded by pine trees. Owing to its isolation, all measurements at Gilpin Creek were taken with battery-powered measurement systems, recharged by photovoltaic cells.

- Baggs, WY: The Baggs site was intended to monitor air outside the Yampa Valley, though the results of data analysis and modeling show that this site sometimes encountered Yampa Valley sources. Baggs is a small town located ~60 km north of Craig, CO on Wyoming State Route 789 (Colorado State Route 13) in the Little Snake River Valley. Aerosol and visibility measurements were acquired ~5 km south of the Baggs populated area atop a small rise ~0.25 km to the west of SR 789. The radar profiler site was located ~7 km north of this site at the base of a small bluff near the Baggs landfill to obtain a regional representation of upper-air winds outside of the Yampa Valley.

- Juniper Mountain, CO: The Juniper Mountain site was also intended to monitor air outside of the Yampa Valley, especially that above the morning mixed layer. The site is on a mountain peak ~800 m above the Yampa River floor at the western end of the Valley, ~45 km west of Craig, CO and ~150 km west of Buffalo Pass. A limestone quarry is located near the base of the eastern side of the mountain, but only repeater stations are located at its summit. Data analysis shows that this site can be affected by Yampa Valley sources when flows are from the east.

- Hayden VOR, CO: The Hayden VOR (aircraft navigation transmitter) site was intended to measure contributions from a combination of regional and local sources within the Yampa Valley at an elevation comparable to local generating station plumes. It is located ~5 km northwest of the town of Hayden, and 11 km west-northwest of the Hayden generating station at ~400 m above the Yampa River. It is accessed by an unpaved access road with negligible traffic.

- Hayden Waste Water: The Hayden Waste Water site was intended to measure the accumulated pollutants from local sources within the Yampa Valley. It is located along the Yampa River just west of the town of Hayden, CO. The site is ~200 m north of U.S. Highway 40, which experiences light to moderate traffic volumes throughout the day. It is in a low part of the Valley and provides measurements within the surface layer that often forms at night and persists through the morning. The radar profiler located at this site characterized flows within the Yampa Valley and the meteorology that affects generating station

emissions. There are potential interferences from ammonia emissions near this site, due to the sewage treatment operations.

The following visual documentation sites obtained different views of local and regional haze within and near the Wilderness using time-lapse video and 35-mm slides:

- Cedar Mountain: The Cedar Mountain site is ~15 km north of the Craig Power Station and commands a view of visible emissions from the station. The CEDZ video view to the south documented changes in the visible characteristics and movements of visible plumes from the generating station.

- Chavez Mountain: The Chavez Mountain site is on the southern slopes of the Yampa Valley and commands good views of the Hayden Generating Station and of the Wilderness from within the Valley. Three views were located at this site: 1) the CHBZ video view to the east-northeast recorded visibility along sight paths to the southern end of the Mt. Zirkel Wilderness Area, Buffalo Pass, and Storm Peak; 2) the CHZZ video view toward the north-northeast recorded visibility along sight paths to most of the Mt. Zirkel Wilderness Area, including the Gilpin Creek location; and 3) the CHHZ video view to the north-northwest included sight paths in the central portion of the Yampa Valley, and to more distant northern peaks. Visible emissions from the Hayden Generating Station were in the left part of the CHHZ view.

- Storm Peak: The Storm Peak site is located atop Mt. Werner in the Steamboat Springs ski area, ~12 km south of the Wilderness. The certification of visibility impairment was determined from views photographed at this site with cameras operated by the U.S. Forest Service and the Colorado Department of Public Health and Environment. The two video views acquired as part of the MZVS approximately correspond to these camera views: 1) the STPH video view to the north-northeast documented sight paths to Hahns Peak and the western edge of the Wilderness; 2) the STPY view to the west-northwest documented sight paths over and within the Yampa Valley. As shown in Table 2.1.1 and Figure 2.1.2, these corresponded to the 35-mm camera views acquired by the U.S. Forest Service and the Colorado Department of Public Health and Environment.

- Juniper Mountain: Cameras at the Juniper Mountain site were collocated with the visibility and air quality monitoring instruments. The JUNZ video view to the east documented conditions within the Yampa Valley in the opposite direction from that viewed by the STPY view at Storm Peak. It also provided a greater resolution of the western end of the Yampa Valley, as opposed to the eastern end documented from Storm Peak. Color slide views to the northeast (JUNZ), the southwest (JUNS), and to the west (JUNW) documented the regional appearances of haze outside of the Yampa Valley.

- Gilpin Creek: Gilpin Creek 35-mm slides of the GLCZ view to the southwest of the monitoring site documented haze in the northern portion of the Wilderness.

- Craig BLM: The Craig 35-mm CRAI views obtained by the Bureau of Land Management documented haze along sight paths at the western end of the Yampa Valley.

A radar profiler and RASS was located off Forest Road 400, ~2 km northeast of the village of Clark, CO, near the Elk River. This site was chosen to characterize terrain-induced upslope and downslope flows caused by diurnal changes in heating and cooling, as well as channeling in one of the narrow river valleys that punctuate the western side of the Mt. Zirkel range. The Craig meteorological tower, instrumented at 6 m and 60 m above ground level (AGL), was located ~1 km directly south of the Craig generating station. The tower provides upper-air winds near the height of the Craig generating station stacks. Its data were not used as input to meteorological models. These data were reserved to be compared with wind fields calculated by the CALMET diagnostic model.

Surface-based meteorological measurements of wind speed, wind direction, temperature, and relative humidity were acquired from existing networks operated by the National Weather Service (NWS), the U.S. Forest Service (USFS), and the Bureau of Land Management via satellite downlink throughout the study period. Surface meteorological monitors available to MZVS from all sources are located within the regional modeling domain, as shown in Figure 2.1.3. Twice-daily NWS upper-air soundings were available from Lander, WY, Salt Lake City, UT, Grand Junction, CO, and Denver, CO for the regional domain.

Precipitation data, used to estimate wet deposition in the CALPUFF model, were obtained from National Oceanic and Atmospheric Administration COOP sites and NWS sites. Figure 2.1.4 shows the locations of available precipitation measurements.

To complete the data base, aerosol data were obtained from the National Parks Service IMPROVE network for stations at Buffalo Pass and other sites in the region. PM_{10} and continuous air quality measurements were obtained from the Colorado Department of Public Health and Environment via the EPA AIRS network.

2.2 Measurement Periods

Ambient measurements were taken for a one-year period from 12/01/94 through 11/30/95. Twelve-hour average (0600 to 1800 MST) aerosol and sulfur dioxide filter sampling did not commence until 02/06/95, and continued every day (weather permitting) through 11/30/95 at the Buffalo Pass, Gilpin Creek, and Juniper Mountain sites.

Imbedded in the annual measurements were three intensive operating periods (IOP). These included winter (02/06/95 through 03/02/95), summer (08/03/95 through 09/02/95), and fall (09/15/95 through 10/15/95). Morning (0600 to 1200 MST) and afternoon (1200 to 1800 MST) aerosol and sulfur dioxide measurements were taken at the Buffalo Pass, Juniper

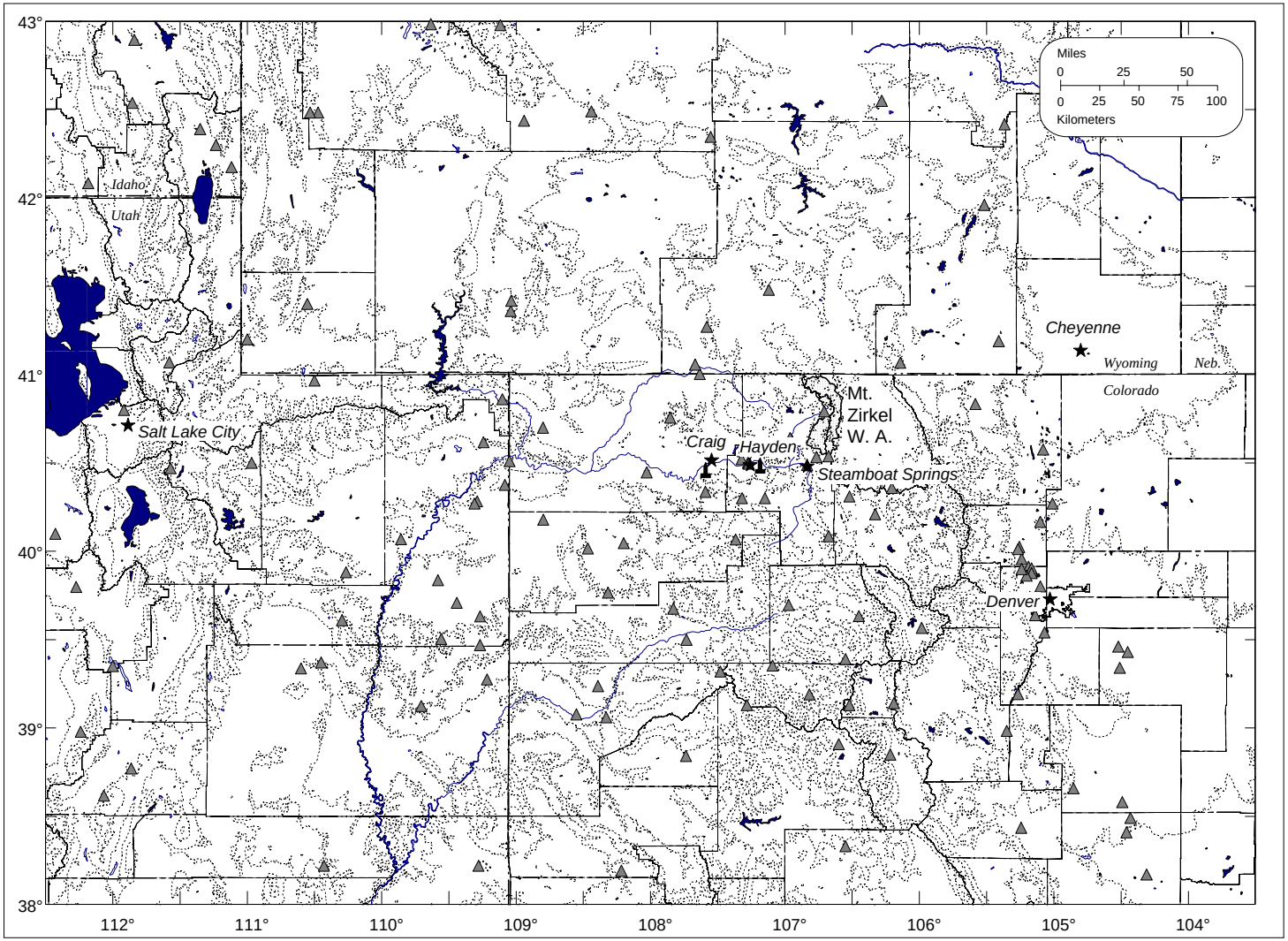

Figure 2.1.3. Meteorological monitoring sites (▲) in the mesoscale and regional domains

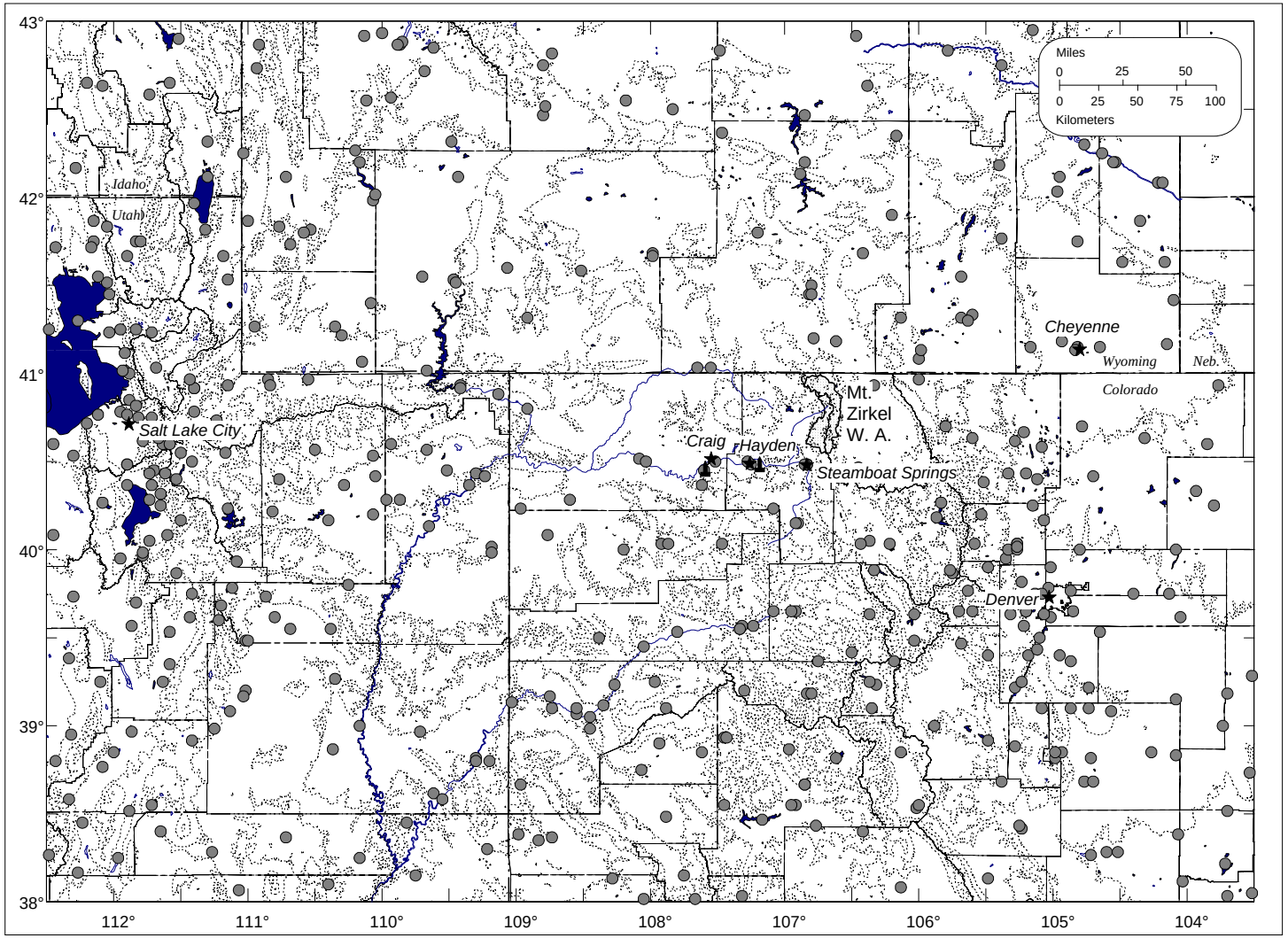

Figure 2.1.4. Precipitation measurement sites (•) in the mesoscale and regional domains.

Mountain, Baggs, Hayden VOR, and Hayden Waste Water sites during these periods. Morning and afternoon denuder difference filter-based measurements of nitric acid, and ammonia precursor gases were acquired at the Buffalo Pass, Juniper Mountain, and Hayden VOR sites. Continuous sulfur dioxide, sulfate, and optical absorption measurements were taken during the IOPs at the Buffalo Pass sites, and ozone was measured during the summer and fall IOPs at the Hayden VOR site.

The weather during the 1995 study period was compared to the climatology of northwestern Colorado to determine if study period meteorological parameters differed significantly from long-term averages. The concern was that if the meteorology for the 1995 study period was unique, it would not be possible to draw conclusions about visibility impairment and its causes that would be generally applicable to past and future years. The following climatological variables can affect the frequency of perceptible nonweather visibility events:

- Frequency and intensity of storms: These are indicated by monthly quantities of precipitation. More frequent storms imply fewer opportunities to enjoy vistas in and around the Wilderness. Greater moisture, especially in clouds and fogs, engenders transformation of sulfur dioxide to sulfate particles that affect light extinction.

- Atmospheric clarity and sunlight: These are indicated by cloud cover and solar radiation. Sunlight is needed to illuminate targets, but when it is scattered into polluted sight paths it increases path radiance and impairs visibility. Cloud cover can obscure vistas when it is low and deep.

- Transport and mixing: These phenomena are indicated by wind direction, wind speed, and surface temperature. Lower surface temperatures often inhibit vertical mixing, while higher surface temperatures indicate more rapid coupling of surface and elevated layers. Wind direction affects the transport of pollutants from sources to sight paths.

Analysis of measurements from long-term networks in and near the Yampa Valley showed that the 1995 monitoring period differed from long-term averages and frequencies by no more than expected for any year. Every year experiences deviations from long-term averages. For most years, 4% to 5% of the days contribute to that year's uniqueness. For this study, a year is considered to be atypical when the fraction of days on which a meteorological variable significantly deviates from long-term averages exceeds 7%. No more than 6% of the days during the study period showed major deviations from long-term averages and frequencies for the variables described above (Doesken, 1996). Deviations were found during the winter, spring, and summer; autumn was not unique. Nonrepresentative winter days were due to the absence of extreme cold and the presence of persistent warm periods with zonal flows aloft. Unusual days during the spring and continuing into June experienced persistent wet, cloudy weather. Unusual days during the summer were due to an absence of active convection with warmer than normal temperatures.

Observations of uniform and layered haze from 35-mm slides of the Storm Peak view of Hahns Peak taken during the study period were compared with those from previous years to examine the frequency and intensity of haze over a longer time period (see Section 2.2.4). The prior years' classifications (Air Resource Specialists, 1994) were used by Watson *et al.* (1995) to select the intensive operating periods defined above.

2.2.1 Frequency and Intensity of Precipitation Events

The Steamboat Springs, Hayden, and Craig precipitation stations experienced approximately the same precipitation patterns. Figure 2.2.1 compares the number of days with precipitation during each MZVS month with long-term averages. Precipitation was below average during seven months and above average during five months. Over a long period of time, the expectation is that approximately 55% of all months will have lower than average precipitation, and 45% of all months will have equal or above average precipitation.

Most monthly precipitation totals and the observed number of days with measurable precipitation were within one standard deviation of the mean. May was the wettest May on record for the upper Yampa Valley. Twenty-five days with measurable precipitation during May was exceptional, and was indicative of more cloudiness and humidity than normal for that month.

Based on three-month seasonal precipitation totals for the Steamboat Springs station, winter precipitation (December - February) was 81% of the 1961-1990 average and ranked the twenty-seventh driest winter in 89 years of record. Spring precipitation (March-May) totaled 10.78 inches, 170% of average and ranked third wettest. Summer precipitation (June - August) was 51% of average, the ninth driest summer on record (Hayden and Craig were each about 75% of average). Autumn precipitation (September - November) was 128% of average and ranked fourteenth wettest on record. For the study period, precipitation totals were 10-20% above average across the area. May was primarily responsible for this surplus, both in terms of the number of days with precipitation and the total accumulation. Annual precipitation at Steamboat Springs was 26.06 inches, 111% of average. In 89 years of recorded data at Steamboat Springs, 26 have been wetter. The wettest December - November twelve-month period occurred in 1956-57 when more than 36 inches of precipitation was recorded.

Cool temperatures and more snow in April raised snowpack values slightly above average by May 1. The majority of the snowpack in the mountains surrounding the Yampa Valley normally melts in May, but the cool and extraordinarily wet month of May allowed very little melting and left June 1 snowpack above average, near record levels. Yampa Valley snow-cover was present throughout the winter months and melted during early March near Hayden and later in March at Steamboat Springs. Frequent snows in April and May did not produce a lasting snow-cover in the lower valley areas. Snow-cover duration was well within the normal range throughout the year, except for earlier than normal melting during March to the west of Steamboat Springs. This is consistent with below-average winter precipitation and above-average temperatures. Over the entire twelve-month study period,

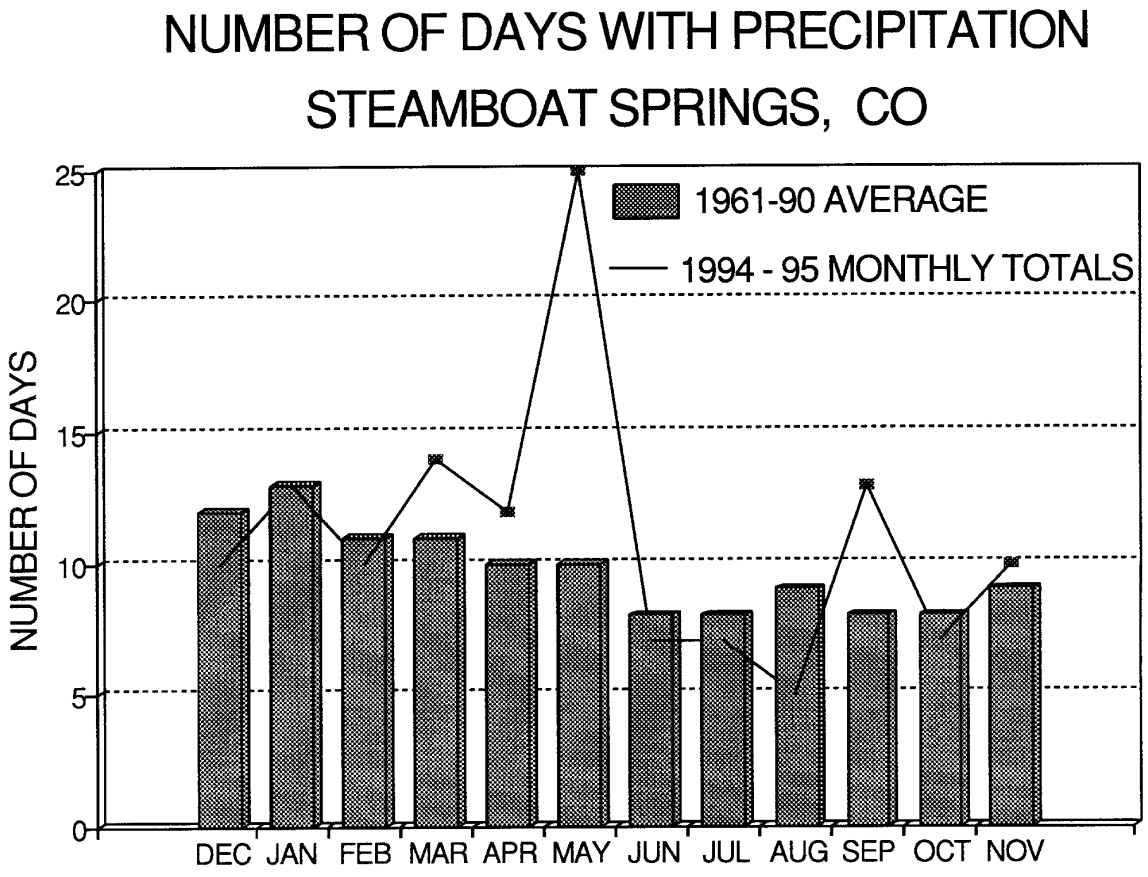

Figure 2.2.1. Number of days of precipitation during the study period compared to 1961-90 averages at Steamboat Springs. CO..

Steamboat Springs reported 139 days with snow-covered ground compared to a long-term average of 135 days. Farther west at Hayden, 107 days of snow-cover were reported, compared to an average of 116. Both are within the standard deviation of long-term measurements.

2.2.2 Cloud Cover and Solar Radiation

Winter and autumn cloud cover was close to average for Grand Junction, CO, the nearest station with a continuous record, as shown in Table 2.2.1. Grand Junction is normally much drier and sunnier than the Yampa Valley. The spring months differed from long-term averages with 13 fewer clear days and 12 more cloudy days. The summer months showed more clear days and fewer partly cloudy days than average.

Solar radiation measurements from Steamboat Springs obtained by the Joint Center for Energy Management are shown in Figure 2.2.2. These are consistent with the Grand Junction cloud cover observations. Solar radiation was close to average, except during April and May when storms occurred more often and were more intense.

Table 2.2.1
Daily Sky Cover Comparison, Grand Junction, Colorado
December 1994 - November 1995 versus 1962-1992 Averages

Month	Year	Number of Days		
		Clear	Partly Cloudy	Cloudy
December	1994	12	5	14
January	1995	2	7	22
February	1995	11	7	10
Winter Totals		25	19	46
Winter Averages[a]		27	22	41
March	1995	8	8	15
April	1995	3	14	13
May	1995	2	8	21
Spring Totals		12	30	49
Spring Averages[a]		26	29	37
June	1995	12	10	8
July	1995	22	2	7
August	1995	15	12	4
Summer Totals		49	24	19
Summer Averages[a]		42	32	18
September	1995	14	11	5
October	1995	20	5	6
November	1995	11	7	12
Autumn Totals		45	23	23
Autumn Averages[a]		42	24	25

Clear = 0-30% sky cover
Partly Cloudy = 30-80% sky cover
Cloudy = 80-100% sky cover
[a]1962-1992 averaging period

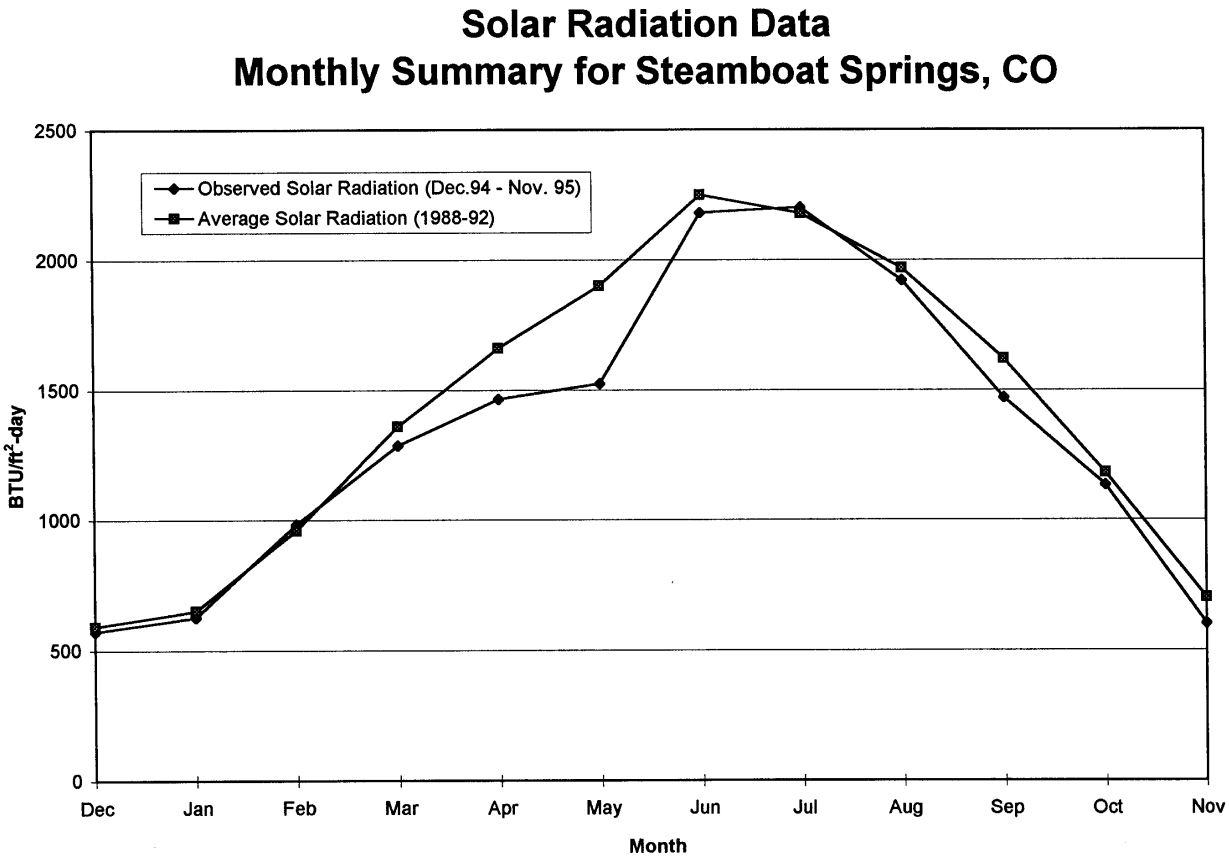

Figure 2.2.2. Monthly average solar radiation during the MZVS compared to 1988-1992 averages at Steamboat Springs, CO.

2.2.3 Temperatures and Winds

Figures 2.2.3 and 2.2.4 compare monthly average temperatures from the Hayden and Craig weather stations with long-term values. Surface and upper-air temperatures during the study period were similar to long-term averages, except for extremely warm weather during February and November, a very cool May and June, and a hot August. Few daily extreme values approached a record maximum or minimum. February was the fourth warmest in 76 years of record at the Hayden site. Temperatures for the MZVS period at the Hayden weather station were 1.1 °F above the 1988-1994 average and 1.5 °F above the 1961-1990 average.

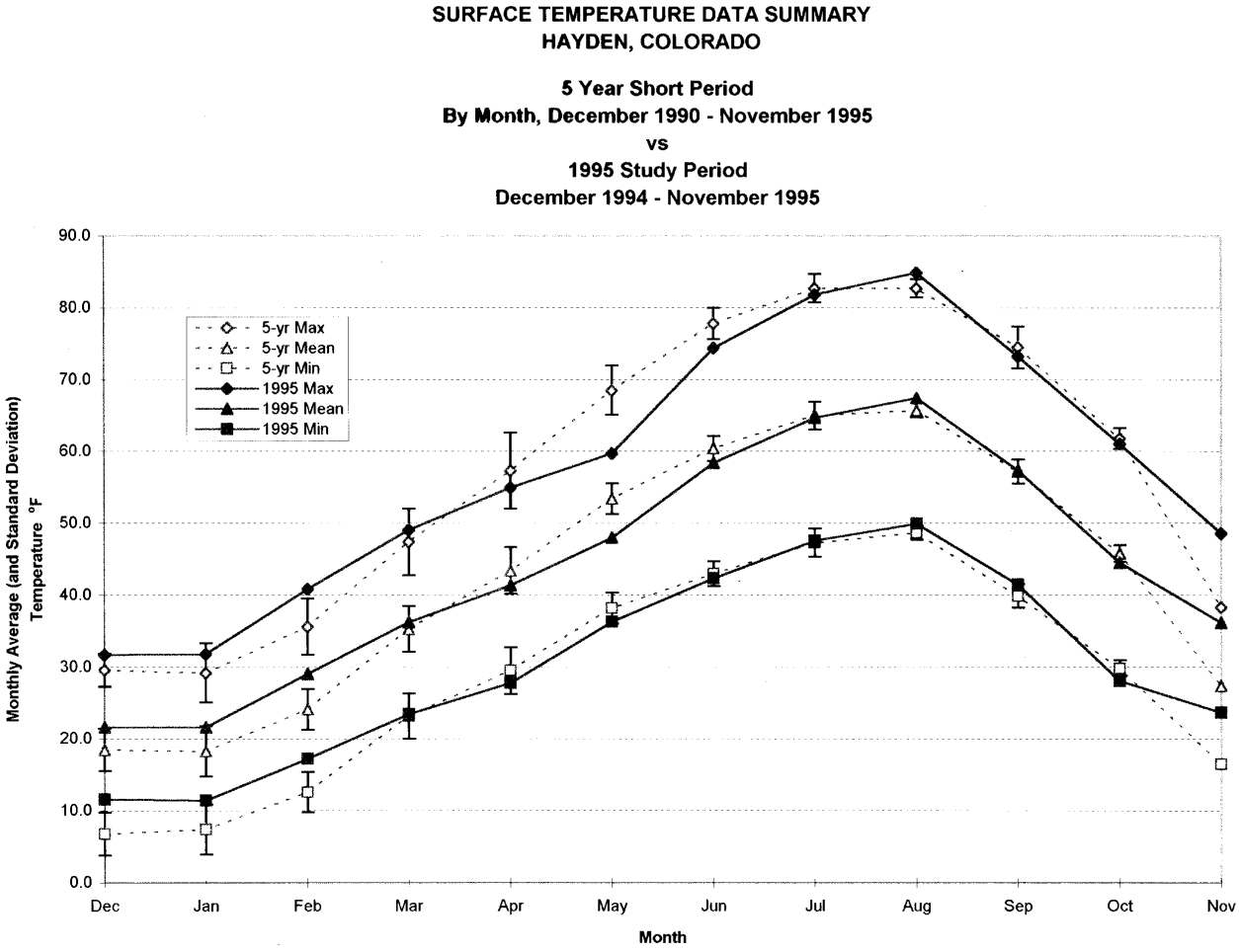

Figure 2.2.3. Monthly surface temperatures during the study period compared to long term averages at Hayden, CO.

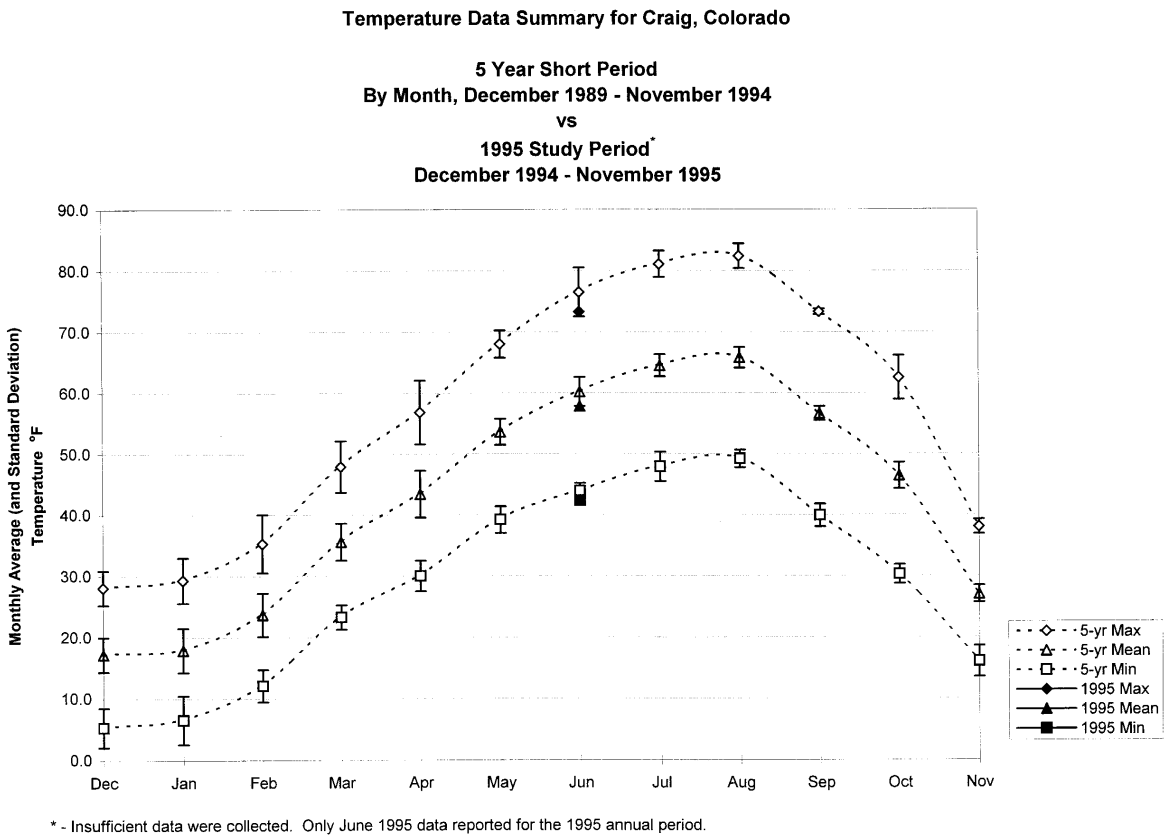

Figure 2.2.4. Monthly surface temperatures during the study period compared to long term averages at Craig, CO.

Figure 2.2.5 plots temperatures measured at 700 mb (approximately 3,000 m above MSL) at Grand Junction, CO. There were warmer temperatures during February, August, and November 1995, and cooler than average values during May and June. All other months were within the normal expected range of 700 mb monthly mean temperatures. Persistent, cooler than average spring temperatures and the lack of extreme cold during the winter months were the most notable temperature excursions during the study period. February temperatures approached the warmest on record. Approximately one in six winters are comparably mild, based on long-term records.

Surface wind speeds and directions are summarized for the Craig and Hayden 10 m towers in Table 2.2.2. These are similar to the data examined by Watson *et al.* (1995) to determine where and when samples were to be taken during the MZVS. Little variability has been recorded from year to year, particularly in areas like the Yampa Valley where topography controls much of the local wind patterns. January 1995 had approximately 7% more westerly and west-northwesterly winds than the 1989-1994 period. March winds showed more frequent surface westerly winds, fewer easterly winds, and higher speeds during 1995 than during the prior five years. This is consistent with the earlier than average

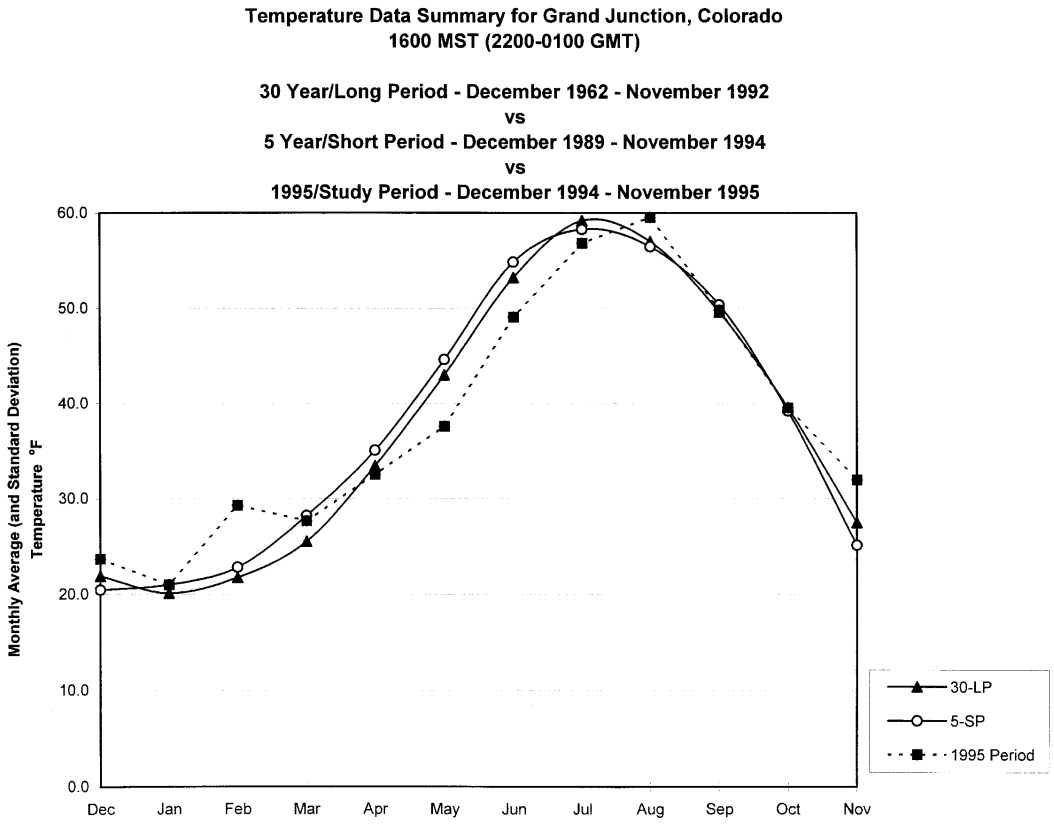

Figure 2.2.5. Monthly 700 mb temperatures during the study period compared to long term averages at Grand Junction, CO.

snow melt noted at Hayden. The stormy, wet weather of May was accompanied by fewer easterly winds and more westerly winds than average, but wind speeds did not differ significantly from long-term averages. June 1995 experienced fewer strong west and southwest winds than usual. October brought windier conditions than average with more winds out of the west-northwest. For the study period, there were more westerly winds and fewer easterly winds than indicated in the 1989-1994 frequencies. The frequency of observed winds from the southwest (225°) through the northwest (315°) was 31.2% of all observations during the study year compared to 29.0% for the 1989-1994 period. Easterly winds (northeast through southeast) accounted for 43.5% of all observations during the study year compared to 45.1% during the 1989-1994 period. Wind speeds as a whole were nearly identical to the 1989-1994 period.

Upper-air winds at 700 mb from Grand Junction, CO, are presented in Table 2.2.3 and give some indication of deviations from long-term regional transport patterns for the study period. There was a greater frequency of winds from the south during the study period that was most evident during the winter. Upper air wind speeds during the study period were higher than the multi-year averages, especially during October. Winds from the southwest were prevalent during all seasons. At most upper-air measuring sites in the U.S., 700-mb measurements are high enough above the surface to represent regional flows. However, the

Grand Junction soundings may be affected by Grand Mesa, which rises to approximately 700 mb 12 miles due east of the sampling location.

Synoptic weather classes offer another method of examining regional differences between the study year and longer time periods. Changnon *et al.* (1993) classified synoptic weather patterns during the cold months into seven classifications based on daily 500-mb weather maps as described in Table 2.2.4. The frequencies of each pattern for the colder months of the study period are compared with similar frequencies from 1951 to 1985 in Table 2.2.5.

There were no major differences between the study period and the long-term frequencies for the SWS, NWM, and unclassifiable patterns. The NWZ and DR patterns were more frequent than prior years, compensated by lower frequencies of the NWW, SWC, and SWT patterns. The timing of these patterns was consistent with the relatively mild and dry winter of 1994-95 followed by the wet spring. NWZ and DR patterns are normally associated with above-average temperatures. The NWZ pattern is associated with more westerly winds at the surface, which is consistent with the Hayden wind summary. DR is a consistently dry pattern and is usually associated with stable surface air masses over much of the Great Basin region. NWZ can be either dry or wet for the Mt. Zirkel area depending on the fetch of the zonal flow pattern and the availability of Pacific moisture. SWT is normally a cold and wet weather pattern for the region, while SWC is cold and unsettled but with little precipitation.

Table 2.2.2
Wind Speed (mph) and Wind Direction (°North) Frequencies at Hayden and Craig, CO

SITE	ANALYZED PERIOD	OVERALL PERIOD		MONTH																							
				December		January		February		March		April		May		June		July		August		September		October		November	
		WS (mph)	WD (°N)	WS (mph)	WD (°N)	WS (mph)	WD (°N)	WS (mph)	WD (°N)	WS (mph)	WD (°N)	WS (mph)	WD (°N)	WS (mph)	WD (°N)	WS (mph)	WD (°N)	WS (mph)	WD (°N)	WS (mph)	WD (°N)	WS (mph)	WD (°N)	WS (mph)	WD (°N)	WS (mph)	WD (°N)
Hayden (surface data)	SP	7.7	143.0	6.7	122.0	6.5	120.0	6.8	138.0	7.3	157.0	8.2	254.0	8.0	144.0	8.5	179.0	8.5	148.0	8.2	115.0	8.6	146.0	7.5	193.0	7.0	143.0
Hayden (surface data)	AP	7.7	155.0	7.0	120.0	6.8	132.0	7.1	138.0	8.1	215.0	8.1	246.0	8.0	242.0	7.8	132.0	7.9	145.0	8.5	127.0	8.2	115.0	8.3	253.0	7.1	173.0
Craig (surface data)	SP	4.9	235.0	3.6	225.0	3.4	216.0	4.0	216.0	5.5	235.0	6.2	248.0	5.8	231.0	6.5	233.0	6.1	231.0	5.2	220.0	5.5	243.0	4.6	247.0	4.1	234.0
Craig (surface data)	AP	*	*	3.2	218.0	4.6	221.0	4.2	203.0	7.0	226.0	*	*	*	*	*	*	*	*	*	*	*	*	*	*	*	*

SP=Short Period (Jan 1992 - Nov 1995)

AP=Annual Study Period (Dec 1994 - Mar 1995)

* - Insufficient data were reported to include April 95 - November 95 Craig data in the combined period statistical summaries

Table 2.2.3
700 mb Wind Speed (mph) and Wind Direction (°North) Frequencies at Grand Junction, CO

ANALYZED PERIOD		OVERALL PERIOD		MONTH																							
				December		January		February		March		April		May		June		July		August		September		October		November	
		WS (mph)	WD (°N)	WS (mph)	WD (°N)	WS (mph)	WD (°N)	WS (mph)	WD (°N)	WS (mph)	WD (°N)	WS (mph)	WD (°N)	WS (mph)	WD (°N)	WS (mph)	WD (°N)	WS (mph)	WD (°N)	WS (mph)	WD (°N)	WS (mph)	WD (°N)	WS (mph)	WD (°N)	WS (mph)	WD (°N)
LP	0400	15.5	255.6	18.2	266.5	18.3	267.9	16.9	272.6	17.3	260.1	17.0	248.8	15.2	245.6	14.1	242.1	11.4	244.9	11.4	247.7	14.2	245.0	14.7	257.5	17.4	259.0
LP	1600	14.8	255.9	17.1	260.5	17.9	266.1	15.9	265.7	15.7	252.6	16.1	249.5	14.9	249.0	14.1	245.9	10.6	266.3	10.6	266.3	13.7	248.6	14.0	251.8	16.6	255.7
SP	0400	15.8	255.3	17.8	261.5	17.1	268.9	17.7	255.7	17.1	263.2	16.1	263.8	16.6	231.5	16.1	242.1	12.4	253.8	11.8	246.3	13.8	249.5	15.9	267.3	17.2	261.9
SP	1600	15.2	255.4	16.9	256.7	16.6	262.1	16.7	250.6	14.8	255.8	15.4	256.4	16.2	238.0	15.7	244.6	12.7	273.6	11.4	269.3	13.5	260.3	15.0	251.9	18.0	255.3
AP	0400	16.9	248.7	17.6	233.2	18.3	246.8	18.7	275.1	21.5	243.4	18.0	268.0	17.6	242.7	15.5	221.9	14.1	237.1	13.4	238.7	15.0	258.0	16.6	276.6	0.0	0.0
AP	1600	16.0	249.9	17.1	240.5	17.1	249.2	18.9	269.4	16.2	235.8	18.0	259.3	17.4	246.1	17.3	224.9	11.5	245.1	11.8	262.2	13.3	253.8	17.8	260.5	0.0	0.0

LP = Long Period (Dec 1962 - Nov 1992)

SP=Short Period (Jan 1992 - Nov 1995)

AP=Annual Study Period (Dec 1994 - Nov 1995)

Table 2.2.4
Characteristics of Synoptic Weather Patterns in Northern Colorado

Potential Precipitation Distribution	Synoptic Pattern	Airflow Direction	Latitude Constraints	Longitude Constraints	Meridional or Zonal Feature
Dry	DR	Weak NW 310° - 360	Main flow north of 50° N	Ridge crest 110° - 125° W	Meridional
West-to-North Wet	NWM	Strong NW to N 310° - 360	Main flow between 40° and 50° N	Ridge crest 117° W - 135° W	Meridional
	NWW	Strong WNW 290° - 320	Main flow between 35° and 50° N	Small ridge crest if any 115° - 136° W	Zonal
	NWZ	Weak or strong W 260° - 280	No constraints	No constraints	Zonal
West-to-South Wet	SWT	Strong SW 200° - 260	Main flow between 35° and 47° N	Bottom of trough (NW-SW flow) between 115° - 127° W	Meridional
	SWS	Weak NW north 300° - 340 weak WSW south 210° - 260	Flow divided north of 50° N and south of 40° N	Largest split in flows 115° - 125° W	Meridional
	SWC	Strong N-turns SW; flow around low - south to east	Cutoff low between 45° and 32° N	Cutoff low between 105° and 125° W	Meridional

Reprinted from Monthly Weather Review, Vol. 121, No. 3, March 1993

Table 2.2.5
Frequency of Synoptic Patterns over Colorado
(Number of Days by Month By Predominant Weather Pattern)

Month	Year	Snoptic Pattern* (No. of Occurrences) NWZ	NWW	DR	SWS	SWC	SWT	NWM	Not Identifiable
Dec	1994	1	1	5	4	5	10	4	1
Jan	1995	1	3	8	4	2	3	10	0
Feb	1995	5	5	9	2	2	1	4	0
Mar	1995	5	3	6	1	5	7	2	2
Apr	1995	5	3	3	2	7	5	4	1
No summer identification									
Oct	1995	5	9	5	1	1	4	6	0
Nov	1995	4	10	6	0	1	3	6	0
Total		26	34	42	14	23	33	36	4
Percent (%) of Days		12%	16%	20%	7%	11%	15%	17%	2%
1951-1985 Averages		3%	22%	11%	5%	17%	25%	15%	2%
Departure from Average		9%	-6%	9%	2%	-6%	-10%	2%	0%

* Abbreviation reference provided in Table 2-4

Colorado Climate Center 3/5/96

Color Slide Comparisons

Color slides showed that the 1995 study period differed from longer-term distributions by no more than prior years with respect to the frequencies of layered and uniform hazes with different intensities. No cases of layered hazes that completely obscured the background target were found in 1995 photographs, contrasted to three to nine occurrences in prior years.

Air Resource Specialists (1994) visually reviewed, chronologically numbered, and assigned a four-digit qualitative slide condition code to each slide available from 1991 through 1994. The same procedure was completed for the slides available during the study period. This code identifies weather conditions, observed hazes or plumes, unusable or missing observations, and intensity of noted haze events. Ground-based, elevated, and multiple layers were accounted for separately and, together, reflect the total number of layered hazes observed during a period. A uniform haze code of *slight* was assigned when the most distant terrain features were clearly visible. Uniform haze codes of *moderate* and *considerable* were assigned as the perception of color and terrain detail diminished. Periods when weather or clouds concealed the scene (i.e., a uniform haze description could not be made) were identified as *weather concealed*.

Codes were subjectively determined by viewing each slide on a light table with the naked eye and an eight-power hand-held lens. The classification scheme used to analyze these slides was identical to the scheme used to classify 1990 to 1994 slides, but differed from the more detailed video and slide classification scheme described in Section 3 that was used to analyze all 1995 study images. These differing classification codes are not comparable. Results are summarized in Table 2.2.6.

Thirty-six occurrences of layered haze were observed (5% of all valid observations) during the study period. Typically 35 to 40 occurrences are reported annually, with the exception of 1994 when 78 occurrences were documented. During 1994, numerous forest fires caused the increased frequency of hazes. During the study period only slight and moderate hazes were observed from the Storm Peak 35-mm cameras. No considerable layered hazes were observed. In previous years, an average of four considerable haze events were documented annually. Layered haze occurred most often during the summer and fall months (June through October), with October having the most notable frequency. Layered haze appeared most often as a dark, ground-based layer in the 0900 MST slide that dissipated as the day progressed. The frequencies and intensities of uniform haze during the study period were comparable with those found during the previous four years. A larger number of weather-obscured views were encountered during 1995 than during the prior years.

2.2.4 Intensive Operating Periods

The winter Intensive Operating Period (IOP) (02/06/95 to 03/02/95) was characterized by temperatures 8 to 10 °F warmer than average across the study area both near

Table 2.2.6
Color Slide Classifications of Hahns Peak from Storm Peak from 1991 through 1995

Time Period	Year*	Usable Observations	Scene Concealed by Weather	Layered Haze Intensity				Uniform Haze Intensity		
				No Layered Haze	Barely Visible	Clearly Visible	Obscures Background	Slight Intensity	Moderate Intensity	Considerable Intensity
ALL DATA	1991	644	176	433	17	14	4	222	189	57
	1992	689	187	464	14	21	3	174	232	96
	1993	1027	372	608	21	22	4	217	375	63
	1994	910	265	582	44	25	9	180	393	72
	1995	775	297	473	25	11	0	162	256	60
	TOTAL	4045 (100%)	1297 (32%)	2560 (63%)	121 (3%)	93 (3%)	20 (1%)	955 (24%)	1445 (36%)	348 (9%)

* Represents annual period of January 1 - December 31

the surface and aloft. A four-day period in early February with clear skies, light winds, snow-cover, and warm temperatures aloft presented an excellent example of a typical winter air stagnation situation similar to what can be expected several times during a winter season. A stormy period in mid-February with clouds, snow, and strong winds was also typical for the area but was the only period during the month with widespread cloud cover and precipitation. The most unusual aspect of February's climate was the long air stagnation episode that lasted for most of the final two weeks of the month. The period was characterized by nearly calm surface winds during the day in the Yampa Valley, clear skies, near-record warm daytime temperatures (despite snow-cover), strong shallow nocturnal inversions and drainage flows, and very warm temperatures aloft with lighter than normal winds. For the IOP as a whole, there were more days with potential local and regional air stagnation than normal and few disturbances to mix the air in the Yampa Valley horizontally or vertically.

The summer IOP (08/03/95 to 09/02/95) was 2 to 4 °F warmer than average with above-average readings persisting for the entire month. Precipitation totals were very low (45% to 60% of average). The first ten days of August were relatively cloud-free with large day-night temperature fluctuations. Dry convection occurred each day in the boundary layer, but little horizontal mixing was evident. Mid-August brought three weather disturbances that resulted in an exchange of air masses across the region. A relatively moist air mass reached the area and lingered for several days before gradually drying out as the month ended. The higher humidity supported afternoon and evening convective showers, but no strong storm systems with deep convection occurred. Overall, convection in August was less vigorous than normal, and air mass changes in the Yampa Valley were fewer than expected. Aloft, there was a higher frequency of moderate westerly winds and a lower frequency of light southerly winds. Surface wind patterns observed at Hayden for the month were normal. All of this is indicative of a drier and more stable regional air mass than that which commonly occurs during August.

The fall IOP (09/15/95 to 10/15/95) experienced a variety of weather conditions, including several strong synoptic-scale storms and periods of sunny, dry weather with chilly nights and distinct local nocturnal temperature inversions. No single weather pattern persisted for more than a few days at a time. Regional air mass exchanges and vertical mixing may have been more frequent than is typical for this time of year, since winds aloft were slightly stronger than average and the storm systems that crossed the region were vigorous. However, the mix of stormy and placid weather patterns and the accompanying fluctuations in temperature were all within the range of conditions that is expected during the early autumn season.

2.3 Measurement Durations and Variability

Light scattering, wind speed, temperature, relative humidity, ozone, and Buffalo Pass sulfur dioxide and light absorption measurements are reported as hourly averages, both for consistency with data from other networks and because one hour is on the order of changes in atmospheric processes and emissions rates. Aerosol samples, however, had to be acquired over six- and twelve-hour intervals to obtain sufficient deposits for chemical analysis. The

0600 to 1200 and 1200 to 1800 MST daylight hours were selected by Watson *et al.* (1995) because: 1) they covered daylight hours when haze could be observed; 2) surface easterly flows often occurred during the morning while westerly flows occurred during the afternoon; and 3) surface-based layers usually coupled to upper-air layers between 1000 and 1200 MST. With the hourly nephelometer data, it is possible to examine the diurnal variation in particle scattering for each of the intensive operating periods when six-hour samples were taken to determine how variable conditions might be within the six-hour aerosol averaging periods.

Figures 2.3.1 through 2.3.6 show the range of values and the 25th, 50th, and 75th percentiles of total light scattering for each hour during the three intensive operating periods during which six-hour aerosol samples were acquired. With the exception of the Hayden Waste Water site, light scattering changed by no more than a few Mm^{-1} during the aerosol sampling periods. The six-hour aerosol samples adequately represent the light-scattering particles present during the measurement period, especially for afternoon samples. Light scattering particles appear to be consistent during the afternoon samples, though the afternoon scattering was often significantly different from that during the morning period. The maxima and minima show greater variation than the percentiles, though these do not always correspond to the same sample, as will be examined in Section 3. These diurnal variations are related to meteorological and emissions changes discussed in Section 6, and they were repeatable most of the time during the different seasons of the study period.

Light scattering at Buffalo Pass during the winter was close to that of clean air throughout the day. Diurnal variation was minor, with greater variability during the morning sampling period than during the afternoon period. Hourly light scattering during the summer was ~5 Mm^{-1} more than the winter values for the 50th and 75th percentiles for all hours. Although the total light scattering remained fairly uniform over the entire day, the periods of greatest variability occurred during the daylight hours. The 50th percentile during the fall was higher than that found during winter, but lower than that for the summer. Again, most of the variability occurred during the morning.

Winter light scattering at Gilpin Creek was ~4 Mm^{-1} higher than that at Buffalo Pass throughout the day. Gilpin Creek experienced more diurnal changes than Buffalo Pass, with most of the variability during the morning. During the summer intensive operating period, light scattering at Gilpin Creek was ~10 Mm^{-1} larger than that seen in the winter throughout the day, but with lower diurnal variability than found during the winter. Fall light scattering was higher than that of winter and lower than that of summer throughout the day with similar variabilities during the morning and afternoon. Gilpin Creek aerosol samples were of 12-hour duration even during intensive periods, and it is apparent from these diurnal variations that, at least during the most intense hazes, a majority of the particles were probably obtained during the first half of the six-hour interval.

The Juniper Mountain site is most similar in elevation to the Gilpin Creek site, and the patterns of the medians at these two sites are most comparable. Again, the highest 50th percentiles of light scattering were observed during the summer, the lowest during the winter, with the fall levels in between.

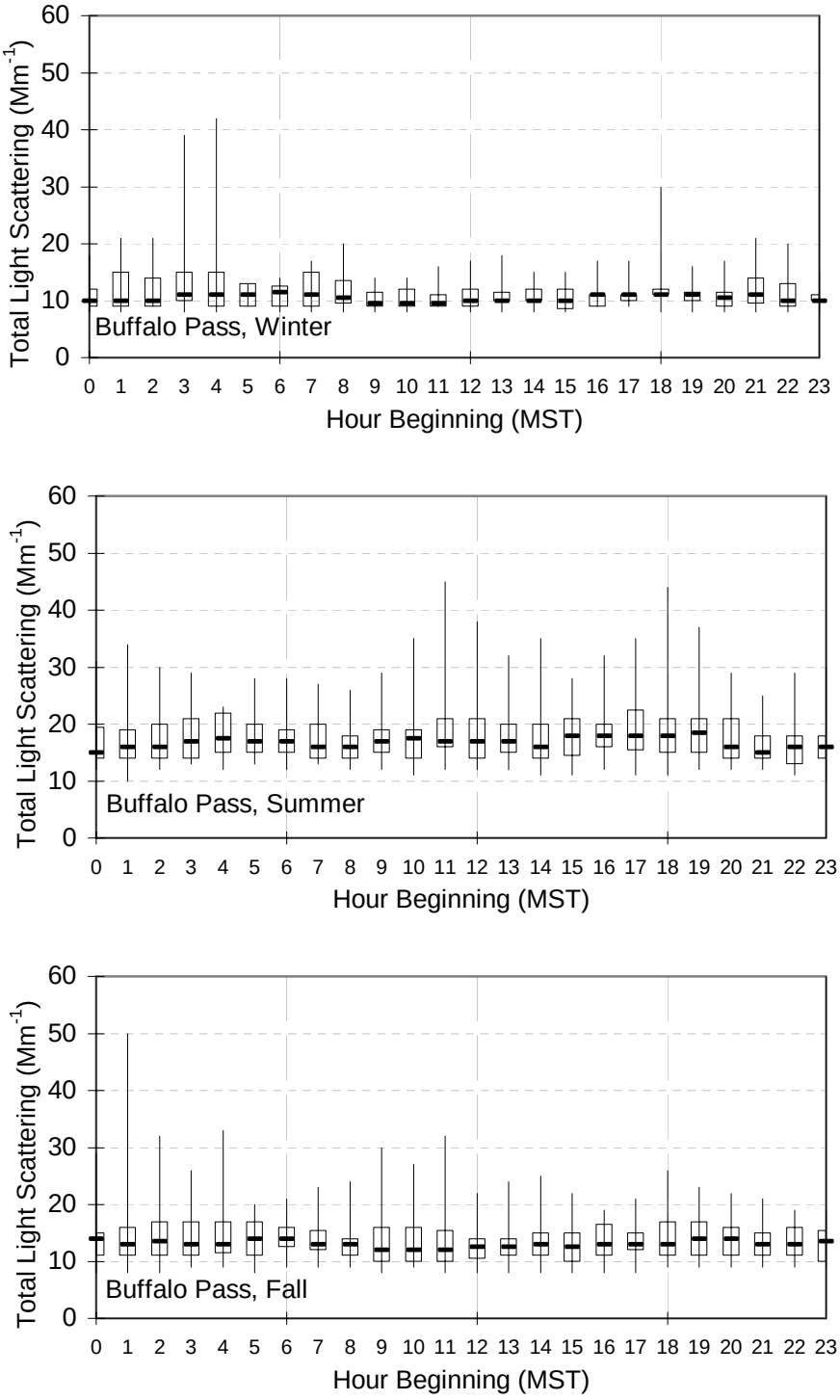

Figure 2.3.1 Hourly variations in total light scattering at Buffalo Pass during winter, summer, and fall intensive operating periods. Bottoms, centers, and tops of boxes indicate 25th, 50th, and 75th percentiles. Bottoms and tops of vertical bars indicate hourly minima and maxima for the time period. Data are for RH<90%.

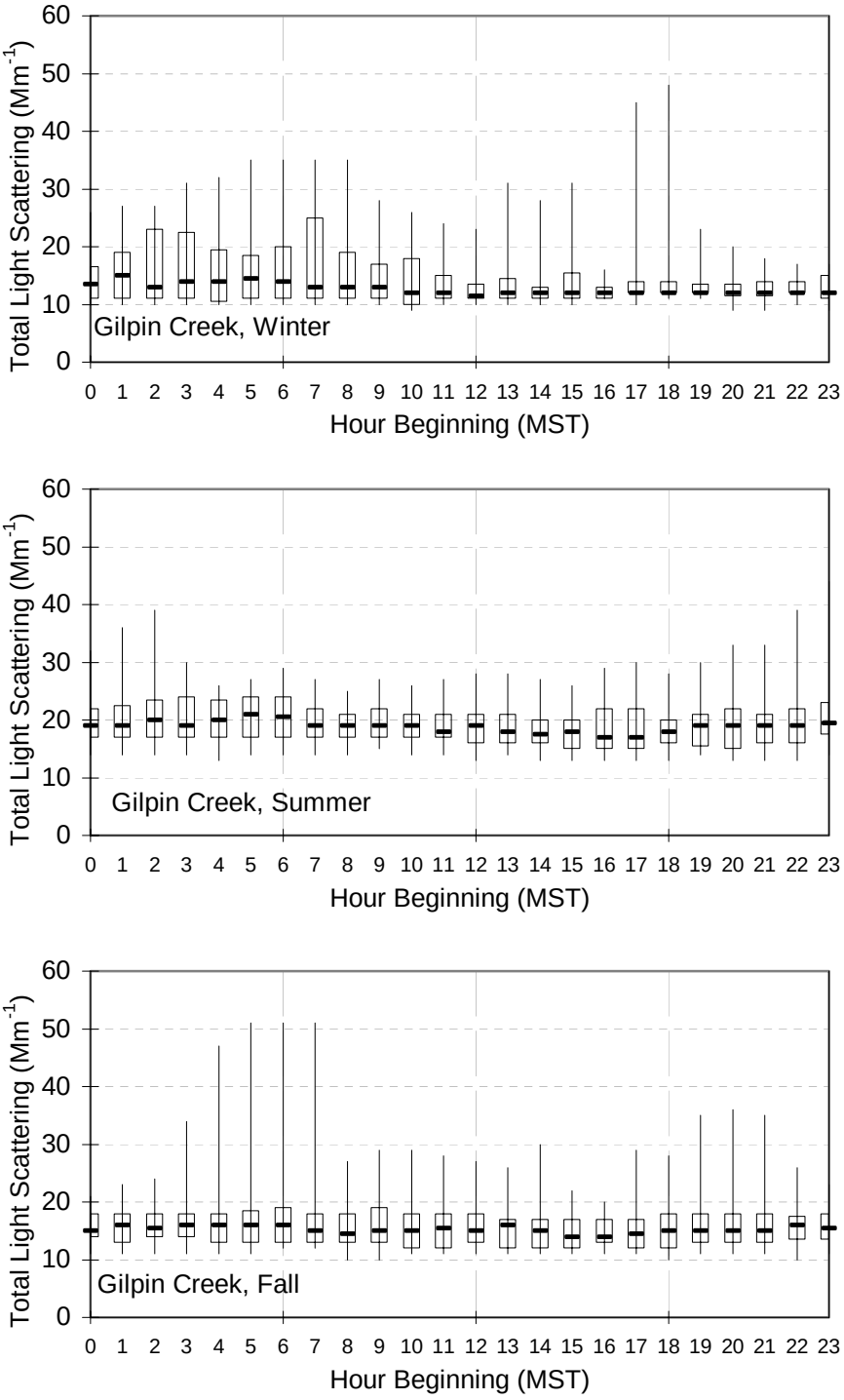

Figure 2.3.2 Hourly variations in total light scattering at Gilpin Creek during winter, summer, and fall intensive operating periods. Bottoms, centers, and tops of boxes indicate 25th, 50th, and 75th percentiles. Bottoms and tops of vertical bars indicate hourly minima and maxima for the time period. Data are for RH<90%.

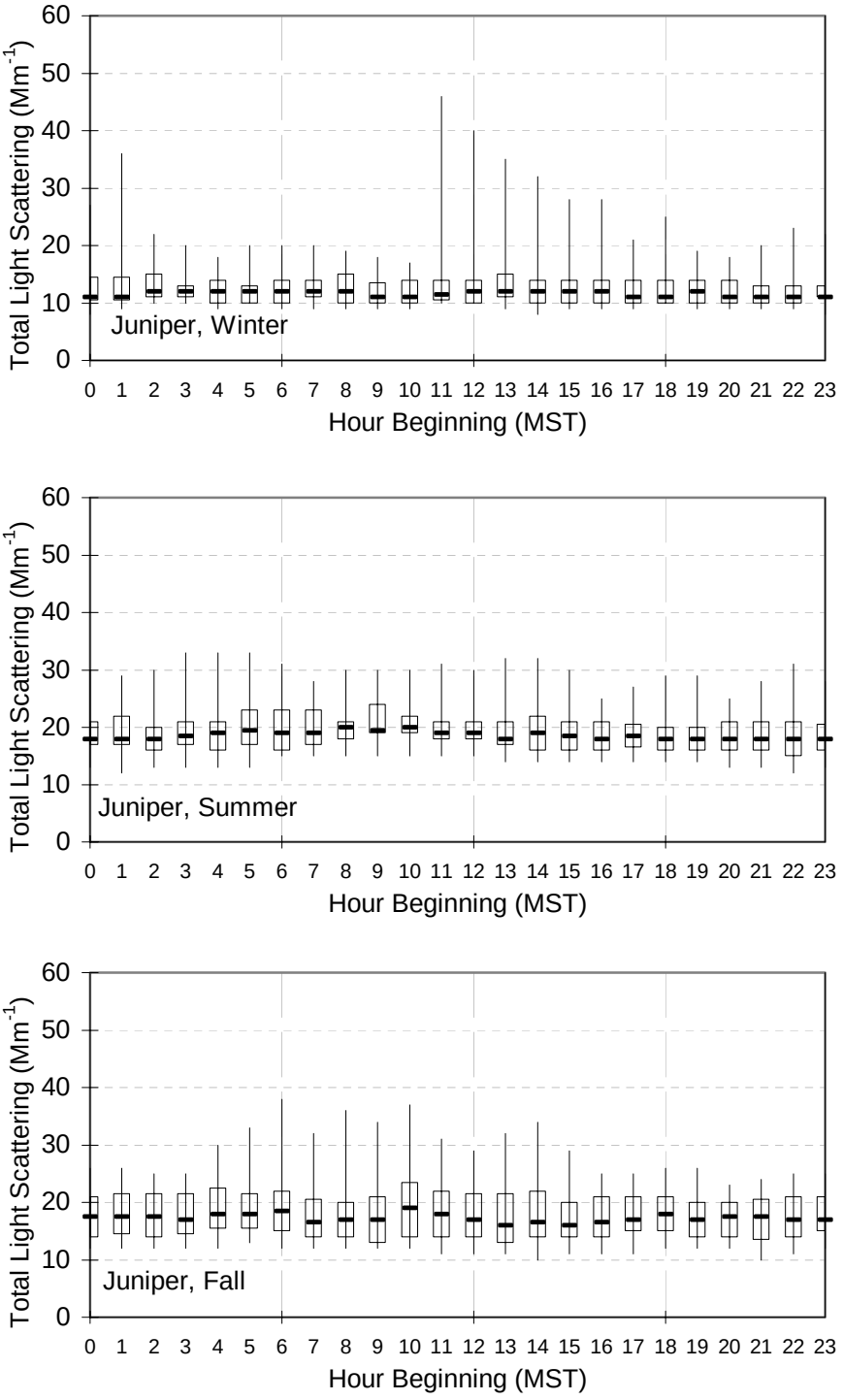

Figure 2.3.3 Hourly variations in total light scattering at Juniper Mountain during winter, summer, and fall intensive operating periods. Bottoms, centers, and tops of boxes indicate 25th, 50th, and 75th percentiles. Bottoms and tops of vertical bars indicate hourly minima and maxima for the time period. Data are for RH<90%.

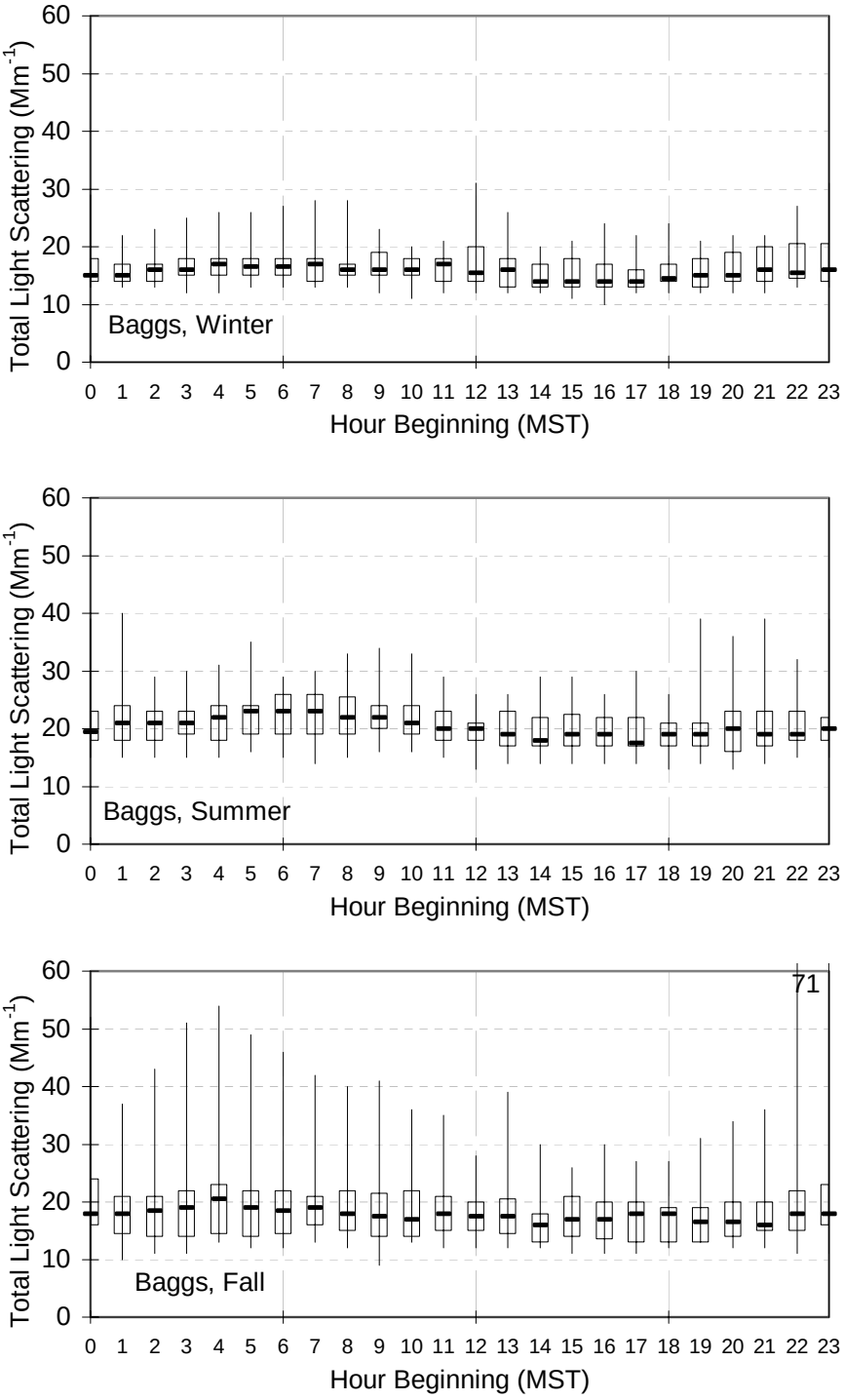

Figure 2.3.4 Hourly variations in total light scattering at Baggs during winter, summer, and fall intensive operating periods. Bottoms, centers, and tops of boxes indicate 25th, 50th, and 75th percentiles. Bottoms and tops of vertical bars indicate hourly minima and maxima for the time period. Data are for RH<90%.

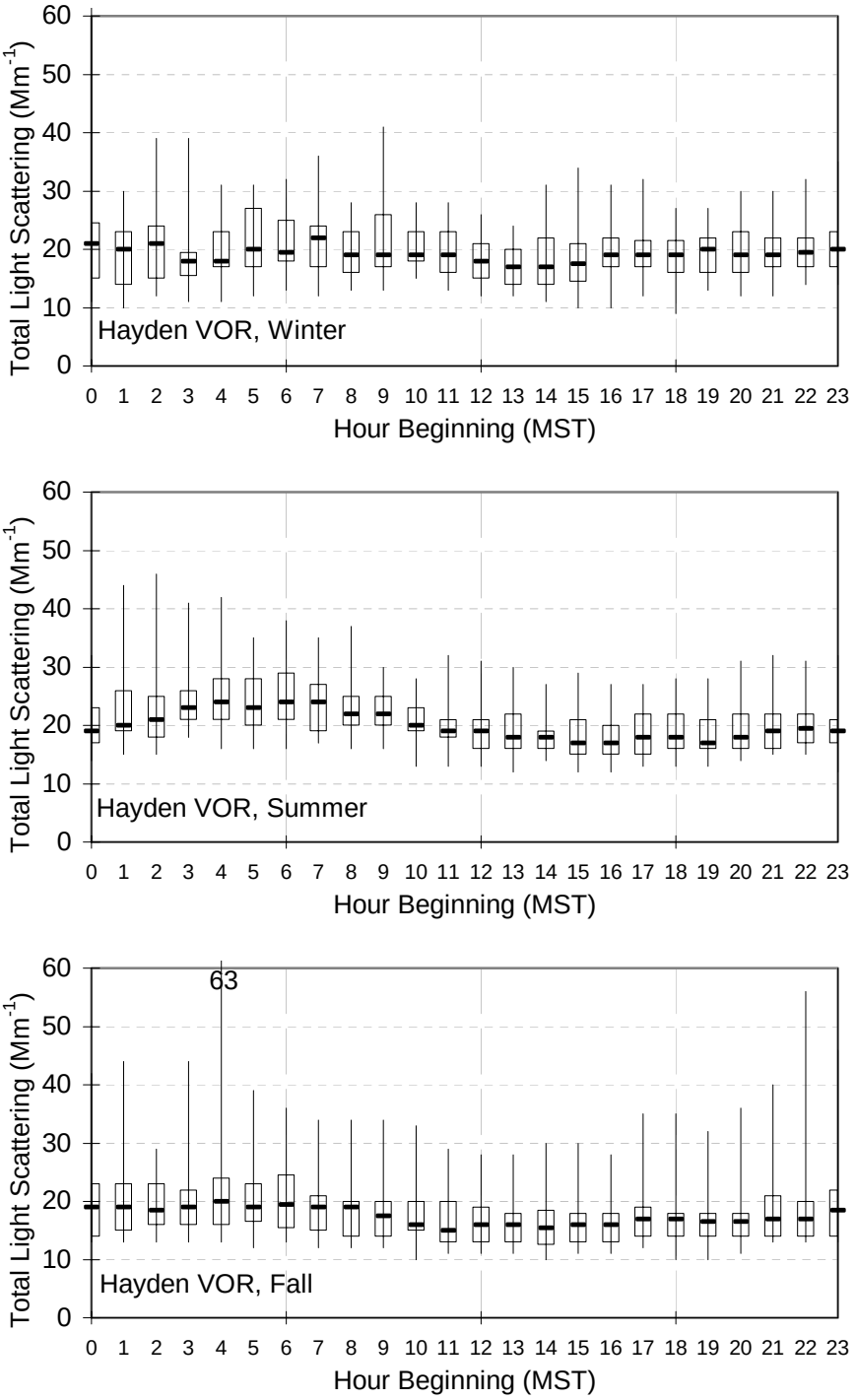

Figure 2.3.5 Hourly variations in total light scattering at Hayden VOR during winter, summer, and fall intensive operating periods. Bottoms, centers, and tops of boxes indicate 25th, 50th, and 75th percentiles. Bottoms and tops of vertical bars indicate hourly minima and maxima for the time period. Data are for RH<90%.

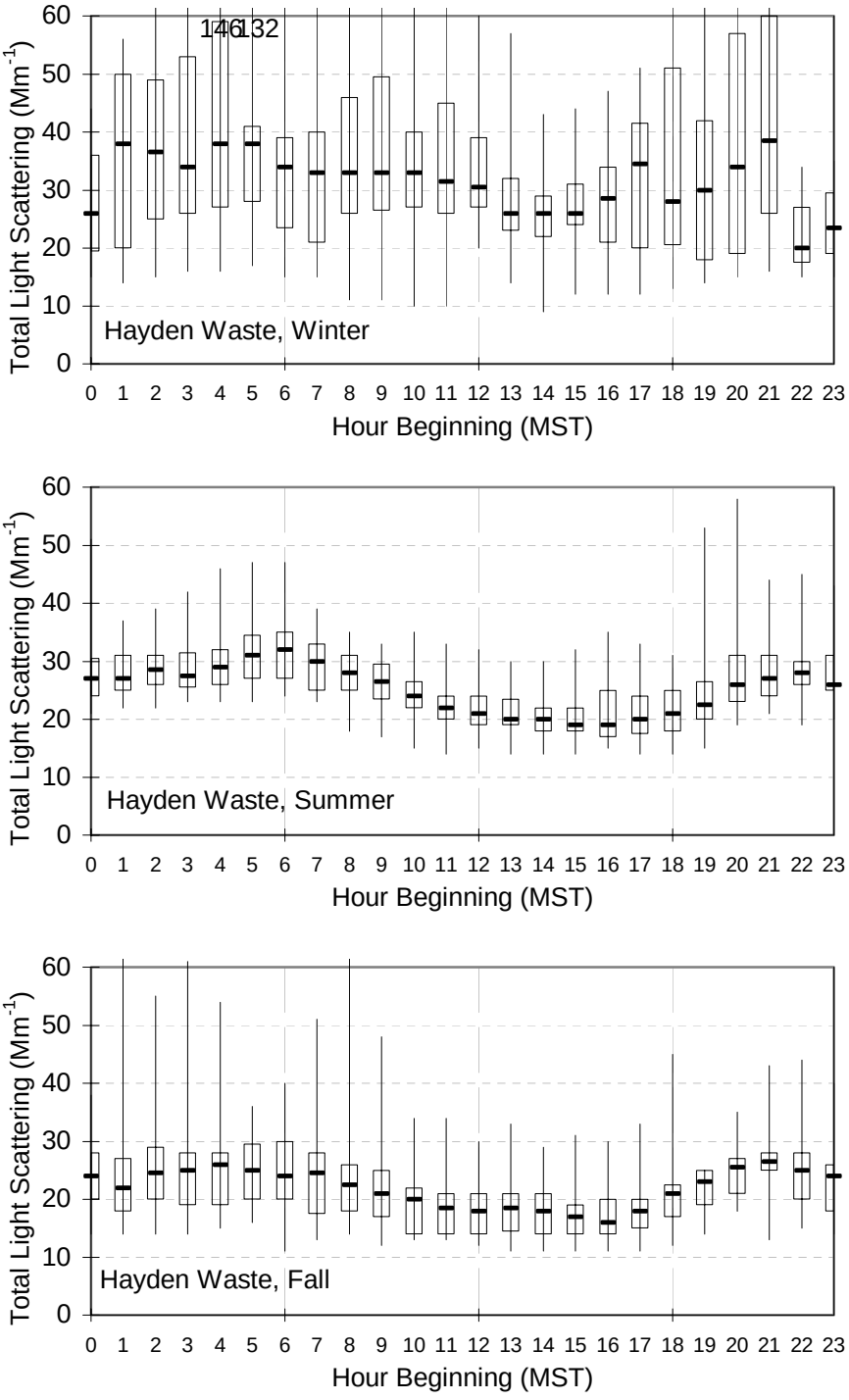

Figure 2.3.6 Hourly variations in total light scattering at Hayden Wastewater during winter, summer, and fall intensive operating periods. Bottoms, centers, and tops of boxes indicate 25th, 50th, and 75th percentiles. Bottoms and tops of vertical bars indicate hourly minima and maxima for the time period. Data are for RH<90%.

Light scattering at Baggs during the winter was higher than at Buffalo Pass, Gilpin Creek, and Juniper Mountain. Morning periods experienced higher scattering than afternoon periods during all seasons. Hour-to-hour changes are more pronounced during the summer than during the winter. The fall showed higher variability, with larger maxima and smaller minima than either the winter or summer, even though the 50th percentiles were between those of winter and summer.

The Hayden Waste Water site showed the most diurnal variability of all sites, in terms of deviations from the 50^{th} percentiles as well as maxima and minima. This was especially evident during the winter, where a not-easily-repeatable pattern can be discerned. During winter, scattering was often more than three times that measured at Buffalo Pass during all hours. During all seasons, the morning aerosol sample was dominated by particle concentrations accumulated prior to 1000 MST, though the afternoon samples experienced more uniform fine particle concentrations.

Over the region, light scattering observed at the Wilderness and background sites follows the same pattern (fairly uniform scattering over a day, low scattering in winter, high scattering in summer, in between scattering in the fall) and, during summer, has the same magnitude. The two Hayden sites track each other (elevated mornings and lower afternoons), and during summer afternoons, show the same total light scattering magnitudes as all of the other sites.

These analyses show that the six-hour aerosol samples represent the fine particles that cause light scattering in afternoon samples for all but the most extreme cases. For these extremes, that are of one to three-hour duration, source apportionment and extinction budget estimates will underestimate contributions to extinction during the shorter term period even though they may be reasonable for the six-hour average. These periods are evident from the hourly light scattering measurements, and will be considered in analysis of specific cases.

For morning samples at the lower-elevation sites (Hayden Waste Water, Hayden VOR, and Baggs), Figures 2.3.4 through 2.3.6 show that the majority of fine particles causing scattering were acquired during the first three or four hours (0600 to ~1000 MST) of the measurement period. The final two hours are more representative of the afternoon samples. At the higher-elevation sites (Juniper Mountain, Gilpin Creek, and Buffalo Pass), Figures 2.3.1 through 2.3.3 show that scattering during the morning hours was more uniform throughout the sample, though it often differed from the afternoon sample. The morning average reasonably represents the entire six-hour morning period at the elevated sites.

2.4 Measurement Precision, Accuracy, and Validity

Watson *et al.* (1995) described several validation levels assigned to data in the process of acquisition and analysis. Prior to use in data analysis, data sets were processed to remove information when instruments malfunctioned and to flag data corresponding to deviations from normal operating conditions. For the first data analysis objective, data were submitted to other validation tests that are described along with their detailed results in

Appendix A. Andersen (1995a; 1995b) performed two field performance audits and one laboratory audit to evaluate accuracy relative to independent standards, and the quantitative results of these audits are also summarized in Appendix A. Meteorological and air quality validity and accuracy were found to be within norms for similar monitoring networks, despite the remote locations and harsh weather conditions encountered during the monitoring period. Owing to the very low levels measured, precisions commonly exceeded 30% of measured values for aerosol concentrations. These precisions were better (<20%) for the higher concentrations that contributed most to light extinction and were within the uncertainties attained by extinction efficiency and source apportionment models.

Surface and upper-air meteorological data from the MZVS network and other data sets were subjected to both quantitative and qualitative screening that identified data outliers and ascertained the representativeness of the measurements for characterizing transport conditions in the region. Surface wind speeds, wind directions, temperature, and relative humidity measurements were spatially plotted and examined for consistency, given differences in terrain, elevation, and time of year. Only data from the National Weather Service (NWS) Craig site consistently reported winds with exceptionally high speeds compared to the other sites in the study domain. Though the cause of the problem was not determined, this site was not essential, and the Craig NWS data were excluded in subsequent analyses.

Upper-air wind and temperature measured by the MZVS radar profilers and RASS were compared with twice-a-day soundings from nearby NWS rawinsondes. Values at different elevations were comparable at altitudes greater than 2,000 m AGL where synoptic-scale forcing was the dominant process affecting aloft winds and temperatures. Terrain effects were evident at lower altitudes and were consistent with expected channeling by terrain at all sites. Profiler data affected by ground clutter and precipitation interferences were removed from data files as part of the data evaluation.

Interferences for nephelometer measurements were evaluated with respect to: 1) aerosol heating, 2) changes in ambient temperature and relative humidity, and 3) coarse particle scattering. The OPTEC NGN-2 nephelometer reported an average heating of 0.06 ± 1.07 °C on the sampled aerosol. The effect of heating on relative humidity in the nephelometer scattering chamber was negligible, in the range of 1% to 5% for ambient relative humidities between 10% and 100%, respectively, for 0.5 °C heating of a sampled aerosol. The effects of aerosol heating on the OPTEC light scattering measurements are well within the instrument measurement precisions. The ambient temperature dependence of the OPTEC nephelometer response was less than ±5% for ambient temperatures between -20 °C and +40 °C.

The effect of angular truncation in light scattering measured by the OPTEC nephelometers in the extreme backward (0-5 degrees) and forward (175-180 degrees) directions is less than 5% for fine particles (geometric mean diameter = 1.25 μm) and approaches 50% for coarse particles (geometric mean diameter = 10 μm).

The TSI Three-Color nephelometer measured particle scattering at 450 nm (blue), 550 nm (green) and 700 nm (red) after drawing air through a $PM_{2.5}$ inlet. Since this nephelometer was located in a heated shelter and illuminated the sampled aerosol in a closed chamber, relative humidities were typically <60% in the sample chamber, regardless of ambient relative humidities. The combination of higher humidity and the removal of fog and cloud droplets by the inlet meant that this was a closer measure of dry particle scattering, as opposed to the wet particle scattering measured by the OPTEC nephelometer. This particle drying was intentional to gain a better understanding of the size distributions present during different aerosol measurement periods.

Comparisons of collocated measurements from the OPTEC particle scattering (total scattering minus clean air scattering) and the TSI green particle scattering showed that both measurements are equivalent, within expected precisions, for ambient relative humidity less than 70%. For these low humidity cases, the one-to-one correspondence between OPTEC and TSI green particle scattering confirms the assumption that coarse particle scattering was negligible at Buffalo Pass during summer and fall. Since the area was snow-covered during other parts of the year, it is safe to extrapolate this assumption to the entire monitoring period at Buffalo Pass. This result further confirms that the effect of angular truncation on OPTEC measurements is negligible.

The ratios of OPTEC to TSI particle scattering increased from unity at 70% relative humidity to two or three when relative humidity exceeded 90%. This shows that liquid water is a major component of fine particles when relative humidity exceeds 70%, consistent with observations from other visibility studies (Watson *et al.*, 1988; 1990).

Aerosol measurements on filters were evaluated by comparing collocated measurements, examining the adsorption of carbon gases and volatilized particulate carbon on quartz backup filters, comparing the sums of chemical concentrations to measured mass concentrations, calculating cation and anion balances, estimating ammonium nitrate volatilization from front and backup filters, estimating interferences from coarse particle nitrate, and evaluating denuder efficiencies.

For each comparison, correlations and linear regression statistics were computed and scatter plots were prepared. Suspect measurements were flagged and samples were chemically reanalyzed. Statistical outliers were identified, documented, and assigned flags of valid, suspect, or invalid. All validation actions are documented in the data base as part of the data validation summary.

With respect to collocated measurements, good agreement (correlation coefficient, r=0.9) was found for sulfur dioxide (SO_2) measurements between the TECO 43 continuous monitor and filter pack samples. Poorer agreement (r=0.68) was found between the DRI high sensitivity sulfur analyzer and filter pack values. The high sensitivity instrument was originally intended to quantify SO_2 at levels as low as 20 ppt, but it was found during the winter intensive operating period that levels were high enough to be detected with more conventional instruments such as the TECO 43. Therefore, SO_2 measurements from the

TECO 43 were used for data analysis when they were available after 08/03/95, with the high sensitivity SO_2 measurement used prior to that time.

The continuous particulate sulfur channel on the high sensitivity monitor showed no relationship with filter pack particulate sulfate by ion chromatography or particulate sulfur by x-ray fluorescence, even though the two filter-based measurements agreed with each other very well most of the time. The continuous sulfate measurements at Buffalo Pass were deemed unreliable and were not used for subsequent data analysis.

Precisions, lower quantifiable limits (LQL), and number of measurements above LQLs are reported in Appendix A. Major chemical components of mass, sulfate, nitrate, sulfur dioxide, aluminum, silicon, and potassium exceeded LQLs for more than 80% of the samples. With high sensitivity x-ray fluorescence analysis, selenium concentrations were detected above the nominal LQL of 0.00025 $\mu g/m^3$ on more than 43% of the samples. The minimum detection limits of the selected chemical analysis methods were sufficiently low to establish valid chemical concentrations and their associated precisions.

The laboratory audit results and laboratory intercomparisons established the accuracy of organic and elemental (i.e, light absorbing) carbon measurements. As discussed by Watson *et al.* (1995), the collection of particulate organic carbon on quartz-fiber filters is subject to error from both adsorption of organic vapor (positive artifact) and volatilization of particulate organic carbon (negative artifact) during sampling. Organic carbon measured on quartz backup filters were often 60% or more of the carbon measured on the front quartz-fiber filters, and the relationship between the front and backup filter organic carbon measurements varied at all concentration levels. This does not mean, however, that all of the carbon on the backup filter is a positive bias to the front filter, as subtracting organic carbon on the backup filter from the deposit on the front filter results in an inability to account for $PM_{2.5}$ mass and measured particle scattering. Dynamic blank concentrations for organic carbon were a large fraction of the low organic carbon concentrations found in the study area, and were highly variable. This blank variability often resulted in organic carbon precisions on the order of ±30%. While this precision is poorer than desired, it is on the order of other uncertainties in the source apportionment and light extinction modeling for which the chemical data are used. Additional work is needed to better understand the uncertainties associated with the sampling of organic carbon (Chow, 1995).

Internal consistency tests were performed for: 1) sulfate versus sulfur, 2) chloride versus chlorine, 3) soluble potassium versus total potassium, and 4) light absorption versus elemental carbon. These comparisons show that chemical species measured by different chemical analysis methods (e.g., x-ray fluorescence, ion chromatography, atomic absorption spectrophotometry, thermal/optical carbon, densitometer) on different filter substrates exhibit consistency within one standard deviation of the measurement intervals for more than 90% of the data points. Relative deviations are larger for low concentrations that are within three times the LQLs of each measurement method.

Ammonium was the major positive ion and that sulfate and nitrate were the major negative ions. Cation and anion comparisons showed that positive and negative ions

balanced when sulfate was assumed to be present as ammonium sulfate ($(NH_4)_2SO_4$), but not when it was assumed to be ammonium bisulfate (NH_4HSO_4) or sulfuric acid (H_2SO_4). The ion balance is consistent with sulfate in the form of ammonium sulfate for nearly every sample. This indicates that ammonia was sufficiently abundant in the study region to neutralize sulfuric acid particles when these samples were taken.

Significant fractions (~45%) of ammonium nitrate volatilized during the warmer season (March through August) when temperatures were higher. This volatilization decreased to 28% of ammonium nitrate during the colder season (February, March, September, October). Data analysis incorporated the backup absorbent filter to adequately estimate the particulate ammonium nitrate and its contribution to mass concentration.

Reasonable correlations (r=0.80) were found between total and $PM_{2.5}$ particulate nitrate measurements. Coarse particle nitrate (i.e., the difference between total and $PM_{2.5}$ particulate nitrate) was found to be insignificant since over 90% of the collocated nitrate concentrations differed by no more than one or two precision intervals. $PM_{2.5}$ ammonium measurements acquired with ammonia denuder difference and particle samplers were comparable within stated precisions.

3.0 FREQUENCY, CHARACTER, AND INTENSITY OF HAZE

This section documents the frequency with which different levels of light scattering occur, and how these relate to frequencies measured within and near Class I areas. Visual observations of uniform and layered hazes are summarized. Hourly measurements of light scattering at each of the MZVS measurement sites are compared and examined to identify periods of extreme light scattering that need to be studied in greater detail. For the six- and twelve-hour periods for which particle absorption measurements were available, the relative contributions of the different components of light extinction are summarized and compared for each sampling site during Intensive Operating Periods.

Light reflected from an object is transmitted through the atmosphere, where its intensity is attenuated when it is scattered and absorbed by gases and particles. The sum of these scattering and absorption coefficients yields the extinction coefficient (b_{ext}) expressed in units of inverse megameters ($Mm^{-1}=1/10^6$ m). Typical extinction coefficients range from ~10 Mm^{-1} in pollution-free air to ~1,000 Mm^{-1} in extremely polluted air (Trijonis *et al.*, 1990). The inverse of b_{ext} corresponds to the distance (in 10^6 m) at which the original intensity of transmitted light is reduced by approximately two-thirds.

Light is scattered when diverted from its original direction by matter (Malm, 1979; Watson and Chow, 1994). The presence of atmospheric gases, such as oxygen and nitrogen, would limit horizontal visual range to ~400 km (if such a sight path were possible); these gases obscure many of the attributes of a target at less than half this distance. This "Rayleigh" or clean air scattering is the major component of light extinction in areas where pollution levels are low, and it can be accurately estimated from temperature and pressure measurements (Edlen, 1953; Penndorf, 1957). Values for clean air scattering at each of the MZVS sites are as follows for the range of wavelengths measured with the OPTEC nephelometer:

Buffalo Pass:	8.4 Mm^{-1}
Gilpin Creek:	8.8 Mm^{-1}
Juniper Mountain:	9.2 Mm^{-1}
Baggs:	9.5 Mm^{-1}
Hayden VOR:	9.4 Mm^{-1}
Hayden Waste Water:	9.6 Mm^{-1}

Light is also scattered by particles suspended in the atmosphere, and the efficiency of this scattering per unit mass concentration is largest for particles with sizes comparable to the wavelength of light (~500 nm). Light is absorbed by nitrogen dioxide (NO_2) gas (Dixon, 1940), black carbonaceous particles (Horvath, 1993), and nontransparent geological material. NO_2 concentrations in excess of 60 $\mu g/m^3$ (30 ppbv) are needed to exceed Rayleigh scattering, and these levels are not found in pristine areas.

Sunlight illuminating the view path is also scattered toward the observer. This air light, also termed the "path radiance," increases with distance from the target while the light reflected from the target decreases due to scattering and absorption (Richards, 1990). For a given composition of the intervening atmosphere, a viewing distance to the target is achieved

where the scattered air light overwhelms the transmitted light and the object can no longer be discerned from the horizon sky against which it is viewed. This distance is termed the "visual range" and, under homogeneous illumination and uniform atmospheric composition, is inversely related to the extinction coefficient (visual range = $3.91/b_{ext}$). This "Koschmeider formula" is not perfect because it involves several assumptions that are not always true (Koschmeider, 1924). In particular, the Koschmeider formula assumes that the observer's eye can distinguish contrast differences between the target and horizon sky of 2%, regardless of the nature of the target, the angle of illumination, and the observer's eye.

Light extinction measurements do not fully represent the way people perceive a view. This perception depends on complex interactions among physiological, psychological, and cultural variables that are not completely defined, let alone measurable (Henry *et al.*, 1987; Malm *et al.*, 1981). Pleasing vistas often contain details such as color and texture that make them interesting. Sharp delineations, specifically different colored strata or jagged edges in rock outcroppings, are often considered to provide a pleasing view, as they do in and around the Mt. Zirkel Wilderness. Daytime classifications of scenes recorded by video and color slide, though less quantitative than light scattering and absorption measurements, are important complements to the objective measures. Since visibility is appreciated as an event, rather than an average, frequencies and durations of different extinction levels are more meaningful quantifiers than are long-term averages.

3.1 Light Scattering and Extinction in the Mt. Zirkel Wilderness and Other Class I Areas

The **I**nteragency **M**onitoring of **Pro**tected **V**isual **E**nvironments (IMPROVE) network and IMPROVE protocol monitoring sites have obtained optical, aerosol, and photographic measurements at several Class I wilderness areas and national parks throughout the United States since 1987. Figure 3.1.1 shows IMPROVE sites that acquired light scattering (b_{scat}) measurements with OPTEC nephelometers identical to those used in the MZVS and light extinction (b_{ext}) measurements with sight path transmissometers.

As will be shown in Section 3.5, particle absorption accounts for no more than 20% of b_{ext} in the MZVS study area and is often negligible. Light scattering is, therefore, an adequate surrogate for total light extinction, and at most might be increased by 2 or 3 Mm^{-1} to account for particle absorption. Scattering and extinction values are summarized in Table 3.1.1 for the MZVS study period as 10th, 50th, and 90th percentile values for b_{scat}. Following IMPROVE reporting conventions, data are filtered for weather events by eliminating values corresponding to relative humidity exceeding 90%. The percentiles reported in Table 3.1.1 represent hours when visibility is not directly influenced by rain, snow, or fog at the monitoring site or along a sight path. At high elevation mountain sites, such as Buffalo Pass, as much as 60% of hourly values collected during the winter are weather affected.

Table 3.1.1 shows that the Buffalo Pass, Gilpin Creek, and Juniper Mountain sites experience among the lowest light scattering and extinction of all IMPROVE and IMPROVE

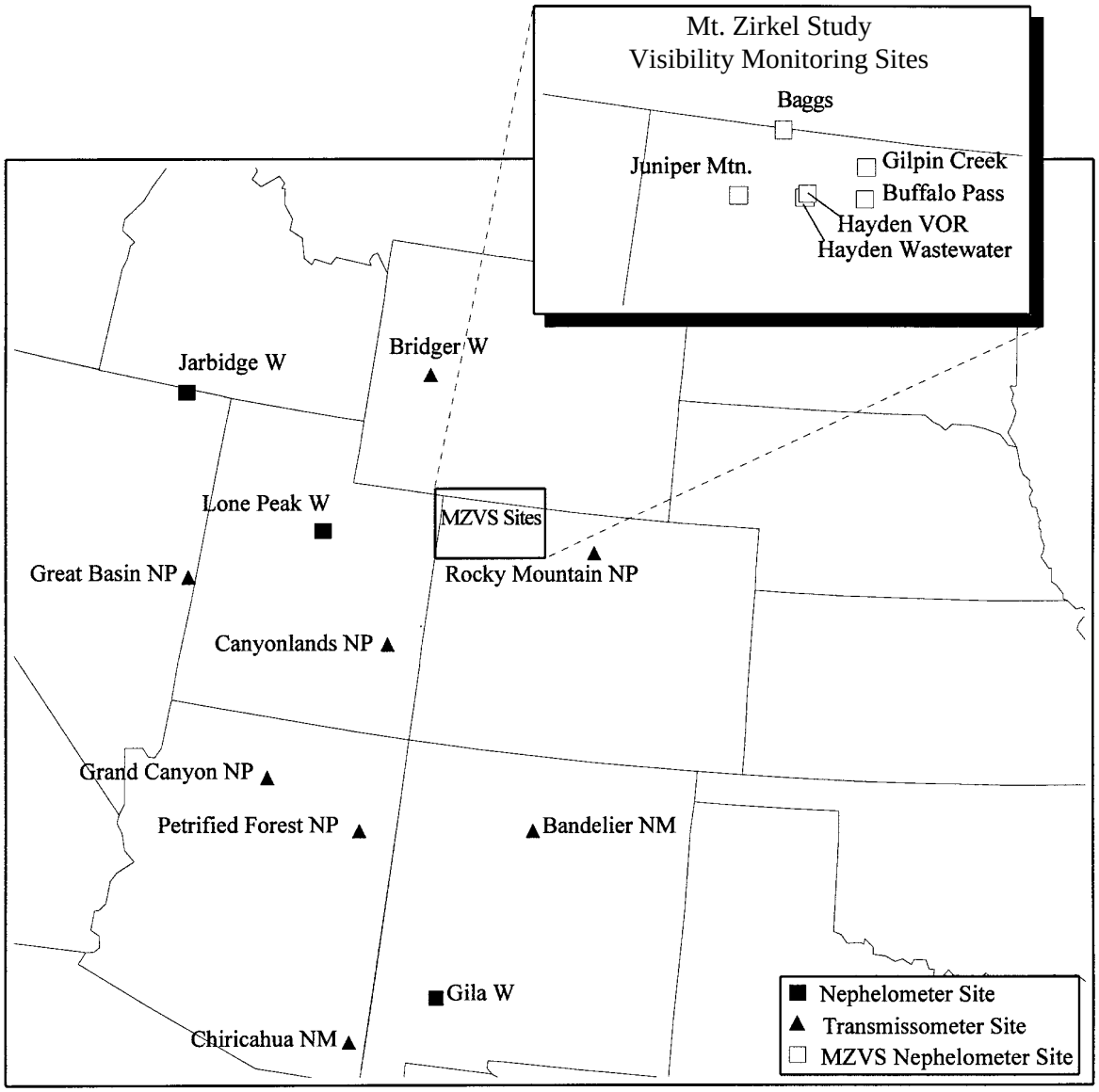

Figure 3.1.1. Locations of MZVS and IMPROVE visibility monitoring sites.

Table 3.1.1
Comparison of Mt. Zirkel Visibility Study Light Scattering with Measurements in Other Class 1 Areas

Site Name	Site Abbr.	Light scattering or extinction coefficients at 10th, 50th, and 90th percentiles (Mm^{-1})														
		Dec 1994–Nov 1995			Jan-Mar 1995			Apr-Jun 1995			Jul-Sep 1995			Oct-Nov 1995		
		10th	50th	90th	10th	50th	90th	10th	50th	90th	10th	50th	90th	10th	50th	90th
NEPHELOMETER		b_{scat}	b_{scat}	b_{scat}	b_{scat}	b_{scat}	b_{scat}	b_{scat}	b_{scat}	b_{scat}	b_{scat}	b_{scat}	b_{scat}	b_{scat}	b_{scat}	b_{scat}
MZVS Sites:																
Buffalo Pass	BUPZ	10	14	22	9	11	20	11	14	23	12	16	23	9	12	17
Gilpin Creek	GLCZ	12	16	24	11	13	24	13	17	26	14	18	25	11	14	19
Juniper Mountain	JUNZ	11	16	23	9	11	18	13	16	24	14	18	25	12	15	21
Baggs	BAGZ	13	18	27	13	16	29	14	18	28	15	20	28	12	15	22
Hayden VOR	VORZ	13	18	28	12	17	27	14	18	30	15	19	28	12	15	21
Hayden Waste Water	SEWZ	15	24	43	15	27	58	16	24	37	17	24	35	13	19	32
IMPROVE and IMPROVE Protocol Sites:																
Jarbidge Wilderness	JARB	10	15	27	10	12	19	12	18	28	14	23	36	10	14	25
Lone Peak Wilderness	LOPE	12	19	35	11	15	38	15	23	35	13	20	33	13	18	36
Gila Wilderness	GILA	10	18	35	9	12	21	13	19	33	16	26	59	12	19	34
TRANSMISSOMETER		b_{ext}	b_{ext}	b_{ext}	b_{ext}	b_{ext}	b_{ext}	b_{ext}	b_{ext}	b_{ext}	b_{ext}	b_{ext}	b_{ext}	b_{ext}	b_{ext}	b_{ext}
IMPROVE and IMPROVE Protocol Sites:																
Canyonlands NP	CANY	16	24	32	14	18	26	19	25	37	19	26	33	23	26	31
Grand Canyon NP South Rim	GRCA	18	26	39	18	21	28	19	26	38	26	33	43	18	24	38
Grand Canyon NP In-Canyon	GRCW	22	30	42	19	23	33	26	32	41	28	35	46	25	30	41
Bridger Wilderness	BRID	17	23	33	16	19	27	19	25	34	21	27	37	18	22	28
Rocky Mountain NP	ROMO	16	22	34	15	20	29	18	23	41	18	25	36	20	23	31
Bandelier NM	BAND	22	32	45	21	26	35	26	32	45	32	37	50	20	29	44
Petrified Forest NP	PEFO	24	37	51	15	30	40	27	37	48	34	44	56	32	39	55
Chiricahua NM	CHIR	29	42	58	27	33	44	39	37	65	40	50	69	40	42	44
Great Basin NP	GRBA	16	25	34	11	13	19	21	26	35	22	28	35	19	23	32

protocol sites. During the MZVS, the 90th percentile scattering values at the Buffalo Pass site were less than three times that of clean air, even when allowances are made for particle absorption. Only the Jarbidge Wilderness in northern Nevada is comparable to the highest light scattering measurements at these sites. The highest values at other sites are 1.5 to 2 times those measured near the Mt. Zirkel Wilderness, regardless of time of year.

At Buffalo Pass, Gilpin Creek, and Juniper Mountain, the median nonweather-related light scattering was least during the winter and highest during the summer, while at Baggs and Hayden VOR, the median nonweather-related light scattering was least during the fall and highest during the summer. At the Hayden Waste Water site adjacent to the Yampa River, the poorest median visibility values occurred during the winter months. The nearest Class I nephelometers and transmissometers exhibited the same seasonal patterns in median values as those measured at the Buffalo Pass site, with lower scattering and extinction during winter and higher values during spring and summer.

3.2 Frequencies of Observed Hazes

Time-lapse videotapes (SVHS format) were reviewed on a high-resolution monitor, and 35-mm slides were reviewed on a light table with a hand lens to assign a seven-digit scene classification code that documents conditions according to the descriptions in Table 3.2.1. Though video and 35-mm cameras are the only practical methods to record the daylight appearance of haze for later examination, they are not entirely equivalent to the scene an observer would view. The video and slide records are of restricted view and have exposure, color, and resolution limitations as compared to the human eye. An on-site observer would scan all directions horizontally and vertically and would use his or her senses and interpretive skills to assess the type and intensity of a haze. Visibility impairment is often more noticeable when viewing a scene in person than it is when viewing a time-lapse or photographic image. On the other hand, the time-lapse videos offer rapid temporal contrasts that may not register when viewed over many hours, and many of the haze events recorded during the MZVS are clearly visible in these records.

Uniform haze intensities are judged by the reduction of clarity and contrast in terrain features in a view. Since there is always some obscuration of distant targets, even in clean air, a uniform haze code of "slight" (Code 1) was assigned when a terrain feature ~60 km away was clearly visible. A uniform haze code of "moderate" (Code 2) was assigned when a terrain feature ~60 km away was difficult to discern. A uniform haze code of "considerable" (Code 3*)* was assigned when a terrain feature ~30 km away was difficult to discern. When clouds or precipitation were such that the accurate determination of the level of uniform haze intensity was impossible, the scene was coded as "weather dominates scene."

Each scene would ideally have two easily identifiable terrain features at ~60 km and ~30 m to allow uniform haze intensity codes to be consistent between views. Scene-specific natural terrain features were based on readily visible landmarks in the view as described in Table 3.2.2. It is apparent from Table 3.2.2 that there is considerable variation in distance ($\pm$ 10 km) to each of the targets, so there is variation in the absolute interpretation of these codes.

Table 3.2.1
Scene Classifications

Digit	Observed Condition Code	Description
1	SKY CONDITIONS	SKY CONDITIONS VIEWED AS CHARACTERISTIC OF THE PERIOD.
	0 No clouds	No clouds visible anywhere in the sky.
	1 Scattered clouds < half of sky	Less than one-half of the sky has clouds present.
	2 Overcast > half of sky	More than one-half of the sky has clouds present.
	3 Haze concealing scene	Atmospheric haze conditions are such that determination of the sky value is impossible.
	5 Weather dominates scene	Clouds or precipitation are such that determination of the sky value is impossible.
	8 Observation cannot be determined	Observation cannot be determined due to extreme exposure inconsistencies, lens (or window) condensation, misalignment, or view obstructed by a foreign object.
	9 No observation	No observation taken.
2	LAYERED HAZE TYPE	LAYERED HAZE TYPE OBSERVED DURING THE PERIOD.
	0 No layered haze	No layered haze boundary (intensity of coloration edge) is perceptible.
	1 Ground-based layered haze only	Only a single-layered haze boundary is perceptible with the haze layer extending to the surface.
	2 Elevated layered haze only	An elevated layered haze with two boundaries is perceptible (e.g., horizontal plume).
	3 Multiple haze layers	More than a single ground-based or elevated haze layer (or both) is perceptible.
	5 Weather dominates scene	Clouds or precipitation are such that determination of the presence of layered hazes is impossible.
	9 No observation or cannot be determined	To be used with sky condition of 9 or if a layered haze value cannot be determined due to reasons other than weather.
3	UNIFORM HAZE INTENSITY	MAXIMUM UNIFORM HAZE OBSERVED DURING THE PERIOD.
	1 Slight haze intensity	Terrain features at 60 km are clearly perceptible.
	2 Moderate haze intensity	Perception of the 60 km target is difficult to discern.
	3 Considerable haze intensity	Perception of the 30 km target is difficult to discern.
	5 Weather dominates scene	Clouds or precipitation are such that determination of the level of uniform haze intensity is impossible.
	8 Terrain features not available	To be used if terrain features at 30 km or 60 km cannot be determined.
	9 No observation or cannot be determined	To be used with sky condition code of 9 or if a uniform haze value cannot be determined due to reasons other than weather.
4	LAYERED HAZE INTENSITY	MAXIMUM LAYERED HAZE INTENSITY OBSERVED DURING THE PERIOD.
	0 No layered haze	No layered haze is perceptible.
	1 Slight layered haze	Perception of layered haze is difficult to discern.
	2 Moderate layered haze	Perception of layered haze is clearly discernable.
	3 Considerable layered haze	Perception of layered haze has such intensity that the haze appears opaque and background features are obscured.
	5 Weather dominates scene	Clouds or precipitation are such that determination of the presence of layered hazes is impossible.
	9 No observation or cannot be determined	To be used with sky condition of 9 or if a layered haze intensity value cannot be determined due to reasons other than weather.
5	VISUAL ANOMALIES	VISUAL ANOMALY SEEN DURING THE PERIOD.
	0 No anomaly	No anomaly is visible anywhere in the view.
	1 Stack emission	A stack emission is visible from either Craig or Hayden power plants.
	2 Naturally-caused smoke or fire	A smoke plume due to fire is visible.
	3 Fog	Naturally-occurring fog is clearly visible.
	4 Blowing snow	Blowing snow is visible across the entire view or part of the view.
	5 Weather dominates scene	Clouds or precipitation are such that determination of anomalous features is impossible.
	6 Blowing dust	Blowing dust or soil is visible across the entire view or part of the view.
	7 Other natural features	Any other unusual, naturally-caused feature is visible in the view.

	8 Other Man-made features	Any other unusual, man-made feature is visible in the view.
	9 No observation or cannot be determined	To be used with sky condition code of 9 or if an anomalous feature cannot be clearly identified due to reasons other than weather.

Table 3.2.1 (continued)
Scene Classifications

Digit	Observed Condition Code	Description
6	INSTRUMENT EFFECTS	PRESENCE OF WEATHER WHICH COULD EFFECT THE INSTRUMENTS DURING THE PERIOD.
	0 No effect	No apparent weather related effects on visibility or aerosol instruments at monitoring sites within the view or collocated with the camera.
	1 Weather effects	Probable weather related effects on visibility or aerosol instruments at monitoring sites within the view.
	5 Weather dominates scene	Clouds or precipitation are such that determination of instrument effects are impossible.
	8 N/A	No aerosol or visibility monitoring sites in view.
	9 No observation or cannot be determined	To be used with sky condition code of 9 or if scene features cannot be clearly identified due to reasons other than weather.
7	STACK/COOLING TOWER PLUME DYNAMICS	STACK OR COOLING TOWER DYNAMICS WHICH CHARACTERIZE THE PERIOD.
	0 No plume	No steam or other emissions are visible.
	1 Up valley - decoupled	Observed steam plumes or stack emissions generally flow up valley but either plume dynamics or observed plume and cloud motions indicate a decoupling of air flows in the scene.
	2 Down valley - decoupled	Observed steam plumes or stack emissions generally flow down valley but either plume dynamics or observed plume and cloud motions indicate a decoupling of air flows in the scene.
	3 Up valley - coupled	Observed steam plumes or stack emissions generally flow up valley but neither plume dynamics nor observed plume or cloud motions indicate any flow decoupling.
	4 Down valley - coupled	Observed steam plumes or stack emissions generally flow down valley but neither plume dynamics nor observed plume or cloud motions indicate any flow decoupling.
	5 Weather dominates scene	Clouds or precipitation are such that determination of plume features is impossible.
	6 Vertical plume	Observed steam or stack emissions rise vertically; no dominant direction observed, decoupling may or may not be present.
	7 Other	Observed steam plumes or stack emissions have characteristics that cannot be described by any of the above codes.
	8 N/A	Power plant not in the view.
	9 No observation or cannot be determined	To be used with sky condition code of 9 or if plume features cannot be clearly identified due to reasons other than weather.

Table 3.2.2
Criteria for Determining Uniform Haze Intensities
for the Mt. Zirkel Visibility Study

Relative Haze Intensity Code

Site	Slight [1]		Moderate [2]		Considerable [3]	
	Referenced Topographic Feature	Approx. Distance	Referenced Topographic Feature	Approx. Distance	Referenced Topographic Feature	Approx. Distance
Storm Peak - Hahns Peak	Hahns Peak	60 km	Hahns Peak	60 km	End of valley floor	30 km
Storm Peak - Yampa Valley	Elkhead Mtns.	60 km	Elkhead Mtns.	60 km	Wolf Mtn.	30 km
Buffalo Pass	Medicine Bow Mtns.	50 km	Medicine Bow Mtns.	50 km	Sheep Mtn.	29 km
Gilpin Creek	N/A	N/A	N/A	N/A	Pilot Knob	37 km
Chavez Mountain - Buffalo Pass View	Mt. Zirkel	55 km	Mt. Zirkel	55 km	Rocky Peak	30 km
Chavez Mountain - Zirkel View	Mt. Zirkel	55 km	Mt. Zirkel	55 km	Pilot Knob	30 km
Chavez Mountain - Hayden View	Black Mtn.	50 km	Black Mtn.	50 km	Agner Mtn.	30 km
Cedar Mountain	Pyramid Peak	55 km	Pyramid Peak	55 km	Wilson Mesa	40 km
Juniper Mountain - East View	Pagoda Peak	60 km	Pagoda Peak	60 km	Cedar Mtn.	35 km
Juniper Mountain - North View	Bakers Peak	65 km	Bakers Peak	65 km	Big Gulch Rim	30 km
Juniper Mountain - West View	Tanks Peak	60 km	Tanks Peak	60 km	Cross Mtn.	30 km
Juniper Mountain - South View	N/A	N/A	N/A	N/A	Colorow Mtn.	28 km

[1]Slight haze intensity-Terrain features at 60 km are clearly perceptible.
[2]Moderate haze intensity-Perception of the 60 km target is difficult to discern.
[3]Considerable haze intensity-Perception of the 30 km target is difficult to discern.

When the time-lapse images were viewed to evaluate uniform or layered hazes, the worst-case condition that could be clearly identified during the nominal 0600 to 1200 MST (a.m.) and 1200 to 1800 MST (p.m.) periods was recorded. The actual classification period extended from sunrise to sunset, which was slightly longer or shorter than these intervals depending on the time of year. When a moderate layered haze was observed for one hour during the early morning, but the layer dissipated as the morning progressed, the morning was assigned the code for a moderate layered haze. This code was given even though the major fraction of the period might correspond to a slight uniform haze in order to call attention to the time and location of such a haze.

Still photographs were not as useful as videos for classification because they represent an instantaneous record of conditions observed at 0900, 1200, and 1500 MST rather than a continuous evolution of visibility events. Slide and video classifications of the same view do not necessarily match. For example, a haze layer observed on a video between sunrise and 0800 that dissipated by 0830 would not be observed on a corresponding 0900 35-mm slide.

The assigned uniform haze code is partially indeterminate for the Gilpin Creek (GLCZ) and Juniper Mountain south (JUNS) view because prominent landmarks could not be seen at or near the 60 km or 30 km distances. For example, for the Juniper Mountain south view, a uniform haze code of 8 means that the 30 km feature was clearly visible, but there is no way to classify a view beyond this distance. A uniform haze code of 8 was used where this situation occurred, and results are represented by N/A in Table 3.2.2.

The result of this coding process is a digital file for each site in the MZVS data base that contains a seven-digit code for each slide or each half-day of videotape. These classifications can only be used to document the presence of observed conditions, and in some cases the sources of those conditions. Several of the layered hazes, for example, could be directly attributed to excessive primary particle emissions from a power generating station during a malfunction or to a prescribed burn. For most situations, however, the videos and 35-mm slides could not identify the source of a haze, especially uniform hazes, nor could they determine the chemical composition or full spatial extent of that haze. Naturally-occurring fogs and clouds along sight paths, as well as manmade pollution, could be the reasons that distant targets were obscured, but these causes must be determined by other aspects of the MZVS.

To illustrate how these classification codes appear visually, an abbreviated VHS video has been prepared as part of the MZVS data base, with examples of each time-lapse video view shown in Figure 2.1.2; slight, moderate, and considerable hazes; primary source emissions; and the appearance of haze under different illumination and weather conditions.

Detailed plots of haze classifications are contained in quarterly data reports (Air Resource Specialists, 1995). Figures 3.2.1 through 3.2.4 summarize by month the number of slight, moderate, and considerable hazes observed for uniform and layered situations excluding those concealed by poor weather. The Storm Peak views of Hahns Peak and the Yampa Valley represent views that can be seen from the Mt. Zirkel Wilderness. The

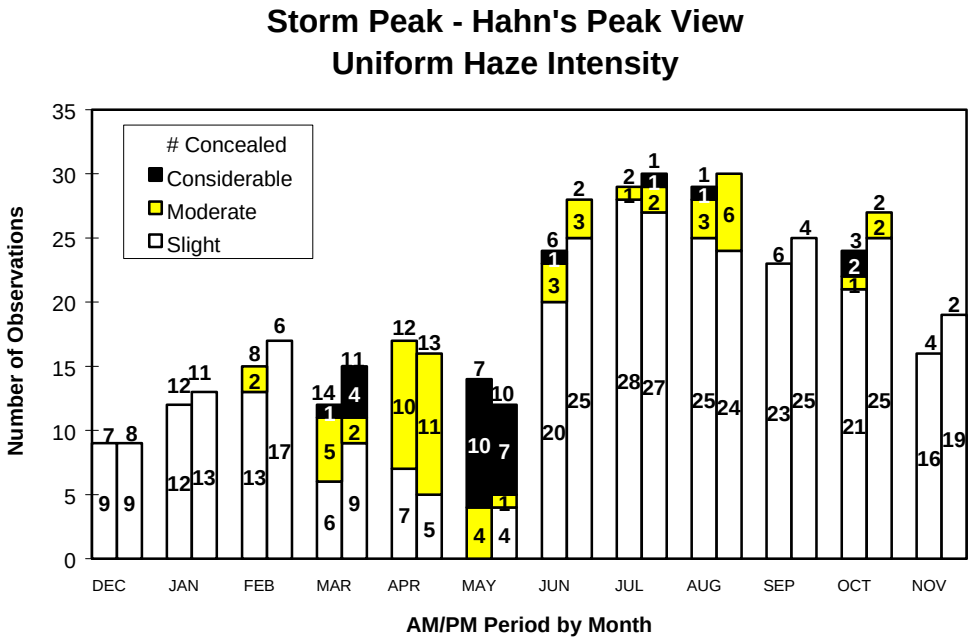

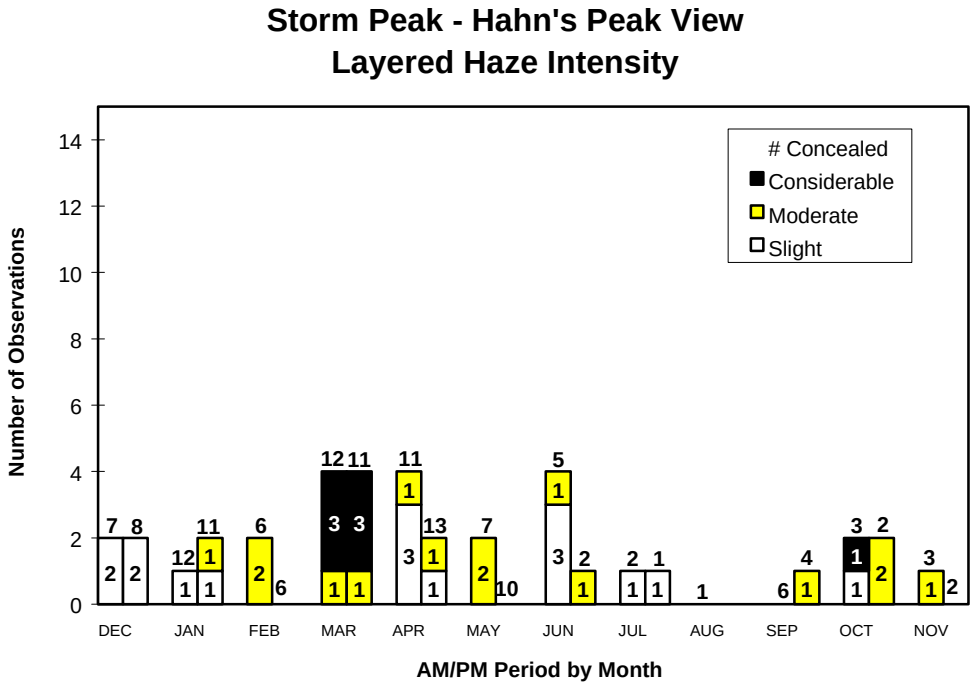

Figure 3.2.1. Observation frequencies of slight, moderate, and considerable uniform and layered hazes in the Hahns Peak video view from Storm Peak.

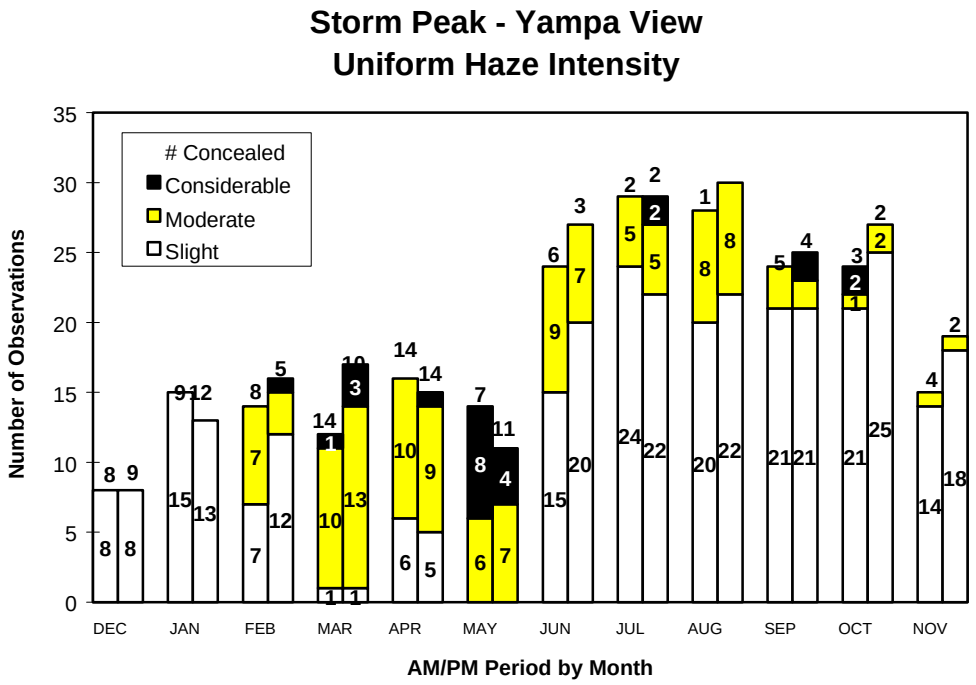

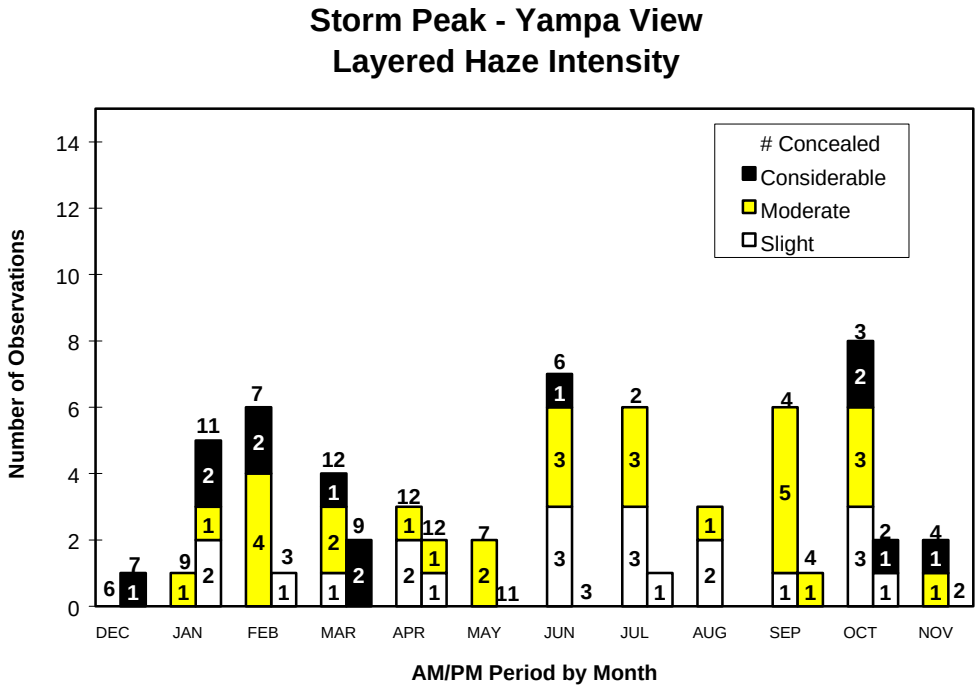

Figure 3.2.2 Observation frequencies of slight, moderate, and considerable uniform and layered hazes in the Yampa Valley video view from Storm Peak.

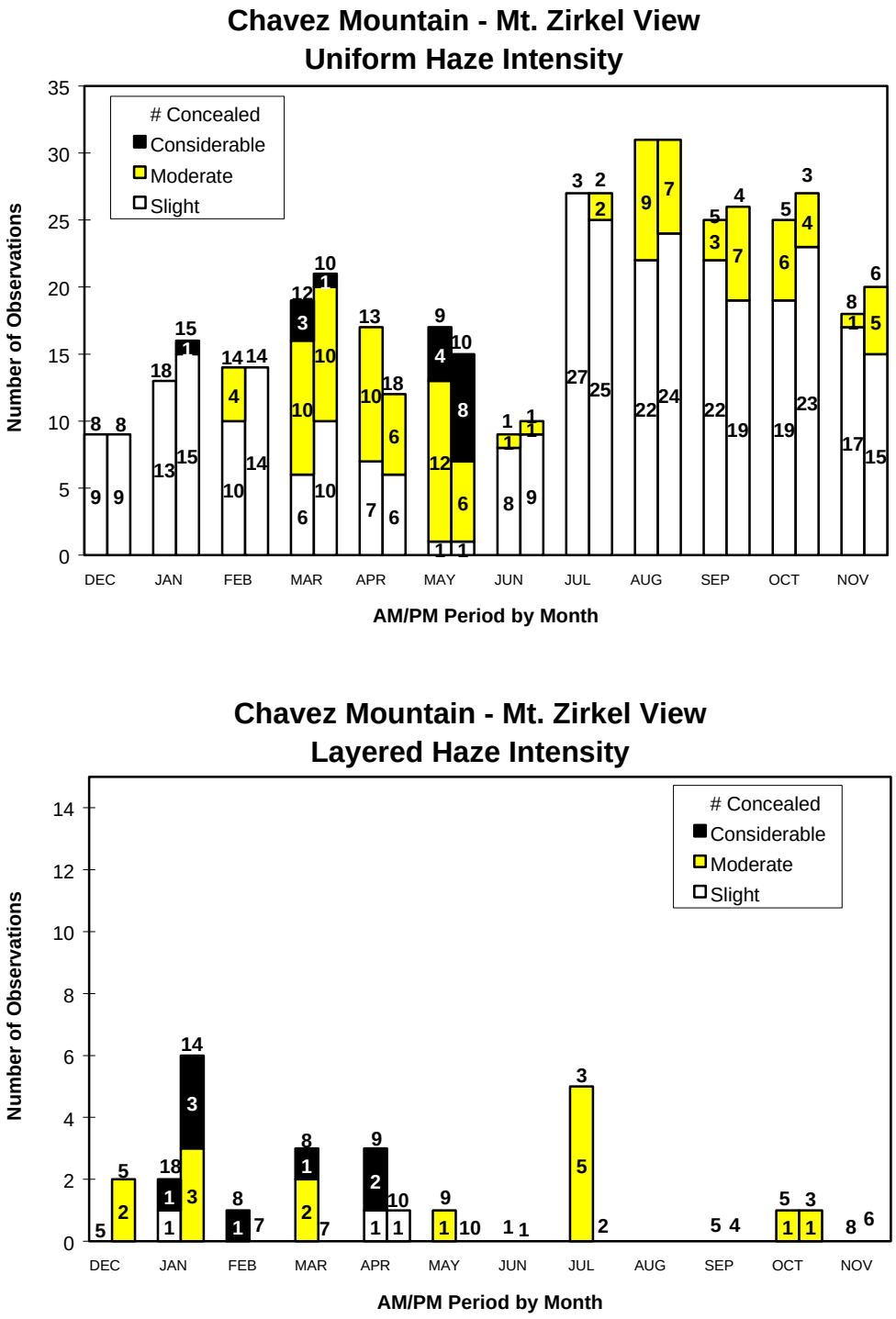

Figure 3.2.3 Observation frequencies of slight, moderate, and considerable uniform and layered hazes in the Mt. Zirkel video view from Chavez Mt.

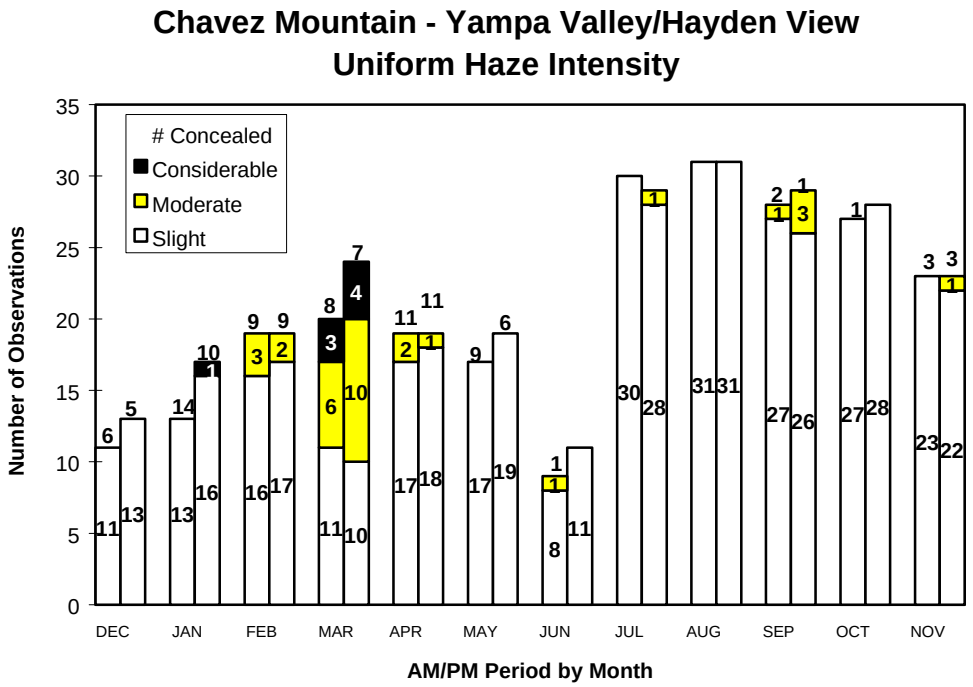

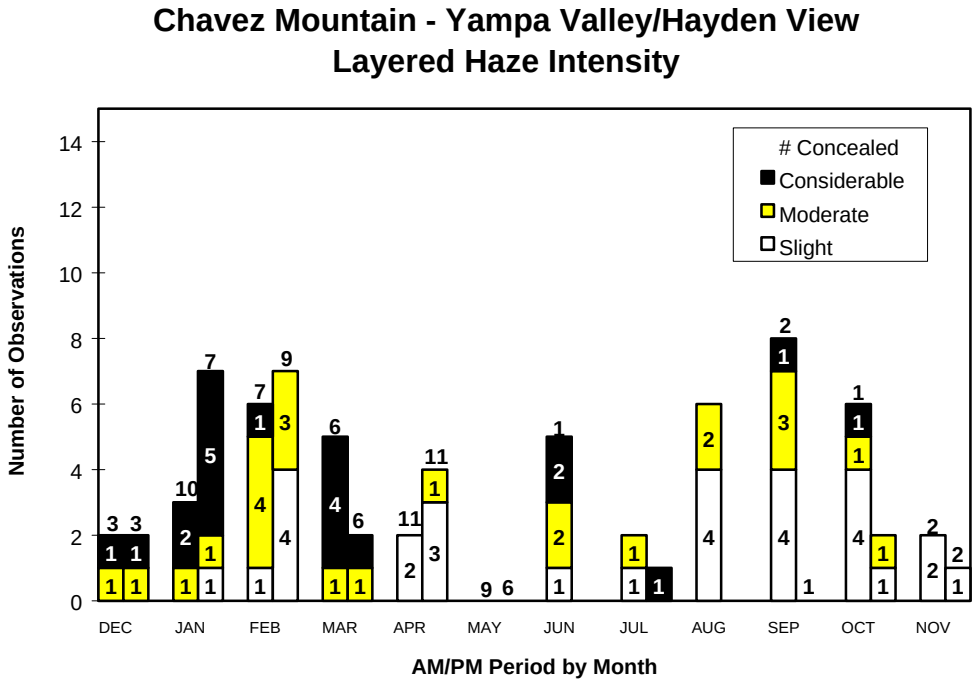

Figure 3.2.4 Observation frequencies of slight, moderate, and considerable uniform and layered hazes in the Hayden video view of the Yampa Valley from Chavez Mt.

Chavez Mountain views of Mt. Zirkel and the Hayden Generating Station represent what can be seen from within the Yampa Valley. Each view is different and incorporates different

terrain features, lighting conditions, and viewing angles. What can be seen from one site may not be visible from another, or the scene may look considerably different.

Weather commonly concealed the views during the winter and spring months, particularly at the higher elevation Storm Peak site. Weather-concealed classifications decreased in June when wetter winter and spring storm patterns shifted to drier summer patterns. Sight paths for the Chavez video views across the Yampa Valley and toward Mt. Zirkel often included morning pollutant accumulations in the valley, and uniform haze classifications for these views tend toward the moderate and considerable categories.

3.2.1 Uniform Haze

The frequencies shown in Figures 3.2.1 through 3.2.4 indicate that slight uniform hazes were observed most of the time during all but the spring months. As noted in Section 2.2, March, April, and May contained an unsettled period with numerous storms. Classifications during this period were difficult owing to the extreme weather. Many of the codes could be influenced by precipitation events, clouds, or unusual lighting along the sight path that might obscure distant targets. Views were commonly limited to several hours a day as precipitation ebbed and clouds lifted, especially during May. A number of considerable hazes were noted for all views in May except for the Chavez Mountain view of Hayden.

No moderate or considerable uniform hazes were observed from Storm Peak during December, January, September, and November. Views from the Yampa Valley sites contained several occurrences of moderate and considerable hazes, but the slight category was most prevalent. Slight hazes were most often observed during July and August for all views. Data recovery from the Chavez Mountain videos was limited during June owing to a lightning strike that disabled the monitoring equipment.

During the winter (February) Intensive Operating Period (IOP), moderate uniform hazes were observed in the Storm Peak/Hahns Peak view during the morning periods on 02/07/95 and 02/28/95. Moderate hazes were observed in the Storm Peak/Yampa view during the morning periods on 02/05/95, 02/07/95, 02/19/95, 02/21/95, 02/22/95, 02/23/95, and 02/25/95, and during the afternoon periods on 02/19/95, 02/21/95, and 02/23/95. One considerable haze was observed in the Yampa view during the afternoon on 02/28/95. The Storm Peak views exhibited patterns similar to those in views from the Yampa Valley sites (CHBZ, CHZZ, and CHHZ) on 02/07/95, 02/21/95, 02/22/95, 02/23/95, and 02/28/95. These observations indicate that a range of uniform haze conditions occurred during the winter IOP.

During the summer (August) IOP, slight uniform hazes dominated all views, but most views observed moderate hazes more often during August than during any other summer or fall month. Considerable hazes were seldom observed. High elevation and Yampa Valley views exhibited similar patterns. Events of moderate uniform haze were observed on 08/08/95, 08/11/95, and 08/20/95 through 08/24/95, from both the high elevation and the Yampa Valley sites.

During the fall (mid-September to mid-October) IOP, slight uniform hazes were seen most of the time, but moderate and considerable uniform hazes were sometimes observed

from all sites, specifically on 09/18/95, 09/19/95, 09/24/95, 10/01/95, 10/02/95, 10/08/95, and 10/12/95.

3.2.2 Layered Haze

Layered hazes were not seen as often as uniform hazes, but they were observed throughout the year in one or more of the views. The maximum number of layered hazes observed from any site during any month was nine and the minimum was zero. Generally the number of slight, moderate, and considerable layered haze intensities were the same. No intensity level was dominant. Layered hazes were observed many more times during the "a.m." period than the "p.m." period, particularly in the summer months.

For the Storm Peak views, layered haze occurrences were evenly distributed throughout the year. Considerable layered hazes were observed most often during cold months. On several occasions in late December and January, layered hazes observed in the Yampa Valley could be visually traced to visible plumes of primary particles from the Hayden Station. These events are described in Section 5.5. No considerable hazes were found during July, August, or September. Layered hazes were most often identified in the Storm Peak/Yampa view (STPY), owing to its elevation, broad vistas, and solar orientation. For this view, winter and fall IOPs experienced the highest frequencies of moderate and considerable haze layers.

Slight layered hazes were not easily discerned from the Chavez Mountain view of Mt. Zirkel; therefore, moderate and considerable hazes were recorded more frequently. Very few layered hazes were observed from the CHZZ view during the summer months.

The Chavez Mountain view of Hayden included the Hayden Station, and layers observed in the view were commonly associated with its emissions. Layers occurred more often in the "a.m." period, but layers were also observed in the "p.m." period particularly during January and February.

These observations show that visibility is very good near the Mt. Zirkel Wilderness area most of the time. Most of the observed hazes were uniform with no defined edge. Layered hazes were most commonly observed during the morning, and along sight paths through the Yampa Valley. Uniform and layered hazes were observed during the winter, summer, and fall IOPs.

3.3 Frequencies of Light Scattering in the MZVS

Frequency distributions of light scattering values for each OPTEC nephelometer in the network were calculated for those hours when the relative humidity was < 95% and the data were not flagged for weather interference. The 25th, 50th, and 75th percentiles of total light scattering for each site for each month are shown in Figure 3.3.1. These plots elaborate

on the percentiles in Table 3.1.1 by providing: 1) percentiles for each month of the study; 2) maximum and minimum scattering, as well as percentiles; and 3) a less exclusive relative humidity screen of 95%.

Consistent with the comparisons in Table 3.1.1, light scattering at Buffalo Pass, Gilpin Creek, and Juniper Mountain were the lowest observed at any of the sites with respect to 50^{th} and 80^{th} percentiles as well as the hourly maxima. This was the case for each month of the study. The highest hourly light scattering value of 59 Mm^{-1} was found at the Buffalo Pass site during June, with the highest value of 61 Mm^{-1} found at the Gilpin Creek site in March. The Baggs, Hayden VOR, and Hayden Waste Water sites experienced maximum hourly scattering values of ~60 Mm^{-1} during most of the months, and their 50^{th} and 75^{th} percentile values were commonly larger that the corresponding percentiles at Buffalo Pass, Gilpin Creek, and Juniper Mountain

The variability of light scattering between sites was highest during the winter when Buffalo Pass showed the lowest light scattering and Hayden Waste Water showed the highest scattering. During the winter, the lowest 25% of the light scattering at Buffalo Pass, Gilpin Creek, and Juniper Mountain were very close to the clean air scattering values; Baggs and Hayden VOR light scattering were ~50% larger than clean air scattering, and light scattering at Hayden Waste Water was approximately double that of clean air. The high Hayden Waste Water scattering compared to the lower regional background values implies that Yampa Valley particle sources had a large impact at that site during winter.

During the summer, light scattering at Buffalo Pass, Gilpin Creek, Juniper Mountain, Baggs, and Hayden VOR were all higher compared to their winter values or to clean air scattering. Hayden Waste Water experienced a decrease in light scattering between the winter and summer. During summer, the light scattering frequencies for the different sites were more similar to each other than during the winter.

During the fall, light scattering at all sites was lower than during the summer. Hayden Waste Water and Hayden VOR achieved their lowest values of the year, with minima that were ~4 Mm^{-1} larger than clean air scattering. The other four sites experienced values equal to, or slightly larger than, their winter values.

Non-weather light scattering during the IOPs, indicated by heavy dark lines at the bottom of Figure 3.3.1, showed the frequencies of different light scattering levels to be similar to, or slightly larger than, values seen in other months related to the winter, summer, and fall. The intensive operating periods were representative of the variations of total light scattering observed over their seasons.

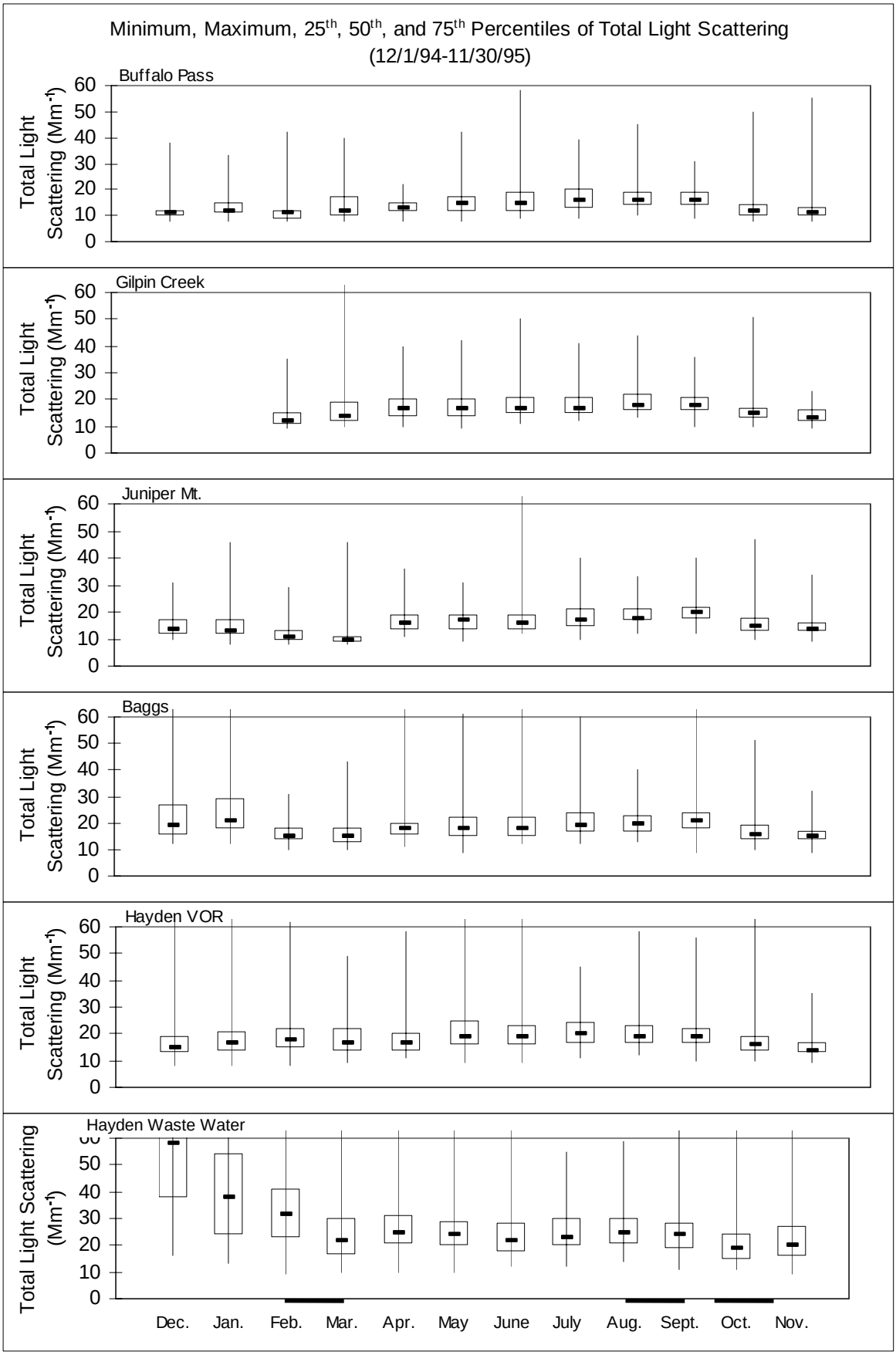
Minimum, Maximum, 25th, 50th, and 75th Percentiles of Total Light Scattering
(12/1/94-11/30/95)
Buffalo Pass
Gilpin Creek
Juniper Mt.
Baggs
Hayden VOR
Hayden Waste Water
Total Light Scattering (Mm-1)
0
10
20
30
40
50
60
Dec.
Jan.
Feb.
Mar.
Apr.
May
June
July
Aug.
Sept.
Oct.
Nov.

Figure 3.3.1. The monthly variation in total light scattering at all sites (RH < 95%). The heavy lines at the bottom indicate the intensive operating periods

Table 3.1.1
Comparison of Mt. Zirkel Visibility Study Light Scattering with Measurements in Other Class 1 Areas

Site Name	Site Abbr.	Light scattering or extinction coefficients at 10th, 50th, and 90th percentiles (Mm^{-1})													
		Dec 1994–Nov 1995			Jan-Mar 1995			Apr-Jun 1995			Jul-Sep 1995			Oct-Nov 1995		
		10th	50th	90th	10th	50th	90th	10th	50th	90th	10th	50th	90th	10th	50th	90th
NEPHELOMETER		b_{scat}	b_{scat}	b_{scat}	b_{scat}	b_{scat}	b_{scat}	b_{scat}	b_{scat}	b_{scat}	b_{scat}	b_{scat}	b_{scat}	b_{scat}	b_{scat}	b_{scat}
MZVS Sites:																
Buffalo Pass	BUPZ	10	14	22	9	11	20	11	14	23	12	16	23	9	12	17
Gilpin Creek	GLCZ	12	16	24	11	13	24	13	17	26	14	18	25	11	14	19
Juniper Mountain	JUNZ	11	16	23	9	11	18	13	16	24	14	18	25	12	15	21
Baggs	BAGZ	13	18	27	13	16	29	14	18	28	15	20	28	12	15	22
Hayden VOR	VORZ	13	18	28	12	17	27	14	18	30	15	19	28	12	15	21
Hayden Waste Water	SEWZ	15	24	43	15	27	58	16	24	37	17	24	35	13	19	32
IMPROVE and IMPROVE Protocol Sites:																
Jarbidge Wilderness	JARB	10	15	27	10	12	19	12	18	28	14	23	36	10	14	25
Lone Peak Wilderness	LOPE	12	19	35	11	15	38	15	23	35	13	20	33	13	18	36
Gila Wilderness	GILA	10	18	35	9	12	21	13	19	33	16	26	59	12	19	34
TRANSMISSOMETER		b_{ext}	b_{ext}	b_{ext}	b_{ext}	b_{ext}	b_{ext}	b_{ext}	b_{ext}	b_{ext}	b_{ext}	b_{ext}	b_{ext}	b_{ext}	b_{ext}	b_{ext}
IMPROVE and IMPROVE Protocol Sites:																
Canyonlands NP	CANY	16	24	32	14	18	26	19	25	37	19	26	33	23	26	31
Grand Canyon NP South Rim	GRCA	18	26	39	18	21	28	19	26	38	26	33	43	18	24	38

Grand Canyon NP In-Canyon	GRCW	22	30	42	19	23	33	26	32	41	28	35	46	25	30	41
Bridger Wilderness	BRID	17	23	33	16	19	27	19	25	34	21	27	37	18	22	28
Rocky Mountain NP	ROMO	16	22	34	15	20	29	18	23	41	18	25	36	20	23	31
Bandelier NM	BAND	22	32	45	21	26	35	26	32	45	32	37	50	20	29	44
Petrified Forest NP	PEFO	24	37	51	15	30	40	27	37	48	34	44	56	32	39	55
Chiricahua NM	CHIR	29	42	58	27	33	44	39	37	65	40	50	69	40	42	44
Great Basin NP	GRBA	16	25	34	11	13	19	21	26	35	22	28	35	19	23	32

3.4 Visibility Episodes

Figure 3.4.1 documents hourly light scattering from clean air and suspended particles at each site for the entire MZVS measurement period. These plots were used as the primary method of identifying visibility episodes, and events within those episodes. Aerosol filter samples corresponding to these episodes were chemically analyzed, and five of them were examined with detailed data analysis and modeling.

Figure 3.4.1 includes light scattering measured with the OPTEC nephelometer, with values corresponding to RH<90% plotted with a heavy line and values corresponding to RH>90% plotted with a thin line; RH values are plotted with a dotted line. No data are plotted for periods of missing or invalid measurements. Many of the light scattering readings exceed the graphical scale when RH>90%, indicating the presence of fogs or clouds that dominated the light scattering measurement. These events are confirmed most of the time by collocated photographs and videos that show the sight path to be completely obscured at these high relative humidities.

Figure 3.4.1 shows substantial obscuration due to weather from December through May, especially at the Buffalo Pass and Gilpin Creek sites. Many, but not all, of these weather events occurred simultaneously at all sites during winter and spring, indicating the widespread and frequent storms discussed in Section 2.2. The unusual frequency of storms during May that was identified in Section 2.2 is clearly evident in the nephelometer traces for that month. There were very few periods during which visibility was not obscured by storm clouds, and these were commonly of short duration. Fogs and clouds near the sampling sites were more spatially diverse during summer and fall, however, and occurred more frequently at the Buffalo and Gilpin Creek sites than at the other sites.

For much of the time when clouds or fogs did not dominate extinction, the nephelometer traces at Buffalo Pass, Gilpin Creek, and Juniper Mountain were at or near the clean air scattering limit of ~10 Mm^{-1}, consistent with the frequency distributions in Table 3.1.1 and Figure 3.3.1. Hour-to-hour excursions in light scattering are often abrupt, and they often rise and fall in conjunction with RH. This was especially true when RH varied between ~60% and 90%. This covariation is consistent with major components of the suspended particles being water soluble, and growing into size ranges that scatter light more efficiently when they extract water from a humid atmosphere. It is also consistent with the formation of aerosol sulfate in clouds which are often present at high humidity.

In addition to these plots, $PM_{2.5}$ mass concentrations and continuous sulfur dioxide and light absorption measurements at Buffalo Pass were examined to select visibility episodes for more detailed analysis. Tabulations of wildfire acreage available through September 1995 were also used to ensure that some episodes included and excluded major wildfire activity. These sample analysis periods are designated in Figure 3.4.1 by solid bars corresponding to the 0600 to 1800 MST daylight period during which aerosol samples were taken. They fulfill one or more of the following criteria delineated by Watson *et al.* (1995) for sample selection:

- Visibility is Impaired: Nonweather-related light scattering increased, as indicated by the OPTEC nephelometer traces.

- Visibility is Not Impaired: These are events with some elevated scattering and $PM_{2.5}$ mass, but not obvious or considerable hazes. These were usually selected from samples before or after events when light scattering was high.

- Plume Transport to Receptors. Plume transport was identified from continuous sulfur dioxide and light absorption measurements at Buffalo Pass. Some cases of plume transport to the Hayden VOR site were identified from videos.

- Specific Atmospheric and Emissions Conditions: These events include: 1) samples for which there is evidence of direct plume impact without major traversal of complex terrain (e.g., impacts at Waste Water and VOR); 2) evidence of direct plume impact with traversal of complex terrain (e.g., impacts at Juniper Mountain and Buffalo Pass); 3) long-range transport from distant sources (e.g., fires or haze from outside of the Yampa Valley); 4) mixing of plumes in clouds; and 5) plume accumulation in the Valley during nighttime and early morning and subsequent upslope transport. These events were chosen using videos, relative humidity data, and the everyday plume model animation discussed in Section 5.4 (which shows the plume transport direction).

- Measurements Evaluation: Sulfur dioxide and sulfate filter samples at Buffalo Pass were selected to compare with elevated sulfur levels measured with the continuous monitors. Organic and elemental carbon samples at Buffalo Pass were selected to compare with elevated light absorption levels measured with the continuous monitors. Aerosol samples were selected for which the $PM_{2.5}$ mass concentrations were much higher than those measured at other sampling sites.

The following episodes resulted from this selection criteria.

- 02/23/95: Figure 3.4.1 shows an increase in the Buffalo Pass light scattering during an IOP. This was accompanied by a sharp 22 ppb spike of sulfur dioxide with low black carbon concentrations. Conditions were moist, especially at higher elevations. This was the only nonweather light scattering excursion near the Wilderness that was observed during the winter IOP.

- 03/26/95–03/31/95: Light scattering was elevated at all sites during this non-IOP, indicating a regionwide event. Videos showed weather obscuration, punctuated by cloud clearing during which distant targets were moderately obscured. A 20-ppb sulfur dioxide spike occurred at Buffalo Pass on the morning of 03/30/95, but visibility was obscured by weather at this time. A morning scattering spike on 03/28/95 was not accompanied by an sulfur dioxide levels. Conditions were moist throughout the region.

- 05/06/95–05/07/95: Light scattering was elevated at all sites during this non-IOP, achieving ~30 Mm^{-1} at Buffalo Pass and Gilpin Creek. Sulfur dioxide was not available at Buffalo Pass. Conditions were moist, with weather obscuration at Buffalo Pass and Gilpin Creek.

- 06/14/95–06/16/95: A consistently high scattering of ~30 to 40 Mm^{-1} was recorded throughout the network during this dry, non-IOP period, indicating a regionwide event. Sulfur dioxide measurements were not available at Buffalo Pass.

- 06/29/95–07/01/95: Scattering coefficients of ~40 to 60 Mm^{-1} were recorded at Juniper and Baggs, on 06/30/95, with rapid decrease on 7/1 during this non-IOP period. Scattering at Buffalo Pass and Gilpin Creek was ~30 Mm^{-1} over this period, which was accompanied by clouds or fog at Buffalo Pass. The other sites experienced lower relative humidity, ~50% to 80%, during daylight hours.

- 07/29/95–07/31/95: Scattering was elevated at all sites, approaching 30 Mm^{-1} at Buffalo Pass, during this non-IOP, low humidity period. Scattering was variable from hour to hour at all sites.

- 08/07/95–08/09/95: Scattering increased over previous days to values exceeding 30 Mm^{-1} at Buffalo Pass during this IOP. Relative humidity was commonly low (RH <50%) at all sites during daylight hours.

- 08/14/95: This day was typical of most of the days during the August IOP, and was selected to represent them. A small scattering increase occurred at Buffalo Pass in the morning, coincident with an increase in sulfur dioxide.

- 08/21/95–08/27/95: This is an IOP example of high relative humidity conditions followed by a period of lower relative humidities. Light scattering ranged from ~20 to ~40 Mm^{-1} at Gilpin Creek during this period, with substantial hour-to-hour variability. There was a marked correspondence between light scattering and relative humidity at Hayden VOR and Hayden Waste Water. The latter half of the period was included to examine a relatively clean period for comparison.

- 09/02/95: An increase in light scattering at Buffalo Pass was partially accompanied by an increase in sulfur dioxide during this IOP period.

- 09/17/95–09/21/95: This IOP episode commenced with low relative humidities, increasing to RH>90% with accompanying increases in scattering. Weather commonly obscured views of the Wilderness during this episode. Several correspondences between excursions in light scattering and sulfur dioxide concentrations were measured at Buffalo Pass.

- 09/24/95: This IOP episode experienced morning peaks in light scattering at most of the sites and a distinct peak in light scattering during the late afternoon at Gilpin Creek.

- 09/27/95: This was a dry IOP episode with correspondence between light scattering and sulfur dioxide. Two light scattering spikes were recorded at most of the sites.

- 09/30/95–10/02/95: Light scattering was elevated throughout the network during this IOP event. Relative humidity decreased from >90% to <50% during the afternoon during the latter part of this episode. Changes in light scattering were accompanied by changes in sulfur dioxide concentrations on 10/01/95.

- 10/07/95–10/14/95: This episode is important because a wide variety of conditions were observed. The light scattering was elevated at all of the sites from the 10/07/95 through the 10/12/95 and then dropped to near Rayleigh on 10/13/95 and 10/14/95. There were two large peaks (10/08/95 and 10/12/95) in light scattering superimposed on the elevated light scattering and corresponding to peaks in the relative humidity. Also during this elevated period there were intermittent spikes of sulfur dioxide at Buffalo Pass. The 10/13/95 and 10/14/95 dates were of interest because the light scattering was very low while there were high sulfur dioxide concentrations present at Buffalo Pass. This is one of the primary episodes for modeling.

- 10/16/95–10/19/95: There was elevated light scattering throughout the network that decreased toward 10/19/95 at all sites except Buffalo Pass and Gilpin Creek, which showed peaks in their light scattering. A prescribed burn was seen in the 10/19/95 video of the Yampa Valley from Cedar Mountain.

- 10/22/95–10/23/95: There was high relative humidity throughout the region and large peaks in light scattering at several of the sites. There were coincident sulfur dioxide and light-scattering peaks on 10/23/95 at Buffalo Pass.

All of the episodes listed above were subjected to full chemical analyses of aerosol samples and ELSIE and CMB modeling. In addition, five of these episodes (08/07/95–08/09/95, 08/21/95–08/27/95, 09/17/95–09/21/95, 10/07/95–10/14/95, and 10/16/95–10/19/95) were submitted to more detailed data analysis and CALMET/CALPUFF modeling. These five episodes represent a range of meteorological and emissions conditions that can be compared and contrasted with each other. Other episodes listed above contain meteorological situations that are similar, though not identical, to these five episodes. Of the entire 54 days identified as visibility episodes, these modeled periods include 29 of those days, and the majority of those that occurred during the IOPs. In addition to the periods modeled, the 09/27/95 episode was examined in more detail since it represented one of the few times when b_{scat} and sulfur dioxide had corresponding peaks during dry conditions.

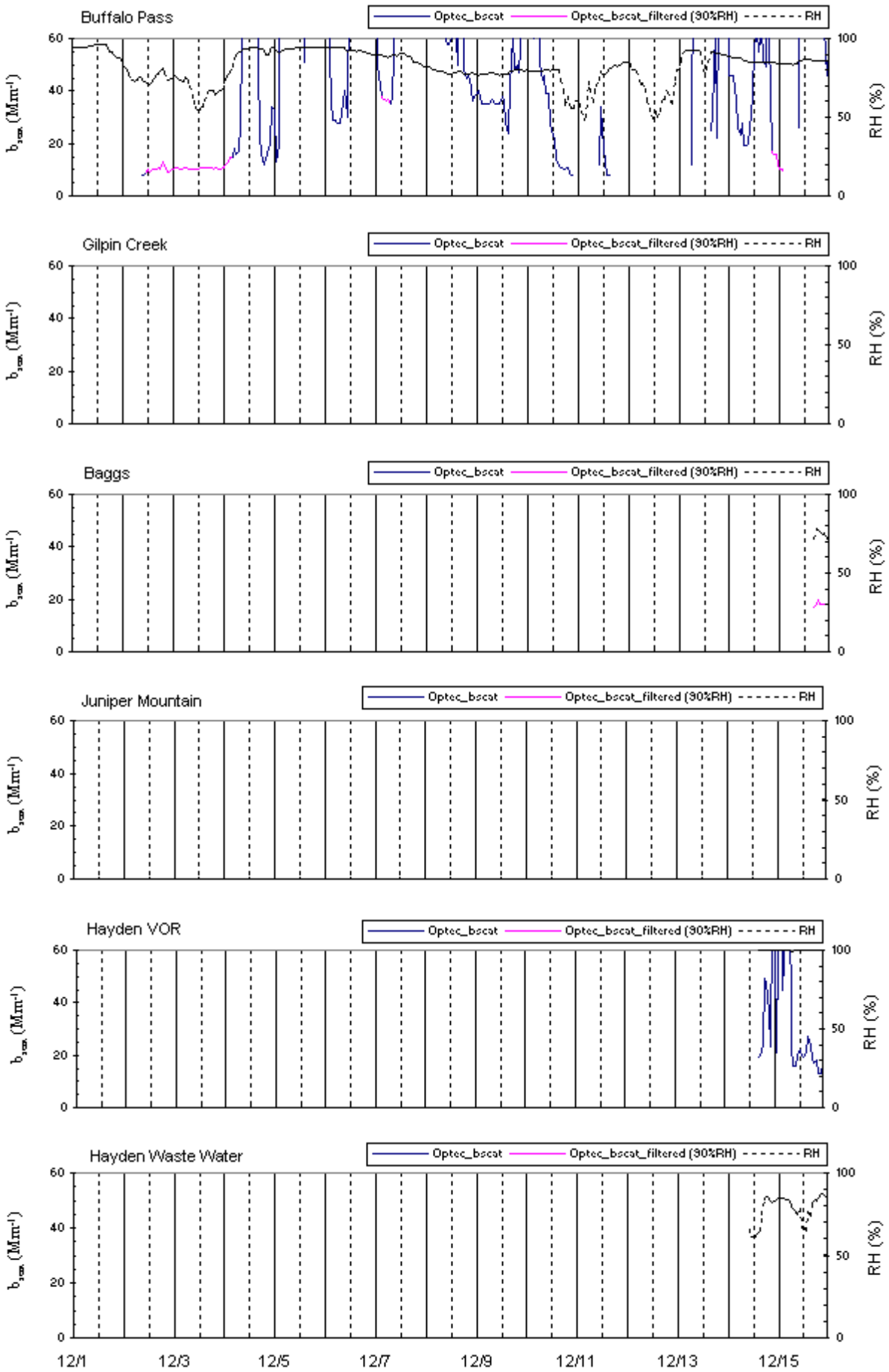
Buffalo Pass
Optec_bscat
Optec_bscat_filtered (90%RH)
RH
Gilpin Creek
Baggs
Juniper Mountain
Hayden VOR
Hayden Waste Water
b_{scat} (Mm^{-1})
RH (%)
0
20
40
60
50
100
12/1
12/3
12/5
12/7
12/9
12/11
12/13
12/15

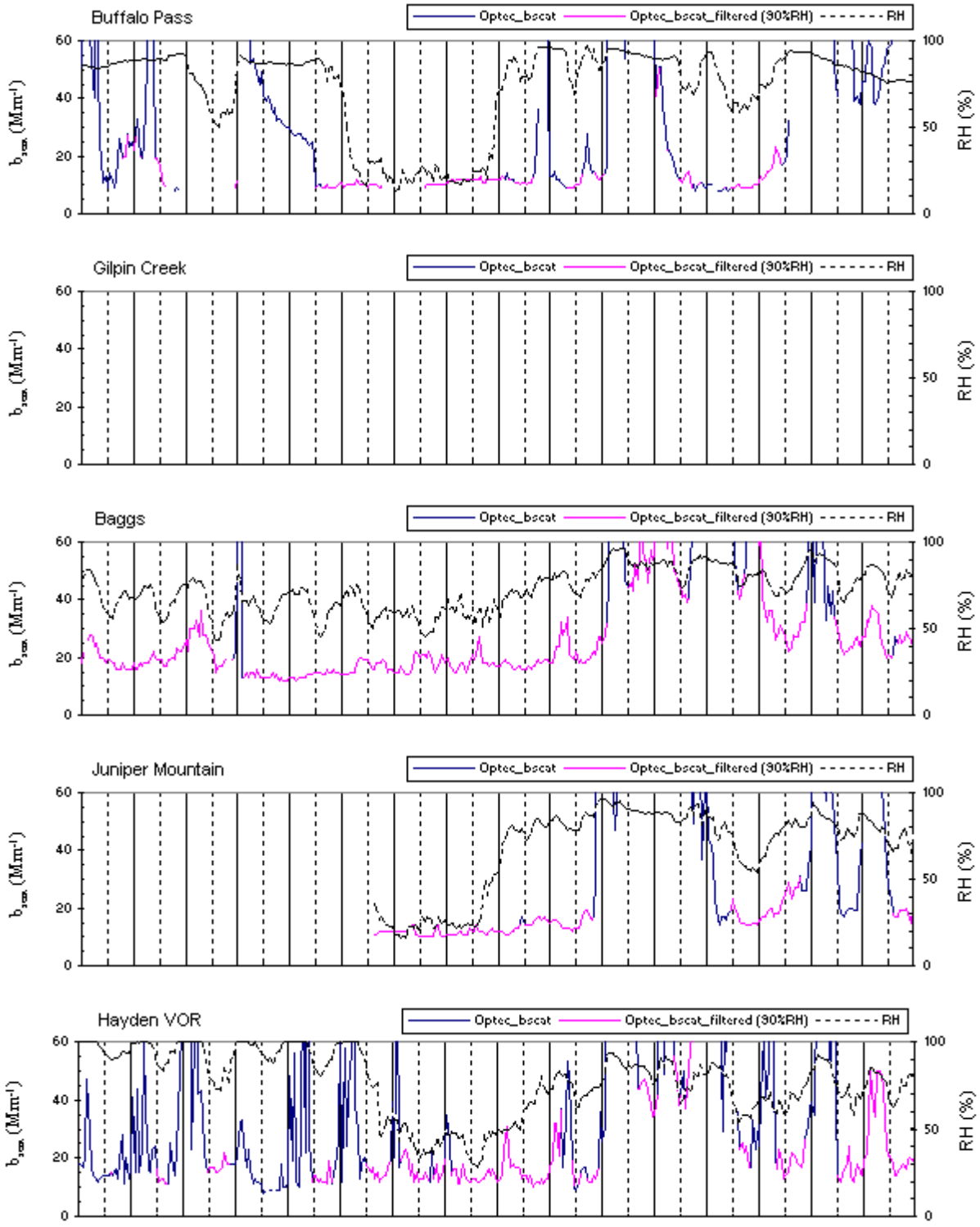
Buffalo Pass
Optec_bscat
Optec_bscat_filtered (30%RH)
RH
b_{scat} (Mm^{-1})
RH (%)
0
20
40
60
0
50
100
Gilpin Creek
Optec_bscat
Optec_bscat_filtered (30%RH)
RH
b_{scat} (Mm^{-1})
RH (%)
0
20
40
60
0
50
100
Baggs
Optec_bscat
Optec_bscat_filtered (30%RH)
RH
b_{scat} (Mm^{-1})
RH (%)
0
20
40
60
0
50
100
Juniper Mountain
Optec_bscat
Optec_bscat_filtered (30%RH)
RH
b_{scat} (Mm^{-1})
RH (%)
0
20
40
60
0
50
100
Hayden VOR
Optec_bscat
Optec_bscat_filtered (30%RH)
RH
b_{scat} (Mm^{-1})
RH (%)
0
20
40
60
0
50
100

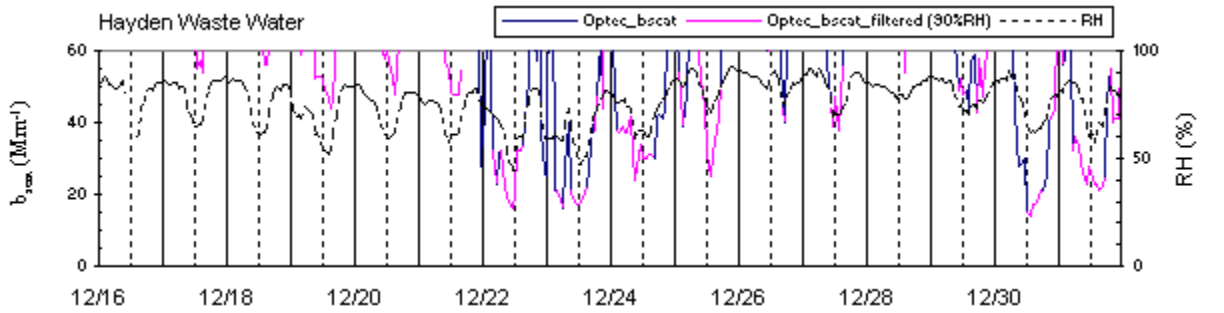
Hayden Waste Water
Optec_bscat
Optec_bscat_filtered (90%RH)
RH
b_{sca} (Mm^{-1})
RH (%)
0
20
40
60
0
50
100
12/16
12/18
12/20
12/22
12/24
12/26
12/28
12/30

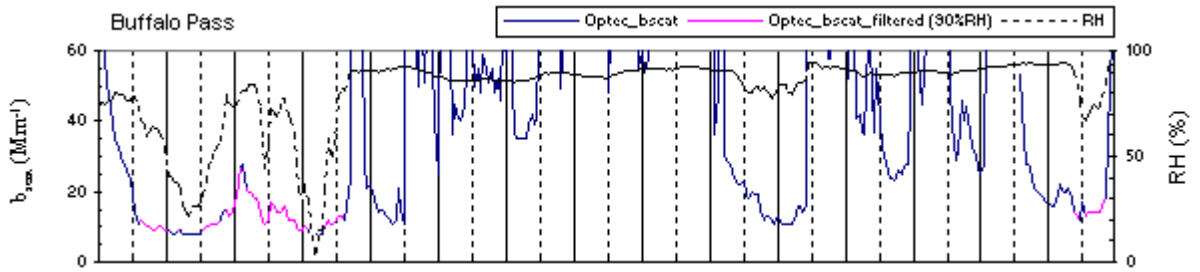
Buffalo Pass
Optec_bscat
Optec_bscat_filtered (90%RH)
RH
b_{sca} (Mm^{-1})
RH (%)
0
20
40
60
0
50
100

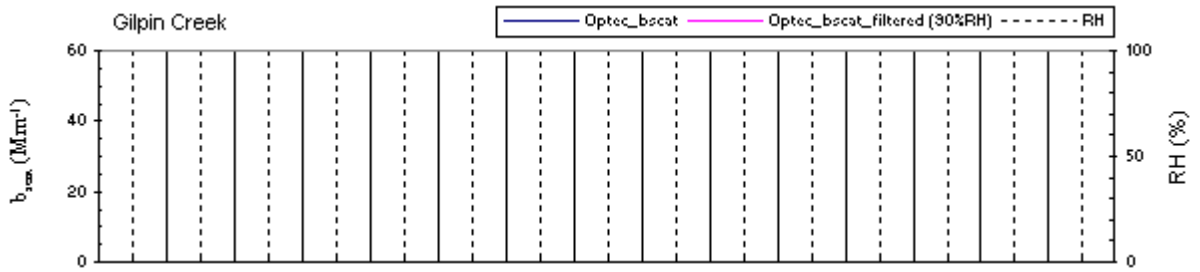
Gilpin Creek
Optec_bscat
Optec_bscat_filtered (90%RH)
RH
b_{sca} (Mm^{-1})
RH (%)
0
20
40
60
0
50
100

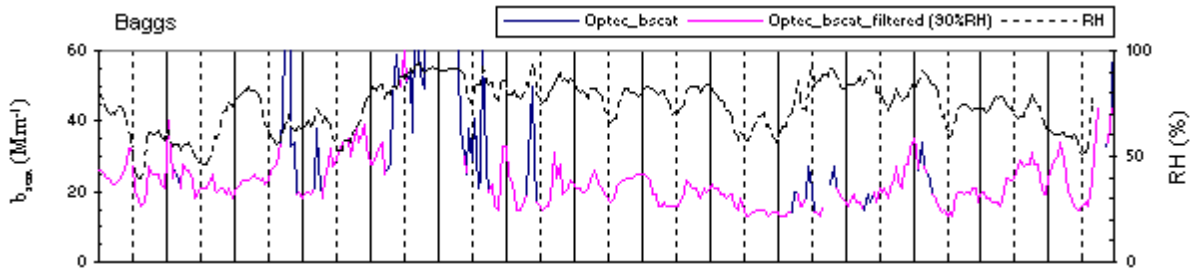
Baggs
Optec_bscat
Optec_bscat_filtered (90%RH)
RH
b_{sca} (Mm^{-1})
RH (%)
0
20
40
60
0
50
100

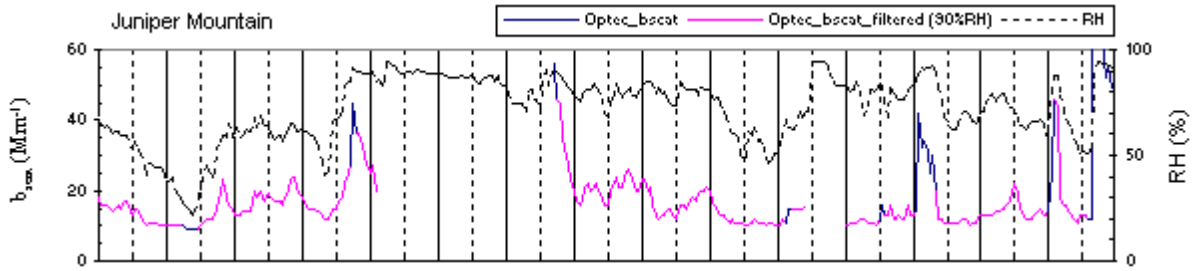
Juniper Mountain
Optec_bscat
Optec_bscat_filtered (90%RH)
RH
b_{sca} (Mm^{-1})
RH (%)
0
20
40
60
0
50
100

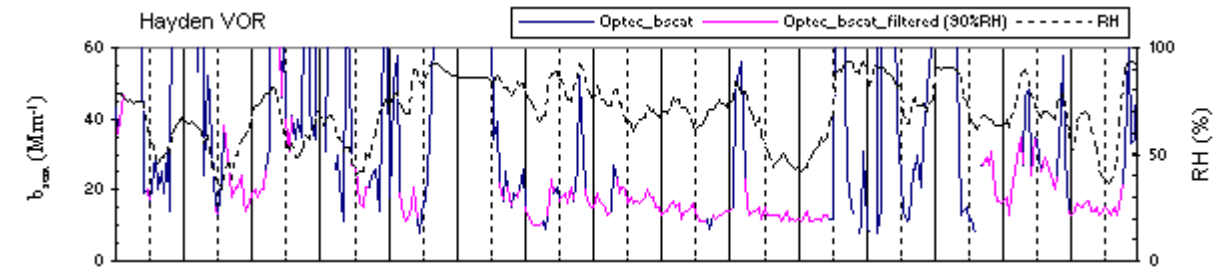
Hayden VOR
Optec_bscat
Optec_bscat_filtered (30%RH)
RH
b_{scat} (Mm^{-1})
RH (%)
0
20
40
60
0
50
100

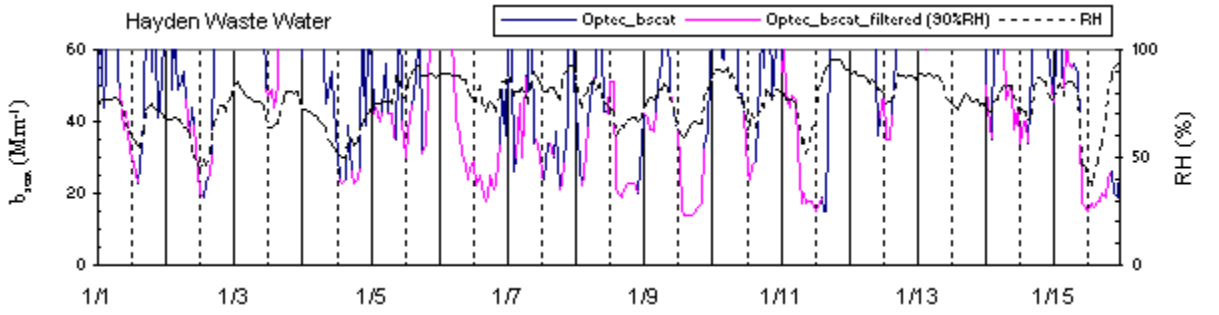
Hayden Waste Water
Optec_bscat
Optec_bscat_filtered (30%RH)
RH
b_{scat} (Mm^{-1})
RH (%)
0
20
40
60
0
50
100
1/1
1/3
1/5
1/7
1/9
1/11
1/13
1/15

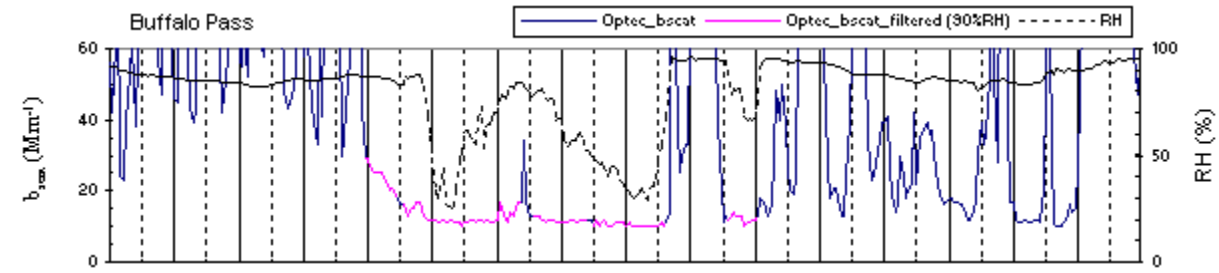
Buffalo Pass
Optec_bscat
Optec_bscat_filtered (30%RH)
RH
b_{scat} (Mm^{-1})
RH (%)
0
20
40
60
0
50
100

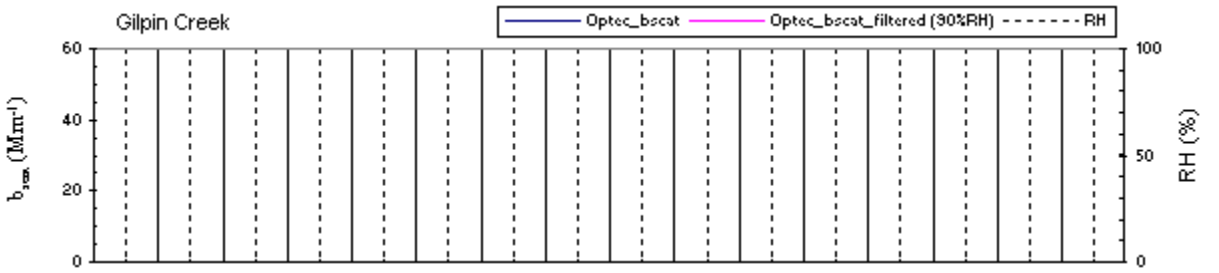
Gilpin Creek
Optec_bscat
Optec_bscat_filtered (30%RH)
RH
b_{scat} (Mm^{-1})
RH (%)
0
20
40
60
0
50
100

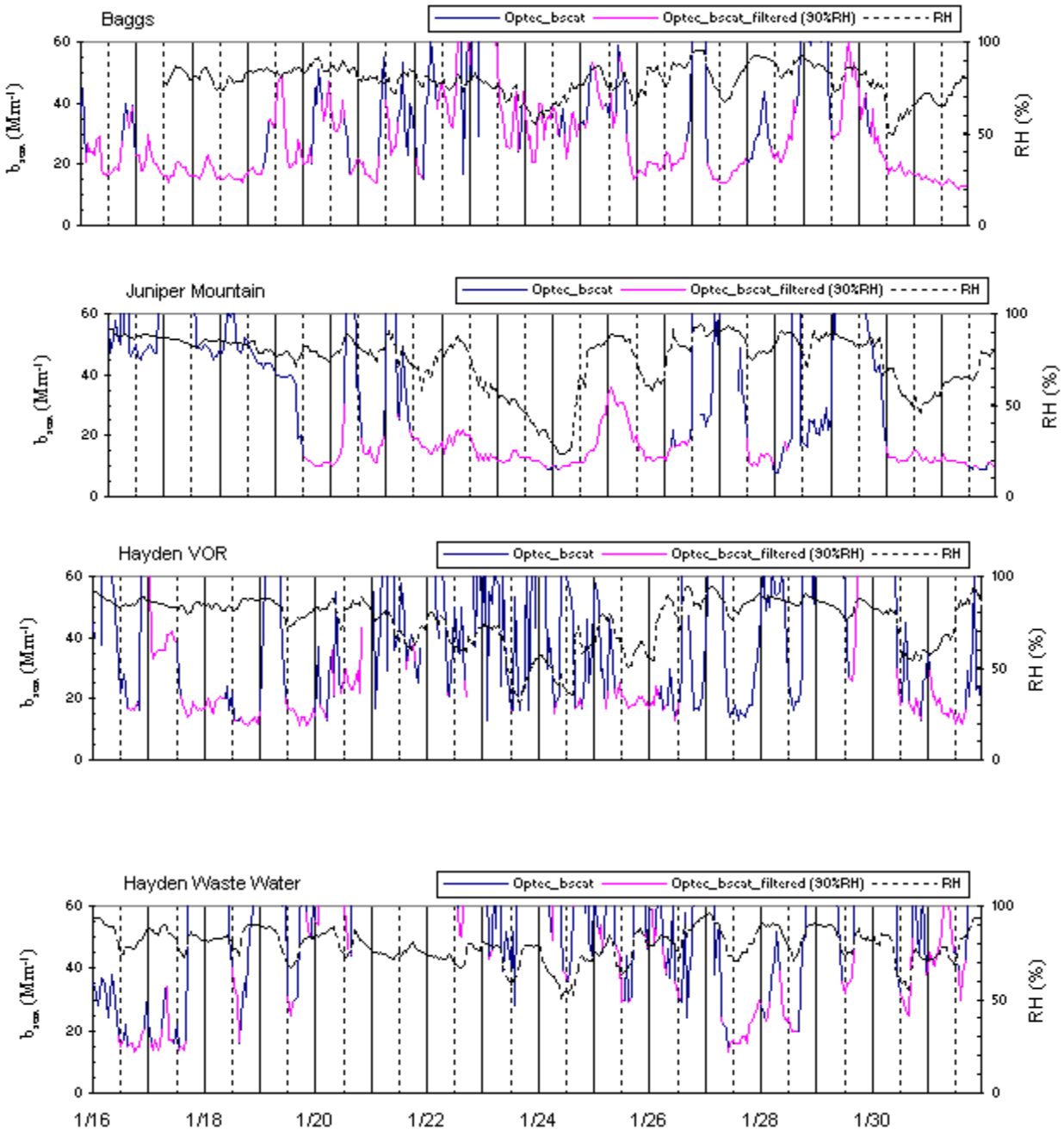
Baggs
Optec_bscat
Optec_bscat_filtered (30%RH)
RH
b_{sca} (Mm^{-1})
RH (%)
Juniper Mountain
Hayden VOR
Hayden Waste Water
1/16
1/18
1/20
1/22
1/24
1/26
1/28
1/30

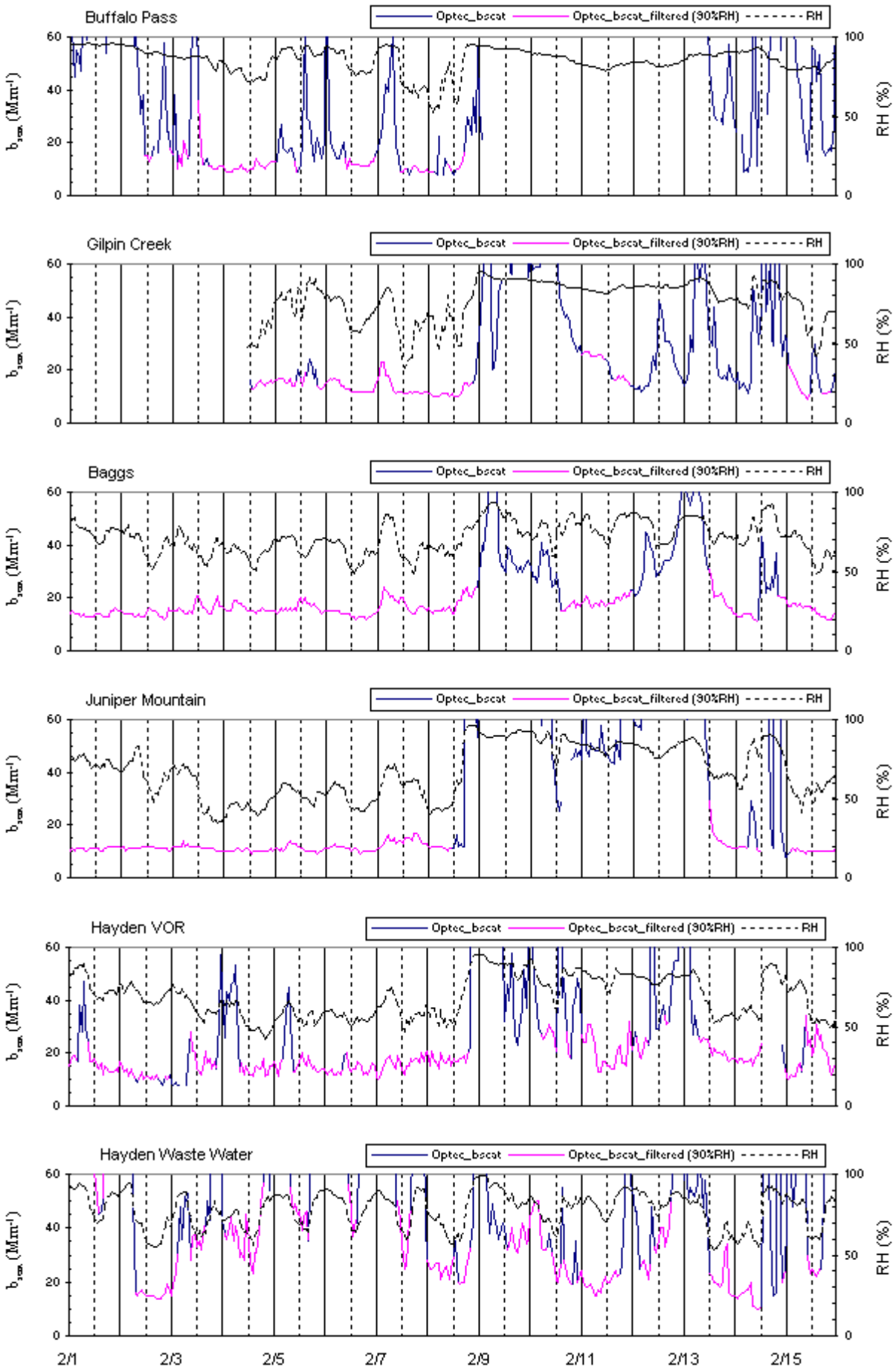
Buffalo Pass
Optec_bscat
Optec_bscat_filtered (90%RH)
RH
b_{scat} (Mm^{-1})
RH (%)
0
20
40
60
0
50
100
Gilpin Creek
Optec_bscat
Optec_bscat_filtered (90%RH)
RH
b_{scat} (Mm^{-1})
RH (%)
Baggs
Optec_bscat
Optec_bscat_filtered (90%RH)
RH
b_{scat} (Mm^{-1})
RH (%)
Juniper Mountain
Optec_bscat
Optec_bscat_filtered (90%RH)
RH
b_{scat} (Mm^{-1})
RH (%)
Hayden VOR
Optec_bscat
Optec_bscat_filtered (90%RH)
RH
b_{scat} (Mm^{-1})
RH (%)
Hayden Waste Water
Optec_bscat
Optec_bscat_filtered (90%RH)
RH
b_{scat} (Mm^{-1})
RH (%)
2/1
2/3
2/5
2/7
2/9
2/11
2/13
2/15

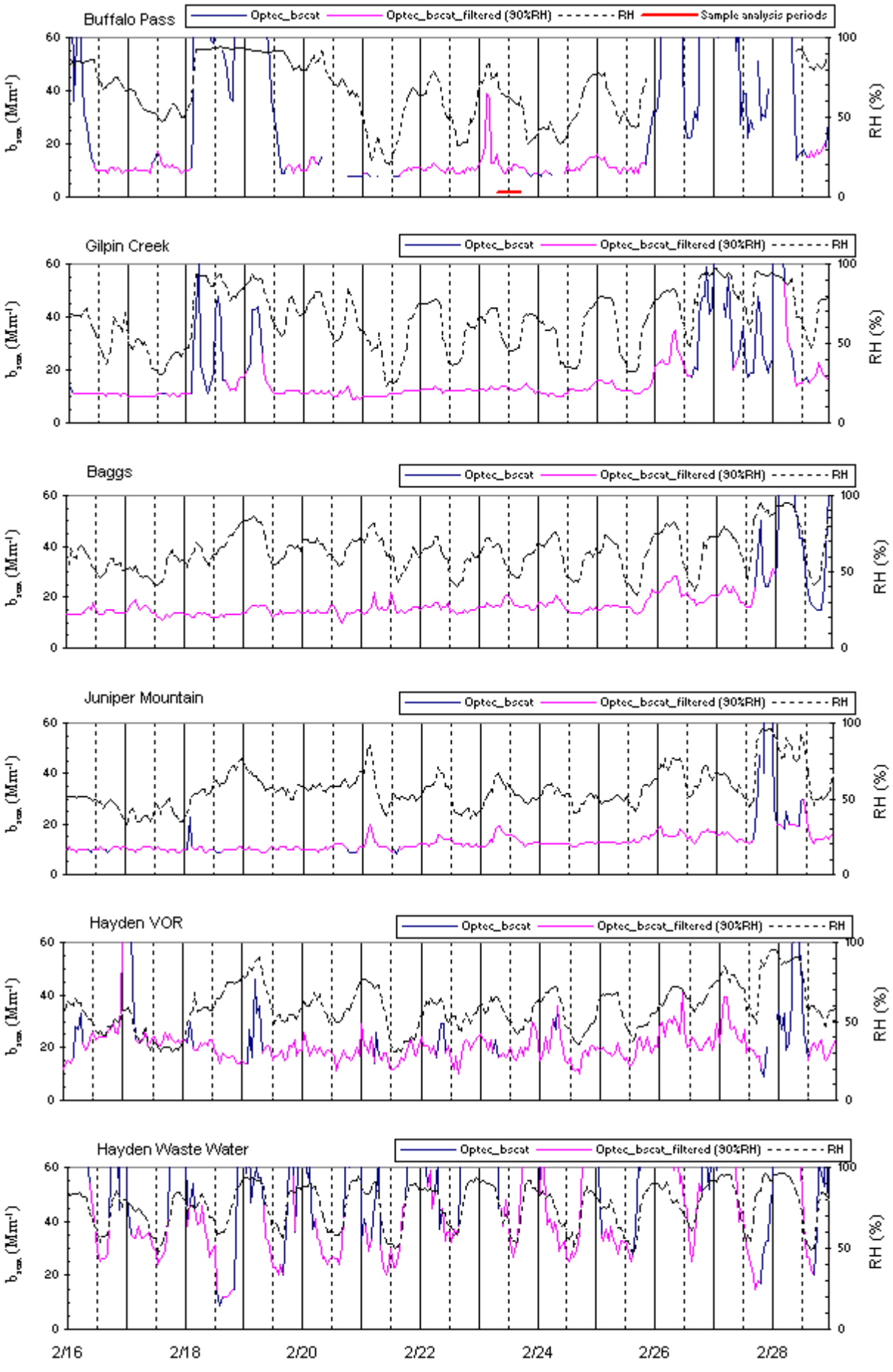
Buffalo Pass
Optec_bscat
Optec_bscat_filtered (90%RH)
RH
Sample analysis periods
Gilpin Creek
Baggs
Juniper Mountain
Hayden VOR
Hayden Waste Water
b_{scat} (Mm^{-1})
RH (%)
0
20
40
60
0
50
100
2/16
2/18
2/20
2/22
2/24
2/26
2/28

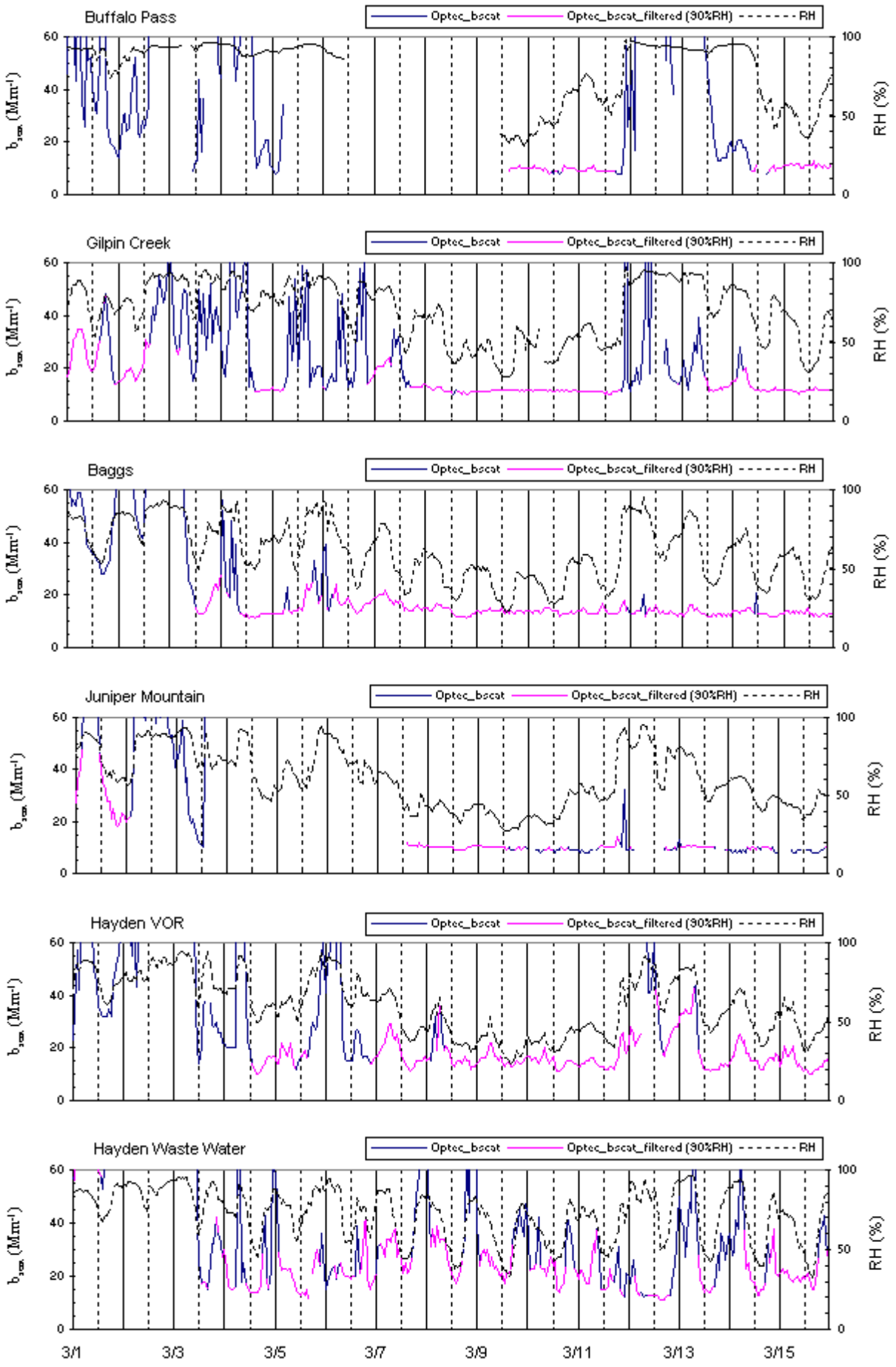
Buffalo Pass
Gilpin Creek
Baggs
Juniper Mountain
Hayden VOR
Hayden Waste Water
Optec_bscat
Optec_bscat_filtered (90%RH)
RH
b_{scat} (Mm^{-1})
RH (%)
0
20
40
60
50
100
3/1
3/3
3/5
3/7
3/9
3/11
3/13
3/15

3.5 Components of Light Extinction

This section examines the relative contributions of clean air scattering, particle scattering, and particle absorption for different levels of light extinction. Continuous measurements of total light scattering were made at the six monitoring sites described in Section 2. Six- or twelve-hour, daytime filter measurements of light absorption were made at the same sites. The clean-air (Rayleigh) scatter contribution to light scattering was calculated for each measurement site (see the Section 3 introduction for the constant Rayleigh components for each site); and the particle scattering, Rayleigh scattering, and absorption components of light extinction were calculated for the time period of each filter sample. The variation in these components of light extinction were examined as a function of season, intensive monitoring period, location, and amount of light extinction.

Figure 3.5.1 shows the contributions to light extinction for each site for each intensive operating period (IOP). For each site and IOP, the average contributions of the above components are shown for four extinction categories: < 15 Mm^{-1}, 15-20 Mm^{-1}, 20-30 Mm^{-1}, and > 30 Mm^{-1}. Shown below each stacked bar in Figure 3.5.1 is the percentage of the total number of samples at that site for that intensive period falling into the listed extinction category. Figure 3.5.2 shows similar data averaged over seasons for the three sites that operated between intensive monitoring periods.

From Figures 3.5.1 and 3.5.2, it is clear that winter is the cleanest season at the Wilderness (Buffalo Pass and Gilpin Creek) and "background" (Baggs and Juniper Mountain) sites, while it is the haziest season at the Yampa Valley (Hayden) sites. About 90% of the valid Buffalo Pass sample periods during winter had light extinction less than 15 Mm^{-1}; while 75% of the Hayden Waste Water sample periods were above 30 Mm^{-1}. This is consistent with the strong stability in winter which traps fresh emissions in the valleys, except during storms when emissions are rapidly dispersed. From the low winter extinction levels at Buffalo Pass and Juniper Mountain, it is clear that the regional contributors to extinction are minimal in the winter. On the other hand, some of the haziest days at all sites but Buffalo Pass are in the winter, indicating the possible effects of local sources. Gilpin Creek provides an excellent example of this since it is impacted by local wood-burning in the valley below the site, as evidenced by large light scattering during the winter.

Figures 3.5.1 and 3.5.2 show the relative contributions to extinction of scattering and absorption by particles. In general, absorption accounts for less than 20% of total extinction

and less than about one-third of particle extinction. However, there are a few exceptions worth noting. During the winter intensive period at Gilpin Creek, there were a few sample periods when absorption dominated the particle extinction. In addition during the non-intensive spring period from April through June at Gilpin Creek, most of the sample periods were above 30 Mm^{-1}, and the absorption dominated the particle extinction and made up almost half the total extinction. During the same period, the absorption component was high at Buffalo Pass and Juniper Mountain as well. It is likely that during both winter and spring, the Gilpin Creek site was affected by burning (either open or wood stoves) in the Elk River Valley below the site. In addition, it is likely that there were regional fires that affected most sites on some days. The fire inventory (see Section 6.2) showed a major fire of 141 km^2 to the west of the Valley during June, and numerous smaller fires up to 3 km^2 in April and May.

During the summer and fall, except for one sample at Gilpin Creek, absorption was a smaller fraction of particle and total extinction than during the winter and spring. This is consistent with the increased importance of haze due to secondary aerosols during those months. On the worst days during the summer intensive, however, the absolute amount of the absorption component at most sites was higher than during the other intensive operating periods, again indicating the importance of fires to the extinction budget.

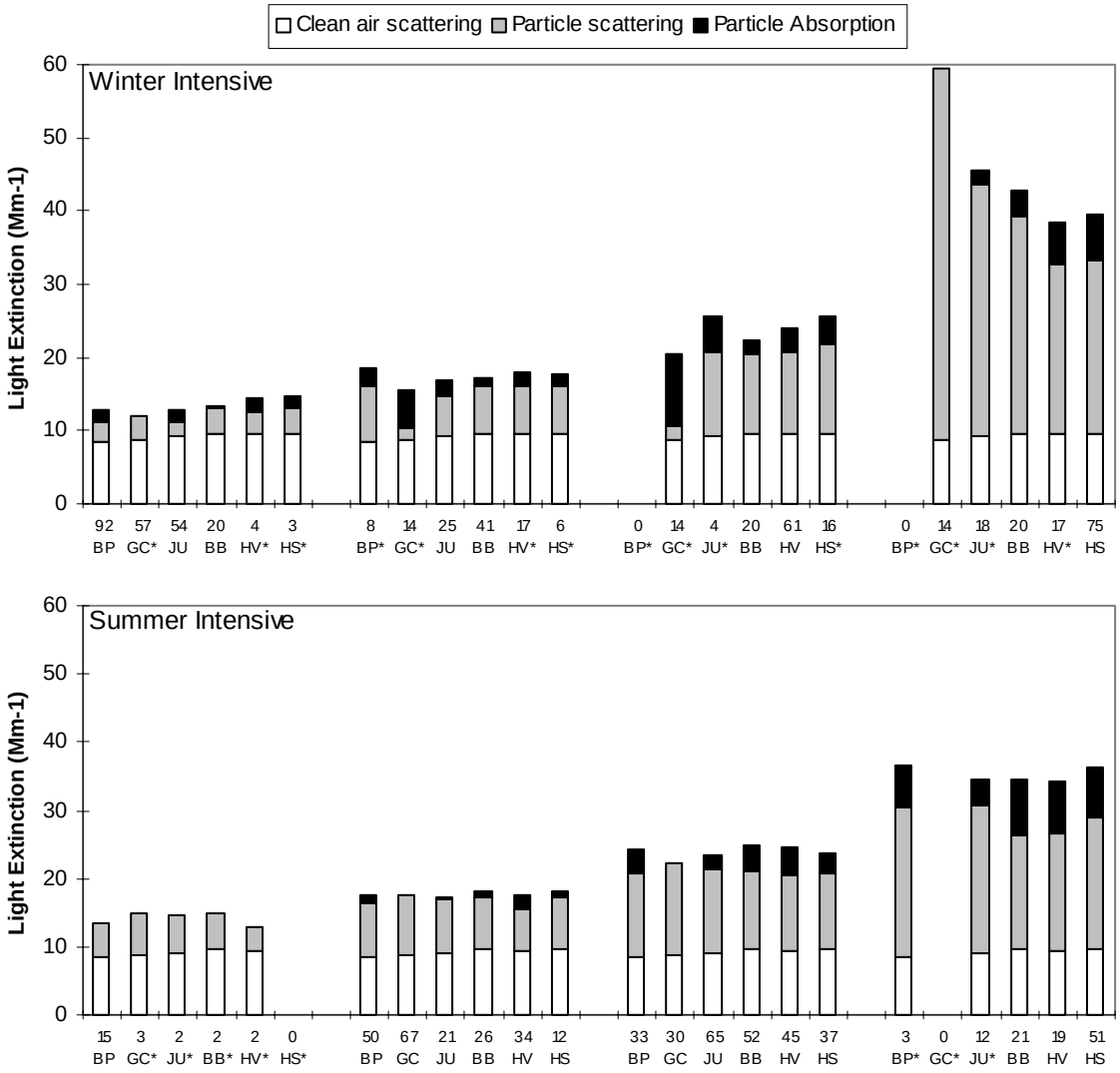
Clean air scattering
Particle scattering
Particle Absorption
Winter Intensive
Light Extinction (Mm-1)
0
10
20
30
40
50
60
92 BP
57 GC*
54 JU
20 BB
4 HV*
3 HS*
8 BP*
14 GC*
25 JU
41 BB
17 HV*
6 HS*
0 BP*
14 GC*
4 JU*
20 BB
61 HV
16 HS*
0 BP*
14 GC*
18 JU*
20 BB
17 HV*
75 HS
Summer Intensive
Light Extinction (Mm-1)
0
10
20
30
40
50
60
15 BP
3 GC*
2 JU*
2 BB*
2 HV*
0 HS*
50 BP
67 GC
21 JU
26 BB
34 HV
12 HS
33 BP
30 GC
65 JU
52 BB
45 HV
37 HS
3 BP*
0 GC*
12 JU*
21 BB
19 HV
51 HS

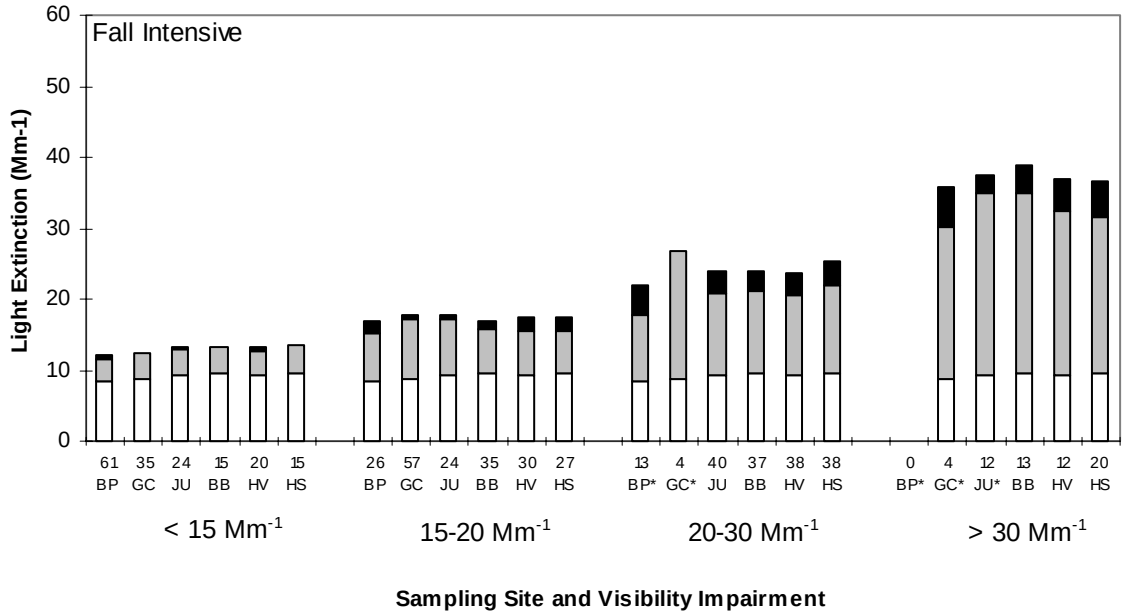

Figure 3.5.1 The components of light extinction during the intensive operating periods divided into 4 categories based on the magnitude: <15 Mm^{-1}, 15-20 Mm^{-1}, 20-30 Mm^{-1}, and >30 Mm^{-1}. The number above the site abbreviation is the percent of the valid samples during the intensive in the average. An * by the site abbreviation means there are five or fewer samples in the average.

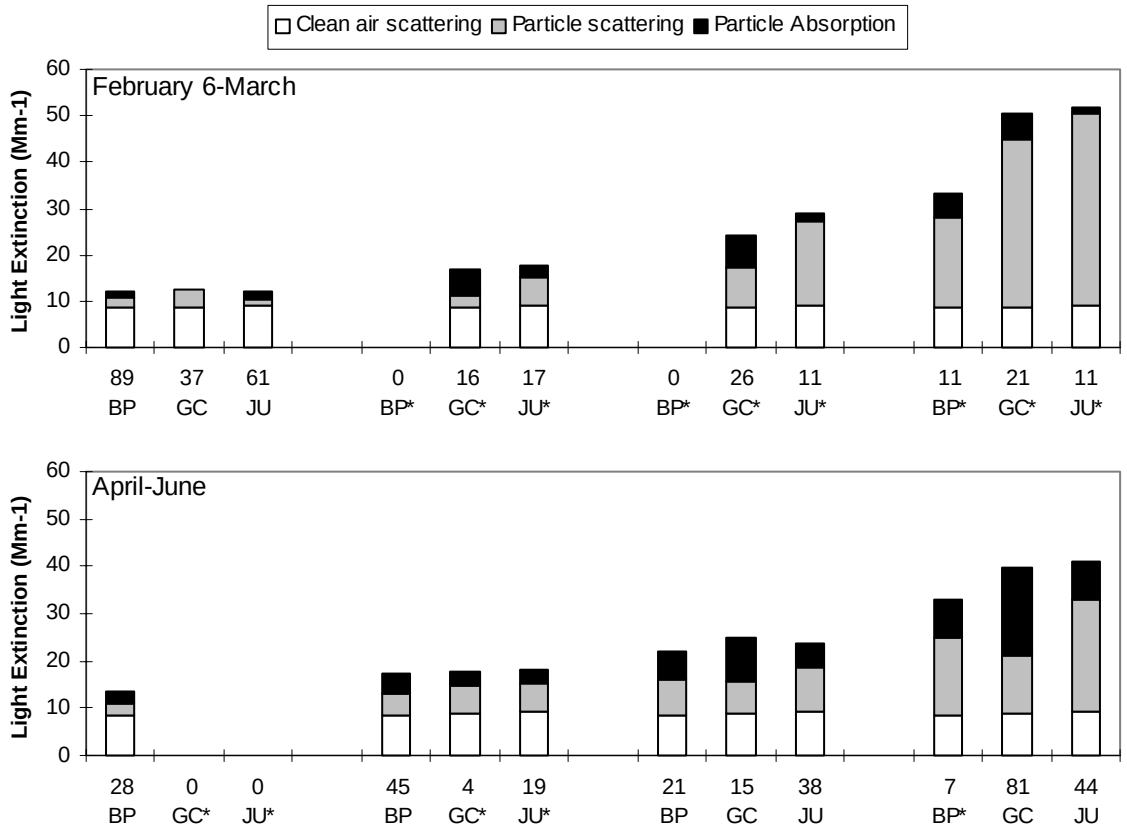

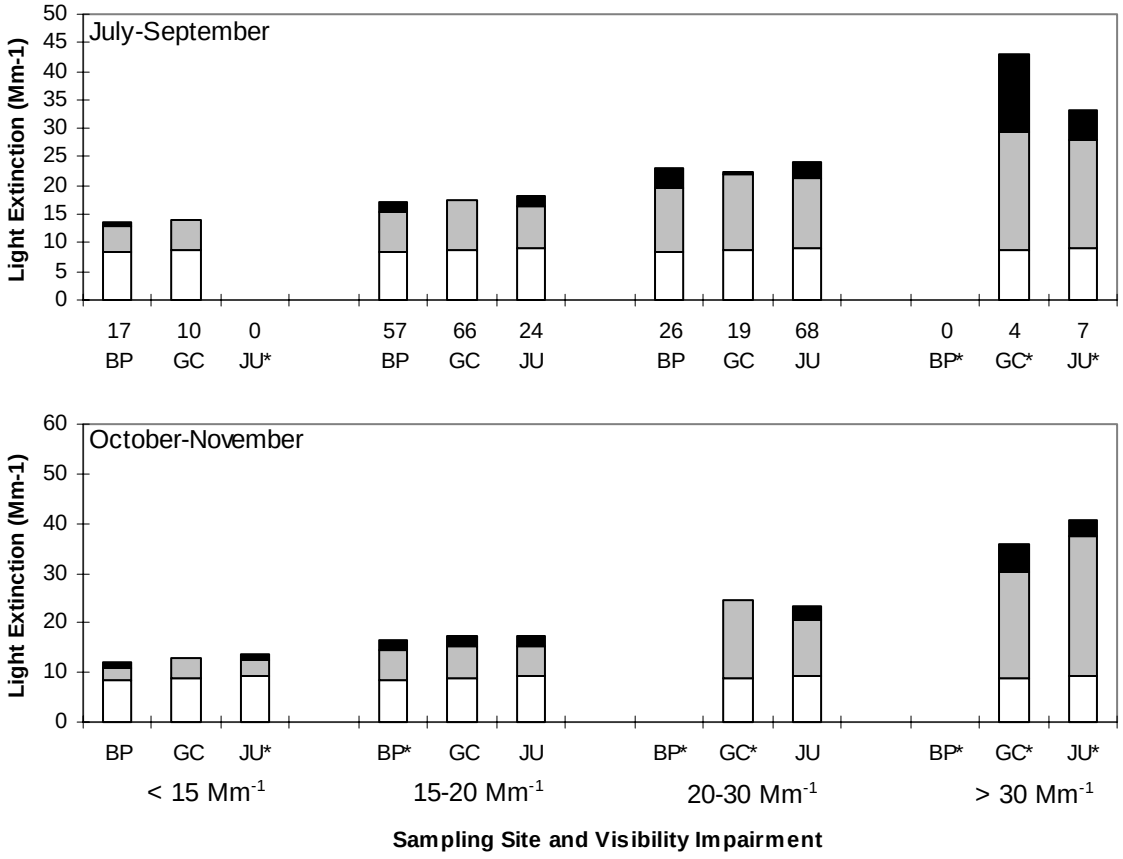

Figure 3.5.2 The components of light extinction during different seasons divided into 4 categories based on the magnitude: <15 Mm^{-1}, 15-20 Mm^{-1}, 20-30 Mm^{-1}, and >30 Mm^{-1}. The number above the site abbreviation is the percent of the valid samples during period in the average. An * by the site abbreviation means there are five or fewer samples in the average.

4.0 CHEMICAL COMPONENTS OF LIGHT EXTINCTION

Since the chemical components of the suspended particles can be used to determine the sources and the light extinction properties of particles in the atmosphere, it is important to understand the chemical characteristics of the suspended particles. Different chemical components possess different light extinction properties. These properties are expressed as chemical-specific "efficiencies" for the chemical components that constitute the majority of suspended particle mass. Efficiencies are expressed in square meters per gram (m^2/g) of suspended material, and they approximate the number of inverse megameters (Mm^{-1}) that correspond to each $\mu g/m^3$ of each chemical component. Watson and Chow (1994) note that elemental carbon absorbs light with efficiencies commonly in the range of 8 to 12 m^2/g, whereas suspended dust scatters light with efficiencies commonly in the range of 0.4 to 1.0 m^2/g. Other scattering efficiency ranges are 3 to 9 m^2/g for sulfate or nitrate and 3 to 5 m^2/g for organic carbon.

Particle scattering efficiencies are most sensitive to the size distribution of particles, and this distribution changes with relative humidity depending on the hygroscopic nature of each chemical substance. Efficiency estimates are also complicated by the mixture of several chemical species in the same particle, a mixture that is largely unknown for a specific situation. Changes in extinction differ depending on whether particle size or particle number changes for a given change in chemical concentration.

This section estimates scattering and absorption efficiencies for different chemical components, and estimates uncertainties associated with different assumptions about size and composition. It summarizes the particle compositions at each aerosol measurement location to identify the major components of $PM_{2.5}$ that can be associated with scattering and absorption efficiencies. Individual contributions from each chemical component are tabulated, and frequency distributions are examined to determine which chemical components contribute to different levels of total light extinction. Chemical compositions measured by the Buffalo Pass IMPROVE monitor are compared with compositions from other Class I areas.

4.1 Light Scattering Efficiencies

The Elastic Light Scattering Interactive Efficiencies (ELSIE) model (Sloane, 1984; 1986; Sloane *et al.*, 1991; Lowenthal *et al.*, 1995) is used to estimate the light extinction caused by hygroscopic aerosols of mixed chemical composition. Appendix B.4 provides details on the use of ELSIE in the MZVS and compares the derived efficiencies with those found by other methods.

4.1.1 ELSIE Model

The ELSIE model was applied with the following assumptions and parameter selections:

- A unimodal-lognormal particle size distribution was assumed based on a specified geometric mean diameter (D_g) and standard deviation for all chemical components. If the actual size distribution is non-unimodal or non-lognormal, the

light extinction coefficients will be overestimated at some sizes and underestimated at other sizes. Appendix B shows that light extinction is very sensitive to D_g for D_g <0.3 μm, and small changes in the geometric mean diameter could result in large errors in the total estimated light extinction.

- Unimodal-lognormal distributions are estimated from the ratios between the TSI nephelometer particle scattering measured at different wavelengths (blue/green and green/red).

- Particles are assumed to be spherical. This is a good assumption if the particles have been nucleated or condensed into droplets. However, at low relative humidities, suspended dust and elemental carbon particles may have irregular shapes that deviate from sphericity and change their light extinction properties.

- Particle light extinction coefficients are assumed to equal the number of particles multiplied by each one's extinction cross section. This implies that no particle blocks light that would hit another particle, and light is not multiply scattered. This assumption is reasonable for the MZVS because particle concentrations are low. Significant multiple scattering would result in an underestimate extinction efficiencies.

- $PM_{2.5}$ mass is assumed to be composed of six chemical components: ammonium sulfate, ammonium nitrate, organics, elemental carbon, suspended dust (using the definitions of Zhang *et al*., 1994), and liquid water. This assumption neglects other components that were not directly measured or have very low extinction coefficients. As shown below, these components are the major constituents of $PM_{2.5}$ found during the MZVS.

- The particle absorption cross section is assumed to be the difference between the particle extinction and scattering cross sections. This is a fairly good assumption since only particles are considered by ELSIE.

- The wavelength of light is assumed to be monochromatic (550 nm), corresponding to the green light scattering of the TSI nephelometer. This wavelength is also in the middle of the visible light range of the OPTEC nephelometer. Particles scatter and absorb light, and their efficiencies vary with wavelength. Sunlight is composed of many wavelengths. Actual extinction in the atmosphere will vary depending on the illumination (which varies by time of day and cloud-cover).

- Particles in a size range are assumed to have the same density. ELSIE calculates the number of particles in each size range from the particle size, volume-averaged density, and the total aerosol volume in the size range.

- Liquid water growth functions are empirically derived, and may differ from actual liquid water uptake by soluble particles. There is no definitive way to determine how particles of differing composition and structure grow as the relative humidity increases. Some particles become droplets within a short time after relative humidity rises, while other particles require a longer reaction time.

- The size of particles is assumed to be constant rather than the number when chemical compositions are changed in ELSIE calculations.

- The aerosol is assumed to be internally and homogeneously mixed. Sensitivity tests in Appendix B.4 show that an externally mixed assumption yields particle scattering coefficients (b_{sp}) that are 14% lower than those obtained with the internally mixed assumption. In reality, the aerosol is probably some combination of externally and internally mixed particles.

Appendix B.4 examines the quantitative effects of these assumptions in some detail, enhancing rather than repeating the observations published by Lowenthal et al. (1995). The most critical assumptions for applying ELSIE for the MZVS are those related to the particle size distribution. The estimated b_{sp} is most sensitive to variations in particle size for the particle diameters less than 0.3 μm that apparently occurred in the MZVS. These limitations are further evaluated in the following discussions.

4.1.2 Particle Size Distributions and Mean Geometric Diameters

The aerosol size distribution for each six-hour average $PM_{2.5}$ sample at the Buffalo Pass site was inferred from the ratio of the average measured b_{sp} in the blue wavelength (450 nm) to the average measured b_{sp} in the green wavelength (550 nm) (i.e., B/G ratio). A unimodal-lognormal particle size distribution was assumed with geometric mean diameter (D_g) and a geometric standard deviation equal to 2.0. Particle scattering (b_{sp}) was estimated at the blue and green wavelengths over a range of D_g from 0.05 to 1.0 μm. The inferred D_g was that which produced an estimated B/G that corresponded most closely to the measured B/G. The inferred D_g for a given sample reflects its chemical composition and water content.

Table 4.1.1 shows the relationship between the measured B/G and inferred D_g (Size1) for each sample at Buffalo Pass. The first "ER" column in Table 4.1.1 shows the percent deviation of the calculated from measured particle scattering. These deviations are sometimes very large, exceeding a factor of two or more for some samples. The final three columns in Table 4.1.1 show the geometric mean particle diameters (Size2) that best reproduce the measured particle scattering for each sample, and the B/G ratios that would correspond to this diameter. The deviations between measured and calculated values are much smaller for these cases, as would be expected. For most cases, the difference in B/G

Table 4.1.1
Comparison of $b_{sp}(g)$ Estimated from Sizes (D_g) Inferred from Measured $b_{sp}(b)/b_{sp}(g)$ Ratios

(sizes (D_g) which give best agreement between measured
and estimated $b_{sp}(g)$ and $b_{sp}(b)/b_{sp}(g)$ ratios)

Date	Start Hour (MST)	Meas. b_{sp}[a]	Meas. B/G[b]	Size1[c]	ER[d]	Size2[e]	B/G[f]	ER[g]
08/07/95	6	17.52	1.55	0.17	-0.6	0.15	1.60	16.6
08/07/95	12	14.84	1.49	0.20	-6.6	0.20	1.49	-7.2
08/08/95	6	17.72	1.57	0.18	-1.1	0.20	1.53	-17.1
08/08/95[h]	12	17.39	1.46	0.24	-108.7	0.15	1.62	-13.8
08/09/95[h]	6	7.57	1.32	0.35	-310.2	0.10	1.80	17.8
08/09/95[h]	12	8.60	1.28	0.41	-341.9	0.10	1.79	14.5
08/14/95	6	6.39	1.52	0.18	-3.7	0.20	1.49	-13.2
08/14/95	12	3.92	1.50	0.20	-48.6	0.15	1.60	-4.9
08/21/95[h]	6	15.09	1.42	0.28	-83.6	0.15	1.63	11.3
08/21/95[h]	12	16.27	1.39	0.29	-65.1	0.20	1.52	-17.2
08/22/95	6	10.97	1.36	0.30	-72.4	0.20	1.51	-17.1
08/22/95[h]	12	12.36	1.40	0.28	-123.2	0.15	1.61	-11.5
08/23/95	6	9.93	1.37	0.29	-70.6	0.15	1.60	17.6
08/23/95[h]	12	14.18	1.39	0.29	-100.4	0.15	1.62	5.6
08/24/95[h]	6	11.48	1.44	0.26	-251.4	0.10	1.79	11.1
08/24/95	12	11.69	1.57	0.17	-17.4	0.15	1.60	-1.8
08/25/95	6	6.79	1.49	0.21	-122.5	0.10	1.77	26.9
08/25/95	12	8.06	1.57	0.17	-70.7	0.10	1.78	30.2
08/26/95	6	7.75	1.54	0.18	-57.5	0.15	1.61	-19.4
08/26/95	12	6.77	1.57	0.18	-50.6	0.15	1.62	-21.6
08/27/95	6	11.05	1.52	0.20	-3.1	0.20	1.52	-5.6
08/27/95	12	9.21	1.54	0.19	-33.1	0.15	1.62	4.5
09/02/95	6	14.61	1.43	0.24	19.1	0.35	1.30	-2.1
09/02/95	12	14.99	1.44	0.22	30.3	0.45	1.17	0.5
09/17/95	6	7.44	1.52	0.19	22.9	0.25	1.43	-0.6
09/17/95	12	7.56	1.56	0.18	13.8	0.20	1.53	3.4
09/18/95	6	5.40	1.62	0.15	49.7	0.25	1.45	7.1
09/18/95	12	10.92	1.57	0.18	59.8	0.60	1.16	13.1
09/19/95	6	3.37	1.52	0.19	17.3	0.25	1.42	-11.0
09/19/95	12	10.74	1.56	0.17	43.1	0.30	1.36	1.3
09/20/95	6	6.26	1.54	0.17	18.0	0.20	1.49	3.1
09/20/95	12	9.16	1.48	0.22	48.6	0.50	1.22	17.8
09/21/95	6	6.43	1.58	0.16	59.7	0.50	1.21	8.0
09/21/95	12	7.30	1.62	0.15	73.6	0.60	1.16	28.2
09/24/95	6	9.65	1.56	0.18	42.4	0.30	1.38	1.6
09/24/95	12	8.13	1.53	0.18	59.5	0.40	1.26	26.2
09/27/95	6	8.00	1.49	0.20	40.2	0.40	1.26	5.1
09/27/95	12	9.18	1.49	0.22	33.2	0.35	1.32	2.4

Table 4.1.1 (continued)
Comparison of $b_{sp}(g)$ Estimated from Sizes (D_g) Inferred from Measured $b_{sp}(b)/b_{sp}(g)$ Ratios.

(sizes (D_g) which give best agreement between measured
and estimated $b_{sp}(g)$ and $b_{sp}(b)/b_{sp}(g)$ ratios)

Date	Start Hour	Meas. b_{sp}[a]	Meas. B/G[b]	Size1[c]	ER[d]	Size2[e]	B/G[f]	ER[g]
09/30/95	6	1.02	1.59	0.14	21.5	0.15	1.57	16.9
09/30/95	12	8.00	1.59	0.15	35.0	0.20	1.47	4.5
10/01/95	6	10.13	1.58	0.16	57.9	0.50	1.21	3.9
10/01/95	12	6.46	1.55	0.18	15.4	0.20	1.52	5.4
10/02/95	6	11.13	1.55	0.19	50.2	0.60	1.17	0.7
10/02/95	12	3.72	1.48	0.21	-19.8	0.20	1.50	-11.9
10/07/95	6	4.65	1.44	0.22	-69.9	0.15	1.57	-9.8
10/07/95	12	5.46	1.44	0.26	45.5	0.50	1.23	23.1
10/08/95	6	16.55	1.53	0.19	60.3	0.60	1.16	25.3
10/08/95	12	6.76	1.50	0.22	53.0	0.50	1.24	19.7
10/09/95	6	5.56	1.43	0.24	6.9	0.25	1.42	4.6
10/09/95	12	6.24	1.43	0.23	17.5	0.30	1.34	-0.7
10/10/95	6	9.52	1.44	0.23	64.8	0.45	1.17	50.9
10/10/95	12	6.70	1.44	0.22	37.0	0.40	1.25	13.5
10/11/95	6	3.82	1.42	0.24	-35.3	0.20	1.48	-15.0
10/11/95	12	3.83	1.41	0.25	-178.1	0.10	1.75	21.2
10/12/95	6	15.92	1.49	0.20	-24.3	0.15	1.59	13.2
10/12/95	12	12.00	1.53	0.17	26.3	0.95	1.03	-2.1
10/13/95	6	2.38	1.57	0.15	-41.1	0.10	1.73	26.8
10/13/95	12	1.78	1.52	0.19	-123.0	0.10	1.76	17.5
10/14/95	6	2.52	1.45	0.21	-67.5	0.15	1.57	-11.4
10/14/95	12	1.55	1.48	0.20	-183.3	0.10	1.75	-2.6
10/16/95	6	2.81	1.42	0.24	-86.0	0.15	1.59	-6.4
10/17/95	6	8.93	1.46	0.24	40.1	0.50	1.22	12.5
10/18/95	6	6.95	1.44	0.23	35.0	0.40	1.26	11.7
10/19/95	6	5.39	1.46	0.22	64.6	0.40	1.26	48.7
10/22/95	6	2.82	1.58	0.15	61.2	0.40	1.26	12.9
10/23/95	6	6.55	1.66	0.14	70.8	0.50	1.23	8.4

[a] Measured $b_{sp}(g)$.
[b] Measured ratio of $b_{sp}(b)/b_{sp}(g)$.
[c] Size1: D_g corresponding to measured $b_{sp}(b)/b_{sp}(g)$ ratios.
[d] Error (Measured b_{sp} - Estimated b_{sp})/Measured b_{sp} based on Size1 and TSI nephelometer RH.
[e] Optimum size (D_g) corresponding to best agreement between estimated and measured b_{sp} and $b_{sp}(b)/b_{sp}(g)$.
[f] Estimated $b_{sp}(b)/b_{sp}(g)$ ratio which corresponds to best agreement between measured and estimated $b_{sp}(g)$ over a range of D_g.
[g] Error (Measured b_{sp} - Estimated b_{sp})/Measured b_{sp} corresponding to optimum size.
[h] Samples where b_{sp} was overpredicted.

ratios for the two calculation methods is small, and well within measurement precisions. The difference in particle geometric mean diameters is also small for most cases, on the order 0.05 μm for most cases. These results show how sensitive the calculated particle scattering is to particle size in this size range.

4.1.3 Liquid Water Content

The volume of liquid water is estimated using a growth function, which is the relationship between particle composition and relative humidity derived empirically for chemically-complex aerosols (Hanel, 1976; Hanel and Lehmann, 1981; Sloane, 1984; Sloane, 1986). This function depends on the volume-averaged density and fractional solubility of the dry aerosol. The changes in the scattering efficiencies for different chemical components as a function of the relative humidity growth function are shown in Figure 4.1.1. As the relative humidity increases, the scattering efficiencies of the various components increase.

Figure 4.1.1. Relationships between relative humidity (1/1-RH/100)) and specific scattering efficiencies of ammonium sulfate, ammonium nitrate, organic carbon, and soil.

4.1.4 Comparisons Between Measured and Calculated Light Extinction

Comparisons between the results of the ELSIE model and measured total light extinction at each site are shown in Figure 4.1.2. Each plot contains a solid line indicating the one-to-one line and two dashed lines indicating the slope with a non-zero or zero intercept. Measurement uncertainties as well as model-calculated uncertainties associated with the X- and Y-axes are shown for comparison. As intercepts are low compared to the measured concentrations, the slope closely represents the ratio of Y over X. Points are not plotted for weather obscured situations; a total of 28 points were removed because the relative humidity exceeded 90%.

Comparisons of calculated and measured b_{ext} are within the measured and calculated uncertainties most of the time at all sites except Gilpin Creek. The measurement uncertainty for each 6-hour or 12-hour sampling period was approximated by the standard error of the average derived from hourly measurements. The measurement and modeled uncertainties are often large. More than 70% of the data overlap with the one-to-one line within one standard deviation of each measurement.

Figure 4.1.2 Scatter plots of calculated versus measured particle light scattering between 2/23/95 and 10/23/95 at all six sites during the Mt. Zirkel Visibility Study.

The disagreements for Gilpin Creek data do not have an obvious explanation. Uncertainties associated with these values are large, owing to long averaging times and a large portion of the light extinction being due to organics and elemental carbon, which have large measurement uncertainties. For Gilpin Creek, fewer than 50% of the data points were explained well by the ELSIE modeling.

Scatter plots comparing calculated particle scattering and absorption were also generated and are included in Appendix B. These plots show that the calculated particle light scattering (b_{sp}) agreed with the measured b_{sp} within one standard deviation for more than

80% of the samples at the Baggs and Hayden Waste Water sites, with correlation coefficients (r) of 0.78 to 0.81. The particle scattering comparisons were in poorer agreement at the Gilpin Creek and Buffalo Pass sites (r = 0.35 to 0.37).

4.2 Chemical Composition of Suspended Particles

Tables 4.2.1a-f summarize average and maximum concentrations of the chemical components measured in the MZVS. The period from which these samples were obtained spanned 02/16/95 to 10/29/95, and the dates correspond to the episodes identified in Section 3.4. Since the sample selection process was intentionally biased toward the sampling periods with elevated light extinction, the averages in Tables 4.2.1a-f are higher than the averages that would be found in a random selection of samples or in a long-term sampling network.

Various plots of the individual measurements are available in Appendix E, and examination of these plots is consistent with the general discussion of averages and maxima presented here. Tables 4.2.1a-f show which chemical components are the largest contributors to $PM_{2.5}$ mass, and therefore those chemicals that are likely to be the major causes of particle scattering and absorption. Organic carbon and sulfate were the major chemical components in most of the samples. Ammonium was a large component in most samples. Nitrate was a minor component all of the time. Suspended dust elements and elemental carbon were minor components in most samples, but they were large components on some samples.

$PM_{2.5}$ mass concentrations were low most of the time, averaging from 3.8 ± 1.6 $\mu g/m^3$ at the Baggs site to 5.7 ± 2.1 $\mu g/m^3$ at the Hayden VOR site. Elevated $PM_{2.5}$ concentrations were found at the Buffalo Pass site (20.5 ± 0.04 $\mu g/m^3$) during the morning (0600-1200 MST) of 08/24/95, and at the Hayden Waste Water site during the afternoon (1200-1800 MST) of 02/24/95 (15.5 ± 2.6 $\mu g/m^3$) as well as during the morning of 02/26/95 (14.3 ± 0.8 $\mu g/m^3$), and at the Gilpin Creek site (14.8 ± 2.7 $\mu g/m^3$) during the daytime (0600-1800 MST) of 07/30/95.

On average, the sum of species to $PM_{2.5}$ mass ratios ranged from 0.57 at the Juniper Mountain site to 1.05 at the Baggs site, which is consistent with the findings of other studies (e.g., Chow *et al.*, 1996). The major species accounted for most of the measured mass, most of the time.

Organic carbon was the largest component of $PM_{2.5}$, followed by sulfate, ammonium, elemental carbon, and nitrate. Average organic carbon concentrations ranged from 0.92 ± 0.77 $\mu g/m^3$ at the Buffalo Pass site to 2.1 ± 1.0 $\mu g/m^3$ at the Baggs site. Maximum organic carbon ranged from 3.0 $\mu g/m^3$ at the Buffalo Pass site to 6.3 $\mu g/m^3$ at the Gilpin Creek site.

Average elemental carbon concentrations ranged from 0.26 ± 0.22 $\mu g/m^3$ at the Buffalo Pass site to 0.96 ± 0.81 $\mu g/m^3$ at the Gilpin Creek site. Maximum elemental carbon ranged from 0.93 $\mu g/m^3$ at the Juniper Mountain site to 3.8 $\mu g/m^3$ at the Gilpin Creek site. The average organic to total carbon ratio (i.e, OC/TC, where TC is the sum of organic plus elemental carbon) of 0.63 at the Gilpin Creek site is 15% to 25% lower than the OC/TC ratios at the other sites.

Average sulfate concentrations were similar among all sites, ranging from 0.81 ± 0.48 $\mu g/m^3$ at the Buffalo Pass site to 1.1 ± 0.7 $\mu g/m^3$ at the Hayden VOR and Hayden Waste

Table 4.2.1a

Maximum and Average Six- and/or Twelve-Hour Concentrations ($\mu g/m^3$)

for $PM_{2.5}$ Mass and Major Chemical Constituents at the Buffalo Pass Site

between 02/16/95 and 10/29/95

Species	Average	Maximum	Std. Dev.	Total No. in Average
Mass	4.70156	20.40620	2.96880	64
b_{abs} (Mm^{-1})	2.46988	9.45875	2.09006	80
Cl^-	0.00939	0.13100	0.01963	94
NO_3^-	0.08824	0.58320	0.08603	94
$SO_4^=$	0.80650	2.08860	0.48207	94
K^+	0.01785	0.08840	0.01707	93
NH_4^+	0.26732	0.91110	0.19323	80
Total Ammonia (NH_3+NH_4^+)	0.48132	1.08010	0.22800	61
Denuded NH_4^+	0.34537	0.86240	0.20725	62
OC	0.91746	3.01890	0.76931	94
EC	0.25718	1.12240	0.21750	94
Backup OC	0.82601	3.45320	0.63063	94
Backup EC	0.22790	1.42330	0.25629	94
Na	0.01094	0.05420	0.01095	95
Mg	0.01003	0.06450	0.01230	95
Al	0.07503	1.09240	0.12049	95
Si	0.17366	1.29020	0.19768	95
P	0.00027	0.00280	0.00057	95
S	0.28736	0.77340	0.17124	95
Cl	0.00208	0.04260	0.00533	95
K	0.03799	0.18260	0.03382	95
Ca	0.03569	0.27520	0.03961	95
Ti	0.00476	0.04180	0.00769	95
V	0.00026	0.00300	0.00045	95
Cr	0.00032	0.00400	0.00054	95
Mn	0.00125	0.01030	0.00156	95
Fe	0.06144	0.48340	0.07656	95
Co	0.00007	0.00180	0.00021	95
Ni	0.00021	0.00300	0.00051	95
Cu	0.00263	0.03110	0.00457	95
Zn	0.00641	0.09950	0.01079	95
Ga	0.00005	0.00040	0.00009	95
As	0.00022	0.00260	0.00036	95
Se	0.00018	0.00100	0.00017	95
Br	0.00154	0.00500	0.00097	95
Rb	0.00016	0.00130	0.00020	95
Sr	0.00048	0.00270	0.00050	95

Yt	0.00005	0.00060	0.00008	95
Zr	0.00023	0.00180	0.00032	95
Mo	0.00012	0.00330	0.00035	95
Pd	0.00054	0.00290	0.00067	95
Ag	0.00038	0.00290	0.00067	95
Cd	0.00064	0.01950	0.00210	95
In	0.00064	0.00360	0.00089	95
Sn	0.00145	0.00690	0.00164	95
Sb	0.00134	0.00660	0.00164	95
Ba	0.00687	0.02400	0.00667	95
La	0.00292	0.01950	0.00469	95
Au	0.00009	0.00080	0.00018	95
Hg	0.00006	0.00040	0.00011	95
Tl	0.00008	0.00200	0.00022	95
Pb	0.00089	0.00690	0.00109	95
U	0.00009	0.00100	0.00015	95
SO_2	1.21173	10.43410	1.39658	90
Total Nitrate (HNO_3+NO_3^+)	0.59743	1.65900	0.37924	57
Denuded NO_3^-	0.18451	1.06870	0.17628	49
Volatilized NO_3^-	0.04770	0.24310	0.03854	94
Sum of Species	2.71472	9.11390	1.55614	95

Table 4.2.1b

Maximum and Average Six- and/or Twelve-Hour Concentrations ($\mu g/m^3$)

for $PM_{2.5}$ Mass and Major Chemical Constituents at the Gilpin Creek Site

between 02/16/95 and 10/29/95

Species	Average	Maximum	Std. Dev.	Total No. in Average
Mass	4.31739	14.84160	2.66618	47
b_{abs} (Mm^{-1})	4.89930	23.84787	7.98182	41
Cl^-	0.04914	1.56970	0.24259	42
NO_3^-	0.21888	0.43580	0.10010	42
$SO_4^=$	0.90165	1.87740	0.44388	42
K^+	0.03639	0.34820	0.06868	40
NH_4^+	0.25866	0.66380	0.15840	24
Total Ammonia (NH_3+NH_4^+)	0.00000	0.00000	0.00000	0
Denuded NH_4^+	0.00000	0.00000	0.00000	0
OC	1.19512	6.34810	1.55933	42
EC	0.96276	3.78950	0.80705	42
Backup OC	0.40688	2.51090	0.70146	44
Backup EC	0.39569	2.23920	0.59977	44

Na	0.02778	0.09950	0.02862	45
Mg	0.01607	0.08680	0.01876	45
Al	0.03122	0.20150	0.03969	45
Si	0.11197	0.68600	0.13275	45
P	0.00037	0.00450	0.00095	45
S	0.32539	0.75540	0.15496	45
Cl	0.00123	0.01800	0.00324	45
K	0.03349	0.11030	0.02838	45
Ca	0.03049	0.18540	0.03405	45
Ti	0.00195	0.02410	0.00483	45
V	0.00048	0.00330	0.00092	45
Cr	0.00090	0.01000	0.00212	45
Mn	0.00089	0.00700	0.00133	45
Fe	0.03040	0.18780	0.03622	45
Co	0.00023	0.00120	0.00034	45
Ni	0.00026	0.00240	0.00050	45
Cu	0.00065	0.00280	0.00070	45
Zn	0.00165	0.01070	0.00200	45
Ga	0.00027	0.00570	0.00087	45
As	0.00033	0.00210	0.00054	45
Se	0.00024	0.00100	0.00024	45
Br	0.00132	0.00560	0.00103	45
Rb	0.00013	0.00070	0.00017	45
Sr	0.00046	0.00270	0.00049	45
Yt	0.00015	0.00080	0.00021	45
Zr	0.00112	0.03550	0.00526	45
Mo	0.00036	0.00150	0.00049	45
Pd	0.00301	0.01110	0.00308	45
Ag	0.00170	0.00840	0.00238	45
Cd	0.00182	0.00930	0.00276	45
In	0.00316	0.01060	0.00341	45
Sn	0.00591	0.02270	0.00665	45
Sb	0.00566	0.01740	0.00565	45
Ba	0.02692	0.07410	0.02366	45
La	0.02039	0.08060	0.02535	45
Au	0.00040	0.00190	0.00063	45
Hg	0.00037	0.00170	0.00051	45
Tl	0.00025	0.00130	0.00036	45
Pb	0.00125	0.01050	0.00191	45
U	0.00024	0.00130	0.00035	45
SO_2	0.62695	2.32200	0.53375	46
Total Nitrate (HNO_3+NO_3^+)	0.00000	0.00000	0.00000	0
Denuded NO_3^-	0.00000	0.00000	0.00000	0
Volatilized NO_3^-	0.00000	0.00000	0.00000	0
Sum of Species	3.36565	9.08700	2.59966	50

Table 4.2.1c

Maximum and Average Six- and/or Twelve-Hour Concentrations ($\mu g/m^3$)
for $PM_{2.5}$ Mass and Major Chemical Constituents at the Juniper Mountain Site
between 02/16/95 and 10/29/95

Species	Average	Maximum	Std. Dev.	Total No. in Average
Mass	4.49806	12.80610	2.53299	47
b_{abs} (Mm^{-1})	2.88798	8.79618	2.18607	47
Cl^-	0.00565	0.11750	0.01868	45
NO_3^-	0.06508	0.16290	0.03589	45
$SO_4^=$	0.88045	1.75590	0.43821	45
K^+	0.02307	0.13010	0.02330	45
NH_4^+	0.29379	0.62480	0.17690	31
Total Ammonia (NH_3+NH_4^+)	0.48705	1.50460	0.26834	33
Denuded NH_4^+	0.29423	1.24800	0.23662	32
OC	1.27004	3.13630	0.77866	45
EC	0.42322	0.92750	0.21945	45
Backup OC	0.84690	3.79930	0.77763	45
Backup EC	0.24870	0.62900	0.18410	45
Na	0.01090	0.03590	0.00997	47
Mg	0.00850	0.03780	0.00880	47
Al	0.12730	1.61140	0.26300	47
Si	0.13471	0.83480	0.12482	47
P	0.00007	0.00120	0.00023	47
S	0.33671	0.66280	0.16151	47
Cl	0.00237	0.02430	0.00493	47
K	0.03493	0.12300	0.02621	47
Ca	0.03727	0.13320	0.02948	47
Ti	0.00199	0.01960	0.00311	47
V	0.00024	0.00110	0.00032	47
Cr	0.00046	0.00600	0.00099	47
Mn	0.00083	0.00430	0.00082	47
Fe	0.03602	0.20770	0.03340	47
Co	0.00006	0.00040	0.00009	47
Ni	0.00021	0.00190	0.00038	47
Cu	0.00205	0.01240	0.00242	47
Zn	0.02476	0.34120	0.05470	47
Ga	0.00003	0.00030	0.00007	47
As	0.00030	0.00210	0.00041	47
Se	0.00015	0.00050	0.00011	47
Br	0.00179	0.00410	0.00109	47
Rb	0.00011	0.00060	0.00011	47
Sr	0.00048	0.00290	0.00052	47

Yt	0.00006	0.00040	0.00008	47
Zr	0.00016	0.00070	0.00014	47
Mo	0.00010	0.00050	0.00013	47
Pd	0.00055	0.00240	0.00066	47
Ag	0.00016	0.00130	0.00031	47
Cd	0.00040	0.00220	0.00064	47
In	0.00070	0.00370	0.00092	47
Sn	0.00181	0.00900	0.00201	47
Sb	0.00207	0.00730	0.00189	47
Ba	0.00593	0.02140	0.00641	47
La	0.00540	0.04090	0.00857	47
Au	0.00009	0.00120	0.00022	47
Hg	0.00010	0.00040	0.00013	47
Tl	0.00004	0.00030	0.00007	47
Pb	0.00098	0.00500	0.00096	47
U	0.00007	0.00030	0.00009	47
SO_2	0.43146	3.14260	0.49617	47
Total Nitrate (HNO_3+NO_3^+)	0.86043	2.56740	0.52146	26
Denuded NO_3^-	0.16202	1.01810	0.19528	29
Volatilized NO_3^-	0.04914	0.22310	0.03698	46
Sum of Species	2.56426	6.24400	1.84731	58

Table 4.2.1f

Maximum and Average Six- and/or Twelve-Hour Concentrations ($\mu g/m^3$)

for $PM_{2.5}$ Mass and Major Chemical Constituents at the Hayden Waste Water Site between 02/16/95 and 10/29/95

Species	Average	Maximum	Std. Dev.	Total No. in Average
Mass	5.39501	15.46500	2.57460	66
b_{abs} (Mm^{-1})	4.26912	14.73817	3.31286	55
Cl^-	0.01792	0.41550	0.05207	66
NO_3^-	0.24583	2.28100	0.45127	66
$SO_4^=$	1.07634	4.53790	0.60427	66
K^+	0.01970	0.07580	0.01705	66
NH_4^+	0.35115	1.37480	0.23870	43
Total Ammonia (NH_3+NH_4^+)	0.00000	0.00000	0.00000	0
Denuded NH_4^+	0.00000	0.00000	0.00000	0
OC	1.68601	4.16320	0.97143	66
EC	0.47893	1.49410	0.26897	66
Backup OC	1.12226	7.43730	1.27564	67
Backup EC	0.22898	4.41880	0.65717	67

Na	0.04215	0.18240	0.04321	66
Mg	0.01342	0.05310	0.01301	66
Al	0.10145	0.57180	0.09108	66
Si	0.15827	0.71770	0.12327	66
P	0.00043	0.00300	0.00076	66
S	0.40579	1.32470	0.19650	66
Cl	0.00129	0.03070	0.00444	66
K	0.03549	0.13550	0.02697	66
Ca	0.03690	0.14820	0.02853	66
Ti	0.00382	0.02260	0.00392	66
V	0.00065	0.00250	0.00059	66
Cr	0.00032	0.00240	0.00047	66
Mn	0.00099	0.00390	0.00067	66
Fe	0.05455	0.26350	0.04514	66
Co	0.00007	0.00040	0.00012	66
Ni	0.00048	0.00650	0.00092	66
Cu	0.00267	0.01960	0.00297	66
Zn	0.01005	0.08360	0.01522	66
Ga	0.00021	0.00120	0.00032	66
As	0.00034	0.00250	0.00045	66
Se	0.00080	0.00500	0.00086	66
Br	0.00846	0.44030	0.05357	66
Rb	0.00014	0.00060	0.00016	66
Sr	0.00096	0.01720	0.00214	66
Yt	0.00010	0.00070	0.00014	66
Zr	0.00042	0.00450	0.00072	66
Mo	0.00010	0.00070	0.00017	66
Pd	0.00089	0.00590	0.00143	66
Ag	0.00109	0.00630	0.00154	66
Cd	0.00057	0.00700	0.00106	66
In	0.00151	0.01210	0.00229	66
Sn	0.00233	0.01950	0.00348	66
Sb	0.00103	0.00810	0.00180	66
Ba	0.00565	0.03370	0.00885	66
La	0.00595	0.03720	0.01022	66
Au	0.00026	0.00180	0.00041	66
Hg	0.00009	0.00080	0.00017	66
Tl	0.00008	0.00070	0.00017	66
Pb	0.00152	0.04910	0.00596	66
U	0.00018	0.00110	0.00027	66
SO_2	9.27529	71.79830	14.50151	71
Total Nitrate (HNO_3+NO_3^+)	0.00000	0.00000	0.00000	0
Denuded NO_3^-	0.00000	0.00000	0.00000	0
Volatilized NO_3^-	0.12214	0.69390	0.14093	66
Sum of Species	3.86058	8.92120	2.04227	72

Water sites. Maximum sulfate concentrations were two to four times higher than their averages, ranging from 1.9 $\mu g/m^3$ at the Gilpin Creek and Baggs sites to 4.3 $\mu g/m^3$ at the Hayden VOR site or 4.5 $\mu g/m^3$ at the Hayden Waste Water site.

Nitrate concentrations were 10% to 25% of the corresponding sulfate abundance at each site. Average nitrate concentrations were 0.25 ± 0.45 $\mu g/m^3$ at the Hayden Waste Water site, 0.22 ± 0.10 $\mu g/m^3$ at the Gilpin Creek site, and between 0.07 to 0.10 $\mu g/m^3$ at the remaining sites. A maximum nitrate concentration of 2.3 $\mu g/m^3$ was found at the Hayden Waste Water site during the morning of 02/26/95, which is 4 to 14 higher than the maximum nitrate concentrations measured at the other sites.

Average ammonium concentrations were also similar among all sites, ranging from 0.24 ± 0.12 $\mu g/m^3$ at the Baggs site to 0.49 ± 0.38 $\mu g/m^3$ at the Hayden VOR site. Major crustal components such as aluminum (Al), silicon (Si), potassium (K), calcium (Ca), and iron (Fe) were low most of the time, on the order of one-tenth to one-hundredth of 1 $\mu g/m^3$.

Observations drawn from examination of the individual chemical compositions and time series plots in Appendix E are as follows:

- Total carbon aerosol constituted over 50% of the $PM_{2.5}$ mass during the warmer months (May through August) and constituted only 20% to 30% of $PM_{2.5}$ during the cooler months (February, March, September, October). Organic carbon (OC) was the major component of total carbon (TC) in all samples, with OC/TC ratios in the range of 0.6 to 0.8. Organic carbon concentrations varied by threefold from the colder to warmer seasons, being highest during August and lowest during February and October.

- $PM_{2.5}$ ammonium nitrate concentrations were a small fraction of $PM_{2.5}$ for nearly all samples, in the range of 1% to 5% of $PM_{2.5}$.

- The abundance of crustal components varied significantly and accounted for 5% to 30% of the $PM_{2.5}$ mass depending on location and sampling period.

- High carbon concentrations were measured sporadically at different sites. The maximum organic carbon concentration for the entire study period was found at the Gilpin Creek site on 06/29/95 (6.3 ± 1.6 $\mu g/m^3$), while concurrent measurements at the other sites were below 1.5 $\mu g/m^3$. The maximum elemental carbon of 3.8 ± 2.1 $\mu g/m^3$ was found at the Gilpin Creek site on 09/02/95, which was three times the maxima observed at the other sites. Juniper Mountain also reported its maximum elemental carbon (0.93 ± 0.15 $\mu g/m^3$) during the morning of 09/02/95, with less than 1 $\mu g/m^3$ of elemental carbon at the other sites. The maximum organic carbon concentration of 3.0 ± 0.65 $\mu g/m^3$ at the Buffalo Pass site (reported on the morning of 10/12/95) was twice that of corresponding measurements at the other sites. Concurrent elemental carbon concentrations were also elevated (> 1 $\mu g/m^3$) at Buffalo Pass and Gilpin Creek.

- Elemental carbon was higher at the Gilpin Creek site than at the other sites, with concentrations exceeding 1 $\mu g/m^3$ on over 40% of the samples. Since elemental

carbon has a high extinction efficiency, these high concentrations would have a significant impact on light extinction.

4.3 Light Extinction by Chemical Components

Tables 4.3.1–4.3.6 present all six- and/or twelve-hour averaged measured and calculated values for the various components of light extinction during episodes. Table 4.3.7 summarizes the frequency with which each chemical component contributed extinction, while Table 4.3.8 presents the maximum and average contributions to extinction. As with the $PM_{2.5}$ mass and chemical data, averages are biased towards sampling periods with elevated light extinction and will not be representative of averages found in a random selection of samples or in a long-term sampling network.

Table 4.3.7 shows that organics are the largest chemical contributor to light extinction at five out of the six sites most of the time. At Gilpin Creek, elemental carbon was often a the major contributor to extinction, with organics being the second highest contributor. Elemental carbon was the second largest chemical contributor to light extinction at four of the remaining five sites. At Buffalo Pass, however, ammonium sulfate was the second largest contributor to extinction instead of the third as occurred at the other five sites. Soils and ammonium nitrates were the least important chemical contributors to light extinction.

Even though the major chemical components were elevated during certain periods, the total light extinction was not necessarily elevated. For example, the concentrations of major chemical components were elevated at all sites during the period between 08/07/95 and 08/09/95, but the light extinction was not elevated.

Since ammonium sulfate concentrations were similar throughout the network during a given period, the light extinction due to ammonium sulfate might be expected to be fairly constant across the network during a measurement period. However, Tables 4.3.1 through 4.3.8 show that the contribution of ammonium sulfate to total light extinction was more pronounced at the Buffalo Pass site. Of the 27 cases where ammonium sulfate accounted for more than 25% of the total light extinction, 55.6% were at the Buffalo Pass site, 3.7% were at the Juniper Mountain site, 14.8% were at the Hayden VOR site, 11.1% were at the Hayden Waste Water site, 11.1% were at the Gilpin Creek site, and 3.7% were at the Baggs site.

These situations were found during the four episode periods of 03/26/95 to 03/31/95, 08/21/95 to 08/27/95, 09/17/95 to 09/21/95, and 09/30/95 to 10/02/95. This demonstrates that the relative proportion of light extinction due to a chemical component to the total light extinction is more important than the absolute concentration of the component. Therefore, an increment of a light scattering or absorbing component added to the overall aerosol loading

Table 4.3.1
Measured and Calculated Component Contributions to Total Light Extinction at Buffalo Pass

Site	Date	Hr	RH	Cln Air	bsp	Ebsp	babs	Ebabs	bext	Ebext	Esul	Enit	Eoc	Eec	Esoil	Unid.
B. Pass	2/23	6	69	8.4	3.2 ± 1.0	2.8 ± 1.4	1.4 ± 1.2	3.3 ± 0.9	13.1 ± 1.7	14.4 ± 1.6	1.5 ± 0.1	1.1 ± 0.1	0.0 ± 1.4	3.3 ± 0.9	0.2 ± 0.0	-1.3 ± 2.4
B. Pass	2/23	12	61	8.4	2.7 ± 0.3	2.6 ± 1.3	2.9 ± 1.3	2.5 ± 0.8	14.1 ± 1.6	13.6 ± 1.5	1.7 ± 0.1	0.5 ± 0.1	0.3 ± 1.3	2.5 ± 0.8	0.2 ± 0.0	0.5 ± 2.2
B. Pass	3/26	6	87	8.4	61.8 ± 27.1	9.1 ± 1.1	2.4 ± 0.7	1.1 ± 0.5	72.6 ± 11.9	18.7 ± 1.2	6.4 ± 0.3	0.7 ± 0.1	1.7 ± 1.1	1.1 ± 0.5	0.3 ± 0.0	53.9 ± 11.9
B. Pass	3/27	6	86	8.4	34.7 ± 7.1	15.5 ± 1.2	3.2 ± 0.7	2.1 ± 0.8	46.2 ± 4.8	26.0 ± 1.4	12.1 ± 0.6	1.1 ± 0.1	2.0 ± 1.0	2.1 ± 0.8	0.3 ± 0.0	20.2 ± 5.0
B. Pass	3/28	6	86	8.4	16.9 ± 2.0	18.1 ± 1.3	2.4 ± 0.7	1.9 ± 0.8	27.8 ± 2.9	28.4 ± 1.5	12.1 ± 0.6	1.9 ± 0.2	3.8 ± 1.1	1.9 ± 0.8	0.3 ± 0.0	-0.7 ± 3.2
B. Pass	3/29	6	88	8.4	38.2 ± 4.3	21.8 ± 1.4	--- ± ---	1.0 ± 0.5	--- ± ---	31.1 ± 1.5	14.8 ± 0.8	6.6 ± 0.4	0.0 ± 1.2	1.0 ± 0.5	0.3 ± 0.0	--- ± ---
B. Pass	3/30	6	85	8.4	33.0 ± 4.7	17.7 ± 1.3	4.7 ± 0.7	0.8 ± 0.5	46.1 ± 4.5	27.0 ± 1.4	16.0 ± 0.9	0.8 ± 0.1	0.4 ± 0.9	0.8 ± 0.5	0.5 ± 0.0	19.2 ± 4.7
B. Pass	3/31	6	82	8.4	19.8 ± 1.0	15.4 ± 1.1	4.9 ± 0.7	0.7 ± 0.4	33.1 ± 2.9	24.5 ± 1.2	11.1 ± 0.6	1.5 ± 0.1	1.8 ± 0.9	0.7 ± 0.4	1.0 ± 0.0	8.6 ± 3.1
B. Pass	5/6	6	72	8.4	28.7 ± 11.4	9.9 ± 0.8	4.7 ± 0.7	1.2 ± 0.5	41.8 ± 10.4	19.5 ± 1.0	3.4 ± 0.2	0.6 ± 0.1	3.1 ± 0.8	1.2 ± 0.5	2.8 ± 0.1	22.3 ± 10.5
B. Pass	5/7	6	85	8.4	196.9 ± 97.4	14.2 ± 1.1	4.0 ± 0.7	1.3 ± 0.6	209.4 ± 75.0	23.9 ± 1.2	7.3 ± 0.4	1.5 ± 0.1	2.3 ± 1.0	1.3 ± 0.6	3.0 ± 0.1	185.4 ± 75.0
B. Pass	6/14	6	28	8.4	18.2 ± 0.5	13.9 ± 1.2	9.5 ± 0.8	0.6 ± 0.4	36.1 ± 5.3	22.9 ± 1.3	2.5 ± 0.1	0.5 ± 0.0	9.8 ± 1.2	0.6 ± 0.4	1.1 ± 0.0	13.2 ± 5.5
B. Pass	6/15	6	54	8.4	14.8 ± 1.0	11.6 ± 0.9	8.0 ± 0.8	1.3 ± 0.6	31.2 ± 4.6	21.4 ± 1.0	6.4 ± 0.3	0.3 ± 0.1	4.3 ± 0.8	1.3 ± 0.6	0.7 ± 0.0	9.8 ± 4.7
B. Pass	6/16	6	38	8.4	12.0 ± 0.6	7.3 ± 0.7	7.3 ± 0.9	5.4 ± 1.9	27.7 ± 3.9	21.1 ± 2.0	3.2 ± 0.2	0.4 ± 0.0	2.6 ± 0.6	5.4 ± 1.9	0.9 ± 0.0	6.6 ± 4.4
B. Pass	6/29	6	99	8.4	1227.0 ± 422.4	86.4 ± 10.8	3.8 ± 0.7	0.0 ± 0.3	1239.3 ± 364.0	94.8 ± 10.8	38.1 ± 2.3	5.1 ± 1.4	42.2 ± 10.4	0.0 ± 0.3	0.9 ± 0.1	1144.5 ± 364.1
B. Pass	6/30	6	75	8.4	14.5 ± 1.1	12.6 ± 1.2	6.3 ± 0.8	1.4 ± 0.6	29.3 ± 4.6	22.4 ± 1.4	4.2 ± 0.2	0.4 ± 0.1	7.6 ± 1.2	1.4 ± 0.6	0.3 ± 0.0	6.9 ± 4.8
B. Pass	7/1	6	76	8.4	14.0 ± 1.2	9.0 ± 1.1	3.9 ± 0.7	1.7 ± 0.5	26.3 ± 4.5	19.1 ± 1.2	3.0 ± 0.2	0.5 ± 0.1	5.2 ± 1.1	1.7 ± 0.5	0.3 ± 0.0	7.2 ± 4.6
B. Pass	7/29	6	24	8.4	11.4 ± 1.6	9.7 ± 0.9	3.1 ± 0.7	3.6 ± 0.7	23.0 ± 4.0	21.7 ± 1.2	1.8 ± 0.1	0.2 ± 0.0	6.8 ± 0.9	3.6 ± 0.7	0.8 ± 0.0	1.3 ± 4.2
B. Pass	7/30	6	38	8.4	13.7 ± 0.7	8.8 ± 0.8	3.8 ± 0.7	2.6 ± 0.6	26.0 ± 4.3	19.8 ± 1.0	2.8 ± 0.1	0.2 ± 0.0	4.9 ± 0.8	2.6 ± 0.6	0.8 ± 0.0	6.2 ± 4.4
B. Pass	7/31	6	---	8.4	--- ± ---	--- ± ---	--- ± ---	--- ± ---	--- ± ---	--- ± ---	--- ± ---	--- ± ---	--- ± ---	--- ± ---	--- ± ---	--- ± ---
B. Pass	8/7	6	36	8.4	--- ± ---	14.2 ± 1.6	6.6 ± 1.5	6.3 ± 2.3	51.6 ± 9.1	28.9 ± 2.8	3.0 ± 0.2	0.4 ± 0.1	9.5 ± 1.6	6.3 ± 2.3	1.3 ± 0.0	22.7 ± 9.6
B. Pass	8/7	12	35	8.4	16.4 ± 1.8	9.2 ± 1.2	4.7 ± 1.4	5.5 ± 2.1	29.6 ± 5.1	23.2 ± 2.4	2.9 ± 0.2	0.2 ± 0.1	4.9 ± 1.2	5.5 ± 2.1	1.2 ± 0.0	6.4 ± 5.6
B. Pass	8/8	6	48	8.4	17.4 ± 2.4	15.5 ± 1.6	6.3 ± 1.4	0.0 ± 0.7	32.1 ± 4.9	23.9 ± 1.7	4.4 ± 0.2	0.2 ± 0.1	9.0 ± 1.6	0.0 ± 0.7	1.9 ± 0.1	8.2 ± 5.2
B. Pass	8/8	12	46	8.4	21.9 ± 2.2	12.9 ± 1.3	6.2 ± 1.4	6.7 ± 2.4	36.5 ± 5.9	28.0 ± 2.7	4.4 ± 0.2	0.5 ± 0.1	5.6 ± 1.3	6.7 ± 2.4	2.3 ± 0.1	8.5 ± 6.5
B. Pass	8/9	6	31	8.4	9.1 ± 0.8	12.7 ± 1.4	3.1 ± 1.4	0.1 ± 0.7	20.6 ± 3.6	21.2 ± 1.5	1.1 ± 0.1	0.6 ± 0.1	7.3 ± 1.4	0.1 ± 0.7	3.8 ± 0.1	-0.6 ± 3.9
B. Pass	8/9	12	28	8.4	7.9 ± 0.9	15.1 ± 1.6	5.1 ± 1.5	1.3 ± 0.9	21.4 ± 3.4	24.9 ± 1.8	2.2 ± 0.1	0.5 ± 0.1	9.4 ± 1.6	1.3 ± 0.9	3.0 ± 0.1	-3.4 ± 3.9
B. Pass	8/14	6	56	8.4	7.2 ± 0.9	8.4 ± 1.5	1.6 ± 1.4	2.9 ± 0.9	17.2 ± 3.3	19.7 ± 1.7	1.7 ± 0.1	0.5 ± 0.1	5.2 ± 1.5	2.9 ± 0.9	1.1 ± 0.0	-2.5 ± 3.8
B. Pass	8/14	12	62	8.4	3.9 ± 0.9	7.4 ± 1.6	0.0 ± 1.4	2.1 ± 0.8	12.3 ± 2.6	17.9 ± 1.8	1.4 ± 0.1	0.4 ± 0.1	5.1 ± 1.6	2.1 ± 0.8	0.5 ± 0.0	-5.6 ± 3.1
B. Pass	8/21	6	85	8.4	18.1 ± 0.8	28.3 ± 2.8	1.4 ± 1.3	0.0 ± 0.7	27.9 ± 5.2	36.7 ± 2.9	12.3 ± 0.7	1.0 ± 0.3	13.6 ± 2.7	0.0 ± 0.7	1.4 ± 0.0	-8.8 ± 5.9
B. Pass	8/21	12	68	8.4	18.1 ± 2.2	17.2 ± 1.7	2.8 ± 1.2	1.5 ± 0.9	29.3 ± 5.4	27.2 ± 1.9	7.9 ± 0.4	0.4 ± 0.1	7.7 ± 1.6	1.5 ± 0.9	1.2 ± 0.0	2.2 ± 5.7
B. Pass	8/22	6	86	8.4	11.2 ± 1.3	14.7 ± 2.1	1.4 ± 1.2	2.5 ± 1.1	21.0 ± 4.1	25.6 ± 2.4	7.9 ± 0.4	1.0 ± 0.2	5.6 ± 2.1	2.5 ± 1.1	0.2 ± 0.0	-4.5 ± 4.7

B. Pass	8/22	12	71	8.4	11.6 ± 0.7	19.0 ± 2.1	2.5 ± 1.1	2.9 ± 1.3	22.5 ± 4.0	30.3 ± 2.5	4.7 ± 0.3	0.4 ± 0.1	13.1 ± 2.1	2.9 ± 1.3	0.8 ± 0.0	-7.8 ± 4.7
B. Pass	8/23	6	83	8.4	9.9 ± 1.4	10.6 ± 1.8	1.4 ± 1.2	3.1 ± 1.3	19.7 ± 3.8	22.2 ± 2.3	6.5 ± 0.4	0.6 ± 0.2	2.7 ± 1.8	3.1 ± 1.3	0.8 ± 0.0	-2.5 ± 4.4
B. Pass	8/23	12	86	8.4	25.2 ± 7.9	27.5 ± 2.7	3.1 ± 1.4	1.6 ± 1.0	36.7 ± 7.5	37.5 ± 2.9	12.2 ± 0.7	0.8 ± 0.3	10.0 ± 2.6	1.6 ± 1.0	4.5 ± 0.1	-0.8 ± 8.0
B. Pass	8/24	6	94	8.4	19.7 ± 1.6	93.6 ± 6.3	4.7 ± 1.4	3.3 ± 1.4	32.8 ± 5.6	105.4 ± 6.4	27.4 ± 1.4	3.5 ± 0.5	39.5 ± 6.0	3.3 ± 1.4	23.3 ± 0.7	-72.6 ± 8.5
B. Pass	8/24	12	76	8.4	16.9 ± 1.4	18.2 ± 1.7	3.1 ± 1.3	4.9 ± 1.9	28.4 ± 5.2	31.4 ± 2.5	11.1 ± 0.6	0.4 ± 0.2	5.7 ± 1.6	4.9 ± 1.9	1.0 ± 0.0	-3.1 ± 5.8
B. Pass	8/25	6	72	8.4	6.4 ± 0.4	10.7 ± 1.6	0.0 ± 1.4	3.9 ± 1.6	14.8 ± 3.3	23.0 ± 2.3	3.0 ± 0.2	0.6 ± 0.1	6.5 ± 1.6	3.9 ± 1.6	0.6 ± 0.0	-8.2 ± 4.0
B. Pass	8/25	12	50	8.4	6.7 ± 0.3	11.5 ± 1.4	1.5 ± 1.3	2.5 ± 1.2	16.7 ± 3.3	22.4 ± 1.8	2.9 ± 0.2	0.8 ± 0.1	6.9 ± 1.4	2.5 ± 1.2	1.0 ± 0.0	-5.7 ± 3.8
B. Pass	8/26	6	46	8.4	5.7 ± 0.6	14.9 ± 1.7	1.6 ± 1.4	2.9 ± 0.9	15.7 ± 3.0	26.2 ± 1.9	3.1 ± 0.2	0.6 ± 0.1	10.0 ± 1.7	2.9 ± 0.9	1.2 ± 0.0	-10.4 ± 3.6
B. Pass	8/26	12	37	8.4	6.6 ± 0.5	12.9 ± 1.5	3.2 ± 1.4	1.4 ± 0.7	18.2 ± 3.3	22.7 ± 1.7	2.3 ± 0.1	0.4 ± 0.1	6.6 ± 1.5	1.4 ± 0.7	3.5 ± 0.1	-4.5 ± 3.7
B. Pass	8/27	6	55	8.4	9.4 ± 0.6	13.8 ± 1.6	4.7 ± 1.4	2.0 ± 0.8	22.5 ± 3.8	24.3 ± 1.8	3.5 ± 0.2	0.9 ± 0.1	7.0 ± 1.6	2.0 ± 0.8	2.4 ± 0.1	-1.8 ± 4.2
B. Pass	8/27	12	55	8.4	9.4 ± 1.0	15.3 ± 1.8	1.6 ± 1.4	1.1 ± 0.7	19.5 ± 3.7	24.8 ± 1.9	2.8 ± 0.2	0.7 ± 0.1	9.7 ± 1.8	1.1 ± 0.7	2.1 ± 0.1	-5.4 ± 4.1
B. Pass	9/2	6	53	8.4	13.7 ± 0.4	11.1 ± 1.4	3.1 ± 1.4	4.3 ± 1.0	25.3 ± 4.2	23.8 ± 1.7	5.2 ± 0.3	0.4 ± 0.1	4.4 ± 1.4	4.3 ± 1.0	1.1 ± 0.0	1.5 ± 4.6
B. Pass	9/2	12	43	8.4	15.2 ± 1.1	9.7 ± 1.3	3.2 ± 1.4	5.5 ± 1.2	26.9 ± 4.7	23.7 ± 1.8	5.4 ± 0.3	0.3 ± 0.1	2.1 ± 1.3	5.5 ± 1.2	1.9 ± 0.1	3.3 ± 5.1
B. Pass	9/17	6	40	8.4	6.2 ± 0.3	6.4 ± 1.5	1.6 ± 1.4	1.6 ± 0.9	16.3 ± 3.3	16.4 ± 1.8	2.3 ± 0.1	0.4 ± 0.1	3.1 ± 1.5	1.6 ± 0.9	0.7 ± 0.0	-0.2 ± 3.8
B. Pass	9/17	12	41	8.4	7.2 ± 0.7	7.9 ± 1.3	0.0 ± 1.4	0.4 ± 0.6	15.7 ± 3.5	16.8 ± 1.5	3.0 ± 0.2	0.3 ± 0.1	4.1 ± 1.3	0.4 ± 0.6	0.5 ± 0.0	-1.1 ± 3.8
B. Pass	9/18	6	99	8.4	789.1 ± 500.1	102.2 ± 21.4	0.0 ± 1.4	0.6 ± 0.7	797.5 ± 277.9	111.2 ± 21.4	57.5 ± 3.8	6.6 ± 2.8	36.4 ± 20.9	0.6 ± 0.7	1.6 ± 0.1	686.3 ± 278.7
B. Pass	9/18	12	96	8.4	851.2 ± 491.6	40.0 ± 5.7	1.6 ± 1.4	0.9 ± 0.7	861.3 ± 281.2	49.3 ± 5.8	28.4 ± 1.6	3.9 ± 0.7	7.0 ± 5.5	0.9 ± 0.7	0.6 ± 0.0	812.0 ± 281.2
B. Pass	9/19	6	92	8.4	98.2 ± 86.8	11.0 ± 3.7	0.0 ± 1.5	1.1 ± 0.7	106.6 ± 38.4	20.6 ± 3.7	4.4 ± 0.4	1.0 ± 0.4	5.2 ± 3.6	1.1 ± 0.7	0.5 ± 0.0	86.0 ± 38.6
B. Pass	9/19	12	75	8.4	12.4 ± 1.5	11.8 ± 1.9	1.6 ± 1.4	2.2 ± 0.8	22.4 ± 4.4	22.4 ± 2.0	4.4 ± 0.3	0.6 ± 0.2	6.4 ± 1.8	2.2 ± 0.8	0.4 ± 0.0	0.0 ± 4.9
B. Pass	9/20	6	100	8.4	1960.7 ± 608.2	242.8 ± 45.6	0.0 ± 1.4	3.1 ± 0.9	1969.2 ± 469.2	254.4 ± 45.6	53.0 ± 5.6	26.0 ± 5.7	161.4 ± 44.9	3.1 ± 0.9	2.4 ± 0.3	1714.8 ± 471.4
B. Pass	9/20	12	99	8.4	740.2 ± 354.8	156.8 ± 29.6	3.2 ± 1.4	0.8 ± 0.7	751.8 ± 217.8	166.0 ± 29.6	90.1 ± 5.7	16.3 ± 4.0	48.8 ± 28.7	0.8 ± 0.7	1.5 ± 0.1	585.8 ± 219.8
B. Pass	9/21	6	90	8.4	31.6 ± 9.0	13.3 ± 2.7	0.0 ± 1.4	1.2 ± 0.7	40.0 ± 8.7	22.9 ± 2.8	12.2 ± 0.7	0.5 ± 0.3	0.3 ± 2.6	1.2 ± 0.7	0.4 ± 0.0	17.1 ± 9.2
B. Pass	9/21	12	82	8.4	7.7 ± 1.1	6.5 ± 1.0	0.0 ± 0.7	0.4 ± 0.3	16.1 ± 3.2	15.3 ± 1.1	4.3 ± 0.2	0.3 ± 0.1	1.5 ± 1.0	0.4 ± 0.3	0.3 ± 0.0	0.7 ± 3.4
B. Pass	9/24	6	94	8.4	669.9 ± 194.9	29.0 ± 5.7	1.6 ± 1.4	0.6 ± 0.8	679.9 ± 157.5	37.9 ± 5.8	14.4 ± 0.8	0.8 ± 0.5	13.3 ± 5.6	0.6 ± 0.8	0.4 ± 0.0	642.0 ± 157.6
B. Pass	9/24	12	57	8.4	7.2 ± 0.8	4.6 ± 1.6	0.0 ± 1.4	1.8 ± 1.1	15.7 ± 3.5	14.9 ± 2.0	2.7 ± 0.2	0.3 ± 0.1	1.4 ± 1.6	1.8 ± 1.1	0.2 ± 0.0	0.8 ± 4.0
B. Pass	9/27	6	62	8.4	8.4 ± 0.7	6.2 ± 1.5	3.3 ± 1.4	3.0 ± 0.9	20.1 ± 3.5	17.5 ± 1.7	3.5 ± 0.2	0.4 ± 0.1	1.6 ± 1.4	3.0 ± 0.9	0.6 ± 0.0	2.6 ± 3.9
B. Pass	9/27	12	42	8.4	8.7 ± 0.5	6.1 ± 1.3	3.2 ± 1.4	0.5 ± 0.7	20.4 ± 3.5	15.0 ± 1.5	3.2 ± 0.2	0.3 ± 0.1	2.1 ± 1.3	0.5 ± 0.7	0.5 ± 0.0	5.4 ± 3.8
B. Pass	9/30	6	95	8.4	812.2 ± 184.5	7.4 ± 6.2	0.0 ± 1.3	1.0 ± 0.9	820.7 ± 178.1	16.8 ± 6.3	3.2 ± 0.6	2.5 ± 0.7	0.8 ± 6.1	1.0 ± 0.9	0.9 ± 0.0	803.8 ± 178.2
B. Pass	9/30	12	96	8.4	1608.9 ± 265.6	49.5 ± 7.4	1.5 ± 1.3	5.9 ± 2.5	1618.9 ± 331.1	63.8 ± 7.8	32.9 ± 1.8	4.9 ± 0.7	10.5 ± 7.1	5.9 ± 2.5	1.1 ± 0.0	1555.1 ± 331.2
B. Pass	10/1	6	95	8.4	758.4 ± 329.9	33.7 ± 6.8	3.4 ± 1.5	2.5 ± 1.4	770.2 ± 211.7	44.6 ± 7.0	18.8 ± 1.1	4.3 ± 0.7	8.2 ± 6.7	2.5 ± 1.4	2.4 ± 0.1	725.7 ± 211.9
B. Pass	10/1	12	87	8.4	6.9 ± 1.3	15.7 ± 3.2	1.6 ± 1.4	0.7 ± 0.8	16.9 ± 3.2	24.8 ± 3.3	5.6 ± 0.4	3.1 ± 0.3	5.4 ± 3.1	0.7 ± 0.8	1.5 ± 0.0	-7.9 ± 4.6
B. Pass	10/2	6	91	8.4	49.2 ± 14.5	21.2 ± 3.1	1.6 ± 1.4	0.5 ± 0.7	59.2 ± 12.8	30.2 ± 3.2	7.6 ± 0.5	7.3 ± 0.5	5.1 ± 3.1	0.5 ± 0.7	1.2 ± 0.0	29.1 ± 13.2
B. Pass	10/2	12	65	8.4	2.7 ± 0.6	5.6 ± 1.5	0.0 ± 1.4	1.4 ± 0.8	11.2 ± 2.6	15.5 ± 1.7	1.8 ± 0.1	0.8 ± 0.1	2.1 ± 1.5	1.4 ± 0.8	0.9 ± 0.0	-4.3 ± 3.1
B. Pass	10/7	6	42	8.4	3.1 ± 0.2	7.1 ± 1.6	1.7 ± 1.5	5.2 ± 2.2	13.2 ± 2.5	20.8 ± 2.8	1.5 ± 0.1	0.3 ± 0.1	3.1 ± 1.6	5.2 ± 2.2	2.3 ± 0.1	-7.6 ± 3.7
B. Pass	10/7	12	43	8.4	3.9 ± 0.2	2.5 ± 1.3	1.6 ± 1.4	0.1 ± 0.7	13.9 ± 2.4	11.1 ± 1.4	1.6 ± 0.1	0.2 ± 0.1	0.0 ± 1.3	0.1 ± 0.7	0.7 ± 0.0	2.8 ± 2.8
B. Pass	10/8	6	88	8.4	42.9 ± 10.4	19.4 ± 3.5	0.0 ± 1.4	1.5 ± 1.0	51.3 ± 10.8	29.3 ± 3.7	6.3 ± 0.4	2.7 ± 0.3	9.5 ± 3.5	1.5 ± 1.0	0.9 ± 0.0	22.0 ± 11.4
B. Pass	10/8	12	39	8.4	4.9 ± 0.9	3.2 ± 1.4	0.0 ± 1.4	0.1 ± 0.7	13.3 ± 2.7	11.7 ± 1.6	1.7 ± 0.1	0.2 ± 0.1	0.8 ± 1.4	0.1 ± 0.7	0.5 ± 0.0	1.6 ± 3.2
B. Pass	10/9	6	50	8.4	4.7 ± 0.4	4.8 ± 1.6	0.0 ± 1.4	1.6 ± 1.0	13.2 ± 2.9	14.8 ± 1.9	1.3 ± 0.1	0.2 ± 0.1	2.7 ± 1.6	1.6 ± 1.0	0.5 ± 0.0	-1.6 ± 3.5
B. Pass	10/9	12	41	8.4	5.4 ± 0.4	4.8 ± 1.6	0.0 ± 1.5	2.8 ± 1.4	13.8 ± 3.1	16.0 ± 2.2	1.2 ± 0.1	0.4 ± 0.1	2.3 ± 1.6	2.8 ± 1.4	0.8 ± 0.0	-2.1 ± 3.8
B. Pass	10/10	6	50	8.4	8.1 ± 0.7	3.4 ± 1.2	1.6 ± 1.4	1.4 ± 0.7	18.1 ± 3.5	13.3 ± 1.4	1.5 ± 0.1	0.5 ± 0.1	0.8 ± 1.2	1.4 ± 0.7	0.7 ± 0.0	4.9 ± 3.8
B. Pass	10/10	12	40	8.4	4.6 ± 0.3	3.9 ± 1.2	1.6 ± 1.4	2.6 ± 0.8	14.6 ± 2.8	14.9 ± 1.4	1.5 ± 0.1	0.4 ± 0.1	1.5 ± 1.2	2.6 ± 0.8	0.5 ± 0.0	-0.3 ± 3.1
B. Pass	10/11	6	35	8.4	2.7 ± 0.4	4.3 ± 1.5	0.0 ± 1.4	2.6 ± 1.3	11.2 ± 2.4	15.4 ± 2.0	0.7 ± 0.1	0.2 ± 0.1	3.1 ± 1.5	2.6 ± 1.3	0.5 ± 0.0	-4.2 ± 3.1
B. Pass	10/11	12	30	8.4	2.9 ± 0.3	8.4 ± 1.6	3.5 ± 1.6	3.7 ± 1.7	14.9 ± 2.5	20.6 ± 2.3	1.0 ± 0.1	0.3 ± 0.1	5.0 ± 1.6	3.7 ± 1.7	2.1 ± 0.1	-5.7 ± 3.4

B. Pass	10/12	6	57	8.4	56.2 ± 37.3	22.9 ± 2.8	--- ± ---	9.3 ± 3.7	--- ± ---	40.5 ± 4.6	5.9 ± 0.3	0.7 ± 0.1	12.8 ± 2.7	9.3 ± 3.7	3.5 ± 0.1	--- ± ---
B. Pass	10/12	12	92	8.4	260.1 ± 167.7	35.2 ± 4.8	3.3 ± 1.5	8.7 ± 3.4	271.8 ± 93.2	52.3 ± 5.8	16.2 ± 0.9	0.9 ± 0.3	17.5 ± 4.7	8.7 ± 3.4	0.6 ± 0.0	219.6 ± 93.4
B. Pass	10/13	6	77	8.4	2.2 ± 0.5	7.2 ± 2.5	0.0 ± 1.4	3.3 ± 1.6	10.7 ± 2.5	19.0 ± 3.0	1.5 ± 0.2	0.7 ± 0.2	4.4 ± 2.5	3.3 ± 1.6	0.6 ± 0.0	-8.3 ± 3.9
B. Pass	10/13	12	47	8.4	0.4 ± 0.3	4.6 ± 1.5	0.0 ± 1.4	1.4 ± 0.9	8.8 ± 2.4	14.4 ± 1.8	0.7 ± 0.1	0.2 ± 0.1	3.3 ± 1.5	1.4 ± 0.9	0.3 ± 0.0	-5.6 ± 3.0
B. Pass	10/14	6	38	8.4	1.9 ± 0.5	4.0 ± 1.5	3.1 ± 1.3	2.7 ± 1.4	13.4 ± 2.4	15.0 ± 2.0	0.6 ± 0.1	0.3 ± 0.1	2.0 ± 1.5	2.7 ± 1.4	1.1 ± 0.0	-1.7 ± 3.1
B. Pass	10/14	12	42	8.4	-0.1 ± 0.2	4.5 ± 1.6	0.0 ± 1.3	2.3 ± 1.3	8.3 ± 2.4	15.3 ± 2.0	0.7 ± 0.1	0.2 ± 0.1	3.0 ± 1.6	2.3 ± 1.3	0.7 ± 0.0	-7.0 ± 3.1
B. Pass	10/15	6	38	8.4	0.4 ± 0.2	2.0 ± 1.5	7.3 ± 1.3	2.6 ± 2.7	16.2 ± 2.4	13.1 ± 3.1	0.5 ± 0.1	0.5 ± 0.1	0.0 ± 1.5	2.6 ± 2.7	1.0 ± 0.0	3.1 ± 3.9
B. Pass	10/15	12	32	8.4	-0.2 ± 0.2	6.9 ± 2.1	0.0 ± 1.3	1.5 ± 1.8	8.2 ± 2.3	16.8 ± 2.8	0.5 ± 0.1	0.4 ± 0.1	4.9 ± 2.1	1.5 ± 1.8	1.1 ± 0.0	-8.6 ± 3.6
B. Pass	10/16	6	32	8.4	3.1 ± 0.6	4.4 ± 0.6	2.3 ± 0.7	1.9 ± 0.5	13.8 ± 2.4	14.7 ± 0.8	1.6 ± 0.1	0.3 ± 0.0	1.3 ± 0.6	1.9 ± 0.5	1.1 ± 0.0	-0.8 ± 2.5
B. Pass	10/17	6	46	8.4	7.3 ± 0.4	5.0 ± 0.7	2.8 ± 0.8	0.9 ± 0.4	18.5 ± 3.1	14.3 ± 0.8	1.8 ± 0.1	0.3 ± 0.0	2.1 ± 0.7	0.9 ± 0.4	0.8 ± 0.0	4.2 ± 3.2
B. Pass	10/18	6	41	8.4	5.8 ± 0.2	4.1 ± 0.7	1.4 ± 0.6	1.7 ± 0.5	15.7 ± 3.0	14.2 ± 0.8	1.7 ± 0.1	0.3 ± 0.0	1.5 ± 0.6	1.7 ± 0.5	0.6 ± 0.0	1.5 ± 3.1
B. Pass	10/19	6	43	8.4	4.3 ± 1.0	1.9 ± 0.6	1.4 ± 0.6	0.9 ± 0.4	14.2 ± 2.7	11.2 ± 0.7	0.6 ± 0.0	0.3 ± 0.0	0.6 ± 0.6	0.9 ± 0.4	0.4 ± 0.0	2.9 ± 2.8
B. Pass	10/20	6	22	8.4	5.7 ± 1.0	4.1 ± 1.0	0.8 ± 0.7	2.5 ± 2.3	14.9 ± 2.9	15.0 ± 2.5	0.6 ± 0.0	0.2 ± 0.0	2.3 ± 1.0	2.5 ± 2.3	1.0 ± 0.0	-0.1 ± 3.8
B. Pass	10/21	6	35	8.4	7.0 ± 1.0	3.8 ± 0.9	2.3 ± 0.7	1.9 ± 1.8	17.7 ± 3.1	14.1 ± 2.0	1.2 ± 0.1	0.3 ± 0.0	1.3 ± 0.9	1.9 ± 1.8	1.0 ± 0.0	3.6 ± 3.7
B. Pass	10/22	6	89	8.4	53.6 ± 16.6	5.4 ± 1.3	0.8 ± 0.7	0.9 ± 0.4	62.8 ± 16.2	14.7 ± 1.4	4.6 ± 0.3	0.5 ± 0.2	0.0 ± 1.3	0.9 ± 0.4	0.3 ± 0.0	48.0 ± 16.3
B. Pass	10/23	6	86	8.4	220.9 ± 111.0	9.9 ± 1.2	1.5 ± 0.7	0.5 ± 0.4	230.9 ± 85.1	18.8 ± 1.2	9.4 ± 0.5	0.4 ± 0.1	0.0 ± 1.1	0.5 ± 0.4	0.2 ± 0.0	212.1 ± 85.1
B. Pass	10/24	6	61	8.4	2.8 ± 0.2	2.1 ± 0.9	0.8 ± 0.7	3.1 ± 2.8	12.0 ± 2.1	13.6 ± 2.9	1.5 ± 0.1	0.2 ± 0.1	0.1 ± 0.9	3.1 ± 2.8	0.2 ± 0.0	-1.5 ± 3.6
B. Pass	10/25	6	56	8.4	2.9 ± 0.2	4.2 ± 1.1	2.3 ± 0.7	5.1 ± 4.3	13.7 ± 2.1	17.7 ± 4.5	1.4 ± 0.1	0.3 ± 0.1	2.2 ± 1.1	5.1 ± 4.3	0.3 ± 0.0	-4.0 ± 4.9
B. Pass	10/26	6	66	8.4	12.6 ± 2.3	12.7 ± 2.5	0.9 ± 0.8	10.2 ± 8.5	21.9 ± 4.2	31.3 ± 8.9	1.3 ± 0.1	0.4 ± 0.1	10.4 ± 2.5	10.2 ± 8.5	0.6 ± 0.0	-9.4 ± 9.8
B. Pass	10/27	6	66	8.4	30.9 ± 17.4	3.5 ± 1.1	0.0 ± 0.7	2.5 ± 2.3	39.3 ± 13.6	14.4 ± 2.6	1.1 ± 0.1	0.5 ± 0.1	1.2 ± 1.1	2.5 ± 2.3	0.8 ± 0.0	24.9 ± 13.9
B. Pass	10/28	6	51	8.4	1.4 ± 0.2	2.1 ± 0.8	0.8 ± 0.7	0.5 ± 0.8	10.6 ± 2.1	11.1 ± 1.1	0.6 ± 0.1	0.4 ± 0.1	0.1 ± 0.8	0.5 ± 0.8	1.1 ± 0.0	-0.5 ± 2.4
B. Pass	10/29	6	61	8.4	0.7 ± 0.4	3.6 ± 1.0	0.0 ± 0.7	3.2 ± 2.8	9.2 ± 2.1	15.2 ± 3.0	0.8 ± 0.1	0.4 ± 0.1	1.5 ± 1.0	3.2 ± 2.8	0.8 ± 0.0	-6.0 ± 3.7

Table 4.3.2
Measured and Calculated Component Contributions to Total Light Extinction at Gilpin Creek

Site	Date	Hr	RH	Cln Air	bsp	Ebsp	babs	Ebabs	bext	Ebext	Esul	Enit	Eoc	Eec	Esoil	Unid.
Gilpin Cr.	2/23	6	54	8.8	4.2 ± 0.2	--- ± ---	0.0 ± 5.2	--- ± ---	13.0 ± 5.3	--- ± ---	--- ± ---	--- ± ---	--- ± ---	--- ± ---	--- ± ---	--- ± ---
Gilpin Cr.	3/26	6	66	8.8	9.8 ± 1.8	3.2 ± 6.4	5.8 ± 5.1	2.8 ± 2.5	24.4 ± 5.2	14.8 ± 6.9	2.4 ± 0.4	0.7 ± 0.4	0.0 ± 6.4	2.8 ± 2.5	0.2 ± 0.0	9.6 ± 8.6
Gilpin Cr.	3/27	6	67	8.8	13.3 ± 1.8	5.7 ± 6.6	6.0 ± 5.2	6.8 ± 3.1	28.0 ± 5.3	21.2 ± 7.3	2.1 ± 0.4	0.4 ± 0.4	2.6 ± 6.6	6.8 ± 3.1	0.5 ± 0.0	6.8 ± 9.0
Gilpin Cr.	3/28	6	55	8.8	10.5 ± 0.7	5.8 ± 5.9	5.8 ± 5.1	2.0 ± 2.6	25.1 ± 5.2	16.6 ± 6.5	4.0 ± 0.4	1.5 ± 0.3	0.0 ± 5.9	2.0 ± 2.6	0.3 ± 0.0	8.5 ± 8.3
Gilpin Cr.	3/29	6	---	8.8	--- ± ---	--- ± ---	--- ± ---	--- ± ---	--- ± ---	--- ± ---	--- ± ---	--- ± ---	--- ± ---	--- ± ---	--- ± ---	--- ± ---
Gilpin Cr.	3/30	6	73	8.8	28.5 ± 4.4	11.8 ± 7.1	11.7 ± 5.1	1.8 ± 2.5	48.9 ± 5.4	22.4 ± 7.5	9.1 ± 0.6	1.4 ± 0.4	0.0 ± 7.0	1.8 ± 2.5	1.2 ± 0.0	26.6 ± 9.2
Gilpin Cr.	3/31	6	67	8.8	17.2 ± 0.9	10.6 ± 6.7	11.8 ± 5.2	4.1 ± 2.6	37.8 ± 5.3	23.5 ± 7.1	7.7 ± 0.6	1.8 ± 0.4	0.0 ± 6.6	4.1 ± 2.6	1.1 ± 0.0	14.3 ± 8.9
Gilpin Cr.	5/6	6	60	8.8	21.2 ± 4.5	14.8 ± 5.9	18.3 ± 5.4	8.2 ± 3.3	48.2 ± 5.5	31.7 ± 6.8	4.9 ± 0.4	1.1 ± 0.3	5.2 ± 5.9	8.2 ± 3.3	3.6 ± 0.1	16.5 ± 8.8
Gilpin Cr.	5/7	6	71	8.8	79.5 ± 58.3	9.4 ± 6.6	18.2 ± 5.3	6.9 ± 3.0	106.4 ± 10.2	25.1 ± 7.3	4.3 ± 0.5	1.2 ± 0.4	0.0 ± 6.6	6.9 ± 3.0	3.9 ± 0.1	81.3 ± 12.5
Gilpin Cr.	6/14	6	26	8.8	20.8 ± 0.8	22.0 ± 5.6	22.5 ± 5.0	12.8 ± 4.6	52.1 ± 5.1	43.5 ± 7.3	3.1 ± 0.3	1.1 ± 0.3	16.9 ± 5.6	12.8 ± 4.6	0.8 ± 0.0	8.6 ± 8.9
Gilpin Cr.	6/15	6	41	8.8	17.9 ± 0.9	18.2 ± 5.5	23.0 ± 5.1	11.0 ± 4.1	49.7 ± 5.2	38.0 ± 6.8	5.4 ± 0.4	1.0 ± 0.3	10.9 ± 5.5	11.0 ± 4.1	0.9 ± 0.0	11.7 ± 8.6
Gilpin Cr.	6/16	6	26	8.8	13.7 ± 0.5	10.8 ± 5.1	23.8 ± 5.3	10.8 ± 4.1	46.3 ± 5.4	30.4 ± 6.6	3.1 ± 0.3	0.7 ± 0.2	6.4 ± 5.1	10.8 ± 4.1	0.7 ± 0.0	16.0 ± 8.5
Gilpin Cr.	6/29	6	67	8.8	10.2 ± 0.4	33.8 ± 7.4	17.4 ± 5.1	12.2 ± 4.4	36.4 ± 5.2	54.7 ± 8.6	3.0 ± 0.4	0.8 ± 0.4	29.7 ± 7.4	12.2 ± 4.4	0.2 ± 0.1	-18.3 ± 10.1
Gilpin Cr.	6/30	6	54	8.8	13.9 ± 0.6	13.3 ± 5.9	17.9 ± 5.3	6.3 ± 2.9	40.6 ± 5.4	28.3 ± 6.6	3.1 ± 0.3	1.2 ± 0.3	8.6 ± 5.8	6.3 ± 2.9	0.4 ± 0.0	12.2 ± 8.5
Gilpin Cr.	7/1	6	52	8.8	17.4 ± 0.8	4.5 ± 5.9	17.8 ± 5.2	10.4 ± 6.3	43.9 ± 5.3	23.7 ± 8.6	2.5 ± 0.3	0.7 ± 0.3	1.0 ± 5.8	10.4 ± 6.3	0.4 ± 0.1	20.2 ± 10.1
Gilpin Cr.	7/29	6	25	8.8	12.0 ± 1.2	17.4 ± 5.4	0.0 ± 5.1	30.6 ± 17.3	20.8 ± 5.2	56.8 ± 18.1	2.2 ± 0.3	0.7 ± 0.2	14.2 ± 5.4	30.6 ± 17.3	0.4 ± 0.0	-36.1 ± 18.9
Gilpin Cr.	7/30	6	33	8.8	16.2 ± 1.0	13.2 ± 5.3	0.0 ± 5.0	24.8 ± 14.1	24.9 ± 5.1	46.7 ± 15.0	3.0 ± 0.3	0.5 ± 0.2	9.1 ± 5.3	24.8 ± 14.1	0.6 ± 0.0	-21.8 ± 15.9
Gilpin Cr.	7/30	6	33	8.8	16.2 ± 1.0	--- ± ---	0.0 ± 5.0	--- ± ---	24.9 ± 5.1	--- ± ---	--- ± ---	--- ± ---	--- ± ---	--- ± ---	--- ± ---	--- ± ---
Gilpin Cr.	7/31	6	37	8.8	9.7 ± 1.4	5.5 ± 5.3	0.0 ± 5.2	16.6 ± 9.5	18.4 ± 5.3	30.8 ± 10.9	1.7 ± 0.3	0.5 ± 0.3	2.8 ± 5.3	16.6 ± 9.5	0.5 ± 0.0	-12.4 ± 12.1
Gilpin Cr.	8/7	6	29	8.8	14.8 ± 0.4	18.5 ± 5.4	0.0 ± 5.2	15.9 ± 5.7	23.6 ± 5.3	43.2 ± 7.9	3.3 ± 0.3	0.8 ± 0.2	13.9 ± 5.4	15.9 ± 5.7	0.5 ± 0.0	-19.6 ± 9.5
Gilpin Cr.	8/8	6	---	8.8	--- ± ---	--- ± ---	--- ± ---	--- ± ---	--- ± ---	--- ± ---	--- ± ---	--- ± ---	--- ± ---	--- ± ---	--- ± ---	--- ± ---
Gilpin Cr.	8/9	6	29	8.8	9.1 ± 0.5	--- ± ---	0.0 ± 4.9	--- ± ---	17.8 ± 5.0	--- ± ---	--- ± ---	--- ± ---	--- ± ---	--- ± ---	--- ± ---	--- ± ---
Gilpin Cr.	8/14	6	49	8.8	6.2 ± 0.4	10.6 ± 5.3	0.0 ± 5.2	7.6 ± 4.8	15.0 ± 5.3	27.0 ± 7.1	1.5 ± 0.3	0.7 ± 0.3	8.2 ± 5.2	7.6 ± 4.8	0.3 ± 0.0	-12.0 ± 8.9
Gilpin Cr.	8/21	6	54	8.8	13.9 ± 0.5	20.9 ± 5.9	0.0 ± 5.2	9.1 ± 3.6	22.7 ± 5.3	38.8 ± 6.9	5.0 ± 0.4	0.5 ± 0.3	15.2 ± 5.9	9.1 ± 3.6	0.2 ± 0.1	-16.1 ± 8.7
Gilpin Cr.	8/22	6	57	8.8	12.4 ± 0.5	9.4 ± 5.5	0.0 ± 5.2	2.7 ± 2.2	21.2 ± 5.3	20.8 ± 5.9	4.0 ± 0.4	0.4 ± 0.3	4.6 ± 5.5	2.7 ± 2.2	0.3 ± 0.0	0.3 ± 7.9
Gilpin Cr.	8/23	6	62	8.8	12.6 ± 0.8	21.0 ± 6.6	0.0 ± 4.9	12.2 ± 4.5	21.3 ± 5.0	42.0 ± 8.0	5.3 ± 0.4	0.7 ± 0.4	14.8 ± 6.6	12.2 ± 4.5	0.2 ± 0.0	-20.7 ± 9.5
Gilpin Cr.	8/24	6	73	8.8	13.6 ± 1.1	3.2 ± 6.5	0.0 ± 5.3	6.3 ± 2.9	22.3 ± 5.3	18.3 ± 7.2	1.8 ± 0.4	0.5 ± 0.4	0.5 ± 6.5	6.3 ± 2.9	0.3 ± 0.0	4.0 ± 8.9
Gilpin Cr.	8/25	6	57	8.8	9.7 ± 1.4	6.4 ± 5.6	0.0 ± 5.1	10.0 ± 3.9	18.4 ± 5.2	25.2 ± 6.8	2.6 ± 0.3	0.5 ± 0.3	3.0 ± 5.5	10.0 ± 3.9	0.2 ± 0.0	-6.7 ± 8.5
Gilpin Cr.	8/26	6	39	8.8	8.2 ± 0.6	6.9 ± 5.3	0.0 ± 5.0	9.3 ± 5.7	17.0 ± 5.1	25.0 ± 7.8	2.7 ± 0.3	0.6 ± 0.3	3.4 ± 5.3	9.3 ± 5.7	0.2 ± 0.0	-8.0 ± 9.3
Gilpin Cr.	8/27	6	49	8.8	12.4 ± 0.7	4.3 ± 5.5	0.0 ± 4.9	6.8 ± 4.4	21.2 ± 5.0	19.9 ± 7.0	3.5 ± 0.3	0.5 ± 0.3	0.1 ± 5.5	6.8 ± 4.4	0.2 ± 0.0	1.2 ± 8.7
Gilpin Cr.	9/2	6	43	8.8	15.2 ± 0.7	14.3 ± 5.6	0.0 ± 5.1	34.5 ± 19.5	24.0 ± 5.2	57.5 ± 20.3	5.0 ± 0.4	0.4 ± 0.3	8.5 ± 5.6	34.5 ± 19.5	0.3 ± 0.1	-33.5 ± 20.9

Gilpin Cr.	9/17	6	35	8.8	8.3 ± 0.2	4.3 ± 5.1	0.0 ± 5.1	4.4 ± 3.5	17.1 ± 5.2	17.5 ± 6.2	3.0 ± 0.3	0.8 ± 0.2	0.0 ± 5.1	4.4 ± 3.5	0.4 ± 0.0	-0.4 ± 8.1
Gilpin Cr.	9/18	6	90	8.8	114.6 ± 80.0	12.4 ± 12.4	0.0 ± 5.2	4.6 ± 3.5	123.3 ± 13.3	25.8 ± 12.9	10.3 ± 1.1	1.8 ± 0.9	0.0 ± 12.3	4.6 ± 3.5	0.4 ± 0.1	97.5 ± 18.5
Gilpin Cr.	9/19	6	72	8.8	10.9 ± 1.9	3.9 ± 6.8	0.0 ± 5.2	4.6 ± 3.5	19.7 ± 5.3	17.3 ± 7.7	2.6 ± 0.4	1.1 ± 0.4	0.0 ± 6.8	4.6 ± 3.5	0.3 ± 0.1	2.3 ± 9.3
Gilpin Cr.	9/20	6	88	8.8	143.3 ± 79.5	7.5 ± 11.5	0.0 ± 5.0	3.1 ± 3.1	152.1 ± 13.5	19.3 ± 11.9	5.6 ± 0.9	1.5 ± 0.9	0.0 ± 11.4	3.1 ± 3.1	0.4 ± 0.1	132.7 ± 18.0
Gilpin Cr.	9/21	6	68	8.8	6.3 ± 0.7	3.3 ± 6.7	0.0 ± 5.0	4.1 ± 3.3	15.1 ± 5.1	16.2 ± 7.5	2.4 ± 0.4	0.6 ± 0.4	0.2 ± 6.7	4.1 ± 3.3	0.1 ± 0.1	-1.1 ± 9.0
Gilpin Cr.	9/24	6	69	8.8	10.8 ± 1.1	--- ± ---	0.0 ± 5.3	--- ± ---	19.6 ± 5.4	--- ± ---	--- ± ---	--- ± ---	--- ± ---	--- ± ---	--- ± ---	--- ± ---
Gilpin Cr.	9/27	6	43	8.8	10.5 ± 0.5	5.1 ± 5.6	0.0 ± 5.0	5.3 ± 3.9	19.3 ± 5.1	19.2 ± 6.8	3.6 ± 0.3	1.1 ± 0.3	0.0 ± 5.6	5.3 ± 3.9	0.5 ± 0.0	0.1 ± 8.5
Gilpin Cr.	9/30	6	96	8.8	1637.7 ± 431.2	8.6 ± 28.4	0.0 ± 5.2	0.0 ± 2.5	1646.5 ± 89.1	17.4 ± 28.5	8.2 ± 2.6	0.0 ± 2.4	0.0 ± 28.2	0.0 ± 2.5	0.5 ± 0.1	1629.1 ± 93.6
Gilpin Cr.	10/1	6	66	8.8	12.7 ± 2.2	4.4 ± 7.2	0.0 ± 5.2	15.3 ± 6.2	21.4 ± 5.3	28.5 ± 9.5	3.0 ± 0.4	0.9 ± 0.4	0.3 ± 7.2	15.3 ± 6.2	0.2 ± 0.0	-7.1 ± 10.8
Gilpin Cr.	10/2	6	57	8.8	9.3 ± 2.1	8.0 ± 6.1	0.0 ± 5.2	9.9 ± 6.0	18.1 ± 5.3	26.7 ± 8.6	2.3 ± 0.3	1.3 ± 0.3	4.2 ± 6.1	9.9 ± 6.0	0.3 ± 0.0	-8.6 ± 10.1
Gilpin Cr.	10/7	6	---	8.8	--- ± ---	--- ± ---	--- ± ---	--- ± ---	--- ± ---	--- ± ---	--- ± ---	--- ± ---	--- ± ---	--- ± ---	--- ± ---	--- ± ---
Gilpin Cr.	10/8	6	51	8.8	18.0 ± 3.7	9.0 ± 6.7	0.0 ± 5.2	5.3 ± 3.2	26.8 ± 5.4	23.0 ± 7.5	2.5 ± 0.3	0.8 ± 0.3	4.8 ± 6.7	5.3 ± 3.2	0.8 ± 0.0	3.7 ± 9.2
Gilpin Cr.	10/9	6	39	8.8	6.7 ± 0.1	2.8 ± 5.7	0.0 ± 5.2	2.1 ± 2.6	15.4 ± 5.3	13.7 ± 6.3	1.7 ± 0.3	0.5 ± 0.3	0.0 ± 5.7	2.1 ± 2.6	0.6 ± 0.0	1.7 ± 8.2
Gilpin Cr.	10/10	6	37	8.8	8.5 ± 0.5	12.7 ± 5.5	0.0 ± 5.2	12.7 ± 7.5	17.3 ± 5.3	34.2 ± 9.3	1.4 ± 0.3	0.6 ± 0.3	9.9 ± 5.5	12.7 ± 7.5	0.9 ± 0.0	-17.0 ± 10.7
Gilpin Cr.	10/11	6	31	8.8	4.4 ± 0.2	3.4 ± 6.1	0.0 ± 5.0	10.0 ± 4.4	13.2 ± 5.1	22.2 ± 7.5	0.9 ± 0.2	0.4 ± 0.3	1.8 ± 6.1	10.0 ± 4.4	0.3 ± 0.0	-9.0 ± 9.1
Gilpin Cr.	10/12	6	62	8.8	21.3 ± 2.0	1.5 ± 6.8	5.8 ± 5.0	3.6 ± 4.0	35.9 ± 5.2	13.9 ± 7.9	0.7 ± 0.3	0.0 ± 0.3	0.0 ± 6.8	3.6 ± 4.0	0.8 ± 0.0	22.0 ± 9.4
Gilpin Cr.	10/13	6	50	8.8	2.5 ± 0.2	2.1 ± 6.0	0.0 ± 5.1	0.2 ± 2.6	11.3 ± 5.1	11.0 ± 6.6	0.8 ± 0.3	0.5 ± 0.3	0.0 ± 6.0	0.2 ± 2.6	0.8 ± 0.0	0.2 ± 8.3
Gilpin Cr.	10/14	6	34	8.8	3.2 ± 0.2	2.4 ± 5.6	0.0 ± 5.1	0.0 ± 2.6	12.0 ± 5.2	11.1 ± 6.1	1.3 ± 0.3	0.6 ± 0.3	0.0 ± 5.5	0.0 ± 2.6	0.5 ± 0.0	0.9 ± 8.0
Gilpin Cr.	10/16	6	27	8.8	6.0 ± 0.8	--- ± ---	0.0 ± 5.2	--- ± ---	14.7 ± 5.3	--- ± ---	--- ± ---	--- ± ---	--- ± ---	--- ± ---	--- ± ---	--- ± ---
Gilpin Cr.	10/17	6	36	8.8	10.1 ± 0.4	--- ± ---	0.0 ± 5.2	--- ± ---	18.8 ± 5.3	--- ± ---	--- ± ---	--- ± ---	--- ± ---	--- ± ---	--- ± ---	--- ± ---
Gilpin Cr.	10/18	6	33	8.8	8.1 ± 0.2	--- ± ---	0.0 ± 5.1	--- ± ---	16.8 ± 5.2	--- ± ---	--- ± ---	--- ± ---	--- ± ---	--- ± ---	--- ± ---	--- ± ---
Gilpin Cr.	10/19	6	---	8.8	--- ± ---	--- ± ---	--- ± ---	--- ± ---	--- ± ---	--- ± ---	--- ± ---	--- ± ---	--- ± ---	--- ± ---	--- ± ---	--- ± ---
Gilpin Cr.	10/22	6	---	8.8	--- ± ---	--- ± ---	--- ± ---	--- ± ---	--- ± ---	--- ± ---	--- ± ---	--- ± ---	--- ± ---	--- ± ---	--- ± ---	--- ± ---
Gilpin Cr.	10/23	6	---	8.8	--- ± ---	--- ± ---	--- ± ---	--- ± ---	--- ± ---	--- ± ---	--- ± ---	--- ± ---	--- ± ---	--- ± ---	--- ± ---	--- ± ---

Table 4.3.3
Measured and Calculated Component Contributions to Total Light Extinction at Juniper Mt.

Site	Date	Hr	RH	Cln Air	bsp	Ebsp	babs	Ebabs	bext	Ebext	Esul	Enit	Eoc	Eec	Esoil	Unid.
Junpr.Mt.	2/23	6	62	9.2	8.318 + 0.51	--- + ---	--- + ---	--- + ---	--- + ---	--- + ---	--- + ---	--- + ---	--- + ---	--- + ---	--- + ---	--- + ---
Junpr.Mt.	2/23	12	53	9.2	5.2 ± 0.5	10.5 ± 1.2	0.0 ± 1.4	6.1 ± 1.0	14.3 ± 1.7	25.8 ± 1.5	1.8 ± 0.1	1.1 ± 0.1	6.9 ± 1.2	6.1 ± 1.0	0.6 ± 0.1	-11.5 ± 2.3
Junpr.Mt.	3/26	6	69	9.2	--- ± ---	--- ± ---	--- ± ---	--- ± ---	--- ± ---	--- ± ---	--- ± ---	--- ± ---	--- ± ---	--- ± ---	--- ± ---	--- ± ---
Junpr.Mt.	3/27	6	59	9.2	--- ± ---	7.6 ± 0.6	4.0 ± 0.7	1.4 ± 0.5	--- ± ---	18.1 ± 0.7	4.9 ± 0.2	0.1 ± 0.1	2.3 ± 0.5	1.4 ± 0.5	0.2 ± 0.0	--- ± ---
Junpr.Mt.	3/28	6	64	9.2	--- ± ---	6.7 ± 0.5	3.6 ± 0.7	1.1 ± 0.4	--- ± ---	17.0 ± 0.6	5.2 ± 0.3	0.3 ± 0.1	1.0 ± 0.5	1.1 ± 0.4	0.3 ± 0.0	--- ± ---
Junpr.Mt.	3/29	6	82	9.2	--- ± ---	10.6 ± 0.7	2.9 ± 0.7	0.7 ± 0.2	--- ± ---	20.5 ± 0.8	7.5 ± 0.4	0.6 ± 0.1	1.7 ± 0.6	0.7 ± 0.2	0.7 ± 0.1	--- ± ---
Junpr.Mt.	3/30	6	---	9.2	--- ± ---	--- ± ---	--- ± ---	--- ± ---	--- ± ---	--- ± ---	--- ± ---	--- ± ---	--- ± ---	--- ± ---	--- ± ---	--- ± ---
Junpr.Mt.	3/31	6	59	9.2	--- ± ---	--- ± ---	6.3 ± 1.8	--- ± ---	--- ± ---	--- ± ---	--- ± ---	--- ± ---	--- ± ---	--- ± ---	--- ± ---	--- ± ---
Junpr.Mt.	5/6	6	---	9.2	--- ± ---	--- ± ---	--- ± ---	--- ± ---	--- ± ---	--- ± ---	--- ± ---	--- ± ---	--- ± ---	--- ± ---	--- ± ---	--- ± ---
Junpr.Mt.	5/7	6	74	9.2	--- ± ---	14.4 ± 0.7	5.8 ± 0.8	3.1 ± 1.0	--- ± ---	26.6 ± 1.2	5.6 ± 0.3	0.9 ± 0.1	3.2 ± 0.6	3.1 ± 1.0	4.7 ± 0.1	--- ± ---
Junpr.Mt.	6/14	6	19	9.2	22.5 ± 1.8	10.2 ± 0.7	8.8 ± 0.8	2.8 ± 0.9	40.5 ± 0.8	22.2 ± 1.2	4.1 ± 0.2	0.2 ± 0.0	5.1 ± 0.7	2.8 ± 0.9	0.8 ± 0.0	18.2 ± 1.4
Junpr.Mt.	6/15	6	38	9.2	20.6 ± 0.3	13.4 ± 0.9	8.6 ± 0.8	4.9 ± 1.6	38.3 ± 0.8	27.4 ± 1.8	3.8 ± 0.2	0.4 ± 0.0	7.1 ± 0.9	4.9 ± 1.6	2.0 ± 0.1	10.9 ± 2.0
Junpr.Mt.	6/16	6	30	9.2	16.8 ± 1.4	3.9 ± 0.6	2.3 ± 0.7	1.2 ± 0.4	28.3 ± 0.7	14.2 ± 0.7	0.3 ± 0.0	0.0 ± 0.0	3.4 ± 0.6	1.2 ± 0.4	0.1 ± 0.0	14.1 ± 1.0
Junpr.Mt.	6/29	6	69	9.2	8.3 ± 0.3	10.7 ± 1.1	6.4 ± 1.0	4.7 ± 1.6	23.9 ± 1.0	24.6 ± 1.9	1.8 ± 0.1	0.3 ± 0.1	7.1 ± 1.1	4.7 ± 1.6	1.5 ± 0.1	-0.8 ± 2.2
Junpr.Mt.	6/30	6	---	9.2	--- ± ---	--- ± ---	--- ± ---	--- ± ---	--- ± ---	--- ± ---	--- ± ---	--- ± ---	--- ± ---	--- ± ---	--- ± ---	--- ± ---
Junpr.Mt.	7/1	6	71	9.2	16.4 ± 6.5	--- ± ---	--- ± ---	--- ± ---	--- ± ---	--- ± ---	--- ± ---	--- ± ---	--- ± ---	--- ± ---	--- ± ---	--- ± ---
Junpr.Mt.	7/29	6	---	9.2	--- ± ---	--- ± ---	--- ± ---	--- ± ---	--- ± ---	--- ± ---	--- ± ---	--- ± ---	--- ± ---	--- ± ---	--- ± ---	--- ± ---
Junpr.Mt.	7/30	6	29	9.2	31.0 ± 3.4	--- ± ---	--- ± ---	--- ± ---	--- ± ---	--- ± ---	--- ± ---	--- ± ---	--- ± ---	--- ± ---	--- ± ---	--- ± ---
Junpr.Mt.	7/31	6	---	9.2	--- ± ---	--- ± ---	--- ± ---	--- ± ---	--- ± ---	--- ± ---	--- ± ---	--- ± ---	--- ± ---	--- ± ---	--- ± ---	--- ± ---
Junpr.Mt.	8/7	6	24	9.2	16.3 ± 1.1	13.9 ± 1.4	4.9 ± 1.4	5.4 ± 1.8	30.4 ± 1.4	28.5 ± 2.2	2.9 ± 0.2	0.3 ± 0.1	9.7 ± 1.4	5.4 ± 1.8	1.0 ± 0.1	1.9 ± 2.7
Junpr.Mt.	8/7	12	20	9.2	13.0 ± 0.2	11.8 ± 1.2	3.2 ± 1.4	6.3 ± 2.1	25.3 ± 1.4	27.3 ± 2.4	2.4 ± 0.1	0.3 ± 0.1	8.5 ± 1.2	6.3 ± 2.1	0.5 ± 0.1	-1.9 ± 2.8
Junpr.Mt.	8/8	6	33	9.2	19.7 ± 0.5	17.7 ± 1.6	4.8 ± 1.4	6.1 ± 2.0	33.6 ± 1.4	33.0 ± 2.6	4.2 ± 0.2	0.4 ± 0.1	11.6 ± 1.5	6.1 ± 2.0	1.5 ± 0.1	0.6 ± 2.9
Junpr.Mt.	8/8	12	26	9.2	16.5 ± 0.5	12.9 ± 1.2	3.2 ± 1.4	7.4 ± 2.4	28.9 ± 1.4	29.6 ± 2.7	2.8 ± 0.2	0.4 ± 0.1	8.0 ± 1.2	7.4 ± 2.4	1.7 ± 0.1	-0.7 ± 3.1
Junpr.Mt.	8/9	6	22	9.2	9.5 ± 0.3	11.5 ± 1.3	1.6 ± 1.4	6.1 ± 2.0	20.3 ± 1.4	26.8 ± 2.4	0.8 ± 0.1	0.4 ± 0.1	9.2 ± 1.3	6.1 ± 2.0	1.0 ± 0.1	-6.5 ± 2.8
Junpr.Mt.	8/9	12	22	9.2	12.0 ± 0.2	11.6 ± 1.2	1.6 ± 1.4	6.9 ± 2.3	22.8 ± 1.4	27.7 ± 2.6	1.7 ± 0.1	0.4 ± 0.1	8.4 ± 1.2	6.9 ± 2.3	1.2 ± 0.1	-4.9 ± 2.9
Junpr.Mt.	8/14	6	49	9.2	6.4 ± 0.4	--- ± ---	--- ± ---	--- ± ---	--- ± ---	--- ± ---	--- ± ---	--- ± ---	--- ± ---	--- ± ---	--- ± ---	--- ± ---
Junpr.Mt.	8/14	12	56	9.2	--- ± ---	--- ± ---	--- ± ---	--- ± ---	--- ± ---	--- ± ---	--- ± ---	--- ± ---	--- ± ---	--- ± ---	--- ± ---	--- ± ---
Junpr.Mt.	8/21	6	62	9.2	15.6 ± 0.7	14.0 ± 1.6	0.0 ± 1.7	5.0 ± 1.6	24.8 ± 1.7	28.2 ± 2.3	4.4 ± 0.3	0.4 ± 0.2	8.7 ± 1.6	5.0 ± 1.6	0.4 ± 0.1	-3.4 ± 2.9
Junpr.Mt.	8/21	12	48	9.2	19.2 ± 1.0	12.7 ± 1.0	2.1 ± 0.9	4.1 ± 1.3	30.4 ± 0.9	25.9 ± 1.7	4.1 ± 0.2	0.4 ± 0.1	6.8 ± 1.0	4.1 ± 1.3	1.4 ± 0.1	4.5 ± 1.9
Junpr.Mt.	8/22	6	64	9.2	16.0 ± 1.5	11.3 ± 1.2	1.6 ± 1.4	4.2 ± 1.4	26.7 ± 1.4	24.6 ± 1.8	4.4 ± 0.2	0.4 ± 0.1	6.2 ± 1.2	4.2 ± 1.4	0.2 ± 0.1	2.1 ± 2.3
Junpr.Mt.	8/22	12	---	9.2	--- ± ---	--- ± ---	--- ± ---	--- ± ---	--- ± ---	--- ± ---	--- ± ---	--- ± ---	--- ± ---	--- ± ---	--- ± ---	--- ± ---
Junpr.Mt.	8/23	6	70	9.2	19.2 ± 0.6	14.8 ± 1.4	3.2 ± 1.4	4.6 ± 1.5	31.5 ± 1.4	28.6 ± 2.1	5.4 ± 0.3	0.4 ± 0.1	8.1 ± 1.4	4.6 ± 1.5	0.8 ± 0.1	2.9 ± 2.5

Junpr.Mt.	8/23	12	57	9.2	14.7 ± 0.3	--- ± ---	3.2 ± 1.4	--- ± ---	27.1 ± 1.4	--- ± ---	--- ± ---	--- ± ---	--- ± ---	--- ± ---	--- ± ---	--- ± ---	--- ± ---	--- ± ---	--- ± ---	--- ± ---	--- ± ---	--- ± ---	--- ± ---	--- ± ---
Junpr.Mt.	8/24	6	67	9.2	12.7 ± 1.0	11.3 ± 1.2	3.1 ± 1.4	3.4 ± 1.1	25.0 ± 1.4	23.9 ± 1.7	4.4 ± 0.2	0.1 ± 0.1	6.5 ± 1.2	3.4 ± 1.1	0.2 ± 0.1	1.0 ± 2.2								
Junpr.Mt.	8/24	12	54	9.2	9.3 ± 0.5	10.9 ± 1.3	0.0 ± 1.4	4.1 ± 1.3	18.5 ± 1.4	24.2 ± 1.9	2.5 ± 0.2	0.1 ± 0.1	8.1 ± 1.3	4.1 ± 1.3	0.2 ± 0.1	-5.7 ± 2.3								
Junpr.Mt.	8/25	6	56	9.2	10.9 ± 1.5	9.3 ± 0.9	2.1 ± 0.9	6.8 ± 2.2	22.2 ± 0.9	25.3 ± 2.4	2.7 ± 0.1	0.2 ± 0.1	6.0 ± 0.9	6.8 ± 2.2	0.3 ± 0.1	-3.1 ± 2.6								
Junpr.Mt.	8/25	12	---	9.2	--- ± ---	--- ± ---	--- ± ---	--- ± ---	--- ± ---	--- ± ---	--- ± ---	--- ± ---	--- ± ---	--- ± ---	--- ± ---	--- ± ---	--- ± ---	--- ± ---	--- ± ---	--- ± ---	--- ± ---	--- ± ---	--- ± ---	--- ± ---
Junpr.Mt.	8/26	6	45	9.2	10.2 ± 0.4	9.8 ± 1.3	1.6 ± 1.4	3.5 ± 0.7	21.0 ± 1.4	22.5 ± 1.4	2.9 ± 0.2	0.3 ± 0.1	6.3 ± 1.2	3.5 ± 0.7	0.3 ± 0.1	-1.5 ± 2.0								
Junpr.Mt.	8/26	12	33	9.2	--- ± ---	--- ± ---	--- ± ---	--- ± ---	--- ± ---	--- ± ---	--- ± ---	--- ± ---	--- ± ---	--- ± ---	--- ± ---	--- ± ---	--- ± ---	--- ± ---	--- ± ---	--- ± ---	--- ± ---	--- ± ---	--- ± ---	--- ± ---
Junpr.Mt.	8/27	6	40	9.2	8.6 ± 0.2	--- ± ---	--- ± ---	--- ± ---	--- ± ---	--- ± ---	--- ± ---	--- ± ---	--- ± ---	--- ± ---	--- ± ---	--- ± ---	--- ± ---	--- ± ---	--- ± ---	--- ± ---	--- ± ---	--- ± ---	--- ± ---	--- ± ---
Junpr.Mt.	8/27	12	38	9.2	10.2 ± 0.2	--- ± ---	--- ± ---	--- ± ---	--- ± ---	--- ± ---	--- ± ---	--- ± ---	--- ± ---	--- ± ---	--- ± ---	--- ± ---	--- ± ---	--- ± ---	--- ± ---	--- ± ---	--- ± ---	--- ± ---	--- ± ---	--- ± ---
Junpr.Mt.	9/2	6	42	9.2	15.0 ± 0.4	15.2 ± 1.4	4.8 ± 1.4	8.4 ± 1.4	29.0 ± 1.4	32.8 ± 2.0	5.1 ± 0.3	0.6 ± 0.1	8.0 ± 1.3	8.4 ± 1.4	1.5 ± 0.1	-3.9 ± 2.4								
Junpr.Mt.	9/2	12	29	9.2	11.3 ± 0.4	9.1 ± 1.1	3.2 ± 1.4	5.4 ± 0.9	23.7 ± 1.4	23.7 ± 1.4	3.9 ± 0.2	0.3 ± 0.1	4.4 ± 1.1	5.4 ± 0.9	0.4 ± 0.1	-0.1 ± 2.0								
Junpr.Mt.	9/17	6	31	9.2	--- ± ---	--- ± ---	--- ± ---	--- ± ---	--- ± ---	--- ± ---	--- ± ---	--- ± ---	--- ± ---	--- ± ---	--- ± ---	--- ± ---	--- ± ---	--- ± ---	--- ± ---	--- ± ---	--- ± ---	--- ± ---	--- ± ---	--- ± ---
Junpr.Mt.	9/17	12	---	9.2	--- ± ---	--- ± ---	0.0 ± 0.0	--- ± ---	--- ± ---	--- ± ---	--- ± ---	--- ± ---	--- ± ---	--- ± ---	--- ± ---	--- ± ---	--- ± ---	--- ± ---	--- ± ---	--- ± ---	--- ± ---	--- ± ---	--- ± ---	--- ± ---
Junpr.Mt.	9/18	6	77	9.2	104.8 ± 56.3	--- ± ---	--- ± ---	--- ± ---	--- ± ---	--- ± ---	--- ± ---	--- ± ---	--- ± ---	--- ± ---	--- ± ---	--- ± ---	--- ± ---	--- ± ---	--- ± ---	--- ± ---	--- ± ---	--- ± ---	--- ± ---	--- ± ---
Junpr.Mt.	9/18	12	69	9.2	16.3 ± 2.6	--- ± ---	--- ± ---	--- ± ---	--- ± ---	--- ± ---	--- ± ---	--- ± ---	--- ± ---	--- ± ---	--- ± ---	--- ± ---	--- ± ---	--- ± ---	--- ± ---	--- ± ---	--- ± ---	--- ± ---	--- ± ---	--- ± ---
Junpr.Mt.	9/19	6	94	9.2	--- ± ---	--- ± ---	--- ± ---	--- ± ---	--- ± ---	--- ± ---	--- ± ---	--- ± ---	--- ± ---	--- ± ---	--- ± ---	--- ± ---	--- ± ---	--- ± ---	--- ± ---	--- ± ---	--- ± ---	--- ± ---	--- ± ---	--- ± ---
Junpr.Mt.	9/19	12	---	9.2	--- ± ---	--- ± ---	--- ± ---	--- ± ---	--- ± ---	--- ± ---	--- ± ---	--- ± ---	--- ± ---	--- ± ---	--- ± ---	--- ± ---	--- ± ---	--- ± ---	--- ± ---	--- ± ---	--- ± ---	--- ± ---	--- ± ---	--- ± ---
Junpr.Mt.	9/20	6	76	9.2	21.2 ± 2.4	--- ± ---	--- ± ---	--- ± ---	--- ± ---	--- ± ---	--- ± ---	--- ± ---	--- ± ---	--- ± ---	--- ± ---	--- ± ---	--- ± ---	--- ± ---	--- ± ---	--- ± ---	--- ± ---	--- ± ---	--- ± ---	--- ± ---
Junpr.Mt.	9/20	12	70	9.2	13.7 ± 1.1	--- ± ---	--- ± ---	--- ± ---	--- ± ---	--- ± ---	--- ± ---	--- ± ---	--- ± ---	--- ± ---	--- ± ---	--- ± ---	--- ± ---	--- ± ---	--- ± ---	--- ± ---	--- ± ---	--- ± ---	--- ± ---	--- ± ---
Junpr.Mt.	9/21	6	73	9.2	30.3 ± 14.6	--- ± ---	--- ± ---	--- ± ---	--- ± ---	--- ± ---	--- ± ---	--- ± ---	--- ± ---	--- ± ---	--- ± ---	--- ± ---	--- ± ---	--- ± ---	--- ± ---	--- ± ---	--- ± ---	--- ± ---	--- ± ---	--- ± ---
Junpr.Mt.	9/21	12	50	9.2	--- ± ---	--- ± ---	--- ± ---	--- ± ---	--- ± ---	--- ± ---	--- ± ---	--- ± ---	--- ± ---	--- ± ---	--- ± ---	--- ± ---	--- ± ---	--- ± ---	--- ± ---	--- ± ---	--- ± ---	--- ± ---	--- ± ---	--- ± ---
Junpr.Mt.	9/24	6	72	9.2	17.0 ± 0.9	9.0 ± 1.7	1.6 ± 1.4	3.7 ± 1.4	27.8 ± 1.4	22.0 ± 2.3	4.7 ± 0.3	0.5 ± 0.1	3.5 ± 1.7	3.7 ± 1.4	0.3 ± 0.1	5.8 ± 2.6								
Junpr.Mt.	9/24	12	35	9.2	10.2 ± 0.5	6.6 ± 1.4	0.0 ± 1.4	4.9 ± 1.8	19.3 ± 1.4	20.7 ± 2.3	2.6 ± 0.1	0.2 ± 0.1	3.7 ± 1.4	4.9 ± 1.8	0.2 ± 0.1	-1.4 ± 2.7								
Junpr.Mt.	9/27	6	42	9.2	11.7 ± 0.3	7.2 ± 1.1	1.6 ± 1.4	4.2 ± 0.8	22.4 ± 1.4	20.6 ± 1.3	3.1 ± 0.2	0.3 ± 0.1	3.1 ± 1.0	4.2 ± 0.8	0.7 ± 0.1	1.8 ± 1.9								
Junpr.Mt.	9/27	12	28	9.2	13.2 ± 0.4	13.3 ± 1.2	4.9 ± 1.4	6.6 ± 1.1	27.2 ± 1.4	29.1 ± 1.7	3.0 ± 0.2	0.6 ± 0.1	6.4 ± 1.2	6.6 ± 1.1	3.3 ± 0.1	-1.9 ± 2.2								
Junpr.Mt.	9/30	6	79	9.2	763.8 ± 373.2	--- ± ---	--- ± ---	--- ± ---	--- ± ---	--- ± ---	--- ± ---	--- ± ---	--- ± ---	--- ± ---	--- ± ---	--- ± ---	--- ± ---	--- ± ---	--- ± ---	--- ± ---	--- ± ---	--- ± ---	--- ± ---	--- ± ---
Junpr.Mt.	9/30	12	---	9.2	--- ± ---	--- ± ---	--- ± ---	--- ± ---	--- ± ---	--- ± ---	--- ± ---	--- ± ---	--- ± ---	--- ± ---	--- ± ---	--- ± ---	--- ± ---	--- ± ---	--- ± ---	--- ± ---	--- ± ---	--- ± ---	--- ± ---	--- ± ---
Junpr.Mt.	10/1	6	82	9.2	--- ± ---	--- ± ---	--- ± ---	--- ± ---	--- ± ---	--- ± ---	--- ± ---	--- ± ---	--- ± ---	--- ± ---	--- ± ---	--- ± ---	--- ± ---	--- ± ---	--- ± ---	--- ± ---	--- ± ---	--- ± ---	--- ± ---	--- ± ---
Junpr.Mt.	10/1	12	---	9.2	--- ± ---	--- ± ---	--- ± ---	--- ± ---	--- ± ---	--- ± ---	--- ± ---	--- ± ---	--- ± ---	--- ± ---	--- ± ---	--- ± ---	--- ± ---	--- ± ---	--- ± ---	--- ± ---	--- ± ---	--- ± ---	--- ± ---	--- ± ---
Junpr.Mt.	10/2	6	50	9.2	4.4 ± 0.1	--- ± ---	--- ± ---	--- ± ---	--- ± ---	--- ± ---	--- ± ---	--- ± ---	--- ± ---	--- ± ---	--- ± ---	--- ± ---	--- ± ---	--- ± ---	--- ± ---	--- ± ---	--- ± ---	--- ± ---	--- ± ---	--- ± ---
Junpr.Mt.	10/2	12	42	9.2	4.2 ± 0.2	--- ± ---	--- ± ---	--- ± ---	--- ± ---	--- ± ---	--- ± ---	--- ± ---	--- ± ---	--- ± ---	--- ± ---	--- ± ---	--- ± ---	--- ± ---	--- ± ---	--- ± ---	--- ± ---	--- ± ---	--- ± ---	--- ± ---
Junpr.Mt.	10/7	6	37	9.2	4.5 ± 0.2	5.0 ± 1.3	0.0 ± 1.4	2.3 ± 0.9	13.7 ± 1.4	16.4 ± 1.6	1.5 ± 0.1	0.2 ± 0.1	2.5 ± 1.3	2.3 ± 0.9	0.8 ± 0.1	-2.8 ± 2.2								
Junpr.Mt.	10/7	12	---	9.2	--- ± ---	--- ± ---	--- ± ---	--- ± ---	--- ± ---	--- ± ---	--- ± ---	--- ± ---	--- ± ---	--- ± ---	--- ± ---	--- ± ---	--- ± ---	--- ± ---	--- ± ---	--- ± ---	--- ± ---	--- ± ---	--- ± ---	--- ± ---
Junpr.Mt.	10/8	6	63	9.2	20.5 ± 1.9	6.4 ± 1.5	3.3 ± 1.4	3.8 ± 1.4	33.0 ± 1.4	19.4 ± 2.1	2.3 ± 0.2	0.7 ± 0.1	2.9 ± 1.5	3.8 ± 1.4	0.5 ± 0.1	13.6 ± 2.5								
Junpr.Mt.	10/8	12	33	9.2	6.8 ± 0.8	4.8 ± 1.3	5.1 ± 1.5	2.5 ± 1.0	21.1 ± 1.5	16.5 ± 1.7	1.3 ± 0.1	0.2 ± 0.1	2.9 ± 1.3	2.5 ± 1.0	0.4 ± 0.1	4.6 ± 2.2								
Junpr.Mt.	10/9	6	34	9.2	8.7 ± 0.4	3.8 ± 1.2	1.7 ± 1.5	2.1 ± 0.9	19.5 ± 1.5	15.1 ± 1.5	1.1 ± 0.1	0.3 ± 0.1	1.6 ± 1.2	2.1 ± 0.9	0.8 ± 0.1	4.4 ± 2.1								
Junpr.Mt.	10/9	12	28	9.2	9.7 ± 0.2	3.0 ± 1.1	3.3 ± 1.5	1.6 ± 0.7	22.2 ± 1.5	13.8 ± 1.3	1.2 ± 0.1	0.3 ± 0.1	0.8 ± 1.1	1.6 ± 0.7	0.6 ± 0.1	8.4 ± 2.0								
Junpr.Mt.	10/10	6	35	9.2	12.3 ± 0.4	6.9 ± 1.1	3.3 ± 1.4	4.0 ± 0.8	24.8 ± 1.4	20.0 ± 1.3	1.2 ± 0.1	0.3 ± 0.1	4.7 ± 1.1	4.0 ± 0.8	0.7 ± 0.1	4.7 ± 2.0								
Junpr.Mt.	10/10	12	---	9.2	--- ± ---	--- ± ---	--- ± ---	--- ± ---	--- ± ---	--- ± ---	--- ± ---	--- ± ---	--- ± ---	--- ± ---	--- ± ---	--- ± ---	--- ± ---	--- ± ---	--- ± ---	--- ± ---	--- ± ---	--- ± ---	--- ± ---	--- ± ---
Junpr.Mt.	10/11	6	25	9.2	6.9 ± 0.3	--- ± ---	--- ± ---	--- ± ---	--- ± ---	--- ± ---	--- ± ---	--- ± ---	--- ± ---	--- ± ---	--- ± ---	--- ± ---	--- ± ---	--- ± ---	--- ± ---	--- ± ---	--- ± ---	--- ± ---	--- ± ---	--- ± ---
Junpr.Mt.	10/11	12	20	9.2	7.0 ± 0.4	10.0 ± 1.5	5.0 ± 1.5	3.6 ± 1.4	21.2 ± 1.5	22.8 ± 2.0	3.6 ± 0.2	0.3 ± 0.1	4.7 ± 1.5	3.6 ± 1.4	1.5 ± 0.1	-1.6 ± 2.5								
Junpr.Mt.	10/12	6	38	9.2	17.7 ± 0.6	14.6 ± 1.7	5.0 ± 1.5	3.4 ± 1.3	31.8 ± 1.5	27.2 ± 2.1	2.5 ± 0.1	0.4 ± 0.1	6.0 ± 1.7	3.4 ± 1.3	5.7 ± 0.3	4.6 ± 2.6								
Junpr.Mt.	10/12	12	44	9.2	19.8 ± 1.6	11.1 ± 2.7	2.7 ± 2.4	4.9 ± 1.9	31.7 ± 2.4	25.2 ± 3.3	0.7 ± 0.1	0.5 ± 0.2	9.2 ± 2.7	4.9 ± 1.9	0.7 ± 0.1	6.5 ± 4.1								

Junpr.Mt.	10/13	6	68	9.2	--- ± ---	--- ± ---	0.0 ± 3.6	--- ± ---	18.5 ± 3.6	--- ± ---	--- ± ---	--- ± ---	--- ± ---	--- ± ---	--- ± ---	--- ± ---	--- ± ---	--- ± ---	--- ± ---	--- ± ---	--- ± ---
Junpr.Mt.	10/13	12	---	9.2	--- ± ---	--- ± ---	--- ± ---	--- ± ---	--- ± ---	--- ± ---	--- ± ---	--- ± ---	--- ± ---	--- ± ---	--- ± ---	--- ± ---	--- ± ---	--- ± ---	--- ± ---	--- ± ---	--- ± ---	--- ± ---
Junpr.Mt.	10/14	6	33	9.2	3.3 ± 0.3	3.5 ± 1.3	0.0 ± 1.4	1.6 ± 0.7	12.5 ± 1.4	14.3 ± 1.4	0.6 ± 0.1	0.3 ± 0.1	2.3 ± 1.3	1.6 ± 0.7	0.3 ± 0.1	-1.8 ± 2.0						
Junpr.Mt.	10/14	12	30	9.2	1.7 ± 0.2	1.6 ± 1.1	0.0 ± 0.0	0.0 ± 0.4	10.8 ± 0.0	10.8 ± 1.2	0.4 ± 0.1	0.2 ± 0.1	0.8 ± 1.1	0.0 ± 0.4	0.2 ± 0.1	0.0 ± 1.2						
Junpr.Mt.	10/16	6	25	9.2	4.3 ± 0.3	5.0 ± 1.4	0.0 ± 2.2	3.5 ± 0.8	13.5 ± 2.2	17.7 ± 1.6	2.4 ± 0.2	0.5 ± 0.1	0.9 ± 1.4	3.5 ± 0.8	1.2 ± 0.1	-4.2 ± 2.7						
Junpr.Mt.	10/17	6	34	9.2	12.0 ± 0.6	5.1 ± 0.6	2.5 ± 0.7	2.8 ± 0.5	23.6 ± 0.7	17.1 ± 0.8	1.7 ± 0.1	0.3 ± 0.0	2.5 ± 0.6	2.8 ± 0.5	0.6 ± 0.0	6.6 ± 1.1						
Junpr.Mt.	10/18	6	28	9.2	9.9 ± 0.6	4.6 ± 0.5	2.5 ± 0.7	2.1 ± 0.4	21.5 ± 0.7	15.9 ± 0.7	1.6 ± 0.1	0.4 ± 0.0	1.8 ± 0.5	2.1 ± 0.4	0.8 ± 0.0	5.7 ± 1.0						
Junpr.Mt.	10/19	6	---	9.2	--- ± ---	--- ± ---	--- ± ---	--- ± ---	--- ± ---	--- ± ---	--- ± ---	--- ± ---	--- ± ---	--- ± ---	--- ± ---	--- ± ---	--- ± ---	--- ± ---	--- ± ---	--- ± ---	--- ± ---	--- ± ---
Junpr.Mt.	10/22	6	91	9.2	603.9 ± 109.7	4.1 ± 1.2	0.8 ± 0.7	0.4 ± 0.2	613.9 ± 0.7	13.6 ± 1.2	0.8 ± 0.2	0.6 ± 0.2	1.9 ± 1.2	0.4 ± 0.2	0.7 ± 0.1	600.3 ± 1.4						
Junpr.Mt.	10/23	6	84	9.2	38.9 ± 2.5	8.3 ± 0.9	2.5 ± 0.7	1.5 ± 0.3	50.5 ± 0.7	18.9 ± 0.9	6.0 ± 0.3	0.5 ± 0.1	1.4 ± 0.8	1.5 ± 0.3	0.3 ± 0.1	31.6 ± 1.2						

Table 4.3.4
Measured and Calculated Component Contributions to Total Light Extinction at Baggs

Site	Date	Hr	RH	Cln Air	bsp	Ebsp	babs	Ebabs	bext	Ebext	Esul	Enit	Eoc	Eec	Esoil	Unid.
Baggs	2/23	6	62	9.5	8.311 + 0.8	9.6 + 1.9	1.6 + 1.4	6.3 + 1.2	19.4 + 2.2	25.4 + 2.3	2.3 + 0.1	1.3 + 0.1	5.7 + 1.9	6.3 + 1.2	0.4 + 0.2	-6.0 + 3.2
Baggs	2/23	12	48	9.5	8.0 ± 0.6	7.5 ± 1.8	1.6 ± 1.4	3.8 ± 0.8	19.1 ± 2.2	20.9 ± 2.0	3.3 ± 0.2	1.2 ± 0.1	2.7 ± 1.8	3.8 ± 0.8	0.4 ± 0.2	-1.7 ± 3.0
Baggs	8/7	6	23	9.5	17.5 ± 0.6	17.4 ± 2.2	11.8 ± 1.6	4.4 ± 1.7	38.8 ± 1.6	31.3 ± 2.8	3.1 ± 0.2	0.4 ± 0.1	12.6 ± 2.2	4.4 ± 1.7	1.3 ± 0.2	7.4 ± 3.2
Baggs	8/7	12	13	9.5	15.8 ± 0.3	11.4 ± 1.8	11.1 ± 1.5	5.0 ± 1.3	36.5 ± 1.5	25.9 ± 2.2	2.5 ± 0.1	0.3 ± 0.1	7.9 ± 1.8	5.0 ± 1.3	0.8 ± 0.2	10.5 ± 2.7
Baggs	8/8	6	32	9.5	23.0 ± 2.3	21.3 ± 2.3	14.4 ± 1.6	3.8 ± 1.5	46.9 ± 1.6	34.7 ± 2.7	3.9 ± 0.2	0.7 ± 0.1	14.1 ± 2.2	3.8 ± 1.5	2.6 ± 0.2	12.2 ± 3.1
Baggs	8/8	12	24	9.5	16.0 ± 0.8	21.8 ± 2.8	10.4 ± 1.6	11.9 ± 3.8	35.9 ± 1.6	43.2 ± 4.7	2.2 ± 0.1	0.7 ± 0.1	16.6 ± 2.8	11.9 ± 3.8	2.2 ± 0.2	-7.3 ± 5.0
Baggs	8/9	6	30	9.5	10.5 ± 0.6	13.7 ± 2.0	3.3 ± 1.5	0.5 ± 0.5	23.3 ± 1.5	23.7 ± 2.0	1.4 ± 0.1	0.3 ± 0.1	9.7 ± 2.0	0.5 ± 0.5	2.3 ± 0.2	-0.4 ± 2.5
Baggs	8/9	12	14	9.5	9.1 ± 0.3	13.1 ± 1.9	3.5 ± 1.5	4.7 ± 1.7	22.1 ± 1.5	27.3 ± 2.6	1.6 ± 0.1	0.4 ± 0.1	9.1 ± 1.9	4.7 ± 1.7	1.9 ± 0.2	-5.2 ± 3.0
Baggs	8/14	6	50	9.5	6.5 ± 0.4	10.7 ± 2.2	0.0 ± 1.5	7.5 ± 1.4	16.0 ± 1.5	27.6 ± 2.6	1.0 ± 0.1	0.6 ± 0.1	8.4 ± 2.2	7.5 ± 1.4	0.6 ± 0.2	-11.6 ± 3.0
Baggs	8/21	6	---	9.5	--- ± ---	--- ± ---	--- ± ---	--- ± ---	--- ± ---	--- ± ---	--- ± ---	--- ± ---	--- ± ---	--- ± ---	--- ± ---	--- ± ---
Baggs	8/21	12	---	9.5	--- ± ---	--- ± ---	--- ± ---	--- ± ---	--- ± ---	--- ± ---	--- ± ---	--- ± ---	--- ± ---	--- ± ---	--- ± ---	--- ± ---
Baggs	8/22	6	56	9.5	14.8 ± 0.8	16.1 ± 2.4	5.4 ± 1.6	2.8 ± 1.2	29.8 ± 1.6	28.4 ± 2.6	5.1 ± 0.3	0.3 ± 0.1	10.3 ± 2.3	2.8 ± 1.2	0.4 ± 0.2	1.3 ± 3.1
Baggs	8/22	12	37	9.5	12.5 ± 0.3	17.5 ± 2.2	5.5 ± 1.6	6.0 ± 2.2	27.5 ± 1.6	33.0 ± 3.1	4.5 ± 0.2	0.3 ± 0.1	12.5 ± 2.2	6.0 ± 2.2	0.3 ± 0.2	-5.5 ± 3.5
Baggs	8/23	6	58	9.5	14.8 ± 0.6	15.3 ± 2.4	3.7 ± 1.6	3.1 ± 1.2	28.0 ± 1.6	27.9 ± 2.7	3.8 ± 0.2	0.2 ± 0.1	10.8 ± 2.4	3.1 ± 1.2	0.4 ± 0.2	0.1 ± 3.1
Baggs	8/23	12	41	9.5	12.5 ± 0.5	12.4 ± 2.0	5.5 ± 1.6	1.8 ± 0.8	27.5 ± 1.6	23.7 ± 2.2	4.7 ± 0.3	0.2 ± 0.1	7.1 ± 2.0	1.8 ± 0.8	0.3 ± 0.2	3.8 ± 2.7
Baggs	8/24	6	60	9.5	15.5 ± 1.0	19.4 ± 2.6	5.4 ± 1.6	4.0 ± 1.5	30.4 ± 1.6	32.9 ± 3.0	5.6 ± 0.3	0.4 ± 0.1	13.0 ± 2.5	4.0 ± 1.5	0.4 ± 0.2	-2.6 ± 3.4
Baggs	8/24	12	56	9.5	12.6 ± 1.6	18.1 ± 2.6	3.6 ± 1.6	2.8 ± 1.1	25.8 ± 1.6	30.4 ± 2.9	2.9 ± 0.2	0.4 ± 0.1	14.3 ± 2.6	2.8 ± 1.1	0.5 ± 0.2	-4.6 ± 3.3
Baggs	8/25	6	64	9.5	19.5 ± 1.2	19.4 ± 2.7	5.2 ± 1.5	3.1 ± 1.2	34.2 ± 1.5	32.1 ± 3.0	3.3 ± 0.2	0.3 ± 0.1	15.5 ± 2.7	3.1 ± 1.2	0.4 ± 0.2	2.1 ± 3.4
Baggs	8/25	12	32	9.5	16.5 ± 0.8	17.3 ± 2.3	5.3 ± 1.6	2.1 ± 0.9	31.3 ± 1.6	28.9 ± 2.5	3.4 ± 0.2	0.2 ± 0.1	13.3 ± 2.3	2.1 ± 0.9	0.4 ± 0.2	2.4 ± 2.9
Baggs	8/26	6	47	9.5	11.5 ± 0.8	19.7 ± 2.6	1.8 ± 1.5	9.7 ± 1.7	22.8 ± 1.5	38.9 ± 3.1	4.4 ± 0.2	0.4 ± 0.1	14.5 ± 2.5	9.7 ± 1.7	0.3 ± 0.2	-16.2 ± 3.4
Baggs	8/26	12	24	9.5	7.8 ± 0.4	13.2 ± 2.1	1.8 ± 1.5	9.5 ± 1.7	19.1 ± 1.5	32.2 ± 2.7	3.0 ± 0.2	0.4 ± 0.1	9.4 ± 2.1	9.5 ± 1.7	0.4 ± 0.2	-13.1 ± 3.1
Baggs	8/27	6	41	9.5	14.1 ± 0.8	14.9 ± 2.3	1.8 ± 1.5	4.1 ± 0.9	25.4 ± 1.5	28.5 ± 2.5	3.0 ± 0.2	0.4 ± 0.1	11.0 ± 2.3	4.1 ± 0.9	0.5 ± 0.2	-3.1 ± 2.9
Baggs	8/27	12	24	9.5	9.3 ± 0.4	13.3 ± 2.1	3.6 ± 1.6	6.4 ± 1.3	22.4 ± 1.6	29.2 ± 2.4	3.0 ± 0.2	0.3 ± 0.1	9.6 ± 2.1	6.4 ± 1.3	0.3 ± 0.2	-6.8 ± 2.9

Baggs	9/2	6	42	9.5	19.3 ± 0.3	19.9 ± 2.4	3.5 ± 1.5	7.6 ± 1.4	32.3 ± 1.5	37.0 ± 2.8	5.7 ± 0.3	0.5 ± 0.1	13.2 ± 2.4	7.6 ± 1.4	0.5 ± 0.2	-4.7 ± 3.2
Baggs	9/2	12	33	9.5	14.1 ± 1.5	12.1 ± 2.1	1.7 ± 1.5	1.8 ± 0.6	25.4 ± 1.5	23.4 ± 2.2	2.8 ± 0.2	0.3 ± 0.1	8.5 ± 2.0	1.8 ± 0.6	0.4 ± 0.2	2.0 ± 2.6
Baggs	9/17	6	36	9.5	10.6 ± 0.5	17.0 ± 2.5	3.6 ± 1.6	4.4 ± 1.0	23.7 ± 1.6	30.9 ± 2.6	1.9 ± 0.1	0.4 ± 0.1	14.0 ± 2.4	4.4 ± 1.0	0.7 ± 0.2	-7.2 ± 3.1
Baggs	9/17	12	28	9.5	10.6 ± 0.8	18.7 ± 2.5	3.7 ± 1.6	4.2 ± 1.0	23.9 ± 1.6	32.4 ± 2.7	2.7 ± 0.2	0.3 ± 0.1	14.0 ± 2.5	4.2 ± 1.0	1.6 ± 0.2	-8.5 ± 3.1
Baggs	9/18	6	89	9.5	39.1 ± 5.9	35.4 ± 4.8	5.4 ± 1.6	5.1 ± 1.1	54.0 ± 1.6	50.1 ± 5.0	13.7 ± 0.8	0.9 ± 0.3	20.2 ± 4.8	5.1 ± 1.1	0.7 ± 0.3	3.9 ± 5.2
Baggs	9/18	12	82	9.5	21.8 ± 2.0	22.6 ± 3.4	3.6 ± 1.6	6.2 ± 1.2	34.9 ± 1.6	38.3 ± 3.6	7.9 ± 0.4	0.5 ± 0.2	13.5 ± 3.4	6.2 ± 1.2	0.7 ± 0.3	-3.4 ± 4.0
Baggs	9/19	6	85	9.5	475.6 ± 397.7	26.4 ± 3.8	1.8 ± 1.5	7.3 ± 1.3	486.9 ± 1.5	43.2 ± 4.1	9.0 ± 0.5	1.5 ± 0.3	15.5 ± 3.8	7.3 ± 1.3	0.4 ± 0.3	443.7 ± 4.4
Baggs	9/19	12	54	9.5	13.0 ± 1.5	15.0 ± 2.5	3.7 ± 1.6	9.0 ± 1.6	26.2 ± 1.6	33.6 ± 3.0	2.1 ± 0.1	0.4 ± 0.1	11.8 ± 2.5	9.0 ± 1.6	0.8 ± 0.2	-7.4 ± 3.4
Baggs	9/20	6	78	9.5	26.1 ± 3.6	16.3 ± 3.0	1.8 ± 1.5	6.4 ± 1.3	37.4 ± 1.5	32.2 ± 3.2	6.3 ± 0.4	0.6 ± 0.2	9.1 ± 2.9	6.4 ± 1.3	0.3 ± 0.2	5.2 ± 3.6
Baggs	9/20	12	60	9.5	13.3 ± 0.8	8.9 ± 2.2	1.8 ± 1.6	3.6 ± 0.9	24.6 ± 1.6	22.1 ± 2.4	3.6 ± 0.2	0.2 ± 0.1	4.9 ± 2.2	3.6 ± 0.9	0.2 ± 0.2	2.5 ± 2.9
Baggs	9/21	6	61	9.5	5.6 ± 0.7	7.4 ± 2.3	0.0 ± 1.6	4.0 ± 0.9	15.2 ± 1.6	20.9 ± 2.5	2.1 ± 0.2	0.2 ± 0.1	5.1 ± 2.3	4.0 ± 0.9	0.1 ± 0.2	-5.7 ± 2.9
Baggs	9/21	12	36	9.5	4.3 ± 0.4	6.2 ± 2.0	0.0 ± 1.6	0.0 ± 0.6	13.8 ± 1.6	15.8 ± 2.0	0.9 ± 0.1	0.2 ± 0.1	4.7 ± 2.0	0.0 ± 0.6	0.4 ± 0.2	-1.9 ± 2.6
Baggs	9/24	6	46	9.5	12.6 ± 1.4	11.5 ± 1.6	2.7 ± 0.8	2.3 ± 1.0	24.9 ± 0.8	23.3 ± 1.9	4.3 ± 0.2	0.3 ± 0.1	6.3 ± 1.6	2.3 ± 1.0	0.6 ± 0.1	1.6 ± 2.0
Baggs	9/24	12	31	9.5	8.8 ± 0.2	6.7 ± 2.1	1.8 ± 1.6	0.0 ± 0.6	20.1 ± 1.6	16.2 ± 2.2	3.2 ± 0.2	0.1 ± 0.1	3.1 ± 2.1	0.0 ± 0.6	0.3 ± 0.2	3.9 ± 2.7
Baggs	9/27	6	---	9.5	--- ± ---	--- ± ---	--- ± ---	--- ± ---	--- ± ---	--- ± ---	--- ± ---	--- ± ---	--- ± ---	--- ± ---	--- ± ---	--- ± ---
Baggs	9/27	12	---	9.5	--- ± ---	--- ± ---	--- ± ---	--- ± ---	--- ± ---	--- ± ---	--- ± ---	--- ± ---	--- ± ---	--- ± ---	--- ± ---	--- ± ---
Baggs	9/30	6	89	9.5	--- ± ---	15.0 ± 5.2	0.0 ± 1.6	2.5 ± 1.2	13.3 ± 1.6	27.0 ± 5.3	2.4 ± 0.3	0.6 ± 0.3	11.7 ± 5.1	2.5 ± 1.2	0.3 ± 0.3	-13.7 ± 5.5
Baggs	9/30	12	69	9.5	15.0 ± 0.7	13.8 ± 3.1	1.8 ± 1.6	0.0 ± 0.5	26.3 ± 1.6	23.3 ± 3.2	4.0 ± 0.2	0.2 ± 0.1	9.2 ± 3.1	0.0 ± 0.5	0.3 ± 0.2	3.0 ± 3.5
Baggs	10/1	6	63	9.5	14.3 ± 4.3	8.5 ± 2.6	0.0 ± 1.6	3.5 ± 1.6	23.8 ± 1.6	21.6 ± 3.1	2.9 ± 0.2	0.3 ± 0.1	4.9 ± 2.6	3.5 ± 1.6	0.4 ± 0.2	2.2 ± 3.5
Baggs	10/1	12	37	9.5	4.5 ± 0.2	8.9 ± 2.5	1.9 ± 1.6	1.2 ± 0.8	15.9 ± 1.6	19.6 ± 2.6	0.9 ± 0.1	0.1 ± 0.1	7.5 ± 2.5	1.2 ± 0.8	0.3 ± 0.2	-3.7 ± 3.1
Baggs	10/2	6	61	9.5	8.8 ± 0.7	7.0 ± 2.2	0.0 ± 1.6	4.1 ± 0.9	18.3 ± 1.6	20.6 ± 2.4	1.8 ± 0.1	0.8 ± 0.1	3.9 ± 2.2	4.1 ± 0.9	0.4 ± 0.2	-2.3 ± 2.9
Baggs	10/2	12	29	9.5	5.0 ± 0.4	7.6 ± 2.0	0.0 ± 1.6	1.1 ± 0.6	14.5 ± 1.6	18.2 ± 2.1	1.0 ± 0.1	0.5 ± 0.1	5.9 ± 2.0	1.1 ± 0.6	0.3 ± 0.2	-3.7 ± 2.6
Baggs	10/7	6	45	9.5	6.5 ± 0.5	5.9 ± 2.2	0.0 ± 1.6	1.9 ± 1.1	16.0 ± 1.6	17.3 ± 2.5	1.7 ± 0.1	0.2 ± 0.1	3.0 ± 2.2	1.9 ± 1.1	1.0 ± 0.2	-1.3 ± 3.0
Baggs	10/7	12	27	9.5	7.3 ± 0.6	5.3 ± 2.1	1.8 ± 1.6	1.9 ± 1.1	18.7 ± 1.6	16.7 ± 2.3	1.6 ± 0.1	0.2 ± 0.1	2.8 ± 2.1	1.9 ± 1.1	0.8 ± 0.2	1.9 ± 2.8
Baggs	10/8	6	66	9.5	25.1 ± 3.6	13.4 ± 3.0	5.5 ± 1.6	8.6 ± 3.4	40.1 ± 1.6	31.5 ± 4.5	3.2 ± 0.2	1.2 ± 0.2	8.2 ± 3.0	8.6 ± 3.4	0.8 ± 0.2	8.6 ± 4.8
Baggs	10/8	12	27	9.5	8.0 ± 0.5	5.7 ± 2.1	1.8 ± 1.6	1.9 ± 1.0	19.3 ± 1.6	17.0 ± 2.4	1.3 ± 0.1	0.1 ± 0.1	3.7 ± 2.1	1.9 ± 1.0	0.5 ± 0.2	2.3 ± 2.8
Baggs	10/9	6	43	9.5	8.5 ± 0.3	5.5 ± 2.2	3.6 ± 1.6	1.2 ± 0.8	21.6 ± 1.6	16.2 ± 2.4	1.6 ± 0.1	0.3 ± 0.1	3.0 ± 2.2	1.2 ± 0.8	0.7 ± 0.2	5.4 ± 2.9
Baggs	10/9	12	26	9.5	7.6 ± 0.2	6.7 ± 2.3	0.0 ± 1.6	1.8 ± 1.1	17.2 ± 1.6	18.0 ± 2.6	1.1 ± 0.1	0.3 ± 0.1	4.4 ± 2.3	1.8 ± 1.1	1.0 ± 0.2	-0.8 ± 3.0
Baggs	10/10	6	40	9.5	11.5 ± 0.2	8.7 ± 2.0	3.6 ± 1.6	1.7 ± 0.7	24.6 ± 1.6	19.9 ± 2.1	1.5 ± 0.1	0.4 ± 0.1	6.0 ± 2.0	1.7 ± 0.7	0.8 ± 0.2	4.8 ± 2.7
Baggs	10/10	12	25	9.5	7.8 ± 0.3	8.5 ± 2.0	3.7 ± 1.6	2.5 ± 0.7	21.0 ± 1.6	20.5 ± 2.1	1.1 ± 0.1	0.5 ± 0.1	6.3 ± 2.0	2.5 ± 0.7	0.7 ± 0.2	0.5 ± 2.7
Baggs	10/11	6	36	9.5	7.8 ± 0.2	7.0 ± 2.3	3.6 ± 1.6	1.1 ± 0.8	20.9 ± 1.6	17.7 ± 2.4	1.1 ± 0.1	0.1 ± 0.1	5.1 ± 2.3	1.1 ± 0.8	0.7 ± 0.2	3.3 ± 2.9
Baggs	10/11	12	19	9.5	9.3 ± 0.6	11.3 ± 2.6	3.7 ± 1.6	1.7 ± 1.0	22.6 ± 1.6	22.6 ± 2.8	1.4 ± 0.1	0.2 ± 0.1	8.5 ± 2.6	1.7 ± 1.0	1.2 ± 0.2	0.0 ± 3.2
Baggs	10/12	6	36	9.5	16.1 ± 0.3	11.4 ± 2.5	7.3 ± 1.6	4.1 ± 1.8	32.9 ± 1.6	25.0 ± 3.0	3.6 ± 0.2	0.2 ± 0.1	6.7 ± 2.4	4.1 ± 1.8	0.9 ± 0.2	7.9 ± 3.4
Baggs	10/12	12	40	9.5	15.5 ± 1.7	9.2 ± 2.4	3.7 ± 1.6	0.0 ± 0.6	28.7 ± 1.6	18.7 ± 2.4	2.5 ± 0.1	0.3 ± 0.1	4.9 ± 2.3	0.0 ± 0.6	1.5 ± 0.2	10.0 ± 2.9
Baggs	10/13	6	56	9.5	3.8 ± 0.3	5.5 ± 2.4	1.8 ± 1.6	1.9 ± 1.1	15.1 ± 1.6	16.9 ± 2.6	0.8 ± 0.1	0.3 ± 0.1	3.9 ± 2.4	1.9 ± 1.1	0.5 ± 0.2	-1.8 ± 3.1
Baggs	10/13	12	25	9.5	2.5 ± 0.2	3.4 ± 2.0	0.0 ± 1.8	0.1 ± 0.6	12.0 ± 1.8	13.0 ± 2.1	0.6 ± 0.1	0.1 ± 0.1	2.1 ± 2.0	0.1 ± 0.6	0.6 ± 0.2	-1.0 ± 2.7
Baggs	10/14	6	37	9.5	4.1 ± 0.3	2.6 ± 2.0	1.8 ± 1.6	0.8 ± 0.7	15.5 ± 1.6	13.0 ± 2.1	0.7 ± 0.1	0.2 ± 0.1	1.2 ± 2.0	0.8 ± 0.7	0.5 ± 0.2	2.5 ± 2.7
Baggs	10/14	12	28	9.5	2.6 ± 0.3	7.5 ± 2.4	1.8 ± 1.6	2.2 ± 1.1	14.0 ± 1.6	19.2 ± 2.6	0.8 ± 0.1	0.2 ± 0.1	6.2 ± 2.4	2.2 ± 1.1	0.4 ± 0.2	-5.2 ± 3.1

Table 4.3.5
Measured and Calculated Component Contributions to Total Light Extinction at Hayden VOR

Site	Date	Hr	RH	Cln Air	bsp	Ebsp	babs	Ebabs	bext	Ebext	Esul	Enit	Eoc	Eec	Esoil	Unid.
Hdn.VOR	2/16	6	---	9.4	--- + ---	--- + ---	--- + ---	--- + ---	--- + ---	--- + ---	--- + ---	--- + ---	--- + ---	--- + ---	--- + ---	--- + ---
Hdn.VOR	2/16	12	47	9.4	--- ± ---	--- ± ---	--- ± ---	--- ± ---	--- ± ---	--- ± ---	--- ± ---	--- ± ---	--- ± ---	--- ± ---	--- ± ---	--- ± ---
Hdn.VOR	2/17	6	37	9.4	13.5 ± 0.5	--- ± ---	3.4 ± 0.8	--- ± ---	26.4 ± 4.2	--- ± ---	--- ± ---	--- ± ---	--- ± ---	--- ± ---	--- ± ---	--- ± ---
Hdn.VOR	2/17	12	35	9.4	13.1 ± 0.8	2.2 ± 3.0	2.8 ± 2.4	6.9 ± 2.4	25.3 ± 4.7	18.4 ± 3.9	0.7 ± 0.2	0.8 ± 0.1	0.2 ± 3.0	6.9 ± 2.4	0.4 ± 0.0	6.8 ± 6.1
Hdn.VOR	2/19	6	68	9.4	18.6 ± 7.9	--- ± ---	4.1 ± 0.9	--- ± ---	32.1 ± 6.4	--- ± ---	--- ± ---	--- ± ---	--- ± ---	--- ± ---	--- ± ---	--- ± ---
Hdn.VOR	2/19	12	---	9.4	--- ± ---	--- ± ---	--- ± ---	--- ± ---	--- ± ---	--- ± ---	--- ± ---	--- ± ---	--- ± ---	--- ± ---	--- ± ---	--- ± ---
Hdn.VOR	2/23	6	55	9.4	8.3 ± 0.8	10.5 ± 1.6	--- ± ---	3.2 ± 0.7	--- ± ---	23.1 ± 1.7	3.2 ± 0.2	1.8 ± 0.1	4.8 ± 1.6	3.2 ± 0.7	0.7 ± 0.0	--- ± ---
Hdn.VOR	2/23	12	47	9.4	9.4 ± 0.9	--- ± ---	--- ± ---	--- ± ---	--- ± ---	--- ± ---	--- ± ---	--- ± ---	--- ± ---	--- ± ---	--- ± ---	--- ± ---
Hdn.VOR	2/24	6	67	9.4	17.1 ± 3.1	19.1 ± 4.3	2.9 ± 2.5	12.0 ± 3.8	29.4 ± 5.3	40.6 ± 5.7	4.2 ± 0.4	2.1 ± 0.2	12.0 ± 4.2	12.0 ± 3.8	0.9 ± 0.0	-11.2 ± 7.8
Hdn.VOR	2/24	12	43	9.4	--- ± ---	--- ± ---	--- ± ---	--- ± ---	--- ± ---	--- ± ---	--- ± ---	--- ± ---	--- ± ---	--- ± ---	--- ± ---	--- ± ---
Hdn.VOR	2/26	6	70	9.4	19.8 ± 2.7	16.7 ± 2.6	6.8 ± 1.5	3.7 ± 1.3	35.9 ± 5.2	29.9 ± 2.9	8.3 ± 0.5	4.7 ± 0.3	2.4 ± 2.5	3.7 ± 1.3	1.2 ± 0.0	6.1 ± 6.0
Hdn.VOR	2/26	12	60	9.4	11.8 ± 0.8	14.9 ± 2.5	1.8 ± 1.5	4.7 ± 1.7	22.9 ± 4.0	29.0 ± 3.0	4.1 ± 0.3	2.0 ± 0.1	8.0 ± 2.5	4.7 ± 1.7	0.8 ± 0.0	-6.1 ± 5.0
Hdn.VOR	8/7	6	31	9.4	16.3 ± 0.7	12.2 ± 2.2	12.4 ± 1.5	6.5 ± 2.2	38.1 ± 9.5	28.1 ± 3.1	2.3 ± 0.2	0.3 ± 0.1	8.5 ± 2.2	6.5 ± 2.2	1.0 ± 0.0	10.0 ± 10.0
Hdn.VOR	8/7	12	17	9.4	13.1 ± 0.2	11.9 ± 1.9	11.5 ± 1.5	4.1 ± 1.4	34.0 ± 8.7	25.4 ± 2.4	3.5 ± 0.2	0.3 ± 0.1	6.7 ± 1.9	4.1 ± 1.4	1.4 ± 0.0	8.6 ± 9.0
Hdn.VOR	8/8	6	31	9.4	18.6 ± 0.7	14.6 ± 2.1	12.8 ± 1.7	3.7 ± 1.3	40.8 ± 10.5	27.7 ± 2.4	4.3 ± 0.2	0.4 ± 0.1	8.4 ± 2.0	3.7 ± 1.3	1.6 ± 0.0	13.1 ± 10.8
Hdn.VOR	8/8	12	27	9.4	18.1 ± 0.8	17.0 ± 2.1	12.7 ± 1.5	3.7 ± 1.3	40.2 ± 10.3	30.2 ± 2.5	3.5 ± 0.2	0.6 ± 0.1	10.9 ± 2.1	3.7 ± 1.3	2.1 ± 0.1	10.0 ± 10.6
Hdn.VOR	8/9	6	41	9.4	19.1 ± 2.2	15.9 ± 2.1	6.3 ± 1.4	4.5 ± 1.6	34.8 ± 10.8	29.8 ± 2.6	3.1 ± 0.2	0.6 ± 0.1	8.7 ± 2.1	4.5 ± 1.6	3.5 ± 0.1	5.0 ± 11.1
Hdn.VOR	8/9	12	16	9.4	8.3 ± 0.4	17.9 ± 2.4	3.3 ± 1.4	5.0 ± 1.7	20.9 ± 6.8	32.3 ± 2.9	1.7 ± 0.1	0.5 ± 0.1	13.7 ± 2.4	5.0 ± 1.7	1.9 ± 0.1	-11.3 ± 7.4
Hdn.VOR	8/14	6	52	9.4	6.6 ± 0.9	7.5 ± 2.1	1.6 ± 1.4	6.6 ± 1.2	17.6 ± 6.2	23.5 ± 2.4	1.6 ± 0.2	0.5 ± 0.1	4.7 ± 2.1	6.6 ± 1.2	0.8 ± 0.0	-6.0 ± 6.7
Hdn.VOR	8/14	12	38	9.4	3.4 ± 0.3	9.3 ± 2.1	0.0 ± 1.4	6.2 ± 1.2	12.8 ± 4.9	24.9 ± 2.4	1.2 ± 0.1	0.4 ± 0.1	7.3 ± 2.1	6.2 ± 1.2	0.4 ± 0.0	-12.0 ± 5.4
Hdn.VOR	8/21	6	62	9.4	17.6 ± 1.5	25.3 ± 2.8	4.7 ± 1.4	4.7 ± 1.6	31.7 ± 10.0	39.4 ± 3.2	7.6 ± 0.4	1.2 ± 0.1	13.5 ± 2.7	4.7 ± 1.6	3.0 ± 0.1	-7.6 ± 10.5
Hdn.VOR	8/21	12	43	9.4	16.4 ± 0.7	18.4 ± 2.3	4.7 ± 1.4	4.6 ± 1.6	30.5 ± 9.8	32.4 ± 2.8	6.2 ± 0.3	0.7 ± 0.1	9.9 ± 2.3	4.6 ± 1.6	1.5 ± 0.0	-1.8 ± 10.2
Hdn.VOR	8/22	6	71	9.4	18.9 ± 2.3	18.9 ± 2.8	3.1 ± 1.4	5.0 ± 1.7	31.5 ± 10.9	33.3 ± 3.3	5.4 ± 0.3	0.8 ± 0.1	12.1 ± 2.8	5.0 ± 1.7	0.6 ± 0.0	-1.8 ± 11.4
Hdn.VOR	8/22	12	47	9.4	12.3 ± 0.3	13.2 ± 2.2	1.6 ± 1.4	3.8 ± 1.3	23.3 ± 8.0	26.4 ± 2.6	4.0 ± 0.2	0.4 ± 0.1	8.3 ± 2.2	3.8 ± 1.3	0.5 ± 0.0	-3.1 ± 8.4
Hdn.VOR	8/23	6	66	9.4	15.8 ± 0.7	16.3 ± 2.4	1.6 ± 1.4	1.0 ± 0.7	26.8 ± 9.6	26.7 ± 2.5	6.5 ± 0.4	0.7 ± 0.1	7.4 ± 2.4	1.0 ± 0.7	1.7 ± 0.1	0.1 ± 9.9
Hdn.VOR	8/23	12	61	9.4	12.9 ± 0.7	14.9 ± 2.3	0.0 ± 1.3	3.4 ± 1.2	22.3 ± 8.6	27.7 ± 2.6	5.0 ± 0.3	0.5 ± 0.1	8.6 ± 2.3	3.4 ± 1.2	0.8 ± 0.0	-5.4 ± 9.0
Hdn.VOR	8/24	6	69	9.4	16.3 ± 2.5	20.8 ± 2.8	3.2 ± 1.4	5.3 ± 1.8	28.8 ± 9.9	35.5 ± 3.3	6.3 ± 0.4	0.7 ± 0.1	12.6 ± 2.7	5.3 ± 1.8	1.1 ± 0.0	-6.7 ± 10.4
Hdn.VOR	8/24	12	51	9.4	8.9 ± 0.4	18.3 ± 2.4	1.6 ± 1.4	5.0 ± 1.7	19.9 ± 7.0	32.6 ± 3.0	3.9 ± 0.2	0.5 ± 0.1	11.9 ± 2.4	5.0 ± 1.7	2.0 ± 0.1	-12.7 ± 7.6
Hdn.VOR	8/25	6	72	9.4	13.9 ± 1.0	23.2 ± 2.8	3.1 ± 1.3	5.2 ± 1.8	26.4 ± 8.8	37.8 ± 3.4	9.5 ± 0.5	0.9 ± 0.1	11.3 ± 2.8	5.2 ± 1.8	1.5 ± 0.0	-11.4 ± 9.4
Hdn.VOR	8/25	12	32	9.4	8.4 ± 0.5	20.1 ± 2.7	3.5 ± 1.5	5.1 ± 1.8	21.3 ± 6.8	34.7 ± 3.2	3.9 ± 0.2	0.6 ± 0.1	14.8 ± 2.7	5.1 ± 1.8	0.8 ± 0.0	-13.4 ± 7.5
Hdn.VOR	8/26	6	54	9.4	13.6 ± 1.5	24.1 ± 2.7	3.1 ± 1.4	4.5 ± 1.0	26.1 ± 8.9	38.0 ± 2.9	4.8 ± 0.3	0.9 ± 0.1	15.8 ± 2.7	4.5 ± 1.0	2.6 ± 0.1	-11.9 ± 9.3
Hdn.VOR	8/26	12	23	9.4	6.8 ± 0.2	13.5 ± 2.0	0.0 ± 1.4	5.0 ± 1.0	16.2 ± 6.2	27.8 ± 2.2	3.2 ± 0.2	0.8 ± 0.1	8.4 ± 2.0	5.0 ± 1.0	1.1 ± 0.0	-11.7 ± 6.5
Hdn.VOR	8/27	6	46	9.4	15.4 ± 1.9	22.8 ± 2.4	1.5 ± 1.3	2.4 ± 0.7	26.4 ± 9.4	34.6 ± 2.5	4.8 ± 0.3	3.9 ± 0.3	12.9 ± 2.4	2.4 ± 0.7	1.3 ± 0.0	-8.2 ± 9.8
Hdn.VOR	8/27	12	29	9.4	7.4 ± 0.3	15.8 ± 2.1	4.8 ± 1.4	6.1 ± 1.2	21.6 ± 6.3	31.3 ± 2.4	3.1 ± 0.2	0.6 ± 0.1	9.6 ± 2.1	6.1 ± 1.2	2.5 ± 0.1	-9.7 ± 6.8
Hdn.VOR	9/2	6	---	9.4	--- ± ---	--- ± ---	--- ± ---	--- ± ---	--- ± ---	--- ± ---	--- ± ---	--- ± ---	--- ± ---	--- ± ---	--- ± ---	--- ± ---

Hdn.VOR	9/2	12	27	9.4	--- ± ---	--- ± ---	0.0 ± 3.0	--- ± ---	22.3 ± 8.9	--- ± ---	--- ± ---	--- ± ---	--- ± ---	--- ± ---	--- ± ---	--- ± ---	--- ± ---
Hdn.VOR	9/17	6	35	9.4	8.6 ± 1.4	17.8 ± 2.4	3.1 ± 1.4	2.7 ± 0.8	21.1 ± 7.1	30.0 ± 2.5	2.6 ± 0.2	0.3 ± 0.1	13.4 ± 2.4	2.7 ± 0.8	1.6 ± 0.0	-8.9 ± 7.5	
Hdn.VOR	9/17	12	22	9.4	6.9 ± 0.6	12.3 ± 2.0	1.6 ± 1.4	1.7 ± 0.7	17.9 ± 6.3	23.4 ± 2.2	2.5 ± 0.2	0.3 ± 0.1	8.0 ± 2.0	1.7 ± 0.7	1.4 ± 0.0	-5.5 ± 6.7	
Hdn.VOR	9/18	6	84	9.4	69.6 ± 21.6	41.2 ± 4.2	1.6 ± 1.4	5.8 ± 1.1	80.6 ± 35.2	56.4 ± 4.4	18.0 ± 1.0	3.4 ± 0.3	18.8 ± 4.1	5.8 ± 1.1	1.0 ± 0.0	24.2 ± 35.5	
Hdn.VOR	9/18	12	80	9.4	23.9 ± 2.7	20.6 ± 3.4	3.2 ± 1.4	4.4 ± 1.0	36.5 ± 12.7	34.5 ± 3.5	7.6 ± 0.5	0.7 ± 0.2	11.6 ± 3.3	4.4 ± 1.0	0.7 ± 0.0	2.1 ± 13.1	
Hdn.VOR	9/19	6	89	9.4	1942.3 ± 764.2	64.5 ± 5.4	4.9 ± 1.4	5.9 ± 1.2	1956.6 ± ####	79.8 ± 5.5	46.1 ± 2.6	3.0 ± 0.3	14.3 ± 4.7	5.9 ± 1.2	1.1 ± 0.1	1876.7 ± ####	
Hdn.VOR	9/19	12	49	9.4	12.9 ± 1.5	12.7 ± 2.3	3.4 ± 1.5	3.6 ± 0.9	25.7 ± 8.7	25.7 ± 2.4	2.7 ± 0.2	0.7 ± 0.1	8.1 ± 2.2	3.6 ± 0.9	1.2 ± 0.0	0.1 ± 9.0	
Hdn.VOR	9/20	6	77	9.4	19.8 ± 1.6	14.2 ± 2.8	3.1 ± 1.4	2.1 ± 0.7	32.3 ± 11.2	25.7 ± 2.9	5.1 ± 0.3	0.7 ± 0.2	7.1 ± 2.8	2.1 ± 0.7	1.2 ± 0.0	6.5 ± 11.5	
Hdn.VOR	9/20	12	65	9.4	13.3 ± 1.3	15.4 ± 2.6	3.1 ± 1.4	5.8 ± 1.1	25.8 ± 8.5	30.6 ± 2.8	4.1 ± 0.3	0.6 ± 0.1	9.8 ± 2.6	5.8 ± 1.1	1.0 ± 0.0	-4.8 ± 9.0	
Hdn.VOR	9/21	6	85	9.4	12.4 ± 1.3	12.2 ± 3.5	1.6 ± 1.4	1.2 ± 0.7	23.4 ± 8.5	22.9 ± 3.6	4.7 ± 0.4	0.9 ± 0.2	6.2 ± 3.5	1.2 ± 0.7	0.3 ± 0.0	0.6 ± 9.2	
Hdn.VOR	9/21	12	44	9.4	4.3 ± 0.8	9.3 ± 2.0	1.6 ± 1.4	4.2 ± 1.0	15.3 ± 5.1	22.9 ± 2.3	4.0 ± 0.2	0.3 ± 0.1	4.5 ± 2.0	4.2 ± 1.0	0.6 ± 0.0	-7.6 ± 5.6	
Hdn.VOR	9/24	6	63	9.4	10.3 ± 0.6	9.8 ± 2.6	3.2 ± 1.4	3.1 ± 1.3	22.8 ± 7.3	22.3 ± 2.9	3.1 ± 0.2	0.7 ± 0.1	5.3 ± 2.6	3.1 ± 1.3	0.8 ± 0.0	0.6 ± 7.9	
Hdn.VOR	9/24	12	30	9.4	7.3 ± 0.2	7.5 ± 2.1	1.5 ± 1.3	2.2 ± 1.0	18.2 ± 6.1	19.1 ± 2.3	2.4 ± 0.2	0.2 ± 0.1	4.3 ± 2.1	2.2 ± 1.0	0.5 ± 0.0	-0.9 ± 6.6	
Hdn.VOR	9/27	6	45	9.4	11.3 ± 0.8	11.2 ± 2.0	1.5 ± 1.3	4.8 ± 1.0	22.2 ± 7.7	25.4 ± 2.2	3.6 ± 0.2	0.6 ± 0.1	5.7 ± 2.0	4.8 ± 1.0	1.3 ± 0.0	-3.2 ± 8.0	
Hdn.VOR	9/27	12	24	9.4	13.9 ± 2.4	15.4 ± 2.1	3.0 ± 1.3	9.0 ± 1.6	26.4 ± 9.0	33.8 ± 2.6	3.3 ± 0.2	0.8 ± 0.1	9.9 ± 2.0	9.0 ± 1.6	1.5 ± 0.0	-7.5 ± 9.4	
Hdn.VOR	9/30	6	96	9.4	1022.1 ± 578.0	22.7 ± 10.9	1.6 ± 1.4	1.5 ± 0.9	1033.1 ± 648.1	33.6 ± 10.9	1.9 ± 1.1	1.9 ± 0.7	18.7 ± 10.8	1.5 ± 0.9	0.1 ± 0.1	999.6 ± 648.2	
Hdn.VOR	9/30	12	69	9.4	16.4 ± 1.1	14.8 ± 3.2	3.3 ± 1.4	4.7 ± 1.9	29.1 ± 9.7	29.0 ± 3.7	4.9 ± 0.3	0.6 ± 0.1	8.8 ± 3.2	4.7 ± 1.9	0.5 ± 0.0	0.1 ± 10.4	
Hdn.VOR	10/1	6	68	9.4	36.1 ± 11.6	20.4 ± 3.0	5.0 ± 1.5	2.3 ± 1.1	50.5 ± 19.7	32.1 ± 3.2	11.3 ± 0.6	0.8 ± 0.1	5.9 ± 2.9	2.3 ± 1.1	2.4 ± 0.1	18.4 ± 19.9	
Hdn.VOR	10/1	12	38	9.4	5.3 ± 0.4	7.1 ± 2.5	0.0 ± 1.5	1.2 ± 0.8	14.7 ± 5.9	17.7 ± 2.6	1.1 ± 0.1	0.4 ± 0.1	4.8 ± 2.5	1.2 ± 0.8	0.8 ± 0.0	-3.0 ± 6.4	
Hdn.VOR	10/2	6	59	9.4	7.3 ± 0.8	10.8 ± 2.3	1.6 ± 1.4	2.4 ± 0.8	18.3 ± 6.4	22.7 ± 2.5	2.0 ± 0.2	1.4 ± 0.1	6.3 ± 2.3	2.4 ± 0.8	1.2 ± 0.0	-4.4 ± 6.8	
Hdn.VOR	10/2	12	32	9.4	2.3 ± 0.2	6.4 ± 2.0	0.0 ± 1.5	3.0 ± 0.8	11.7 ± 4.3	18.8 ± 2.2	1.0 ± 0.1	0.5 ± 0.1	4.1 ± 2.0	3.0 ± 0.8	0.7 ± 0.0	-7.2 ± 4.8	
Hdn.VOR	10/7	6	52	9.4	9.6 ± 2.2	9.5 ± 2.3	0.0 ± 1.3	1.8 ± 0.9	19.0 ± 7.4	20.6 ± 2.5	2.0 ± 0.2	0.4 ± 0.1	3.3 ± 2.3	1.8 ± 0.9	3.8 ± 0.1	-1.6 ± 7.8	
Hdn.VOR	10/7	12	25	9.4	7.4 ± 0.3	8.3 ± 2.2	1.5 ± 1.3	1.7 ± 0.9	18.4 ± 6.3	19.4 ± 2.3	2.0 ± 0.1	0.3 ± 0.1	4.2 ± 2.1	1.7 ± 0.9	1.8 ± 0.1	-1.0 ± 6.7	
Hdn.VOR	10/8	6	61	9.4	21.6 ± 1.9	12.8 ± 2.7	6.6 ± 1.5	3.0 ± 1.3	37.6 ± 11.9	25.2 ± 3.0	3.2 ± 0.2	1.9 ± 0.2	4.7 ± 2.7	3.0 ± 1.3	2.9 ± 0.1	12.5 ± 12.2	
Hdn.VOR	10/8	12	25	9.4	7.9 ± 0.4	9.6 ± 2.4	3.2 ± 1.4	2.0 ± 1.0	20.6 ± 6.5	21.0 ± 2.6	1.7 ± 0.1	0.4 ± 0.1	6.2 ± 2.4	2.0 ± 1.0	1.4 ± 0.0	-0.4 ± 7.0	
Hdn.VOR	10/9	6	41	9.4	7.8 ± 0.4	8.6 ± 2.4	5.0 ± 1.5	3.0 ± 1.3	22.1 ± 6.5	20.9 ± 2.7	1.7 ± 0.1	0.4 ± 0.1	4.2 ± 2.4	3.0 ± 1.3	2.3 ± 0.1	1.2 ± 7.1	
Hdn.VOR	10/9	12	22	9.4	7.8 ± 0.3	11.7 ± 2.6	3.1 ± 1.4	3.1 ± 1.3	20.3 ± 6.5	24.2 ± 2.9	1.3 ± 0.1	0.7 ± 0.1	7.0 ± 2.6	3.1 ± 1.3	2.7 ± 0.1	-3.9 ± 7.1	
Hdn.VOR	10/10	6	37	9.4	10.1 ± 0.2	9.9 ± 2.1	1.7 ± 1.4	2.2 ± 0.8	21.2 ± 7.1	21.6 ± 2.2	1.4 ± 0.1	0.9 ± 0.1	5.6 ± 2.1	2.2 ± 0.8	2.0 ± 0.1	-0.4 ± 7.5	
Hdn.VOR	10/10	12	24	9.4	9.1 ± 0.5	8.6 ± 2.0	1.7 ± 1.4	4.1 ± 1.0	20.2 ± 6.8	22.2 ± 2.2	1.1 ± 0.1	0.5 ± 0.1	4.8 ± 2.0	4.1 ± 1.0	2.2 ± 0.1	-2.0 ± 7.2	
Hdn.VOR	10/11	6	38	9.4	7.3 ± 0.5	8.2 ± 2.4	3.3 ± 1.4	3.4 ± 1.4	19.9 ± 6.5	21.1 ± 2.8	0.9 ± 0.1	0.3 ± 0.1	5.2 ± 2.4	3.4 ± 1.4	1.8 ± 0.1	-1.1 ± 7.1	
Hdn.VOR	10/11	12	15	9.4	4.9 ± 0.2	8.7 ± 2.3	1.7 ± 1.5	2.2 ± 1.1	16.0 ± 5.6	20.3 ± 2.5	1.1 ± 0.1	0.7 ± 0.1	5.3 ± 2.3	2.2 ± 1.1	1.6 ± 0.0	-4.3 ± 6.1	
Hdn.VOR	10/12	6	33	9.4	18.4 ± 0.6	14.2 ± 2.5	5.0 ± 1.5	4.4 ± 1.8	32.8 ± 10.3	28.0 ± 3.1	4.5 ± 0.2	0.5 ± 0.1	7.1 ± 2.5	4.4 ± 1.8	2.2 ± 0.1	4.8 ± 10.7	
Hdn.VOR	10/12	12	57	9.4	18.4 ± 1.0	16.9 ± 2.9	3.3 ± 1.5	6.9 ± 2.6	31.2 ± 10.3	33.3 ± 3.9	5.3 ± 0.3	0.6 ± 0.1	7.8 ± 2.9	6.9 ± 2.6	3.1 ± 0.1	-2.1 ± 11.0	
Hdn.VOR	10/13	6	53	9.4	4.4 ± 0.4	3.4 ± 2.2	0.0 ± 1.4	2.3 ± 1.1	13.8 ± 5.2	15.1 ± 2.4	1.1 ± 0.1	0.4 ± 0.1	0.7 ± 2.2	2.3 ± 1.1	1.2 ± 0.0	-1.2 ± 5.8	
Hdn.VOR	10/13	12	25	9.4	2.9 ± 0.2	5.2 ± 2.1	0.0 ± 1.4	4.2 ± 1.7	12.3 ± 4.6	18.8 ± 2.7	0.8 ± 0.1	0.4 ± 0.1	2.8 ± 2.1	4.2 ± 1.7	1.1 ± 0.0	-6.4 ± 5.3	
Hdn.VOR	10/14	6	33	9.4	4.9 ± 0.3	4.3 ± 2.0	1.6 ± 1.4	4.7 ± 1.8	15.9 ± 5.7	18.4 ± 2.7	0.8 ± 0.1	0.3 ± 0.1	2.0 ± 2.0	4.7 ± 1.8	1.2 ± 0.0	-2.5 ± 6.3	
Hdn.VOR	10/14	12	26	9.4	3.6 ± 0.7	4.1 ± 1.9	0.0 ± 1.4	2.6 ± 1.1	13.0 ± 4.8	16.1 ± 2.2	0.7 ± 0.1	0.2 ± 0.1	2.4 ± 1.9	2.6 ± 1.1	0.7 ± 0.0	-3.1 ± 5.2	

Table 4.3.6
Measured and Calculated Component Contributions to Total Light Extinction at Hayden Waste Water

Site	Date	Hr	RH	Cln Air	bsp	Ebsp	babs	Ebabs	bext	Ebext	Esul	Enit	Eoc	Eec	Esoil	Unid.
Hdn.WW	2/16	6	---	9.6	--- + ---	--- + ---	--- + ---	--- + ---	--- + ---	--- + ---	--- + ---	--- + ---	--- + ---	--- + ---	--- + ---	--- + ---
Hdn.WW	2/16	12	57	9.6	16.9 ± 0.8	24.0 ± 3.5	10.9 ± 2.4	13.6 ± 4.9	37.4 ± 6.7	47.2 ± 6.0	3.4 ± 0.4	6.8 ± 0.4	11.5 ± 3.4	13.6 ± 4.9	2.3 ± 0.1	-9.8 ± 9.0
Hdn.WW	2/17	6	65	9.6	24.2 ± 0.8	11.6 ± 2.0	8.5 ± 1.5	5.8 ± 2.2	42.3 ± 8.0	27.0 ± 3.0	2.2 ± 0.3	5.9 ± 0.4	2.9 ± 2.0	5.8 ± 2.2	0.6 ± 0.0	15.4 ± 8.5
Hdn.WW	2/17	12	55	9.6	19.9 ± 2.2	15.3 ± 1.9	9.6 ± 1.5	4.8 ± 1.9	39.1 ± 7.1	29.7 ± 2.7	2.8 ± 0.3	6.2 ± 0.4	5.4 ± 1.9	4.8 ± 1.9	0.9 ± 0.0	9.3 ± 7.6
Hdn.WW	2/19	6	82	9.6	32.4 ± 4.6	21.4 ± 3.0	4.9 ± 1.4	2.8 ± 1.3	46.9 ± 10.3	33.8 ± 3.2	6.2 ± 0.5	5.6 ± 0.4	9.2 ± 2.9	2.8 ± 1.3	0.4 ± 0.0	13.1 ± 10.8
Hdn.WW	2/19	12	63	9.6	14.9 ± 2.4	7.6 ± 1.9	6.4 ± 1.4	1.5 ± 0.9	30.9 ± 6.2	18.7 ± 2.1	2.3 ± 0.3	3.1 ± 0.2	1.6 ± 1.9	1.5 ± 0.9	0.6 ± 0.0	12.3 ± 6.5
Hdn.WW	2/23	6	77	9.6	55.1 ± 12.0	27.1 ± 2.8	8.5 ± 1.5	5.8 ± 1.2	73.2 ± 16.4	42.6 ± 3.0	8.2 ± 0.6	11.6 ± 0.5	4.9 ± 2.7	5.8 ± 1.2	2.5 ± 0.1	30.6 ± 16.7
Hdn.WW	2/23	12	---	9.6	--- ± ---	--- ± ---	--- ± ---	--- ± ---	--- ± ---	--- ± ---	--- ± ---	--- ± ---	--- ± ---	--- ± ---	--- ± ---	--- ± ---
Hdn.WW	2/24	6	71	9.6	24.6 ± 1.5	15.5 ± 2.1	7.9 ± 1.4	4.4 ± 1.8	42.1 ± 8.0	29.5 ± 2.8	4.9 ± 0.4	5.7 ± 0.4	3.8 ± 2.1	4.4 ± 1.8	1.2 ± 0.0	12.5 ± 8.5
Hdn.WW	2/24	12	57	9.6	19.2 ± 1.4	29.2 ± 2.7	8.3 ± 1.5	10.3 ± 3.6	37.1 ± 6.9	49.0 ± 4.5	3.9 ± 0.3	4.3 ± 0.2	16.2 ± 2.6	10.3 ± 3.6	4.8 ± 0.1	-11.9 ± 8.2
Hdn.WW	2/26	6	78	9.6	67.7 ± 10.7	41.8 ± 3.3	13.6 ± 1.6	6.2 ± 2.3	91.0 ± 18.7	57.5 ± 4.0	8.4 ± 0.6	15.8 ± 1.0	15.0 ± 3.1	6.2 ± 2.3	2.6 ± 0.1	33.4 ± 19.2
Hdn.WW	2/26	12	66	9.6	28.1 ± 3.1	23.4 ± 2.4	6.5 ± 1.4	6.7 ± 2.5	44.1 ± 9.1	39.7 ± 3.5	7.1 ± 0.5	4.7 ± 0.2	10.8 ± 2.4	6.7 ± 2.5	0.8 ± 0.0	4.4 ± 9.7
Hdn.WW	8/7	6	37	9.6	20.1 ± 0.6	15.9 ± 1.8	13.8 ± 1.4	5.4 ± 2.0	43.4 ± 7.0	30.9 ± 2.7	3.8 ± 0.2	0.4 ± 0.1	10.1 ± 1.8	5.4 ± 2.0	1.7 ± 0.1	12.5 ± 7.5
Hdn.WW	8/7	12	18	9.6	15.2 ± 0.5	17.4 ± 1.9	12.1 ± 1.4	6.4 ± 2.4	36.9 ± 6.0	33.4 ± 3.0	4.0 ± 0.2	0.4 ± 0.1	12.0 ± 1.9	6.4 ± 2.4	1.1 ± 0.0	3.5 ± 6.7
Hdn.WW	8/8	6	39	9.6	23.1 ± 1.2	22.4 ± 2.3	14.7 ± 1.5	5.7 ± 2.1	47.4 ± 7.8	37.7 ± 3.1	4.7 ± 0.3	0.4 ± 0.1	15.8 ± 2.2	5.7 ± 2.1	1.5 ± 0.0	9.7 ± 8.4
Hdn.WW	8/8	12	26	9.6	20.1 ± 0.6	18.1 ± 1.9	13.2 ± 1.4	3.9 ± 1.5	42.8 ± 6.8	31.6 ± 2.5	2.9 ± 0.2	0.5 ± 0.1	12.5 ± 1.9	3.9 ± 1.5	2.3 ± 0.1	11.2 ± 7.3
Hdn.WW	8/9	6	49	9.6	19.9 ± 1.6	15.7 ± 1.9	8.9 ± 1.4	4.1 ± 1.6	38.4 ± 6.9	29.4 ± 2.5	2.8 ± 0.2	0.7 ± 0.1	9.5 ± 1.9	4.1 ± 1.6	2.7 ± 0.1	9.1 ± 7.3
Hdn.WW	8/9	12	16	9.6	11.1 ± 0.5	12.1 ± 1.7	0.0 ± 1.3	4.2 ± 1.6	20.7 ± 5.0	25.8 ± 2.3	1.8 ± 0.2	0.4 ± 0.1	7.9 ± 1.7	4.2 ± 1.6	2.0 ± 0.1	-5.2 ± 5.5
Hdn.WW	8/14	6	56	9.6	11.1 ± 2.2	9.4 ± 1.9	3.0 ± 1.3	7.0 ± 1.4	23.7 ± 5.1	26.0 ± 2.4	1.7 ± 0.2	0.5 ± 0.1	6.1 ± 1.9	7.0 ± 1.4	1.2 ± 0.0	-2.4 ± 5.6
Hdn.WW	8/14	12	37	9.6	5.4 ± 0.2	7.1 ± 1.8	0.0 ± 1.3	6.6 ± 1.3	15.0 ± 3.4	23.4 ± 2.2	1.2 ± 0.2	0.3 ± 0.1	5.1 ± 1.8	6.6 ± 1.3	0.5 ± 0.0	-8.4 ± 4.1
Hdn.WW	8/21	6	76	9.6	--- ± ---	30.1 ± 5.5	7.0 ± 3.0	5.4 ± 2.6	41.6 ± 8.9	45.1 ± 6.0	9.1 ± 0.9	0.9 ± 0.3	18.4 ± 5.4	5.4 ± 2.6	1.7 ± 0.1	-3.5 ± 10.7
Hdn.WW	8/21	12	36	9.6	22.9 ± 2.8	18.2 ± 2.8	6.8 ± 2.0	7.2 ± 2.8	39.3 ± 7.9	35.0 ± 3.9	5.2 ± 0.4	0.4 ± 0.1	11.7 ± 2.8	7.2 ± 2.8	0.9 ± 0.0	4.2 ± 8.8
Hdn.WW	8/22	6	---	9.6	--- ± ---	--- ± ---	--- ± ---	--- ± ---	--- ± ---	--- ± ---	--- ± ---	--- ± ---	--- ± ---	--- ± ---	--- ± ---	--- ± ---
Hdn.WW	8/22	12	46	9.6	--- ± ---	--- ± ---	--- ± ---	--- ± ---	--- ± ---	--- ± ---	--- ± ---	--- ± ---	--- ± ---	--- ± ---	--- ± ---	--- ± ---
Hdn.WW	8/23	6	65	9.6	22.4 ± 1.7	14.7 ± 2.0	5.7 ± 1.3	3.6 ± 1.5	37.7 ± 7.4	27.9 ± 2.5	5.6 ± 0.4	0.5 ± 0.1	7.8 ± 2.0	3.6 ± 1.5	0.9 ± 0.0	9.8 ± 7.8
Hdn.WW	8/23	12	59	9.6	17.6 ± 1.3	25.3 ± 2.6	5.8 ± 1.3	7.9 ± 2.8	32.9 ± 6.3	42.8 ± 3.9	5.4 ± 0.3	1.4 ± 0.1	17.7 ± 2.6	7.9 ± 2.8	0.8 ± 0.0	-9.8 ± 7.4
Hdn.WW	8/24	6	69	9.6	20.9 ± 3.2	15.4 ± 2.2	5.8 ± 1.3	6.2 ± 2.3	36.3 ± 7.5	31.2 ± 3.1	5.2 ± 0.4	0.9 ± 0.1	8.9 ± 2.1	6.2 ± 2.3	0.5 ± 0.0	5.2 ± 8.2
Hdn.WW	8/24	12	49	9.6	12.4 ± 0.8	15.1 ± 1.9	4.4 ± 1.3	1.0 ± 0.7	26.4 ± 5.4	25.7 ± 2.1	4.2 ± 0.3	0.3 ± 0.1	9.7 ± 1.9	1.0 ± 0.7	0.9 ± 0.0	0.7 ± 5.8
Hdn.WW	8/25	6	68	9.6	16.9 ± 1.3	15.6 ± 2.3	5.8 ± 1.3	3.1 ± 1.3	32.3 ± 6.2	28.3 ± 2.6	4.1 ± 0.3	0.4 ± 0.1	9.9 ± 2.2	3.1 ± 1.3	1.1 ± 0.0	3.9 ± 6.7
Hdn.WW	8/25	12	32	9.6	9.8 ± 0.6	13.4 ± 1.9	4.9 ± 1.4	4.4 ± 1.8	24.3 ± 4.8	27.4 ± 2.6	4.0 ± 0.3	0.4 ± 0.1	8.5 ± 1.9	4.4 ± 1.8	0.6 ± 0.0	-3.2 ± 5.5
Hdn.WW	8/26	6	54	9.6	17.6 ± 1.9	12.7 ± 2.0	3.1 ± 1.3	3.8 ± 0.9	30.2 ± 6.5	26.1 ± 2.2	3.8 ± 0.3	0.5 ± 0.1	7.5 ± 2.0	3.8 ± 0.9	0.9 ± 0.0	4.2 ± 6.9
Hdn.WW	8/26	12	25	9.6	9.2 ± 0.2	11.5 ± 1.8	1.5 ± 1.3	3.2 ± 0.9	20.4 ± 4.2	24.2 ± 2.0	2.8 ± 0.2	0.3 ± 0.1	7.9 ± 1.8	3.2 ± 0.9	0.4 ± 0.0	-3.9 ± 4.7
Hdn.WW	8/27	6	52	9.6	20.9 ± 2.2	12.5 ± 1.9	3.1 ± 1.3	2.2 ± 0.8	33.6 ± 7.2	24.3 ± 2.1	5.5 ± 0.3	0.4 ± 0.1	5.5 ± 1.9	2.2 ± 0.8	1.0 ± 0.0	9.3 ± 7.5
Hdn.WW	8/27	12	33	9.6	11.2 ± 0.4	13.0 ± 1.9	3.1 ± 1.4	3.0 ± 0.9	23.9 ± 5.2	25.7 ± 2.1	3.0 ± 0.2	0.4 ± 0.1	8.7 ± 1.9	3.0 ± 0.9	0.9 ± 0.0	-1.7 ± 5.6

Hdn.WW	9/2	6	---	9.6	--- ± ---	--- ± ---	--- ± ---	--- ± ---	--- ± ---	--- ± ---	--- ± ---	--- ± ---	--- ± ---	--- ± ---	--- ± ---	--- ± ---	--- ± ---	--- ± ---	--- ± ---	--- ± ---	--- ± ---	--- ± ---
Hdn.WW	9/2	12	---	9.6	--- ± ---	--- ± ---	--- ± ---	--- ± ---	--- ± ---	--- ± ---	--- ± ---	--- ± ---	--- ± ---	--- ± ---	--- ± ---	--- ± ---	--- ± ---	--- ± ---	--- ± ---	--- ± ---	--- ± ---	--- ± ---
Hdn.WW	9/17	6	46	9.6	13.1 ± 1.1	11.8 ± 2.1	5.3 ± 1.6	3.4 ± 1.0	28.0 ± 5.6	24.7 ± 2.3	2.5 ± 0.2	0.4 ± 0.1	7.8 ± 2.1	3.4 ± 1.0	1.1 ± 0.0	3.3 ± 6.0
Hdn.WW	9/17	12	23	9.6	9.9 ± 0.4	9.8 ± 2.3	--- ± ---	0.0 ± 0.9	--- ± ---	19.4 ± 2.5	2.4 ± 0.3	0.6 ± 0.1	6.1 ± 2.3	0.0 ± 0.9	0.7 ± 0.0	--- ± ---
Hdn.WW	9/18	6	81	9.6	54.9 ± 11.8	31.0 ± 3.2	3.0 ± 1.3	7.4 ± 1.4	67.5 ± 16.4	48.0 ± 3.5	12.1 ± 0.7	3.5 ± 0.3	14.5 ± 3.1	7.4 ± 1.4	0.9 ± 0.0	19.6 ± 16.8
Hdn.WW	9/18	12	73	9.6	20.2 ± 1.1	26.5 ± 4.3	3.0 ± 1.3	7.9 ± 1.8	32.8 ± 7.0	44.0 ± 4.7	6.1 ± 0.6	1.0 ± 0.2	19.1 ± 4.3	7.9 ± 1.8	0.3 ± 0.0	-11.1 ± 8.4
Hdn.WW	9/19	6	83	9.6	96.9 ± 36.6	44.9 ± 3.3	4.7 ± 1.4	5.0 ± 1.1	111.2 ± 32.0	59.5 ± 3.5	31.5 ± 1.7	2.1 ± 0.2	10.2 ± 2.9	5.0 ± 1.1	1.1 ± 0.0	51.7 ± 32.2
Hdn.WW	9/19	12	48	9.6	13.2 ± 1.5	11.7 ± 1.9	4.7 ± 1.4	6.4 ± 1.3	27.6 ± 5.4	27.8 ± 2.3	3.1 ± 0.3	0.6 ± 0.1	7.2 ± 1.9	6.4 ± 1.3	0.9 ± 0.0	-0.2 ± 5.9
Hdn.WW	9/20	6	80	9.6	24.2 ± 1.4	18.3 ± 3.1	4.8 ± 1.4	3.2 ± 0.9	38.6 ± 8.0	31.1 ± 3.2	8.1 ± 0.6	1.2 ± 0.2	8.4 ± 3.0	3.2 ± 0.9	0.7 ± 0.0	7.5 ± 8.6
Hdn.WW	9/20	12	62	9.6	16.6 ± 1.9	11.6 ± 2.0	3.1 ± 1.4	2.0 ± 0.7	29.3 ± 6.4	23.2 ± 2.1	4.7 ± 0.3	0.5 ± 0.1	5.9 ± 2.0	2.0 ± 0.7	0.5 ± 0.0	6.1 ± 6.8
Hdn.WW	9/21	6	75	9.6	8.2 ± 1.0	10.9 ± 2.2	1.6 ± 1.4	0.0 ± 0.6	19.4 ± 4.3	20.5 ± 2.3	5.7 ± 0.4	0.4 ± 0.1	4.4 ± 2.2	0.0 ± 0.6	0.5 ± 0.0	-1.1 ± 4.9
Hdn.WW	9/21	12	44	9.6	5.7 ± 0.9	6.1 ± 1.7	1.6 ± 1.4	0.0 ± 0.6	16.9 ± 3.6	15.7 ± 1.8	2.6 ± 0.2	0.2 ± 0.1	2.7 ± 1.7	0.0 ± 0.6	0.6 ± 0.0	1.2 ± 4.1
Hdn.WW	9/24	6	65	9.6	14.9 ± 1.6	9.1 ± 2.4	1.6 ± 1.4	2.2 ± 1.2	26.1 ± 6.0	20.9 ± 2.7	3.4 ± 0.3	0.5 ± 0.1	4.6 ± 2.4	2.2 ± 1.2	0.6 ± 0.0	5.2 ± 6.6
Hdn.WW	9/24	12	29	9.6	--- ± ---	9.2 ± 2.2	1.5 ± 1.3	3.6 ± 1.7	--- ± ---	22.3 ± 2.8	2.1 ± 0.2	0.2 ± 0.1	6.6 ± 2.2	3.6 ± 1.7	0.2 ± 0.0	--- ± ---
Hdn.WW	9/27	6	51	9.6	15.2 ± 1.7	10.4 ± 1.9	4.5 ± 1.3	4.5 ± 1.1	29.3 ± 6.0	24.6 ± 2.2	4.1 ± 0.3	0.5 ± 0.1	5.1 ± 1.9	4.5 ± 1.1	0.8 ± 0.0	4.7 ± 6.4
Hdn.WW	9/27	12	27	9.6	15.6 ± 1.6	10.3 ± 1.8	4.5 ± 1.3	5.3 ± 1.2	29.7 ± 6.1	25.2 ± 2.1	3.4 ± 0.2	0.6 ± 0.1	5.5 ± 1.8	5.3 ± 1.2	0.8 ± 0.1	4.5 ± 6.4
Hdn.WW	9/30	6	86	9.6	4.1 ± 0.8	7.5 ± 3.8	0.0 ± 1.4	2.8 ± 1.4	13.7 ± 3.5	19.9 ± 4.0	0.9 ± 0.5	0.3 ± 0.2	6.1 ± 3.7	2.8 ± 1.4	0.1 ± 0.0	-6.2 ± 5.3
Hdn.WW	9/30	12	65	9.6	16.9 ± 1.1	11.9 ± 2.4	3.1 ± 1.4	2.4 ± 1.3	29.6 ± 6.2	23.9 ± 2.7	6.9 ± 0.4	0.4 ± 0.1	3.9 ± 2.3	2.4 ± 1.3	0.7 ± 0.0	5.7 ± 6.8
Hdn.WW	10/1	6	69	9.6	25.6 ± 6.4	14.9 ± 2.7	3.2 ± 1.4	4.7 ± 2.0	38.3 ± 9.0	29.1 ± 3.4	6.3 ± 0.4	0.8 ± 0.1	7.1 ± 2.7	4.7 ± 2.0	0.7 ± 0.0	9.2 ± 9.6
Hdn.WW	10/1	12	37	9.6	5.2 ± 0.3	9.6 ± 2.3	0.0 ± 1.4	5.3 ± 2.3	14.8 ± 3.5	24.5 ± 3.3	1.4 ± 0.2	0.3 ± 0.1	7.3 ± 2.3	5.3 ± 2.3	0.6 ± 0.0	-9.7 ± 4.8
Hdn.WW	10/2	6	67	9.6	16.2 ± 4.3	8.0 ± 2.1	3.2 ± 1.4	1.2 ± 0.7	29.0 ± 6.6	18.8 ± 2.2	4.0 ± 0.3	1.0 ± 0.1	2.4 ± 2.0	1.2 ± 0.7	0.7 ± 0.0	10.2 ± 7.0
Hdn.WW	10/2	12	33	9.6	4.2 ± 0.3	8.0 ± 1.8	1.6 ± 1.4	0.2 ± 0.7	15.4 ± 3.3	17.8 ± 2.0	0.9 ± 0.2	0.8 ± 0.1	6.2 ± 1.8	0.2 ± 0.7	0.2 ± 0.0	-2.4 ± 3.8
Hdn.WW	10/7	6	56	9.6	13.2 ± 1.8	9.8 ± 2.2	3.0 ± 1.3	4.7 ± 2.0	25.9 ± 5.6	24.1 ± 3.0	2.7 ± 0.2	0.5 ± 0.1	5.1 ± 2.2	4.7 ± 2.0	1.4 ± 0.0	1.8 ± 6.3
Hdn.WW	10/7	12	24	9.6	7.2 ± 0.4	7.4 ± 1.9	3.0 ± 1.3	0.8 ± 0.8	19.9 ± 4.1	17.8 ± 2.1	2.1 ± 0.2	0.3 ± 0.1	4.0 ± 1.9	0.8 ± 0.8	1.1 ± 0.0	2.1 ± 4.6
Hdn.WW	10/8	6	62	9.6	25.4 ± 2.3	13.7 ± 2.5	6.1 ± 1.4	7.5 ± 3.1	41.1 ± 8.2	30.9 ± 3.9	4.3 ± 0.3	1.5 ± 0.1	6.9 ± 2.4	7.5 ± 3.1	0.9 ± 0.0	10.3 ± 9.1
Hdn.WW	10/8	12	27	9.6	10.1 ± 0.5	2.9 ± 1.6	3.1 ± 1.4	2.5 ± 1.3	22.8 ± 4.6	15.0 ± 2.1	1.4 ± 0.2	0.4 ± 0.1	0.6 ± 1.6	2.5 ± 1.3	0.5 ± 0.0	7.8 ± 5.0
Hdn.WW	10/9	6	54	9.6	12.2 ± 1.2	8.4 ± 2.1	3.1 ± 1.4	5.6 ± 2.4	24.9 ± 5.4	23.6 ± 3.2	2.7 ± 0.2	0.4 ± 0.1	4.5 ± 2.1	5.6 ± 2.4	0.7 ± 0.0	1.3 ± 6.3
Hdn.WW	10/9	12	24	9.6	8.4 ± 0.3	7.4 ± 1.9	3.2 ± 1.4	2.6 ± 1.3	21.2 ± 4.2	19.6 ± 2.3	1.5 ± 0.2	0.2 ± 0.1	4.2 ± 1.9	2.6 ± 1.3	1.5 ± 0.0	1.6 ± 4.8
Hdn.WW	10/10	6	51	9.6	15.7 ± 1.9	8.1 ± 1.9	6.4 ± 1.4	3.8 ± 0.9	31.7 ± 6.2	21.5 ± 2.1	1.8 ± 0.2	0.5 ± 0.1	4.7 ± 1.9	3.8 ± 0.9	1.0 ± 0.0	10.3 ± 6.6
Hdn.WW	10/10	12	25	9.6	9.7 ± 0.6	7.5 ± 1.8	3.2 ± 1.4	3.1 ± 0.9	22.5 ± 4.7	20.2 ± 2.0	1.3 ± 0.2	0.6 ± 0.1	4.7 ± 1.7	3.1 ± 0.9	0.9 ± 0.0	2.3 ± 5.1
Hdn.WW	10/11	6	45	9.6	9.4 ± 1.0	4.6 ± 3.2	3.3 ± 1.4	3.0 ± 1.9	22.3 ± 4.5	17.2 ± 3.7	1.3 ± 0.3	0.7 ± 0.2	1.6 ± 3.2	3.0 ± 1.9	1.0 ± 0.0	5.1 ± 5.8
Hdn.WW	10/11	12	20	9.6	5.6 ± 0.6	5.6 ± 1.8	1.6 ± 1.4	2.5 ± 1.3	16.8 ± 3.6	17.7 ± 2.2	1.3 ± 0.2	0.3 ± 0.1	2.9 ± 1.8	2.5 ± 1.3	1.1 ± 0.0	-0.9 ± 4.3
Hdn.WW	10/12	6	48	9.6	21.9 ± 1.7	8.6 ± 2.0	6.2 ± 1.4	5.9 ± 2.5	37.7 ± 7.4	24.1 ± 3.2	4.0 ± 0.3	0.3 ± 0.1	3.3 ± 2.0	5.9 ± 2.5	1.1 ± 0.0	13.6 ± 8.0
Hdn.WW	10/12	12	55	9.6	19.4 ± 1.8	9.5 ± 2.1	4.7 ± 1.4	2.8 ± 1.4	33.7 ± 6.9	21.9 ± 2.5	4.7 ± 0.3	0.3 ± 0.1	3.5 ± 2.1	2.8 ± 1.4	1.0 ± 0.0	11.8 ± 7.4
Hdn.WW	10/13	6	59	9.6	10.2 ± 2.5	8.0 ± 2.1	3.1 ± 1.3	4.9 ± 2.1	22.9 ± 5.0	22.5 ± 3.0	3.6 ± 0.3	0.6 ± 0.1	3.0 ± 2.1	4.9 ± 2.1	0.8 ± 0.0	0.4 ± 5.8
Hdn.WW	10/13	12	27	9.6	3.9 ± 0.2	2.1 ± 1.8	0.0 ± 1.4	3.2 ± 1.6	13.5 ± 3.3	15.0 ± 2.4	0.9 ± 0.2	0.2 ± 0.1	0.2 ± 1.8	3.2 ± 1.6	0.8 ± 0.0	-1.5 ± 4.1
Hdn.WW	10/14	6	47	9.6	6.9 ± 0.9	6.9 ± 2.1	3.1 ± 1.3	7.3 ± 3.0	19.6 ± 4.1	23.8 ± 3.6	1.4 ± 0.2	0.4 ± 0.1	4.5 ± 2.0	7.3 ± 3.0	0.6 ± 0.0	-4.2 ± 5.5
Hdn.WW	10/14	12	27	9.6	2.1 ± 0.5	2.5 ± 1.8	0.0 ± 1.4	3.8 ± 1.8	11.7 ± 3.3	15.9 ± 2.6	0.5 ± 0.2	0.1 ± 0.1	1.5 ± 1.8	3.8 ± 1.8	0.4 ± 0.0	-4.2 ± 4.2

Table 4.3.7

Calculated Component Contributions to Calculated Extinction

	<15 Mm^{-1}			15 - <20 Mm^{-1} [a]				20 - <30 Mm^{-1} [a]					- 60 Mm^{-1} [a]			
	0-10%	10-25%	25-50%	>50%	0-10%	10-25%	25-50%	>50%	0-10%	10-25%	25-50%		0-10%	10-25%	25-50%	>50%
Buffalo Pass			# of incidents in category: 19				# of incidents in category: 14				# of incidents in category:				# of incidents in category: 14	
Clean Air (Rayleigh)	0	0	5	14	0	0	7	7	0	0	19		1	1	12	0
Organics	6	11	2	0	2	7	5	0	2	8	10		4	4	6	0
Elemental Carbon	5	13	1	0	7	7	0	0	12	7	1		12	2	0	0
Ammonium Sulfate	12	7	0	0	1	11	2	0	3	12	5		0	6	6	2
Ammonium Nitrate	19	0	0	0	13	1	0	0	20	0	0		13	1	0	0
Soil	17	2	0	0	13	1	0	0	17	3	0		11	3	0	0
Gilpin Creek			# of incidents in category: 3				# of incidents in category: 11				# of incidents in category:				# of incidents in category: 10	
Clean Air (Rayleigh)	0	0	1	2	0	0	7	4	0	6	6		0	3	6	1
Organics	3	0	0	0	6	3	2	0	6	2	2		4	2	3	1
Elemental Carbon	2	0	1	0	0	1	9	1	1	4	3		1	3	6	0
Ammonium Sulfate	2	1	0	0	4	7	0	0	3	10	1		3	5	2	0
Ammonium Nitrate	3	0	0	0	11	0	0	0	14	0	0		10	0	0	0
Soil	3	0	0	0	11	0	0	0	14	0	0		9	1	0	0
Juniper Mt.			# of incidents in category: 5				# of incidents in category: 3				# of incidents in category:				# of incidents in category: 10	

Clean Air (Rayleigh)	0	0		1	4	0	0		2	1	0	0		17	5	0	0		10	0
Organics	2	2		1	0	0	2		1	0	1	12		9	(	1	3		6	0
Elemental Carbon	1	4		0	0	0	3		0	0	1	17		4	(	1	9		0	0
Ammonium Sulfate	4	1		0	0	1	2		0	0	9	13		0	(	2	7		1	0
Ammonium Nitrate	5	0		0	0	3	0		0	0	22	0		0	(	10	0		0	0
Soil	5	0		0	0	3	0		0	0	21	1		0	(	9	1		0	0
Baggs			# of incidents in category: 5					# of incidents in category: 13					# of incidents in category: 5				# of incidents in category: 13		
Clean Air (Rayleigh)	0	0		2	3	0	0		7	6	0	1		20	4	0	3		10	0
Organics	0	1		4	0	1	9		2	0	0	4		21	(	0	0		13	0
Elemental Carbon	4	1		0	0	2	9		2	0	12	11		2	(	2	9		2	0
Ammonium Sulfate	5	0		0	0	12	1		0	0	11	14		0	(	3	9		1	0
Ammonium Nitrate	5	0		0	0	13	0		0	0	25	0		0	(	13	0		0	0
Soil	5	0		0	0	13	0		0	0	25	0		0	(	13	0		0	0
Hayden VOR			# of incidents in category: 6					# of incidents in category: 12					# of incidents in category: 3				s in category: 14		
Clean Air (Rayleigh)	0	0		1	5	0	1		10	1	0	2		21	(	0	1		13	0
Organics	1	3		2	0	0	7		5	0	0	4		19	(	0	3		11	0
Elemental Carbon	1	5		0	0	3	7		2	0	5	17		1	(	2	12		0	0
Ammonium Sulfate	6	0		0	0	6	6		0	0	9	13		1	(	1	12		1	2
Ammonium Nitrate	6	0		0	0	12	0		0	0	22	1		0	(	14	0		0	0
Soil	6	0		0	0	11	1		0	0	21	2		0	(	12	2		0	0
Hayden Waste Water			# of incidents in category: 4					# of incidents in category: 7					# of incidents in category: 1				# of incidents in category: 20		
Clean Air (Rayleigh)	0	0		2	2	0	0		3	4	0	0		18	3	0	3		17	0
Organics	2	0		2	0	0	6		1	0	2	11		8	(	0	6		14	0
Elemental Carbon	0	4		0	0	4	1		2	0	3	17		1	(	1	19		0	0
Ammonium Sulfate	4	0		0	0	4	2		1	0	6	14		1	(	3	16		1	0
Ammonium Nitrate	4	0		0	0	7	0		0	0	21	0		0	(	20	0		0	0

Soil	4	0	0	0	7	0	0	0	21	0	0 (	20	0	0	0

[a] Categories determined by measured extinction.
[b] % of calculated extinction due to component (since the measured and calculated values differ, some of the <15 Mm^{-1} Rayleigh values are classified as 25-50% although they should be greater than 50%).

Table 4.3.8

Average, Maximum, and Minimum Calculated Light Extinction by Chemical Components for All Sites

Site		Esul	Enit	Eoc	Eec	Esoil	Unid.
Buffalo Pass	ave	3.72 ± 3.60	0.63 ± 0.85	4.37 ± 3.46	2.45 ± 1.94	1.07 ± 0.90	1.21 ± 8.01
	min	0.47 ± 0.07	0.15 ± 0.09	0.00 ± 1.16	0.00 ± 0.72	0.19 ± 0.01	-10.43 ± 3.60
	max	16.04 ± 0.85	6.58 ± 0.42	13.64 ± 2.71	10.21 ± 8.48	4.51 ± 0.13	24.91 ± 13.90
	# in ave	77	77	77	77	77	77
Gilpin Creek	ave	3.11 ± 1.77	0.76 ± 0.36	5.29 ± 6.65	9.30 ± 7.58	0.55 ± 0.57	-1.60 ± 14.75
	min	0.67 ± 0.34	0.00 ± 0.34	0.00 ± 5.08	0.00 ± 2.56	0.09 ± 0.05	-36.08 ± 18.86
	max	9.11 ± 0.64	1.79 ± 0.40	29.68 ± 7.40	34.48 ± 19.47	3.60 ± 0.11	26.56 ± 9.23
	# in ave	37	37	37	37	37	37

Juniper Mt.	ave	2.98 ± 1.71	0.38 ± 0.20	5.10 ± 2.91	3.93 ± 1.97	0.98 ± 1.12	2.43 ± 7.61
	min	0.35 ± 0.04	0.04 ± 0.04	0.83 ± 1.10	0.05 ± 0.41	0.08 ± 0.04	-11.46 ± 2.33
	max	7.48 ± 0.38	1.12 ± 0.11	11.62 ± 1.53	8.44 ± 1.40	5.74 ± 0.25	31.61 ± 1.19
	# in ave	42	42	42	42	42	42
Baggs	ave	2.91 ± 2.14	0.39 ± 0.26	8.50 ± 4.33	3.64 ± 2.74	0.69 ± 0.54	-0.81 ± 6.04
	min	0.62 ± 0.08	0.13 ± 0.09	1.18 ± 1.99	0.00 ± 0.55	0.11 ± 0.21	-16.18 ± 3.44
	max	13.69 ± 0.75	1.26 ± 0.12	20.20 ± 4.76	11.94 ± 3.81	2.58 ± 0.18	12.24 ± 3.11
	# in ave	57	57	57	57	57	57
Hayden VOR	ave	3.53 ± 2.29	0.79 ± 0.78	7.51 ± 3.59	4.03 ± 1.94	1.45 ± 0.82	-2.19 ± 6.97
	min	0.67 ± 0.19	0.24 ± 0.07	0.23 ± 3.01	1.00 ± 0.67	0.29 ± 0.02	-13.43 ± 7.52
	max	11.33 ± 0.59	4.73 ± 0.25	15.80 ± 2.67	12.04 ± 3.78	3.80 ± 0.11	18.40 ± 19.95
	# in ave	69	69	69	69	69	69
Hayden Waste Water	ave	3.51 ± 1.89	1.12 ± 1.68	7.00 ± 4.25	4.25 ± 2.49	0.98 ± 0.71	2.92 ± 6.96
	min	0.53 ± 0.17	0.14 ± 0.08	0.21 ± 1.79	0.00 ± 0.62	0.10 ± 0.03	-11.91 ± 8.23
	max	9.06 ± 0.89	6.79 ± 0.44	19.14 ± 4.29	13.60 ± 4.91	4.82 ± 0.14	15.36 ± 8.54
	# in ave	66	66	66	66	66	66

will have a greater impact at certain sites than others due to the differing concentrations of the particulate matter the added component is superimposed upon.

A similar comparison was made for organic carbon light extinction. Of the 142 cases where organic carbon was estimated to account for more than 25% of the total light extinction (not including the Gilpin Creek samples, which are subject to local wood smoke and a high carbon artifact), 26.1% were found at the Hayden VOR site, 17.6% at the Hayden Waste Water site, 12.0% at the Juniper Mountain site, 28.2% at the Baggs site, and 16.2% at the Buffalo Pass site. Most of the highest cases overlap the sulfate episodes, demonstrating that elevated light extinction is usually due to a combination of components.

Since the episodes selected for chemical analysis were chosen with a bias towards independent cases of noticeable visibility impairment caused by potentially different sources and during different meteorological conditions, the average of the chosen episodes is not representative of the overall conditions observed during the field portion of the MZVS. Therefore the results of the chemical analyses and the ELSIE modeling are presented here on an episode-by-episode basis to emphasize the different conditions that can lead to visibility degradation. The episodes are summarized below:

- 02/23/95: This IOP day was chosen due to a sharp peak in the Buffalo Pass light scattering accompanied by a sharp 22-ppb spike of sulfur dioxide. The conditions were moist, especially at higher elevations. Chemically, the highest nitrate of the MZVS occurred at Hayden Waste Water during the morning, and the organics were uncharacteristically high for a winter sample. Although the elemental carbon was high, the soluble potassium indicative of vegetative burning was low. Also, although the selenium and sulfur dioxide, generating station emissions markers, were high at all of the sites, the sulfate remained low and regional in nature. Optically, the air (Rayleigh scattering) dominated the light extinction. At most of the sites, the organics and elemental carbon components were responsible for most of the particulate light scattering. Hayden Waste Water was an exception, with ammonium nitrate and ammonium sulfate causing the largest portion of the explained extinction.

- 03/26/95–03/31/95: Light scattering was elevated at all sites during this non-IOP. Videos showed weather obscuration, punctuated by cloud clearing during which distant targets were moderately obscured. A 20-ppb sulfur dioxide spike occurred on the morning of 03/30/95. Also, a morning scattering peak occurred on 03/28/95 but was not accompanied by a sulfur dioxide peak. The conditions were moist throughout the region. Chemically, sulfates and soils increased during the episode with maximums at Buffalo Pass on 03/30/95 and 03/31/95. Buffalo Pass consistently showed higher selenium and sulfur dioxide concentrations than the other sites during the entire episode. Characteristic of a winter sample, the organics were low and the elemental carbon was associated with soluble potassium. Although the sulfates reached their maximums at the end of the episode, the organics, elemental carbon, and soluble potassium all peaked on 03/27/95. Since sulfate was the primary component of the aerosol, it was not surprising that most of the light scattering observed during this episode was caused by ammonium sulfate. The Rayleigh scattering was also a major

contributor to the overall light extinction. The large unexplained component was probably a function of the high relative humidities causing high nephelometer readings.

- 05/06/95–05/07/95: Light scattering was elevated at all sites during this moist non-IOP. This episode was interesting because Gilpin Creek had higher selenium, sulfur dioxide, sulfate, organics, and elemental carbon than Buffalo Pass on 05/06/95. In contrast 05/07/95 displayed regional sulfate with more sulfur dioxide at Juniper Mountain than at the other sites. Although the organics were low, there was a moderate amount of elemental carbon associated with soluble potassium. The soil concentrations were elevated at all of the sites. Although the ammonium sulfate and Rayleigh components were the largest contributors to the light extinction at Buffalo Pass and Juniper Mountain, the elemental carbon contribution was larger than the ammonium sulfate contribution at Gilpin Creek. Again, due to the moisture, the unexplained portions of the measured light extinction were high at Buffalo Pass and Gilpin Creek.

- 06/14/95–06/16/95: A consistently high light scattering was found across the network during this dry period. High sulfate concentrations were observed at the sites. Buffalo Pass and Gilpin Creek track each other for selenium, sulfur dioxide, and sulfate, but Juniper Mountain led both sites by a day. The sulfate at Juniper Mountain peaked on 06/14/95 and the decreased through the rest of the episode. The sulfate concentrations at Buffalo Pass and Gilpin Creek, however, peaked on 06/15/95 and then decreased. The organics and soluble potassium started very high, but decreased through the period. Again, Gilpin Creek had higher organics, elemental carbon, and soluble potassium than the other sites. This led to Gilpin Creek having the highest light extinction of the three sites, with most of the extinction being due to the organics and elemental carbon portions of the aerosol. The light extinction due to ammonium sulfate peaked on 06/15/95 at Buffalo Pass when it was approximately the same as the Rayleigh component. At Buffalo Pass and Juniper Mountain, which exhibited higher light extinction than Buffalo Pass, the light extinction on 06/14/95 and 06/16/95 was primarily due to Rayleigh and the organics and elemental carbon fractions.

- 06/29/95–07/01/95: Very high light scattering coefficients were measured at Juniper Mountain and Baggs on 06/30/95, with rapid decrease on 07/01/95. These changes are reflected to a lesser extent in measurements from the other sites. Buffalo Pass was moist, while the other sites were relatively dry during daylight hours. The sulfate measurement at Juniper Mountain for 06/30/95 was invalid, but Buffalo Pass and Gilpin Creek both showed peaks in sulfate, sulfur dioxide, and selenium on that day. The peak in sulfate corresponded to a peak in organics at Buffalo Pass. The contributions to light extinction are highly elevated at Buffalo Pass on 06/29/95 due to the high relative humidities (the nephelometer data was invalid for this period due to the weather). On 06/30/95 and 07/01/95, both Buffalo Pass and Gilpin Creek's light extinction were dominated by Rayleigh scattering and extinction due to organics and elemental carbon.

- 07/29/95–07/31/95: Scattering was elevated during this non-IOP at all of the sites during low relative humidity conditions. There was a lot of variability in the light

scattering at all sites. The sulfates at Buffalo Pass and Gilpin Creek were of approximately the same magnitude during this day. The Gilpin Creek site did show selenium and sulfur dioxide on 07/29/95 and 07/31/95. The organics and elemental carbon decreased during this episode. Accordingly, the light extinction due to organics and elemental carbon decreased during this period, but it was still the primary component at Gilpin Creek and was on the order of Rayleigh scattering at Buffalo Pass. The ammonium sulfate contribution to light extinction was small at both sites (~3-4 Mm^{-1}).

- 08/07/95–08/09/95: This episode had elevated light scattering at all sites during a period of low relative humidity. The light-scattering peaks were much less defined at Gilpin Creek than at the other sites. This was one of the primary episodes for modeling. This period showed the greatest forest fire impact of the MZVS. It had very high organics, elemental carbon, and soluble potassium due to the nearby forest fires listed in the fire inventory. In addition to the high fire components, this period also had high (~1.5 $\mu g/m^3$) sulfate at all of the sites (i.e. regional), high selenium and sulfur dioxide at Hayden Waste Water and Hayden VOR in the mornings, increased selenium and sulfur dioxide at Buffalo Pass on the afternoons of 08/08/95 and 08/09/95, and increased soils. The light extinction during this period was high (>30 Mm^{-1}) for 08/07/95 and 08/08/95 and decreased only slightly on 08/09/95. Although the sulfates observed during this period were high, their contribution to light extinction was overwhelmed by that of the elemental carbon and organics (up to 30 Mm^{-1} at some of the sites).

- 08/14/95: A small morning increase in light scattering at Buffalo Pass was coincident with an increase in sulfur dioxide. Sulfate was low (~0.5 $\mu g/m^3$) at all sites during both the morning and afternoon samples although the selenium and sulfur dioxide were high at Buffalo Pass, Baggs, Hayden VOR, and Hayden Waste Water during the morning period. The soluble potassium was low despite the high elemental carbon, and the organics were lower than in the previous episode. However, there was enough elemental carbon and organics to dominate the light extinction. The contributions due to ammonium sulfate were approximately a fifth of those due to Rayleigh.

- 08/21/95–08/27/95: This was an example of high relative humidity conditions followed by a period of lower relative humidities. The light scattering was elevated and there were clear peaks in the light scattering at all of the sites. The peaks in the Gilpin Creek light scattering were some of the clearest observed during the MZVS. This was one of the primary episodes for modeling. Chemically, there were high sulfates, selenium, organics, and elemental carbon throughout the period. Every morning the sulfur dioxide and selenium were higher at Baggs, Hayden Waste Water, and Hayden VOR than in the afternoon. During 08/21/95–08/25/95, the wet period, the sulfate, sulfur dioxide, and selenium concentrations at Buffalo Pass increased every afternoon, while during 08/26/95–08/27/95, the dry period, the sulfates, sulfur dioxide, and selenium decreased at Buffalo Pass during the afternoon. Interestingly, ammonium sulfate was the primary contributor to light extinction at Buffalo Pass through 08/24/95, but not afterwards when the contributions due to organics and elemental carbon,

on the order of Rayleigh, were higher than the ammonium sulfate contributions. Although the light extinction due to sulfate was noticeable at the other sites, the light scattering due to organics and elemental carbon and Rayleigh scattering dominated the light extinction.

- 09/02/95: An increase in light scattering at Buffalo Pass was partially accompanied by an increase in sulfur dioxide during the same period. This period was characterized by high sulfates throughout the network and a slight increase in sulfate at Buffalo Pass in the afternoon. Again the generating station emissions markers were higher in the morning at Baggs, Hayden VOR and Hayden Waste Water than in the afternoon. Also, all of the sites had high elemental carbon concentrations although the soluble potassium and organics were only of moderate levels (~2 $\mu g/m^3$ for organics). As expected, the elemental carbon and organics together were the largest contributors to light extinction at all of the sites. However, at Buffalo Pass, the light extinction due to ammonium sulfate was close to being on the order of the Rayleigh and elemental carbon and organics components.

- 09/17/95–09/21/95: This episode started off with low relative humidities and by the second day had very high relative humidities. (Weather affected portions of this episode.) There were some good examples of the interaction between fog and aerosols and several correspondences at Buffalo Pass between sulfur dioxide and light scattering during this episode. This was the highest priority episode for modeling. Chemically, the sulfates in this episode started out looking regional (09/17/95), but showed dramatic local influences on 09/18/95 and 09/19/95, including the highest sulfates and selenium observed during the MZVS (sulfates >4.0 $\mu g/m^3$ and selenium >2.5 ng/m^3, respectively, at both Hayden VOR and Hayden Waste Water). 09/20/95 and 09/21/95 showed a more regional signature, with slight local influences. During this entire period, Hayden VOR and Hayden Waste Water had higher sulfur dioxide and selenium in the mornings than in the afternoons and Buffalo Pass had increased sulfates and sulfur dioxide every afternoon except 09/21/95. The nitrates at the valley sites were also slightly elevated on the morning of 09/18/95. The organics started high and decreased through the period. There was significant elemental carbon at the sites and some corresponding soluble potassium. The light scattering on 09/17/95 was fairly low with both Buffalo Pass and Gilpin Creek having Rayleigh scattering as the primary component of light extinction. However, when the periods had high relative humidity, the light extinction rose dramatically and was dominated by organics and ammonium sulfate. For example, on the afternoon of 09/18/95, the sulfate was responsible for approximately 30 Mm^{-1} of light extinction. The afternoon of 09/19/95 was drier, and all of the sites showed much lower relative humidities and ammonium sulfate and organics contributions to light extinction. On the morning of 09/21/95, Buffalo Pass showed a large contribution to light extinction from ammonium sulfate due to a large concentration of sulfate at the site and high humidity. The Hayden Waste Water site showed a similar peak in sulfate, but did not have the corresponding humidity, so had a much lower light scattering due to ammonium sulfate than the corresponding sample at Buffalo Pass.

- 09/24/95: This episode had morning peaks in light scattering at most of the sites and a distinct peak in light scattering during the late afternoon at Gilpin Creek. This episode showed regional sulfate, low organics, and some elemental carbon and soluble potassium at all sites. Although Buffalo Pass had increased sulfur dioxide and selenium in the afternoon, the sulfate decreased slightly. The light extinction at Buffalo Pass also decreased in the afternoon, but dramatically instead of slightly as the small decrease in the concentration of sulfate would suggest. Again, the high relative humidity caused a large light extinction due to the sulfate component at Buffalo Pass. This sulfate component of light extinction dominated the contributions of the other components. The other sites showed lower light extinctions than Buffalo Pass in the morning and higher light extinctions than Buffalo Pass in the afternoon, although the observed extinction decreased at all sites in the afternoon.

- 09/27/95: This was a fairly dry episode with correspondence between light scattering and sulfur dioxide. There were two peaks observed in the light scattering at most sites. Again this episode displayed regional sulfate with increased sulfur dioxide and selenium in the morning at Hayden VOR and Hayden Waste Water, and selenium and sulfur dioxide at both Gilpin Creek and Buffalo Pass. Organics, elemental carbon, and soluble potassium were elevated at Juniper Mountain, Hayden VOR, and Hayden Waste Water during the afternoon. Buffalo Pass showed the same increased organics and soluble potassium as the other sites, but the elemental carbon decreased. The total light extinction was dominated by organics, elemental carbon, and Rayleigh at all of the sites except Buffalo Pass, where ammonium sulfate was on the order of, or higher than, the combined organics and elemental carbon components.

- 09/30/95–10/02/95: Light scattering was elevated throughout the network. The relative humidity changed from very high to mid-range during the course of this episode. SO_2 and light scattering were correlated at Buffalo Pass on 10/01/95. This episode started with one of the cleanest IOP periods and ended with a clean period. However, the sulfates peaked on the afternoon of 09/30/95 and the morning of 10/01/95. The selenium and sulfur dioxide were at their maximum on the morning of 10/01/95 and decreased through the rest of the period. There was a strong generating station signature at all of the sites (except Juniper Mountain where the sample was invalid), but Buffalo Pass did not show a corresponding increase in its afternoon sulfate concentrations, except when regional sulfate appeared at all sites on the afternoon of 09/30/95. Gilpin Creek showed very high elemental carbon and soluble potassium concentrations during this period. Also, the organics were decreasing towards their low winter values. The high relative humidities greatly increased the light extinction at the elevated sites as evidenced by the high unexplained components. It also amplified the extinction due to ammonium sulfate and ammonium nitrate when they were present. Corresponding to the large sulfate concentration at Buffalo Pass on the afternoon of 09/30/95 was a 30 Mm^{-1} contribution to light extinction from ammonium sulfate. The mornings of 10/01/95 and 10/02/95 also showed significant contributions to light extinction from ammonium sulfate and ammonium nitrate.

At the lower elevation sites, the light extinction was dominated by the combined organics and elemental carbon contributions.

- 10/07/95–10/14/95: This episode was important because a wide variety of conditions were observed. The light scattering was elevated at all of the sites from 10/07/95 through 10/12/95 and then dropped to near Rayleigh on 10/13/95 and 10/14/95. There were two large peaks (10/08/95 and 10/12/95) in light scattering superimposed on the elevated light scattering and corresponding to peaks in the relative humidity. Also during this elevated period there were intermittent spikes of sulfur dioxide at Buffalo Pass. The 10/13/95 and 10/14/95 dates were of interest because the light scattering was very low while there were high sulfur dioxide concentrations present at Buffalo Pass. This was one of the primary episodes for modeling. Chemically, this period was very clean as far as sulfates were concerned. The sulfate was low and regional in nature. The two large peaks in light scattering corresponded to the two periods where sulfates were elevated. There was a regional increase in sulfate on 10/08/95. Juniper Mountain experienced an increase in sulfate on the afternoon of 10/11/95, while the other sites did not experience the increase until the morning of 10/12/95, when Juniper Mountain began to decrease. On 10/13/95 and 10/14/95, the concentrations of selenium and sulfur dioxide were elevated at all sites, but the sulfate concentrations were very low (< 0.5 $\mu g/m^3$). Also, the sulfates at Buffalo Pass did not increase on the afternoons of 10/07/95 and 10/09/95 despite elevated sulfur dioxide and selenium at Hayden VOR and Hayden Waste Water in the morning. The organics, elemental carbon, and soluble potassium were elevated for typical fall/winter samples on 10/08/95, 10/10/95, and 10/12/95 (note the correspondence of two of those days to the sulfate peaks). However, 10/13/95 and 10/14/95 were far more representative of winter organics concentrations (< 1 $\mu g/m^3$). It is also interesting to note that the soil component of the aerosol was elevated until afternoon of 10/12/95. The light extinction during this episode followed the trends in the chemical composition fairly well since the relative humidity was low. There were peaks in light scattering on the morning of 10/08/95 and 10/12/95 which were dominated by organics and elemental carbon. Ammonium sulfate was a significant contributor at Buffalo Pass, but it was not as significant as the organics and elemental carbon. Also, there was a peak in light scattering due to organics and elemental carbon at Gilpin Creek on 10/10/95. The rest of the days had light extinctions on the order of 20 Mm^{-1} and were dominated by the Rayleigh scattering component.

- 10/16/95–10/19/95: There was elevated light scattering throughout the network that decreased toward 10/19/95 at all sites except Buffalo Pass and Gilpin Creek which showed peaks in their light scattering. A prescribed burn was seen in the 10/19/95 video of the Yampa Valley from Cedar Mountain. Corresponding to the fire, the soluble potassium and elemental carbon were slightly elevated. The organics and soils were low, and became lower as the period progressed. The Buffalo Pass and Juniper Mountain sulfate concentrations were very similar, although Buffalo Pass had higher sulfur dioxide. The light extinction at both Buffalo Pass and Juniper Mountain peaked on 10/17/95 with Rayleigh being the dominant contributor. The organics and elemental carbon contributions were

slightly higher at Juniper Mountain than at Buffalo Pass, while the ammonium sulfate contributions were approximately the same at both sites.

- 10/22/95–10/23/95: There was high relative humidity throughout the region and large peaks in light scattering at several of the sites. There were coincident SO_2 and light-scattering peaks on 10/23/95 at Buffalo Pass. This period was the cleanest period chosen for analysis during the MZVS. The soils, organics, elemental carbon, and soluble potassium were all very low. However, the Buffalo Pass sulfates, sulfur dioxide, and selenium were elevated with respect to Juniper Mountain during this period. The light extinction was also very elevated, due to the high relative humidities (e.g., high unexplained component). After Rayleigh, the contribution to light extinction from ammonium sulfate was the highest explained contribution to light extinction at Buffalo Pass on 10/22/95 and at Juniper Mountain on 10/23/95. On 10/23/95, the light extinction due to ammonium sulfate was higher than the Rayleigh contribution and much higher than any other explained component.

4.4 Comparison with Other Class I Areas

Table 4.4.1 compares the IMPROVE measurements for several keys species at Mt. Zirkel, Bridger, and Lone Peak Wilderness Areas and at Canyonlands, Mesa Verde, and Rocky Mountain National Parks during March through August, 1995. Figure 3.1.1 shows the locations of these sampling sites. During the spring (March through May), the average (50%) and 10% level concentrations at the Mt. Zirkel wilderness sites were approximately 10% to 30% less than the other sites. However, at the 90% level, these species concentrations were similar among all sites. The Lone Peak Wilderness Area exhibited the highest concentrations of most of the species examined, with 1.6 $\mu g/m^3$ of sulfate, 0.9 $\mu g/m^3$ of nitrate, 0.00044 $\mu g/m^3$ of selenium, and 7.1 Mm^{-1} of light absorption (b_{abs}).

The chemical concentrations were increased in the Mt. Zirkel Wilderness Area during the summer (June through August). On average, the Bridger Wilderness Area reported 15% to 30% lower concentrations than the Mt. Zirkel Wilderness Area. Nitrate concentrations remained approximately constant between the spring and summer at most of the sites, while light absorption increased at all of the sites in summer. Except for the constant low sulfate concentrations (0.5 $\mu g/m^3$) at the Bridger Wilderness Area, sulfate concentrations at the 50% level ranged from 0.7 $\mu g/m^3$ at the Mt. Zirkel Wilderness Area to 0.9 $\mu g/m^3$ at the Mesa Verde and Rocky Mountain National Parks. These summer levels increased by 40% to 90% as compared to spring. In contrast, the sulfur dioxide concentrations experienced a 30% to 45% reduction during the summer as compared to the spring.

Average silicon concentrations varied from 0.05 $\mu g/m^3$ to 0.13 $\mu g/m^3$ during the spring and from 0.097 $\mu g/m^3$ to 0.20 $\mu g/m^3$ during the summer. The highest 90% level silicon concentration of 0.5 $\mu g/m^3$ was found at the Rocky Mountain National Park.

The concentrations presented in Table 4.4.1 are comparable to the statistics presented in Tables 4.2.1a-f, which show average concentrations of 0.8 to 1.1 $\mu g/m^3$ for sulfate, 0.07 to 0.25 $\mu g/m^3$ for nitrate, and 0.11 to 0.25 $\mu g/m^3$ for silicon.

Table 4.4.1 Comparison of 1995 IMPROVE Measurements for Major Chemical Components

Table 4.4.1

Comparison of 1995 IMPROVE Measurements for Major Chemical Compounds

(all concentrations are derived from twice-weekly 24-hour filter samples in ng/m^3 except for b_{abs} which is in Mm^{-1})

Site	Mt. Zirkel Wilderness Area			Bridger Wilderness Area			Canyonlands National Park			Lone Peak Wilderness Area			Mesa Verde National Park			Rocky Mountain National Park		
Percentile[a]	10%	50%	90%	10%	50%	90%	10%	50%	90%	10%	50%	90%	10%	50%	90%	10%	50%	90%
Spring (March-May) 1995																		
SO_4	175.7	461.5	######	232.1	468.45	926.2	259.2	505.65	1,134.2	239.8	592.7	1,589	262.0	561.2	1,091.4	198	497.4	######
NO_3	16.3	98.5	344.8	38.3	90.2	265.1	37.3	109.25	199.1	67	305.6	898	33.8	78.8	244	30.6	167.2	597.5
SO_2	NA	NA	NA	NA	NA	NA	33.4	247.9	763.6	NA	NA	NA	35.4	266.2	897.1	0.7	57.6	300.7
b_{abs}	<MDL[b]	1.1026	3.0531	0.5542	1.2167	0.2451	0.4949	1.4291	3.0543	1.0035	4.3625	7.0677	51.35	286.07	312.81	54.91	179.29	361.86
Se	0.05	0.09	0.26	0.05	0.14	0.26	0.11	0.18	0.33	0.08	0.23	0.44	0.09	0.16	0.30	<MDL[b]	0.10	0.19
Si	22.41	80.98	243.22	21.17	56.53	254.22	29.33	124.55	379.46	28.91	94.30	243.24	27.55	130.42	325.35	30.56	86.85	304.29
Summer (June-August) 1995																		
SO_4	429.3	723.6	######	251.0	510.55	901.2	465.5	804.7	1,463.9	403.2	868.2	######	519.3	919.9	1,788.8	362.7	924.1	######
NO_3	55.8	96.2	183.5	42.5	83.85	144.6	49.6	95.6	228.5	101.3	158.4	354.2	45.2	95	227.1	55.4	171.7	649.1
SO_2	NA	NA	NA	NA	NA	NA	<MDL[b]	<MDL[b]	414.9	NA	NA	NA	<MDL[b]	<MDL[b]	487.8	<MDL[b]	<MDL[b]	217.3
b_{abs}	1.0215	2.2074	5.3713	0.7410	1.9333	4.2068	1.9410	2.9443	5.2933	4.0900	6.9500	9.6762	164.37	335.81	589.06	319.07	624.73	979.62
Se	0.14	0.19	0.27	<MDL	0.21	0.31	<MDL[b]	0.22	0.28	<MDL[b]	0.26	0.38	0.12	0.26	0.37	0.15	0.22	0.33
Si	59.54	190.31	322.19	49.60	97.40	217.08	75.35	164.31	227.39	85.21	197.84	364.04	63.07	125.47	345.32	82.40	201.19	495.91

[a] The concentrations at the specified percentile.

[b] Minimum detectable limits.

5.0 YAMPA VALLEY PLUME BEHAVIOR

As defined in Section 1, plumes are coherent bodies of pollutants that are detectable either by visible observation or by instrumentation. For example, sulfur dioxide detected at levels above background is a good indication of being in a generating station plume, even though particle levels may be so low that no plume can be seen.

The most visible plumes within the Yampa Valley are those from the Hayden and Craig coal-fired generating stations. The most noticeable of these are steam emissions from the cooling towers that rapidly evaporate upon dilution with ambient air. Primary particles that pass through electrostatic precipitators are the main cause of visible emissions from stacks. These primary particle plumes become more visible when precipitators malfunction. The majority of pollutant emissions from generating stations are sulfur dioxide and nitric oxide that can be detected instrumentally but not visually. Sulfur dioxide and oxides of nitrogen, along with ammonia, can change into particulate ammonium sulfate and ammonium nitrate that contribute to light extinction. These transformation rates are highly variable, but they can be expected to be low in clear air and rapid when plumes encounter fogs or clouds. For this reason it is important to know whether or not plumes containing precursor gases encountered fogs and clouds. Prescribed burns and wildfires also cause visible plumes within and outside the Yampa Valley. Emissions from motor vehicles and residential burning can accumulate at night and during the morning near the floor of the Yampa Valley, to be mixed above the surface when the morning sun heats the surface layer. The time and nature of this coupling must be understood to determine how these pollutants might be transported to the wilderness.

This section examines the behavior of plumes in the Yampa Valley, with special emphasis on emissions from the major generating stations. It summarizes the visual character of these plumes and develops a conceptual model of how they might mix with surface pollutants below the nighttime inversion, and how these mixed emissions might couple to upper-air westerly winds. Primary emission events from generating stations that occurred during malfunctions and/or upsets, and were seen on video but not necessarily detected by nephelometers, are tabulated and described. Continuous emission rates of sulfur dioxide and oxides of nitrogen from the five generating units are plotted to identify emission variations and plant downtime. The results of everyday modeling of generating station plumes are summarized to determine how frequently they might arrive at the Wilderness, whether or not they would cause perceptible haze. Finally, for the episodes selected in Section 3, emissions and meteorology are examined to understand the conditions under which emissions from various sources might mix to cause the haze observed during those episodes.

5.1 Plume Observations

The Chavez Mountain (CHHZ) video of Hayden station and the Cedar Mountain (CEDZ) video of the Craig station were examined to determine where and when visible plumes mixed to the surface, traveled up-valley toward the Wilderness, or down-valley away from the Wilderness.

Monthly plots were made for each morning (0600 to 1200 MST) and afternoon (1200 to 1800 MST) periods (Air Resource Specialists, 1995; 1996) to show up-valley and down-valley flows and whether these were consistent with upper-air flows. Plume directions were discerned from the directions of the visible plumes, and upper-air flows were inferred from cloud movements. For example, if the steam plume from a generating unit flowed down-valley but clouds were observed to flow up-valley, the flow was called decoupled. If all flow indicators moved in the same direction, the flow was classified as coupled. Condensed steam plumes were more visible for the entire day during cold periods. During dry summer afternoons, steam plumes were often not visible, and unless primary particle emissions were visible, plume movement was not classified. Hayden primary particle emissions were visible most of the time, but Craig primary particle emissions were commonly not visible. When both steam and particle emissions were clearly visible, the plume classification was made for the particle emissions. Plume movement was not classified when the video view was obscured by weather. April, May, and June had the highest frequency of obscured views.

Figures 5.1.1 and 5.1.2 summarize the flow frequencies from the individual monthly plots for the Hayden station and the Craig station, respectively. These plots show that up-valley and down-valley plume movement occurred regularly in the Yampa Valley during the study period with down-valley movement most commonly occurring from shortly after sunset to late morning. Up-valley movement occurred from late morning until sunset. This is the case for both generating station plumes.

Morning down-valley plume movements were commonly decoupled. The visible plumes moved down-valley with the drainage flow, while upper levels of the atmosphere moved with the synoptic flow. The plumes seldom penetrated the inversion layer. Afternoon up-valley plume movements are commonly coupled, and visible plumes mix with upper flows most of the time. During stormy periods, however, plume movements and upper-air flows were commonly coupled. Hayden plumes experienced more down-valley movement than the Craig plumes.

Bifurcated plumes were observed on some days. A buoyant portion of the plume would pass through the surface layer and be transported up-valley, while the portion of the plume in the surface layer moved down-valley. Plumes were seen to pass into valley fogs on several occasions, which will be described later in this section. At times, small clouds would form at the condensation level above and slightly downwind of the stacks.

5.2 Mesoscale Mixing and Flows

Upper-air wind and temperature measurements in the Yampa Valley are examined to: 1) describe the potential for local and regional transport of emissions and haze; 2) compare mixing depth estimates computed using CALMET to observation-based estimates; and 3) describe a conceptual model of the mechanisms that mix and transport emissions from

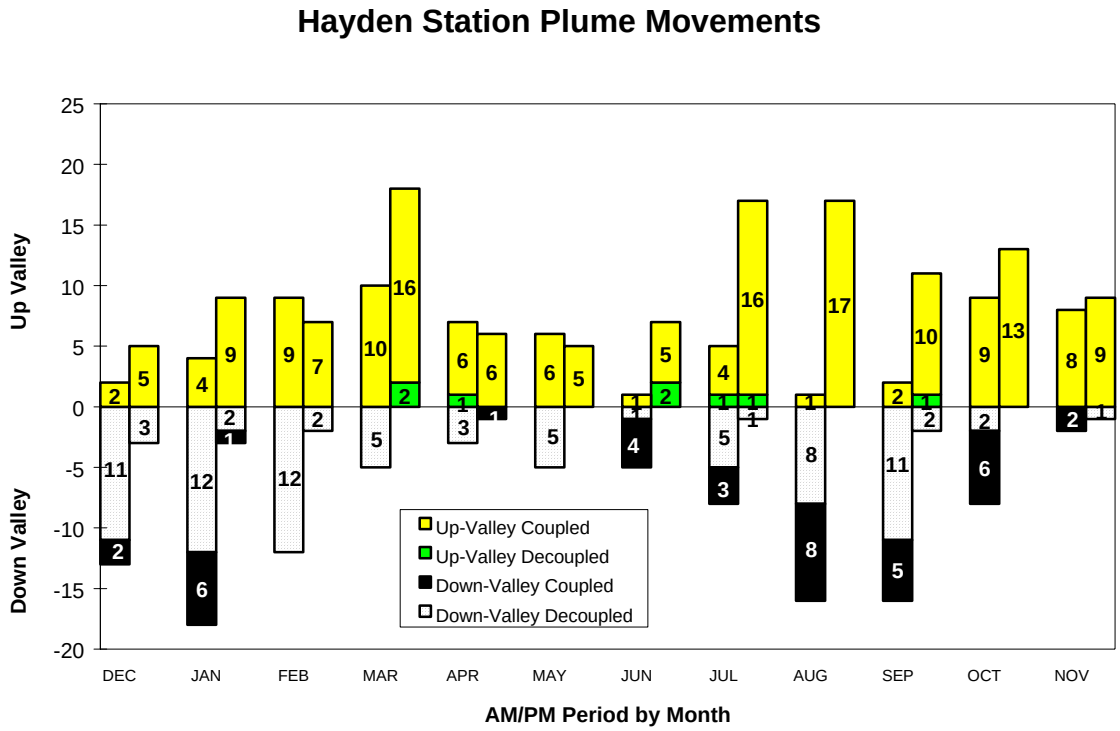

Figure 5.1.1. Hayden station plume movements.

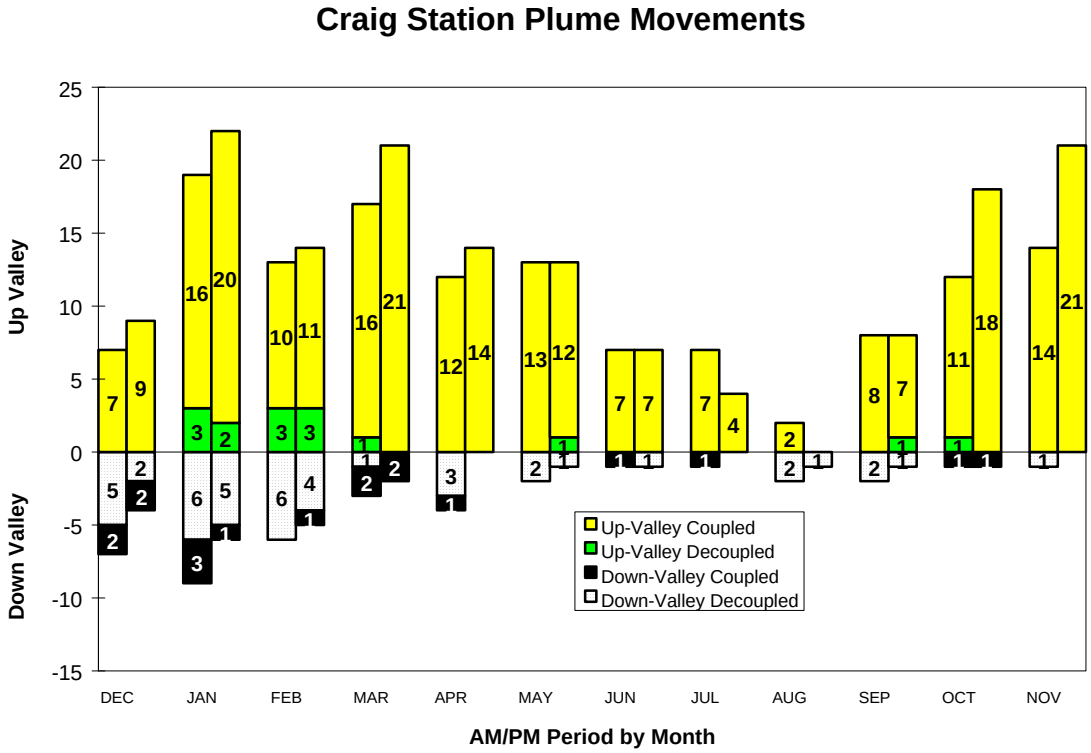

Figure 5.1.2. Craig station plume movements.

elevated and ground-level emitters, especially power stations, in the Yampa Valley. The Hayden (SEWZ), Clark (CLAZ), and Baggs (BAGZ) radar profiler measurements up to 3000 m AGL and RASS virtual temperature measurements up to 900 m AGL are used in these analyses.

5.2.1 Climatology of Winds Aloft

Figure 5.2.1 shows a time-height cross section of these annually averaged (12/01/94 to 11/30/95) winds at Hayden. Several wind regimes were persistent enough that they survived the averaging:

- Drainage flow is shown as a low-level (below 400 m AGL) easterly wind at night starting on average at 2000 MST and ending the following morning at 0900. This flow was produced when cold, dense air flowed downward into the Yampa Valley from the surrounding valleys and mountains. During this time, the low-level winds became decoupled from the prevailing westerly flow aloft. At 2000 MST, the drainage flow was quite shallow (i.e., 150 m deep) and typically deepened to 350 m by the next morning. Temperature profiles from the RASS showed a temperature inversion at the top of the drainage flow, which would tend to trap emissions in or just above the cold, stable air.

- Above 600 m AGL, the winds were synoptically driven most of the time, which produced west-southwesterly to westerly flow all day. These persistent westerly winds make it likely that background haze in the area comes from the west most of the time and rarely travels across the mountains from the east.

- During the daytime (1000 to 1800 MST), vertical mixing caused the winds below about 500 m to become coupled with the prevailing westerly winds (i.e., synoptic flow) most of the time. During this part of the day, air at all levels moved up the Yampa Valley toward Buffalo Pass and the southern end of the Wilderness area most of the time.

The flow reversal from easterly winds (drainage flow) to westerly winds (coupled) was a regular feature observed at the Hayden upper-air site. The coupling occurred when the drainage flow ceased and the heating of the valley and surrounding mountain sides mixed low-level and aloft air. This flow reversal occurred on 63% of the days from June through September and on 37% of the days from December through May. Figure 5.2.2 shows an annual frequency distribution of the time when winds became coupled (i.e., when the drainage flow ceased) at the Hayden site. Most of the time (70%), winds became coupled between 0900 and 1300 MST. On other less frequent occasions, the drainage flow ended early, while on other days it persisted throughout the day. As discussed further in Section 5.2.3, this low-level flow reversal may allow the accumulation of emissions during the night and morning hours and the subsequent transport of emissions toward the east when the low-level and upper flows recouple in mid-day.

Figure 5.2.1 Time-height cross sections of annually averaged winds at Hayden, Colorado.

Figure 5.2.2 Frequency distribution of the times when the low-level winds (below about 400 m AGL) became coupled with the prevailing synoptic winds at the Hayden site from 12/01/94-11/30/95.

To examine the similarities and differences in the winds at the upper-air sites, the winds from each pair of upper-air sites were correlated. This was performed over an eight-month period from February through September by correlating the wind speeds and east-west and north-south components of the wind from two sites at each altitude. Figure 5.2.3 shows plots of these correlation coefficients as a function of altitude; two distinct wind regimes were observed:

- A synoptically driven region was apparent above ~3,300 m MSL, where the correlation of the winds from all three sites is high (above 0.7). This indicates that the large-scale synoptic forcing affecting all three of these sites was similar, which was expected given that the sites were within 100 km of each other.

- A terrain-influenced region is evident below ~3,300 m MSL, where the local topography altered the winds. Correlations begin to decrease starting at the height of the local ridgeline; decreasing from about 0.7 at 3,300 m MSL to less than 0.5 at the lower levels near the ground in the valleys.

These wind differences between the regions were examined further by computing wind roses at the three profiler sites for selected episode periods of interest (08/21/95–08/27/95; 09/17/95–09/19/95; 09/27/95; 10/09/95–10/11/95; and 10/16/95–10/19/95). Wind roses were computed using hourly radar profiler winds at ~300 m AGL during the daytime (1000 to 1800 MST) and nighttime (1900 to 0900 MST). Wind roses were also computed for higher altitude winds at the level at Buffalo Pass (3,224 m MSL). The wind roses shown in Figures 5.2.4, 5.2.5, and 5.2.6 indicate the following:

- At Baggs, the winds were stronger during both the day and night than at either Clark or Hayden most of the time. Drainage flows did not appear to dominate the low-level winds as seen at Hayden. However, the lower level flows at night were more southerly than the southwesterly flows prevailing during the day. This may be due to terrain influences on the flows trapped at lower levels at night by the nocturnal inversion. Consequently, the air was channeled northward along the western side of the mountains. This southerly flow may allow emissions from the Craig area to be transported northward towards Baggs during the overnight hours. Baggs should be used as a background site only when the Yampa Valley emissions are transported in another direction, typically during the afternoon.

- At Clark, low-level winds (274 m AGL) were weak, with 73% of the wind speeds less than 2 m/s. Low-level winds were influenced by the surrounding terrain and strongly decoupled from the aloft winds at night and to some extent during the day

as well. The low-level winds at night also tended to align along the north-south Elk River valley. During the daytime, the low-level winds were also weaker than at other sites; thus, there was not much forcing to push air up the Elk River valley toward Gilpin Creek from the south.

Figure 5.2.3 Profiles of correlation coefficient for wind speed and the east west and north-south components of the wind for (a) Baggs and Clark, (b) Clark and Hayden, and (c) Hayden and Baggs.

Figure 5.2.4 Wind roses computed for the Baggs radar profiler site for 8/21/95-8/27/95; 9/17/95-9/19/95; 9/27/95; 10/9/95-10/11/95; and 10/16/95-10/19/95

Figure 5.2.5 Wind roses computed for the Clark radar profiler site for 8/21/95-8/27/95; 9/17/95-9/19/95; 9/27/95; 10/9/95-10/11/95; and 10/16/95-10/19/95.

Figure 5.2.6 Wind roses computed for the Hayden radar profiler site for 8/21/95-8/27/95; 9/17/95-9/19/95; 9/27/95; 10/9/95-10/11/95; and 10/16/95-10/19/95.

At Hayden, low-level winds at night were strongly decoupled from the aloft flow at 268 m AGL. The drainage flow was a common feature as shown by the easterly (east, east-northeast, east-southeast) winds occurring more than 65% of the time during the night hours. In addition, the winds were substantially stronger than winds at Clark, with speeds greater than 5.5 m/s more than 20% of the time and wind speeds less than 2 m/s only occurring 12% of the time. During the daytime, the low-level and aloft winds became coupled with prevailing westerly synoptic flow, which transports air up the Yampa Valley.

5.2.2 Mixing Depths during Episodes

The planetary boundary layer (PBL) is the portion of the atmosphere that is influenced by thermal and frictional forces arising from contact between the air and the earth's surface. These forces, in turn, cause significant diurnal changes in the depth of the PBL, which can range from about 100 to 300 m AGL at night to 1.5 to 2.5 km AGL during the day.

Mixing depth is defined as the altitude above the surface through which vigorous vertical mixing of heat, moisture, momentum, and pollutants occurs (Holzworth, 1972). During the daytime, the mixing depth is the altitude of a temperature inversion capping a well-mixed convective boundary layer. A plume emitted into a convective boundary layer (CBL) will be mixed vertically as well as diluted. At night, the top of the mixed layer is generally considered to be the depth of the stable boundary layer that forms when the

temperature of the air near the ground decreases in response to the radiational cooling of the earth's surface.

Mixing depths were estimated from the radar profiler data for two purposes. First, observation-derived mixing depths were used to help develop the meteorological inputs for the CALMET model. Specifically, observation-derived mixing depths were used to help interpolate temperature data from the NWS upper-air sites at Lander, WY and Grand Junction, CO (see Section 5.3 for more details). Second, mixing depths were used to help understand the diurnal change in the PBL and to identify times when plumes would be trapped in the stable boundary layer or mixed aloft into the prevailing synoptic flow. The techniques used to estimate mixing depths from observations are described below; and comparisons of observation-derived mixing depths with CALMET estimates are presented. The mixing depths are used further in Section 5.2.3 to describe a conceptual model of plume behavior.

Besides measuring winds and temperature, the radar profiler's reflectivity measurements can be used to compute the refractive index structure parameter (C_n^2). This parameter measures the variations in the refractive index of the atmosphere that are produced when turbulence creates gradients in humidity. Dye *et al.* (1994) showed that mixing depths estimated from C_n^2 and RASS during ozone episodes agreed well with mixing depths independently estimated from pollutant, temperature, and turbulence data collected by aircraft. Mixing depths for the MZVS were estimated from C_n^2 during the day using an algorithm developed by Dye *et al.* (1995b). During the morning, virtual temperature (T_v) data from RASS were used to identify the top of the stable layer (note that T_v data were unavailable at night).

Mixing depths were computed for Hayden using the C_n^2 and T_v data for 28 days (03/26/95–03/31/95; 08/04/95–08/09/95; 08/21/95–08/25/95; 09/17/95–09/22/95; 09/27/95; and 09/30/95–10/02/95). These mixing depths were then compared to those computed by the CALMET preprocessor. Figure 5.2.7 shows the average diurnal change in the observation-derived and CALMET mixing depths during these 28 days. This figure illustrates that, on an average basis, CALMET estimates are within several hundred meters of the observation-derived mixing depth estimates. The timing of the rise, fall, and peak mixing depths differ by one to two hours, but the rise and fall rates and peaks are similar. This is generally considered good agreement based on past comparisons of model and observation-based mixing depth estimates (Dye *et al.*, 1994; Haney *et al.*, 1995). This figure indicates that CALMET provides a reasonable estimate of mixing heights, on average, of the CBL, but tends to estimate an earlier growth of the morning convective boundary layer, and a later evening decrease in mixing than measured.

5.2.3 Conceptual Model of Plume Entrainment, Mixing, and Transport

This section presents a generalized conceptual model of the atmospheric processes that mix and transport emissions from Yampa Valley sources based on data collected during the MZVS. Meteorological conditions that result in transport of pollutants affecting visibility in the MZWA have been examined previously by Latimer (1994) and Orgill (1981). During the daytime, they found that the thermally-induced upslope flow can couple with the general southwesterly to westerly synoptic-scale flow and cause air to be transported out of the Yampa Valley toward the MZWA. At night, the formation of downslope, down-valley winds

decoupled the low-level flow from the westerly winds aloft and recirculated air from the eastern end of the Valley back to the western end. The conceptual model resulting from the 1995 MZVS data is consistent with that described by Latimer (1994) and Orgill (1981). This conceptual model seems to apply during all seasons in the absence of overriding synoptic influences (e.g., frontal passage).

The aloft wind data from the Hayden radar profiler were averaged for detailed data analysis periods (08/21/95–08/27/95; 09/17/95–09/19/95; 09/27/95; 10/09/95–10/11/95; and 10/16/95–10/19/95). In addition, mixing depths and the plume heights estimated by CALMET for the Hayden station were averaged over this same period to provide an indication of plume height and local mixing. Results for the Craig station are expected to be similar. Since observation-derived mixing depths were not available for all of the days or at night, the CALMET mixing depths were used. Figure 5.2.8 shows the average aloft conditions and plume heights during these periods. Although this figure shows averaged conditions, the wind patterns on the individual days were similar, with minor exceptions, such as the drainage flow did not begin in the evening on 2 of the 28 days.

The key atmospheric processes that mixed and transported emissions are discussed below. The plume behavior has been divided into three stages, based on the data shown in Figure 5.2.8, and a schematic drawing describing plume behavior is shown in Figure 5.2.9.

Figure 5.2.7	Average mixing depth estimates from CALMET and computed from the Hayden profiler's C_n^2 and virtual temperature data the 28 selected days associated with haze episodes.
Figure 5.2.8	Time-height cross section of averaged winds at Hayden, Colorado for the intensive study days: 8/21/95-8/27/95; 9/17/95-9/19/95; 9/27/95; 10/9/95-10/11/95; and 10/16/95-10/19/95.
Figure 5.2.9	Schematic showing plume behavior based on the analyses of aloft wind and temperature data, mixing depth and plumes heights, and the time-lapse video.

Drainage Flow

At about 1900 MST, the westerly flow that persists during the afternoon changes to easterly flow as the cold air from the surrounding valleys and mountains drains into the Yampa Valley. This drainage flow deepens from about 300 m AGL by 2300 MST to about 450 m AGL by 0700 MST. The mixing depth is quite shallow at night, but the thermal buoyancy allows the plumes from the power stations to ascend into the stable air in the drainage flow. An inversion typically exists at the top of the flow and traps the plume in the drainage flow. Fairly brisk easterly winds at 200 to 400 m AGL (average of 3.5 m/s) transport the emissions to the west at Hayden. These winds may be lighter at Craig, which is in a wider part of the valley and less affected by drainage. These wind speeds could carry the emissions from the Hayden and Craig units between 20 and 80 km to the west in the Yampa Valley. During the night, the emissions may flow up toward Baggs or remain in the Valley. This downslope flow may lead to an accumulation of emissions to the west of Hayden and

Craig. On several episodes days, fog was observed in the downslope flow, which may accelerate the conversion of SO_2 to sulfate.

5.2.3.1 Stage 2, Transition

This stage begins near sunrise when the convective boundary layer starts growing. The plume rise data suggest that between 0600 and 0700 MST, the plume ascends higher and reaches up to 600 m AGL. As the plume rises, it is initially carried westward by the downslope flow and then transported eastward by the prevailing synoptic flow aloft. A bifurcation of the plume may occur as it ascends through these two wind regimes with emissions transported in two directions. As noted in Section 5.1, this characteristic was observed in the time-lapse video on several mornings when the plume was visible.

5.2.3.2 Stage 3, Coupling

As the day continues, the drainage flow ends at about 1000 MST and the convective boundary layer continues deepening and reaches 1,600 m AGL by 1400 MST. Low-level winds couple with the synoptic flow aloft as aloft air mixes downward and the low-level air upward, causing the valley emissions to start flowing up the valley. Rigorous mixing in the CBL tends to dilute and mix emissions from the plumes throughout the developing boundary layer. At this time during several episodes, the plume mixed into clouds, which would accelerate the conversion process. As the CBL grows, these diluted emissions are mixed with any "background" air that was transported into the region aloft during the nighttime and early morning. In addition, surface-based anthropogenic pollutants would also be mixed upwards into the developing boundary layer. Thus, the aloft air in the boundary layer could contain a mix of pollutants from various sources. By 1200 MST, the mixed layer typically grows to about 1,300 m AGL, and the air with its background and local pollutant burden would now be transported eastward at the level of Buffalo Pass or higher.

5.3 Generating Station Emissions Variability

The Hayden station, near Hayden, CO, consists of two units, Unit 1 with a 184 MW capacity and a 76 m (250 ft) stack with a 7.6 m (25 ft) diameter and Unit 2 with a 262 MW capacity and a 120 m (395 ft) stack with a 9.4 m (31 ft) diameter. Hot-side electrostatic precipitators process emissions for both units. Bituminous coal with a nominal average sulfur content of 0.46% is obtained from the Seneca mine.

The Craig station, near Craig, CO, consists of three units, each with a 180 m (600 ft) stack. Units 1 and 2 are 428 MW units. These two units, also known as the Yampa Project, are equipped with electrostatic precipitators and wet limestone scrubbers that remove sulfur dioxide with ~ 67% efficiency. Unit 3 is a 408 MW unit and is equipped with a dry sulfur dioxide scrubber with ~ 85% efficiency and a baghouse that removes particles from the flue gas stream. During the study period, the Yampa Project burned bituminous coal from the Trapper Mine while Unit 3 used coal from the Colowyo Mine. Under normal operating conditions, the Craig station burns pulverized coal with a sulfur content of 0.24% to 0.65%.

Continuous SO_2 and NO_x emissions monitors were operated in the stacks of all units, and hourly emission rates for these chemicals along with hourly loads were obtained,

validated, and entered into the MZVS data base. Hours when the data for load, gas flows, and emission rate appeared inconsistent were identified, and the nature of the apparent inconsistency described. These descriptions and the corresponding plots were sent to the generating station operator for review. A review by generating station engineers indicated that many of the inconsistencies were caused by documented instrument malfunctions. Best estimates of the actual emission rates during times of apparent inconsistencies were developed with each generating station engineer to provide a continuous hourly record for modeling.

Figures 5.3.1 through 5.3.3 show time series plots of daily averages of the hourly emission rates for the Hayden station, Yampa Project (Units 1 and 2), and Craig Unit 3. When the generating stations were down for maintenance and other outages, the load and emissions are either small (in the daily averages) or zero.

Table 5.3.1 summarizes the total load from each station for each of the days selected for aerosol analysis and dispersion modeling. Hayden's daily emissions for these samples ranged from a low of 19.6 tons/day on 10/17/95 to a high of 56.8 tons/day on 03/30/95. The sulfur dioxide emission rates varied little from the 46 ton/day average, except for 09/02/95 and 10/07/95 through 10/11/95 when Unit 1 was down and from 10/17/95 through 10/22/95

when Unit 2 was down. Figure 5.3.1 shows a relatively constant load and sulfur dioxide emission rate throughout the study period, and especially on those days selected for detailed analysis.

The load and emissions at the Craig station were more variable than those at Hayden, both in terms of 24-hour averages and on an hourly basis. Figure 5.3.4 shows an example of hourly load and emissions from the Yampa Project during June 1995, with a very clear diurnal cycle that peaks during the daytime and reduces to nearly half of maximum load at

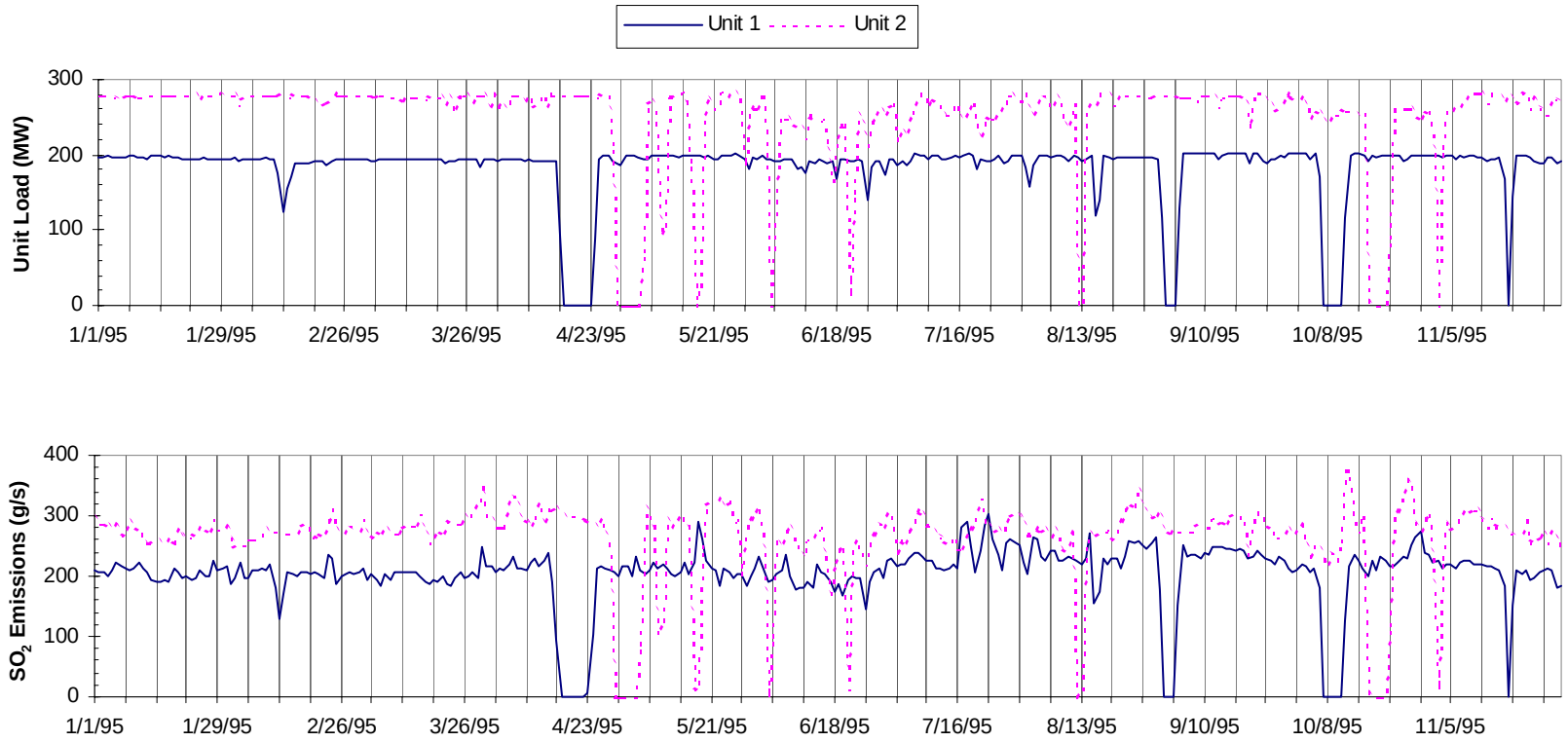

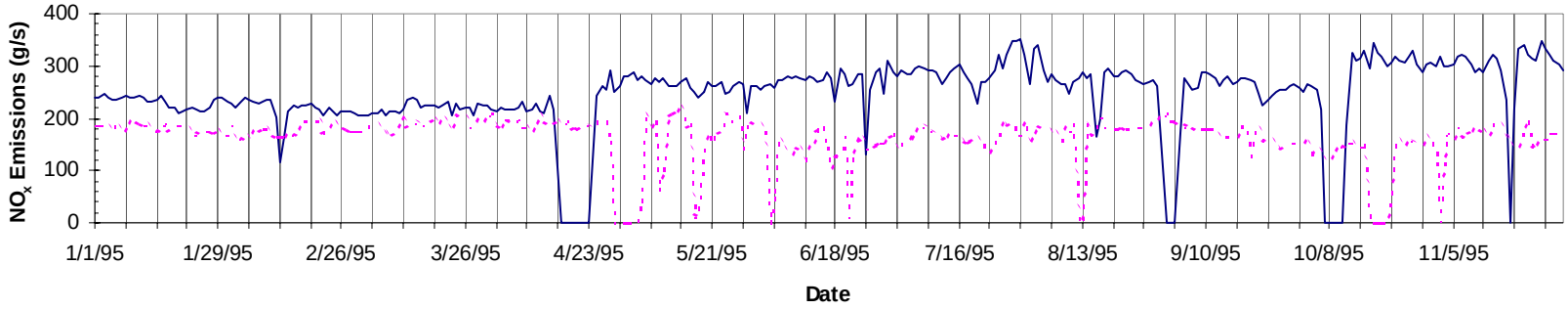

Figure 5.3.1. Daily load, sulfur dioxide emissions, and oxides of nitrogen emissions from units 1 and 2 of the Hayden station.

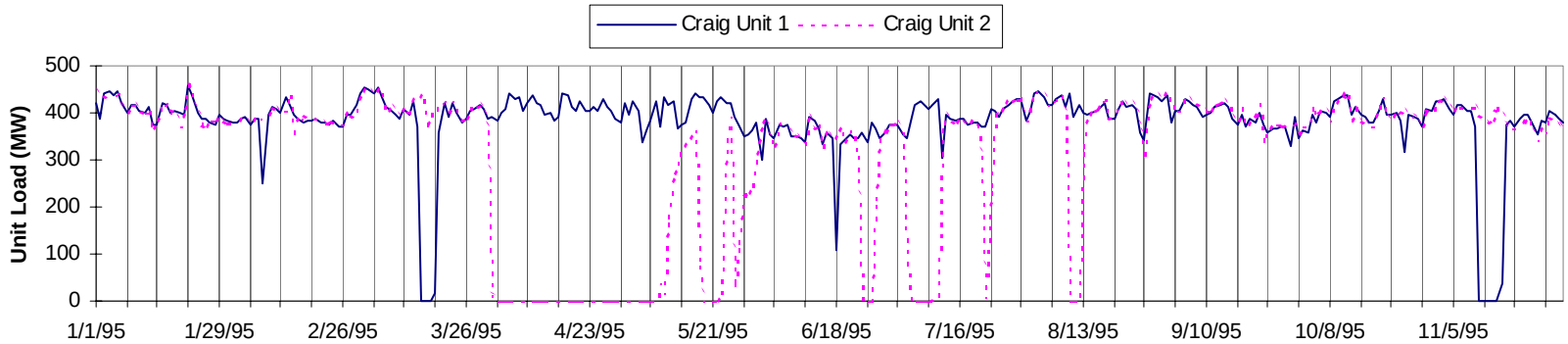

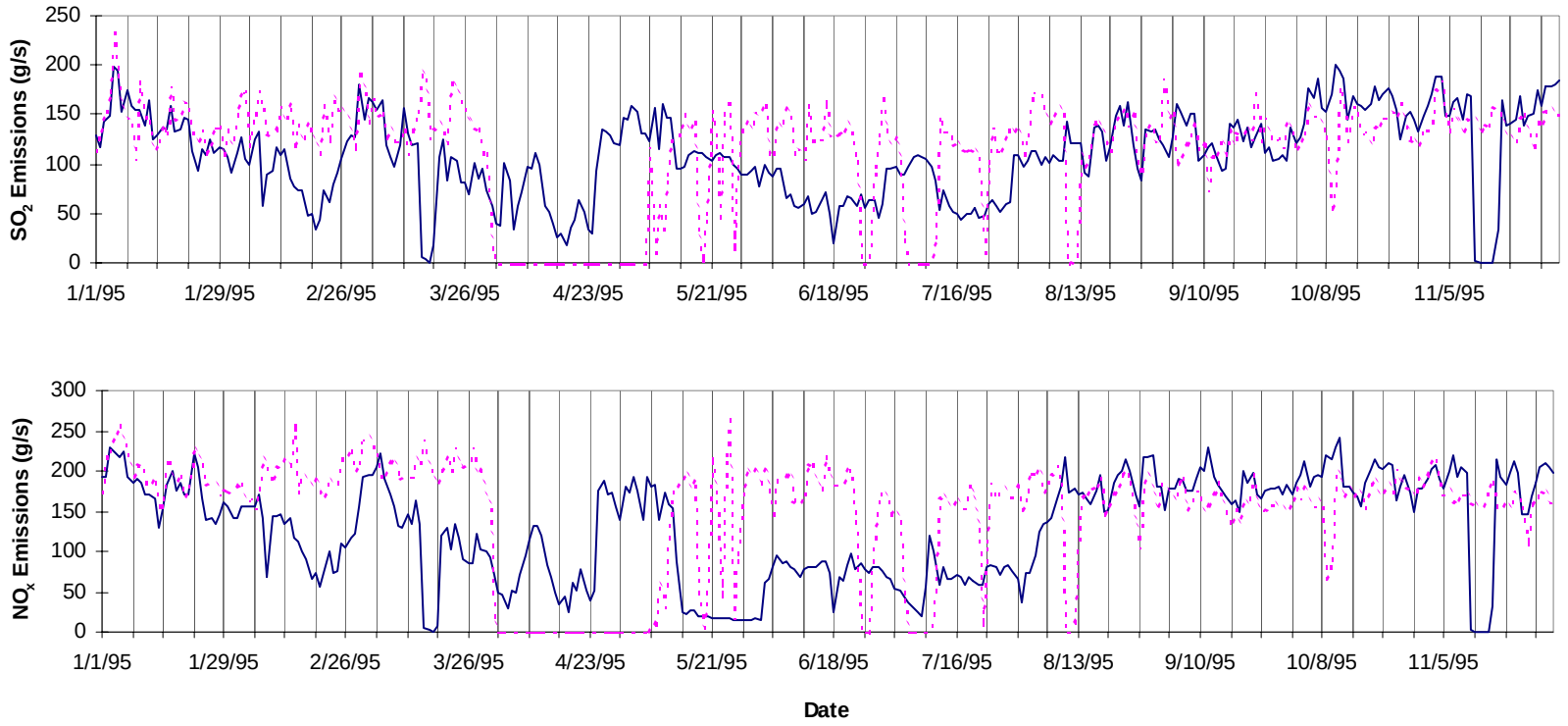

Figure 5.3.2. Daily load, sulfur dioxide emissions, and oxides of nitrogen emissions from units 1 and 2 of the Craig station.

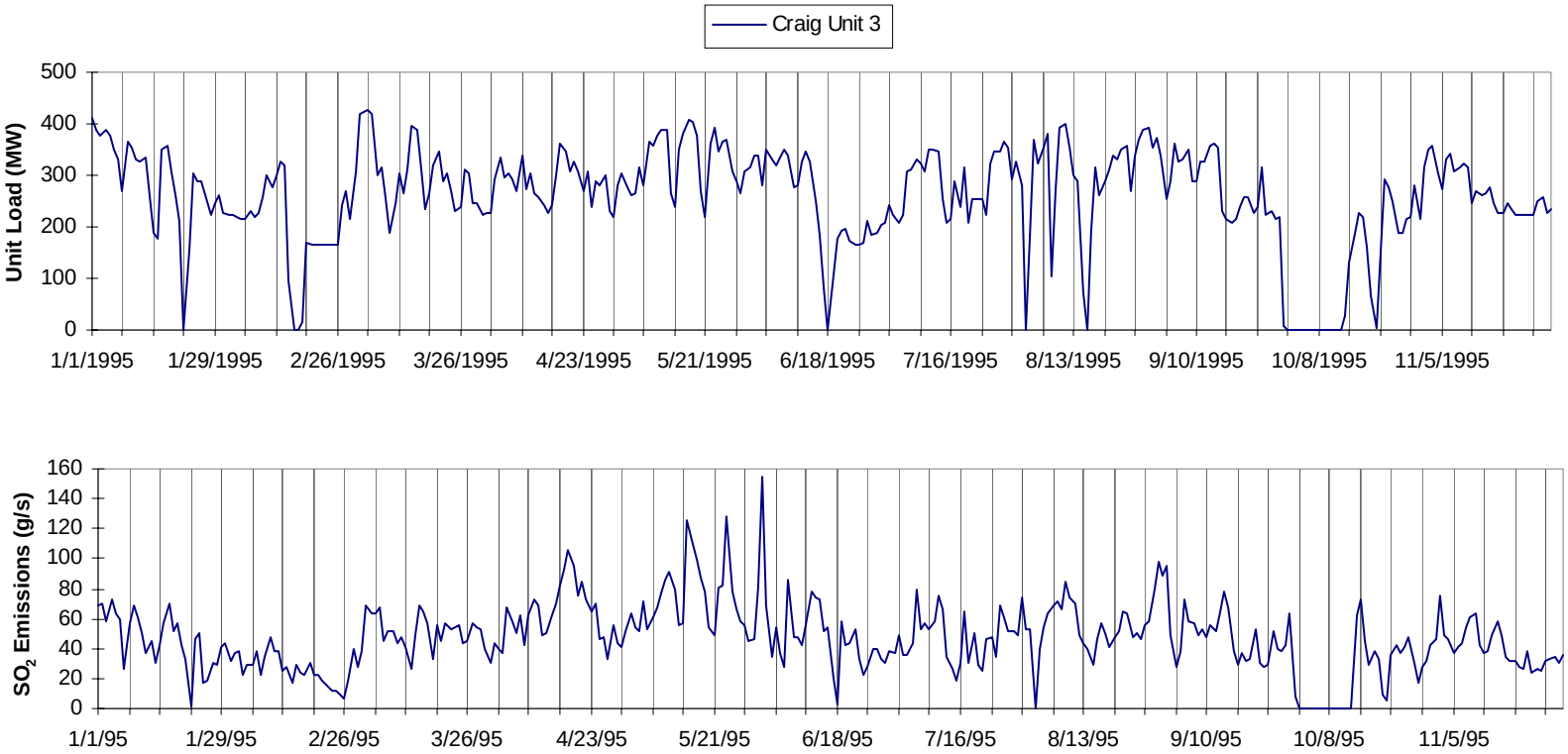
Craig Unit 3
Unit Load (MW)
500
400
300
200
100
0
1/1/1995
1/29/1995
2/26/1995
3/26/1995
4/23/1995
5/21/1995
6/18/1995
7/16/1995
8/13/1995
9/10/1995
10/8/1995
11/5/1995
SO2 Emissions (g/s)
160
140
120
100
80
60
40
20
0
1/1/95
1/29/95
2/26/95
3/26/95
4/23/95
5/21/95
6/18/95
7/16/95
8/13/95
9/10/95
10/8/95
11/5/95

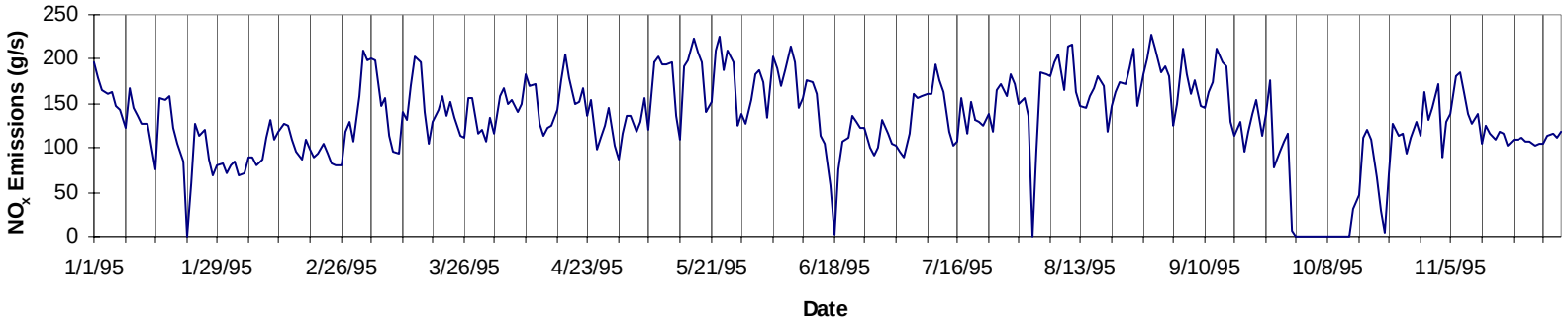

Figure 5.3.3. Daily load, sulfur dioxide emissions, and oxides of nitrogen emissions from unit 3 of the Craig station.

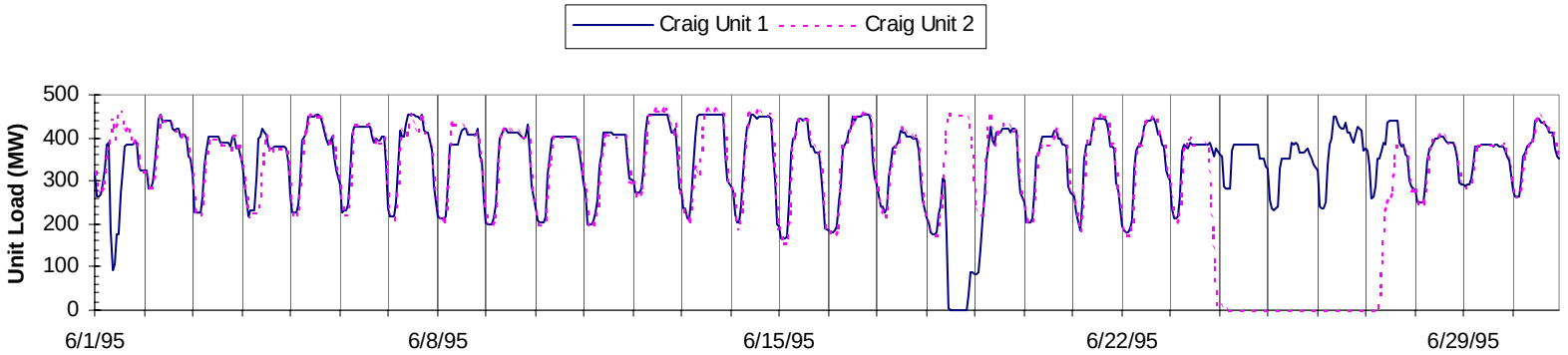

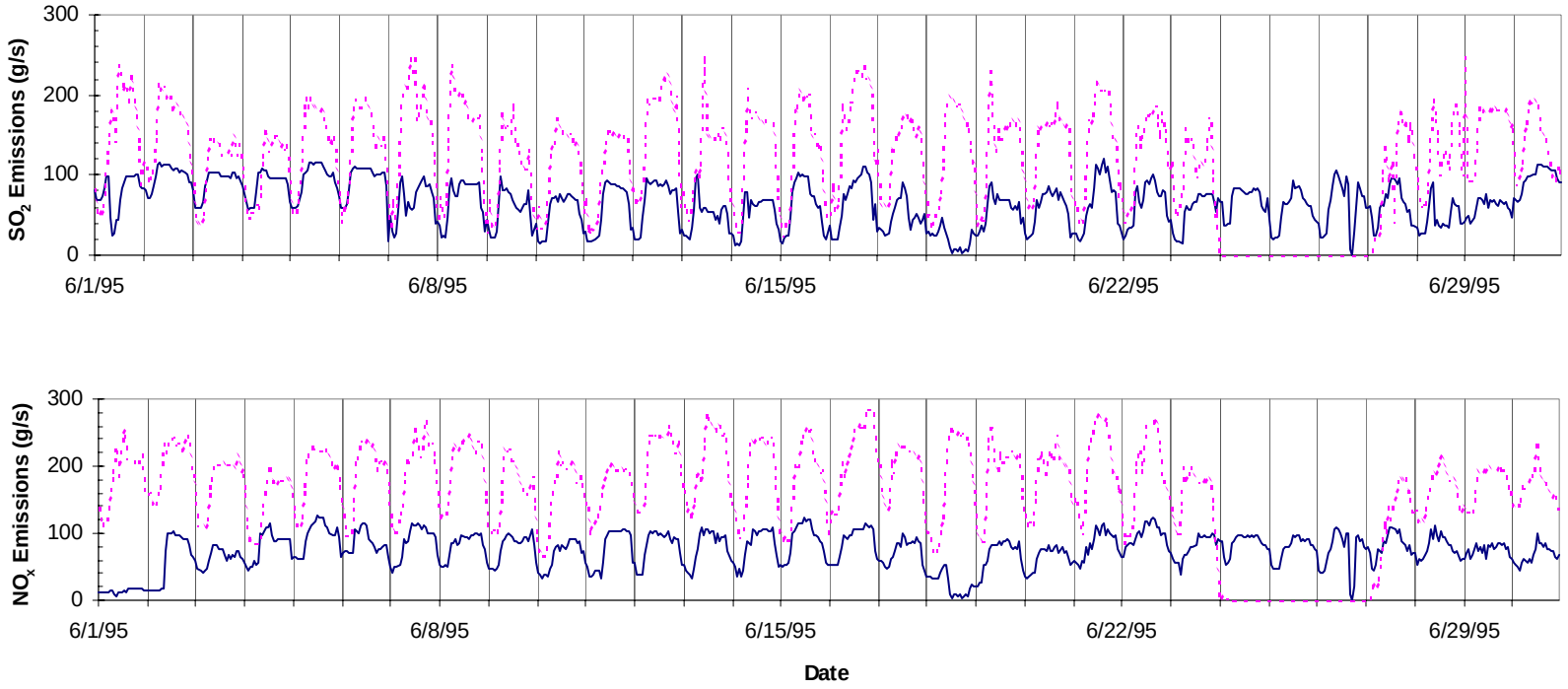

Figure 5.3.4. Example of diurnal variability in emissions from units 1 and 2 at the Craig station during June, 1995.

Table 5.3.1
Daily Power Plant Load and Sulfur Dioxide Emissions for Selected Episodes[a]

Date	Hayden SO_2 (tons/day)	Hayden Load (MW)	Craig SO_2 (tons/day)	Craig Load (MW)
02/23/95	49.878	461.458	18.6725	923.125
03/26/95	47.2892	474.333	26.8246	1013.58
03/27/95	46.9564	463	25.9415	1124.29
03/28/95	48.7088	473.583	27.8983	1122.71
03/29/95	48.9917	462.125	25.9526	1080.38
03/30/95	56.789	473.5	23.0464	1056.29
03/31/95	48.8051	457.292	20.2449	976.583
05/05/95	28.2978	260.875	19.3411	602.333
05/06/95	49.117	464.167	17.6004	675.708
06/14/95	46.9332	440.083	23.8498	1064.17
06/15/95	46.1559	437.375	22.8562	913.25
06/16/95	41.3792	403.6	27.6207	905.875
06/29/95	44.9596	421.917	24.3916	906.417
06/30/95	50.234	458.542	21.4526	953
07/01/95	50.3202	460.958	19.6373	957.833
07/29/95	53.4172	472.75	22.8688	1214.71
07/30/95	52.6976	472	25.7309	1153.17
07/31/95	49.121	464	18.3058	1090.96
08/07/95	49.3845	476.458	31.5884	1236.63
08/08/95	46.6347	465.5	30.985	975.792
08/09/95	44.7934	441.458	32.1734	1089.21
08/14/95	45.4913	453.417	21.6301	1078.21
08/21/95	47.7322	472.042	32.7356	1129.38
08/22/95	47.8904	475.625	35.5566	1191.29
08/23/95	51.5561	474.625	34.2117	1163.58
08/24/95	55.0072	474.667	33.1302	1183.46
08/25/95	54.2985	475.417	30.4033	1174.88
08/26/95	57.3993	476.167	22.8557	998.458
08/27/95	54.4951	475.333	21.714	992.75
09/02/95	25.8279	278.125	28.6365	1140.96
09/17/95	51.7488	481.083	27.1519	968.625
09/18/95	51.5032	479.375	30.0985	1011.33
09/19/95	50.1767	479	26.3678	957.375

Table 5.3.1
Daily Power Plant Load and Sulfur Dioxide Emissions for Selected Episodes[a]

Date	Hayden SO_2 (tons/day)	Hayden Load (MW)	Craig SO_2 (tons/day)	Craig Load (MW)
09/20/95	44.3572	423.375	29.2384	1006.33
09/21/95	50.0244	480.208	26.2809	1029.21
09/24/95	49.2171	458.083	27.0426	961.958
09/27/95	47.3009	461.792	25.4729	978.042
09/30/95	45.1189	477.5	26.8624	772.875
10/01/95	46.0842	472.958	22.3946	701.25
10/02/95	47.935	477.708	23.9256	731.083
10/07/95	21.3857	246.25	28.3195	808.583
10/08/95	20.6918	239.333	27.0468	777.167
10/09/95	22.3685	252.292	21.2478	839.958
10/10/95	21.3598	254.042	26.5626	852.542
10/11/95	24.6125	261.125	35.3411	874.708
10/12/95	48.314	374.583	32.8334	872
10/13/95	55.5974	459.208	25.5428	778.875
10/14/95	49.683	456	36.9895	847.167
10/16/95	48.8257	454.625	32.1333	960.375
10/17/95	19.6558	197.75	30.0854	970.75
10/18/95	21.3839	199.917	30.3054	966.875
10/19/95	20.0926	195.375	33.3134	975.833
10/22/95	31.6192	289.292	34.0529	933.333
10/23/95	48.6978	458.708	34.5835	1094.13

[a] For comparison, the median daily values for 1995 were 46.0 tons/day SO_2 and 461.0 MW/hr for Hayden and 26.4 tons/day SO_2 and 986.4 MW/hr for Craig.

night. Daily sulfur dioxide emissions for the aerosol analysis days ranged from 18.3 tons/day on 07/31/95 to 37 tons/day on 10/14/95 and showed greater variability around the average 26.4 tons/day than for the Hayden station.

5.4 Everyday Plume Transport Modeling

The CALMET/CALPUFF model was run for every hour of the study from the beginning of January 1995 to the end of November 1995 for which radar profiler data were available from at least one of the Hayden, Baggs, and Clark sites. The objective of this modeling was to simulate the transport and dispersion of SO_2 emitted from the two stacks of the Hayden station (Units 1 and 2), the two stacks of the Yampa Project (Craig Units 1 and 2), and from Craig Unit 3. SO_2 is invisible, so this gas has no direct effects on the visual appearance of the plume or on the visual appearance of the atmosphere downwind of the sources. SO_2 is of interest because it is a marker for the emissions from the above stacks; i.e., it can be used as an indicator of the presence of those emissions and their dilution. SO_2 is also a precursor for sulfate, which forms particles in the atmosphere. Sulfate formed from SO_2 emissions are of concern because previous studies have shown that they are capable of increasing light scattering by particles enough to cause perceptible effects downwind of major SO_2 sources.

The use of SO_2 as a marker for Yampa Valley generating stations is supported by two observations: 1) the emission inventory shows that there are no other sources of SO_2 of comparable magnitude in the mesoscale modeling domain, and 2) SO_2 concentrations at the sites to the west and north of the Hayden station and Yampa Project were always very small except when the everyday plume transport modeling showed that the plumes from the local generating stations were transported to these monitoring sites. The limitations on using SO_2 as a quantitative marker for the stack emissions are discussed in Section 5.4.9.

The everyday CALMET/CALPUFF modeling was performed to address the following questions:

1. Does the CALMET/CALPUFF modeling system simulate the transport and dispersion of SO_2 with sufficient accuracy that study conclusions can be based on model results?

2. What is the spatial variability of the cumulative frequency distributions of SO_2 concentrations in and near the MZWA? In particular, do the measurements of SO_2 at the Buffalo Pass and Gilpin Creek monitoring sites near the MZWA boundary satisfactorily represent the effects of the five generating station units listed above on SO_2 concentrations in the MZWA?

3. What are the contributions of each of the five generating station units listed above to SO_2 concentrations in the MZWA?

The second and third questions cannot easily be resolved by measurements. The compositions of the emissions from the five generating station units are similar enough that their relative impacts cannot be satisfactorily determined from measurements of the atmospheric composition at receptor sites. Also, wilderness regulations do not permit

establishing monitoring sites within the wilderness, so the air quality within the MZWA must be inferred from modeling results combined with measurements made near the wilderness boundary. Therefore, the modeling described in this section was performed to estimate concentrations within regularly spaced grids as well as at discrete receptors. Figure 5.4.1 shows the locations of receptors near and within the Wilderness at which concentrations were estimated. They were also estimated for each of the six aerosol monitoring sites shown in Figure 2.2.1.

5.4.1 Results of Everyday Plume Transport Modeling

Hourly SO_2 concentrations calculated by the CALMET/CALPUFF models from the hourly emissions of the Hayden station, Yampa Project, and Craig Unit 3 showed satisfactory agreement with the measured SO_2 concentrations. Therefore, study conclusions can be based on model results. Comparisons of modeled and measured sulfur dioxide concentrations described below show:

- Filter measurements of the presence or absence of SO_2 were consistent with model predictions at all sites except Juniper Mountain, where the model predicted higher SO_2 peaks than were observed.

- Time series plots of modeled SO_2 at Buffalo Pass were consistent with hourly SO_2 measurements at Buffalo Pass from August through November 1995. Both data sets showed that SO_2 arrived in pulses with a duration of less than one to a few hours separated by intervals with no SO_2. The calculated magnitude and frequency of SO_2 pulses was in qualitative agreement with the measurements. The agreement between the timing of the modeled and measured pulses was often good and sometimes excellent.

- The cumulative frequency distribution (CFD) of the modeled and measured hourly SO_2 for August through November 1995 agreed within 0.5 ppbv for all percentiles except the highest 2 percent of the readings. The highest measured and calculated hourly SO_2 concentrations were 9.7 and 6.2 ppbv, respectively. At the 1 percentile frequency of occurrence, the measured and calculated values of the CFD were 4.7 and 4.0 ppbv, respectively.

CFDs of modeled SO_2 concentrations at receptor sites along the Continental Divide in and near the MZWA showed that SO_2 concentrations were greatest at the southern end of the MZWA and decreased uniformly with distance north in the MZWA. Thus, the model results indicate that the Buffalo Pass site experienced higher SO_2 concentrations than any site near the Continental Divide in the MZWA and that receptor sites near the southern end of MZWA provide an upper limit for the concentrations of SO_2 in the MZWA. For receptors along sight paths, the everyday modeling yielded the following results:

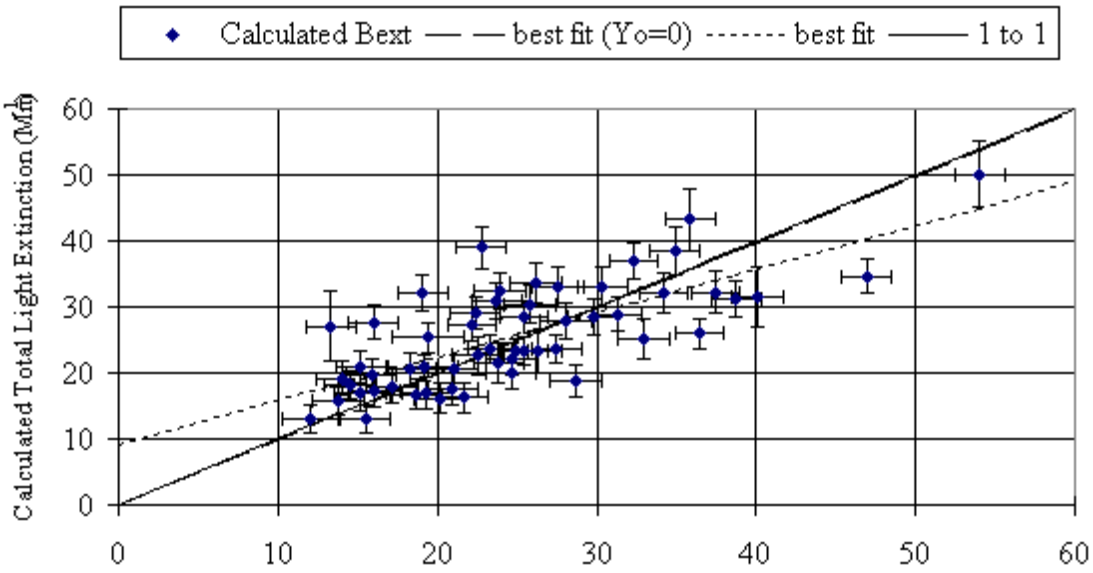

Figure 5.4.1 Locations of discrete receptors in and near the MZWA at which SO_2 concentrations were calculated

- The annual average modeled SO_2 concentration at Davis Peak, in the northern part of the MZWA was 0.19 ppbv. This was less than half the annual average of 0.43 ppbv at Buffalo Pass, just outside the southern boundary of the MZWA.

- The CFD of modeled SO_2 at Gilpin Creek was similar to the CFD for higher receptor sites along the Continental Divide the same distance north in the MZWA.

- The highest modeled SO_2 concentrations were observed at Mad Creek, a low elevation receptor site in a canyon in the southwest corner of the MZWA. The distance to the generating stations is at a minimum in this corner of the MZWA.

Time series plots of the modeled hourly SO_2 concentrations from each of the five units showed that SO_2 from all units tended to be present or absent at Buffalo Pass at the same times. It was extremely rare for SO_2 from the Hayden station to be present without SO_2 from the Yampa Project, and vice versa. CFDs show that the percentage contributions of each generating station unit to SO_2 concentrations at each receptor site were essentially the same for all receptor sites. Also, these percentage contributions did not change when calculated only for hours with SO_2 concentrations greater than 2 ppbv. The annual average percentage contributions calculated for Buffalo Pass and Davis Peak are shown in Table 5.4.1.

When the relative contributions of each generating station unit to calculated ambient SO_2 concentrations (in pptv or parts per trillion by volume) at Buffalo Pass and Davis Peak were divided by the emission rate for that unit (in grams/second), the dilution ratios in Table 5.4.2 were calculated. The first number gives the annual average and the second the month-to-month variability

During times of transport with limited mixing, the ambient concentrations and the dilution ratios in Table 5.4.2 will become larger. The finding that the relative contributions of each generating station were the same for all hours or only for hours with SO_2 concentrations greater than 2 ppbv indicates that all dilution ratios would increase by approximately the same factor if they were calculated for hours that the modeled hourly SO_2 concentration was greater than 2 ppbv at the receptor site. Thus, the relative values of the dilution ratios in Table 5.4.2 can be used to estimate the relative ambient concentration reductions during SO_2 pulses that would result from emissions reductions.

Modification of CALPUFF to output plume rise data showed that the plume rise for Hayden Unit 2 was greater than for Unit 1. The higher plume rise caused the dilution of the Hayden Unit 2 emissions to be greater when mixed to the surface than for Hayden Unit 1.

Analyses of the data from Buffalo Pass presented in Section 6 show that, with rare exceptions, measurable haze pulses were associated with SO_2 pulses only when the RH was greater than about 80 percent. Calculations were done to determine the number of hours each month that satisfied these conditions. During the hours between 0600 and 1800 in January through November, there were 310 hours (8 percent of the hours) when the modeled SO_2 concentration was greater than 1 ppbv and the measured RH was greater than 80 percent at

Table 5.4.1
Annual Average Percentage Contributions of Each Generating Station Unit to Calculated SO_2 Concentrations at Buffalo Pass and Davis Peak

Generating Station Unit	Percentage Contribution to Modeled SO_2 at the Surface in the MZWA
Hayden Unit 1	40 to 45
Hayden Unit 2	35 to 40
Craig Unit 1	6 to 8
Craig Unit 2	7 to 9
Craig Unit 3	3 to 4

Table 5.4.2
Calculated Annual Average Dilution Ratios for Each Generating Station Unit for Buffalo Pass and Davis Peak

Generating Station Unit	Dilution Ratio for Buffalo Pass (pptv s/g)	Dilution Ratio for Davis Peak (pptv s/g)
Hayden Unit 1	0.90 ± 0.19	0.36 ± 0.11
Hayden Unit 2	0.62 ± 0.18	0.26 ± 0.09
Craig Unit 1	0.29 ± 0.08	0.18 ± 0.03
Craig Unit 2	0.34 ± 0.10	0.20 ± 0.05
Craig Unit 3	0.31 ± 0.09	0.19 ± 0.05

Buffalo Pass. The month-to-month variability was large, ranging from 61 hours in May, which was an unusually wet month, to 8 hours in August. When the SO_2 threshold was increased to 2 ppbv, the number of hours decreased to 125 (3 percent of the hours), with a maximum of 36 hours in May and a minimum of 2 hours in April and August. During many of these hours, the monitoring site would be in clouds or the views obscured by clouds.

5.4.2 CALMET/CALPUFF Modeling Procedures

This section outlines the procedures used for the everyday plume transport modeling. In general, these procedures were the same as used for the regional and mesoscale modeling of selected episodes described in Section 6.7. However, there were some differences, which are highlighted here. Appendix B.2 contains a complete description of the procedures used for both applications of the CALMET/CALPUFF modeling system.

The everyday plume transport modeling was performed only for the mesoscale modeling domain, shown in Figure 2.1.1. With one exception, the meteorological, terrain, and land use data were the same as used for the modeling of selected episodes. This exception is that land-use codes were varied by time of year in the everyday modeling; and the codes for snow-cover were used for the higher elevations during late fall, winter, and spring months as described in Appendix B.2.2.3.

Including wet deposition in the CALMET/CALPUFF calculations requires hourly precipitation data, but these data were available only for the Hayden Waste Water site. Daily precipitation data were available for additional sites, but it would have required an unreasonable amount of effort to use these data as the basis for estimates of the hourly precipitation data for the eleven months modeled. In addition, precipitation data were not available for the ridge that contains the MZWA, where the precipitation amounts are much greater than in nearby areas at lower elevations. Therefore, the everyday plume transport modeling was performed using the CALMET option of zero precipitation, and wet deposition was not included in the CALPUFF simulations. The effect of this simplification on the CALPUFF results is that the model will overpredict SO_2 concentrations in SO_2-containing air parcels that had been exposed to rain. Precipitation and wet deposition were included in the simulations of selected episodes described in Section 6.7.

The hourly surface wind fields calculated by CALMET were reviewed to ensure that they were not distorted by invalid meteorological data. For selected hours, the observed surface winds speeds and directions were superimposed on a map of the modeling domain showing the wind speeds and directions calculated by CALMET for each grid cell. The Craig airport frequently reported invalid winds, so this site was deleted from the input data and from the project data base.

The CALPUFF modeling was performed with the default chemistry mechanism, puff splitting, and dry deposition. The SO_2 concentrations reported in this section were calculated using the slug formulation. The puff formulation was used only to calculate the hourly SO_2 concentrations in each grid cell for the animation described in Section 5.4.8.

5.4.3 Calculation of Plume Height

The CALPUFF model does not contain an option to output the results of the calculated plume heights in computer-readable format. This information is available only in an optional line-printer-style output file. Therefore, code was added to CALPUFF to allow the output of a new file with the results of the plume rise calculations along with the more important input parameters that enter into the plume rise calculation. The plume height data were a key input to the local trajectory analyses in Section 5.6.

Figure 5.4.2 shows a sample of the plume height data for Hayden station Units 1 and 2 for the time period from 08/03/95, the beginning of the summer intensive, through 10/15/95, the end of the fall intensive. The bottom and top of the boxes show the 25^{th} and 75^{th} percentile values of the plume height. The median value is shown by the bar through the box and the mean by the plus sign within the box. The length of the whiskers is 1.5 times the distance between the 25^{th} and 50^{th} percentile values and data points within the range of the whiskers are not shown. The symbols above and below the whiskers show all outliers in the plume rise values.

These data indicate that the calculated plume height for Hayden Unit 2 is greater than for Unit 1. As a result, the model indicates that a smaller fraction of the Unit 2 emissions mix to ground level than is the case for Hayden Unit 1 emissions.

5.4.4 Sensitivity Tests for Input Parameters

Sensitivity tests were performed to evaluate the effect on model execution times and model results of different values for a few model input parameters. The results are summarized here.

The effect of snow level on wind fields calculated by CALMET was evaluated by performing simulations for the month of June with snow on all grid cells above 2,500 m MSL (8,200 ft MSL) elevation and with no snow, as documented in Table 5.4.3. June was selected for this test because the month began with most of the MZWA covered by snow and ended with the snow melted from most sunny slopes. Side-by-side comparison of the wind fields on screen showed no significant differences. Comparison of cumulative frequency distributions (CFDs) for SO_2 concentrations calculated by CALPUFF with and without snow-cover also showed no significant differences.

The effect of selecting the slug or puff formulation in CALPUFF was evaluated. Differences in the model output were noted, especially at sites such as Hayden VOR, which is close to the Hayden station. At this site, the slug formulation indicated spikes in SO_2 concentrations that did not occur in the results using the puff formulation. At Buffalo Pass, the puff formulation sometimes indicated small concentrations that lingered after major spikes in SO_2 concentrations, while the slug formulation did not show these lingering concentrations CALPUFF was run using both formulations for the month of September. Side-by-side comparison of the animation of the results from each simulation showed very similar results. The execution time was more than a factor of ten greater for the slug

Figure 5.4.2 Calculated plume heights for Hayden station units 1 and 2 for the time period from 8/3/95-10/15/95.

Table 5.4.3
Snow Levels Used in the CALMET Simulations

Month	Minimum Elevation for Snow Cover (ft)	Minimum Elevation for Snow Cover (m)
January and February	All cells snow covered	All cells snow covered
March	7,700	2,316
April, May, June[a], and November	8,200	2,500
June[a] through October	No snow cover	No snow cover

a CALMET was run for June with two different snow levels.

formulation than for the puff formulation when hourly SO_2 concentrations at all grid cells were calculated. Therefore, the CALPUFF simulations to calculate hourly concentrations in grid cells were performed using the puff formulation to keep the elapsed time for the simulations within a reasonable range.

The CALPUFF execution time is decreased by more than a factor of 10 if SO_2 concentrations are calculated only at the discrete receptor sites. This made it feasible to rerun the model using the slug formulation to calculate SO_2 concentrations at the discrete receptors. In summary, SO_2 concentrations at all grid cells were calculated using the puff formulation and the concentrations at the discrete receptor sites were calculated using the slug formulation.

Model simulations with and without the puff-splitting option enabled required the same execution time and, in all cases examined, gave the same results. This is an unexpected result that may be indicative of a bug in the model. The puff-splitting option was enabled in all simulations.

Simulations with and without dry deposition showed the expected effects. At Buffalo Pass, the calculated SO_2 concentrations were decreased by a few percent when dry deposition was enabled. Including the dry deposition calculations increased the model execution time, but the increase was small enough to permit including dry deposition in all model runs.

5.4.5 Model Results that Evaluate Model Performance

This and the following two sections present model results that address the three questions listed at the beginning of Section 5.4.

Model performance was evaluated by comparing calculated SO_2 concentrations resulting from the five stacks of the Hayden and Craig stations with measured SO_2 concentrations. Time series plots comparing the measured and modeled hourly SO_2 concentrations for the complete MZVS study period are in Appendix E. The most accurate SO_2 concentrations were measured by the Thermo-Environmental pulsed fluorescence monitor operated at Buffalo Pass from 08/03/95, the beginning of the summer intensive, to 11/09/95. Both the modeled and measured data indicate that the SO_2 typically arrives in pulses lasting from one to a few hours separated by intervals with no measurable SO_2. The model and the measurements gave similar values for the magnitudes of the SO_2 pulses. The agreement between the timing of the modeled and measured pulses was often good and sometimes excellent.

Figure 5.4.3 shows the highest 30 percent of the cumulative frequency distributions (CFDs) of the modeled and measured hourly SO_2 concentrations at Buffalo Pass from 08/03/95 through 11/09/95. During this time period, the maximum measured concentration was 9.7 ppbv and the highest calculated concentration was 6.2 ppbv. At the 1 percentile level, the measured concentration was 4.7 ppbv and the modeled concentration was 4.0 ppbv, and at the 2 percentile level, 3.5 ppbv was measured and 3.1 ppbv calculated. The two curves agree with each other to within 0.5 ppbv for all percentiles greater than 2.

Similar comparisons between calculated and measured hourly SO_2 concentrations were prepared for the months of August, September, and October. For percentiles greater than 2 percent, the modeled and measured CFDs always agreed within 1.5 ppbv. There was a tendency for the model to overpredict the SO_2 concentration in September and underpredict the SO_2 concentration in October. For ideal agreement, the calculated SO_2 concentrations would be slightly greater than the measured concentrations because: 1) wet deposition was not included in the model calculations, and 2) the chemical mechanism used in the simulations does not simulate the rapid conversion of SO_2 to sulfate that can occur in clouds.

This comparison did not show any evidence that sources other than those modeled contributed significant amounts of SO_2 to the concentrations measured at Buffalo Pass. The measured pulses of SO_2 can be attributed to the five generating station units that were modeled, and the SO_2 concentrations were too small to measure between these pulses.

A series of bar graphs in Appendix E compare all SO_2 concentrations measured by analysis of filter samples with average data for the same time period calculated by the model. At all sites except Juniper Mountain and Hayden VOR, the measured and modeled data are in reasonable agreement. At Juniper Mountain, the model predicted times of high SO_2 concentrations that were not observed. At Hayden VOR, SO_2 concentrations as high as 90 $\mu g/m^3$ (34 ppbv) were observed on a filter sample, but the highest modeled concentration was 20 $\mu g/m^3$ (7.5 ppbv). Both the model and measurements agree that SO_2 from the modeled generating stations is frequently transported to the Baggs site.

The measured SO_2 concentrations at Juniper Mountain during time periods when the modeled concentrations are zero indicate that roughly 1/2 ppbv of SO_2 at this site may be due to sources other than the Hayden and Craig stations.

In summary, the CFDs for modeled and measured hourly SO_2 concentration data at Buffalo Pass show very good quantitative agreement. Time series plots show that the model does an excellent job of simulating the general features of the time variation in the hourly SO_2 concentrations. The agreement between the exact times of the SO_2 pulses in the measured and calculated data was often good and sometimes excellent. Therefore, it was concluded that the everyday plume transport model results were sufficiently accurate that study conclusions could be based on them.

5.4.6 Model Results that Evaluate the Spatial Distribution of SO_2

Figure 5.4.4 shows the highest 30 percent of the CFDs of the calculated SO_2 concentrations at the receptor sites in and near the MZWA January through November 1995. The locations of the receptor sites are shown in Figure 5.4.1. With the exception of Mad Creek, the CFDs form a regular progression. The highest SO_2 concentrations are observed at Buffalo Pass near the southern end of the MZWA and the lowest concentrations at Davis Peak, which is in the northern part of the MZWA. The CFD for the calculated SO_2 concentrations at Gilpin Creek fall between the CFD for Mt. Zirkel and the CFD for the

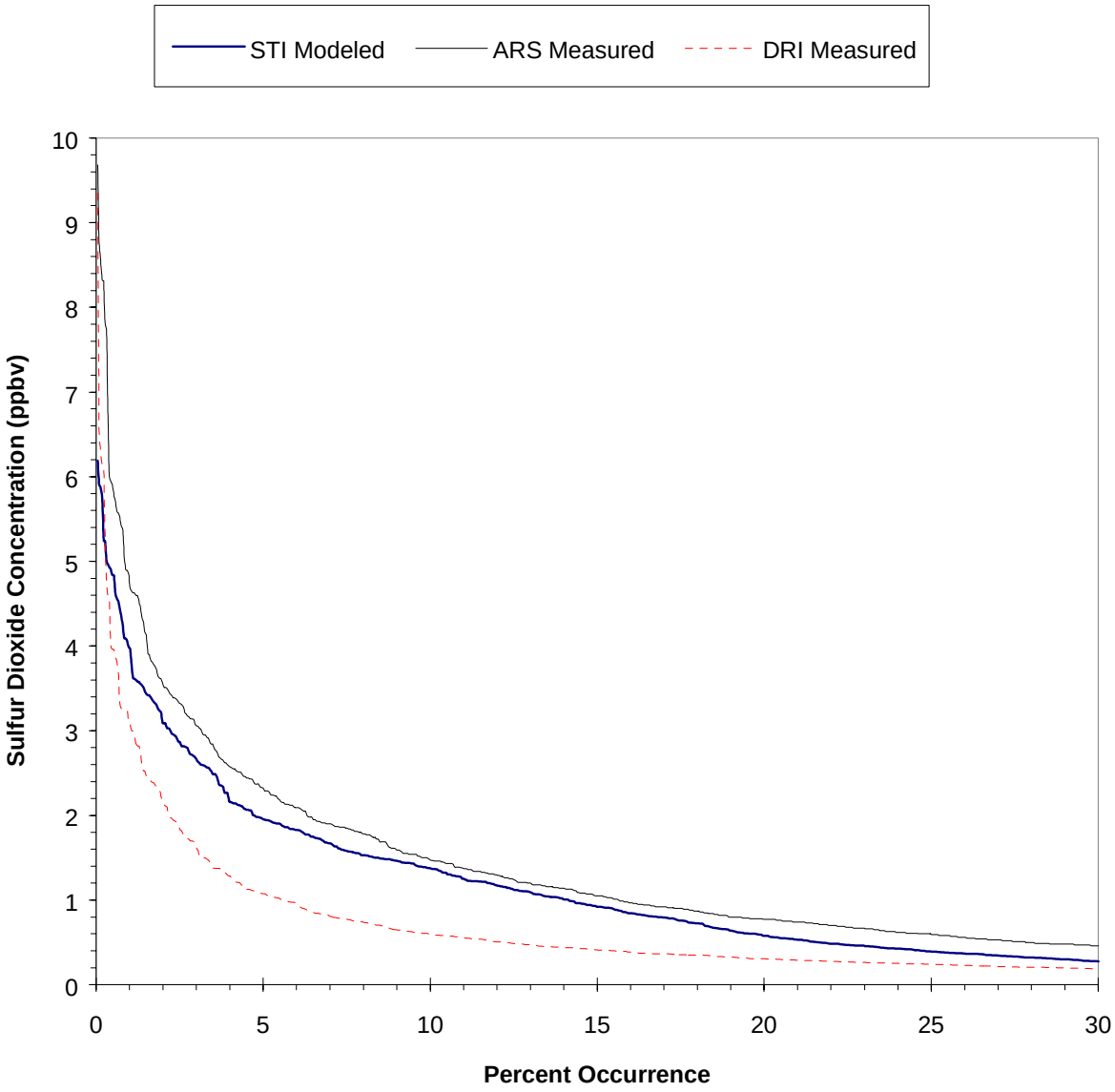

Figure 5.4.3 Cumulative frequency distributions of SO_2 from August 3 to November 9. Comparison of modeled and measured at Buffalo Pass.

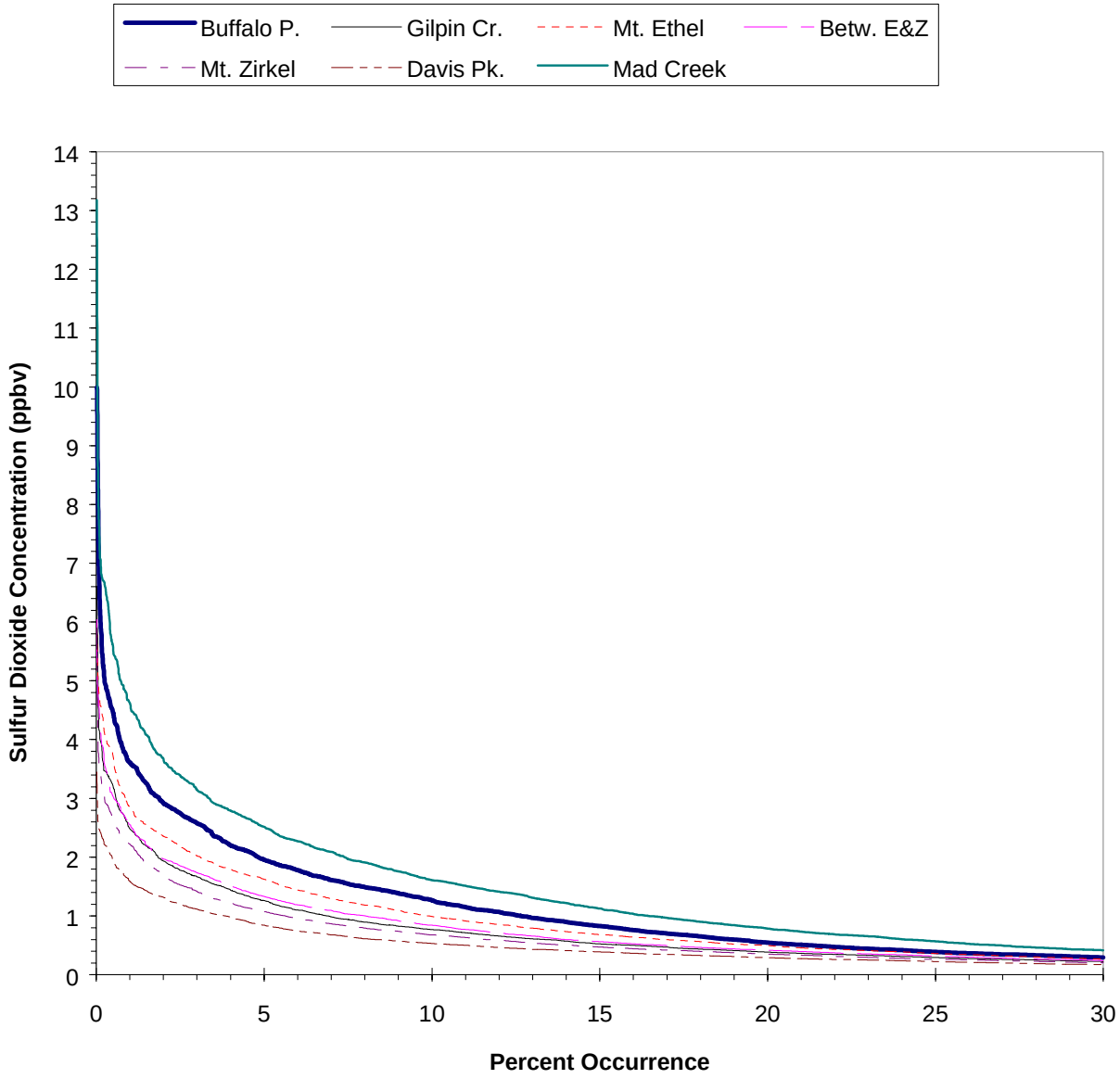

Figure 5.4.4 Cumulative frequency distribution of hourly SO_2 concentrations calculated at receptor sites in and near the MZWA for January through November, 1995.

receptor site between Mt. Zirkel and Mt. Ethel. This agrees with the north-south positions of these receptor sites.

The Mad Creek receptor site is at a low elevation in the southwestern corner of the MZWA. It is 32 km (20 mi) from the Hayden station, compared with 43 km (27 mi) for the Buffalo Pass monitoring station. Thus, the distance from the Hayden station to Buffalo Pass is 35 percent greater than the distance to the Mad Creek receptor site. Davis Peak is 63 km (39 mi) from the Hayden station. This distance is 47 percent greater than the distance to Buffalo Pass. The highest hourly SO_2 concentration in Figure 5.4.4 is 13.2 ppbv at Mad

Creek. This value is 32 percent greater than the highest hourly SO_2 concentration modeled at Buffalo Pass. The highest modeled hourly SO_2 concentration at Davis Peak was 3.4 ppbv.

Cumulative frequency distributions like the one shown in Figure 5.4.4 have been prepared for each month from January through November 1995. With few exceptions, the CFDs for each month were in the same order as in Figure 5.4.4. The exceptions occurred in limited percentile ranges for a few sites during a few months. Therefore, the same spatial pattern of SO_2 concentrations shown in Figure 5.4.4 was calculated by the everyday plume transport modeling for each season of the year.

Two factors contribute to the observed progression of SO_2 concentrations shown in Figure 5.4.4. The first is distance. With the exception of the two receptor sites at Gilpin Creek and between Mt. Zirkel and Mt. Ethel, the SO_2 concentrations decrease uniformly with increasing distance from the Hayden station. The same is true for the distances from the Yampa Project and Craig Unit 3, but the percentage changes in distance are not as great.

The second factor is the most common transport directions. The wind roses in Figures 5.2.5 and 5.2.6 show that the winds measured by the profilers at Hayden Waste Water and Clark are predominantly from the west or west-southwest. Southwest winds would be required for the straight-line transport of emissions from the Hayden station to Davis Peak, and they are less common than winds from the west or west-southwest that transport the generating station emissions to the central or southern portions of the MZWA.

The relative values of the SO_2 concentrations calculated for Gilpin Creek and Buffalo Pass were supported by the SO_2 concentrations measured by the filter samplers. For all samples analyzed for SO_2 during which data were available for the same time period at both sites, the concentration at Buffalo Pass was, on average, a factor of 1.9 ± 1.8 greater than at Gilpin Creek. The uncertainty in this ratio was due to the fact that the SO_2 concentrations were highly variable.

These model results indicate that the measurements at the Buffalo Pass monitoring site provide an upper bound for the effects of SO_2 that may occur in all parts of the MZWA, except for the southwest corner. Also, the distribution of modeled SO_2 concentrations decrease gradually from south to north at the receptor sites near the Continental Divide. This result indicates that the Buffalo Pass monitoring data satisfactorily represent the effects of SO_2 in the high-elevation portions of the southern end of the MZWA.

The southwest corner is the part of the MZWA that is closest to the Hayden station and the Yampa Project, and is in the transport path from the Yampa Valley to Buffalo Pass. The distributions of SO_2 concentrations indicated that the highest modeled concentrations occurred at this site. This site has a lower elevation and is less frequently in clouds than is Buffalo Pass. SO_2 is rapidly converted to sulfate in clouds, so the relation between SO_2 concentrations and sulfate haze may be different at this low elevation site, where clouds are less frequently present than at higher elevations. It is not known how the incidence of sulfate hazes at this site compares with the observations of sulfate haze at Buffalo Pass.

The Gilpin Creek site is at a low elevation near the middle of the MZWA. The modeled distributions of SO_2 concentrations were similar to those at the nearby higher elevations in the MZWA.

5.4.7 Model Results that Apportion SO_2 to Sources

CALPUFF simulations were performed for the SO_2 emissions of each of the five stacks of the Hayden and Craig stations separately and for all five stacks combined. The results from these simulations were used to estimate the apportionment of the SO_2 concentrations at each of several receptor sites to each of the stacks. The cumulative frequency distributions in Figures 5.4.5 through 5.4.8 show the apportionments derived from the model results for January through November for Buffalo Pass, Gilpin Creek, Davis Peak, and Mad Creek (See Figure 5.4.1 for locations). These discrete receptors were selected because they represent the range of conditions found in the MZWA. Buffalo Pass is near the Continental Divide near the southern end of the MZWA and shows the highest modeled SO_2 concentrations of any receptor site near the Continental Divide. Davis Peak is near the Continental Divide in the northern part of the MZWA, and shows the lowest modeled SO_2 concentrations of any receptor site. Gilpin Creek is near the middle of the MZWA, and shows intermediate SO_2 concentrations. Mad Creek is at a low elevation in the southwestern corner of the MZWA, and shows the highest SO_2 concentrations of any discrete receptor.

All cumulative frequency distributions in Figures 5.4.5 through 5.4.8 show similar source apportionments. The relative contributions of the five modeled generating station units are much the same at all locations in and near the MZWA. CFDs like those in Figures 5.4.5 through 5.4.8 were prepared for each month of the year, and no monthly or seasonal trends in the data were identified.

Figures 5.4.9 through 5.4.13 show time series plots of the calculated SO_2 concentrations at Buffalo Pass. These plots include the time periods listed in Section 5.6 selected for intensive analysis. To make the plots easier to read, data from the two Hayden station units have been combined in one line and the data from the two Yampa Project units (Craig Units 1 and 2) have been combined in another line. During this period of time, the emissions from the Hayden and Craig stations always arrived at Buffalo Pass together; there was no time period when SO_2 was attributed to only one of these generating stations. This result is typical; no time period has been identified when the model calculations indicated that only one of the two generating stations contributed significant SO_2 concentrations to a

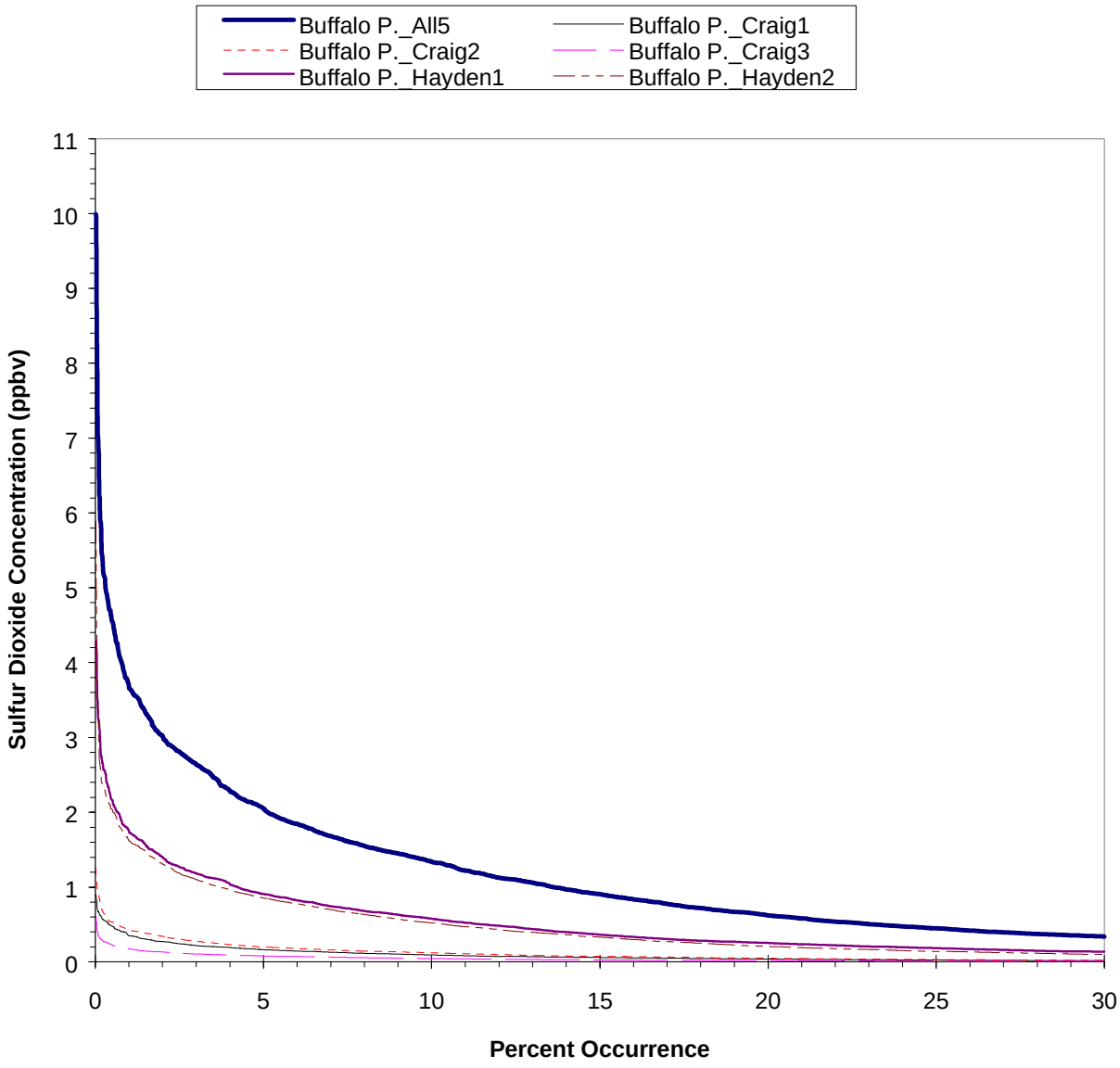

Figure 5.4.5 Cumulative frequency distributions showing the January through November, 1995 apportionment of the calculated hourly SO_2 concentrations at Buffalo Pass to sources.

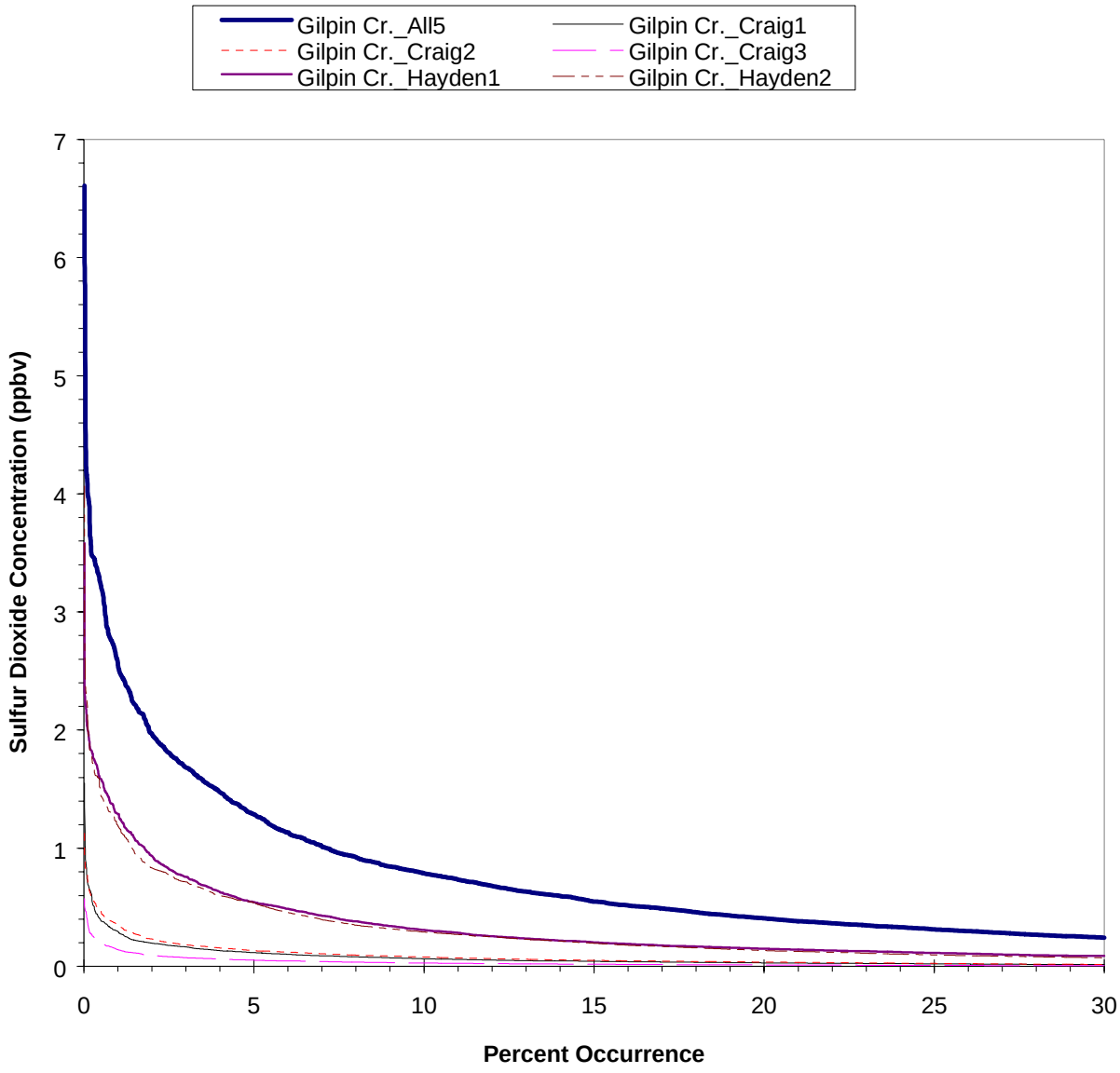

Figure 5.4.6 Cumulative frequency distributions showing the January through November, 1995 apportionment of the calculated hourly SO_2 concentrations at Gilpin Creek to sources.

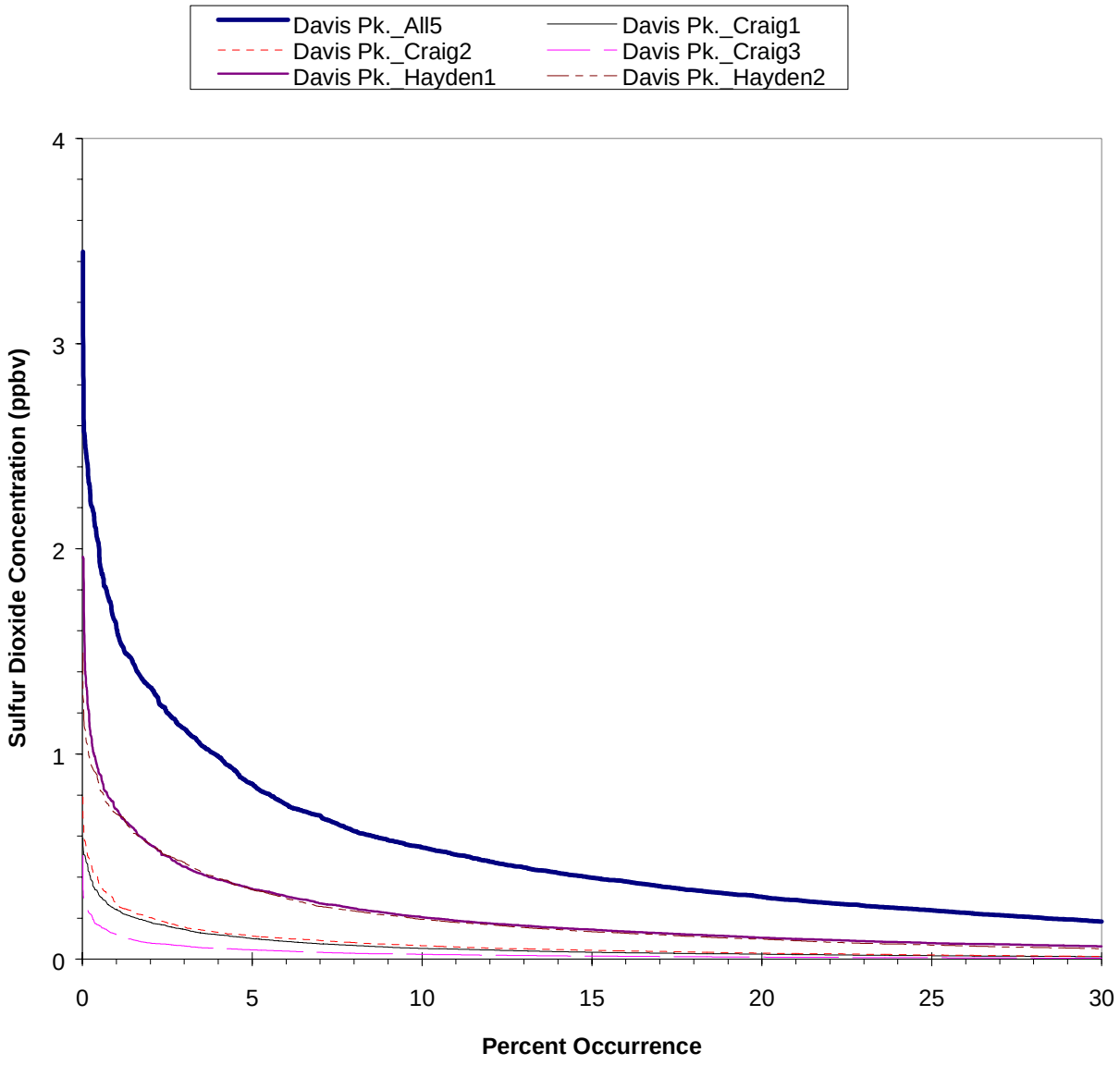

Figure 5.4.7 Cumulative frequency distributions showing the January through November, 1995 apportionment of the calculated hourly SO_2 concentrations at Davis Peak to sources.

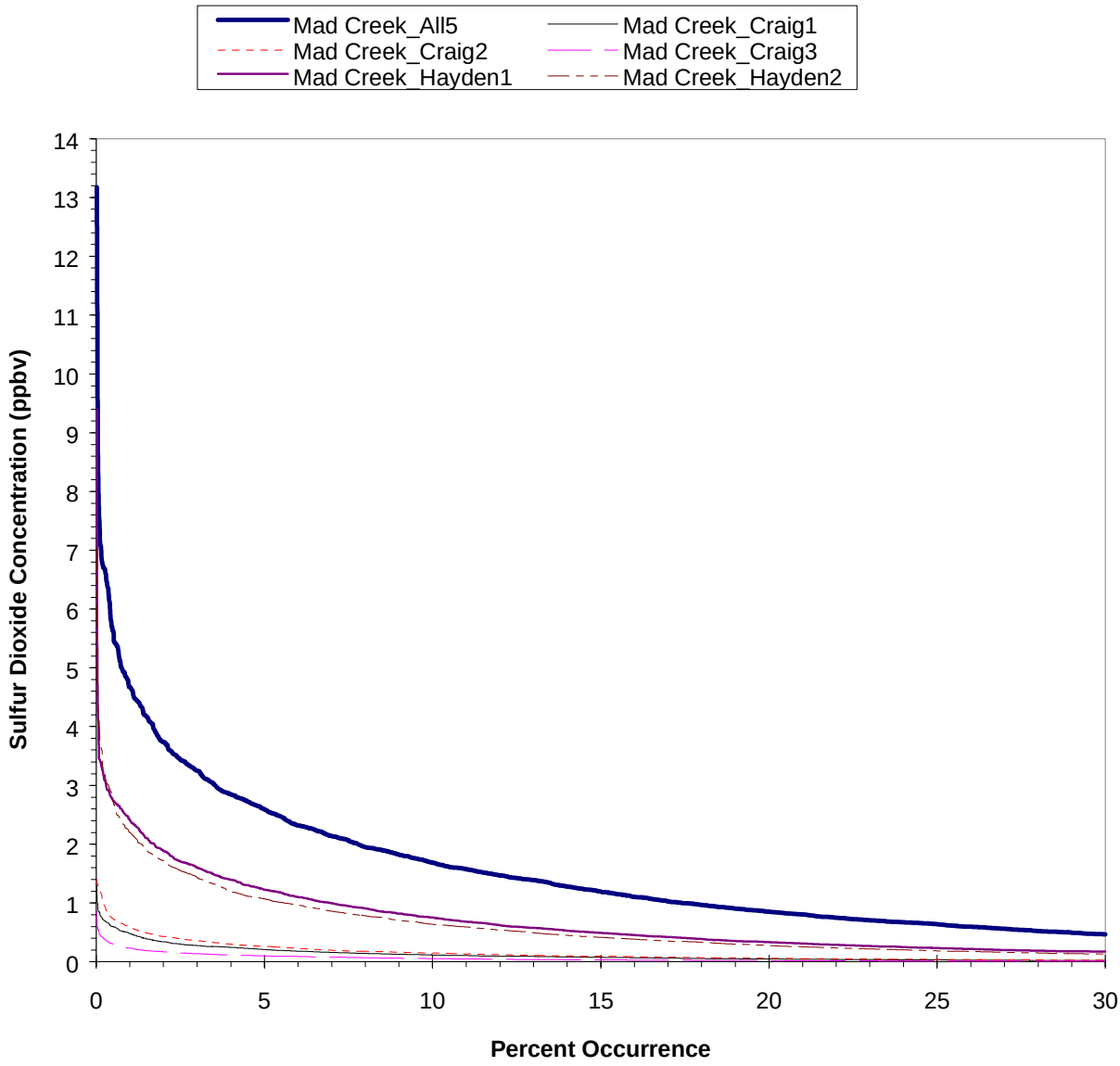

Figure 5.4.8 Cumulative frequency distributions showing the January through November, 1995 apportionment of the calculated hourly SO_2 concentrations at Mad Creek to sources.

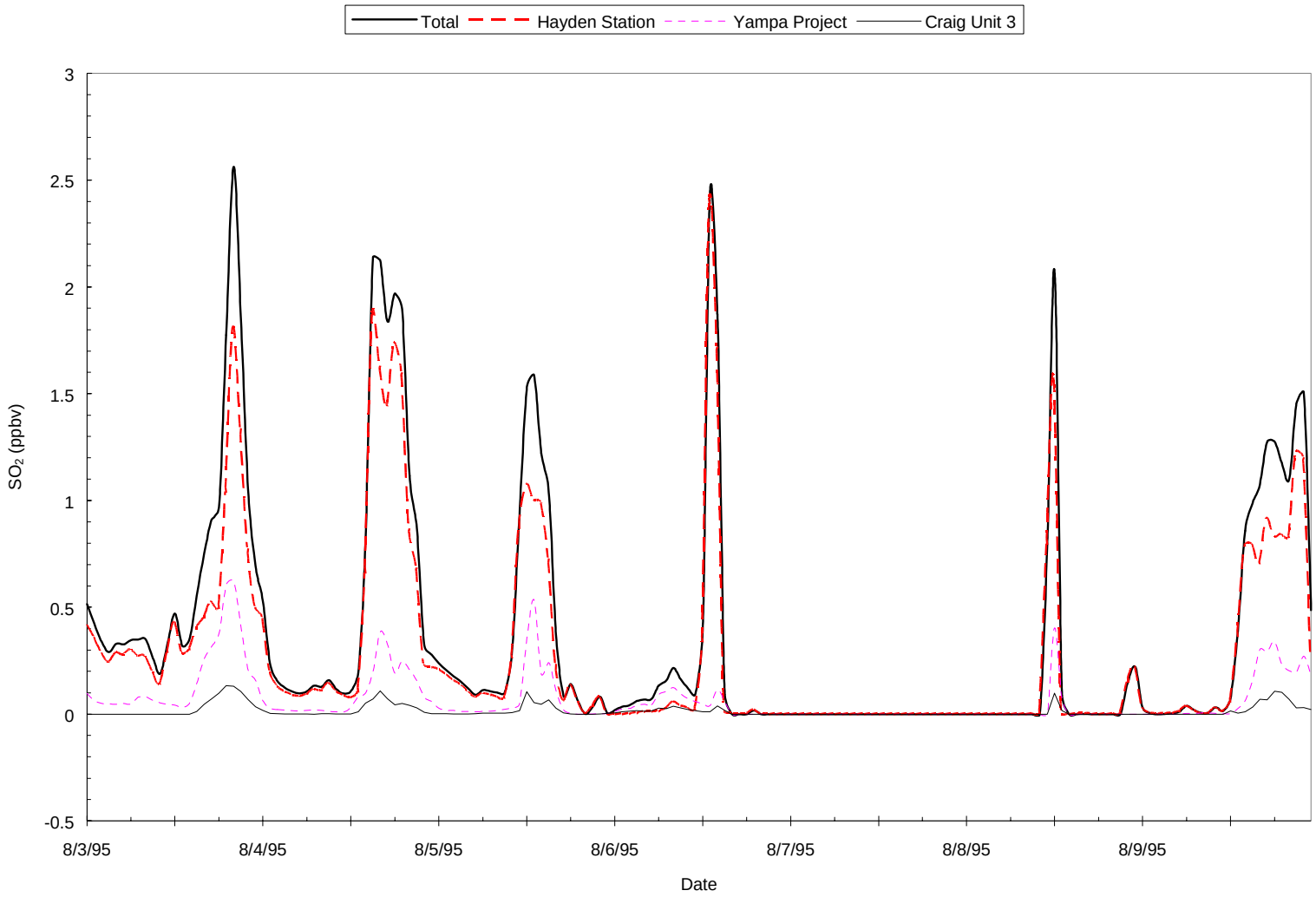

Figure 5.4.9 Time series plot of calculated hourly SO_2 concentrations at Buffalo Pass showing the apportionment to sources for August 3 to 9, 1995.

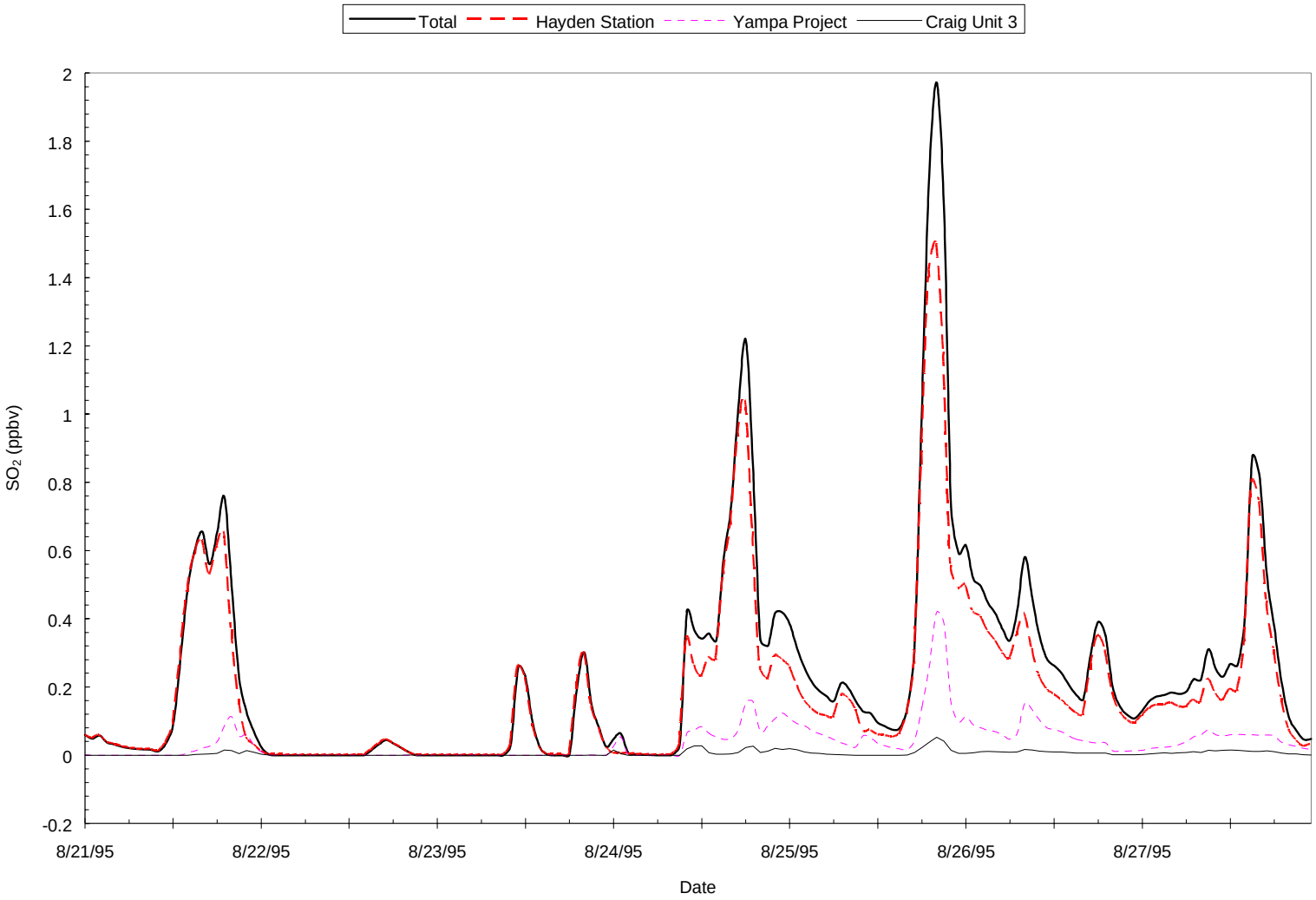

Figure 5.4.10 Time series plot of calculated hourly SO_2 concentrations at Buffalo Pass showing the apportionment to sources for August 21 to 27, 1995.

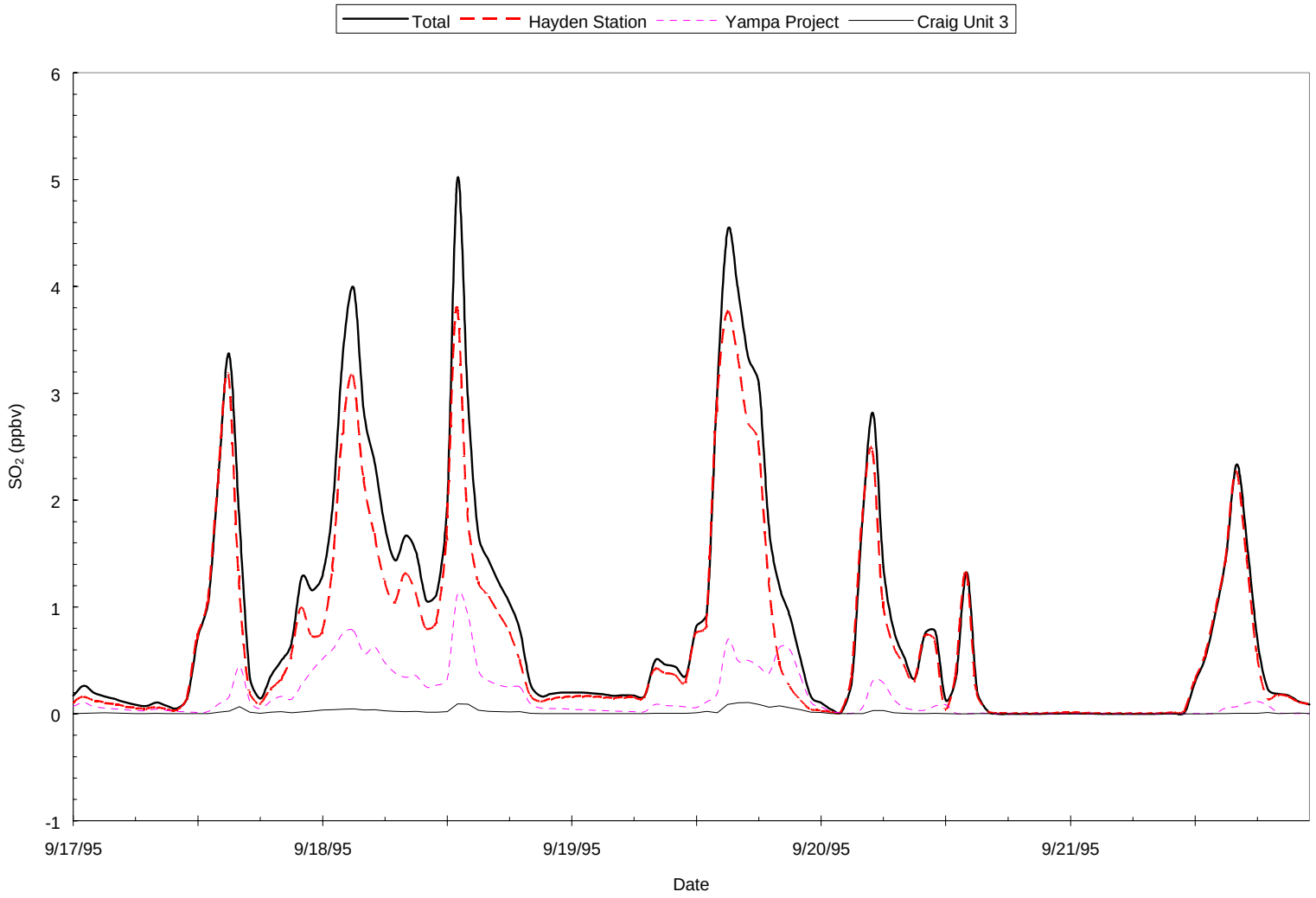

Figure 5.4.11 Time series plot of calculated hourly SO_2 concentrations at Buffalo Pass showing the apportionment to sources for September 17 to 21, 1995.

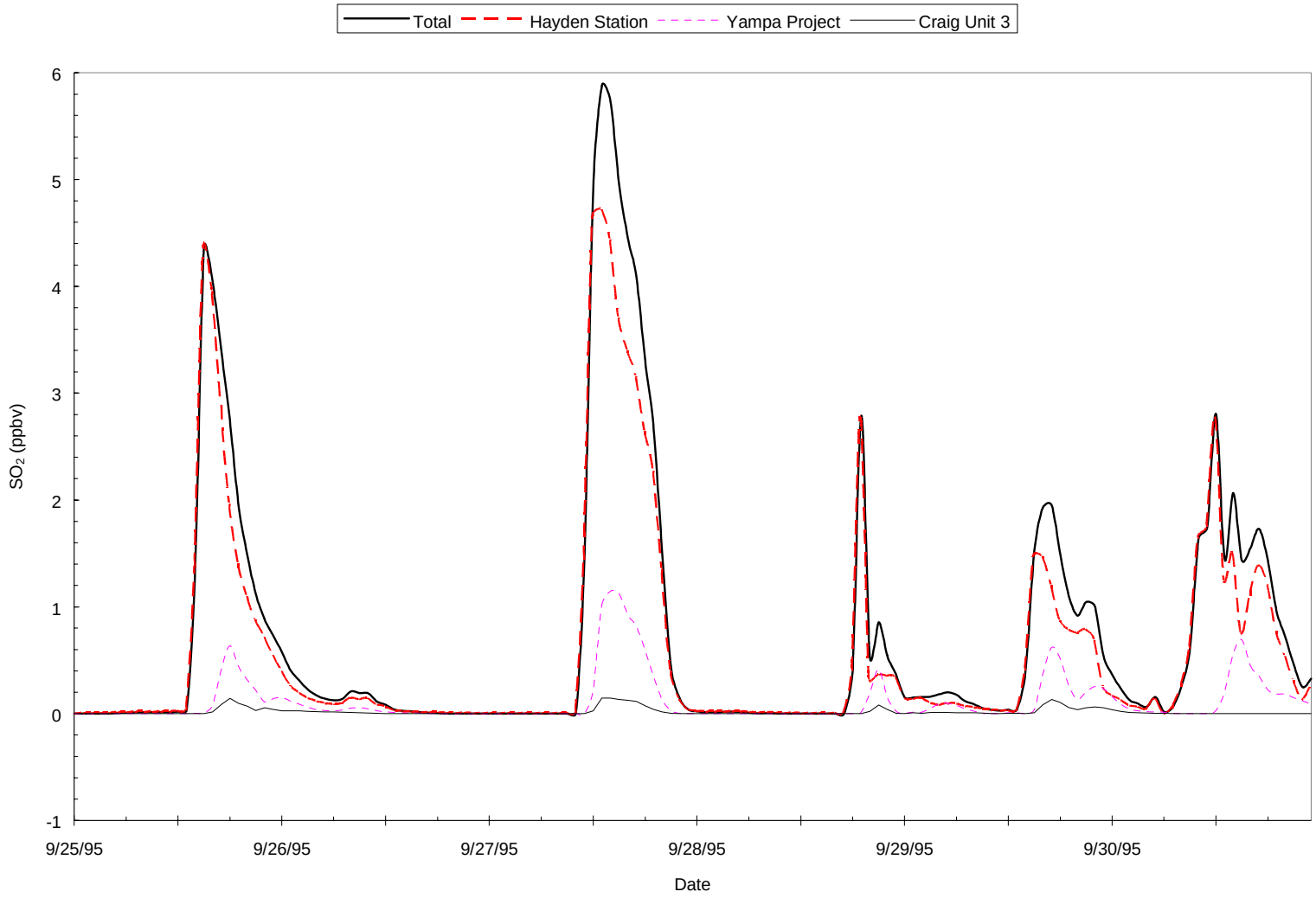

Figure 5.4.12 Time series plot of calculated hourly SO_2 concentrations at Buffalo Pass showing the apportionment to sources for September 25 to 30, 1995.

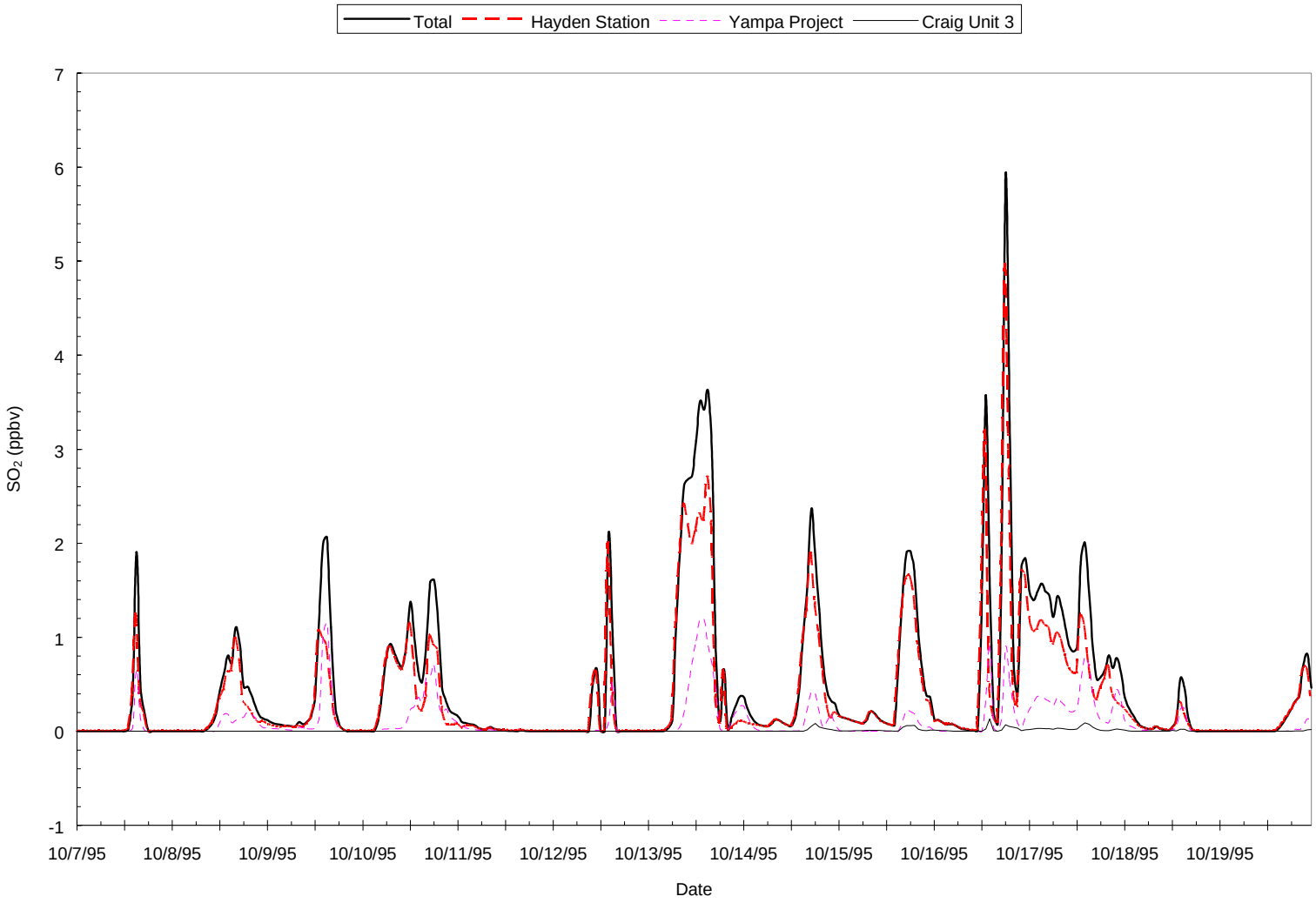

Figure 5.4.13 Time series plot of calculated hourly SO_2 concentrations at Buffalo Pass showing the apportionment to sources for October 7 to 19, 1995.

receptor site in or near the MZWA. However, time series plots have not been prepared for the complete January through November time period for all receptor sites, so the possibility that only one source contributed to a significant SO_2 event has not been ruled out.

The fact that SO_2 from the Hayden and Craig stations arrived simultaneously at Buffalo Pass eliminated the possibility of an experimental observation of the conversion of SO_2 from only one of these sources into sulfate. Had the SO_2 from the two sources frequently arrived at different times, it might have been possible to have estimated separate efficiencies for the conversion of SO_2 into sulfate for each of these generating stations directly from the monitoring data.

Numerical data for the source apportionment of calculated hourly SO_2 concentrations at Buffalo Pass and Davis Peak are presented in Figures 5.4.14 through 5.4.18. The purpose of these data is to further quantify the absolute and relative contributions of each of the five generating station units to SO_2 at two locations in the MZWA. These two sites were selected because they should bracket the range of conditions encountered in the high country of the MZWA.

The top half of Figure 5.4.14 shows the monthly average and study average calculated hourly SO_2 concentrations attributed to each of the five generating station units as well as the total attributed to all units. The data are presented in both tabular and graphical form. The bottom half of Figure 5.4.14 shows the percentage contributions, which were obtained by dividing the monthly average for each unit by the monthly average for the total SO_2 concentration. The column at the right indicates the number of hours of data each month. These hours were used to weight the monthly averages when calculating the average for the 11-month study. The monthly average calculated SO_2 concentrations show significant variability from month to month, but the calculated percentage contributions show much less variability.

Figure 5.4.15 shows the results of the same calculation when only hours with calculated SO_2 concentrations at Buffalo Pass greater than 2 ppbv were included instead of all hours. The right column of the tables shows the number of hours each month hourly SO_2 concentrations exceeded 2 ppbv. These values show significant month-to-month variability. The percentage contributions show less variability, and are quite similar to the percentage contributions calculated for all hours.

Figures 5.4.16 and 5.4.17 show the results of the same calculations for Davis Peak. The average concentrations in the top half of Figures 5.4.14 and 5.4.16 are always smaller at Davis Peak than at Buffalo Pass. On average, the concentrations differ by about a factor of two. The percentage contributions are very much the same for the two receptor sites and for the two concentration ranges evaluated.

Figure 5.4.14 Monthly average absolute and relative contributions for each power station unit to SO_2 concentrations at Buffalo Pass for all data.

Figure 5.4.15 Monthly average absolute and relative contributions for each power station unit to SO_2 concentrations at Buffalo Pass for hours with SO_2 concentrations greater than 2 ppbv.

Figure 5.4.16 Monthly average absolute and relative contributions for each power station unit to SO_2 concentrations at Davis Peak for all data.

Figure 5.4.17 Monthly average absolute and relative contributions for each power station unit to SO_2 concentrations at Davis Peak for hours with SO_2 concentrations greater than 2 ppbv.

Figure 5.4.18 Dilution ratios for Buffalo Pass and Davis Peak for all hours.

The ratio of the calculated SO_2 concentrations in the MZWA to the emission rates were calculated for each generating station unit to estimate an average dilution ratio for each unit. These dilution ratios are of greatest interest during times of peak SO_2 concentrations when effects on visibility may occur, but are difficult to calculate for short time periods because of the hourly variability in the emission rates. Therefore, they were calculated for all data and are shown in Figure 5.4.18. No data are shown for Craig Unit 2 in April because the unit was down most of the month. These dilution ratios give the calculated average ambient concentration of SO_2 in parts per trillion by volume that would result from an emission rate of 1 g/s. The smaller number for Davis Peak than Buffalo Pass indicates that there is more dilution on transport to Davis Peak.

These dilution ratios are a measure of the dilution of the emissions in the atmosphere and are independent of the emission rates. When emissions are transported with little dilution, these ratios and the ambient concentrations become large. The times of poor dilution are of greatest interest for visibility studies, so it is desired to obtain information about dilution ratios at these times. The data in Figures 5.4.14 through 5.4.17 show that the percentage contributions of the five units to SO_2 concentrations at Buffalo Pass and Davis Peak were the same for all hours as for hours with SO_2 concentrations greater than 2 ppbv. Thus, one factor can be used to convert the average dilution ratios for all data into the average dilution ratios during hours with SO_2 concentrations greater than 2 ppbv. It is likely that further calculations would show that this is a general result; the average dilution ratios in Figure 5.4.18 calculated from all data provide good guidance for the relative advantages of changing emissions during times of poor dilution. This hypothesis is recommended for use

in scoping calculations, but it should be confirmed by additional calculations before being used as the basis for decisionmaking.

The data in Figure 5.4.18 show a smaller dilution ratio (more dilution) for the emissions from Hayden Unit 2 than for Hayden Unit 1. The data in Figure 5.4.2 show that the plume rise for Unit 2 is greater, so these emissions undergo more dilution when they are mixed to the surface.

5.4.8 Animation of the Model Results

An animation of the SO_2 concentrations at the surface was prepared to provide an easily accessible overview of the locations of the emissions from the five generating station units during all hours of the study. A preliminary version of the animation was produced in November 1995 using nominal stack parameters and emission rates. This version of the animation was used to select background filter samples, i.e., samples from sites to the west or north of the generating stations during times when the animation showed persistent plume transport toward the east. The animation was also used to identify times when surface monitoring sites were likely to be affected by the stack emissions and to evaluate the dimensions of the mesoscale modeling domain. The preliminary mesoscale domain was extended to the west after viewing the preliminary animation to ensure that emissions transported to the west by drainage flows in the Yampa Valley would not be lost from the modeling grid.

The final model results produced in April 1996 were also made available as an animation that is available from DRI or the study sponsors. The steps in the production of the animation were: 1) convert the unformatted CALPUFF output files that contain the hourly surface SO_2 concentration data at each grid cell to ASCII files that can be read by a PC; 2) use a specially prepared Visual Basic program to generate a map of the grid cells each hour in which the color of the cell indicates the SO_2 concentration; 3) use the Voyager Movie program to capture the images created for each hour of data and combine them in an .AVI-format file that can be played back as a movie; and 4) make copies of the animation on CD-ROMs that also contain the Voyager Player software for viewing the animation. An insert in the CD-ROM package contains operating instructions for viewing the animation on a PC and information on the interpretation of the animation.

Surface concentrations were animated because only surface data are available in the CALPUFF model outputs. The only data for concentrations aloft were obtained by modifying CALPUFF to report results along specific sight paths, as described in Section 6.7. For distances shorter than the distance at which the emissions are uniformly mixed to the ground, concentrations aloft (at the puff centers) are greater than at the surface.

5.4.9 Discussion of the Model Results

The everyday plume transport modeling was performed to simulate the transport of SO_2 from the five stacks of the Hayden and Craig generating stations within the mesoscale modeling domain, which surrounds the generating stations and the MZWA. SO_2 is an invisible gas, so the results of this modeling by themselves provide no direct information on the effects of the SO_2 emissions on visibility impairment. These results provide only one link

in the chain of information used to evaluate the effects of the emissions on visibility conditions in the MZWA.

The model results are useful because SO_2 is a marker for the emissions of the five stacks and it is a precursor for sulfate, which can cause perceptible contributions to haze. The conversion of SO_2 to sulfate is addressed in Section 6. This chemical conversion, along with wet and dry deposition will convert SO_2 into other chemical species or remove it from the atmosphere. Therefore, SO_2 is not an inert species and cannot always be used for the quantitative experimental measurement of the dilution of the emissions from the Hayden station and Yampa Project. In clouds and heavy precipitation, substantial amounts of SO_2 can be transformed or removed by wet deposition. However, at other times, the transport distances and times are typically short enough that the amount of SO_2 removed or transformed during transport to the MZWA is of the order of 10 percent. At these times, SO_2 can be used as a semiquantitative marker.

The model results were tested by comparing the calculated SO_2 concentrations with measurements. Consistent results were found, so it was concluded that study conclusions can be based on model results. The model results provided an apportionment to each of the five sources of hourly SO_2 concentrations at ground level for every grid square in the mesoscale modeling domain and each discrete receptor for all hours during January through November 1995 that upper-air wind data were available from at least one of the three radar profilers. Selected portions of these results are summarized above, and the conclusions derived from these results are summarized at the beginning of Section 5.4. It was found that the apportionment of SO_2 to sources was surprisingly insensitive to the location within the MZWA, the month of the year, and the threshold concentration used to select data for apportionment. Therefore, the apportionments reported above and in the summary are recommended for general use.

5.5 Effects of Primary Emissions

In addition to providing a visual record of plume movement. Chavez Mountain (CHHZ) and Cedar Mountain (CEDZ) video views also documented cases in which visible emissions from the Hayden and Craig generating stations were more intense than normal and when they were obvious contributors to layered hazes in the Yampa Valley. This subsection documents when these visible primary particle emissions occurred during the MZVS, the intensity of the plumes and haze layers they caused, and their relationship to recorded deviations from normal plant operating procedures. Deviations from the most common plume intensities were classified with the following codes:

Code No.	Description
1.	Slight: The particulate plume was visible but did not obscure background features or move any significant distance from the generating station.
2.	Moderate: The particulate plume was visible and obscured background features or moved some distance from the generating station – usually out of the camera view.

3. Considerable: The particulate plume was visible, significantly obscured background features, occupied a large area around the generating station, and/or moved a significant distance from the generating station. In this case, the plume was usually visible from other views.

Only cases in which there was a noticeable increase in the intensity of the visible plume were classified. The video reviewers examined thousands of hours of tapes, and they became quite accomplished at identifying such deviations from normal emissions. Tables 5.5.1 and 5.5.2 document these observations for the Hayden and Craig stations, respectively. The tables include the date of the observation, the intensity code, a brief description of what was seen on associated video camera views, and a summary of recorded malfunctions during the event that were provided by each generating station.

As shown in Table 5.5.1, from nearly a year of observations, 34 occurrences of Hayden generating station visible particulate plumes with moderate or considerable intensity were documented. These events were generally characterized by low-level, dark emissions

Table 5.5.1
Observed Primary Plumes at Hayden Station and Malfunction Reports

Date	Code	Visual Observation	Malfunction Report Unit	Time (MST)	Opacity	Deviation
#######	3	Dense plume appears ~1500 MST. Trapped in surface layer and moves SE and E.	1	1524 to 1524	29.3	Flue Gas Conditioning Malperformance
		Meanders below inversion and appears as a polluted layer for rest of day.	2	- - -		None
#######	2	Morning plume moves up and down valley. Gray color. Dissipates by mid-day.	1	824 to 906	61.8	Flue Gas Conditioning Malperformance
			2	824 to 824	20.7	Boiler Upset
1/3/1995	3	Dense particle plume ~1300 MST. Remains at elevation of stack and appears	1	1848 to 1854	29.4	Flue Gas Conditioning Malperformance
		as layer within the Valley. Visible from several views, with direct transport	1	2100 to 2130	27.6	Soot Blowing
		to CHHZ camera.	2	1312 to 1324	28.1	Soot Blowing
#######	2	Dark gray particle plume ~1300 MST. Lower portion of plume moves down-	1	- - -		None
		valley. A portion breaks through the inversion and moves to the SE. Wind	2	1418 to 1418	21.1	Soot Blowing
		change at ~1500 MST carries plume up-valley.	2	1912 to 1954	27.3	Precip Upset
#######	3	Vapor plume appears at 1200 MST, particulate plume at 1400 MST. Flows SE	1	2036 to 2118	26.8	Soot Blowing
		and E and appears as a layered haze for rest of day.	2	1948 to 1948	20.3	Precip Upset
			2	2236 to 2254	20.6	Blowing Air Heaters
#######	3	Gray afternoon plume moves S in early afternoon, then up-valley.	1	2142 to 2148	32.6	Flue Gas Conditioning Malperformance
			2	2254 to 2254	22.3	Soot Blowing
#######	2	Slight to moderate gray during morning, disappearing by afternoon.	1	- - -		None
			2	- - -		None
#######	3	Brown plume moves up-valley all afternoon.	1	- - -		None
			2	- - -		None
3/1/1995	3	Dense gray plume moves south after fog lifts at 1300 MST. Moves up-valley	1	1306 to 2024	23.7	Blowing Air Heaters
		from 1600-1645 MST, then down-valley until dark.	1	2330 to 2354	28.9	Soot Blowing
			2	1354 to 1754	21.7	Blowing Air Heaters
#######	2	Slight particulate plume most of the afternoon with a short burst.	1	1636 to 2042	37.1	Flue Gas Conditioning Malperformance
		Plume dissipated within camera view.	1	2242 to 2254	22.9	Soot Blowing
			2	1636 to 1642	49.5	Flue Gas Conditioning Malperformance
			2	1930 to 2124	31.3	Soot Blowing
			2	2130 to 2200	30.3	Blowing Air Heaters

#######	2	Small bursts of moderate, elevated plume intensity.	1	-		-	-	None
			2	1054	to	1054	21.3	Flue Gas Conditioning Malperformance
#######	2	Slight plume most of day. Dissipates prior to leaving view.	1	1354	to	1354	21.8	Blowing Air Heaters
			2	-		-	-	None
#######	2	Slight plume, with moderate intensity in afternoon.	1	1406	to	1406	22.6	Blowing Air Heaters
			2	-		-	-	None
#######	2	Moderately intense plume moves up valley from sunrise to ~0800 MST.	1	130	to	130	20.3	Soot Blowing
			1	1118	to	1118	39.4	Flue Gas Conditioning Malperformance
			2	1118	to	1124	27.8	Flue Gas Conditioning Malperformance
#######	2	Slight plume with some moderate bursts.	1	1200	to	1342	100.1	Upset Condition
			1	1348	to	1548	100.2	Cold Boiler
			1	1554	to	2354	100.5	Upset Condition
			2	2312	to	2336	47.6	Soot Blowing
#######	2	Variable moderate plume from 1630-1830 MST moves up-valley and down-valley.	1	-		-	-	None
			2	1354	to	1406	26.9	Precip Upset
#######	2	Plume moving down-valley from sunrise to 0600 MST.	1	-		-	-	None
			2	-		-	-	None
#######	3	Considerable visible plume moving down-valley from sunrise to 0600 MST.	1	736	to	736	22.2	Blowing Air Heaters
			2	448	to	636	100.5	Upset Condition
8/1/1995	2	Slight-moderate plume late in the day, moving up-valley.	1	2048	to	2048	20.1	Boiler Upset
			2	1324	to	1606	32.3	Precip Upset
#######	2	Slight-moderate plume moving down-valley from sunrise to 0600 MST.	1	-		-	-	None
			2	24	to	912	100.5	Upset Condition
#######	2	Slight-moderate plume moving up-valley from dawn to 0600 MST.	1	300	to	300	20.1	Blowing Air Heaters
			1	718	to	718	34.9	Boiler Upset
			2	30	to	1036	99.4	Upset Condition
			2	1048	to	1048	22.1	Boiler Upset
#######	2	Slight-moderate plume moving up-valley from 1600 MST to sunset.	1	-		-	-	None
			2	-		-	-	None
#######	2	Moderate plume moving up-valley and toward the Chavez Mt. camera from	1	1524	to	2354	93.6	Upset Condition
		1500 MST to sunset.	2	1706	to	1706	20.4	Precip Upset
#######	3	Considerable, black plume moving up-valley starting at 0500 MST and out of the	1	124	to	124	22.4	Boiler Upset
		the Chavez Mt. view. Plume appears gray as it disperses downwind. At 0900 MST	1	200	to	254	49.7	Soot Blowing
		the plume is not as prominent, but it leaves a yellow-brown layer extending	1	1118	to	1118	26.2	Boiler Upset
		up-valley.	2	600	to	600	26.7	Boiler Upset
#######	2	Slight-moderate plume moving up-valley from sunrise to 0700 MST.	1	230	to	230	22.4	Soot Blowing
			1	524	to	524	23.9	Boiler Upset
			2	524	to	530	22.1	Boiler Upset

#######	2	Moderate plume from sunrise to 0730, moving down-valley. It moves out of the Chavez Mt. view of Hayden, but is not perceptible in other views.	1	-		-	-		None
			2	-		-	-		None
#######	2	Moderate plume from sunrise to 0730 moving down-valley. The layered haze extends beyond the Chavez Mt. view, but is not perceptible in other view.	1	18	to	36		25.2	Soot Blowing
			2	148	to	148		21.5	Blowing Air Heaters
#######	2	Moderate plume moves up-valley from sunrise to 0900 MST, but dissipates before leaving the Chavez Mt. view.	1	118	to	224		30.9	Soot Blowing
			2	218	to	218		24.3	Boiler Upset
			2	306	to	306		23.9	Soot Blowing
#######	2	Moderate plume moves down-valley from sunrise to 0830 MST. The plume leaves the Chavez Mt. view, but is not perceptible in other views.	1	30	to	148		26.0	Soot Blowing
			2	800	to	812		35.5	Boiler Upset
#######	3	Moderate plume from sunrise to 1030 MST. The plume meanders and concentrates below the inversion until 0830 when it moves up-valley.	1	810	to	1124		100.5	Upset Condition
			2	-		-	-		None
#######	2	Slight-moderate plume moves up-valley from 0600 to 0900 MST.	1	-		-	-		None
			2	-		-	-		None
#######	2	Slight-moderate plume moves down-valley from sunrise to 0745 MST.	1	106	to	636		39.5	Monitor Equipment Failure
			2	454	to	518		29.4	Control Equipment (unacceptable)
#######	3	Moderate-considerable plume moves up-valley from sunrise to 1000 MST. It is dark gray and leaves a dark moderate layered haze. It is visible from other views.	1	206	to	312		24.2	Cleaning/Soot Blowing
			2	42	to	718		50.4	Startup/Shutdown
#######	3	Slight-moderate plume moves down-valley from sunrise to 1000 MST. Only perceptible from the Chavez Mt. view.	1	200	to	642		32.3	Control Equipment (unacceptable)
			1	854	to	936		28.4	Cleaning/Soot Blowing
			1	1018	to	1018		21.6	Process Problem (unacceptable)
			2	-		-	-		None

Table 5.5.2
Observed Primary Plumes at Craig Station and Malfunction Reports

Date	Code	Visual Observation	Malfunction Report Unit	Time (MST)		Opacity	Deviation
######	2			0000	to 2400	81.9	Offline due to voltage regulator malfunction
#		Moderate grey plume moves don-valley beneath inversion from 0900	1				
		to 1430 MST.	2	-	-		None
			3	-	-		None
4/1/1995	2	Dark grey slight-moderate plume moves up-valley from 1000 to 1430 MST.		-	-		None
			1				
			2	0000	to 1924	91.2	Annual outage - offline
			3	-	-		None
######	2			-	-		None
#		Slight-moderate gray plume visible from 0900 to 1845 MST. Dissipates	1				
		rapidly and turns to slight by 1200.	2	0624	to 2400	82.9	Detector malfunction
			3	-	-		None
######	3			-	-		None
#		Considerable dark gray, coherent plume moves down-valley from sunrise to	1				
		0830 MST.	2	0000	to 2400	88.5	Offline for repairs
			3	-	-		None
7/4/1995	3			-	-		None
		Light gray moderate plume moves up-valley from 0715 to 0830 MST.	1				
			2	0742	to 2400	88.0	Offline for repairs
			3	-	-		None
######	3				to		Offline due to controls malfunction
#		Light gray considerable plume moves up-valley from 0715 to 0830 MST.	1	0730	1530	62.6	
			2	-	-		None
			3	-	-		None
######	3						None
#		Considerable, light gray plume spreads below inversion forming a flat, thin	1	-	-	-	
		elevated haze from 0700 to 0830 MST.	2	0442	to 0754	75.9	Startup after repairs
			3	-	-		None
######	2			-	-		None
#		Moderate light gray plume moves up-valley at sunrise, then soon moves	1				
		down-valley until 0545 MST, when it shifts to up valley until emissions	2	0000	to 1342	86.6	Offline for repairs
		stop at 0715 MST.	3	-	-		None

######	2				-	-	None
#		Moderate light gray plume moves up-valley from 1000 to 1500 MST.	1				
			2		-	-	None
			3		948	to 1636	81.2	Offline for repairs.

that occur under stable conditions. In a number of events, the plume appears to be trapped under an inversion layer. The emissions have a defined visual effect near the generating station. In addition, when plumes of moderate or considerable intensity were observed, the emissions tend to either be transported for some distance near the surface as a plume or broaden into a near surface haze layer. When visible particulate plumes were observed, layered hazes were not always seen from the Storm Peak views. There were, however, five instances during the winter when Hayden particulate plumes, visible from the CHHZ camera, could be seen as a plume from STPY.

One of these events occurred on 01/03/95. The video record of this event clearly illustrates that coherent plumes can travel many miles into the upper Yampa Valley. On this date, a primary particulate plume associated with a malfunction of the flue gas conditioning system covered a large area of the Yampa Valley between Hayden and Steamboat Springs as an elevated layered haze. In addition, a clearly defined, coherent plume emanating from the Hayden generating station can be seen moving towards Storm Peak from the Storm Peak-Yampa View camera at nearly the same elevation as the camera. The extent to which the plume reaches or rises over the continental divide cannot be determined because it cannot be seen in the Hahns Peak view. However, it is clear that the potential exists for the plume to reach the Storm Peak area.

Other cases of considerable primary particulate plumes that affected the eastern Yampa Valley occurred on 12/27/94, 01/21/95, 01/22/95, 01/29/95, 03/01/95, 06/28/95, 09/24/95, 10/08/95, 11/02/95, and 11/17/95. Each of these Code 3 events is associated with a recorded malfunction with the exception of the afternoon brown plume on 01/29/95. None of these definitively showed up in nephelometer traces (Figure 3.4.1) at Buffalo Pass or Gilpin Creek, though evidence of some of them appear at the Hayden VOR site. These elevated haze layers commonly remain coherent in the valley for a few hours and do not necessarily encounter nearby instruments. Downwind transport of the haze was not always in the direction of the Zirkel Wilderness. On 12/27/94 and 01/21/95 the plume was transported to the southeast. When transport is in the direction of the Wilderness, the haze may not reach or may miss the Gilpin Creek or Buffalo Pass monitoring sites as was the case on 01/03/95 when the plume was observed to be transported east to Storm Peak and southeast as the day progressed.

Most of the remaining Hayden primary emissions events were of short duration and dispersed prior to leaving the Chavez Mt. video view. Many events occurred right after sunrise with the station returning to normal operations by 0600 or 0700 MST. The 01/24/95, 05/26/95, 08/14/95, 09/29/95, and 10/13/95 events, all classified as slight to moderate, do not correspond to any recorded malfunction.

Nine primary particle events were observed for the Craig station. Four of them were classified as Code 3 (06/24/95, 07/04/95, 07/12/95, and 07/23/95). Each of these is associated with a malfunction record, usually taking a unit off-line for repairs. The most notable event at Craig occurred on 07/23/95, when a flat, thin, elevated layer formed in the morning. There is no evidence that any of the layers were detected by the nephelometer, and most of them remained within the Cedar Mountain view prior to dissipating.

These observations show that primary particle plumes from the Hayden station contributed to layered hazes on ~10% of the days studied and plumes from the Craig station contributed on ~3% of the days studied. Many of these were localized and not detected by the visibility monitors, but they were easily discernible from the time-lapse videos. The majority of these events were associated with reported malfunctions at each generating station. Along with elevated layers from fires, primary particle emissions during generating station malfunctions are one of the major causes of elevated haze layers in the Yampa Valley. During this study, the plumes and elevated layers did not appear to retain their coherency by the time they reached visibility monitors at Buffalo Pass or Gilpin Creek.

5.6 Transport and Light Extinction Characteristics during Modeling Periods

Transport patterns and chemical contributions to light extinction are examined here for cases in which light extinction was high at Buffalo Pass, near the Mt. Zirkel Wilderness Area. The major components of light extinction during these events are clean air scattering (b_{sg}), and particle scattering (b_{sp}) and absorption (b_{ap}) from ammonium sulfate and carbonaceous material (including black carbon). These components account for more than 90% of the total extinction during most of these cases. Fine-particle chemical contributions to extinction during these events are consistent with primary particles from fires, ammonium sulfate from regional sources, and ammonium sulfate from Yampa Valley generating stations. On average, ammonium sulfate contribution during these events contributed ~25% of total extinction. On dry days and during most events, the directly attributable contribution of the nearby generating stations appears to be negligible. On moist days, under conditions when Yampa Valley emissions can accumulate during the night and morning hours and subsequently be transported to Buffalo Pass, the contribution to extinction from Yampa Valley generating stations may be large if the emissions pass through fog or clouds.

5.6.1 Measurement Periods and Events for Detailed Study

Five time periods of elevated light extinction at Buffalo Pass were selected for detailed data analysis and modeling. The rationale for selection of these modeling periods is discussed in Section 3.4. These periods ranged from one to thirteen days. During each of these periods, specific days and hours when b_{scat} peaks ("events") occurred were identified for calculation of back-trajectories and other analyses to determine the causes of the light extinction. The modeling periods and events were chosen to represent different mixtures of source contributions to the light extinction and different transport and transformation conditions. These periods and times are listed in Table 5.6.1 with their priority for applying detailed CALMET/CALPUFF dispersion modeling. The first four periods were modeled and the model results are discussed in Section 6.7.

The b_{sp} events were selected using fine-particle light scattering data from the TSI three-wavelength integrating nephelometer along with the total light-scattering data measured

Table 5.6.1
Events Identified for Detailed Data Analysis

Modeling Priority	Modeling Period (1995)	Event Date	Event Time (MST)
1	9/17-9/21	9/18	1300-1400
		9/19	1300-1500
		9/21	1300-1400
2	8/7-8/9	8/8	1400-1600
3	10/7-10/19	10/8	0600-0700
		10/10	0700
		10/12	0800-1300
		10/17	0500
		10/19	1800
4	8/21-8/27	8/21	1600-1800
		8/23	1300
5	9/27	9/27	1900

by the OPTEC nephelometer. The TSI nephelometer is enclosed and was operated with a 2.5 μm inlet, so it did not measure light scattering by coarse particles and cloud droplets, while the OPTEC nephelometer has an open design and responds to all particles. Use of the TSI nephelometer data ensured that the selection of events was based on the presence of fine particles (i.e., haze) and that the detection of these particles was not interfered with by clouds or precipitation. The sample air in the TSI instrument was heated, typically drying the air below 50% relative humidity and causing water to evaporate from the particles. At high ambient humidities, this caused the TSI readings to be smaller than the ambient fine-particle light scattering (See Appendix A.1.2).

Regional (24-72 hour) and local (5-10 hour) back-trajectories were calculated from Buffalo Pass starting at the times noted in Table 5.6.1. For each event, the videos were reviewed to determine the occurrences of fog and clouds, generating station plume movements, and visible causes of the haze (e.g., fires or generating station malfunction conditions). The nephelometer data from surrounding sites were reviewed to assess whether the events were regional or local; tables of fire locations and sizes were used to identify potential contributions from fires; and plots of b_{scat} (both OPTEC and TSI nephelometers), SO_2, relative humidity, and black carbon at Buffalo Pass were reviewed to identify associations with generating station emissions, clouds, and urban or fire emissions. Extinction budget calculations were estimated for the six- or 12-hour periods of the filter

samples for relative humidities corresponding to ambient levels and for the reduced RH of the TSI nephelometer (See Section 4.4). Chemical mass balance receptor modeling was also performed for these days and is discussed in Section 6.5.

Regional back-trajectories for many of the selected events are shown in Figure 5.6.1. Local trajectories are described or shown along with the discussion of the individual events. Summaries of the video observations for the event days and notes about the occurrence of fires are included in Table 5.6.2. Plots of nephelometer, SO_2, black carbon, and RH data for each modeling period are included in the appropriate subsections below. A summary of the light scattering, chemistry, and extinction budget data referenced in this discussion is included in Table 5.6.3.

The regional back-trajectories in Figure 5.6.1 were estimated for the 700 mb height (about 3,000 m MSL), which is approximately the elevation of the Buffalo Pass monitoring site. The trajectories were computed using winds measured by the National Weather Service's (NWS) rawinsonde network, which makes upper-air soundings twice per day at 0500 and 1700 MST. Trajectories were computed by converting the aloft wind speed and direction into a distance and extrapolating backwards for twelve-hour periods, starting from Hayden, CO. Winds from the nearest stations were used to estimate the wind speed and direction for each 12-hour period. Trajectories were computed back 72-hours or until an air parcel reached a data-sparse area (e.g., the Pacific Ocean). Back trajectories on 09/18/95 and 09/21/95 were not computed owing to the unavailability of NWS wind data for these periods.

Figure 5.6.1 Regional back-trajectories at 3,000 m MSL (700 mb) for selected events.

Local back-trajectories from Buffalo Pass were estimated using aloft winds from the radarprofiler at Hayden. Backward trajectories were computed from the time of elevated light extinction at Buffalo Pass. Both constant altitude and "plume-following" back-trajectories were calculated in time increments of one-hour. The "plume-following" trajectories were computed to assess whether generating station emissions were likely to be detected at Buffalo Pass. To calculate the "plume-following" trajectories, we used the winds at the appropriate estimated (Hayden) plume height for the time increment. These trajectories only made sense when the estimated mixing depth was above the height of Buffalo Pass at the time of the event. The plume height and mixing depth estimates from CALMET, combined with the profiler data were used to determine the altitudes that best represented the plume for any time step. This varying-altitude trajectory attempts to "follow" the plume, whereas a constant-altitude trajectory may not coincide with the plume height.

The backward trajectory computation involved a series of calculations. Mixing depth and plume height estimates were overlaid on the wind plots from the radar profiler (see Figure 5.2.8 for an example). During the nighttime when the plume was confined within the drainage flow, winds at plume height were used. During the morning when the winds coupled, but the mixing depth had not yet reached 1,300 m AGL (i.e., Buffalo Pass altitude

above the Hayden radar profile site), winds in the upper portion of the mixed layer were used. When mixing at Hayden occurred above the Buffalo Pass altitude, winds at Buffalo Pass were used in the trajectory calculation.

The Buffalo Pass light scattering, chemistry, and mass data included in Table 5.6.3 came directly from the data archive. The "dry" light scattering data are from the TSI three-color nephelometer and are averaged over the six- or twelve-hour periods of the filter samples. The estimated ambient and "dry" b_{ext} values and the estimated extinction budget percentage contributions were calculated using the ELSIE model as described in Sections 4.1 and 4.3. The ambient calculations are for the average ambient relative humidity during the time of the samples and are derived from Table 4.3.1. The "dry" calculations are for the average relative humidity in the TSI nephelometer for the same sample periods.

5.6.2 09/17/95–09/21/95 Period

This period was selected because of several instances of $PM_{2.5}$ dry nephelometer b_{sp} peaks of 15-20 Mm^{-1} that corresponded with increases in SO_2 and occurred during times when the cloud heights allowed long views underneath. The best evidence of significant contributions from Yampa Valley generating stations to light extinction occurred during this period.

Contributions from fires and other Yampa Valley emissions were also likely. During this period, the generating station emissions were processed by fog and clouds, allowing more rapid conversion of SO_2 to sulfate. These selected events are apparent in Figure 5.6.2 which shows hourly measurements at Buffalo Pass, along with the SO_2 concentrations estimated by the everyday modeling (see Section 5.4).

TABLE 5.6.3

Event Summary of Buffalo Pass Particle Extinction and $PM_{2.5}$ Chemical Contributions to Extinction

		Dry		Amb. est	Rayl eigh		Ambient										Dry est	Dry est										$PM_{2.5}$	Am m.					
	Period	b_{ext}	Ambient	b_{ext}	Scatter	Amb. est	est %	Amb. est	Amb. est	Amb. est	Amb. est	Amb. est	Amb. est	Amb. est	Amb. est	Amb. est	b_{ext}	b_{ext}	dry est.	Dry est	Dry est	Dry est	Dry est	Dry est	Dry est	Dry est	Dry est	Dry est	Dry est	Mass	Sulfate	OC+ EC	6-h			Solu. K
Date	MST	Mm^{-1}	Mm^{-2}	Mm^{-1}	Mm^{-1}	bscat	Ra. ext	sul scat	% sul ext	OC scat	EC abs.	% C ext	nitr. scat.	% Nit. ext.	soil scat	% soil ext	Mm^{-1}	Mm^{-1}	bscat	% Ra. ext	sul scat	% sul ext.	OC scat	EC abs.	% C ext	nitrate scat.	% Nit. ext.	soil scat	% soil ext	µg/m^3	µg/m^3		ug/m3	ppb	ng/m^3	ng/m^3
9/18	6	5.4	102.2	111.1	8.4	110.6	8%	57.5	52%	36.4	0.6	33%	7	6%	2	1%	13	4.1	12.5	64%	1.6	12%	2.1	0.6	21%	0.2	2%	0.1	1%	1.7	0.8	0.62	0.1	0.0	0.1	0
9/18	12	10.9	40.0	49.3	8.4	48.4	17%	28.4	58%	7.0	0.9	16%	4	8%	1	1%	15	5.3	13.7	58%	3.1	21%	1.5	0.9	16%	0.5	3%	0.2	1%	2.7	1.6	0.51	2.2	0.8	0.4	23
9/19	6	3.4	11.0	20.6	8.4	19.4	41%	4.4	21%	5.2	1.1	31%	1	5%	1	2%	13	3.1	11.5	67%	0.9	7%	1.8	1.1	23%	0.2	2%	0.2	2%	1	0.4	0.59	0	0.0	0.1	0
9/19	12	10.7	11.8	22.4	8.4	20.2	38%	4.4	20%	6.4	2.2	38%	1	3%	0	2%	18	7.2	15.6	47%	2.2	12%	4.4	2.2	37%	0.3	2%	0.3	1%	3.9	1.2	1.46	2.3	0.9	0.3	17
9/21	6	6.4	13.3	22.9	8.4	21.7	37%	12.2	53%	0.3	1.2	7%	1	2%	0	2%	13	3.3	11.7	66%	2.8	22%	0.1	1.2	10%	0.1	1%	0.2	1%	2.7	1.4	0.16	1.3	0.5	0	0
9/21	12	5.7	6.5	15.3	8.4	14.9	55%	4.3	28%	1.5	0.4	12%	0	2%	0	2%	12	2.9	11.3	71%	1.7	14%	0.9	0.4	11%	0.1	1%	0.2	1%	1.7	0.9	0.30	--	--	0.1	2
8/8	6	17.7	15.5	23.9	8.4	23.9	35%	4.4	18%	9	0.0	38%	0	1%	2	8%	22	14.0	22.4	38%	3.7	17%	8.3	0	37%	0.1	1%	1.8	8%	6.7	2.0	2.3	0.4	0.2	0.1	38
8/8	12	17.4	12.9	28.0	8.4	21.3	30%	4.4	16%	5.6	6.7	44%	1	2%	2	8%	26	11.4	19.8	32%	3.6	14%	5.1	6.7	45%	0.5	2%	2.1	8%	8.3	2.4	2.1	1.9	0.7	0.3	88
10/8	6	16.5	19.4	29.3	8.4	27.8	29%	6.3	22%	9.5	1.5	38%	3	9%	1	3%	18	7.6	16.0	48%	1.8	10%	4.5	1.5	34%	0.8	5%	0.5	3%		0.9	1.4	0.4	0.2	0	54
10/8	12	6.8	3.2	11.7	8.4	11.6	72%	1.7	15%	0.8	0.1	8%	0	2%	1	4%	11	2.8	11.2	74%	1.4	12%	0.7	0.1	7%	0.2	2%	0.4	4%		0.8	0.2	1.8	0.7	0.1	25
10/10	6	9.5	3.4	13.3	8.4	11.8	63%	1.5	11%	0.8	1.4	17%	1	4%	1	5%	13	2.9	11.3	66%	1.2	9%	0.7	1.4	17%	0.4	3%	0.6	5%		0.7	0.4	2.5	1.0	0.1	27
10/10	12	6.7	3.9	14.9	8.4	12.3	56%	1.5	10%	1.5	2.6	28%	0	3%	1	3%	15	3.5	11.9	58%	1.2	8%	1.4	2.6	28%	0.3	2%	0.5	4%		0.7	0.7	2.0	0.8	0.3	29
10/12	6	15.9	22.9	40.5	8.4	31.3	21%	5.9	15%	12.8	9.3	55%	1	2%	4	9%	37	18.9	27.3	23%	4.3	12%	10.9	9.3	55%	0.5	1%	3.1	9%		2.3	4.0	1.1	0.4	0.2	30
10/12	12	12	35.2	52.3	8.4	43.6	16%	16.2	31%	17.5	8.7	50%	1	2%	1	1%	27	9.8	18.2	31%	3.2	12%	6.1	8.7	55%	0.2	1%	0.3	1%		1.5	2.6	0.5	0.2	0.2	11
10/17	6	8.1	5	14.3	8.4	13.4	59%	1.8	13%	2.1	0.9	21%	0	2%	1	6%	14	4.4	12.8	61%	1.5	11%	1.9	0.9	20%	0.2	2%	0.8	6%		0.8	0.6	1.6	0.6	0.2	15
10/19	6	4.9	1.9	11.2	8.4	10.3	75%	0.6	5%	0.6	0.9	13%	0	3%	0	4%	11	1.7	10.1	76%	0.5	5%	0.6	0.9	14%	0.2	2%	0.4	3%		0.3	0.3	0.8	0.3	0	17
8/21	6	15.1	28.3	36.7	8.4	36.7	23%	12.3	34%	13.6	0.0	37%	1	3%	1	4%	22	13.8	22.2	38%	4.8	22%	7.7	0.0	35%	0.4	2%	0.9	4%	6.1	2.1	1.9	0.2	0.1	0	15
8/21	12	16.3	17.2	27.2	8.4	25.6	31%	7.9	29%	7.7	1.5	34%	0	2%	1	4%	22	12.4	20.8	38%	5.0	22%	6.1	1.5	34%	0.3	1%	1.0	5%	7.4	2.5	1.8	0.5	0.2	0.2	23
8/23	6	9.9	10.6	22.2	8.4	19	38%	6.5	29%	2.7	3.1	26%	1	3%	1	4%	17	5.3	13.7	50%	2.8	17%	1.6	3.1	28%	0.3	2%	0.6	3%	4.2	0.9	0.7	0.1	0.0	0.1	11
8/23	12	13.8	27.5	37.5	8.4	35.9	22%	12.1	32%	10	1.6	31%	1	2%	5	12%	23	12.8	21.2	37%	4.3	19%	5.3	1.6	30%	0.3	1%	2.8	12%	9	1.9	1.6	1.3	0.5	0.5	16
8/27	6	11.1	13.8	24.3	8.4	22.2	35%	3.5	14%	7.0	2.0	37%	1	4%	2	10%	23	12.2	20.6	37%	2.8	12%	6.4	2.0	37%	0.7	3%	2.3	10%	7.3	1.4	1.9	0.3	0.1	0.3	10
9/27	6	8.0	6.2	17.5	8.4	14.6	48%	3.5	20%	1.6	3.0	26%	0	2%	1	3%	16	4.6	13.0	53%	2.4	15%	1.3	3.0	27%	0.3	2%	0.5	3%	3.4	1.2	0.7	0.9	0.3	0.1	15
9/27	12	9.2	6.1	15.0	8.4	14.5	56%	3.2	21%	2.1	0.5	17%	0	2%	1	3%	14	5.3	13.7	59%	2.6	18%	1.9	0.5	17%	0.3	2%	0.5	3%	3.5	1.5	0.6	1.3	0.5	0.2	23
Averages:							39%		24%			29%		3%		5%				51%		14%			28%		2%		4%							

Figure 5.6.2 Hourly b_{sp}, SO_2, black carbon, and RH at Buffalo Pass for 09/17/95–09/21/95.

The period was characterized by high humidity, snow showers, and clouds at or above Buffalo Pass, with periods of lower humidity and long views under the clouds during midday on 09/18/95 and 09/19/95. The high humidity and cloud-cover started on the afternoon of 09/17/95 and started dissipating during midday on 09/21/95. The synoptic flows during this period were mostly westerly. Throughout the modeling period a large wild-fire (43 km^2) burned about 90 km west-southwest of Craig.

This modeling period began with high pressure, warm temperatures, and clear skies over the study region on the morning of 09/17/95. Gradually during the next four days, a strong upper-level trough of low pressure moved through the northern United States and two trailing cold fronts pushed southward through the region. This stormy weather pattern resulted in higher humidity, rain and snow showers, and clouds at or above Buffalo Pass for the remainder of the period.

On 09/18/95, the first cold front brought morning and afternoon clouds and showers to the region. Aloft winds were generally westerly, but changed to northerly for several hours in the evening after the cold front passed. By 09/19/95, high humidity from the previous day's rain produced thick morning fog and fair weather cumulus clouds during the afternoon. Late on 09/20/95, the second surge of cold Canadian air produced light snow over the region. By 09/21/95, the westerly winds aloft transitioned to northwesterly as the upper-level trough moved eastward. The northwesterly flow decreased the humidity over the area and skies cleared by afternoon. Drainage flows occurred during the overnight and early morning hours from 09/17/95–09/20/95, but were not observed on the night of 09/20/95–09/21/95, that had northwesterly flow during the night and morning.

5.6.2.1 09/18/95, 1300-1400 MST Event

During this event, the TSI b_{sp} increased from about 4 Mm^{-1} to over 20 Mm^{-1} for about an hour during midday. The OPTEC nephelometer b_{sp} peaked above 50 Mm^{-1} during the same event (Figure 5.6.2). SO_2 rose from below detection limit (about 0.2 ppb) to 2.5 ppb, and the black carbon from the aethelometer rose from about 0.04 $\mu g/m^3$ to over 0.2 $\mu g/m^3$.

The event occurred during a dip in RH from 100% to 88%. The Storm Peak video of Hahns Peak showed clouds just above the camera site and noticeable pulses of haze occurring in the view at the time of the event. Videos of the Yampa Valley showed that the plumes from both generating stations were emitted into fog in the morning. Video views from Chavez Mountain showed haze rising in the Valley in mid-morning as the mixing height deepened and appear to indicate transport of the haze eastward during mid day.

The "plume-following" trajectory starting at 1300 MST in Figure 5.6.3 is consistent with an accumulation of emissions in the Valley during the early morning drainage flow,

transport of these same emissions back up the Valley in mid-morning, and transport to Buffalo Pass in mid-day, coincident with the b_{sp} peak. For this day, the everyday modeling (see Section 5.4) also indicated a strong SO_2 peak at Buffalo Pass coincident with the measured SO_2 and b_{sp} peaks (Figure 5.6.2).

Figure 5.6.3 Constant altitude and "plume following" back-trajectories from Buffalo Pass on 09/18/95 at 1300 MST.

Measurements during the 09/18/95 event are consistent with a small regional contribution, possibly from the fire, and an increment due to emissions from the Yampa Valley. The increase in carbon along with the b_{sp} peak is indicative of a contribution from Valley sources other than the power stations. The increase in b_{sp} accompanying an increase in SO_2, however, was the largest seen during the study (see Section 6.6) and is consistent with a b_{sp} contribution from sulfate formed from local SO_2 emissions either in the morning fog or in the clouds enroute to Buffalo Pass.

The $PM_{2.5}$ at Buffalo Pass for the afternoon shows an increase in mass from the morning of 1.7 $\mu g/m^3$ to 2.7 $\mu g/m^3$ with a corresponding increase of ammonium plus sulfate from 0.8 $\mu g/m^3$ to 1.6 $\mu g/m^3$ and a decrease in elemental plus organic carbon from 0.62 $\mu g/m^3$ to 0.51 $\mu g/m^3$. The six-hour average SO_2 increased from 0.1 to 2.2 $\mu g/m^3$. The average TSI nephelometer b_{sp} for the six-hour periods of the filter samples increased from 5.4 Mm^{-1} to 10.9 Mm^{-1}. (see Sections 4.2 and 4.3 for discussion of chemical composition and Appendix D for a list of filter chemical concentrations and corresponding light scattering averages). Selenium, which is present in coal combustion ash, increased from 0.1 to 0.4 ng/m^3 between the two samples. Six-hour soluble potassium (a component of wood combustion particles) increased from 0 to 23 ng/m^3. These values are consistent with a significant contribution from Yampa Valley sulfur sources to both sulfate and light extinction at Buffalo Pass.

As seen in the ~250% difference in scattering between the internal and ambient nephelometers, the hygroscopic nature of the sulfur aerosol at high humidities greatly amplifies the scattering associated with the sulfur aerosol. For the six-hour afternoon sampling period of 09/18/95, ammonium sulfate and the accompanying water were estimated to be responsible for 58% of the ambient light extinction and 21% of the dry light extinction. The remainder of the ambient extinction was attributed to elemental and organic carbon (16%), clean air scattering (17%), ammonium nitrate (8%), and soil. If half of the ammonium sulfate contribution (the concentration increase from morning to afternoon) were from the generating stations, the contribution to scattering (and extinction) would be significant for the six-hour average and probably large during the shorter duration of the SO_2 pulse seen in Figure 5.6.2. The CMB analyses in Section 6.5 show this time period to have a "coal-fired generating station" contribution to extinction of about 14%. This was the largest seen for any of the analyzed samples at Buffalo Pass.

5.6.2.2 09/19/95, 1300-1500 MST Event

This event was similar to the one on 09/18/95. Again, an increase in light scattering occurred at Buffalo Pass in the afternoon, and the haze was noticeable in the Storm Peak videos. The afternoon humidity was lower during this event (below 80%), but there were clouds over the mountains. The TSI b_{sp} increased from about 3 Mm^{-1} to about 15 Mm^{-1} during the few-hour event and from 3.4 to 10.7 Mm^{-1} for the six-hour morning and afternoon averaging periods. SO_2 rose from below about 0.2 ppb to 2.5 ppb, and the black carbon reading rose from about 0.01 $\mu g/m^3$ to about 0.15 $\mu g/m^3$ (Figure 5.6.2) during the event. After the event, however, the TSI b_{sp} and the black carbon readings dropped, but not back to their original levels. For the morning and afternoon six-hour filter samples, the mass rose from 1.0 to 3.9 $\mu g/m^3$, the ammonium plus sulfate from 0.43 to 1.21 $\mu g/m^3$, the elemental plus organic carbon from 0.59 to 1.46 $\mu g/m^3$, the selenium from 0.1 to 0.3 ng/m^3, and the soluble potassium from 0.0 to 17 ng/m^3.

The videos showed that the generating station plumes were emitted into morning fog where they could react to form sulfate. The local back-trajectory calculation (Figure 5.6.4) is consistent with accumulation of generating station and other emissions in the Yampa Valley and subsequent transport to Buffalo Pass when the mixing layer deepened in midday. The everyday modeling also showed generating station emissions arriving at Buffalo Pass coincident with the measured SO_2 and b_{sp} peaks.

The data for the 09/19/95 event are again consistent with extinction contributions from the generating stations and from other Valley sources, including the fire. Extinction budget calculations for the six-hour afternoon period attribute 20% of the ambient light extinction and 12% of the dry light extinction to ammonium sulfate, 38% and 37% respectively to carbon compounds, and 38% and 47% to clean air scattering. Although the generating station contributions were probably significant on this day, it appears that there was also a substantial contribution from the fire or other regional sources.

Figure 5.6.4 Constant altitude and "plume following" back-trajectories from Buffalo Pass on 09/19/95 at 1500 MST.

5.6.2.3 09/21/95, 1300-1400 MST Event

This event involved modestly elevated TSI b_{sp} levels (8-10 Mm^{-1}) from mid-morning through early afternoon. The elevated b_{sp} was accompanied by an increase in SO_2 from below the detection limit to 1-2 ppb. During this period, the RH at Buffalo Pass was generally above 80%, and the Storm Peak views were generally obscured by clouds. Both selenium and soluble potassium were below detection limits in the morning six-hour sample and barely detectable in the afternoon. The black carbon reading was not correlated with the b_{sp} levels. The winds prior to the event were light, and the local back-trajectory is inconclusive. The plumes were emitted into fog and clouds in the morning, however; and the correspondence of the b_{sp} and SO_2 indicate a likely generating station contribution. The extinction budget calculations attribute 53% and 22% of the ambient and dry b_{ext}, respectively, to ammonium sulfate for the morning six-hour sample and 28% and 14% for the afternoon sample. Most of the rest of the extinction was due to clean air scattering and some

to carbon compounds. It is unlikely, however, that the levels of b_{sp} measured were visually perceptible due to general obscuration of the views by clouds.

5.6.3 08/07/95–08/09/95 Period

This period was selected because there was elevated b_{sp} throughout the period (10-20 Mm^{-1} on the TSI nephelometer, 10-30 Mm^{-1} on the OPTEC), yet the relative humidity at Buffalo Pass was less than 70% most of the time, and the haze appeared to be regional. SO_2 peaks up to 2 ppb occurred frequently during the second half of the period, yet there was no apparent correlation between SO_2 and b_{sp}. The black carbon readings, however, seemed to be somewhat correlated with b_{sp}. The continuous air quality data for the period are shown in Figure 5.6.5. During this period, there were several small fires a few hundred kilometers southwest of Craig, the largest being 1.6 km^2.

Figure 5.6.5 Hourly b_{sp}, SO_2, black carbon, and RH at Buffalo Pass for 08/07/95–08/09/95.

The synoptic weather pattern during this period favored dry conditions for the first two days. On 08/07/95, an upper-level ridge produced clear to scattered skies, warm temperatures, and southwesterly winds aloft. By 08/08/95, a Pacific cold front approached Idaho, increased the southwesterly winds aloft to 10-20 m/s during the night, and caused the winds to transition to westerly by morning. Clouds increased throughout the day with scattered rain showers occurring during midday. On 08/09/95, cooler temperatures and widely scattered thunderstorms and showers were produced as the cold front passed. Drainage flows occurred during the night and early morning on all three days.

5.6.3.1 08/08/95, 1400-1600 MST Event

On this day, the TSI b_{sp} levels were ~16-18 Mm^{-1} all morning, peaking at ~20 Mm^{-1} in early afternoon, and decreasing to ~12-15 Mm^{-1} by evening. Small increases in the b_{sp} seemed to be correlated with black carbon, but not with SO_2; although the SO_2 started rising during the afternoon b_{sp} peak and peaked a few hours later at 2.5 ppb. The regional back-trajectory for the day (Figure 5.6.1) shows rapid long-range transport from the southwest, coming from southern California 36-48 hours earlier. The local back-trajectory from Buffalo Pass shows strong flow from the west without evidence of recirculation and accumulation in the vicinity of the generating stations. There was no video evidence of the generating station plumes interacting with fog or clouds. Regional haze was indicated by the b_{scat} readings at the other nephelometer sites.

The ambient and dry extinction budgets were similar for this day. For the morning and afternoon six-hour sampling periods, the extinction budget attributed 35% and 30%, respectively, of the extinction to clean air scattering, 38% and 44% to carbon compounds, 18% and 16% to ammonium sulfate, and 8% and 8% to soil. The soluble potassium concentrations were 38 and 88 ng/m^3, respectively, for the morning and afternoon samples; while the selenium concentrations were 0.1 and 0.3 ng/m^3. The sulfate concentrations at Baggs were similar to those at Buffalo Pass, indicating a regional contribution to sulfate. Although the sulfur contribution to the extinction was significant on this day, the lack of change of the nephelometer signals with major changes in SO_2 concentration is evidence of at

most a minor contribution to extinction from the local generating stations. The major cause of the haze during this event appears to be regional transport and fires, not Yampa Valley emissions.

5.6.4 10/07/95–10/19/95 Period

This period was selected because it includes three days (10/08/95, 10/12/95, 10/19/95) with TSI b_{sp} spikes of about 20-30 Mm^{-1}. In addition, there were intermediate multi-day periods of elevated b_{sp} with peaks of about 10 Mm^{-1} on 10/10/95 and 10/17/95. The events on the 10/08/95 and 10/12/95 had relative humidity at Buffalo Pass above 90%, while the others were much dryer. The hourly measurements for Buffalo Pass are shown in Figure 5.6.6.

Figure 5.6.6 Hourly b_{sp}, SO_2, black carbon, and RH at Buffalo Pass for 10/07/95–10/19/95.

There were numerous occurrences of SO_2 spikes at Buffalo Pass from 3 to 10 ppb; however, most of them were not associated with increases in b_{sp}. On the nights of 10/14/95 and 10/15/95, SO_2 concentrations above 8 ppb occurred while b_{sp} readings were less than 1 Mm^{-1}. Throughout this period, the Yampa Valley generating station plumes were not emitted into fog or clouds.

Buffalo Pass b_{sp} peaks during this period were accompanied by increases in black carbon readings. Review of the b_{scat} data from the other nephelometers in the region (see Section 3.4) showed that all of the selected events during this time period except for 10/19/95 were regional in nature, with most sites showing similar elevated concentrations.

From 10/11/95 through the end of the period, there were numerous fires in the region; including a 0.6 km^2 fire northwest of Craig on the 10/11/95 and a 0.6 km^2 fire southwest of Craig from 10/14/95 through 10/16/95. There was a 2 km^2 fire in or near the Yampa Valley from 10/16/95 through 10/18/95; and a fire was visible in the videos north of Hayden on 10/19/95. Over 100 km^2 burned in southern Idaho starting on 10/16/95.

Weather conditions during this thirteen-day period were controlled by a series of weak upper-level ridges and troughs that moved through the region. The period generally had clear skies or scattered clouds and little or no precipitation, except on 10/12/95. For the first four days, westerly flow aloft occurred around a broad ridge of high pressure located over the southwestern United States. This westerly flow transitioned to southwesterly as an upper-level trough moved through the region on 10/12/95 and produced rain and clouds. Behind the trough, a Canadian high-pressure system with westerly winds aloft transported cooler and drier air into the region from 10/13/95 through 10/15/95. On 10/17/95, another weak upper-level trough and associated cold front moved through the region, but it produced few clouds and no change in the prevailing westerly flow. Aloft winds generally remained westerly until 10/19/95, when a third upper-level trough moved over the area and produced strong northwesterly flow from the surface up to about 5,000 m MSL. Cooler and drier air was advected into the region by this northwesterly flow. Most of the days had drainage (i.e., easterly) flow during the night and morning and coupled up-valley flow in the afternoon.

However, on 10/19/95, strong northwesterly flow occurred during the night and early morning.

5.6.4.1 10/08/95, 0600-0700 MST Event

On this morning, the Buffalo Pass TSI b_{sp} peaked at 20 Mm^{-1} in early morning and stayed elevated until mid-morning. There were clouds above Storm Peak, but they did not obscure the views. The Buffalo Pass relative humidity in the morning was over 90%; and it was noticeably hazy below the clouds. Throughout the event, the SO_2 was below detection limit; the black carbon readings were slightly elevated, exceeding 0.1 $\mu g/m^3$ all morning. Regional back-trajectories extended to central California 60 hours before the event. The event occurred before mixing was deep enough for the site to be affected by local same-day emissions. Wind speeds were high enough that carryover of local emissions was not likely. On this day and through 10/12/95, Hayden Unit 1 and Craig Unit 3 were inoperative or operating at very low levels.

Extinction budget calculations for the morning six-hour period attributed 29% of the ambient extinction to clean air scattering, 22% to ammonium sulfate, 38% to carbon compounds, and 9% to ammonium nitrate. The soluble potassium concentration for the morning sample was 54 ng/m^3, indicating a contribution from fires; while the selenium concentration was below the detection limit. Local power stations probably made negligible contributions during this event. The elevated light extinction appears to be regional, with a possible contribution from fires. Some of the soluble potassium may have come from camp fires near the monitoring site

5.6.4.2 10/10/95, 0700 MST Event

The Buffalo Pass TSI b_{sp} peaked at about 10 Mm^{-1} in early morning. Both SO_2 and black carbon concentrations were slightly elevated at the time of the b_{sp} peak (Figure 5.6.6). Relative humidity at Buffalo Pass was below about 60% all morning. Regional back-trajectories passed through central California about 60 hours before the event. The local back-trajectory at the altitude of Buffalo Pass was also from the west. The event was too early to include air that was trapped below the nocturnal inversion in the Yampa Valley, but plume emissions that broke through the inversion might have contributed to the SO_2 concentrations measured. During this event, Hayden Unit 1 and Craig Unit 3 were inoperative or operating at very low levels.

The extinction budget calculations for the morning six-hour period attributed 63% of the ambient extinction to clean air scattering, 11% to ammonium sulfate, 17% to carbon compounds, 4% to ammonium nitrate, and 5% to soil. The soluble potassium concentration for the morning sample was 27 ng/m^3, indicating a contribution from fires; while the selenium concentration was 0.1 ng/m^3 with an uncertainty of 0.2 ng/m^3. It is unlikely that the local generating stations contributed significantly to this event, but they might have had a minor contribution. The event appears to be regional, with a possible contribution from fires.

5.6.4.3 10/12/95, 0800-1300 MST Event

This event took place during moist conditions with clouds above Storm Peak, but with frequent unobstructed views below the clouds. The TSI b_{sp} was about 17 Mm^{-1} for most of the morning, and the Storm Peak videos showed noticeable haze. There were numerous fires in the region on the prior day, some of which can be seen in the Chavez Mt. video. During this event, Hayden Unit 1 and Craig Unit 3 were inoperative or operating at very low levels.

Buffalo Pass SO_2 was measurable, but less than 0.5 ppb throughout the event. Black carbon readings peaked at over 2 $\mu g/m^3$ during the event. The 48-hour regional back-trajectory extended to the California-Mexico border. The local back-trajectory from Buffalo Pass came from the southwest earlier in the morning.

The extinction budget calculations for the morning six-hour period attributed roughly 21% of the ambient extinction to clean air scattering, 15% to ammonium sulfate, 55% to carbon compounds, 2% to ammonium nitrate, and 9% to soil. The soluble potassium concentration for the morning sample was 30 ng/m^3, indicating a contribution from fires; while the selenium concentration was 0.2 ng/m^3 with an uncertainty of 0.2 ng/m^3. The event appears to be regional, with a likely contribution from fires. The contribution of the local generating stations is not likely to be significant.

5.6.4.4 10/17/95, 0500 MST Event

From 10/17/95 through the morning of the 10/19/95, the Buffalo Pass b_{sp} varied in the 8-10 Mm^{-1} range with a peak of about 10 Mm^{-1} at 0500 MST on 10/17/95. Black carbon readings remained above 1 $\mu g/m^3$ most of the time, peaking at about 2 $\mu g/m^3$ at the time of the b_{sp} peak. SO_2 concentrations were highly variable throughout this period, reaching 3-4 ppb near the time of the b_{sp} peak. The variations in SO_2 do not appear to be reflected in the b_{sp} readings. Fires continued in the area throughout this period.

The 72-hour back-trajectory originated in southern California. The local back-trajectory from the early morning came from the west and could have included local SO_2 emissions, if they had penetrated the surface inversion; however, there were no fog or clouds to foster conversion to sulfate. For this day, the everyday modeling predicts the occurrence of over 1 ppb SO_2 at Buffalo Pass during the early morning. The plume rise estimates during the night were between 200 and 350 m AGL, which was located in the cool downslope flow. The plumes should have been confined within this layer of easterly winds. It is unclear by what mechanism the model predicted transport to Buffalo Pass.

The extinction budget calculations for the day-time 12-hour period attributed 59% of the ambient extinction to clean air scattering, 13% to ammonium sulfate, 21% to carbon compounds, 2% to ammonium nitrate, and 6% to soil. The soluble potassium concentration for the sample was 15 ng/m^3, indicating some contribution from fires; while the selenium concentration was 0.2 ng/m^3 with an uncertainty of 0.2 ng/m^3. The event appears to be mostly regional (the 12-hour Juniper Peak ammonium plus sulfate concentration was essentially the same as the Buffalo Pass concentration), with a possible contribution from fires. Because of the dry, regional nature of this event and the small sulfate contribution to extinction, the contribution of the local generating stations is not likely to be significant.

5.6.4.5 10/19/95, 1800 MST Event

The event on this day consisted of a sharp peak in late afternoon, with b_{sp} rising from under 1 Mm^{-1} in mid day to about 27 Mm^{-1} in the early evening. Black carbon peaked sharply during the event at over 0.25 $\mu g/m^3$. The SO_2 concentration peaked at 1 ppb before the event and dropped sharply during the event. Nearby fires causing the haze could be seen in the Storm Peak video north of Hayden. The local back-trajectory suggested transport from the region of the fire. The extinction budget calculations for this day are not representative of the event since they were made for a twelve-hour filter sample that ended at the time of the event.

5.6.5 08/21/95–08/27/95 Period

The period from 08/21/95 through 08/24/95 was chosen to examine b_{sp} events that occurred under moist conditions when SO_2 was present. The rest of the period was modeled to examine a relatively clean period. The 08/21/95-08/24/95 period was generally cloudy and humid, with periods of slightly reduced humidity at Buffalo Pass in midday. Although the generating station plumes were not emitted into fog during the nights and mornings, conditions were quite humid at night; and the plumes were probably mixed into clouds during the day.

SO_2 was present along with daytime increases in the TSI b_{sp} on 08/21/95 and 08/23/95. Clouds were present above Storm Peak in both cases, but there were long views underneath. On both days, haze was clearly visible in the videos from Storm Peak and became noticeably worse at the time of the event. The continuous Buffalo Pass data for this period are shown in Figure 5.6.7.

The synoptic pattern during this period was dominated by a large ridge aloft that produced hot, muggy weather over the region. Aloft winds were generally from the southwest to the northwest, but varied from day to day, as weak weather systems migrated through the region. The 08/21/95 through 08/24/95 period had higher humidities and afternoon cumulus clouds as the southwesterly winds transported moisture-laden air into the region from Mexico (see Figure 5.6.1). On 08/21/95, skies were generally broken to overcast with thunderstorms occurring in the late afternoon. Winds aloft were southwesterly during the morning, but became light and variable during the afternoon. By 08/23/95, morning clouds led to overcast skies and rain showers by afternoon; aloft winds were southwesterly for the entire day. By 08/27/95, the humidity had decreased as aloft northwesterly winds ahead of an upper-level trough brought drier air into the region. An easterly drainage flow was observed during each night and morning.

Figure 5.6.7 Hourly b_{sp}, SO_2, black carbon, and RH at Buffalo Pass for 08/21/95–08/27/95.

5.6.5.1 08/21/95, 1600-1800 MST Event

Buffalo Pass SO_2 rose to ~0.7 ppb and the black carbon increased to ~0.25 $\mu g/m^3$. The local back-trajectory (Figure 5.6.8) is consistent with accumulation of emissions in the Yampa Valley in the morning and transport to the Wilderness area in the afternoon. The

agreement between measured and modeled SO_2 in Figure 5.6.7 supports the trajectory analysis. From the trajectory, it is likely that higher concentrations of Valley emissions were transported north of Buffalo Pass.

Figure 5.6.8 Constant altitude and "plume following" back-trajectories from Buffalo Pass on 08/21/95 at 1700 MST.

The extinction budget calculations for the afternoon six-hour period attributed roughly 31% of the ambient extinction to clean air scattering, 29% to ammonium sulfate, 34% to carbon compounds, 2% to ammonium nitrate, and 4% to soil. The soluble potassium concentration for the afternoon sample was 23 ng/m^3, indicating some contribution from fires; while the selenium concentration was 0.2 ng/m^3 with an uncertainty of 0.1 ng/m^3. B_{sp} levels at the other nephelometer sites on this afternoon were similar to those at Buffalo Pass, but the afternoon Buffalo Pass sulfate concentration (without ammonium – some ammonium data are missing) was higher than at the "upwind" monitor at Juniper Peak (1.8 μg/m^3 vs. 1.3 μg/m^3).

Although much of the haze on this day is clearly regional, the data are consistent with a minor contribution to the Buffalo Pass b_{sp} peak from generating station emissions due to sulfate formation in clouds. This is supported by the trajectories, the coincidence of measured and modeled SO_2 with b_{sp}, the increase (38%) in sulfate above the regional background, the increase in selenium, and the presence of clouds.

5.6.5.2 08/23/95, 1300 MST Event

During this event, the ambient b_{sp} exceeded 50 Mm^{-1}, and the TSI (dry) b_{sp} peaked at about 20 Mm^{-1}. The peaks were sharp and accompanied by a sharp increase in the SO_2 from about 0.7 to 2.7 ppb, and a rise in the black carbon reading from about 0.1 to 0.2 μg/m^3. The event was accompanied by a dramatic increase in haze in the Storm Peak video. During the event, cloud levels were just above the heights of Storm Peak and Buffalo Pass.

As on 08/21/95, the local back-trajectory (Figure 5.6.9) is consistent with accumulation of emissions in the Valley in the morning and transport to the Wilderness area in the afternoon. From the trajectory, it is likely that higher concentrations of Valley emissions were transported north of Buffalo Pass. It is also possible that valley emissions would have interacted with clouds on the way to Buffalo Pass.

Figure 5.6.9 Constant altitude and "plume following" back-trajectories from Buffalo Pass on 08/23/95 at 1300 MST.

The haze event on this day was also detected at lower altitude by the Chavez Mountain video cameras. In those views, the haze appears to travel toward Storm Peak from southwest of the camera site which is southeast of Hayden. It is unclear how Yampa Valley emissions would have gotten to that location, but the SO_2 accompanying the b_{sp} peak should be a good indicator for Yampa Valley generating station emissions.

The extinction budget calculations for the afternoon six-hour period attributed ~22% of the ambient extinction to clean air scattering, 32% to ammonium sulfate, 31% to carbon compounds, 2% to ammonium nitrate, and 12% to soil. The soluble potassium concentration for the afternoon sample was 16 ng/m^3, indicating a relatively small contribution from fires compared to most other events studied, while the selenium concentration was 0.5 ng/m^3 with

an uncertainty of 0.1 ng/m^3, the highest value seen on any of the event days. B_{sp} levels at the other nephelometer sites on this afternoon were similar to the background concentration at Buffalo Pass before the peak (about 10 Mm^{-1}), indicating that the regional haze component was about half the peak value, and the other half was a local contribution.

Although about half of the Buffalo Pass haze event on this day might be regional, the data are consistent with a significant, and possibly large, contribution to the Buffalo Pass peak b_{sp} from generating station emissions.

5.6.6 09/27/95 Period and 1900 MST Event

This event was selected for analysis because it was one of the few times that the Buffalo Pass b_{sp} increased coincident with an increase in SO_2 under dry conditions. The relative humidity was below 75% all day at Buffalo Pass and below 50% all afternoon. Hourly Buffalo Pass measurements are presented in Figure 5.6.10.

Figure 5.6.10 Hourly b_{sp}, SO_2, black carbon, and RH at Buffalo Pass for 09/27/95.

Synoptic weather conditions on 09/27/95 were dominated by a weak upper-level ridge moving through the western United States. Aloft winds during this modeling period were west-southwesterly and generally 5 to 7 m/s stronger than during the modeling periods in August and mid-September. A drainage flow was observed in the morning, but during the afternoon low-level winds (i.e., below about 500 m AGL) were strong (10 m/s). Scattered clouds during the morning thickened by afternoon, but no precipitation was measured. The local back-trajectory analysis crosses the Yampa Valley in the afternoon under steady winds, with no possibility of accumulation due to recirculation in the valley. It is likely, however, that Yampa Valley generating station emissions were transported directly to Buffalo Pass under dry conditions. The regional 48-hour back-trajectory originates in southern California.

During this event, the b_{sp} (both ambient and dry) increased from about 8 to 15 Mm^{-1}, and the SO_2 increased from about 0.5 to 3.5 ppb. A similar b_{sp} spike was seen at all the other nephelometer sites at around the same time. A regional haze increase was noticeable on the Yampa Valley video from Storm Peak and on the Hayden video from Chavez Mountain. In addition to the regional haze, there were frequent noticeable emissions from the Hayden generating station on this afternoon. However, they were emitted in high winds.

The extinction budget calculations for the afternoon six-hour period attribute ~56% of the ambient extinction to clean air scattering, 21% to ammonium sulfate, 17% to carbon compounds, 2% to ammonium nitrate, and 3% to soil. Most of the event, however, occurred after the end of the afternoon sample.

On the same afternoon, the largest increase in b_{sp} was seen at the Hayden Waste Water site, increasing from about 10 to 40 Mm^{-1} and starting earlier in the afternoon than at the other sites. At this site, the selenium in the afternoon sample was undetectable, but the soluble potassium was 58 ng/m^3, which was one of the highest levels seen at the site, indicating burning in or near the Valley. Fires of 0.6 and 0.5 km^2 were reported ~50 km west of Craig on 09/27/95, but it is possible that one was closer.

Although the Buffalo Pass b_{sp} peak was accompanied by SO_2, the SO_2 would have been transported directly from the Valley to the monitor under dry conditions with minimal time to react. The noticeable primary emissions from the Hayden station would also have been transported, but these would have been highly diluted. Although it is possible that the generating stations contributed significantly to the peak b_{sp}, it is more likely that the peak was due to burning somewhere in the region, superimposed on regional haze and transported over the Yampa Valley generating stations in the afternoon.

6.0 SOURCE CONTRIBUTIONS TO LIGHT EXTINCTION

The final technical objective of determining how much different sources and groups of sources contribute to light extinction and perceptible haze in the Wilderness is addressed in this section. Different models are described and applied. This section emphasizes the results of modeling rather than modeling processes, assumptions, and evaluation, which are explained in Appendix B. Uncertainties and limitations of each model, both those found in this study and in prior studies, are recognized as part of the source apportionment process.

6.1 General Modeling Approach

Every model is a simplification of reality. This is especially true for models related to atmospheric pollution, in which complex and random phenomena are simulated by relatively crude mathematical formulations. Even the most complex mathematical models that attempt to incorporate all chemical and physical phenomena contain substantial deviations from the reality of most pollution situations. Even if they accurately contained all of the relevant physics and chemistry, they would still be limited by the inability to measure all of the relevant variables in space in time.

Watson *et al.* (1995) considered several modeling approaches, including air quality models with complex representations of meteorology and aerosol transformation chemistry. These complex models were found to be promising, but they were still in a rapidly evolving state of research. They were incompatible with the MZVS objective of using "established methods and procedures" to determine the causes of haze.

Recognizing that no single model could be used to attain study objectives, the MZVS applied a variety of models that were available in the public domain at the end of 1995. These models were applied to understand as well as to quantify the causes of haze in and near the Mt. Zirkel Wilderness Area. Where a computer code was modified or created to implement a model, the changes were made to simplify the input, output, and operation of the model rather than to modify its physics and chemistry. The modified codes are part of the project data base. Model options are explicitly stated and justified. Appendix B documents and explains many of these choices, reports the results of previously published sensitivity tests where they exist, and reports additional sensitivity tests conducted as part of the MZVS. Many additional tests are desirable, but were impractical with MZVS resources. The provision of models and input data allow critics to assess for themselves the effects of different model configurations on MZVS results and conclusions, and to objectively communicate these differences in separate reports.

The models applied were: 1) the Grand Canyon Visibility Transport Commission Emissions Model (GCVTCEM, Dickson *et al.*, 1995); 2) the Aerosol Evolution Model (AEM, Robinson and Whitbeck, 1985) with Calvert and Stockwell (1983) gas-to-particle conversions as implemented by Seigneur (1987) and equilibrium calculations as implemented by the Simulating Composition of Atmospheric Particles at Equilibrium (SCAPE, Kim *et al.*, 1993a, 1993b); 3) the Chemical Mass Balance source apportionment receptor model (CMB, Watson *et al.*, 1984, 1990, 1991); 4) the

Elastic Light Scattering Interactive Efficiencies (ELSIE) (Sloane *et al.*, 1991; Lowenthal *et al.*, 1995) light extinction model; 5) the CALMET diagnostic meteorological model (U.S. EPA, 1995a); the CALPUFF dispersion and chemical transformation source apportionment model (U.S. EPA, 1995b); 6) the deciview perceptibility model (Malm and Pitchford, 1994); and 7) the contrast transmittance perceptibility model (Richards, 1990). The CMB and CALPUFF source apportionment models were applied independently so that their results could be compared without one biasing the other. In several cases, the results of one model fed into another model by means that are described below. Each researcher was given the conceptual model explained in Section 5 to provide guidance in the selection of model parameters and options.

Modeling for the MZVS followed an eight-step approach. First, emissions rates are examined to determine which sources were likely or unlikely to be important contributors. Watson *et al.* (1995) recognized the potential of episodic emissions such as fires to be large but intermittent contributors, and the size and locations of most fires were compiled for the study period. Several emissions sources, such as geothermal hot springs and residential coal combustion, were thought to be negligible sulfur emitters compared to other sources, but there was no proof of this prior to the study; the MZVS confirmed these assumptions. Watson *et al.* (1995) recognized that most emissions rate models are inaccurate, so the emphasis was placed on knowing where and when emissions occurred with order of magnitude estimates of their intensities. With the exception of sulfur dioxide emissions from Yampa Valley coal-fired generating stations, which were accurately quantified by continuous emissions monitors throughout the study period (Section 5.3), other emissions were estimated from data bases that were not concurrent with the study period. Though the locations and sizes of fires were determined, only order-of-magnitude emission factors were applied.

Second, chemical profiles for major emitters are examined; these were measured as part of the MZVS. The profiles show which emissions contain the major components that cause light extinction: organic carbon, sulfate, ammonium, elemental carbon, nitrate, and geological elements. They also establish relationships between fine particle and sulfur dioxide emissions that are needed to estimate contributions to secondary ammonium sulfate. Isotopic ratios of sulfur emissions from local coal-fired generating stations, motor vehicle exhaust, hot springs, residential coal combustion, residential wood combustion, and background air were compared. Significant differences were found for some sources, but not between sulfur in generating station emissions and that found in background air.

Third, changes in profiles are estimated via an aerosol evolution model that applies established physical and chemical mechanisms to estimate conversions of sulfur dioxide to sulfate in generating station profiles for examples of dry and moist conditions found during the study. These simulations for MZVS conditions confirm the general findings from other studies; sulfur dioxide to sulfate conversion is rapid when generating station plumes pass through fogs or clouds, but nonaqueous transformations are negligible for the transport times found during the study period for air movement from the Yampa Valley to the Wilderness.

Fourth, the Chemical Mass Balance (CMB) receptor model is applied to analyzed samples at each site for the episodes specified in Sections 3.4 and 4.4 using primary source profiles and generating station profiles adjusted for aging by the aerosol evolution model. This modeling results in apportionment of measured organic carbon, elemental carbon, and elements to primary emitters, secondary ammonium sulfate to Yampa Valley generating stations and regional sources, and secondary ammonium nitrate to unnamed sources. Since ammonium nitrate and geological material were minor contributors to extinction, additional efforts to subdivide these categories were not expended. Fires and vehicle exhaust were the major contributors to organic and elemental carbon and the extinction derived from these sources. Fires were the largest contributors when extinction was high. Since specific organic compounds were not measured in MZVS, contributions from secondary organic carbon that might be determined by nitro-PAH (polycyclic aromatic hydrocarbon) measurements, and meat cooking contributions that might be determined by cholesterol measurements are absorbed into the fire and vehicle contributions. These are believed to provide minor biases in the apportionment, within the uncertainties of the source contribution estimates. Contributions to $PM_{2.5}$ primary particles and sulfate from coal-fired power generators were often determined, but they were only large enough to cause detectable changes in light extinction when a profile that was partially aged by the aerosol evolution model in fogs was used. Fully-reacted profiles were inconsistent with the ambient aerosol measurements. Sulfur isotope ratios measured at Buffalo Pass were consistent with those found in background air and in coal-fired generating station emissions, but they did not show a definitive contribution to sulfur from the nearby Hayden and Craig stations.

Fifth, the effects of Yampa Valley generating stations on light extinction at Buffalo Pass is independently inferred from simultaneous changes in light scattering and sulfur dioxide concentrations from August through October 1995. This analysis assumes that gaseous sulfur dioxide accompanies primary and secondary sulfate particles from nearby coal-fired generators. These results are consistent with those of the aerosol evolution model, showing that negligible changes in extinction occurred when generating station plumes reached the Wilderness under dry conditions, but that significant and large changes in scattering occurred when there was evidence of plumes encountering fogs or clouds.

Sixth, the CALMET and CALPUFF models are applied to all source emission rates from the inventory for five of the episodes described in Sections 3.4 and 4.3: 08/07/95–08/09/95, 08/21/95–08/27/95, 09/17/95–09/21/95, 10/07/95–10/14/95, and 10/16/95–10/19/95. CALPUFF contains a chemical transformation mechanism appropriate for dry conversion of sulfur dioxide to sulfate, but it does not have an explicit mechanism for conversion in fogs or clouds. Therefore, absolute agreement with measured secondary sulfate is not sought or expected. If it is assumed that sulfur dioxide emissions from all five Yampa Valley power generation units experience similar conversions, CALPUFF provides a good estimate of the relative contribution from each unit. Though fire emission rates are not well-quantified, their times and locations are. Semiquantitative comparisons with CMB model results can be made. Relative contributions from individual Yampa Valley sources, specifically the five coal-fired power generation units, are estimated by these models.

Seventh, CALPUFF estimates of source contributions along selected sight paths are used to estimate the effects of contributions to light extinction on the perceived haze along these sight paths. Both the deciview and contrast transmittance models are applied to estimate these changes.

Finally, the effects of reductions in sulfate on ammonium nitrate concentrations are estimated with the AEM/SCAPE model for samples at Buffalo Pass, Juniper Mountain, and Hayden VOR that acquired total nitrate and ammonia measurements during intensive operating periods. The purpose of this step is to determine whether or not reductions in sulfate would free up enough ammonia to negate improvements in visibility by increasing ammonium nitrate particles. These calculations show that ammonium nitrate concentrations would not increase with reductions in sulfate for the conditions encountered during the study period.

6.2 Emissions Rate Estimates

The Grand Canyon Visibility Transport Commission (GCVTC) emissions model, and the inventory that resulted from it (Dickson *et al.*, 1995), were used as a basis for estimating primary particle emissions of $PM_{2.5}$ organic carbon, elemental carbon, and other (primarily crustal) materials for the modeling region in Figure 2.1.3. Emissions of gaseous sulfur dioxide, oxides of nitrogen, ammonia, and volatile organic compounds (VOCs) were included in the model since these are precursors of secondary aerosol. The activity information upon which the GCVTC emission rate estimates are based was compiled for 1990, with some updates from the U.S. EPA (1994) trends inventory for fugitive dust and point sources that are applicable to 1991 and 1992.

In the mesoscale domain of Figure 2.1.1, primary particle emissions were estimated during 1993 for the Steamboat Springs PM_{10} nonattainment area (Reddy, 1995). Fire activities and operating schedules for the Yampa Valley generating stations are current for the 1995 study period. It is assumed that emissions locations, times, and magnitudes have not significantly changed between 1990 and the 1995 study period. Special surveys of sulfur emissions from geothermal hot springs, residential coal combustion, and motor vehicles, ammonia from livestock and agricultural operations, and primary particles from residential wood combustion were conducted for the Yampa Valley as part of emissions characterization. Detailed description of emissions modeling methods, results, and outputs are in Appendix B.1.

6.2.1 Regional-Scale and Mesoscale Emissions Rates

Tables 6.2.1 and 6.2.2 show the distribution of emissions by source type for winter and summer conditions in the regional-scale domain. Several observations are presented below. Coal-fired power generators are the major SO_2 emitters in the regional-scale domain, accounting for 53% of emissions during the summer. Similar contributions also occur in the winter. Other significant SO_2 emitters include industrial and commercial fuel combustion (20%), petroleum refining and chemical manufacturing (8%), and copper smelting (7%).

Table 6.2.1
Summer Emissions Rates for the Regional-Scale Domain (tons/day)

Sector 1 Code and Description	SO_X	NO_X	$PM_{2.5}$	$EC_{2.5}$	$OC_{2.5}$	VOC	Biogenics	CO	NH_3
01 UTILITY COAL COMBUSTION	521	666	10			4		74	0
02 INDUSTRIAL & COMMERCIAL FUEL COMBUSTION	197	408	7	0	0	43		75	1
03 COPPER SMELTERS	72	0	2					0	
04 RESIDENTIAL FUEL COMBUSTION	1	13	7	1	4	3		38	0
05 SOLVENT USE	0	0	0	0	0	342			
06 PETRO AND OTHER CHEMICALS	75	19	3	0	0	449		15	4
07 MOBILE SOURCES	54	675	341	21	46	574		4,874	0
08 MANUFACTURING	29	26	20	0	1	2		5	
09 PRESCRIBED AND NATURAL BURNING	0	2	21	1	4	12		41	179
10 NATURAL SOURCES			3		0		8,491		24
11 MISCELLANEOUS	29	24	253	0	2	21		210	20
99 UNSPECIFIED SOURCES			70	10	16	0			322

Table 6.2.1
Summer Emissions Rates for the Regional-Scale Domain (tons/day)

Region Total	978	1,834	736	34	73	1,450	8,491	5,332	549

Table 6.2.2
Winter Emissions for the Regional-Scale Domain (tons/day)

Sector 1 Code and Description	SO_X	NO_X	$PM_{2.5}$	$EC_{2.5}$	$OC_{2.5}$	VOC	Biogenics	CO	NH_3
01 UTILITY COAL COMBUSTION	479	634	9			4		71	0
02 INDUSTRIAL & COMMERCIAL FUEL COMBUSTION	207	430	8	0	0	44		82	1
03 COPPER SMELTERS	72	0	2					0	
04 RESIDENTIAL FUEL COMBUSTION	8	37	79	9	38	32		420	0
05 SOLVENT USE	0	0	0	0	0	286			
06 PETRO AND OTHER CHEMICALS	75	20	3	0	0	431		16	4
07 MOBILE SOURCES	54	709	286	21	46	486		5,823	0
08 MANUFACTURING	25	21	17	0	1	2		5	
09 PRESCRIBED AND NATURAL BURNING	0	2	16	1	3	12		40	105
10 NATURAL SOURCES			3		0		242		
11 MISCELLANEOUS	29	23	232	0	2	18		205	14
99 UNSPECIFIED SOURCES			70	10	16	0			193

Table 6.2.2
Winter Emissions for the Regional-Scale Domain (tons/day)

Region Total	949	1,876	725	41	107	1,315	242	6,662	317

Table 6.2.3
Summer Emissions for the Mesoscale Domain (tons/day)

Sector 1 Code and Description		SO_X	NO_X	$PM_{2.5}$	$EC_{2.5}$	$OC_{2.5}$	VOC	Biogenics	CO	NH_3
01	UTILITY COAL COMBUSTION	62	74	0.7			1		4	
02	INDUSTRIAL & COMMERCIAL FUEL COMBUSTION	0	3	0.1	0.0		0		1	
03	COPPER SMELTERS									
04	RESIDENTIAL FUEL COMBUSTION	0	0	0.1	0.0	0.1	0		1	
05	SOLVENT USE						2			
06	PETRO AND OTHER CHEMICALS						4			
07	MOBILE SOURCES	1	10	8.6	0.2	0.5	7		58	
08	MANUFACTURING			3.8	0.1	0.2				
09	PRESCRIBED AND NATURAL BURNING		0	0.4	0.0	0.1	0		0	6
10	NATURAL SOURCES			0.0				682		18
11	MISCELLANEOUS	0	0	7.1	0.1	0.3	0		3	8
99	UNSPECIFIED SOURCES			1.3	0.4	0.3				9
Region Total		62	87	22	1	1	13	131	67	42

Table 6.2.4
Winter Emissions for the Mesoscale Domain (tons/day)

Sector 1 Code and Description	SO_X	NO_X	$PM_{2.5}$	$EC_{2.5}$	$OC_{2.5}$	VOC	Biogenics	CO	NH_3
01 UTILITY COAL COMBUSTION	63	73	0.8			1		5	
02 INDUSTRIAL & COMMERCIAL FUEL COMBUSTION	0	4	0.1	0.0		0		1	
03 COPPER SMELTERS									
04 RESIDENTIAL FUEL COMBUSTION	0	0	1.5	0.2	0.7	1		8	
05 SOLVENT USE						1			
06 PETRO AND OTHER CHEMICALS						3			
07 MOBILE SOURCES	1	10	5.7	0.2	0.5	6		71	
08 MANUFACTURING			3.6	0.1	0.2	0			
09 PRESCRIBED AND NATURAL BURNING		0	0.3	0.0	0.0	0		0	4
10 NATURAL SOURCES			0.0				12		
11 MISCELLANEOUS	0	0	5.5	0.0	0.2	0		3	5
99 UNSPECIFIED SOURCES			1.3	0.4	0.3				6
Region Total	64	88	19	1	2	12	12	88	14

Motor vehicles account for ~46% of $PM_{2.5}$ emissions in the regional domain during the summer, with contributions distributed among vehicle exhaust, paved road dust, and unpaved road dust. Another 21% of $PM_{2.5}$ in the summer is emitted from fugitive sources, while 11% is emitted from agricultural tilling. During the winter months, residential wood and coal combustion become significant $PM_{2.5}$ sources, constituting 11% of the emissions. The majority of manmade emissions of VOC are from mobile sources (40%), oil and gas production (21%), and solvent usage (24%). Biogenic emissions from plant life dominate the VOC category, however.

Maps of regional emissions densities (Appendix B.1) show the majority of sulfur dioxide emitters to be located along the Colorado Front Range around the Denver metropolitan area on the eastern extreme of the regional domain. Several large sources are located along the Wasatch Front near Salt Lake City and Provo, UT, and in southwestern Wyoming.

Tables 6.2.3 and 6.2.4 summarize the distribution of emissions from different source types for summer and winter in the mesoscale domain. The majority of these emissions are located in the Yampa Valley portion of this domain, especially in and around the towns of Steamboat Springs, Hayden, and Craig, CO.

The Hayden and Craig coal-fired generating stations (Utility Coal Combustion in Tables 6.2.3 and 6.2.4) are the major SO_2 and NO_x emitters in the Yampa Valley, accounting for 98% and 85% of these emissions, respectively, during the summer and winter. These generating stations emit less than 5% of primary emissions during summer and winter, though Tables 5.5.1 and 5.5.2 show that deviations from these averages may occur during malfunctions. Motor vehicles account for approximately 39% of the primary $PM_{2.5}$ during the summer, with the major fraction of this originating from unpaved roads. Another 17% of $PM_{2.5}$ in the inventory is attributed to mineral product operations, while 19% is attributed to agricultural tilling. These fugitive dust emissions estimate are highly uncertain (Chow and Watson, 1994). During the winter months, primary $PM_{2.5}$ emissions from residential heating account for 8% of the total. The major fraction of manmade VOCs is attributed to mobile sources (51%), oil and gas production (19%), and solvent usage (13%).

Maps of nonpoint source emissions in the mesoscale domain (Appendix B.1) show that the majority of emissions are confined to roadways and to populated areas. This is as expected, since population densities and vehicle miles traveled on roads are used to spatially allocate these emissions.

Emissions in the mesoscale domain are a minor fraction of emissions in the regional-scale domain. For the summer estimates, ~6% of the sulfur dioxide, ~5% of the oxides of nitrogen, ~3% of the primary $PM_{2.5}$, ~3% of the elemental carbon, ~1% of the primary organic carbon, and ~8% of the ammonia emissions in the region are from the mesoscale domain.

The spatially- and temporally-averaged emissions rates in Tables 6.2.1 through 6.2.4 were compiled according to standardized procedures and provide a good starting point for the identification of potential contributors to particles that cause light extinction. They are limited, however, for the following reasons:

Meat cooking, a potentially significant primary source of organic carbon (Hildemann *et al.*, 1991), is not included in the inventory.

Several of the source categories in Tables 6.2.1 through 6.2.4 are episodic rather than continuous emitters. This is especially true for fires and fugitive dust emissions. It is also true for many industrial sources of sulfur dioxide that adjust their activities to market demand (see Section 6.3). Prescribed burns and wildfires were given special attention, as described below.

Source categories are not completely segregated. This is especially true for the mobile sources, in which particulate emissions from several vehicle types and emissions points are combined in emissions models. Construction dust estimates, for example, are based on acres under construction rather than on the individual processes involved in construction. While further disaggregation would be useful on an urban scale, the general categories are adequate to meet the MZVS objectives, and no further disaggregation was undertaken.

Many activity levels are not specific to the study period. The most important ones, Yampa Valley power generators and wildfires, were updated with 1995 estimates. Mobile source sulfur emissions were also reevaluated to account for fuel changes.

Emissions factors applied to activity data are of questionable accuracy. Except for ducted emissions, most emissions factors (U.S. EPA, 1995) used in this inventory were derived from a limited number of empirical tests, none of which were performed in the study area.

6.2.2 Emissions Surveys

Surveys (Appendix B.1) were conducted to estimate the magnitudes of Routt and Moffat county emissions of: 1) gaseous sulfur from hot springs, motor vehicle exhaust, and residential coal combustion; 2) gaseous ammonia from livestock, soil biological activity, and generating stations; and 3) primary particles from residential wood and coal heating.

Sulfur emissions from hot springs are minor compared to other sulfur emissions in the region, with less than one ton per year of hydrogen sulfide emitted in the mesoscale domain, as an upper limit. Mobile source SO_2 emissions, the majority of which derive from on-road vehicles, account for less than 1% of the emissions in Routt and Moffat counties.

A significant amount of wood and coal are consumed for home heating by some households in Routt and Moffat counties. Residential heating in the winter months constitute ~9% of primary $PM_{2.5}$ emissions. Sulfur emissions from residential coal burning are less than 1% of the total sulfur emissions in the Routt and Moffat counties during winter months. Though wood and coal are also burned during other times of the year, the quantities are substantially lower than that burned during the winter.

Livestock and soil biological activity are the predominant emission sources of ammonia in these two counties. During the winter months, however, ammonia injection used to enhance particulate matter control at the Hayden station may be one of the largest sources of ammonia in the two counties.

6.2.3 Wildfires and Prescribed Burns

Table 6.2.5 summarizes wildfires and prescribed burns that occurred during the episode periods. The locations of these fires and daily time series plots of acres burned are in Appendix B.1. A complete list of all fire locations, times, and acres burned is part of the MZVS data base.

Little wildfire activity occurred during the winter and spring. Summer was the peak burning period, with lesser activity in the fall. Within the regional domain, wildfires consumed ~207,000 acres from 03/16/95 through 08/31/95. During September and October, another 97,000 acres were burned. Only minor fire activity was recorded within the Routt National Forest during 1995. Most of the wildfires occurred southwest of the Wilderness on Bureau of Land Management lands.

For the regional domain, there were four periods from mid-June through the end of August with more than 5,000 acres of average wildfire activity per day. This was followed by more than 4,000 acres of average wildfire activity per day during the first, third, and fourth weeks of September and the third and fourth weeks of October. For the mesoscale domain, there was significant fire activity at for an eleven-day period from the end of July and through the first week of August when an average of ~450 acres per day burned. There was also a significant event on 09/16/95 with over 3,000 acres burned.

A minor amount of prescribed burning historically occurs in the spring, with the majority occurring in the fall. Prescribed burning events were obtained only for northwestern Colorado, and is a lower limit for all prescribed burning within the region. A two-day intensive prescribed burning episode occurred on 03/07/95 and 03/08/95, burning approximately 1,640 acres. Prescribed burns consumed approximately 10,400 acres during September and October. This acreage is minor in comparison to the wildfire acreage for the same time period.

The relative amount of 1995 fire activity in the mesoscale domain was minor, for most of the time, compared to fire activity in the regional domain. As shown in Table 6.2.5, the total acreage burned during the 02/23/95, 05/06/95–05/07/95, 09/30/95, and 10/01/95–10/02/95 episodes was less than five acres. The largest amount of fire activity occurred during the 09/29/95–09/31/95 period. The second largest amount of fire activity occurred during the 09/17/95–09/21/95 period.

For both of these cases, the fire activity was located

Table 6.2.5
Episodic Fire Activity in the Mt. Zirkel Wilderness Area

Episode Dates	Regional Domain Acres Burned	Mesoscale Domain Acres Burned
02/23/95	—[a]	—[a]
3/26/95 - 3/31/95	21	0
5/6/95 - 5/7/95	—[a]	—[a]
6/14/95 - 6/16/95	21,252	0
6/29/95 - 6/30/95	21	0
07/01/95	9	0
7/29/95 - 7/31/95	17,863	1,440
8/7/95 - 8/9/95	3,430	927
08/14/95	8,581	10
8/21/95 - 8/27/95	1,592	0
09/02/95	1,571	333
9/17/95 - 9/21/95	15,928	315
09/24/95	4,432	0
09/27/95	3,141	153
09/30/95	—[a]	—[a]
10/1/95 - 10/2/95	—[a]	—[a]
10/7/95 - 10/19/95	9,736	1,100
10/22/95 - 10/23/95	5,968	0

[a] The total area burned for this episode was less than five acres.

near the southwest corner of the mesoscale domain. There was major fire activity somewhere in the region during the remainder of the summer and fall episodes selected for detailed analysis.

6.3 Emissions Compositions

Chemical source profiles are the fractional mass abundances of measured chemical species relative to primary $PM_{2.5}$ mass in source emissions. Previous studies (e.g., Core and Houck, 1987; Houck *et al.*, 1989a, 1989b, 1989c, 1989d, 1989e; Chow and Watson, 1994; Watson *et al.*, 1994) have developed source profiles for geological material (e.g., paved and unpaved road dust, soil dust, storage pile), motor vehicle exhaust (e.g., diesel-, leaded-gasoline-, and unleaded-gasoline-fueled vehicles), vegetative burning (e.g., wood stoves, fireplaces, forest fires, and prescribed burning), industrial boiler emissions, and other aerosol sources. These profiles have been acquired mostly in low-altitude (<1,000 m above MSL) urban areas, and they are not specific to the MZVS.

Watson *et al.* (1995) and Bighouse and Houck (1995) describe the samples taken to represent: 1) geological material from paved and unpaved roads and open land; 2) motor vehicle exhaust from light- and heavy-duty gasoline- and diesel-fueled vehicles in the towns closest to the Wilderness; 3) residential coal- and wood-combustion chimneys; 4) simulated forest fires; 5) geothermal hot springs; and 6) four coal-fired power generation units (Units 1 and 2 at the Hayden station and Units 2 and 3 at the Craig station).

6.3.1 Source Types

Samples of residential wood and coal combustion were acquired during mid-March 1995. Samples of generating station, motor vehicle exhaust, hot springs, and forest fires were acquired during July 1995. Geological samples were acquired throughout the study period.

More than 55 $PM_{2.5}$ source samples were collected using the following specialized approaches:

Sweeping and trowling of surface dust from unpaved roads and open land in many locations, vacuuming of dust from paved roads and highways (Houck, 1991) followed by laboratory resuspension sampling of sieved soil samples using a parallel impactor sampling device (Chow *et al.*, 1994a).

Ground-based source sampling for motor vehicle exhaust, forest fires, and geothermal hot springs.

Diluted exhaust sampling for residential wood and coal combustion and coal-fired power generators.

The individual source profiles compiled for the study are assembled in the database and listed in Appendix C. These were submitted to analyses for the particulate chemical components

listed in Table 4.2.1 and gaseous sulfur dioxide (hydrogen sulfide for the hot springs). Ammonia gas was also measured along with particulate matter in generating station tests.

6.3.2 Geological Source Profiles

Twelve of the 30 samples identified by Watson *et al*. (1995) were resuspended and chemically analyzed, as specified in Table 6.3.1. These individual profiles were grouped as indicated in Table 6.3.1 to form six composite geological profiles by calculating the average and standard deviation for all chemical abundances in the designated samples.

Figure 6.3.1 shows the chemical abundances in four of these profiles. In each of the illustrations, the height of each bar indicates the average fractional abundance for the indicated chemical, while the dot shows the standard deviation of the average. When the height of the bar exceeds the position of the dot, and when the height of the bar is much higher than it is in other profiles, the corresponding species is considered as a good marker for that source type.

Though there are slight differences among these profiles, they are not sufficient to distinguish one geological subgroup from other subgroups by CMB receptor modeling. In each of these profiles, aluminum (Al), silicon (Si), potassium (K), calcium (Ca), and iron (Fe) have large abundances with low variabilities. The abundance of total potassium (K) is 15 to 30 times the abundance of soluble potassium (K^+). The abundances of aluminum (Al), potassium (K), calcium (Ca), and iron (Fe) are similar among the profiles, but the silicon (Si) abundances range from 14.4 ± 2.5% in unpaved road dust (MZUPRDC) to 20.1 ± 2.5% in paved road dust (MZPVRDC).

Lead (Pb) is most abundant (0.018 ± 0.009%) in paved road dust, and is as low as 0.004% in the other profiles. Elemental carbon (EC) abundances range from 0.1% to 3% in individual profiles (Appendix C), and are negligible (0.78 ± 0.84%) in the MZGEOLC profile. Organic carbon (OC) abundances vary among the composite paved (7.4 ± 2.2%) and unpaved (4.6 ± 2.2%) road dust samples, with similar abundances between the composite soil dust (6.1 ± 2.6%) and geological (6.5 ± 2.5%) profiles. The organic-to-total-carbon (sum of organic and elemental carbon), OC/TC, ratios are similar among samples with an average ratio of 0.90. The effect of motor vehicle emissions (e.g., brake and tire wear, oil drips) could result in greater abundances of Pb, EC, and OC in these source profiles. Soluble ions such as sulfate ($SO_4^=$) nitrate (NO_3^-) and ammonium (NH_4^+) are generally low, in the range of 0 to 0.3%. Elemental sodium (Na) and chloride (Cl^-) are also low, with less than 0.5% in abundance. The effect of road sanding and salting on soil composition may not be significant.

These source compositions are similar to paved road dust profiles from Denver, CO (Watson *et al.*, 1988a, 1988b, 1988c). Previous source apportionment studies (e.g., Chow *et al.*, 1992; Watson *et al.*, 1994) show that the chemical abundances and variabilities shown in Figure 6.3.1 are sufficient to separate geological contributions from other source types, but they are insufficient to distinguish paved road, unpaved road, and native soil compositions from each other.

Table 6.3.1
Composite Geological Source Profiles
Calculated for the Mt. Zirkel Visibility Study

Mnemonic	Description	Samples Included in Composite
MZCPVRDC	Paved road dust collected near vehicle exhaust sampling locations in the town of Craig, CO.	MZC1PVRD (Craig A) (REST329) MZC2PVRD (Craig B) (REST324) MZC3PVRD (Craig C) (REST325)
MZSPVRDC	Paved road dust collected near vehicle exhaust sampling locations in the town of Steamboat Springs, CO.	MZS1PVRD (Steamboat A) (REST326) MZS2PVRD (Steamboat B) (REST327) MZS3PVRD (Steamboat C) (REST328)
MZPVRDC	Composite of all 6 paved road dust samples (3 from Craig and 3 from Steamboat Springs, CO).	MZC1PVRD MZC2PVRD MZC3PVRD MZS1PVRD MZS2PVRD MZS3PVRD
MZUPRDC	Unpaved road dust from the Buffalo Pass (BP) and Hayden VOR (HV) access roads.	MZBPUPRD (BP access road) (REST358) MZHVUPRD (HV access road) (REST357)
MZSOILC	Soils in the vicinity of Buffalo Pass (BP), Juniper Mountain (JU), Baggs (BB), and Hayden Waste Water (HS) receptor sites.	MZBPSOIL (BP site) (REST359) MZJUSOIL (JU site) (REST360) MZBBSOIL (BB site) (REST362) MZHSSOIL (HS site) (REST361)
MZGEOLC	Composite of all 12 geological samples (6 paved road dust, 2 unpaved road dust, and 4 soil samples).	MZC1PVRD MZBPUPRD MZC2PVRD MZHVUPRD MZC3PVRD MZBPSOIL MZS1PVRD MZJUSOIL MZS2PVRD MZBBSOIL MZS3PVRD MZHSSOIL

Table 6.3.2
Composite Motor Vehicle Source Profiles
Calculated for the Mt. Zirkel Visibility Study

Mnemonic	Description	Samples Included in Composite
MZMVCG1C	Early morning (0800-0900 MST) samples collected at the intersection of Victory Way and Ranney Avenue, Craig, CO.	MZMVCGA (EXST001) MZMVCGB (EXST002) MZMVCGC (EXST003)
MZMVCG2C	Morning (0900-1300 MST) samples collected at the intersection of Victory Way and Ranney Avenue, Craig, CO.	MZMVCGD (EXST004) MZMVCGE (EXST005) MZMVCGF (EXST006)
MZMVCG3C	Afternoon (1400-1800 MST) samples collected at the intersection of Victory Way and Ranney Avenue, Craig, CO.	MZMVCGG (EXST007) MZMVCGH (EXST008) MZMVCGI (EXST009)
MZMVCGC	Composite of all nine early morning, morning, and afternoon samples.	MZMVCGA MZMVCGF MZMVCGB MZMVCGG MZMVCGC MZMVCGH MZMVCGD MZMVCGI MZMVCGE
MZMVSBC	Morning (0800-1200 MST) samples collected at the intersection of Highway 40 and Elk River Road, Steamboat Springs, CO.	MZMVSBA (EXST012) MZMVSBB (EXST013) MZMVSBD (EXST014)
MZMVC	Composite of all 9 Craig and 3 Steamboat Springs samples.	MZMVCGA MZMVCGG MZMVCGB MZMVCGH MZMVCGC MZMVCGI MZMVCGD MZMVSBA MZMVCGE MZMVSBB MZMVCGF MZMVSBD

Table 6.3.3
Composite Residential Wood and Coal Combustion Source Profiles
Calculated for the Mt. Zirkel Visibility Study

Mnemonic	Description	Samples Included in Composite
MZRWCC	Fireplace and stove burning lodgepole pine, spruce/aspen, spruce/firewood.	MZRWC1 (MZST004)
	Fireplace and stove burning lodgepole pine.	MZRWC2 (MZST006)
	Stove burning lodgepole pine and spruce.	MZRWC3 (MZST010)
MZRCCC	Stove burning coal from Trapper Mine.	MZRCC1 (MZST002) MZRCC2 (MZST003)
	Fireplace and stove burning coal from Seneca Mine.	MZRCC3 (MZST008) MZRCC4 (MZST012)

Table 6.3.4
Composite Forest Fire Emissions Source Profiles
Calculated for the Mt. Zirkel Visibility Study

Mnemonic	Description	Samples Included in Composite
MZFFIREC	Pinyon-Juniper range fire five miles north of Dinosaur, CO (5-minute sampling duration).	MZFFIRE1 (PJST001)
	Pinyon-Juniper range fire five miles north of Dinosaur, CO (2-minute sampling duration).	MZFFIRE2 (PJST002)
	Pinyon-Juniper range fire five miles north of Dinosaur, CO (1.5-minute sampling duration).	MZFFIRE3 (PJST003)
	Pinyon-Juniper range fire five miles north of Dinosaur, CO (8-minute sampling duration).	MZFFIRE4 (PJST004)

Table 6.3.5
Composite Geothermal Springs Emissions Source Profiles
Calculated for the Mt. Zirkel Visibility Study

Mnemonic	Description	Samples Included in Composite
MZGSC	Integrated sampling of emissions from Lithia, Iron, Sulfur, Black Sulfur, and Steamboat Springs (75-minute sampling duration).	MZGS1 (GTST001)
	Integrated sampling of emissions from Lithia, Iron, Sulfur, Black Sulfur, and Steamboat Springs (150-minute sampling duration).	MZGS2 (GTST002)
	Integrated sampling of emissions from Lithia, Iron, Sulfur, Black Sulfur, and Steamboat Springs (300-minute sampling duration).	MZGS3 (GTST003)
MZGS2C	Integrated sampling of emissions from Lithia, Iron, Sulfur, Black Sulfur, and Steamboat Springs (150-minute sampling duration).	MZGS2 (GTST002)
	Integrated sampling of emissions from Lithia, Iron, Sulfur, Black Sulfur, and Steamboat Springs (300-minute sampling duration).	MZGS3 (GTST003)

Table 6.3.6
Composite Coal-Fired Boiler Emissions Source Profiles
Calculated for the Mt. Zirkel Visibility Study

Mnemonic	Description	Samples Included in Composite
MZCG2PPC	Composite of four Craig Unit 2 profiles. System is fueled by coal from Trapper Mine and is equipped with limestone wet scrubber and electrostatic precipitator.	MZCG2PP1 (PPST001) MZCG2PP2 (PPST002) MZCG2PP3 (PPST003) MZCG2PP4 (PPST004)
MZCG3PPC	Composite of three Craig Unit 3 profiles. System is fueled by coal from Colowyo Mine and is equipped with dry lime scrubber and fabric baghouse.	MZCG3PP1 (PPST005) MZCG3PP2 (PPST006) MZCG3PP3 (PPST007)
MZCGPPC	Composite of four Craig Unit 2 and three Craig Unit 3 profiles.	MZCG2PP1 MZCG2PP2 MZCG2PP3 MZCG2PP4 MZCG3PP1 MZCG3PP2 MZCG3PP3
MZHD2PPC	Composite of two Hayden Unit 2 profiles.	MZHD2PP1 (PPST013, PPSQ013) MZHD2PP2 (PPST014, PPSQ011)
MZHDPPC	Composite of one Hayden Unit 1 and two Hayden Unit 2 profiles. System is fueled by coal from Seneca Mine and is equipped with ammonia injection and electrostatic precipitator.	MZHD1PP1 (PPST010, PPSQ014) MZHD2PP1 MZHD2PP2
MZPPC	Composite of four Craig Unit 2, three Craig Unit 3, two Hayden Unit 2, and one Hayden Unit 1 profiles	MZCG2PP1 MZCG3PP2 MZCG2PP2 MZCG3PP3 MZCG2PP3 MZHD2PP1 MZCG2PP4 MZHD2PP2 MZCG3PP1 MZHD1PP1

Table 6.3.7
Composite Regional Emissions Source Profiles
Calculated for the Mt. Zirkel Visibility Study

Mnemonic	Description	Samples Included in Composite	
MZBBRC	Composite of 6 regional background samples from the Baggs site.	BBFT090	(08/08/95 1200 MST)
		BBFT158	(09/20/95 0600 MST)
		BBFT159	(09/20/95 1200 MST)
		BBFT160	(09/21/95 0600 MST)
		BBFT168	(09/24/95 1200 MST)
		BBFT181	(09/30/95 1200 MST)
MZJURC	Composite of 5 regional background samples from the Juniper Mountain site.	JUFT228	(08/08/95 1200 MST)
		JUFT256	(08/21/95 0600 MST)
		JUFT257	(08/21/95 1200 MST)
		JUFT259	(08/22/95 0600 MST)
		JUFT323	(09/27/95 0600 MST)
MZRC	Composite of 6 regional background samples from the Baggs site and 5 regional background samples from the Juniper Mountain site.	BBFT090	(08/08/95 1200 MST)
		BBFT158	(09/20/95 0600 MST)
		BBFT159	(09/20/95 1200 MST)
		BBFT160	(09/21/95 0600 MST)
		BBFT168	(09/24/95 1200 MST)
		BBFT181	(09/30/95 1200 MST)
		JUFT228	(08/08/95 1200 MST)
		JUFT256	(08/21/95 0600 MST)
		JUFT257	(08/21/95 1200 MST)
		JUFT259	(08/22/95 0600 MST)
		JUFT323	(09/27/95 0600 MST)

Figure 6.3.1 Geological material source profiles derived for the Mt. Zirkel Visibility Study.

6.3.3 Motor Vehicle Exhaust

Mobile source particulate emissions are among the most difficult to measure with respect to emission rates and chemical composition. This difficulty arises from: 1) different mobile source types (e.g., passenger cars, light-duty gasoline-fueled trucks, heavy-duty diesel-fueled trucks, diesel buses); 2) inadequate characterization of the high emitters within the motor vehicle fleet; 3) a large number of individual emitters within each mobile source subcategory; 4) yearly changes in fuel composition and emission control technology; 5) undefined operating conditions; 6) several emission points on each vehicle (i.e., tailpipe, fuel evaporation, tire wear, brake wear, resuspended dust); and 7) a mixture of primary particles, semivolatile compounds, and secondary particle precursors.

To obtain a representation of all of these variables for conditions in the Yampa Valley, fifteen samples with durations ranging from one to four hours were obtained between 07/17/95 and 07/22/95 during morning (0800-1200 MST) and afternoon (1300-1600 MST) hours at intersections in Craig and Steamboat Springs, CO (Bighouse and Houck, 1995), and specified in Table 6.3.2.

Though dominated by motor vehicle emissions, roadside samples also contain suspended road dust and particles from other sources in the background air. These samples are likely to be affected by vehicle-related resuspended road dust. The geological contribution was minimized by using a $PM_{2.5}$ inlet on the sampling system to remove coarse particles. The remaining geological contribution was removed from each sample by applying the CMB model with Al, Si, K, and Ca as fitting species for the MZGEOLC profile, then subtracting the calculated geological contribution from each chemical species and the measured mass. Ammonium and nitrate were also used as CMB fitting species with secondary ammonium nitrate and sulfate as sources to remove background concentrations of secondary aerosol from these samples. Individual motor vehicle exhaust profiles were calculated based on the remaining concentrations of mass and chemical species, as specified in Table 6.3.2.

Traffic counts (Bighouse and Houck, 1995) were taken during roadside sampling periods for ten minutes out of each hour of the sampling interval to allow differences in vehicle mixtures to be determined. Motor vehicle counts are provided for the following five categories: 1) passenger cars; 2) light-duty gasoline trucks; 3) heavy-duty diesel trucks; 4) commuter buses; and 5) motorcycles. The average traffic count ranged from 500 to 1,200 vehicles per hour; and more than 95% of the vehicles were fueled by gasoline.

Figure 6.3.2 Motor vehicle emission source profiles derived for the Mt. Zirkel Visibility Study.

In Table 6.3.2, profiles MZMVCGC and MZMVSBC represent motor vehicle emissions at Craig and Steamboat Springs, respectively, and the MZMVC abundances are the averages and standard deviations for twelve of the individual motor vehicle profiles. Figure 6.3.2 shows these profiles.

Organic carbon (OC) and elemental carbon (EC) are the most abundant species in motor vehicle exhaust, accounting for over 95% of the total mass. OC abundances in the Table 6.3.2 profiles range from 36.1 ± 29.0% (MZMVSBB) to 69.5 ± 17.2% (MZMVCG3C). Organic-to-total-carbon (TC) ratios range from 0.40 for the MZMVSBC profile to 0.71 for the MZMVCG3C profile, with an average ratio of 0.58 (MZMVC). Watson *et al.* (1994) reported OC/TC ratios of 0.69 for gasoline-fueled vehicle exhaust (PHAUTO), 0.55 for diesel-fueled vehicle exhaust (PHDIES), and 0.52 for a mixture of vehicle types in roadside tests (PHRD) in Phoenix, AZ.

Federal Test Procedure (FTP) dynamometer tests of four closed-loop and four oxidation-catalyst vehicles in Denver, CO (Watson *et al.*, 1990) reported an OC/TC ratio of 0.39 for the cold transient cycle and 0.81 for the cold stabilized cycle. Samples from an underground bus transfer station reported an OC/TC ratio of 0.76 for diesel buses, while *in situ* samples taken from a parking garage during cold winter time (for comparison with the cold transient portion of the FTP cycle) yielded an OC/TC ratio of 0.48 (Watson *et al.*, 1990). These ratios are within one standard deviation of the MZMVC profile (OC/TC = 0.58 ± 0.15) derived from all MZVS samples.

The lead (Pb) abundance is negligible and highly variable (0.024 ± 0.036%) in the MZMVC and other profiles. The abundance of bromine (Br) is also low, in the range of 0.01% to 0.05%. Zinc (Zn) is present in most of these profiles, usually at levels of 0.05% or less. The abundance of chloride (Cl^-) is 1.5% to 3.5%.

After subtraction of ammonium sulfate, the remaining sulfate abundance is 1.5% to 5.0%. The abundance of SO_2 (as a fraction of $PM_{2.5}$ mass) ranges from 0.13 ± 0.02% in the MZMVSBC profile to 0.73 ± 0.06% in the MZMVCGC profile.

6.3.3 Residential Wood and Coal Combustion

The chemical composition of residential wood combustion (RWC) and residential coal combustion (RCC) emissions are expected to vary owing to: 1) differences in appliance types and installation factors (e.g., appliance types, catalyst/noncatalyst, damper control, airtight/nonairtight, chimney system); 2) wood and coal compositions (e.g., species/density/size, moisture content, seasoned/nonseasoned, extent of decomposition); 3) burning practices (e.g., burning rate/duration, load, frequency of fueling, kindling procedure, household trash); and 4) burn conditions (e.g., kindling/charcoal phase, cool/hot burn, damper settings) (Houck, 1991).

Sampling methods for exhaust from residential chimneys also introduce variability owing to: 1) tar-like emissions adhering to chimneys and sampler inlets; 2) low exit velocities; 3) large ranges of particle concentrations in effluents; and 4) large water vapor contents that condense upon contact with cold ambient air (Houck, 1991).

Ten samples were acquired, each one consisting of the diluted effluent from three different residential chimneys. Each chimney was sampled for 10 to 20 minutes on cold (?30 to 55 ?F) winter nights (?2100 to 2400 PST), when the atmosphere was stable and traffic volumes were low (Bighouse and Houck, 1995). Table 6.3.3 shows how the individual

samples were combined to obtain averages and standard deviations for chemical abundances in residential wood (MZRWCC) and coal (MZRCCC) combustion emissions.

As illustrated in Figure 6.3.3, the chemical abundances are notably different between wood- and coal-burning emissions, although the majority of emissions from both sources are composed of carbonaceous material. Organic carbon (OC) is the most abundant constituent, followed by elemental carbon. In these profiles, average OC abundance ranged from 51.4 ± 11.7% in RWC to 69.5 ± 19.2% in RCC, whereas EC ranged from 12.4 ± 4.2% in RWC to 26.1 ± 15.6% in RCC. Note that elemental carbon in RCC is a factor of two higher than in RWC. The OC/TC ratios are similar, however, ranging from 0.73 in RCC to 0.81 in RWC.

Figure 6.3.3 Residential wood and coal combustion source profiles derived for the Mt. Zirkel Visibility Study

The key features of the RWC profiles are that soluble potassium (K^+) is completely in a water-soluble form, exceeding an abundance of 1% in these emissions, and chloride (Cl^-) is 55% higher than those reported in RCC.

On average, the abundances of sulfate ($SO_4^=$), nitrate (NO_3^-), and silicon (Si) in RCC are a factor of four higher than those found in RWC. The abundance of ammonium (NH_4^+) is highly variable, with an average of 1.4 ± 1.3% in RCC and 0.13 ± 0.02% in RWC.

As expected, SO_2 was not detected in any of the RWC samples. Only 50% of the RCC samples reported significant $SO_2/PM_{2.5}$ mass ratios. These ratios are highly variable, ranging from 112 ± 3% (MZRCC3) to 532 ± 27% (MZRCC4). Both samples were acquired from Seneca Mine coal combustion. Sulfate ($SO_4^=$) in these two samples are 2.2 ± 0.07% and 3.7 ± 0.12%, respectively. Variable combustion temperatures in different domestic stoves may have contributed to the variations in emissions. Selenium (Se) is also detected in 50% of the RCC emissions, with 0.011 ± 0.001% (MZRCC2) from Trapper Mine coal and 0.004 ± 0.001% (MZRCC3 from Seneca Mine coal.

Watson *et al.* (1988) acquired six diluted exhaust RWC samples in a controlled laboratory using a combination of fuel types typical of Denver, CO (i.e., 60% mixture of lodgepole pine, ponderosa pine, and spruce, 10 % each of pinion, aspen, and oak, and 5% each of Douglas fir and cedar) in five different types of fireplaces and woodstoves. The key features of these profiles are similar to those found in chimney emissions with 54% to 74% OC and 9% to 29% EC in the Denver study, as compared to 40% to 64% OC and 8% to 16% EC in this study. Among the inorganic species, both studies reported that sulfur (S), chlorine (Cl), and potassium (K) are in the tenth-of-a-percent range.

6.3.4 Forest Fires

According to the Craig Interagency Dispatch Center, approximately 80% of the wildfire burning in the region involves pinion pine and juniper trees. To simulate these burns, short-duration

(2 to 8 minute) samples of forest fire emissions were taken of burning pinion pines and junipers in an area ~8 km north of Dinosaur, CO. Four samples were analyzed and averaged to create the MZFFIREC profile as described in Table 6.3.4.

Similar to other vegetative burning emissions, Figure 6.3.4 shows that the K^+/K ratio of 0.83 was in large contrast to the low soluble to total potassium ratios found in geological material. OC abundances in the individual samples were variable, ranging from 30.7 ± 1.5% (MZFFIRE1) to 66.1 ± 3.3% (MZFFIRE2), with an average OC/TC ratio of 0.94. This is the highest OC/TC ratio observed among all measured source types in the study.

Figure 6.3.4 Forest fire source profile composite derived for the Mt. Zirkel Visibility Study.

The abundance of SO_2 (0.30 ± 0.14%) in MZFFIREC is similar in magnitude to that observed in motor vehicle exhaust. Other inorganic species such as $SO_4^=$, S, Cl^-, Cl, K^+, and K are present in the tenth-of-a-percent level, whereas Na, Mg, Al, Si, and Fe are present in the hundredth-of-a-percent level.

Chow *et al*. (1995) measured profiles for asparagus field burning in California's Imperial Valley with OC/TC ratios of 0.93, similar to the 0.94 ratio found in the forest fire emissions. Organic carbon was the most abundant species in the profile, accounting for 55.6 ± 15% of the total mass. A similar observation was made for charbroil cooking emissions, with 60% to 70% OC abundances and high (>0.95) OC/TC ratios.

6.3.5 Geothermal Hot Springs

Geothermal hot springs release gaseous hydrogen sulfide (H_2S) that can contribute to the sulfur burden in the atmosphere. Samples of 7.5- to 300-minute durations were obtained from five the major hot springs in downtown Steamboat Springs (i.e., Lithia, Iron, Sulfur, Black Sulfur, and Steamboat Springs). These samples were acquired at night when levels of vehicular emissions and resuspended road dust were expected to be low. A silver-nitrate-impregnated cellulose-fiber filter was placed behind a quartz-fiber filter pack to collect H_2S. Figure 6.3.5 illustrates the chemical abundances in the profiles derived from these samples.

The MZGSC and MZCGS2C profiles were formed from averages and standard deviations of the individual profiles as specified in Table 6.3.5. To maintain consistency with other profiles, the abundance of H_2S in Figure 6.3.5 was converted to SO_2, assuming complete oxidation in the atmosphere after release. Since the mass collected on the samples was low and imprecise, chemical abundances were normalized to the sum of species rather than to the measured mass. The oxidized H_2S (i.e., SO_2) is the most abundant species, but its abundance is variable, ranging from 655 ± 506% to 3,378 ± 2,603%. Soluble ions such as $SO_4^=$,NO_3^-, Cl^-, andNH_4^+ are present at 15% to 20% levels, while trace elements such as Al, Si, K, Ca, and Fe are present at 2% to 10% levels. Sulfur is present as 30% of sulfate abundance. The remaining chemical species are below the uncertainty level.

Figure 6.3.5 Geothermal springs source profiles derived for the Mt. Zirkel Visibility Study.

6.3.6 Coal-Fired Boilers

Diluted exhaust samples were taken from Units 2 and 3 of the Craig station and from Units 1 and 2 of the Hayden station. Craig Unit 3 is equipped with a dry lime scrubber system (with >85% efficiency) and a fabric baghouse. Craig Unit 2 has a wet limestone scrubber (to remove SO_2 with ~67% efficiency) and electrostatic precipitators. Craig Unit 1 was not sampled because it is identical to Unit 2. Units 2 and 3 of the Craig station use coal from the Trapper and Colowyo mines, respectively. Units 1 and 2 at the Hayden station include hot-side electrostatic precipitators with ammonia injection. Coal is obtained from the Seneca Mine.

Source samples were drawn from the stack via negative pressure into the dilution chamber for 1 to 10 hours with a dilution ratio of 3:1 to minimize condensation and water droplets in the sampling train (Bighouse and Houck, 1995). Thirteen samples were acquired and ten validated samples were used estimate chemical abundances and standard deviations for each unit as detailed in Table 6.3.6. Figure 6.3.6 presents the chemical abundances for these profiles.

Figure 6.3.6 Coal-fired boiler source profiles derived for the Mt. Zirkel Visibility Study.

The Craig Unit 2 (MZCG2PPC) and Unit 3 (MZCG3PPC) profiles differ significantly. Sulfate is the most abundant constituent in the particle phase, at 12.7 ± 3.1% in Unit 3 and 22.7 ± 6.3% in Unit 2. EC in Unit 2 (8.1 ± 4.3%) is much higher than in Unit 3 (1.2 ± 1.2%). Since abundances of OC are similar (~2%), the average OC/TC ratio varied from 0.22 in Unit 2 to 0.69 in Unit 3.

In Craig Unit 2, the Al (4.2 ± 0.3%) abundance is similar that found in the MZGEOLC geological profile (4.5 ±0.7%), whereas Si (8.0 ± 0.6%), Ca (3.5 ± 0.3%), and Fe (3.1 ± 0.2%) are present at 30% to 50% of the corresponding levels in geological material. Sodium (Na) and magnesium (Mg) are also present at the 1% to 2% level in Craig Unit 2. The abundances of these components in Craig Unit 3 are commonly half of those found in Craig Unit 2. Other elements such as phosphate (P), potassium (K), titanium (Ti), chromium (Cr), manganese (Mn), strontium (Sr), zirconium (Zr), and barium (Ba) are present in Unit 2 emissions at levels of 0.1% to 1.0% and in Craig Unit 3 emissions at levels of 0.002% to 0.2%.

Selenium (Se) is detected in all four Craig Unit 2 profiles, ranging from 0.27 ± 0.008% (MZCG2PP1) to 0.43 ± 0.006% (MZCG2PP2). Selenium is usually in the gaseous phase within hot stack emissions, and it condenses on particles when air is cooled in the dilution chamber. Se is not found in the Craig Unit 3 samples. Abundances of calcium (14.7 ± 6.8%), chloride (1.3 ± 0.4%), and nitrate (0.79 ± 0.72%) in Craig Unit 3 are four times those measured in Craig Unit 2. These differences may have resulted from the dry lime scrubber present in Unit 3.

Sulfur dioxide in these coal-fired boiler emissions are orders of magnitude higher than those found in geothermal springs and residential coal combustion, with Craig Unit 2 (21,297 ± 12,557% in MZCG2PPC) being a factor of three to four higher than Craig Unit 3 (6,100 ± 3,330% in MZCG3PPC). Ammonia is detectable in Craig's boiler emissions, ranging from 7% to 10% of primary $PM_{2.5}$ mass .

For most elements, Hayden Unit 1 (MZHD1PP1) exhibits higher chemical abundances than those of Hayden Unit 2 (MZHD2PPC). The largest difference is found for organic carbon, with 0.49 ± 0.06% in Unit 2 and 34.1 ± 3.6% in Unit 1 emissions. Elemental carbon differences are also large, with 0.40 ± 0.20% in Unit 2 and 4.3 ± 0.8% in Unit 1. The average OC/TC ratio is 0.56 for Unit 2 and 0.89 for Unit 1.

The Al abundance in Hayden Unit 1 of 10.3 ± 0.67% is approximately three times that of Unit 2. The Si abundance in Unit 1 of 16.0 ± 1.0% is similar to that found in geological profiles, and is also three times the Al abundance in Unit 2 emissions. Calcium (Ca) and iron (Fe) are present at 1% to 4% levels. Other elements such as phosphate (P), potassium (K), titanium (Ti), manganese (Mn), strontium (Sr), and zirconium (Zr) are abundances of 0.1% to 1% in Unit 1, are typically present at levels two to three times higher than those found in Unit 2 emissions.

Selenium is detected in all Hayden profiles, with 0.22 ± 0.02% in Hayden Unit 1 (MZHD1PP1) and 0.43 ± 0.004% in Hayden Unit 2 (MZHD2PP2). These abundance levels are similar to those found in Craig Unit 2, but not in Craig Unit 3. The abundances of sulfate (10.0 ± 4.9%), ammonium (9.2 ± 2.4%), chloride (1.9 ± 0.12%) from Hayden Unit 2 are two to six times higher than those from Hayden Unit 1. Nitrate (NO_3^-) and barium (Ba) are also present in the tenth-of-a-percent level in Hayden Unit 2 only.

The gaseous sulfur dioxide abundance is 5,721 ± 348% in Hayden Unit 1, which is similar to the SO_2 abundance in Craig Unit 3 (6,100 ± 3,330%), but almost a factor of three higher than the SO_2 in Hayden Unit 2 (2,075 ± 199%). These levels are lower than the 21,297 ± 12,557% found in Craig Unit 2.

Ammonia abundances in Hayden Units 1 and 2 are much higher than those reported in Craig Units 2 and 3. Abundances ranged from 491 ± 384% in Hayden Unit 2 to 3,365 ± 265% in Hayden Unit 3, compared to 7% to 10% at Craig Units 2 and 3.

6.3.7 Regional Background Sources

Primary and secondary aerosol constituents from distant emitters may potentially impact the Mt. Zirkel Wilderness area. Selected ambient samples (those which were minimally affected by local emissions in the Yampa Valley) from the Baggs and Juniper Mountain sites were used to characterize these "regional background" sources. The following three criteria were used to choose these samples.

Animations of the dispersion of the Hayden and Craig sulfur dioxide plumes, generated with the CALMET/CALPUFF model, were examined for aerosol sampling periods from August through October 1995 at the Baggs and Juniper Mountain sites. A sample was identified as "background" if it was not impacted by the Yampa Valley generating station sulfur dioxide plumes during the sampling period as well as two or three hours before and after the sampling period. Six samples at the Baggs site and five samples at the Juniper Mountain site were identified by this criterion and are shown in Table 6.3.7.

A second criterion for choosing "background" samples unaffected by the local generating stations was low concentrations of sulfur dioxide and selenium. The average concentrations in the six background samples and 50 nonbackground samples at the Baggs site were 1.39 ug/m^3 and 0.0004 ug/m^3 for sulfur dioxide and 0.35 ug/m^3 and 0.0002 ug/m^3 for selenium, respectively. The average concentrations in the five background and 28 nonbackground samples at the Juniper Mountain site were 0.47 ug/m^3 and 0.0001 ug/m^3 for sulfur dioxide and 0.24 ug/m^3 and 0.0002 ug/m^3 for selenium, respectively. The selection of samples at both sites based on the CALMET/CALPUFF model is consistent with the observed ambient sulfur dioxide and selenium concentrations.

Finally, surface wind data associated with the selected background samples were examined for consistency. Five out of the six Baggs background samples experienced winds from the northwest or northerly direction. The sixth sample experienced winds from the south-southwest. At Juniper Mountain, background samples experienced winds from the west or southwest. Thus, based on three independent criteria, the choice of representative background samples at the Baggs and Juniper Mountain sites seems justifiable.

The sum of species was consistently greater than the measured $PM_{2.5}$ mass concentration in the Baggs background samples. This is not unexpected because five out of six $PM_{2.5}$ concentrations were less than 4 ug/m^3 and three were less than 2 ug/m^3. For consistency, fractional abundances were therefore calculated with respect to the sum of species at both sites. These samples were combined to formulate the regional background profiles.

The composite profiles determined at Baggs (MZBBRC), Juniper Mountain (MZJURC), and overall samples (MZRC) are given in Appendix C. The compositions of the Baggs and Juniper Mountain regional profiles are quite similar. Figure 6.3.7 compares the three composite regional background profiles.

Figure 6.3.7 Regional background source profiles composites.

Organic carbon, the most abundant chemical species in the regional profile, ranged from 41.1 ± 8.7% for Juniper Mountain samples to 45.0 ± 19.2% for Baggs samples. The abundance of elemental carbon is also similar, varying from 14.1 ± 4.5% at Juniper Mountain to 10.8 ± 7.8% at Baggs. This resulted in OC/TC ratios of 0.74 for Juniper Mountain samples and 0.80 for Baggs samples.

Enrichment from secondary aerosol is apparent, ranging from 30.4 ± 4.9% at Juniper Mountain to 27.3 ± 10.2% at Baggs for sulfate, from 11.9 ± 1.6% at Juniper Mountain to 10.2 ± 2.7% at Baggs for ammonium, and from 1.6 ± 0.7% at Juniper Mountain to 1.8 ± 0.9% at Baggs for nitrate.

Al and Si abundances are at the 1% to 2% levels, whereas sodium (Na), soluble potassium (K^+), total potassium (K), calcium (Ca), iron (Fe), and zinc (Zn) are present at the 0.1% to 1% level. The abundance of selenium is very low, being 0.006 ± 0.03% at the Baggs site and 0.005 ± 0.004% at the Juniper Mountain site.

The sulfur dioxide abundance is 6.6 ± 7.1% for Juniper Mountain samples and 9.3 ± 3.8% for Baggs samples. The ammonia abundance is low (7.3 ± 8.3%) at the Juniper Mountain site, with no ammonia data available from the Baggs site. Since the chemical abundances in these regional background profiles were so similar, the same ammonia abundance is assumed for the Baggs regional profile (MZBBRC).

6.3.8 Sulfur-32 and Sulfur-34 Isotopic Abundances

Table 6.3.8 compares sulfur isotopic ratios and del values for selected samples from the sources tested in the MZVS and background samples from Baggs and Juniper Mountain. The background samples were selected after reviewing the everyday plume modeling results to determine that there was little likelihood of direct impact from Yampa Valley generating station emissions at these sites. Deviations in the ratios are small so the del values, as described in the footnotes, are often used to compare isotopic abundances. For individual samples, the precision (±) represents analytical uncertainty. For averages, the precision is expressed as the standard deviation of ratios and dels to reflect the variability among samples. These averages and standard deviations are compared to determine the value of isotopic abundances for distinguishing among different sources of sulfur.

There is variability within each of source groupings. Del values for coal-fired generating stations range from 4.44 ± 0.07 to 10.27 ± 0.04. The two samples from Hayden Unit 1 have values that are twice those found for the majority of other samples from the Hayden and Craig stations. The difference in dates between the Hayden Units 1 and 2 samples may have resulted in coal from a different part of the mine being burned. Hackley and Anderson (1986) found lower S^{32}/S^{34} at the tops and bottoms of coal seams while higher ratios were found in the middle. Ranges for del values were -18.7 to 15.6 in coal from the Powder River basin and 4.3 to 8.1 in the Green River basin. The values reported in Table 6.3.8 are within these ranges, and for the majority of samples they are relatively consistent, with an average del of 5.13 ± 1.07 when the Hayden Unit 1 samples are excluded. Including these samples doubles the uncertainty of these del value for coal-fired generating stations.

The two forest fire del values are highly variable, even though they were taken from fires in the same area. Though these samples were taken in smoke plumes, it is conceivable that sulfur

dioxide in ambient air mixed into these plumes and that these samples could be a combination of sulfur dioxide from fires and background air.

The geothermal hot springs del values are substantially different from those in other sources, showing a dearth of sulfur-34 with an average of -17.80 ± 1.81. The del values for motor vehicle exhaust also show consistency with an average of -1.32 ± 1.17. The background sulfate values are among the most variable, ranging from -4.84 ± 0.11 to 6.23 ± 0.04. If the extreme negative value is ignored, the average del is 3.59 ± 2.13.

These del values are comparable to those found in other studies of water and air. Turk *et al.* (1993) measured del values of 4.4 to 6.7 in lakes within the Mt. Zirkel Wilderness, and these contrasted to del values from the Weminuche Wilderness that ranged from -4.5 to -3.5. Turk *et al.* (1993) hypothesized that the sulfur sources differed for these two areas, with the majority of sulfur in the Weminuche Wilderness deriving from the weathering of geological material, especially pyrite, and the majority in the Mt. Zirkel Wilderness resulting from deposition of sulfur in the air. The contrast between the del values for geothermal hot springs and the values for coal-fired generating stations and background air is consistent with this hypothesis.

Table 6.3.8
Sulfur-32 and Sulfur-34 Isotopic Abundances in Source Emissions and Background Air

Sample	Sample Period[a]	Sulfur Form[b]	S^{32}/S^{34} [c]	del[d]
Generating Station				
Hayden Unit 1	07/19/95	SO_2	22.40 ± 0.018	9.82 ± 0.08
Hayden Unit 1	07/19/95	SO_2	22.39 ± 0.009	10.27 ± 0.04
Hayden Unit 1 Average		SO_2	22.40 ± 0.01	10.05 ± 0.32
Hayden Unit 2	07/24/95	SO_2	22.49 ± 0.021	5.78 ± 0.10
Hayden Unit 2	07/24/95	SO_2	22.54 ± 0.018	3.55 ± 0.08
Hayden Unit 2 Average		SO_2	22.52 ± 0.04	4.66 ± 1.58
Craig Unit 2	07/12-13/95	SO_2	22.51 ± 0.029	4.89 ± 0.13
Craig Unit 2	07/12-13/95	SO_2	22.52 ± 0.016	4.44 ± 0.07
Craig Unit 2	07/12-13/95	SO_2	22.46 ± 0.078	7.12 ± 0.35
Craig Unit 2 Average		SO_2	22.50 ± 0.03	5.48 ± 1.44
Craig Unit 2	07/13/95	SO_4	22.45 ± 0.271	7.57 ± 1.21
Craig Unit 3	07/15/95	SO_2	22.50 ± 0.003	5.33 ± 0.01
Craig Unit 3	07/18/95	SO_2	22.52 ± 0.043	4.44 ± 0.19
Craig Unit 3 Average			22.51 ± 0.01	4.89 ± 0.63
Craig Unit 3	07/15/95	SO_4	22.45 ± 0.013	7.57 ± 0.06

Generating Station Averages				
Craig 2&3, Hayden 1&2		SO_2	22.48+ 0.05	6.18 ± 2.41
Craig 2&3, Hayden 2		SO_2	22.50+ 0.02	5.13 ± 1.07
Forest Fire				
Forest Fire	07/30/95	SO_2	22.58+ 0.013	1.77 ± 0.06
Forest Fire	07/30/95	SO_2	22.30+ 0.009	14.35 ± 0.04
Forest Fire Average			22.44 ± 0.20	8.06 ± 8.89
Hot Springs				
Hot Springs	07/22/95	SO_2	23.00 ± 0.026	-16.52 ± 0.11
Hot Springs	07/22/95	SO_2	23.06 ± 0.023	-19.08 ± 0.10
Hot Springs Average			23.03 ± 0.04	-17.80 ± 1.81
Vehicle Exhaust				
Vehicle Exhaust	07/17/95	SO_2	22.67 ± 0.024	-2.21 ± 0.10
Vehicle Exhaust	07/17/95	SO_2	22.66 ± 0.017	-1.77 ± 0.08
Vehicle Exhaust	07/21/95	SO_2	22.62 ± 0.021	0.00 ± 0.09
Vehicle Exhaust Average			22.65 ± 0.03	-1.32 ± 1.17
Residential Coal	03/15/95	SO_4	22.17 ± 0.010	20.30 ± 0.04
Residential Wood	03/15/95	SO_4	22.30 ± 0.021	14.35 ± 0.10
Background Air				
Baggs	08/08/95 AM	SO_2	22.55 ± 0.014	3.10 ± 0.06
Baggs	08/24/95 PM	SO_4	22.48 ± 0.008	6.23 ± 0.04
Baggs	09/20/95 PM	SO_4	22.73 ± 0.025	-4.84 ± 0.11
Baggs	09/30/95 PM	SO_4	22.48 ± 0.006	6.23 ± 0.03
Juniper Mountain	08/21/95 AM	SO_4	22.59 ± 0.035	1.33 ± 0.15
Juniper Mountain	08/08/95 AM	SO_2	22.57 ± 0.027	2.22 ± 0.12
Average of all samples		SO_2/SO_4	22.57 ± 0.09	2.38 ± 4.08
Average w/o Baggs 9/20		SO_2/SO_4	22.54 ± 0.05	3.58 ± 2.13

[a] Period over which samples were taken.

[b] Particulate SO_4 was on Teflon particle filter, gaseous SO_2 was on potassium carbonate backup filter.

[c] Ratio of concentration of Sulfur-32 isotopic abundance to Sulfur-34 isotopic abundance.

[d] $del=100*\{[(22.62)/(S^{32}/S^{34})]^{-1}\}$, related to Canyon Diablo Meteorite standard S^{32}/S^{34}.

[e] Background samples represent periods without of impact from Yampa Valley generating station plumes.

Forrest and Newman (1973) measured background del values of 0.7 to 4.8 in New York state, and McArdle and Liss (1995) found values ranging from 4 to 23 near the coasts of Ireland and Norway. Newman *et al.* (1975) found del values of 5.0 - 0.3 in an oil-fired generating station plume, with del values for background air ranging from 0.7 to 4.8. These are consistent with the MZVS results in Table 6.3.8.

Variability within each grouping of Table 6.3.8 is ~2 del values. This implies that at least 3 del values (the approximate uncertainty of the difference between del values for a given source type) is needed to distinguish source contributions between two sources. It is apparent that sulfur, as SO_2 or sulfate, from coal-fired power generation, motor vehicle exhaust, and geothermal hot springs could be distinguished from each other. It is also apparent that sulfur from motor vehicle exhaust and hot springs could be distinguished from background air. Given the results in Table 6.3.8, however, it is unlikely that sulfur from coal-fired power generation can be distinguished from background air. This is possibly due to the dominance of coal-burning as the major SO_2 emitter in the region, as discussed in Section 6.2.

These conclusions must be tempered by the small number of samples taken over a short time period. The comparison of results from Hayden Units 1 and 2 is revealing, in that it shows how a change in fuel may change the composition of the emissions, not just for isotopic abundances, but for all of the species included in a source profile. The same situation is true of sulfur in vehicle exhaust and other sources. These changes can only be evaluated through a long-term measurement program analyzing many more samples taken over a longer time period than was available for the MZVS.

6.4 Changes in Reactive Species

The Aerosol Evolution Model (AEM) described in Appendix B.5 quantifies changes in the abundances of particulate sulfate, gaseous sulfur dioxide, and inert primary particles as power plumes age during transport between source and receptor. As used here, the AEM is not intended to simulate what actually happened under different conditions in the MZVS, but is meant to explore what could have happened to generating station emissions during transport.

The AEM is an extension of SCAPE, a thermodynamic equilibrium model that partitions total sulfur, nitrogen, and ammonia between gas and aerosol (liquid and solid) phases. On this structure, the AEM imposes gas and liquid phase transformation of sulfur and nitrogen as well as mixing between a plume and ambient background air.

The meteorological situation simulated is that described in Section 5.2.3, wherein generating station plumes are trapped in the Yampa Valley by a nighttime inversion beginning at ~1800 MST until inversion breakup at ~1000 MST the next morning. These aged emissions arrive at Buffalo Pass by ~1200 MST, giving an 18-hour transport time. Base case parameters were selected to represent conditions with minimal interaction of emissions with clouds or fogs. Several deviations from this base case are parametrically examined in Appendix B.5, and the conclusion is the same.

Lacking processing of sulfur dioxide through fogs or clouds, there is insufficient time for significant quantities of sulfate to be formed during transport from the Yampa Valley to the Wilderness.

Base case temperature and relative humidity were assumed to be 15 degrees C and 51%, respectively, for the six-hour averages for 1800 to 2400 MST on 09/17/95 at the Hayden VOR site. An average transport speed of 0.67 m/s would allow emissions from the furthest generating station (Craig) to arrive at Buffalo Pass 18 hours later. Stability class C, which defines the amount of mixing between plume and ambient air, is a compromise between nighttime and daytime stabilities.

An initial aerosol solute concentration of 0.001 $\mu g/m^3$ of sodium chloride (NaCl) is assumed to provide initial nuclei for droplet formation. The AEM requires a nonzero initial solute concentration, and this NaCl concentration was selected instead of the more likely background sulfate so that the AEM can easily separate the generating station sulfate from other nucleating substances. A 0.001 $\mu g/m^3$ NaCl concentration is also assumed in the background air mixed into the plume.

Nominal concentrations in Craig station emissions, determined from continuous emissions monitoring and volumetric flows, are assumed to be 0.369 g/m^3 for SO_2 and 0.504 g/m^3 for NO_x. Corresponding values for the Hayden station are 0.920 g/m^3 for SO_2 and 0.857 g/m^3 for NO_x. The totals of 1.29 g/m^3 SO_2 and 1.36 g/m^3 NO_x were used for initial pollutant concentrations in the AEM, and the NO_x was split into 10% NO_2 and 90% NO by mass.

Base case background air concentrations for ammonia were assumed to be 0.5 $\mu g/m^3$ and 30 ppbv for ozone, consistent with measured values at the Hayden VOR site. The base case hydrogen peroxide concentration was assumed to be 1 ppbv. Tanner and Schorran (1995) measured peroxide concentration in the Grand Canyon National Park varying from 1 to 3 ppbv. Appendix B.5 shows that conversion is only sensitive to peroxide levels at humidities >90%. The lower end of this range was selected for the base case because the Grand Canyon is affected by transport from southern California, and since the Yampa Valley is relatively unpolluted, the lower bound is appropriate.

Background concentrations of oxides of nitrogen were assumed to be 0.5 ppbv, split into 10% NO and 90% NO_2 by volume, similar to levels measured by Carroll *et al.* (1992) in nonurban areas. Simulations are not sensitive to background NO_x concentrations. The base case concentration for formaldehyde was assumed to be 0.2 ppbv. Background levels of formaldehyde ranging from ~0.2 to 0.8 ppbv were observed at a relatively unpolluted site at 1,600 m elevation in Arizona (Farmer and Dawson, 1982). Lowe *et al.* (1981) report levels from ~0.2 to 2 ppbv at a slightly polluted site in West Germany. Mn^{++} and Fe^{+++} concentrations of 10^{-5} moles per liter were assumed for metal ion catalyzed liquid phase reactions; these values are typical of urban cloud (Barrie and Georgii, 1976), and Yampa Valley concentrations are probably lower.

With these base case conditions for SO_2 concentration, stability, and average transport velocity, the SO_2 conversion to sulfate was estimated to be ~0.1%, meaning that 100 ug/m^3 of SO_2

would need to be found at Buffalo Pass to correspond to 0.1 ug/m^3 of particulate sulfate. As shown in Section 5.6, typical SO_2 pulses were often one-twentieth to one-hundredth of this concentration. Appendix B.5 shows that large deviations from every one of the assumed values for this application of the AEM do not significantly change this negligible conversion rate under dry conditions.

The AEM shows significant conversion over short time intervals when humidities are high enough to form fogs and clouds. Table 6.4.1 shows the amount of sulfur dioxide to sulfate conversion for the base case parameters and variations on relative humidity from the base case. The total fractional conversion of SO_2 to sulfate is given after 1, 6, 12, and 18 hours at the specified relative humidity. Also shown is the calculated sulfate contribution to the scattering coefficient, using the chemical specific extinction efficiency estimated in Appendix B.2 and applied in Section 4.4. The scattering efficiency contains a (100-RH) term in its denominator; as a result, it is applied here up to RH=99%, even when the AEM simulations were performed at RH=100%.

In order to discuss the effect of sulfate formation on light extinction, the definitions of Section 1.4 are applied to a nominal scattering coefficient value of 25 Mm^{-1}, which is approximately that of the maximum 90th percentile light scattering value for Buffalo Pass (see Table 3.1.1). Contributions to the total scattering < 0.25 are defined as negligible, from 0.25 to 2.5 Mm^{-1} are defined as minor, from 2.5 to 6.25 Mm^{-1} are defined as significant, from 6.25 to 12.5 Mm^{-1} are defined as large, and > 12.5 Mm^{-1} are defined as major.

Examination of Table 6.4.1 for the base case of RH=51% shows a total conversion of 0.286% occurring in the final six hours. At this relative humidity, there is little or no liquid water and the conversion is through the gas phase, which is dominated by photolytic conversion in the last six-hour daylight period. The contribution to the total scattering coefficient for the base case is < 0.25 Mm^{-1} , and is negligible.

Increasing the relative humidity to 75% and 95% does not change the total conversion of sulfur dioxide to sulfate appreciably but does increase the contribution to scattering through the inverse relation of the above defined efficiency coefficient on relative humidity. The contributions to scattering, however, rise to no more than the minor range.

At a relative humidity value of 99%, liquid phase conversion becomes significant. This, in combination with the inverse relationship of the scattering efficiency on relative humidity, elevated the contribution to the scattering coefficient just into the large range after 18 hours. It is only when relative humidity reaches 100%, indicative of fogs and clouds, that conversion is large enough to provide gas-to-particle conversions that result in major contributions light scattering. Table 6.4.1 shows that, although total conversion increases with time for 100% relative humidity, the scattering coefficient contribution is approximately level for the times indicated. This is because of the interplay between conversion, which tends to increase sulfate concentrations, and mixing between plume and ambient air, which tends to decrease concentrations. These simulations show that even short time periods spent by the

Table 6.4.1
Conversion of Sulfur Dioxide to Sulfate for Different Relative Humidities

	Fraction of SO_2 Converted to SO_4 at Different Aging Periods[a]				Changes in Particle Scattering (Mm^{-1}) for Different Aging Periods[b]			
RH (%)	1 hr	6-hr	12-hr	18-hr	1-hr	6-hr	12-hr	18-hr
51	2.39E-12	5.31E-10	4.08E-06	2.86E-03	1.26E-08	1.94E-07	6.85E-04	1.55E-01
75	1.84E-06	1.85E-06	1.87E-06	2.78E-03	3.10E-02	1.28E-03	3.78E-04	2.49E-01
95	4.87E-07	5.82E-07	1.65E-05	2.88E-03	3.34E-02	1.64E-03	1.13E-02	1.07E+00
99	1.82E-06	6.33E-06	2.73E-04	3.73E-03	5.66E-01	7.35E-02	9.57E-01	6.58E+00
100	2.36E-03	3.27E-02	1.05E-01	2.30E-01	5.72E+02	4.08E+02	3.87E+02	4.20E+02

[a] Base case presented here assumes the following (effects of variations are reported in Appendix B.5):
A power station plume was assumed to contain:
Initial SO_2 concentration of 1.29 g/m^3
Initial NO_x concentration of 1.36 g/m^3 (10% NO_2, 90% NO)
Initial solute concentration of 0.0001 ? g/m^3 NaCl
Background air mixed into the plume assuming C stability and Gaussian dispersion was assumed to contain:
NH_3 concentration of 0.5 ug/m^3
O_3 concentration of 30 ppbv
H_2O_2 concentration of 1 ppbv
NO_x concentration of 0.5 ppbv (90% NO_2, 10% NO)
Formaldehyde concentration of 0.2 ppbv
10^{-5} moles/liter of dissolved Fe^{+++} and Mn^{++} in droplets
Transport velocity was assumed to be 0.67 m/s.

[b] Assumes that sulfate light scattering =0.86 +0.73[1/(100-RH)]*[sulfate concentration]

as derived in Appendix B.4

plume in clouds or fogs, on the order of a few hours, can produce a major contribution to the particle scattering from conversion of sulfur dioxide gas to sulfate particles.

The conclusion that sulfur dioxide to sulfate conversions from Yampa Valley generating station emissions is only significant for aqueous-phase transformations, and not for dry transformations, is not affected by changes in base case assumptions for the AEM. The parametric studies reported in Appendix B.5 show that the only conditions under which physically reasonable model parameters produce significant contributions to the scattering coefficient is for 99% or 100% relative humidity, with only one case at 99%. For relative humidities of 95% or less, the large majority of contributions were in the minor or less ranges. In short, these simulations support the conclusions stated above that only under high relative humidity conditions where the plume has spent time in clouds or fog is the contribution of the generating stations to extinction likely to be large (major); otherwise, the contribution is likely to be negligible (or at most minor).

These transformations were applied to the coal-fired boiler profiles in Section 6.3 to determine how trace elemental, sulfate, ammonium, and sulfur dioxide abundances might change with sample aging under dry and wet conditions. For example, for the Craig Unit 2 profile, ratios to fine particle mass at time t=0 are assumed to be 213 for sulfur dioxide, 0.23 for sulfate, and 0.0034 for selenium. At time t, these concentrations will change because of dilution due to mixing between the plume and the background air and the conversion of sulfur dioxide to sulfate.

$$M = x * M(t=0) + S4' \qquad (6.4.1)$$

$$Se = x * Se(t=0) \qquad (6.4.2)$$

where x denotes the dilution factor produced by mixing, M denotes fine-particle mass concentration, S4´ denotes sulfate concentration expressed as equivalent ammonium sulfate, and Se denotes the selenium concentration. With these values for M and Se, and the model-calculated values for sulfur dioxide and sulfate, the new mass ratios at time t can be determined. These ratios are then used with source profiles to determine aged profiles which, in CMB, fit to receptor data.

With the 09/18/95 afternoon data at Buffalo Pass, best fits were made using wet (RH=100%) base case simulation values after 4-1/4 hours (H_2O_2 = 1 ppbv) and 2-3/4 hours (H_2O_2 = 2 ppbv). Dry case simulation values could be fit only for formaldehyde values of 2 ppbv, which is unlikely for the pristine MZVS study areas. These results also support the above conclusions about dry and wet case conversion.

6.5 Chemical Mass Balance Receptor Modeling

The Chemical Mass Balance (CMB) source apportionment model is described in detail in Appendix B.3. The CMB uses chemical compositions measured at source and receptor to infer source contributions from different source types. Primary motor vehicle exhaust, primary vegetative burning (including residential wood combustion and forest fires), dust, coal-fired generating station

emissions, and regional sulfates and nitrates are potential contributors to the ambient aerosol in the Yampa Valley and at measurement locations near the Mt. Zirkel Wilderness that can be treated by the CMB model with the chemicals measured at source and receptor during the MZVS. Secondary organic carbon and meat cooking, with profiles dominated by organic carbon, cannot be separated by the CMB model from other carbon-containing emitters, namely fires and motor vehicle exhaust, using the MZVS chemical measurements. Contributions from motor vehicle exhaust and fires may be overestimated, while contributions from secondary organic aerosol and meat cooking are not estimated at all.

6.5.1 CMB Sensitivity to Differences in Source Profiles

Coal-fired generating station emissions were represented by "fresh" profiles (i.e., the profiles acquired in the generating station effluent, as described in Section 6.3), and by profiles that were "aged" under dry and moist conditions, as described in Section 6.4. The "aging" process increased the particle sulfate while decreasing the sulfur dioxide and remaining chemical abundances in these profiles.

Chemical species with concentrations greater than their precisions for most of the samples were used to calculate source contribution estimates. Sulfate was used in place of elemental sulfur. Total sulfur (i.e., SOTC = sulfate + equivalent sulfur dioxide), total carbon (i.e., TCTC = OC + EC), and ammonia (i.e., DDN4CC = denuder difference NH_3) were included in the profiles and ambient concentrations but not used in the CMB calculations. Comparing their measured and calculated concentrations helps to validate the CMB results.

Examples of CMB sensitivity to the use of different combinations of source profiles and fitting species source apportionments are presented in Table 6.5.1. Several of these tests were carried out on several samples, but the results do not differ significantly from those reported for this example. The "best fit" is presented in the first column as a reference. The source contribution estimates (SCEs) and CMB performance measures are shown for each trial. The CMB outputs corresponding to the "best fit" case are reported in Tables 6.5.2a to 6.5.2h.

Tables 6.5.1 and 6.5.2a-h indicate that geological, motor vehicle exhaust, vegetative burning, aged coal-fired generating station, regional secondary ammonium sulfate, and secondary ammonium nitrate were the principal contributors to $PM_{2.5}$ mass at the Buffalo Pass site on the afternoon of 09/18/95. The "best fit" for this case assumes that the fresh coal-fired generating station profile from Hayden Unit 2 underwent transformations in a cloud or fog for two to four hours prior to arrival at Buffalo Pass (MZHD2WET). The "best fit" also uses the composite geological profile (MZSOILC), the Craig motor vehicle profile (MZMVCGC), the residential wood combustion profile (MZRWC3), and secondary ammonium sulfate (AMSUL) and secondary ammonium nitrate (AMNIT) profiles (Watson *et al.*, 1995) to represent sources of these substances from outside the Yampa Valley.

Table 6.5.1
Sensitivity of Source Contribution Estimates to Changes in Source Profiles for Samples Acquired at the Buffalo Pass Site during the Afternoon (1200-1800 MST) of 09/18/95

Profile[a]	Best Fit	Trial 1	Trial 2	Trial 3	Trial 4	Trial 5	Trial 6	Trial 7
MZSOIL	0.140 ± 0.032		0.140 ± 0.032	0.14 ± 0.032	0.176 ± 0.037	0.152 ± 0.040	0.136 ± 0.033	0.143 ± 0.028
MZPVRDC		0.106 ± 0.019						
MZMVCGC	0.47 ± 0.34	0.47 ± 0.34	0.47 ± 0.34	0.47 ± 0.34	0.67 ± 0.44	0.68 ± 0.48	0.44 ± 0.33	
MZMVC								0.062 ± 0.24
MZHD2WET	1.04 ± 0.119	1.04 ± 0.12				1.01 ± 0.12	1.25 ± 0.53	1.05 ± 0.12
MZHD2PPC			0.107 ± 0.012					
MZHD2DRY				0.32 ± 0.04				
MZHD2W6					9.0 ± 1.0			
MZRWC3	0.83 ± 0.10	0.83 ± 0.10	0.83 ± 0.10	0.83 ± 0.10	0.80 ± 0.13		0.85 ± 0.11	0.85 ± 0.07
MZFIREC						2.9 ± 1.7		
MZGSC							-0.0198 ± 0.0530	
AMSUL	0.961 ± 0.177	0.96 ± 0.18	1.45 ± 0.14	1.34 ± 0.14		0.99 ± 0.18	0.86 ± 0.30	0.93 ± 0.17
AMNIT	0.20 ± 0.06	0.20 ± 0.05	0.20 ± 0.05	0.20 ± 0.05	0.21 ± 0.06	0.198 ± 0.064	0.21 ± 0.05	0.20 ± 0.04
CHI-SQUARE[b]	1.41	1.49	1.37	1.39	1.41	1.48	1.57	2.53
R-SQUARE[c]	0.91	0.91	0.92	0.92	0.85	0.85	0.89	0.90
PERCENT MASS[d]	129.7	128.6	114	117.5	387.2	207.8	132.3	135.2
CLUSTERS[e]	---	---	---	---	---	---	---	---

[a] See Tables 6.3.1 to 6.3.8 for source profile descriptions.

[b] CHI-SQUARE measures the agreement between calculated and measured concentrations.

[c] R-SQUARE measures the correlation between calculated and measured concentrations. The closer the value of R-SQUARE to unity, the better the correlation.

[d] PERCENT MASS is the sum of source contributions divided by measured mass. The target value is 100. Values significantly less than 100 indicate missing sources,
while values significantly exceeding 100 indicate sources which do not belong.

[e] CLUSTERS refers to UNCERTAINTY/SIMILARITY CLUSTERS which identify the potential for collinearity among the profiles which are contained in the CLUSTER.
When source profile mnemonics are listed, they appeared together in one or more clusters and are probably collinear.

Table 6.5.2a
CMB Results for Samples Acquired at the Buffalo Pass Site during the Afternoon (1200-1800 MST) of 09/18/95 "Best Fit"

```
SOURCE CONTRIBUTION ESTIMATES -  SITE: BP           DATE: 09/18/95    CMB7 33889
SAMPLE DURATION        6       START HOUR        12        SIZE:    F
       R SQUARE       .91    PERCENT MASS     129.7
     CHI-SQUARE      1.41              DF        23

  SOURCE
     * TYPE     SCE(UG/M3)    STD ERR      TSTAT
-------------------------------------------
11     MZSOILC       .1398      .0317     4.4118
13     MZMVCGC       .4708      .3401     1.3844
31     MZHD2WET     1.0369      .1194     8.6874
35     MZRWC3        .8328      .1045     7.9735
50     AMSUL         .9612      .1772     5.4236
52     AMNIT         .2016      .0548     3.6761
-------------------------------------------

MEASURED CONCENTRATION FOR SIZE: F
       2.8+-      .0

       UNCERTAINTY/SIMILARITY CLUSTERS    CMB7 33889     SUM OF CLUSTER SOURCES
-------------------------------------------------------------------------------

-------------------------------------------------------------------------------

SPECIES CONCENTRATIONS -  SITE: BP           DATE: 09/18/95    CMB7 33889
SAMPLE DURATION        6       START HOUR        12        SIZE:    F
       R SQUARE       .91    PERCENT MASS     129.7
     CHI-SQUARE      1.41              DF        23

SPECIES-------I---MEAS-----------------CALC-------------RATIO C/M----RATIO R/U
MSGC   MSGU   T   2.80880+-   .03870   3.64315+-   .36376   1.30+-  .13      2.3
CLIC   CLIU   *    .00960<    .03560    .02261<    .03123   2.36<  9.32      .3
N3IC   N3IU   *    .16540+-   .03050    .15714+-   .03017    .95+-  .25      -.2
S4IC   S4IU   *   1.15780+-   .06380    .99010+-   .15660    .86+-  .14     -1.0
SOIC   SOIU   *   2.17890+-   .15030   2.20491+-   .21178   1.01+-  .12      .1
SO4T   SO4TU      4.42620+-   .23430   4.09819+-   .33316    .93+-  .09      -.8
S32    S32U        .00000+-   .00000    .00000+-   .00000    .00+-  .00 -1000.0
S34    S34U        .00000+-   .00000    .00000+-   .00000    .00+-  .00 -1000.0
N4CC   N4CU   *    .40440+-   .03220    .47062+-   .05682   1.16+-  .17      1.0
DDN4CC DDN4CU      .01360<    .17110    .53265<    .41703  39.17< *****     1.2
KPAC   KPAU   *    .02260+-   .00840    .02262+-   .01698   1.00+-  .84      .0
OCTC   OCTU   *    .40530+-   .31560    .60240+-   .53590   1.49+- 1.76      .3
ECTC   ECTU   *    .10010+-   .07620    .33547+-   .20158   3.35+- 3.25     1.1
TCTC   TCTU        .50540+-   .35970    .94940+-   .48424   1.88+- 1.64      .7
NAXC   NAXU   *    .00000<    .01880    .00042<    .01475    .00<   .00      .0
MGXC   MGXU   *    .00000<    .00830    .00174<    .00672    .00<   .00      .2
ALXC   ALXU   *    .01450+-   .00180    .00983+-   .00349    .68+-  .26     -1.2
SIXC   SIXU   *    .02950+-   .00270    .03001+-   .00658   1.02+-  .24      .1
SUXC   SUXU        .39590+-   .01990    .31043+-   .03616    .78+-  .10     -2.1
CLXC   CLXU   *    .00000<    .00760    .00442<    .00238    .00<   .00      .6
KPXC   KPXU   *    .02260+-   .00130    .02241+-   .00169    .99+-  .09      -.1
CAXC   CAXU   *    .00570+-   .00080    .00679+-   .00297   1.19+-  .55      .4
TIXC   TIXU   *    .00000<    .00870    .00091<    .00783    .00<   .00      .1
CRXC   CRXU   *    .00000<    .00180    .00020<    .00079    .00<   .00      .1
MNXC   MNXU   *    .00000<    .00080    .00025<    .00055    .00<   .00      .3
FEXC   FEXU   *    .00690+-   .00100    .00881+-   .00322   1.28+-  .50      .6
NIXC   NIXU   *    .00020<    .00040    .00023<    .00042   1.15<  3.12      .1
CUXC   CUXU   *    .00210+-   .00150    .00040+-   .00046    .19+-  .26     -1.1
ZNXC   ZNXU   *    .00270+-   .00210    .00069+-   .00043    .26+-  .26      -.9
```

ASXC	ASXU	*	.00020<	.00040	.00000<	.00039	.01<	1.94	-.4
SEXC	SEXU	*	.00040+-	.00010	.00048+-	.00022	1.19+-	.63	.3
BRXC	BRXU	*	.00140+-	.00010	.00017+-	.00023	.12+-	.16	-4.9
RBXC	RBXU	*	.00000<	.00020	.00004<	.00018	.00<	.00	.2
SRXC	SRXU	*	.00020+-	.00020	.00021+-	.00021	1.06+-	1.51	.0
ZRXC	ZRXU	*	.00000<	.00030	.00006<	.00027	.00<	.00	.1
PBXC	PBXU	*	.00000<	.00060	.00063<	.00076	.00<	.00	.6

Table 6.5.2b
CMB Results for Samples Acquired at the Buffalo Pass Site
during the Afternoon (1200-1800 MST) of 09/18/95
Trial 1

```
SOURCE CONTRIBUTION ESTIMATES -  SITE: BP           DATE: 09/18/95    CMB7 33889
SAMPLE DURATION        6       START HOUR        12        SIZE:    F
       R SQUARE       .91    PERCENT MASS     128.6
     CHI-SQUARE      1.49              DF        23

  SOURCE
     * TYPE     SCE(UG/M3)    STD ERR      TSTAT
-------------------------------------------
3      MZPVRDC       .1061      .0192     5.5163
13     MZMVCGC       .4692      .3393     1.3830
31     MZHD2WET     1.0433      .1197     8.7170
35     MZRWC3        .8326      .1033     8.0584
50     AMSUL         .9579      .1777     5.3910
52     AMNIT         .2017      .0548     3.6818
-------------------------------------------

MEASURED CONCENTRATION FOR SIZE: F
       2.8+-      .0

       UNCERTAINTY/SIMILARITY CLUSTERS    CMB7 33889     SUM OF CLUSTER SOURCES
-------------------------------------------------------------------------------

-------------------------------------------------------------------------------

SPECIES CONCENTRATIONS -  SITE: BP           DATE: 09/18/95    CMB7 33889
SAMPLE DURATION        6       START HOUR        12        SIZE:    F
       R SQUARE       .91    PERCENT MASS     128.6
     CHI-SQUARE      1.49              DF        23

SPECIES-------I---MEAS------------------CALC-------------RATIO C/M----RATIO R/U
MSGC   MSGU   T   2.80880+-   .03870   3.61083+-   .36345   1.29+-  .13     2.2
CLIC   CLIU   *    .00960<    .03560    .02255<    .03113   2.35<  9.30      .3
N3IC   N3IU   *    .16540+-   .03050    .15718+-   .03010    .95+-  .25     -.2
S4IC   S4IU   *   1.15780+-   .06380    .98928+-   .15722    .85+-  .14    -1.0
SOIC   SOIU   *   2.17890+-   .15030   2.21844+-   .21309   1.02+-  .12      .2
SO4T   SO4TU      4.42620+-   .23430   4.11644+-   .33504    .93+-  .09     -.8
S32    S32U        .00000+-   .00000    .00000+-   .00000    .00+-  .00 -1000.0
S34    S34U        .00000+-   .00000    .00000+-   .00000    .00+-  .00 -1000.0
N4CC   N4CU   *    .40440+-   .03220    .47069+-   .05694   1.16+-  .17     1.0
DDN4CC DDN4CU      .01360<    .17110    .53593<    .41960  39.41< *****     1.2
KPAC   KPAU   *    .02260+-   .00840    .02253+-   .01693   1.00+-  .84      .0
OCTC   OCTU   *    .40530+-   .31560    .60083+-   .53413   1.48+- 1.75      .3
ECTC   ECTU   *    .10010+-   .07620    .33429+-   .20092   3.34+- 3.24     1.1
TCTC   TCTU        .50540+-   .35970    .94665+-   .48263   1.87+- 1.64      .7
NAXC   NAXU   *    .00000<    .01880    .00043<    .01469    .00<   .00      .0
MGXC   MGXU   *    .00000<    .00830    .00132<    .00670    .00<   .00      .1
ALXC   ALXU   *    .01450+-   .00180    .00853+-   .00325    .59+-  .24    -1.6
SIXC   SIXU   *    .02950+-   .00270    .02771+-   .00533    .94+-  .20     -.3
SUXC   SUXU        .39590+-   .01990    .31017+-   .03623    .78+-  .10    -2.1
CLXC   CLXU   *    .00000<    .00760    .00443<    .00237    .00<   .00      .6
KPXC   KPXU   *    .02260+-   .00130    .02241+-   .00169    .99+-  .09     -.1
CAXC   CAXU   *    .00570+-   .00080    .00567+-   .00198    .99+-  .37     -.0
TIXC   TIXU   *    .00000<    .00870    .00087<    .00781    .00<   .00      .1
CRXC   CRXU   *    .00000<    .00180    .00020<    .00079    .00<   .00      .1
MNXC   MNXU   *    .00000<    .00080    .00018<    .00055    .00<   .00      .2
FEXC   FEXU   *    .00690+-   .00100    .00830+-   .00133   1.20+-  .26      .8
NIXC   NIXU   *    .00020<    .00040    .00023<    .00042   1.15<  3.11      .1
CUXC   CUXU   *    .00210+-   .00150    .00040+-   .00046    .19+-  .26    -1.1
ZNXC   ZNXU   *    .00270+-   .00210    .00072+-   .00043    .27+-  .26     -.9
ASXC   ASXU   *    .00020<    .00040    .00000<    .00039    .00<  1.93     -.4
SEXC   SEXU   *    .00040+-   .00010    .00048+-   .00022   1.20+-  .63      .3
BRXC   BRXU   *    .00140+-   .00010    .00017+-   .00023    .12+-  .16    -4.9
```

RBXC	RBXU	*	.00000<	.00020	.00004<	.00017	.00<	.00	.2
SRXC	SRXU	*	.00020+-	.00020	.00023+-	.00021	1.17+-	1.59	.1
ZRXC	ZRXU	*	.00000<	.00030	.00006<	.00027	.00<	.00	.1
PBXC	PBXU	*	.00000<	.00060	.00063<	.00076	.00<	.00	.7

Table 6.5.2c
CMB Results for Samples Acquired at the Buffalo Pass Site
during the Afternoon (1200-1800 MST) of 09/18/95
Trial 2

```
SOURCE CONTRIBUTION ESTIMATES -  SITE: BP           DATE: 09/18/95    CMB7 33889
SAMPLE DURATION        6       START HOUR        12        SIZE:    F
       R SQUARE       .92    PERCENT MASS     114.0
     CHI-SQUARE      1.37              DF        23

  SOURCE
     * TYPE     SCE(UG/M3)    STD ERR      TSTAT
-------------------------------------------
11     MZSOILC       .1402      .0317     4.4225
13     MZMVCGC       .4726      .3410     1.3862
23     MZHD2PPC      .1074      .0124     8.6930
35     MZRWC3        .8324      .1047     7.9515
50     AMSUL        1.4464      .1354    10.6855
52     AMNIT         .2024      .0547     3.7011
-------------------------------------------

MEASURED CONCENTRATION FOR SIZE: F
       2.8+-      .0

       UNCERTAINTY/SIMILARITY CLUSTERS    CMB7 33889     SUM OF CLUSTER SOURCES
-------------------------------------------------------------------------------

-------------------------------------------------------------------------------

SPECIES CONCENTRATIONS -  SITE: BP           DATE: 09/18/95    CMB7 33889
SAMPLE DURATION        6       START HOUR        12        SIZE:    F
       R SQUARE       .92    PERCENT MASS     114.0
     CHI-SQUARE      1.37              DF        23

SPECIES-------I---MEAS------------------CALC-------------RATIO C/M----RATIO R/U
MSGC   MSGU   T   2.80880+-   .03870   3.20152+-   .34882   1.14+-  .13     1.1
CLIC   CLIU   *    .00960<    .03560    .02266<    .03135   2.36<  9.34      .3
N3IC   N3IU   *    .16540+-   .03050    .15779+-   .03029    .95+-  .25     -.2
S4IC   S4IU   *   1.15780+-   .06380   1.07243+-   .10898    .93+-  .11     -.7
SOIC   SOIU   *   2.17890+-   .15030   2.22977+-   .21417   1.02+-  .12      .2
SO4T   SO4TU      4.42620+-   .23430   4.41709+-   .33924   1.00+-  .09     -.0
S32    S32U        .00000+-   .00000    .00000+-   .00000    .00+-  .00 -1000.0
S34    S34U        .00000+-   .00000    .00000+-   .00000    .00+-  .00 -1000.0
N4CC   N4CU   *    .40440+-   .03220    .45148+-   .04774   1.12+-  .15      .8
DDN4CC DDN4CU      .01360<    .17110    .52733<    .41287  38.77< *****     1.1
KPAC   KPAU   *    .02260+-   .00840    .02261+-   .01705   1.00+-  .84      .0
OCTC   OCTU   *    .40530+-   .31560    .60326+-   .53799   1.49+- 1.76      .3
ECTC   ECTU   *    .10010+-   .07620    .33617+-   .20236   3.36+- 3.26     1.1
TCTC   TCTU        .50540+-   .35970    .95096+-   .48613   1.88+- 1.65      .7
NAXC   NAXU   *    .00000<    .01880    .00042<    .01480    .00<   .00      .0
MGXC   MGXU   *    .00000<    .00830    .00174<    .00675    .00<   .00      .2
ALXC   ALXU   *    .01450+-   .00180    .00981+-   .00349    .68+-  .26    -1.2
SIXC   SIXU   *    .02950+-   .00270    .03003+-   .00659   1.02+-  .24      .1
SUXC   SUXU        .39590+-   .01990    .35677+-   .03532    .90+-  .10    -1.0
CLXC   CLXU   *    .00000<    .00760    .00439<    .00239    .00<   .00      .6
KPXC   KPXU   *    .02260+-   .00130    .02240+-   .00170    .99+-  .09     -.1
CAXC   CAXU   *    .00570+-   .00080    .00679+-   .00298   1.19+-  .55      .4
TIXC   TIXU   *    .00000<    .00870    .00091<    .00786    .00<   .00      .1
CRXC   CRXU   *    .00000<    .00180    .00020<    .00079    .00<   .00      .1
MNXC   MNXU   *    .00000<    .00080    .00025<    .00056    .00<   .00      .3
FEXC   FEXU   *    .00690+-   .00100    .00882+-   .00323   1.28+-  .50      .6
NIXC   NIXU   *    .00020<    .00040    .00023<    .00042   1.15<  3.13      .1
CUXC   CUXU   *    .00210+-   .00150    .00040+-   .00046    .19+-  .26    -1.1
ZNXC   ZNXU   *    .00270+-   .00210    .00069+-   .00043    .26+-  .26     -.9
ASXC   ASXU   *    .00020<    .00040    .00000<    .00039    .01<  1.94     -.4
SEXC   SEXU   *    .00040+-   .00010    .00047+-   .00022   1.18+-  .63      .3
BRXC   BRXU   *    .00140+-   .00010    .00017+-   .00023    .12+-  .16    -4.9
```

RBXC	RBXU	*	.00000<	.00020	.00004<	.00018	.00<	.00	.2
SRXC	SRXU	*	.00020+-	.00020	.00021+-	.00022	1.05+-	1.51	.0
ZRXC	ZRXU	*	.00000<	.00030	.00006<	.00028	.00<	.00	.1
PBXC	PBXU	*	.00000<	.00060	.00063<	.00076	.00<	.00	.6

Table 6.5.2d
CMB Results for Samples Acquired at the Buffalo Pass Site
during the Afternoon (1200-1800 MST) of 09/18/95
Trial 3

SOURCE CONTRIBUTION ESTIMATES - SITE: BP DATE: 09/18/95 CMB7 33889
SAMPLE DURATION 6 START HOUR 12 SIZE: F
R SQUARE .92 PERCENT MASS 117.5
CHI-SQUARE 1.39 DF 23

SOURCE *	TYPE	SCE(UG/M3)	STD ERR	TSTAT
11	MZSOILC	.1402	.0317	4.4208
13	MZMVCGC	.4722	.3408	1.3858
27	MZHD2DRY	.3169	.0365	8.6885
35	MZRWC3	.8326	.1046	7.9565
50	AMSUL	1.3380	.1350	9.9132
52	AMNIT	.2009	.0546	3.6781

MEASURED CONCENTRATION FOR SIZE: F
2.8+- .0

UNCERTAINTY/SIMILARITY CLUSTERS CMB7 33889 SUM OF CLUSTER SOURCES

SPECIES CONCENTRATIONS - SITE: BP DATE: 09/18/95 CMB7 33889
SAMPLE DURATION 6 START HOUR 12 SIZE: F
R SQUARE .92 PERCENT MASS 117.5
CHI-SQUARE 1.39 DF 23

SPECIES	I		MEAS		CALC		RATIO C/M		RATIO R/U
MSGC	MSGU	T	2.80880+-	.03870	3.30080+-	.34798	1.18+-	.12	1.4
CLIC	CLIU	*	.00960<	.03560	.02265<	.03133	2.36<	9.34	.3
N3IC	N3IU	*	.16540+-	.03050	.15657+-	.03021	.95+-	.25	-.2
S4IC	S4IU	*	1.15780+-	.06380	1.05986+-	.10801	.92+-	.11	-.8
SOIC	SOIU	*	2.17890+-	.15030	2.22348+-	.21357	1.02+-	.12	.2
SO4T	SO4TU		4.42620+-	.23430	4.34370+-	.33737	.98+-	.09	-.2
S32	S32U		.00000+-	.00000	.00000+-	.00000	.00+-	.00	-1000.0
S34	S34U		.00000+-	.00000	.00000+-	.00000	.00+-	.00	-1000.0
N4CC	N4CU	*	.40440+-	.03220	.45772+-	.04685	1.13+-	.15	.9
DDN4CC	DDN4CU		.01360<	.17110	.52818<	.41353	38.84<	*****	1.1
KPAC	KPAU	*	.02260+-	.00840	.02261+-	.01703	1.00+-	.84	.0
OCTC	OCTU	*	.40530+-	.31560	.60312+-	.53757	1.49+-	1.76	.3
ECTC	ECTU	*	.10010+-	.07620	.33604+-	.20221	3.36+-	3.26	1.1
TCTC	TCTU		.50540+-	.35970	.95069+-	.48575	1.88+-	1.65	.7
NAXC	NAXU	*	.00000<	.01880	.00042<	.01479	.00<	.00	.0
MGXC	MGXU	*	.00000<	.00830	.00174<	.00674	.00<	.00	.2
ALXC	ALXU	*	.01450+-	.00180	.00982+-	.00349	.68+-	.26	-1.2
SIXC	SIXU	*	.02950+-	.00270	.03002+-	.00659	1.02+-	.24	.1
SUXC	SUXU		.39590+-	.01990	.34796+-	.03354	.88+-	.10	-1.2
CLXC	CLXU	*	.00000<	.00760	.00440<	.00238	.00<	.00	.6
KPXC	KPXU	*	.02260+-	.00130	.02241+-	.00170	.99+-	.09	-.1
CAXC	CAXU	*	.00570+-	.00080	.00679+-	.00298	1.19+-	.55	.4
TIXC	TIXU	*	.00000<	.00870	.00091<	.00786	.00<	.00	.1
CRXC	CRXU	*	.00000<	.00180	.00020<	.00079	.00<	.00	.1
MNXC	MNXU	*	.00000<	.00080	.00025<	.00055	.00<	.00	.3
FEXC	FEXU	*	.00690+-	.00100	.00882+-	.00322	1.28+-	.50	.6
NIXC	NIXU	*	.00020<	.00040	.00023<	.00042	1.15<	3.13	.1
CUXC	CUXU	*	.00210+-	.00150	.00040+-	.00046	.19+-	.26	-1.1
ZNXC	ZNXU	*	.00270+-	.00210	.00069+-	.00043	.26+-	.26	-.9
ASXC	ASXU	*	.00020<	.00040	.00000<	.00039	.01<	1.94	-.4
SEXC	SEXU	*	.00040+-	.00010	.00047+-	.00022	1.18+-	.63	.3
BRXC	BRXU	*	.00140+-	.00010	.00017+-	.00023	.12+-	.16	-4.9

RBXC	RBXU	*	.00000<	.00020	.00004<	.00018	.00<	.00	.2
SRXC	SRXU	*	.00020+-	.00020	.00021+-	.00022	1.05+-	1.51	.0
ZRXC	ZRXU	*	.00000<	.00030	.00006<	.00028	.00<	.00	.1
PBXC	PBXU	*	.00000<	.00060	.00063<	.00076	.00<	.00	.6

Table 6.5.2e
CMB Results for Samples Acquired at the Buffalo Pass Site
during the Afternoon (1200-1800 MST) of 09/18/95
Trial 4

```
SOURCE CONTRIBUTION ESTIMATES -  SITE: BP           DATE: 09/18/95    CMB7 33889
SAMPLE DURATION        6       START HOUR        12        SIZE:    F
       R SQUARE       .85    PERCENT MASS     387.2
     CHI-SQUARE      1.41              DF        24

  SOURCE
     * TYPE     SCE(UG/M3)    STD ERR      TSTAT
-------------------------------------------
11     MZSOILC       .1760      .0368     4.7846
13     MZMVCGC       .6647      .4365     1.5229
32     MZHD2W6      9.0304     1.0139     8.9064
35     MZRWC3        .7993      .1319     6.0615
52     AMNIT         .2051      .0646     3.1734
-------------------------------------------

MEASURED CONCENTRATION FOR SIZE: F
       2.8+-      .0

       UNCERTAINTY/SIMILARITY CLUSTERS    CMB7 33889     SUM OF CLUSTER SOURCES
-------------------------------------------------------------------------------

-------------------------------------------------------------------------------

SPECIES CONCENTRATIONS -  SITE: BP           DATE: 09/18/95    CMB7 33889
SAMPLE DURATION        6       START HOUR        12        SIZE:    F
       R SQUARE       .85    PERCENT MASS     387.2
     CHI-SQUARE      1.41              DF        24

SPECIES-------I---MEAS------------------CALC-------------RATIO C/M----RATIO R/U
MSGC   MSGU   T   2.80880+-   .03870  10.87540+-  1.08965   3.87+-  .39     7.4
CLIC   CLIU   *    .00960<    .03560    .02796<    .04409   2.91< 11.74      .3
N3IC   N3IU   *    .16540+-   .03050    .15966+-   .03975    .97+-  .30     -.1
S4IC   S4IU   *   1.15780+-   .06380   2.84222+-  1.38407   2.45+- 1.20     1.2
SOIC   SOIU   *   2.17890+-   .15030   1.78260+-   .17113    .82+-  .10    -1.7
SO4T   SO4TU      4.42620+-   .23430    .49310+-   .06109    .11+-  .02   -16.2
S32    S32U        .00000+-   .00000    .00000+-   .00000    .00+-  .00 -1000.0
S34    S34U        .00000+-   .00000    .00000+-   .00000    .00+-  .00 -1000.0
N4CC   N4CU   *    .40440+-   .03220   1.59904+-   .41262   3.95+- 1.07     2.9
DDN4CC DDN4CU      .01360<    .17110    .07539<    .05903   5.54< 69.88      .3
KPAC   KPAU   *    .02260+-   .00840    .02167+-   .02398    .96+- 1.12     -.0
OCTC   OCTU   *    .40530+-   .31560    .69654+-   .75645   1.72+- 2.30      .4
ECTC   ECTU   *    .10010+-   .07620    .41082+-   .28386   4.10+- 4.22     1.1
TCTC   TCTU        .50540+-   .35970   1.11843+-   .68319   2.21+- 2.08      .8
NAXC   NAXU   *    .00000<    .01880    .00052<    .02082    .00<   .00      .0
MGXC   MGXU   *    .00000<    .00830    .00214<    .00949    .00<   .00      .2
ALXC   ALXU   *    .01450+-   .00180    .00869+-   .00413    .60+-  .29    -1.3
SIXC   SIXU   *    .02950+-   .00270    .03108+-   .00761   1.05+-  .28      .2
SUXC   SUXU        .39590+-   .01990    .75092+-   .27585   1.90+-  .70     1.3
CLXC   CLXU   *    .00000<    .00760    .00266<    .00335    .00<   .00      .3
KPXC   KPXU   *    .02260+-   .00130    .02239+-   .00238    .99+-  .12     -.1
CAXC   CAXU   *    .00570+-   .00080    .00663+-   .00387   1.16+-  .70      .2
TIXC   TIXU   *    .00000<    .00870    .00085<    .01106    .00<   .00      .1
CRXC   CRXU   *    .00000<    .00180    .00027<    .00111    .00<   .00      .1
MNXC   MNXU   *    .00000<    .00080    .00030<    .00078    .00<   .00      .3
FEXC   FEXU   *    .00690+-   .00100    .00929+-   .00409   1.35+-  .62      .6
NIXC   NIXU   *    .00020<    .00040    .00032<    .00060   1.60<  4.38      .2
CUXC   CUXU   *    .00210+-   .00150    .00055+-   .00065    .26+-  .36     -.9
ZNXC   ZNXU   *    .00270+-   .00210    .00079+-   .00061    .29+-  .32     -.9
ASXC   ASXU   *    .00020<    .00040    .00000<    .00055    .02<  2.73     -.3
SEXC   SEXU   *    .00040+-   .00010    .00015+-   .00030    .37+-  .75     -.8
BRXC   BRXU   *    .00140+-   .00010    .00012+-   .00032    .09+-  .23    -3.8
RBXC   RBXU   *    .00000<    .00020    .00005<    .00025    .00<   .00      .2
```

SRXC	SRXU	*	.00020+-	.00020	.00018+-	.00030	.90+-	1.75	-.1
ZRXC	ZRXU	*	.00000<	.00030	.00006<	.00039	.00<	.00	.1
PBXC	PBXU	*	.00000<	.00060	.00087<	.00107	.00<	.00	.7

Table 6.5.2f
CMB Results for Samples Acquired at the Buffalo Pass Site
during the Afternoon (1200-1800 MST) of 09/18/95
Trial 5

SOURCE CONTRIBUTION ESTIMATES - SITE: BP DATE: 09/18/95 CMB7 33889
SAMPLE DURATION 6 START HOUR 12 SIZE: F
R SQUARE .86 PERCENT MASS 210.4
CHI-SQUARE 1.39 DF 23

SOURCE *	TYPE	SCE(UG/M3)	STD ERR	TSTAT
11	MZSOILC	.1521	.0395	3.8532
13	MZMVCGC	.6793	.4792	1.4176
31	MZHD2WET	1.0147	.1188	8.5410
41	MZFFIREC	2.8718	1.6672	1.7226
50	AMSUL	.9926	.1836	5.4069
52	AMNIT	.1980	.0644	3.0720

MEASURED CONCENTRATION FOR SIZE: F
2.8+- .0

UNCERTAINTY/SIMILARITY CLUSTERS CMB7 33889 SUM OF CLUSTER SOURCES

SPECIES CONCENTRATIONS - SITE: BP DATE: 09/18/95 CMB7 33889
SAMPLE DURATION 6 START HOUR 12 SIZE: F
R SQUARE .86 PERCENT MASS 210.4
CHI-SQUARE 1.39 DF 23

SPECIES	I	T	MEAS		CALC		RATIO C/M		RATIO R/U
MSGC	MSGU	T	2.80880+-	.03870	5.90843+-	1.52592	2.10+-	.54	2.0
CLIC	CLIU	*	.00960<	.03560	.03323<	.04522	3.46<	13.67	.4
N3IC	N3IU	*	.16540+-	.03050	.15445+-	.04028	.93+-	.30	-.2
S4IC	S4IU	*	1.15780+-	.06380	1.00070+-	.15780	.86+-	.14	-.9
SOIC	SOIU	*	2.17890+-	.15030	2.16709+-	.20720	.99+-	.12	-.0
SO4T	SO4TU		4.42620+-	.23430	4.05633+-	.32813	.92+-	.09	-.9
S32	S32U		.00000+-	.00000	.00000+-	.00000	.00+-	.00	-1000.0
S34	S34U		.00000+-	.00000	.00000+-	.00000	.00+-	.00	-1000.0
N4CC	N4CU	*	.40440+-	.03220	.47713+-	.06283	1.18+-	.18	1.0
DDN4CC	DDN4CU		.01360<	.17110	.52122<	.40809	38.33<	*****	1.1
KPAC	KPAU	*	.02260+-	.00840	.00371+-	.02466	.16+-	1.09	-.7
OCTC	OCTU	*	.40530+-	.31560	1.72713+-	.89436	4.26+-	3.98	1.4
ECTC	ECTU	*	.10010+-	.07620	.37795+-	.29401	3.78+-	4.11	.9
TCTC	TCTU		.50540+-	.35970	2.14730+-	.86030	4.25+-	3.47	1.8
NAXC	NAXU	*	.00000<	.01880	.00080<	.02127	.00<	.00	.0
MGXC	MGXU	*	.00000<	.00830	.00260<	.00970	.00<	.00	.2
ALXC	ALXU	*	.01450+-	.00180	.01053+-	.00449	.73+-	.32	-.8
SIXC	SIXU	*	.02950+-	.00270	.03335+-	.00782	1.13+-	.28	.5
SUXC	SUXU		.39590+-	.01990	.31597+-	.03643	.80+-	.10	-1.9
CLXC	CLXU	*	.00000<	.00760	.00765<	.00448	.00<	.00	.9
KPXC	KPXU	*	.02260+-	.00130	.00864+-	.00428	.38+-	.19	-3.1
CAXC	CAXU	*	.00570+-	.00080	.01720+-	.01681	3.02+-	2.98	.7
TIXC	TIXU	*	.00000<	.00870	.00101<	.01130	.00<	.00	.1
CRXC	CRXU	*	.00000<	.00180	.00028<	.00114	.00<	.00	.1
MNXC	MNXU	*	.00000<	.00080	.00026<	.00080	.00<	.00	.2
FEXC	FEXU	*	.00690+-	.00100	.00952+-	.00372	1.38+-	.57	.7
NIXC	NIXU	*	.00020<	.00040	.00033<	.00061	1.65<	4.48	.2
CUXC	CUXU	*	.00210+-	.00150	.00056+-	.00066	.27+-	.37	-.9
ZNXC	ZNXU	*	.00270+-	.00210	.00058+-	.00063	.22+-	.29	-1.0
ASXC	ASXU	*	.00020<	.00040	.00001<	.00056	.06<	2.80	-.3
SEXC	SEXU	*	.00040+-	.00010	.00050+-	.00031	1.24+-	.84	.3
BRXC	BRXU	*	.00140+-	.00010	.00023+-	.00033	.16+-	.24	-3.4

RBXC	RBXU	*	.00000<	.00020	.00004<	.00025	.00<	.00	.1
SRXC	SRXU	*	.00020+-	.00020	.00028+-	.00031	1.42+-	2.11	.2
ZRXC	ZRXU	*	.00000<	.00030	.00007<	.00040	.00<	.00	.1
PBXC	PBXU	*	.00000<	.00060	.00092<	.00110	.00<	.00	.7

Table 6.5.2g
CMB Results for Samples Acquired at the Buffalo Pass Site
during the Afternoon (1200-1800 MST) of 09/18/95
Trial 6

SOURCE CONTRIBUTION ESTIMATES - SITE: BP DATE: 09/18/95 CMB7 33889
SAMPLE DURATION 6 START HOUR 12 SIZE: F
R SQUARE .89 PERCENT MASS 132.3
CHI-SQUARE 1.57 DF 22

SOURCE	*	TYPE	SCE(UG/M3)	STD ERR	TSTAT
11		MZSOILC	.1364	.0326	4.1879
13		MZMVCGC	.4429	.3306	1.3398
31		MZHD2WET	1.2485	.5346	2.3355
35		MZRWC3	.8463	.1061	7.9789
46		MZGSC	-.0198	.0530	-.3731
50		AMSUL	.8565	.2982	2.8717
52		AMNIT	.2061	.0544	3.7883

MEASURED CONCENTRATION FOR SIZE: F
2.8+- .0

UNCERTAINTY/SIMILARITY CLUSTERS CMB7 33889 SUM OF CLUSTER SOURCES

SPECIES CONCENTRATIONS - SITE: BP DATE: 09/18/95 CMB7 33889
SAMPLE DURATION 6 START HOUR 12 SIZE: F
R SQUARE .89 PERCENT MASS 132.3
CHI-SQUARE 1.57 DF 22

SPECIES	I		MEAS		CALC		RATIO C/M		RATIO R/U
MSGC	MSGU	T	2.80880+-	.03870	3.71684+-	.42458	1.32+-	.15	2.1
CLIC	CLIU	*	.00960<	.03560	.01857<	.02944	1.93<	7.80	.2
N3IC	N3IU	*	.16540+-	.03050	.15815+-	.02908	.96+-	.25	-.2
S4IC	S4IU	*	1.15780+-	.06380	.96681+-	.17865	.84+-	.16	-1.0
SOIC	SOIU	*	2.17890+-	.15030	2.20740+-	.37997	1.01+-	.19	.1
SO4T	SO4TU		4.42620+-	.23430	4.03797+-	.57950	.91+-	.14	-.6
S32	S32U		.00000+-	.00000	.00000+-	.00000	.00+-	.00	-1000.0
S34	S34U		.00000+-	.00000	.00000+-	.00000	.00+-	.00	-1000.0
N4CC	N4CU	*	.40440+-	.03220	.47311+-	.06194	1.17+-	.18	1.0
DDN4CC	DDN4CU		.01360<	.17110	.64135<	.50214	47.16<	*****	1.2
KPAC	KPAU	*	.02260+-	.00840	.02266+-	.01599	1.00+-	.80	.0
OCTC	OCTU	*	.40530+-	.31560	.58788+-	.50424	1.45+-	1.68	.3
ECTC	ECTU	*	.10010+-	.07620	.32558+-	.18979	3.25+-	3.12	1.1
TCTC	TCTU		.50540+-	.35970	.92519+-	.45573	1.83+-	1.58	.7
NAXC	NAXU	*	.00000<	.01880	-.00045<	.01395	.00<	.00	-.0
MGXC	MGXU	*	.00000<	.00830	.00156<	.00632	.00<	.00	.1
ALXC	ALXU	*	.01450+-	.00180	.01006+-	.00359	.69+-	.26	-1.1
SIXC	SIXU	*	.02950+-	.00270	.02994+-	.00675	1.01+-	.25	.1
SUXC	SUXU		.39590+-	.01990	.29885+-	.03914	.75+-	.11	-2.2
CLXC	CLXU	*	.00000<	.00760	.00486<	.00224	.00<	.00	.6
KPXC	KPXU	*	.02260+-	.00130	.02241+-	.00161	.99+-	.09	-.1
CAXC	CAXU	*	.00570+-	.00080	.00659+-	.00290	1.16+-	.53	.3
TIXC	TIXU	*	.00000<	.00870	.00094<	.00737	.00<	.00	.1
CRXC	CRXU	*	.00000<	.00180	.00018<	.00074	.00<	.00	.1
MNXC	MNXU	*	.00000<	.00080	.00024<	.00052	.00<	.00	.3
FEXC	FEXU	*	.00690+-	.00100	.00866+-	.00314	1.25+-	.49	.5
NIXC	NIXU	*	.00020<	.00040	.00021<	.00040	1.06<	2.91	.0
CUXC	CUXU	*	.00210+-	.00150	.00038+-	.00043	.18+-	.24	-1.1
ZNXC	ZNXU	*	.00270+-	.00210	.00068+-	.00041	.25+-	.25	-.9
ASXC	ASXU	*	.00020<	.00040	-.00000<	.00036	-.01<	1.82	-.4
SEXC	SEXU	*	.00040+-	.00010	.00056+-	.00022	1.39+-	.64	.7

BRXC	BRXU	*	.00140+-	.00010	.00018+-	.00022	.13+-	.16	-5.1
RBXC	RBXU	*	.00000<	.00020	.00004<	.00016	.00<	.00	.2
SRXC	SRXU	*	.00020+-	.00020	.00022+-	.00020	1.09+-	1.49	.1
ZRXC	ZRXU	*	.00000<	.00030	.00006<	.00026	.00<	.00	.1
PBXC	PBXU	*	.00000<	.00060	.00058<	.00071	.00<	.00	.6

Table 6.5.2h
CMB Results for Samples Acquired at the Buffalo Pass Site
during the Afternoon (1200-1800 MST) of 09/18/95
Trial 7

SOURCE CONTRIBUTION ESTIMATES - SITE: BP DATE: 09/18/95 CMB7 33889
SAMPLE DURATION 6 START HOUR 12 SIZE: F
R SQUARE .90 PERCENT MASS 135.2
CHI-SQUARE 2.53 DF 23

SOURCE	*	TYPE	SCE(UG/M3)	STD ERR	TSTAT
11		MZSOILC	.1434	.0279	5.1443
19		MZMVC	.6211	.2404	2.5833
31		MZHD2WET	1.0508	.1151	9.1336
35		MZRWC3	.8472	.0661	12.8117
50		AMSUL	.9314	.1692	5.5054
52		AMNIT	.2047	.0441	4.6452

MEASURED CONCENTRATION FOR SIZE: F
2.8+- .0

UNCERTAINTY/SIMILARITY CLUSTERS CMB7 33889 SUM OF CLUSTER SOURCES

SPECIES CONCENTRATIONS - SITE: BP DATE: 09/18/95 CMB7 33889
SAMPLE DURATION 6 START HOUR 12 SIZE: F
R SQUARE .90 PERCENT MASS 135.2
CHI-SQUARE 2.53 DF 23

SPECIES	I	T	MEAS		CALC		RATIO C/M		RATIO R/U
MSGC	MSGU	T	2.80880+-	.03870	3.79870+-	.28778	1.35+-	.10	3.4
CLIC	CLIU	*	.00960<	.03560	.01903<	.00804	1.98<	7.40	.3
N3IC	N3IU	*	.16540+-	.03050	.15957+-	.01587	.96+-	.20	-.2
S4IC	S4IU	*	1.15780+-	.06380	.97803+-	.15510	.84+-	.14	-1.1
SOIC	SOIU	*	2.17890+-	.15030	2.23632+-	.21466	1.03+-	.12	.2
SO4T	SO4TU		4.42620+-	.23430	4.13056+-	.33600	.93+-	.09	-.7
S32	S32U		.00000+-	.00000	.00000+-	.00000	.00+-	.00	-1000.0
S34	S34U		.00000+-	.00000	.00000+-	.00000	.00+-	.00	-1000.0
N4CC	N4CU	*	.40440+-	.03220	.46536+-	.05049	1.15+-	.15	1.0
DDN4CC	DDN4CU		.01360<	.17110	.53980<	.42263	39.69<	*****	1.2
KPAC	KPAU	*	.02260+-	.00840	.02301+-	.00018	1.02+-	.38	.0
OCTC	OCTU	*	.40530+-	.31560	.70023+-	.09594	1.73+-	1.37	.9
ECTC	ECTU	*	.10010+-	.07620	.39658+-	.09295	3.96+-	3.16	2.5
TCTC	TCTU		.50540+-	.35970	1.10854+-	.02874	2.19+-	1.56	1.7
NAXC	NAXU	*	.00000<	.01880	.00237<	.00342	.00<	.00	.1
MGXC	MGXU	*	.00000<	.00830	.00159<	.00074	.00<	.00	.2
ALXC	ALXU	*	.01450+-	.00180	.01013+-	.00238	.70+-	.19	-1.5
SIXC	SIXU	*	.02950+-	.00270	.03119+-	.00579	1.06+-	.22	.3
SUXC	SUXU		.39590+-	.01990	.30896+-	.03728	.78+-	.10	-2.1
CLXC	CLXU	*	.00000<	.00760	.00435<	.00029	.00<	.00	.6
KPXC	KPXU	*	.02260+-	.00130	.02221+-	.00051	.98+-	.06	-.3
CAXC	CAXU	*	.00570+-	.00080	.00721+-	.00243	1.27+-	.46	.6
TIXC	TIXU	*	.00000<	.00870	.00093<	.00027	.00<	.00	.1
CRXC	CRXU	*	.00000<	.00180	.00008<	.00009	.00<	.00	.0
MNXC	MNXU	*	.00000<	.00080	.00028<	.00012	.00<	.00	.3
FEXC	FEXU	*	.00690+-	.00100	.00904+-	.00306	1.31+-	.48	.7
NIXC	NIXU	*	.00020<	.00040	.00005<	.00008	.23<	.62	-.4
CUXC	CUXU	*	.00210+-	.00150	.00011+-	.00014	.05+-	.08	-1.3
ZNXC	ZNXU	*	.00270+-	.00210	.00065+-	.00023	.24+-	.21	-1.0
ASXC	ASXU	*	.00020<	.00040	.00003<	.00005	.15<	.37	-.4
SEXC	SEXU	*	.00040+-	.00010	.00046+-	.00009	1.15+-	.36	.4
BRXC	BRXU	*	.00140+-	.00010	.00027+-	.00014	.19+-	.10	-6.5

RBXC	RBXU	*	.00000<	.00020	.00004<	.00002	.00<	.00	.2
SRXC	SRXU	*	.00020+-	.00020	.00015+-	.00005	.75+-	.79	-.2
ZRXC	ZRXU	*	.00000<	.00030	.00004<	.00002	.00<	.00	.1
PBXC	PBXU	*	.00000<	.00060	.00017<	.00022	.00<	.00	.3

Table 6.5.3
Source Apportionment of Samples Collected during the Afternoon (1200-1800 MST) of 09/18/95
Using Regional Background Profile

```
SOURCE CONTRIBUTION ESTIMATES -  SITE: BP           DATE: 09/18/95    CMB7 33889
SAMPLE DURATION        6       START HOUR        12        SIZE:    F
       R SQUARE       .92    PERCENT MASS     110.6
     CHI-SQUARE       .49              DF        26

  SOURCE
     * TYPE     SCE(UG/M3)    STD ERR      TSTAT
-------------------------------------------
31     MZHD2WET      .9818      .1285     7.6395
49     MZRC         1.9545      .3603     5.4248
52     AMNIT         .1704      .0486     3.5081
-------------------------------------------

MEASURED CONCENTRATION FOR SIZE: F
       2.8+-      .0

       UNCERTAINTY/SIMILARITY CLUSTERS    CMB7 33889     SUM OF CLUSTER SOURCES
-------------------------------------------------------------------------------

-------------------------------------------------------------------------------

SPECIES CONCENTRATIONS -  SITE: BP           DATE: 09/18/95    CMB7 33889
SAMPLE DURATION        6       START HOUR        12        SIZE:    F
       R SQUARE       .92    PERCENT MASS     110.6
     CHI-SQUARE       .49              DF        26

SPECIES-------I---MEAS------------------CALC-------------RATIO C/M----RATIO R/U
MSGC   MSGU   T   2.80880+-   .03870   3.10667+-   .33461   1.11+-  .12      .9
CLIC   CLIU   *    .00960<    .03560    .00456<    .01810    .47<  2.58     -.1
N3IC   N3IU   *    .16540+-   .03050    .16600+-   .02104   1.00+-  .22      .0
S4IC   S4IU   *   1.15780+-   .06380    .82811+-   .20835    .72+-  .18    -1.5
SOIC   SOIU   *   2.17890+-   .15030   2.24433+-   .22935   1.03+-  .13      .2
SO4T   SO4TU      4.42620+-   .23430   4.00591+-   .38576    .91+-  .10     -.9
S32    S32U        .00000+-   .00000    .00000+-   .00000    .00+-  .00 -1000.0
S34    S34U        .00000+-   .00000    .00000+-   .00000    .00+-  .00 -1000.0
N4CC   N4CU   *    .40440+-   .03220    .39685+-   .06411    .98+-  .18     -.1
DDN4CC DDN4CU      .01360<    .17110    .64719<    .41992  47.59< *****     1.4
KPAC   KPAU   *    .02260+-   .00840    .00780+-   .00906    .34+-  .42    -1.2
OCTC   OCTU   *    .40530+-   .31560    .84510+-   .29991   2.09+- 1.78     1.0
ECTC   ECTU   *    .10010+-   .07620    .24012+-   .11887   2.40+- 2.18     1.0
TCTC   TCTU        .50540+-   .35970    .00091+-   .00029    .00+-  .00    -1.4
NAXC   NAXU   *    .00000<    .01880    .01325<    .01602    .00<   .00      .5
MGXC   MGXU   *    .00000<    .00830    .00557<    .00820    .00<   .00      .5
ALXC   ALXU   *    .01450+-   .00180    .03079+-   .02778   2.12+- 1.93      .6
SIXC   SIXU   *    .02950+-   .00270    .05923+-   .03673   2.01+- 1.26      .8
SUXC   SUXU        .39590+-   .01990    .28223+-   .07429    .71+-  .19    -1.5
CLXC   CLXU   *    .00000<    .00760    .00259<    .00882    .00<   .00      .2
KPXC   KPXU   *    .02260+-   .00130    .01367+-   .01030    .60+-  .46     -.9
CAXC   CAXU   *    .00570+-   .00080    .01617+-   .01339   2.84+- 2.38      .8
TIXC   TIXU   *    .00000<    .00870    .00076<    .00858    .00<   .00      .1
CRXC   CRXU   *    .00000<    .00180    .00009<    .00095    .00<   .00      .0
MNXC   MNXU   *    .00000<    .00080    .00024<    .00061    .00<   .00      .2
FEXC   FEXU   *    .00690+-   .00100    .01528+-   .01077   2.21+- 1.59      .8
NIXC   NIXU   *    .00020<    .00040    .00011<    .00038    .56<  2.22     -.2
CUXC   CUXU   *    .00210+-   .00150    .00081+-   .00144    .39+-  .74     -.6
ZNXC   ZNXU   *    .00270+-   .00210    .00450+-   .00514   1.67+- 2.30      .3
ASXC   ASXU   *    .00020<    .00040    .00012<    .00079    .58<  4.12     -.1
SEXC   SEXU   *    .00040+-   .00010    .00050+-   .00042   1.25+- 1.09      .2
BRXC   BRXU   *    .00140+-   .00010    .00070+-   .00042    .50+-  .30    -1.6
RBXC   RBXU   *    .00000<    .00020    .00007<    .00036    .00<   .00      .2
SRXC   SRXU   *    .00020+-   .00020    .00032+-   .00040   1.60+- 2.56      .3
```

ZRXC	ZRXU	*	.00000<	.00030	.00013<	.00057	.00<	.00	.2
PBXC	PBXU	*	.00000<	.00060	.00015<	.00119	.00<	.00	.1

Table 6.5.4
Summary of the Absolute Percent Difference
between Measured and Calculated Light Extinction

Site	Relative Humidity < 90%	Number of Samples	Relative Humidity < 80%	Number of Samples	Relative Humidity < 70%	Number of Samples
Baggs	18.6	58	17.1	54	16.8	53
Buffalo Pass	23.8	80	23.5	64	23.7	56
Gilpin Creek	41.4	40	39.7	38	39.7	34
Hayden Waste Water	18.7	66	17.5	61	17.0	55
Hayden VOR	31.0	62	29.8	59	31.3	55
Juniper Mountain	7.42	44	9.23	42	12.7	40
All	23.2	350	22.5	318	23.0	293

Although the best fit solution overestimates mass by 29.7%, the difference between measured (2.8 ± 0.04 ug/m^3) and calculated (3.6 ± 0.4 ug/m^3) mass is not significant because: 1) the measured mass is very low; and 2) the measured mass overlaps within two standard deviations of the calculated value. The CHI-SQUARE of 1.41 is driven mainly by the underestimation of bromine, which is usually an indicator of leaded-gasoline additives. However, lead is not detected in this sample. It is possible that an unidentified source is responsible for the high bromine concentration. Malm (1996) speculated for Project MOHAVE data that bromine levels are often enriched in some vegetative burning sources.

Good agreement between calculated and measured concentrations were obtained for sulfate, sulfur dioxide, and soluble potassium with a ratio of calculated to measured value (i.e., RATIO C/M) being unity within one standard deviation. Both organic and elemental carbon were overestimated, but this did not greatly influence the CHI-SQUARE, as indicated by the low RATIO R/U for these species (i.e., the ratio of the signed difference between the calculated and measured concentrations [the residual], divided by the uncertainty of the residual).

The initial fit (Trial 1) in Table 6.5.2b was similar to the "best fit" (Table 6.5.2a) solution except that a composite paved road dust profile (MZPVRDC) was substituted for the composite soil profile (MZSOILC). As shown in Table 6.5.2, the composite geological profile (MZSOILC) gives a better fit (i.e., lower RATIO R/U) for the crustal components such as aluminum, silicon, and iron, but not by a significant extent. Geological material (0.11 ± 0.02 ug/m^3) appears to be a minor contributor to mass in this sample, however.

In Trial 2 (Table 6.5.2c), a generating station profile representing "fresh" emissions sampled at the Hayden Unit 2 stack (MZHD2PPC) was substituted for a profile aged for two hours under moist conditions (MZHD2WET). This resulted in a tenfold decrease in the estimated generating station contribution to mass (from 1.04 ± 0.1 ug/m^3 to 0.11 ± 0.01 ug/m^3), which equated to a decrease in the estimated generating station contribution to sulfate from 0.28 to 0.01 ug/m^3. Much this mass is compensated by an increase in the AMSUL contribution without significant changes in the CMB performance measures or other source contribution estimates.

In Trial 3 (Table 6.5.2d), a generating station profile aged under dry conditions for six hours (MZHD2DRY) was substituted for the wet-aged profile (MZHD2WET). The estimated generating station contributions to mass (0.32 ug/m^3) and to sulfate (0.08 ug/m^3) were approximately 30% of those calculated with the wet-aged profile (Table 6.5.2a).

In Trial 4 (Table 6.5.2e), a generating station profile aged under wet conditions for six hours (MZHD2W6) instead of two hours (MZHD2WET) was included in the CMB calculations. In this case, the mass was overestimated by a factor of 3.9. These results demonstrate that the gas-to-particle transformation process of generating station emissions under wet conditions in the Yampa Valley can reasonably be explained by two hours of aging in a fog or cloud by the Aerosol Evolution Model, but not by six or more hours of aging using this model.

In Trial 5 (Table 6.5.2f), a composite profile representing the Pinion-Juniper range fire (MZFIREC) was substituted for the residential wood combustion profile (MZRWC3). This resulted in an overestimation of $PM_{2.5}$ mass by a factor of two, which is due mainly to underestimating the measured soluble potassium and overestimating the measured carbon concentrations. An extremely high organic-to-total-carbon ratio of 0.94 was found in this profile as compared to the corresponding ratio of 0.71 in the residential wood combustion profile (MZRWC3). Even though the organic-to-total-carbon ratio is 0.90 for this test sample, further examination of the ambient data indicates that the average organic-to-total-carbon ratios ranged from 0.57 at the Gilpin Creek site to 0.84 at the Buffalo Pass site. The residential wood combustion profile (MZRWC3) is therefore selected in most of the CMB calculations to represent "vegetative burning" emissions in the study region.

In Trial 6 (Table 6.5.2g), a geothermal spring emission profile (MZGSC) was added to the "best fit" combination. No contribution from this source was detected. Note that this profile contains 17.6% chloride, which was not detected in the ambient sample acquired on 09/18/95. Therefore, it is apparent that hot-springs emissions did not impact the Buffalo Pass site on this sampling period.

Finally, in Trial 7 (Table 6.5.2h), a composite motor vehicle profile (MZMVC) was substituted for the motor vehicle profile acquired in Craig (MZMVCGC). The CHI-SQUARE in this case (2.53) is higher than that of the "best fit" (1.41) because key elements such as organic carbon, elemental carbon, and bromine are not explained well by the composite motor vehicle profile (MZMVC). Since the TSTAT (t-statistic) in the "best fit" case is low (1.38), it implies that the motor vehicle source contributions are associated with large uncertainty intervals.

From the results presented in Table 6.5.1 and similar tests on other samples, it is concluded that: 1) the magnitude of source contributions are insensitive to choice of profile; 2) the Craig motor vehicle profile provides a better explanation of measured concentrations than other profiles; 3) the contribution of (background) secondary ammonium nitrate was small (0.20 ug/m^3) and extremely stable with respect to varying the mix of other source profile types; 4) the contribution of secondary ammonium sulfate depends on whether fresh, dry-aged, or wet-aged generating station profiles are used, being larger with fresh or dry profiles and smaller with wet-aged generating station profiles; and 5) coal-fired generating station profiles can only have aged in a cloud or fog for a few hours prior to arriving at Buffalo Pass.

6.5.2 Generating Station Contributions to Sulfate

It is apparent from the tests shown in Table 6.5.1, and in tests with other samples, that the CMB by itself returns equally valid results for coal-fired generating station emissions that are fresh, dry-aged, or wet-aged for a few hours. It is also clear that further wet-aging beyond ~2 hours in a cloud or fog provides unrealistic estimates of $PM_{2.5}$ mass and sulfate concentrations. The measured sulfate concentration for the Buffalo Pass afternoon sample on September 18 was 1.16 ± 0.06 ug/m^3. The results given in Tables 6.5.2c (Trial 2), 6.5.2d (Trial 3), and 6.5.2a ("best fit") indicate that "fresh" emissions would have contributed only 0.01 ?g/m^3 of sulfate, that dry-aged (six hours)

emissions would have contributed 0.08 ug/m^3 of sulfate, and that wet-aged (two hours) emissions would have contributed 0.28 ug/m^3, or 24% of the measured sulfate. Each of these fits to the data yields comparable values for CMB performance measures.

An alternative source apportionment approach uses a regional background profile that excludes the impact of Yampa Valley generating station emissions but includes other source emissions. The disadvantage of this approach is that the source contributions from geological, motor vehicle exhaust, vegetative burning, and secondary ammonium sulfate are combined in the regional source contribution and cannot be individually resolved. However, this approach is a simple means of separating Yampa Valley generating station contributions from those of other sources.

$PM_{2.5}$ measured at the Buffalo Pass site on 09/18/95 (1200-1800 MST) was apportioned using the regional composite profile (MZRC), the wet-aged generating station profile (MZHD2WET), and a profile representing secondary ammonium nitrate (AMNIT). As shown in Table 6.5.3, this solution is better than the one given for the "best fit" in Table 6.5.2a according to the CMB performance measures. The results in Table 6.5.3 show a percent mass of 110.6 as compared to 129.7 in the "best fit", and a CHI-SQUARE of 0.49 as compared to 1.41 in the "best fit" of Table 6.5.2a. The regional contribution is probably more accurate than the sum of the geological, motor vehicle, vegetative burning, and secondary ammonium sulfate contributions shown in Tables 6.5.2a through 6.5.2h.

Note, however, the similarity of the generating station contribution in the regional and "best fit" cases. The generating station contribution to sulfate in the regional apportionment case is 0.28 ug/m^3, which is identical to the generating station contribution in the "best fit" case. As discussed in Section 6.3, secondary ammonium sulfate is enriched in the regional profile, accounting for approximately 40% of the sum of the measured species. Table 6.5.3 shows a ratio of calculated-to-measured sulfate of 0.91 ± 0.1 without the inclusion of the AMSUL profile.

Secondary ammonium nitrate only accounts for 2% of the sum of the measured species in the regional profile, which does not account for the measured ammonium nitrate at the Buffalo Pass site. Tables 6.5.2a and 6.5.3 show that the secondary ammonium nitrate contributions are 0.17 ± 0.05 ug/m^3 for the regional apportionment case and 0.20 ± 0.05 ug/m^3 for the "best fit" case. This implies that a majority (85% in this case) of the ammonium nitrate does not originate from the regional background. Gas-to-particle transformation of nitrogen oxides or nitric acid and ammonia to ammonium nitrate occurred in the Yampa Valley and was transported to the Wilderness.

This independent apportionment lends confidence in the stability and consistency of the CMB modeling. The uncertainty in the "best fit" apportionment can be attributed to the apportionments of the individual non-generating-station sources.

6.5.3 Average Source Contributions to $PM_{2.5}$

A total of 367 CMB source apportionments were conducted for each sampling period at all six sites with valid concentrations of sulfate, nitrate, organic and elemental carbon, and trace elements. For the ambient concentrations used in these apportions, nitrate concentrations were adjusted to include volatilized ammonium and nitrate as explained in Appendix A, and this volatilized portion was also added to the measured $PM_{2.5}$ mass.

Based on the test CMB results discussed above, each apportionment initially included a geological profile, a motor vehicle emissions profile, a vegetative burning profile, and a dry- or wet-aged coal-fired generating station emissions profile. The dry-aged profiles were reacted for six hours while the wet-aged profiles were reacted for two hours. Profiles for secondary ammonium sulfate and secondary ammonium nitrate were also included. Wet-aged profiles were used when there was evidence that generating station plumes had encountered fogs or clouds, and dry-aged profiles were used otherwise. Section 6.6 discusses the evidence of wet and dry processing of generating station plumes. With this choice, generating station contributions to $PM_{2.5}$ mass and sulfate are intended to maximize, rather than to minimize, the source contribution estimates from these sources. If there is a bias to CMB source apportionments as applied here, it is to overestimate rather than to underestimate local generating station contributions.

Although uncertainty/similarity clusters were not found during the sensitivity tests shown in Table 6.5.1, clusters were found for several samples that included vegetative burning and motor vehicle exhaust profiles. This occurs because organic and elemental carbon are the major components of both motor vehicle and vegetative burning emissions, and the OC and EC abundances have large variabilities in these profiles. Since the forest fire profile (MZFIREC) did not explain the measured concentrations as well as the profile obtained from residential wood combustion sampling (i.e., MZRWC3), it may not represent most of the burning that affected receptor concentrations. As a result, the standard errors of motor vehicle exhaust and vegetative burning source contribution estimates are large.

Source contributions to $PM_{2.5}$ mass for each chemically-characterized sample at each site are presented in Appendix D. Figure 6.5.1 compares the average source contributions of each source-type to $PM_{2.5}$ at each measurement site as estimated from CMB analyses. Recall from Section 4.2 that sample selection was biased toward those samples corresponding to elevated light scattering and $PM_{2.5}$ mass concentrations. As a result, the source contribution averages in Figure 6.5.1 are higher than those that would be found for an actual annual average.

On average, the large contributors to $PM_{2.5}$ at all sites were geological material, vehicle exhaust (or other secondary organics), vegetative burning, and secondary ammonium sulfate. Each of these averaged from ~0.5 to ~1.0 ug/m^3 contribution. Average ammonium nitrate and local coal-fired generating station emissions were minor contributors, except at the Hayden VOR and Hayden Waste Water sites, where local generating station contributions were also large. Geological and vehicle exhaust contributions were also larger at these

Yampa Valley sites than their contributions in the other less populated areas that were sampled.

The average geological contribution ranged from 0.69 ± 0.17 ug/m^3 (15% of the total calculated $PM_{2.5}$ mass) at the Gilpin Creek site to 1.56 ± 0.28 ug/m^3 (24% of $PM_{2.5}$ mass) at the Hayden VOR site. The primary motor vehicle contribution ranged from 0.78 ± 0.58 ug/m^3 (19% of $PM_{2.5}$ mass) at the Buffalo Pass site to 1.78 ± 1.18 ug/m^3 (28% of $PM_{2.5}$ mass) at the Hayden VOR site or 1.75 ± 1.23 ug/m^3 (30% of $PM_{2.5}$ mass) at the Hayden Waste Water site. The average motor vehicle contribution at the Gilpin Creek site was high (1.47 ± 1.1 ug/m^3), but Appendix D shows these source contributions estimates having especially high uncertainties. This could be a consequence of the organic carbon sampling artifact resulting from the low sampling flow rate (5 L/min) of the Mini-vol samplers and the long sampling period (12 hours) at the Gilpin Creek site. It could also be due to misapportionment of vegetative burning contributions to the vehicle exhaust category. The average organic carbon at the Gilpin Creek site (1.2 ± 1.6 ug/m^3) is 30% higher than the average at the Buffalo Pass site (0.92 ± 0.77 ug/m^3).

Average contributions from vegetative burning ranged from 0.60 ± 0.56 ug/m^3 (15% of $PM_{2.5}$ mass) at the Baggs site and 0.61 ± 0.35 ug/m^3 (11% of $PM_{2.5}$ mass) at the Hayden Waste Water site to 0.84 ± 0.37 ug/m^3 (19% of $PM_{2.5}$ mass) at the Gilpin Creek site. As discussed in Section 4.2, the Gilpin Creek site reported the highest average elemental carbon concentration (0.96 ± 0.81 ug/m^3), two to four times that measured at the other sites. CMB modeling indicates that the large carbon concentrations result from vegetative burning and motor vehicle contributions.

Average contributions from Yampa Valley coal-fired generating stations constituted ~15% of $PM_{2.5}$ mass at the two Valley sites, being 0.97 ± 0.28 ug/m^3 at the Hayden VOR site and 0.89 ± 0.18 ug/m^3 at the Hayden Waste Water site. Average coal-fired generating station contributions were lowest (2% of $PM_{2.5}$ mass) at the Juniper Mountain site (0.07 ± 0.17 ug/m^3) and at the Gilpin Creek site (0.09 ± 0.03 ug/m^3). These values are less than 10% of those calculated for the valley sites. Local generating station contributions at the Buffalo Pass site were 0.18 ± 0.04 ug/m^3, or 4% of $PM_{2.5}$ mass. At the Baggs site, they were 0.19 ± 0.06 ug/m^3, or 5% of $PM_{2.5}$ mass. Generating station contributions displayed the largest site-to-site variations, being highest near the sources in the Yampa Valley and lowest at the more remote sites.

Average contributions from secondary ammonium sulfate were similar among all sites (1.0 to 1.2 ug/m^3), as would be expected if the majority of this sulfate originated from emissions outside the Yampa Valley. Secondary ammonium nitrate contributions were low, ranging from 0.14 ± 0.12 ug/m^3 (3% of $PM_{2.5}$ mass) at the Juniper Mountain site and 0.14 ± 0.10 ug/m^3 (4% of $PM_{2.5}$ mass) at the Baggs site to 0.46 ± 0.19 ug/m^3 (8% of $PM_{2.5}$ mass) at the Hayden Waste Water site.

6.5.4 Maximum Source Contributions to $PM_{2.5}$

Individual source contribution estimates (Appendix D) were examined to determine where and when the contributions from each source-type was found. For local coal-fired generating stations, the maximum contribution to $PM_{2.5}$ at the Buffalo Pass site was 1.07 ± 0.12 ug/m^3 on 09/19/95 (1200 MST), and the second highest contribution was 1.00 ± 0.12 ug/m^3 on 09/18/95

(1200 MST). At the Gilpin Creek site, the maximum $PM_{2.5}$ contribution was 0.32 ± 0.09 ug/m^3 on 09/27/95 (0600 MST), and the second highest contribution was 0.26 ± 0.04 ug/m^3 on 03/31/95.

During the MZVS, the highest measured $PM_{2.5}$ mass of 20.4 ± 0.04 ug/m^3 was measured on 08/24/95 (0600 MST) at the Buffalo Pass site. This sample reported the highest primary geological (8.5 ± 0.9 ug/m^3) and vegetative burning (9.2 ± 5.5 ug/m^3) source contributions. These estimates are 7 to 12 times higher than the average source contributions shown in Figure 6.5.1. While the contributions from the coal-fired generating station (0.13 ± 0.02 ug/m^3) and secondary ammonium nitrate (0.28 ± 0.2 ug/m^3) are similar to their average contributions, contributions from secondary ammonium sulfate (1.8 ± 0.3 ug/m^3), and primary motor vehicle exhaust (2.4 ± 1.6 ug/m^3) were 1.5 and 3 times higher during the morning of 08/24/95 than the study averages at the Buffalo Pass site. Elevated concentrations were found for black carbon, organic carbon, elemental carbon, and soluble potassium on this sample. CMB performance measures for this sample are within target ranges, with 108.9 for percent mass explained, 0.97 for R^2, and 0.38 for CHI-SQUARE. Even though the average relative humidity during the morning of 08/24/95 was 94%, the measured light extinction is only 32.8 ± 5.6 Mm^{-1}.

6.5.5 Source Contributions to Light Extinction

In addition to estimating contributions from each source type to $PM_{2.5}$ mass, the CMB model also estimated the contributions from each source type to nitrate, sulfate, organic carbon, elemental carbon, and geological concentrations. To obtain the contribution of each source type to extinction, the source-specific contribution to each chemical component was multiplied by the extinction efficiency for that component (Appendix B.2), and the resulting extinctions were summed for each source type. Clean air scattering values for each site were added to complete the extinction budget. Individual contributions to extinction for each sample are tabulated in Appendix D.

Measured (OPTEC nephelometer) and calculated (sum of the individual source contributions) extinction agree to within 23% on average (absolute difference) for all samples with relative humidity less than 90%. Table 6.5.4 summarizes the absolute percent difference between measured and calculated extinction as a function of relative humidity. The absolute difference improved by only 1% to 2% as relative humidity decreased from 90% to 70%. The percent difference between the measured and calculated extinction would be much lower if the "average" rather than "absolute" difference were used in this calculation.

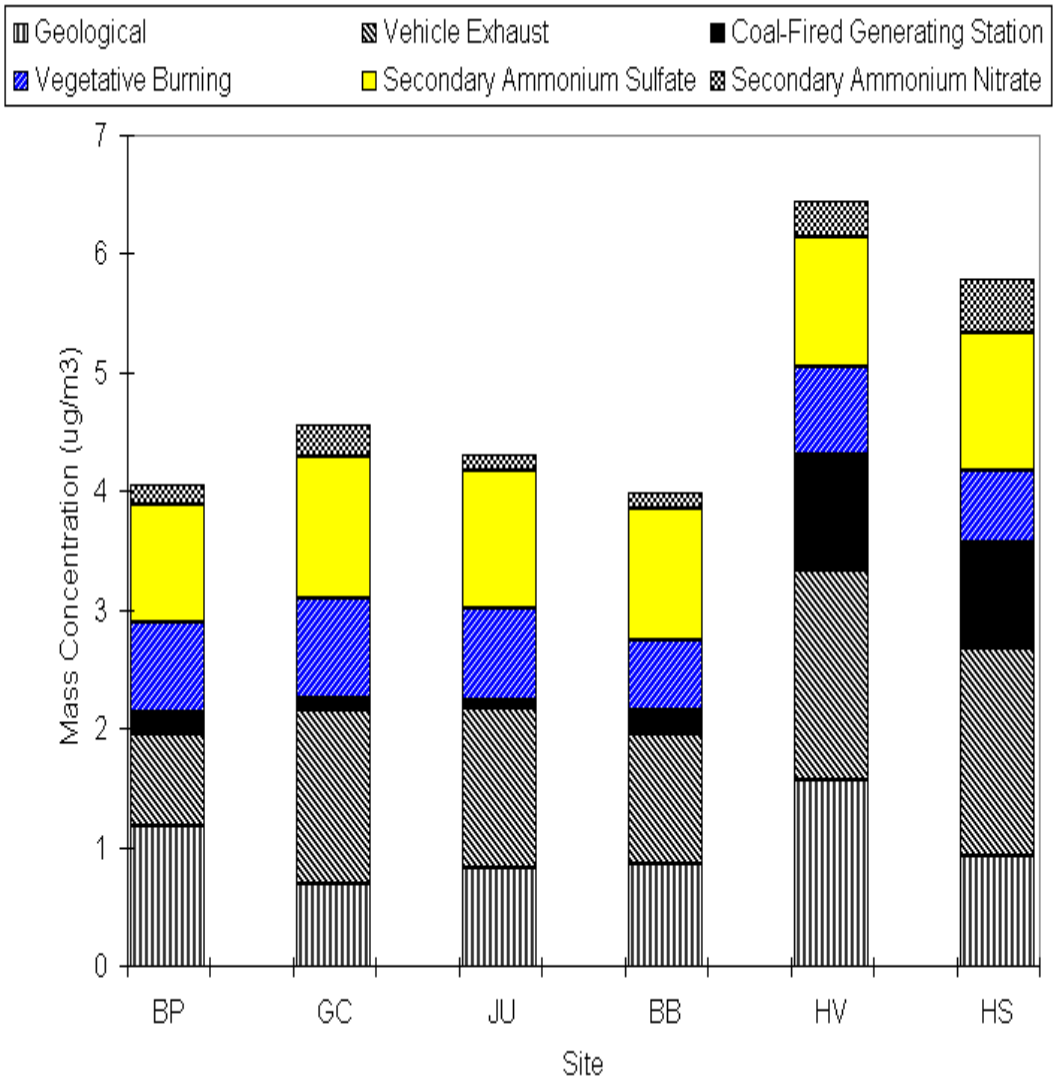

Figure 6.5.1 Average source contributions to $PM_{2.5}$ mass concentrations

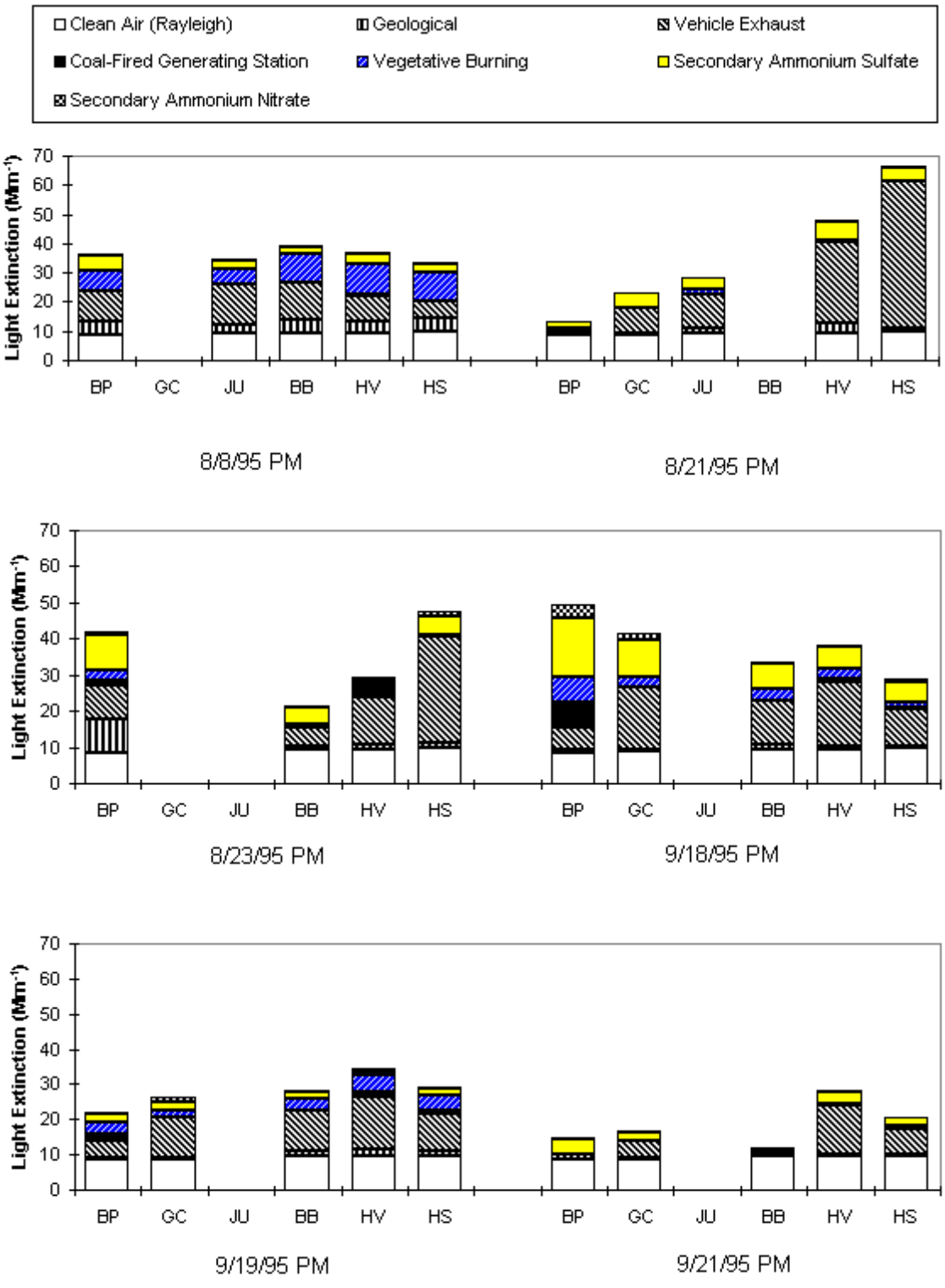

Figure 6.5.2 Chemical mass balance source contributions to extinction during haze events.

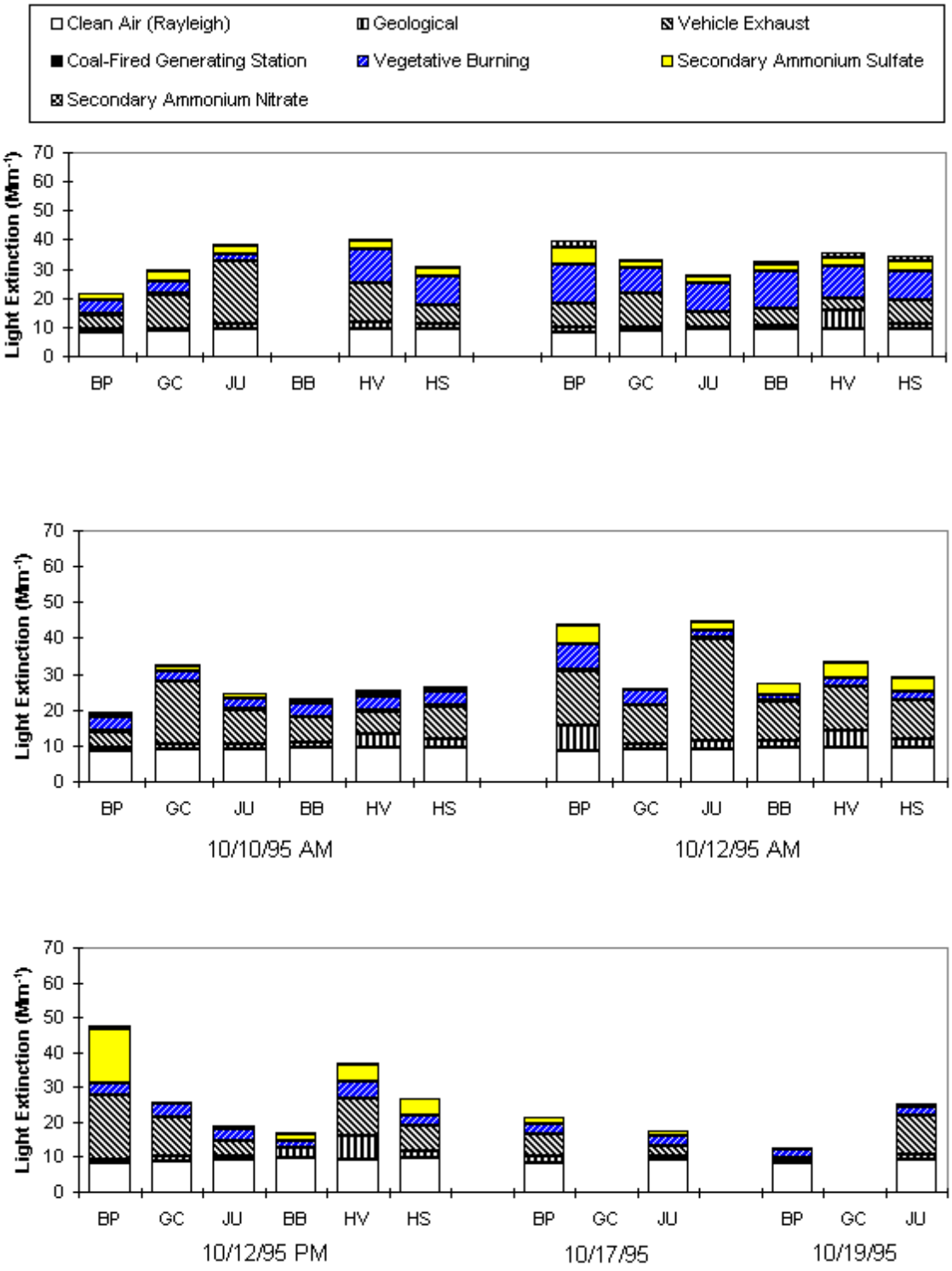

Figure 6.5.2 continued

Table 6.5.5 summarizes the contributions from each source category to extinction for four different categories of measured extinction: <15 Mm^{-1}, 15 to 20 Mm^{-1}, 20-30 Mm^{-1}, and 30 to 60 Mm^{-1}. Extinction higher than 60 Mm^{-1} was most often associated with poor weather, and these were eliminated from the distributions in Table 6.5.5. Several of the occasions when Buffalo Pass samples exhibited higher extinction are examined in greater detail below.

Table 6.5.5 Source Contributions to Calculated Light Extinction

The measured extinction is the sum of six- or twelve-hour averages of particle absorption from Teflon filter transmittance, particle scattering from the OPTEC nephelometer, and site-specific Rayleigh scattering. Within each category, the frequency of contributions to extinction at the minor (<10%), significant (10 to 25%), large (25 to 50%), and major (>50%) levels are made with respect to CMB-calculated (sum of CMB extinction contributions and Rayleigh scattering) extinction to minimize the effects of positive and negative biases to the relative contributions. As noted in Sections 3 and 4, most of the samples submitted to chemical analysis and CMB source apportionment correspond to haze events. The distributions in Table 6.5.5 show more frequent events or poorer visibility than would be found for all situations.

Clean air (Rayleigh) scattering made a large contribution to extinction most of the time at all sites. It was the major contributor for the clearest (<15 Mm^{-1}) periods. Motor vehicle exhaust, which probably also accounts for other carbon sources such as secondary organic aerosol, was a major contributor for a few periods at most sites for all extinction levels. Regional secondary ammonium sulfate was the major contributor on only one occasion at the Buffalo Pass site. Vegetative burning was a large contributor on several occasions when light extinction was highest, but it was most frequently a minor or insignificant contributor in the higher extinction categories. Contributions to extinction from motor vehicle exhaust, vegetative burning, and secondary ammonium sulfate exceeded 1 Mm^{-1} (~10% of clean air extinction) most of the time at all sites for these periods.

Yampa Valley coal-fired generating stations were estimated to be negligible or minor contributors most of the time at all but the Hayden VOR and Hayden Waste Water sites, where they were significant contributors some of the time. The CMB estimated source contributions to extinction that exceeded 1 Mm^{-1} (~10% of Rayleigh scattering) at Buffalo Pass over twelve-hour periods on 03/27/95 and 10/23/95, over six-hour afternoon periods on 08/23/95, 09/18/95, 09/19/95, 09/20/95, and 09/30/95. No contributions exceeding 1 Mm^{-1} were found for morning sampling periods.

Secondary ammonium nitrate was a minor contributor most of the time, and it was seldom a significant contributor. The most frequent cases of significant contribution were found at the Hayden Waste Water site. Secondary ammonium nitrate contributions exceeded 1 Mm^{-1} on 03/26/95, 03/27/95, 03/28/95, 08/24/95, 09/18/95, 09/19/95, 09/20/95, 09/30/95, 10/01/95, 10/02/95, and

10/08/95. There was no preference toward morning or afternoon samples on these dates, but most experienced high humidity and clouds.

Suspended dust was a minor contributor most of the time, and a significant contributor some of the time at all sites. Dust was a more frequent contributor at the lower elevation sites (Baggs, Hayden VOR, Hayden Waste Water), all of which were closer to roads than the higher elevation sites. Most of the samples corresponded to dust contributions exceeding 1 Mm^{-1}.

Table 6.5.6 and Figure 6.5.2 show the individual source contributions to extinction at Buffalo Pass that correspond to the events listed in Table 5.6.1. These show that, for most of the samples, light extinction resulted from several contributors. Most of these contributions reflect the observations made for Table 6.5.5, that vehicle exhaust, fires, regional sulfate, and clean air scattering were the significant and large contributors during most events, with minor or significant contributions from Yampa Valley generating stations and secondary ammonium nitrate on some occasions.

Table 6.5.6 CMB Source Contributions to Extinction at Buffalo Pass for Selected Data Analysis Events

The highest source contribution from each source type does not necessarily correspond to the highest $PM_{2.5}$ concentration or the highest light extinction. The two highest contributions from motor vehicle exhaust were found at the Hayden Waste Water site during the afternoons of 08/21/95 (8.5 ± 4.4 ug/m^3) and 02/24/95 (7.4 ± 4.0 ug/m^3). $PM_{2.5}$ mass concentrations were also elevated at this site with 9.5 ± 0.8 ug/m^3 on 08/21/95 (1200 MST) and 15.9 ± 0.9 ug/m^3 on 02/24/95 (1200-1800 MST). The contribution of motor vehicle exhaust to light extinction was 50 ± 49 Mm^{-1} on 08/21/95 (1200 MST) and 45 ± 46 Mm^{-1} on 02/24/95 (1200 MST), which accounts for 75% to 85% of the total calculated extinction at the Hayden Waste Water site during these two sampling periods.

The three highest coal-fired generating station contributions were found at the Hayden Waste Water site during the mornings of 08/25/95 (6.8 ± 0.7 ug/m^3) and 08/21/95 (5.6 ± 0.7 ug/m^3) and at the Hayden VOR site during the afternoon of 08/23/95 (5.3 ± 0.6 ug/m^3). The measured light extinction in this period ranged from 22 ± 9 Mm^{-1} at the Hayden VOR site on 08/23/95 (1200-1800 MST) to 42 ± 9 Mm^{-1} at the Hayden Waste Water site on 08/21/95 (0600-1200 MST). The contribution of primary motor vehicle exhaust to light extinction ranged from 25% to 50% of the total calculated extinction in these three sampling periods.

Maximum secondary ammonium sulfate contributions were found on the morning of 09/19/95 at the Hayden Waste Water site (4.4 ± 0.5 ug/m^3) and Hayden VOR site (4.3 ± 0.6 ug/m^3), which accounts for approximately 55% of the total calculated extinction. The measured light extinction in these periods was very high, being 111 ± 32 Mm^{-1} at the Hayden Waste Water site and 1,957 ± 1,000 Mm^{-1} at the Hayden VOR site.

The maximum secondary ammonium nitrate contribution (3.6 ± 0.5 ug/m^3) was found at the Hayden Waste Water site on the morning of 02/26/95, which accounts for 27% of the total calculated light extinction. The measured light extinction in this period was also high, with 91 ± 19 Mm^{-1}.

Table 6.5.7
Sulfur-32 and Sulfur-34 Abundances at Buffalo Pass

Sample	Sample Period[a]	Sulfur Form	S^{32}/S^{34} [b]	Diablo Canyon Meteorite del[c]	Background del[d]	Gen. Sta. del[e]	Ambient SO_4 or SO_2 [f] ($\mu g/m^3$)	CMB Gen. Sta. SO_4 or SO_2 [g] ($\mu g/m^3$)	CMB Amm. Sul. SO_4 or SO_2 [g] ($\mu g/m^3$)
Buff. P.	8/8/95 AM	SO_4	22.57 ± 0.015	2.22 ± 0.07	-1.33 ± 2.30	-3.10 ± 1.11	1.41 ± 0.08	0.041 ± 0.015	1.45 ± 0.15
Buff. P.	8/8/95 AM	SO_2	22.54 ± 0.027	3.55 ± 0.12	0.00 ± 2.51	-1.77 ± 1.49	0.43 ± 0.06	0.430 ± 0.040	0.00 ± 0.00
Baggs	8/8/95 AM	SO_2	22.55 ± 0.014	3.10 ± 0.06	-0.44 ± 2.29	-2.22 ± 1.09	0.80 ± 0.07	0.790 ± 0.080	0.00 ± 0.00
Jun. Mt.	8/8/95 AM	SO_2	22.57 ± 0.027	2.22 ± 0.12	-1.33 ± 2.52	-3.10 ± 1.50	0.84 ± 0.08	0.610 ± 0.060	0.00 ± 0.00
Jun. Mt.	8/21/95 AM	SO_4	22.59 ± 0.035	1.33 ± 0.15	-2.21 ± 2.68	-3.98 ± 1.77	1.16 ± 0.06	0.020 ± 0.010	1.16 ± 0.11
Buff. P.	8/23/95 AM	SO_2	22.52 ± 0.005	4.44 ± 0.02	0.89 ± 2.22	-0.89 ± 0.92	0.11 ± 0.04	0.000 ± 0.000	0.00 ± 0.00
Buff. P.	8/24/95 AM	SO_2	22.48 ± 0.004	6.23 ± 0.02	2.67 ± 2.22	0.89 ± 0.91	0.93 ± 0.09	0.900 ± 0.090	0.00 ± 0.00
Buff. P.	8/24/95 PM	SO_2	22.47 ± 0.005	6.68 ± 0.02	3.12 ± 2.23	1.34 ± 0.92	0.86 ± 0.08	0.000 ± 0.000	0.00 ± 0.00
Baggs	8/24/95 PM	SO_4	22.48 ± 0.008	6.23 ± 0.04	2.67 ± 2.24	0.89 ± 0.96	0.85 ± 0.05	0.003 ± 0.001	0.84 ± 0.08
Buff. P.	9/18/95 PM	SO_2	22.59 ± 0.013	1.33 ± 0.06	-2.21 ± 2.28	-3.98 ± 1.06	0.09 ± 0.04	0.090 ± 0.010	0.00 ± 0.00
Baggs	9/20/95 PM	SO_4	22.73 ± 0.025	-4.84 ± 0.11	-8.36 ± 2.46	-10.12 ± 1.42	0.97 ± 0.06	0.010 ± 0.005	0.92 ± 0.09
Baggs	9/30/95 PM	SO_4	22.48 ± 0.006	6.23 ± 0.03	2.67 ± 2.23	0.89 ± 0.94	0.90 ± 0.05	0.010 ± 0.005	0.78 ± 0.07
Buff. P.	10/12/95 PM	SO_2	22.69 ± 0.182	-3.09 ± 0.80	-6.61 ± 8.24	-8.37 ± 7.98	0.99 ± 0.08	0.990 ± 0.100	0.00 ± 0.00

[a] Period over which samples were taken.

[b] Ratio of Sulfur-32 isotopic abundance to Sulfur-34 isotopic abundance.

[c] del=1000*{[(22.62)/(S^{32}/S^{34})]$^{-1}$}, deviation from Canyon Diablo Meteorite standard with S^{32}/S^{34}=22.62.

[d] del=1000*{[(22.54)/(S^{32}/S^{34})]$^{-1}$}, deviation from MZVS background with S^{32}/S^{34}=22.54±0.05.

[e] del=1000*{[(22.50)/(S^{32}/S^{34})]$^{-1}$}, deviation from MZVS generating station with S^{32}/S^{34}=22.50±0.02.

[f] Measured by ion chromatography on the auarta particle filter (SO_4) or on the potassium carbonate backup filter (SO_2).

[g] Contribution to SO_4 or SO_2 calculated by the CMB for this sample.

6.6 Increases in Extinction from Local Generating Stations

Section 5 showed that pulses of sulfur dioxide were commonly detected at Buffalo Pass without corresponding changes in light scattering. Many of these SO_2 pulses occurred under weather-obscured conditions or under dry conditions during which little conversion to sulfate particles was expected. The SO_2 pulses at Buffalo Pass had durations between a fraction of an hour up to ~6 hours. During the August 3 to November 9 period when SO_2 was measured with the TECo 43 monitor, the highest hourly average SO_2 concentration was 9.7 ppbv. There were 34 hours during which the SO_2 concentration exceeded 4 ppbv and 160 hours during which it exceeded 1.9 ppbv. A review of the data for the 160 hours with the highest SO_2 concentrations identified 69 pulses of SO_2 with peak concentrations greater than 1.9 ppbv.

The data recorded by the TSI and OPTEC nephelometers sometimes showed a pulse in light scattering by particles that matched the time history of the SO_2 pulse, but more often, they showed no variation during a sulfur dioxide pulse. An investigation of the relationship between pulses in SO_2 and the accompanying pulses in light scattering, if any, was undertaken because of the following observations and hypotheses:

The every-day plume transport modeling described in Section 5.4 showed that the observed SO_2 pulses could be satisfactorily accounted for by the emissions of the five units at the Hayden and Craig stations. Also, the emissions inventory shows that there are no other SO_2 sources of comparable magnitude in the mesoscale modeling domain. Thus, most (if not all) of the SO_2 pulses are caused by the emissions of the five units at the Hayden and Craig stations.

Determining the presence or absence of a relationship between pulses in light scattering by particles and pulses in SO_2 concentrations at Buffalo Pass would help determine the relationship between the emissions from the Hayden and Craig stations and light scattering by particles in the Wilderness.

The most probable cause of light scattering by particles associated with SO_2 emissions is sulfate formed from the oxidation of SO_2 in the atmosphere. Therefore, determining the relationship between the presence or absence of pulses of light scattering associated with pulses of SO_2 has the potential to provide experimental data for the factors that influence the rate of conversion of SO_2 to sulfate, as well as confirmation of the plume aging calculations of Section 5.3.

6.6.1 b_{sp} Measurements

Sample air entering the inlet of the TSI nephelometer passed through a cyclone with a 2.5 µm particle diameter cutpoint. This cyclone was at the entrance of the sample line, so the particle-size cut was made at ambient conditions. Therefore, the only particles sampled by the TSI nephelometer were fine particles. Cloud droplets, drizzle, and most snowflakes were removed by the cyclone. When the sample inlet was in clouds, the nephelometer sampled only the interstitial aerosol (i.e., the fine particles within the

cloud that did not serve as nuclei on which water condensation took place to form cloud droplets). The data from the TSI nephelometer showed that light scattering by the interstitial aerosol at Buffalo Pass was typically much smaller than the light scattering by aerosol present before the clouds arrived or after they departed. Because of the cyclone on the inlet, a pulse in the reading of the TSI nephelometer reliably indicated that a pulse in the ambient fine particle concentrations occurred. The presence of fine particles was not confused or obscured by the presence of clouds.

The TSI nephelometer has an enclosed design and was operated in a shelter that was typically warmer than the ambient air. As a result, the sample air in this nephelometer was warmer than ambient and the RH in the sample chamber rarely exceeded 60 percent. Therefore, at high humidities, the pulse in light scattering recorded by the TSI nephelometer was less than the actual pulse in light scattering in the ambient air.

The OPTEC nephelometer has an open design, so it responds to a broad range of particle sizes, including cloud droplets. The temperature and RH in the scattering chamber are close to ambient. Therefore, the light scattering values recorded by this instrument are closer to those in the ambient air than the values recorded by the TSI nephelometer. At very high RH, this instrument cannot distinguish between wisps of clouds and pulses of fine particles.

6.6.2 Estimated Changes in b_{sp}

The TSI and OPTEC measurements were examined for the time period surrounding each of the 69 pulses of SO_2 to estimate the magnitude of the pulse in fine-particle light scattering that accompanied each SO_2 pulse. The data for the pulses observed by the two nephelometers are shown in Table 6.6.1 and are plotted in Figures 6.6.1 and 6.6.2. The times shown in Table 6.6.1 are the hour of the maximum SO_2 reading during each pulse. Error bars in the figures indicate the estimated uncertainty in the magnitude of the pulse.

Table 6.6.1 Data for SO_2 Pulses and Accompanying Pulses in Light Scattering by Particles at Buffalo Pass

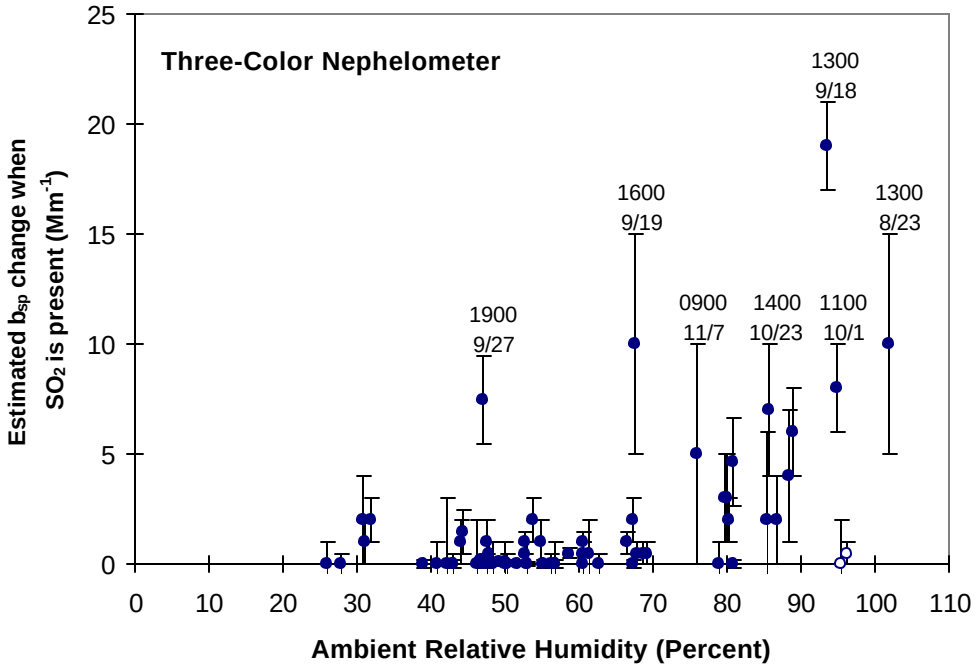

Figure 6.6.1. Changes in light scattering in the presence of sulfur dioxide, measured with the TSI three-color nephelometer. Open circles show two events when the nephelometer was in clouds, so only the interstitial aerosol was sampled.

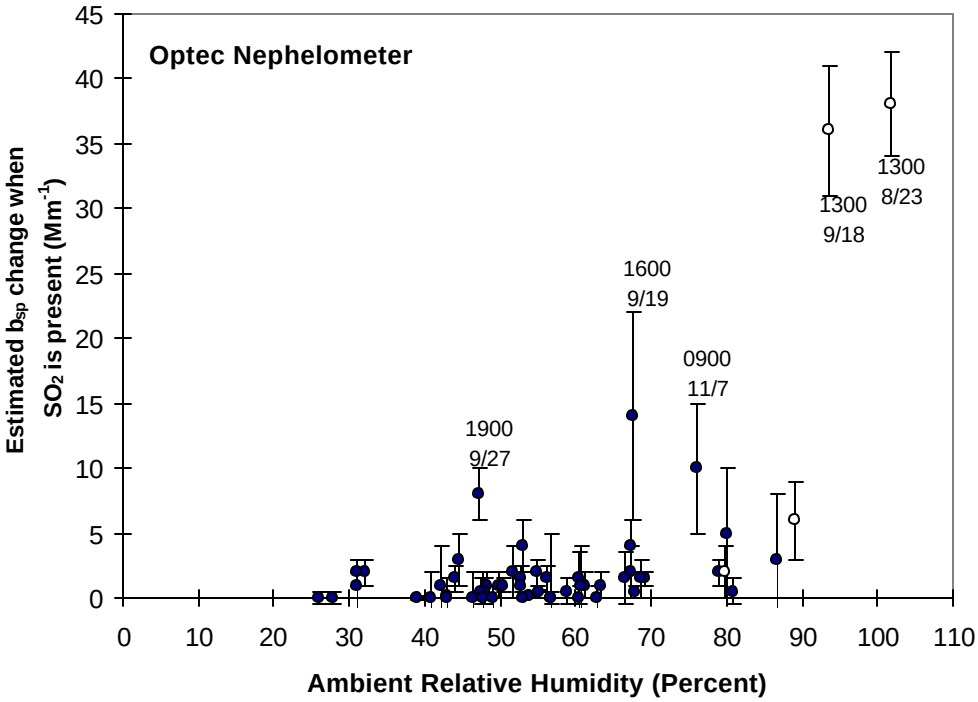

Figure 6.6.2. Changes in light scattering in the presence of sulfur dioxide, measured with the OPTEC nephelometer. Open circles show readings flagged to indicate the presence of meteorological effects.

In some cases, the nephelometer data indicated that the background values of b_{sp} (i.e., the b_{sp} due to sources other than the local sources of SO_2) were varying with time. In these cases, the uncertainties in the estimates of the magnitudes of the b_{sp} pulses associated with the SO_2 pulses were relatively large. Estimates are semiquantitative; different values would be obtained by different analysts. Nevertheless, it is expected that: 1) the estimates for the magnitudes of the pulses by most analysts would fall within the estimated uncertainties; and 2) the estimates of all analysts would follow the general pattern of the results in Figure 6.6.1.

On some occasions, the OPTEC nephelometer reading exceeded 100 Mm^{-1} during a pulse of SO_2, and the validity flag accompanying the data indicated that the nephelometer reading was influenced by the meteorological conditions. In these cases, it was assumed that the readings were mostly due to cloud droplets and no estimate was made of the OPTEC nephelometer response during the SO_2 pulse. On two occasions, the OPTEC nephelometer recorded a pulse with a magnitude between 35 and 40 Mm^{-1} that corresponded well with pulses in the SO_2 and TSI nephelometer data. Because of the corroborating evidence, these OPTEC nephelometer pulses were included in the tabulation in Table 6.6.1 even though the readings were flagged as being influenced by meteorological effects. These two points, and others that were similarly flagged, are shown by the open circles in Figure 6.6.2. The filled circles show data flagged as valid (flag value of V). The data in Figure 6.6.2 indicate that the OPTEC nephelometer recorded data flagged as valid during only one SO_2 pulse when the RH was greater than 80 percent. In comparison, most nonzero pulses in the TSI nephelometer readings that accompanied SO_2 pulses were recorded when the RH was greater than 80 percent.

The following general conclusions can be drawn from the measurements of SO_2 and light scattering at Buffalo Pass:

Atmospheric moisture has a strong effect on the relationship between pulses of light scattering and pulses of SO_2:

- Except for two events, little or no change in b_{sp} was observed during the 46 pulses of SO_2 that occurred when the RH was below 70 percent and TSI nephelometer data were available. The average of the TSI nephelometer readings for these 46 pulses was less than 0.5 Mm^{-1}, which differs from zero by less than the uncertainty in the estimates. (This average would have been smaller if the estimated b_{sp} pulses had not been set to zero when the data

indicated a negative deflection of the nephelometer reading during the SO_2 pulse.)

- Except for two events that occurred in clouds when only interstitial aerosol was sampled (shown by open circles in Figure 6.6.1), the TSI nephelometer recorded a pulse in b_{sp} during every SO_2 pulse when the RH exceeded 80 percent. In the absence of dense clouds, the magnitude of these pulses tended to increase with increasing RH.
- There were two high RH events when the OPTEC nephelometer recorded substantial pulses in b_{sp} at the time of SO_2 pulses. These pulses were flagged to indicate the presence of meteorological effects (RH>90 percent). However, their correspondence with the TSI nephelometer data indicated that these OPTEC nephelometer readings were largely caused by fine particles.

The RH measured at a receptor site at the time of arrival of an SO_2 pulse is a useful indicator of the exposure of that SO_2 to atmospheric conditions associated with rapid oxidation of SO_2 to sulfate.

The pulses in b_{sp} that occurred during SO_2 pulses when the RH was high were sometimes substantial. The largest pulse observed by the TSI nephelometer was 19 Mm^{-1} above a baseline that had a value less than 10 Mm^{-1}. The largest pulses observed by the OPTEC nephelometer were greater than 35 Mm^{-1} above the baseline readings and had peak readings near 60 Mm^{-1}. The difference between the two nephelometer readings was caused by the sample heating in the TSI nephelometer, which evaporated water from the particles.

The largest pulses in SO_2 occurred under conditions where clouds could be in the sight paths. Therefore, it is necessary to view the time-lapse videos as part of the process of determining the effect of the b_{sp} pulses on visibility.

The low values estimated for the b_{sp} pulses from the OPTEC nephelometer data when the RH was below 70% indicate that primary particles from Hayden and Craig stations (e.g., fly ash) are negligible contributors to light extinction at Buffalo Pass most of the time. Owing to its open design, the OPTEC nephelometer would respond to primary particles if they were present in detectable concentrations. When the two outliers mentioned above were excluded, the average of the 43 OPTEC nephelometer readings of b_{sp} pulses corresponding to SO_2 pulses was less than 1 Mm^{-1} when the RH was below 70%. This average decreased when only SO_2 pulses with peaks above 3 ppbv were included. Thus, primary particles that accompanied SO_2 pulses made a contribution to total light scattering that was too small to measure. The peak contributions during the SO_2 pulses were estimated to be less than 1 Mm^{-1}, which is the nominal detection limit of the OPTEC nephelometer, during 08/03/95–11/09/95.

6.6.3 Estimated Changes in Other Components of b_{ext}

An order-of-magnitude calculation shows that NO_2, which is a brown gas, is unlikely to cause a significant change in light extinction in the Wilderness. NO_2 is formed by the oxidation in the atmosphere of NO, which is emitted by combustion sources such as vehicles and generating stations. Experimental

measurements (Hardison, 1970) and model calculations (Richards *et al.*, 1992) indicate that a plume that subtends a visual angle of about 1/3 degree must have a burden of more than 65 ppbv·km of NO_2 in the sight path to be perceptible. Plumes that subtend wider or narrower visual angles must have greater burdens of NO_2 in the sight path for the effects to be perceptible (U.S. EPA, 1988).

The emissions data in Section 5.3 indicate that the NO_x emission rates from the Hayden and Craig stations are comparable to the SO_2 emission rates on a mass basis. NO_2 has a molecular weight of 46 and SO_2 a molecular weight of 64, so on a mole basis, the NO_x emission rates are roughly 1.4 times the SO_2 emission rates. The monitoring data at Buffalo Pass indicate that the SO_2 concentration exceeded 6 ppbv during nine hours in the 08/03/95–11/09/95 time period. If all of the NO_x emitted by the generating stations with 6 ppbv of SO_2 was converted only to NO_2, the NO_2 concentration accompanying the SO_2 would be about 8.4 ppbv. It is necessary for a sight path to have a length of 7.8 km for this concentration to cause a burden of 65 ppbv·km. For this burden of NO_2 to be perceptible, it is necessary that it subtend a viewing angle of about 1/3 degree from the location of the observer.

It is unlikely that these conditions will be satisfied. The highest SO_2 concentrations occur when the dispersion is poor and the plumes are relatively narrow. At these times, the plumes will not be wide enough to produce significant burdens of NO_2 in views across the plume. It is possible that high burdens could be produced in views approximately along the plume, but in this case, the observer is within or close to the plume, so it subtends a viewing angle much larger than 1/3 degree.

Other components of light extinction do not change measurably during the SO_2 pulses. Light scattering by gases remains the same. Generating stations do not emit soot during routine operations, so the change in light absorption by particles accompanying the SO_2 pulses is expected to be negligible most of the time. This expectation is confirmed by the time series plots in Appendix E, showing that SO_2 pulses were often unaccompanied by increases in black carbon concentrations. The most notable exception occurred at 1300 MST on 08/23/95, when an SO_2 pulse was accompanied by an increase in the black carbon.

6.7 Regional Episodic Modeling

Detailed CALMET/CALPUFF modeling results are reported in this subsection. The everyday plume modeling for January through November 1995, described in Section 5.4, was intended to determine where and when Yampa Valley generating station SO_2 emissions encountered the Wilderness and other areas in the mesoscale domain. It was also intended to estimated the frequency of encounters of different magnitude from individual generating units. The everyday modeling was not intended to quantify contributions to light extinction from the local generating stations or other sources.

Detailed CALMET/CALPUFF modeling estimates source contributions to $PM_{2.5}$, to its chemical components, and to light extinction from all source types in the regional domain. Detailed modeling uses all of the CALMET/CALPUFF modeling capabilities. Five episodes consisting of 28 days were modeled in detail. These include the periods of 08/07/95–08/09/95, 08/21/95–08/27/95, 09/17/95–09/21/95, 10/07/95–10/14/95, and 10/16/95–10/19/95. For convenience, the final two episodes were modeled together with the inclusion 10/15/95. Detailed CALMET/CALPUFF modeling results were obtained for

28 days total, with nearly half of all days submitted to aerosol chemical analysis. Through sensitivity simulations described in Appendix B.2, the adequacy and uncertainty of the calculated and source attributions were also evaluated.

6.7.1 Modifications to CALMET/CALPUFF Computer Codes

The Interagency Workgroup on Air Quality Modeling (IWAQM) recommends use of the CALMET/CALPUFF modeling system for source attribution modeling. The most recent computer codes were requested from the CALMET/CALPUFF developers. When modeling commenced at the end of 1995, EPA had made CALMET/CALPUFF (Version 3.0, Modification 1) publicly available. A revision to this computer code (Version 3.0, Modification 3) became available by mid-1996, but it was not practical to recompute the values reported here using the new software. Model input files are available as part of the MAVS data base. Interested parties can use these inputs with subsequent versions of CALMET/CALPUFF to determine whether or not major differences in results and conclusions would result from computer code changes

Changes in the CALMET/CALPUFF (Version 3.0, Modification 1) code that were implemented as part of the MZVS were the following:

New CALMET/CALPUFF pre- and post-processors were developed to process the routine and MZVS field study data for input into CALMET/CALPUFF, and to calculate light extinction and source contributions to concentrations and extinction.

The chemistry and block data routines in CALPUFF were slightly modified, and species arrays were extended, to handle several new categories of inert PM (i.e., EC, OC, other primary PM, and secondary organic aerosol [SOA]) beyond the standard five SO_x and NO_x species.

Elevated receptor sampling within the CALPUFF code was implemented to allow sampling of puffs at user-specified heights above mean sea level (not just at the ground).

An error was corrected in the buoyant area source plume rise calculation.

Additional modifications to the CALMET/CALPUFF modeling system were made for some sensitivity simulations, such as modifications to the CALMET slope flow parameter and enhancement of the CALPUFF SO_2 conversion rate as a function of relative humidity. However, these changes were not used in the final CALMET/CALPUFF source apportionment simulations.

IWAQM recommends default settings for the options contained within the CALMET/CALPUFF modeling system. Several tests, based on the 09/17/95–09/21/95 episode, were performed (Appendix B.2) to evaluate the suitability of several of the recommended settings for simulating transport, dispersion, chemical transformation, and light extinction in the complex terrain of the MZVS study region. The optimal selections were used for all subsequent CALMET/CALPUFF simulations in the everyday and detailed modeling.

6.7.2 Overview of CALMET

The CALMET meteorological model consists of a diagnostic wind field module and separate micrometeorological modules for over-water and over-land boundary layers. When specifying large domains, the user has the option to adjust input winds to a Lambert Conformal Projection coordinate system to account for the earth's curvature, and this option was selected for MZVS modeling.

The diagnostic wind field module uses a two-step approach to compute gridded wind fields. First, an initial-guess wind field (large-scale flow) is adjusted for local kinematic effects of terrain, slope flows, and terrain blocking, to produce a Step 1 wind field. Second, an objective analysis procedure combines observational data into the Step 1 wind field. Options allow gridded prognostic wind fields (such as those produced by the MM4 or CSUMM models) to be used by CALMET. These may better represent regional flows, certain aspects of sea breeze circulations, and slope/valley circulations. However, such prognostic wind fields were not available for the MZVS and were not used.

CALMET reads a "control file" that specifies selections for the model options, input variables, and outputs. Table 6.7.1 documents the selections for this application and compares them with the IWAQM default recommendations. CALMET requires as model inputs: 1) geophysical data (land use and terrain); 2) surface meteorological data; 3) upper-air meteorological data; and 4) precipitation data. The data sources and locations are documented in Section 2.2.

Table 6.7.1
CALMET Modeling Options, Sensitivity Tests Performed, and Optimal Values for the Mt. Zirkel Visibility Study

Parameter	Default	MZVS Optimal	Sensitivity Tests
GRID PARAMETERS			
Grid Resolution (km)			
Mesoscale Region	None	4	4
Regional-Scale Region	None	4	4,16
Grid Projection Type			
Universal Transverse Mercator (UTM) or Lambert Conformal Mapping (LCM)	UTM	LCM	
Model Domain Extent (km x km)			
Mesoscale Region	None	280 x 152	
Regional-Scale Region	None	784 x 560	
LCM Projection Definition			
Latitude Parallels (deg, deg)	30, 60	38, 43	
Reference Longitude/Latitude (deg, deg)	None	107.0, 40.5	
Top of Modeling Domain (km AGL)			
Mesoscale Region	None	2.8	
Regional-Scale Region	None	2.8	

Parameter	Default	MZVS Optimal	Sensitivity Tests
Number of Vertical Layers[1]			
Mesoscale Region	None	13	12,13,25
Regional-Scale region	None	13	

[1] MZVS "optimal" vertical cell faces are (m agl): 0, 20, 70, 182, 294, 406, 518, 630, 840, 1134, 1526, 1918, 2310, 2800

Parameter	Default	MZVS Optimal	Sensitivity Tests
DIAGNOSTIC WIND MODEL (DWM) PARAMETERS			
Model Type (0=objective analysis/1=DWM)	1	1	
Compute Froude Number Adjustment (0=No/1=Yes)	1	1	
Compute Kinematic Effects (0=No/1=Yes)	1	1	
Use O'Brien Procedure to Adjust Vertical Velocity	1	0	
Extrapolate Surface Wind Observations to Upper Layers (1=no extrapolation, 2=power law extrapolation, 3=user input multiplicative factors, 4=similarity theory used) (negative value=ignore layer 1 data at upper-air sites)	1	1	1,4
Minimum surface-upper site distance allowing vert extrapolation (km)	4	4	
Use Gridded Prognostic Model Output	No	No	
Kinematic Effect Parameters			
Empirical factor Controlling Kinematic Effects (Alpha)	0.1	0.1	0.1,0.5
Radius of Influence Parameters			
Use Varying Radius of Influence (True/False)	False	True	
Maximum Radius of Influence Surface Over Land (km)	None	50[2]	
Maximum Radius of Influence Aloft Over Land (km)	None	500[3]	
Maximum Radius of Influence Surface Over Water (km)	None	50	
Minimum Radius of Influence in Wind Field Interpolation (km)	None	0.2	
Slope Flow Parameters (set in code)			
Magnitude of slope flow parameter (Beta2)	±1	±1	±1, ±2

[2] Value for every-day inert SO_2 trajectory modeling is 100 km

[3] Value for every-day inert SO_2 trajectory modeling is 1000 km

Parameter	Default	MZVS Optimal	Sensitivity Tests
Blocking Effect Parameters			
Critical Froude Number (CRITFR)	1.0	1.0	1.0,2.0
Radius of Influence of Terrain Features (TERRAD) (km)	None	20	20,50
Distance Where First Guess Wind Field and Observations are Treated Equally			
Surface Wind Fields (R1) (km)	None	10	10,20,50
Aloft Wind Fields (R2) (km)	None	30	30,50,100,200
Divergence Minimization Procedure			
Maximum Acceptable Divergence (m/s?)	5.E-6	5.E-6	
Maximum Number of Iterations	50	50	
Number of smoothing passes	2 (sfc)/ 4 (aloft)	4 (all layers)	4 (all layers), 2 (1st 8 lyrs)/ 4 (aloft)
Maximum number of stations to use in interpolation	None	2 (sfc)/ 4 (aloft)	4 (all layers), 2 (sfc)/4 (aloft)
Use of Barriers in Wind Interpolation (0=No/1=Yes)	0	14	0,1
Surface Temperature Control for DWM (0=compute internally/1=read from file DIAG.DAT)	0	0	
Surface Site for DWM Temperature	None	Hayden	
Domain Average Lapse Rate Control for DWM (0=compute internally/1=read from file DIAG.DAT)	0	0	

[4] Specification of barriers was not done for every-day inert SO_2 trajectory modeling

Parameter	Default	MZVS Optimal	Sensitivity Tests
Upper-air Station to use for Domain Average Lapse Rate	None	Clark	Hayden, Clark
Depth Domain Average Lapse Rate is computed (m AGL)	200	200	200,1000
Domain average wind components (0=calculate internally/1=read from file DIAG.DAT)	0	0	
Upper-air Station Used for Domain Average Wind for DWM (-1=calculate spatially varying values)	None	-1	
Bottom and Top of Layer for Domain Average Wind (m AGL)	1-2000	1-15005	
Include Lake Breeze Effects	False	False	
MIXING HEIGHT, TEMPERATURE, AND PRECIPITATION PARAMETERS			
Neutral Mechanical Mixing Height Constant (B in Eqn. 2-54)	1.41	1.41	
Convective Mixing Height Constant (E in Eqn. 2-52)	0.15	0.15	
Stable Mixing Height Constant (B_2 in Eqn. 2-57)	2400	2400	
Overwater Mixing Height Constant (c_w in Eqn. 2-64)	0.16	0.16	
Coriolis Parameter (f in Eqn. 2-64) (1/s)	1.E-4	1.E-4	
Minimum Temperature Lapse Rate Above Mixing Height (K/m)	0.001	0.001	
Depth of Layer Above Convective Mixing Height for Lapse Rate Computation (m)	200	200	
Maximum Overland Mixing Height (m)	2500	2500	

[5] Range used for inert SO_2 trajectory modeling was 1-2000 m.

Parameter	Default	MZVS Optimal	Sensitivity Tests
Minimum Overland Mixing Height (m)	20	20	
Maximum Overwater Mixing Height (m)	2500	2500	
Minimum Overwater Mixing Height (m)	50	50	
Conduct Spatial Averaging of Mixing Heights (0=No/1=Yes)	1	1	
Maximum Search Distance for Spatial Averaging (grid cells)	1	5	1,3,5
Half-Angle of upwind-looking Cone for Spatial Averaging (deg.)	30	30	
Layer of Winds Used in Upwind Averaging of Mixing Heights	None	66	
Type of Temperature Interpolation (1=1/r;2=1/r^2)	1	1	
Conduct Spatial Averaging of Temperatures (0=No/1=Yes)	1	1	
Radius of Influence for Temperature Interpolation (grid cells)	1	1	1,3,5
Default Lapse Rate Overwater Below Mixing Height (K/m)	-0.0098	-0.0098	
Default Lapse Rate Overwater Above Mixing Height (K/m)	-0.0045	-0.0045	
Method of Precipitation Interpolation (1=1/r;2=1/r^2;3=1/r^2 *expftn)	2	3	2,3
Radius of Influence for Precip Interpolation in Methods 1 or 2 (km)	100	50	0,50,100
Cutoff Precipitation Rate (mm/hr)	0.01	0.10	0.01, 0.10

[6] Value used for inert SO_2 trajectory modeling is 4

Parameter	Default	MZVS Optimal	Sensitivity Tests

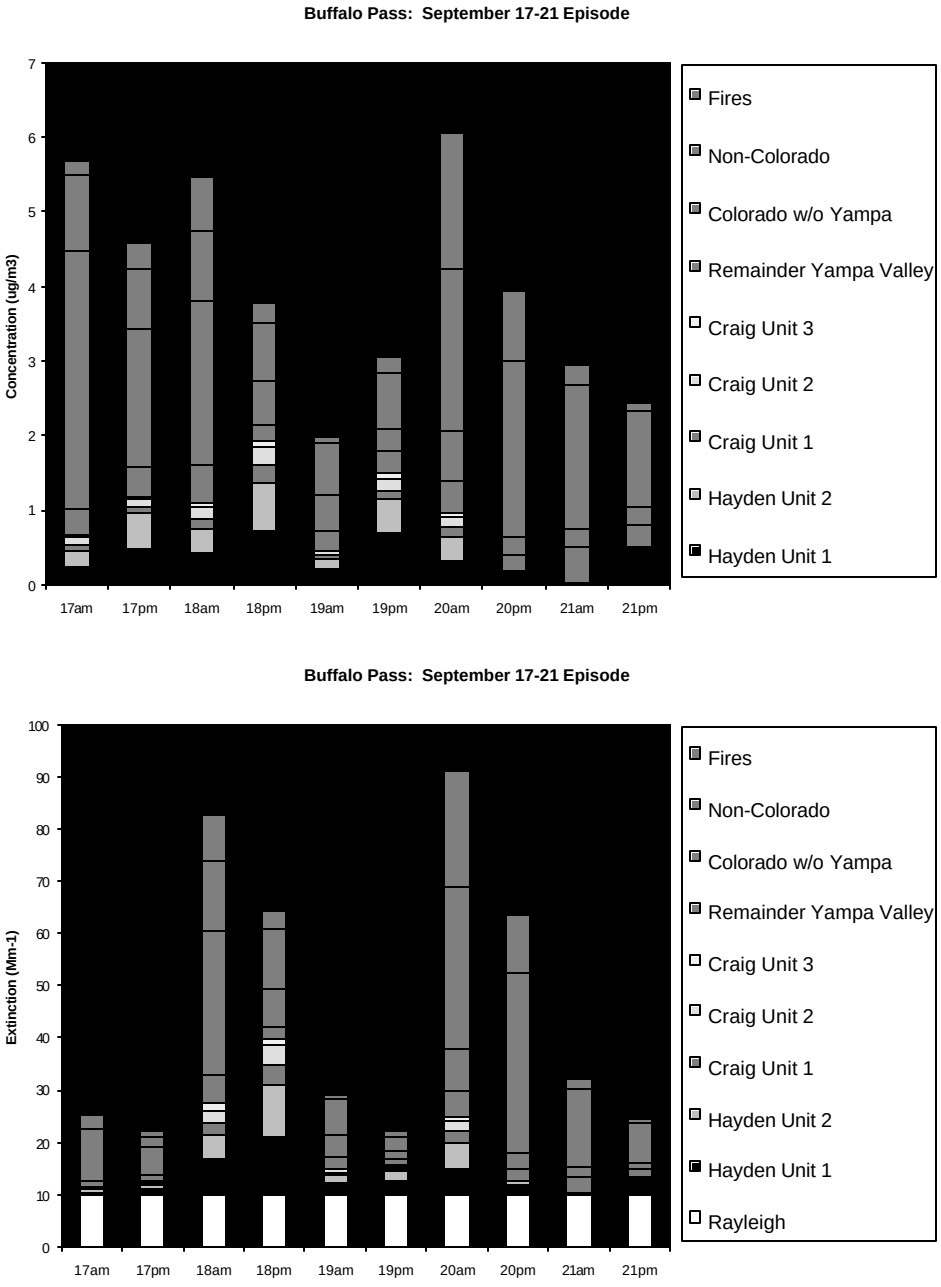

Figure 6.7.1a Source contribution to CALPUFF estimated six-hour average $PM_{2.5}$ concentrations and total extinction for the September 17-21, 1995 episode. Buffalo Pass.

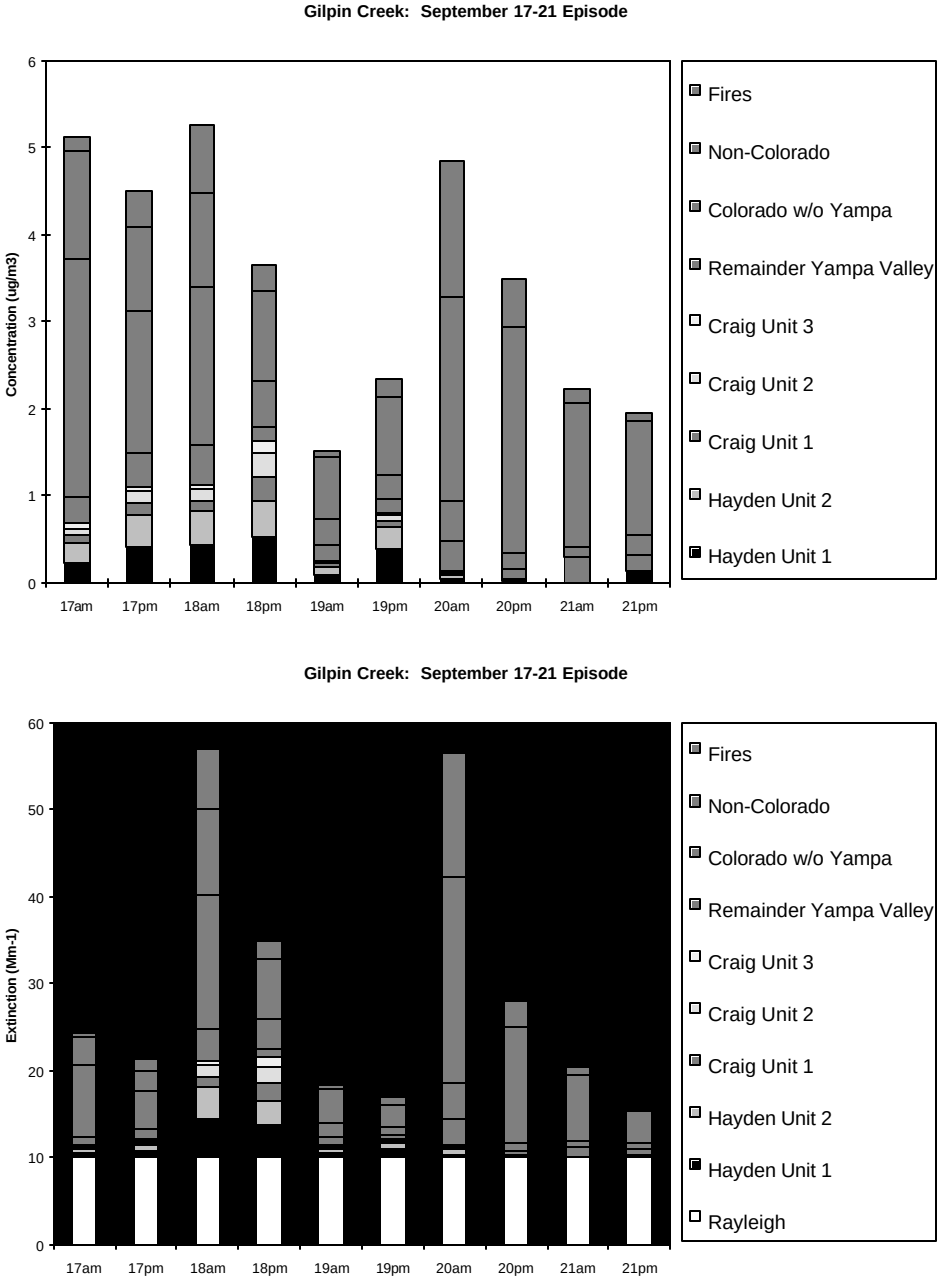

Figure 6.7.1b Source contribution to CALPUFF estimated six-hour average $PM_{2.5}$ concentrations and total extinction for the September 17-21, 1995 episode. Gilpin Creek.

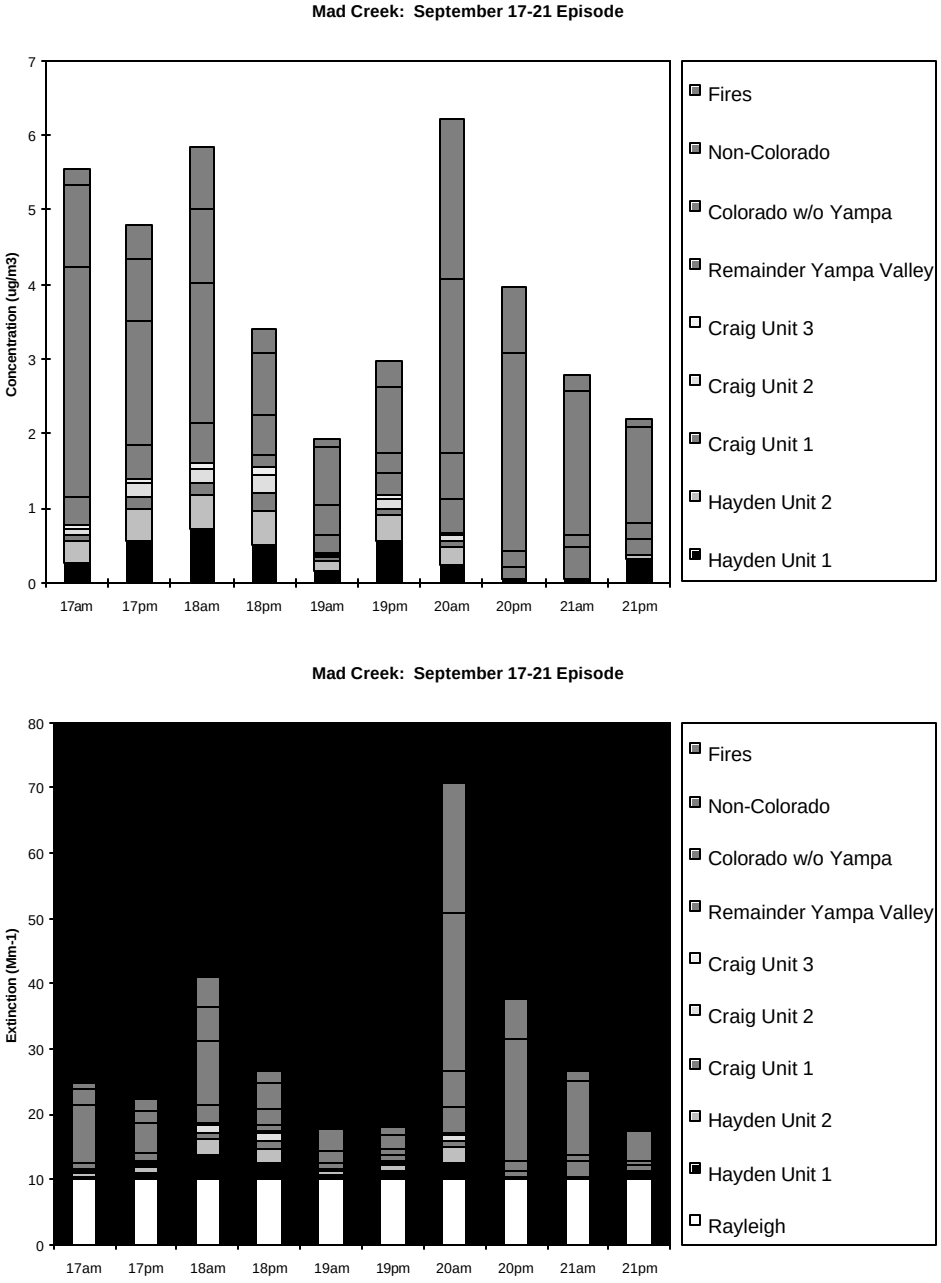

Figure 6.7.1c Source contribution to CALPUFF estimated six-hour average $PM_{2.5}$ concentrations and total extinction for the September 17-21, 1995 episode. Mad Creek.

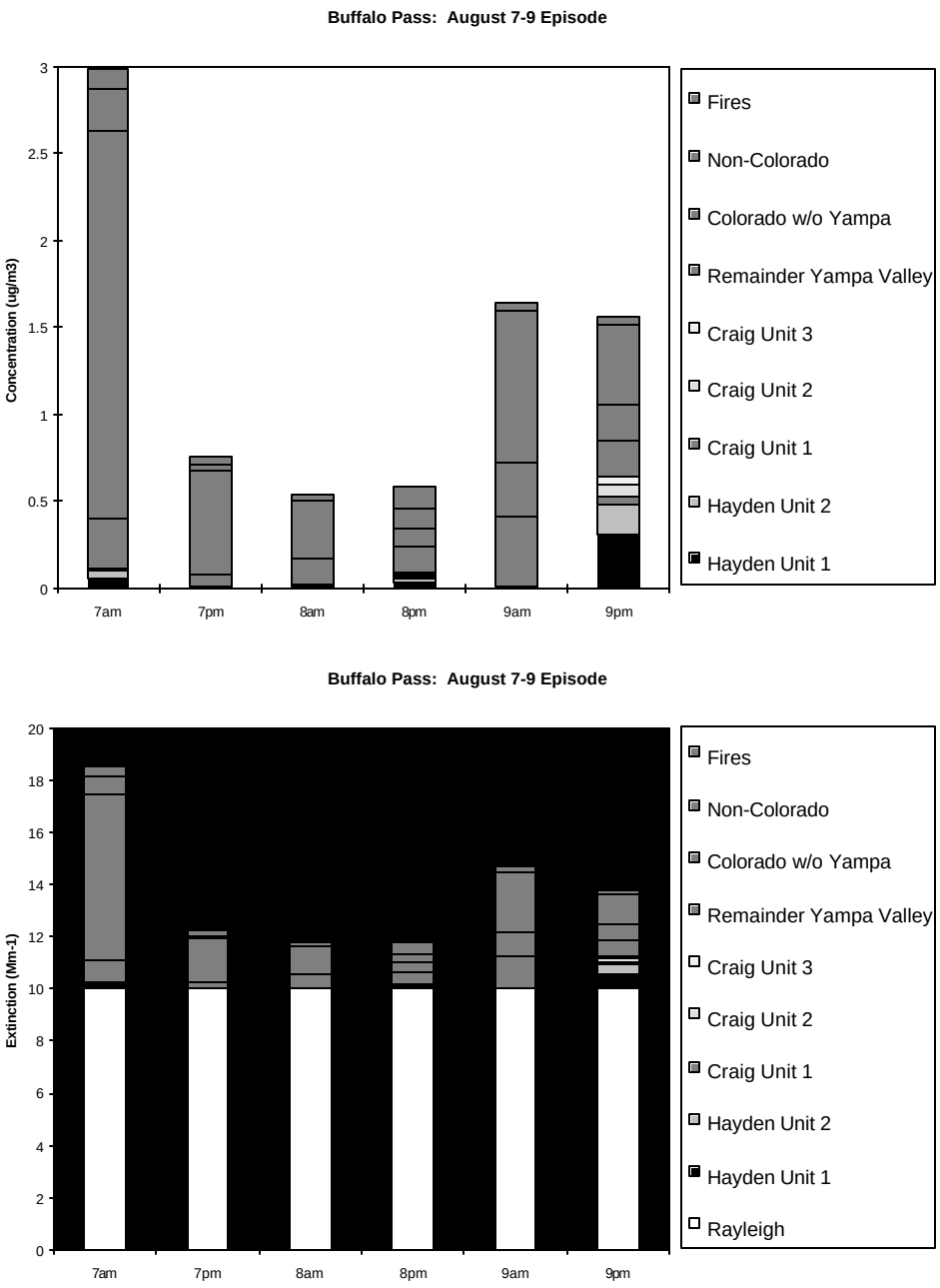

Figure 6.7.2a Source contribution to CALPUFF estimated six-hour average $PM_{2.5}$ concentrations and total extinction for the August 7-9, 1995 episode. Buffalo Pass.

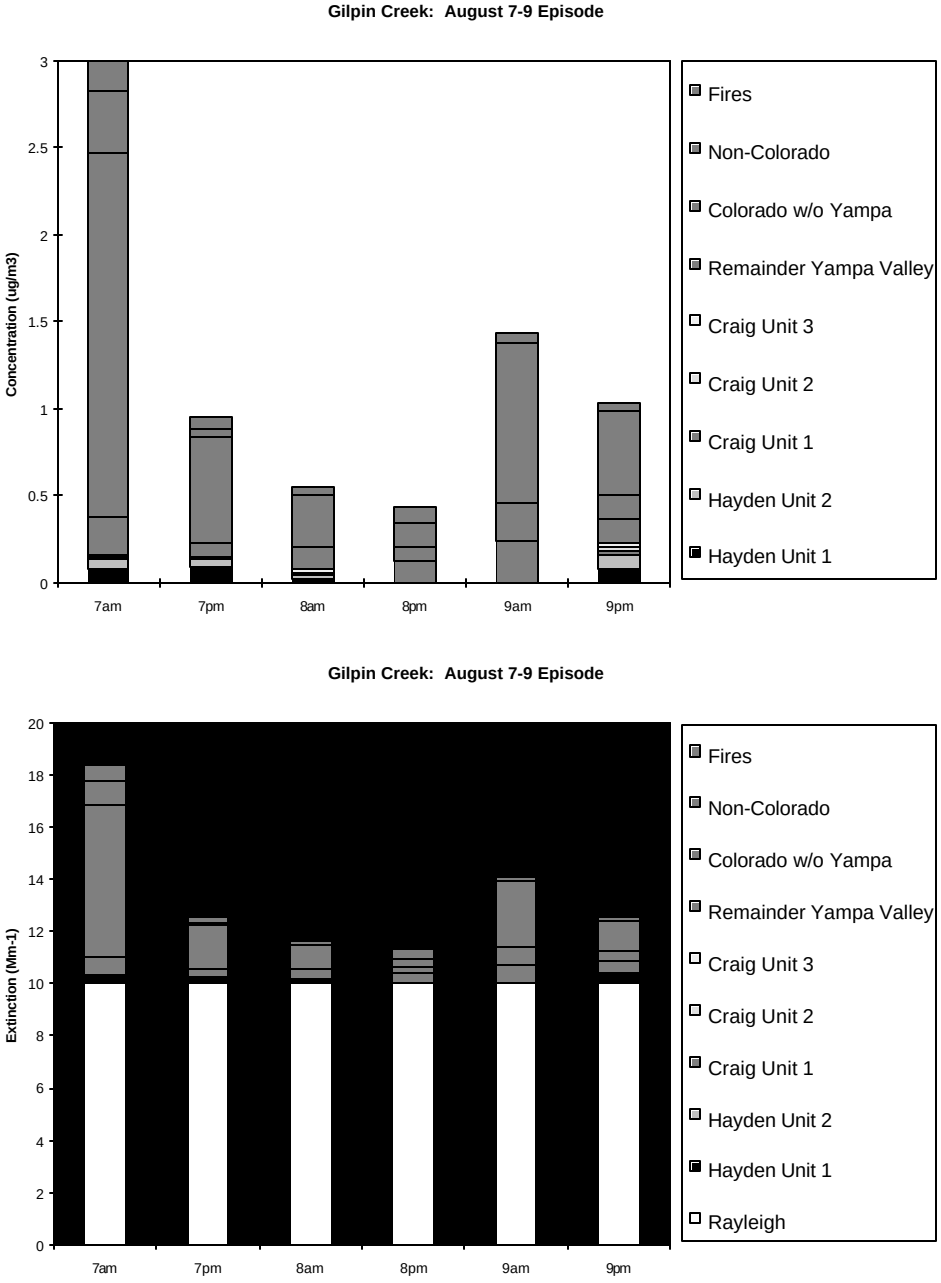

Figure 6.7.2b Source contribution to CALPUFF estimated six-hour average $PM_{2.5}$ concentrations and total extinction for the August 7-9, 1995 episode. Gilpin Creek.

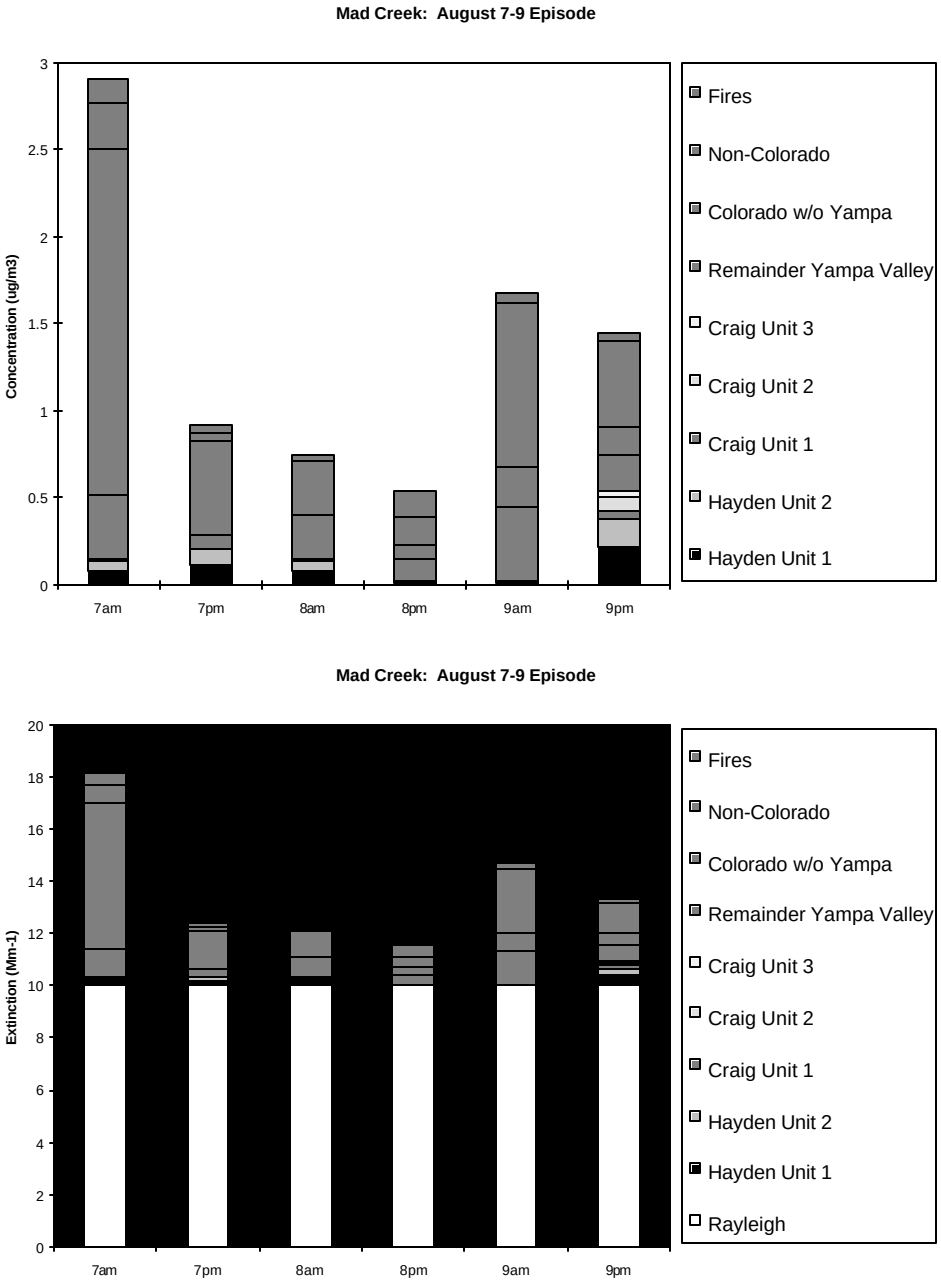

Figure 6.7.2c Source contribution to CALPUFF estimated six-hour average $PM_{2.5}$ concentrations and total extinction for the August 7-9, 1995 episode**.** Mad Creek**.**

6.7.3. CALMET Limitations

CALMET contains two principal submodels: the Diagnostic Wind Model and the Micrometeorological Model. As with all models of complex phenomena, each has significant limitations with respect to representing the real world.

Limitations of the diagnostic wind model are:

While CALMET solves the incompressible mass continuity equation, the method does not explicitly conserve momentum or energy as in prognostic models.

The diagnostic wind model may be viewed as a complex mass-conservative measurement interpolation package. Reliability of the interpolated fields improves as the density of the measurement stations increases; conversely, reliability degrades where measurements are sparse.

Experience has shown that such models have not been successful in representing light wind situations, highly stable or unstable conditions, and situations with significant vertical wind variations, particularly over distances of <1 km. Specific limitations related to the MZVS include CALMET's inability to reproduce the vertical recirculation patterns associated with mountain-valley winds, lee waves, lee wakes, and chaotic light wind situations.

Limitations of the micrometeorological model are:

Micrometeorological parameters required by CALPUFF are calculated by CALMET based on parameterizations that include many variables. Error derives from limitations in the input data, for which direct micrometeorological measurements are sparse or unavailable. Complex terrain greatly exacerbates this problem.

CALMET does not include any adjustment of sun angle to account for the local terrain slope. As a result, the model will not properly account for differential heating of mountain slopes that can produce significant stability, mixing height, and wind direction differences over surfaces with different orientations relative to the sun.

Given these limitations, several atmospheric processes in the MZVS domain, such as the development of local-scale convective cells and venting of material trapped below the inversion by flow up heated slopes, may not be reliably simulated with CALMET. Inaccurate lapse rates, and uncertainties in the estimated micrometeorological variables, lead to inaccuracies in daytime convective mixing height. This is of particular concern for the MZVS modeling owing to the interaction of generating station plumes with the mixing depth. Errors in mixing depth can result in large errors in estimates of plume location and dispersion. On average, however, the CALMET mixing depth estimates compared well with those determined by radar profile measurements (see Section 5.2).

CALMET sensitivity tests (Appendix B.2) conclude that the model performs best when and where terrain-induced flow agrees with observations, for near-surface wind fields away from complex terrain, in

data-rich areas, and aloft (> 1,000 m AGL). The model is questionable near observed calms, when and where observations appear to be locally influenced (< 1 km), distant from observations, and when surface observations directly affect only layer 1 wind fields (leading to potentially very large vertical shear). CALMET breaks down when and where divergence minimization creates spurious high-speed winds near the surface, when and where measured or inferred lapse rates do not agree with diurnal changes in stability, and when and where observations influence near-surface wind fields on opposite sides of terrain features.

6.7.3 Overview of CALPUFF

CALPUFF is a multi-layer, multi-species, nonsteady-state puff dispersion model that simulates the effects of time- and space-varying meteorological conditions on pollutant transport, transformation, and removal. CALPUFF contains algorithms for near-source effects such as building downwash, transitional plume rise, partial plume penetration, and subgrid scale terrain interactions. It also includes longer range effects such as pollutant removal (wet scavenging and dry deposition), chemical transformation, vertical wind shear, over-water transport, and coastal interaction effects. It can accommodate arbitrarily-varying point source and gridded area source emissions. Most of the algorithms contain options to treat physical processes at different levels of detail depending on the model application and the availability meteorological and other data inputs.

CALPUFF calculates species concentrations at user-defined discrete receptor locations and/or receptors located on a Cartesian "sampling grid". Concentrations are calculated at ground level in the Modification 1 code, so the computer code modifications described above were effected to output calculated concentrations at different elevations along sight paths. For the MZVS CALPUFF application, discrete receptors were placed at air quality monitoring sites to assist in model performance evaluation, as well as at several key locations within the Wilderness and along sight paths. To keep model run times manageable, sampling grid receptors were not specified for the detailed modeling as they were for the everyday modeling.

CALPUFF reads inputs from a "control file" that specifies selections for the various model options, input variables, and output options. Table 6.7.2 documents these selections and compares them with IWAQM defaults. Input data files supply: 1) meteorological and geophysical data (CALMET output); 2) time- and space-varying emissions inputs; and 3) ambient ozone concentrations, deposition velocities, chemical transformation rates, and dispersion coefficients. Emissions were generated for elevated point and area sources for twelve specific source regions or types (including fires and coal-fired generating stations). For each source region, CALPUFF was applied to the regional domain with 4 km x 4 km grid squares. Results for the different source regions were superimposed, with adjustments to account for errors due to the assumed chemical linearity (see Section 5.7.6). Species modeled included SO_2, sulfate, NO_x ($NO+NO_2$), HNO_3, particulate nitrate, elemental carbon, primary organic carbon, secondary organic aerosol (SOA), and noncarbonaceous primary $PM_{2.5}$.

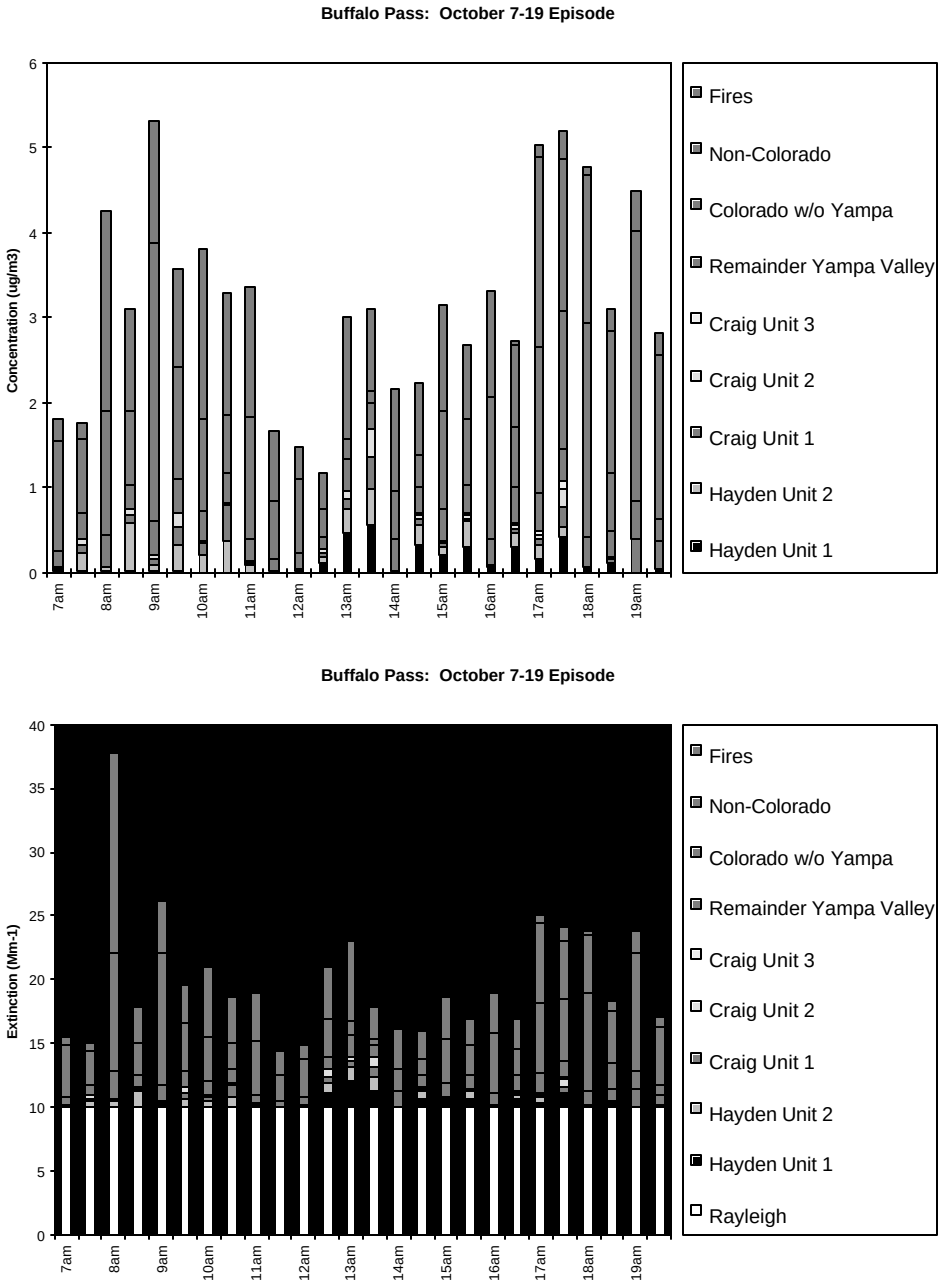

Figure 6.7.3a Source contribution to CALPUFF estimated six-hour average $PM_{2.5}$ concentrations and total extinction for the October 7-19, 1995 episode. Buffalo Pass.

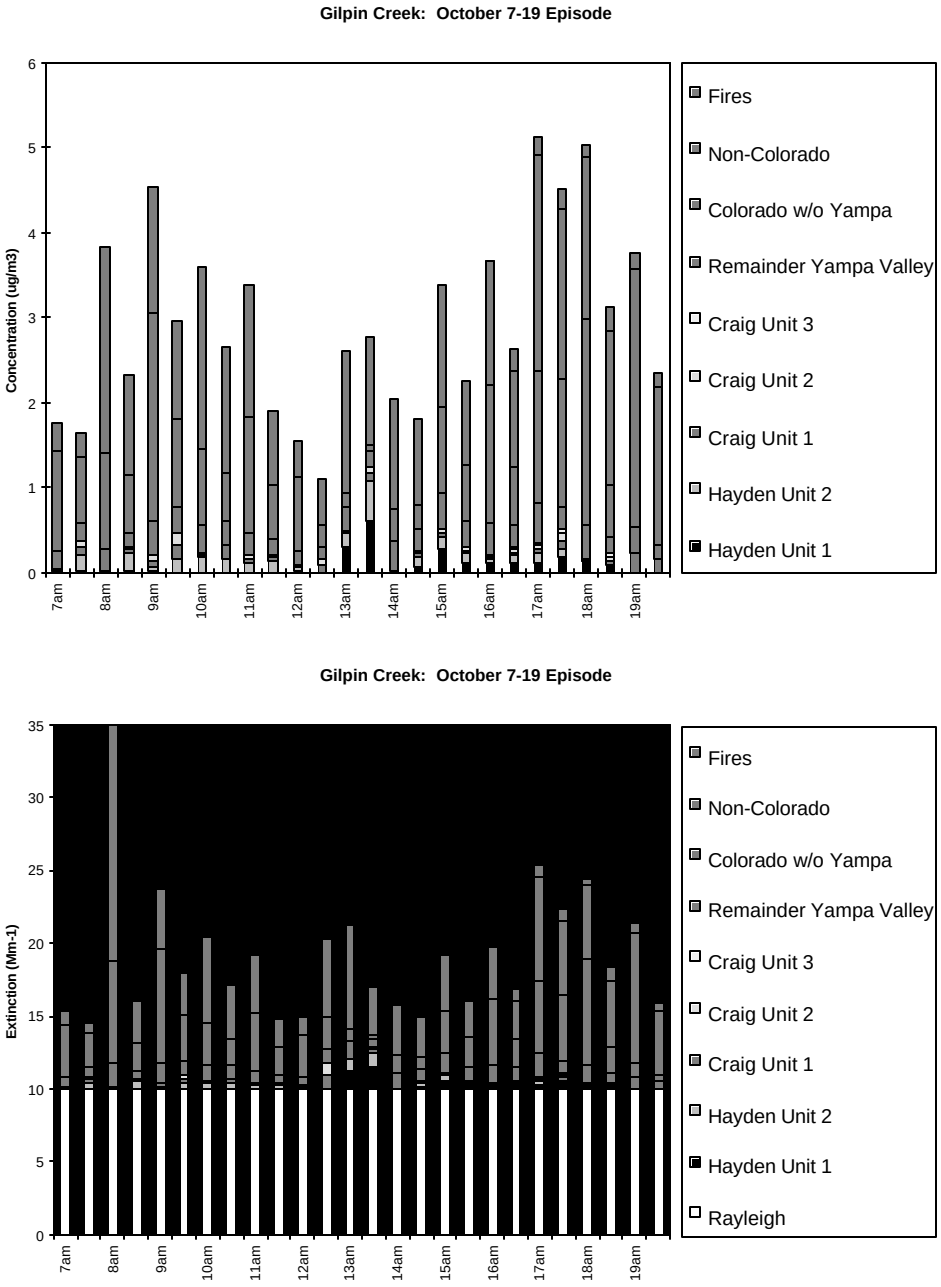

Figure 6.7.3b Source contribution to CALPUFF estimated six-hour average $PM_{2.5}$ concentrations and total extinction for the October 7-19, 1995 episode. Gilpin Creek.

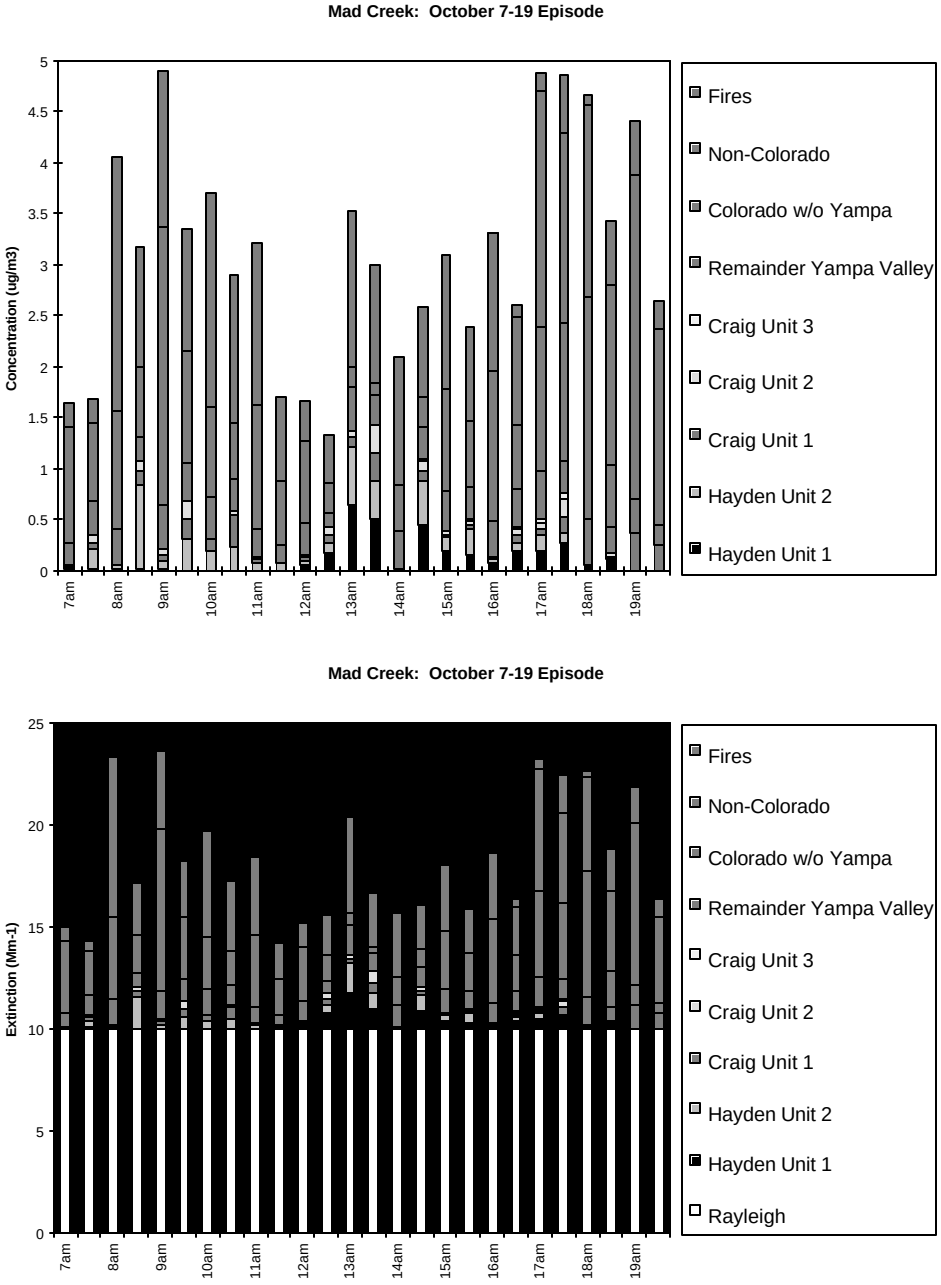

Figure 6.7.3c Source contribution to CALPUFF estimated six-hour average $PM_{2.5}$ concentrations and total extinction for the October 7-19, 1995 episode. Mad Creek.

Table 6.7.2
CALPUFF Modeling Options, Sensitivity Tests Performed, and Optimal Values for the Mt. Zirkel Visibility Study

Parameter	IWAQM Default	MZVS Optimal	Sensitivity Tests
GENERAL RUN CONTROL PARAMETERS			
Starting Date (days before episode)	None	2-3[7]	
Number of Modeled Species[8]	5	9	
Averaging Time (min)	60	60	
TECHNICAL OPTIONS			
Near-Field Vertical Puff Distribution (0=uniform/1=Gaussian)	1	1	
Terrain Adjustment (0=none/1=ISC adjustment/2=CALPUFF adjustment/3=half-height adjustment)	1	0	
Sub-Grid Complex Terrain Adjustment (0=none/1=CTSG model)	None	0	
Near-Field Puff Model (0=puff/1=elongated "slugs")	1	0[9]	
Plume Rise Calculation (0=final rise only/1=transitional rise)	1	0[10]	

[7] Whenever possible, a spinup period of 5 days was used in the every-day inert SO_2 trajectory modeling

[8] SO_2, $SO_4^{=}$, NO_x,. HNO_3, NO_3^{-}, elemental carbon (EC), primary organic carbon (POC), secondary organic aerosol (SOA), other $PM_{2.5}$ (PPM25). Only SO_2 was specified for every-day inert power plant plume trajectory simulations

[9] The slug formulation was used for every-day inert SO_2 trajectory modeling (puffs were used to calculate gridded SO_2 for animation)

[10] Transitional rise was used for every-day inert SO_2 trajectory modeling

Parameter	IWAQM Default	MZVS Optimal	Sensitivity Tests
Stack Tip Downwash (0=no/1=yes)	1	0	
Vertical Wind Shear Used in Plume Rise (0=no/1=yes)	1	1	

Parameter	IWAQM Default	MZVS Optimal	Sensitivity Tests
Puff Shear Splitting (0=no/1=yes)	None	1	0,1
Chemical Mechanism (0=inert/1=MESOPUFF II scheme/2=user-specified rates)	1	1	
Wet Removal (0=no/1=yes)	1	1[11]	0,1
Dry Removal (0=no/1=yes)	1	1	
Dispersion Coefficients (1=user-specified turbulence statistics/2=turbulence statistics from micro-meteorological variables/3=rural PGT using ISCST approx, urban MP/4=rural PGT using MESOPUFF equations, urban MP/5=CTDM equations with user-specified turbulence statistics)	2	2	
PGT Dispersion Coefficients Adjusted for Surface Roughness (0=no/1=yes)	0	0	
Partial Plume Penetration of Elevated Inversion (0=no/1=yes)	None	1	
Test for Regulatory Settings (0=no/1=US EPA short range/2=US EPA long range visibility/3=Victoria EPA)	None	0	
GRID CONTROL PARAMETERS			
Met/Computational Grid Resolution (km)			
Mesoscale Region	None	4	
Regional-Scale Region	None	4	4,16
Model Domain Extent (km x km)			
Mesoscale Region	None	280 x 152	
Regional-Scale Region	None	784 x 560	

[11] Wet deposition was not invoked for every-day inert SO_2 trajectory modeling

Parameter	IWAQM Default	MZVS Optimal	Sensitivity Tests
Column Range of Computational Grid[12]			
Mesoscale Region	None	1-70	
Regional-Scale Region	None	1-196	1-49,1-196
Row Range of Computational Grid[2]			
Mesoscale Region	None	1-38	
Regional-Scale Region	None	1-140	1-35,1-140
Column Range of Sampling Grid[13]			
Mesoscale Region	None	1-70	
Regional-Scale Region	None	None	1-49,73-142,None
Row Range of Sampling Grid			
Mesoscale Region	None	1-38	
Regional-Scale Region	None	None	1-35,55-92,None
Sampling Grid Nesting Factor			
Mesoscale Region	None	1	
Regional-Scale Region	None	1	
Top of Modeling Domain (km AGL)			
Mesoscale Region	None	2.8	
Regional-Scale Region	None	2.8	

[12]Coverage of the computational grid in terms of meteorological grid points; resolution must equal meteorological grid resolution. Full coverage of the meteorological grid was used. Row and column ranges given in this table reflect grid resolution listed above.

[13]Coverage of the sampling grid in terms of meteorological grid points; resolution can be equal or higher than meteorological grid resolution. Sensitivity tests for the regional grid included the entire domain at 16 km resolution, the mesoscale sub-domain at 4 km resolution, and no sampling grid. No sampling grid was used in the final regional production runs.

Parameter	IWAQM Default	MZVS Optimal	Sensitivity Tests
Number of Vertical Layers[14]			
Mesoscale Region	None	13	
Regional-Scale region	None	13	
DRY DEPOSITION PARAMETERS – GASES			
Diffusivity (cm^2/s)			
SO_2	None	0.1509	
NO_x	None	0.1656	
HNO_3	None	0.1628	
ALPHA STAR			
SO_2	None	1.00e3	
NO_x	None	1.00	
HNO_3	None	1.00	
Reactivity			
SO_2	None	8.0	
NO_x	None	8.0	
HNO_3	None	18.0	
Mesophyll Resistance (s/cm)			
SO_2	None	0.0	
NO_x	None	5.0	
HNO_3	None	0.0	
Henry's Law Coefficient			
SO_2	None	4.0e-2	
NO_x	None	3.5	
HNO_3	None	8.0e-8	

[14] MZVS "optimal" vertical cell faces are (m agl): 0, 20, 70, 182, 294, 406, 518, 630, 840, 1134, 1526, 1918, 2310, 2800

Parameter	IWAQM Default	MZVS Optimal	Sensitivity Tests
DRY DEPOSITION PARAMETERS – PARTICLES			
Geometric Mass Mean Diameter (microns)	None	0.48	
Geometric Standard Deviation (microns)	2.00	2.00	
MISC. DRY DEPOSITION PARAMETERS			
Reference cuticle resistance (s/cm)	30	30	
Reference ground resistance (s/cm)	10	10	
Reference pollutant reactivity	8	8	
Unirrigated Vegetation State (1=active and unstressed/2=active and stressed/3=inactive)	1	1	
WET DEPOSITION PARAMETERS			
Scavenging Coefficient - Liquid Precip (s^{-1})			
SO_2	3.0e-5	3.0e-5	
NO_x	0.0	0.0	
HNO_3	6.0e-5	6.0e-5	
SO_4, NO_3, other PM	10.0e-5	10.0e-5	
Scavenging Coefficient - Frozen Precip (s^{-1})			
SO_2	0.0	0.0	
NO_x	0.0	0.0	
HNO_3	0.0	0.0	
SO_4, NO_3, other PM	3.0e-5	3.0e-5	

Parameter	IWAQM Default	MZVS Optimal	Sensitivity Tests
CHEMISTRY PARAMETERS			
Ozone Data[15] (0=use constant background value/1=use hourly values from file)	1	0 & 1	
Background Ozone Concentration in ppb (used if no ozone file read, or if all ozone data is missing)	80	40	
Background ammonia concentration (ppb)	10	Episode-specific	
Nighttime SO_2 loss rate (percent/hr)	0.2	0.2	
Nighttime NO_x loss rate (percent/hr)	2.0	2.0	
Nighttime HNO_3 formation rate (percent/hr)	2.0	2.0	
DISPERSION PARAMETERS			
Use Heffter Formulas for $?_z$ (0=no/1=yes)	1	1	
Critical Horizontal Puff Size to use Heffter Formulas (m)	550	550	
Stability Class for Puffs Above Boundary Layer	5	5	
Vertical Dispersion Constant for Stable Conditions	0.01	0.01	
Vertical Dispersion Constant for Neutral/Unstable Conditions	0.10	0.10	
Range of Urban Land Use Categories	10-19	10-19	
Maximum Travel Distance of Puff in One Sampling Step (Met Grid Units)	5	1	

[15]A single background value for ozone (40 ppb) was used for the August 7-9 episode due to lack of data at the Hayden VOR site for that period.

Parameter	IWAQM Default	MZVS Optimal	Sensitivity Tests
Maximum Number of Puffs Released from Each Source during 1 Time Step	99	99	
Maximum Number of Sampling Steps per Time Step	5	5	
Wind Speed Power Law Exponents for Stabilities A-F	0.07, 0.07 0.10, 0.15 0.35, 0.55	0.07, 0.07 0.10, 0.15 0.35, 0.55	
Potential Temperature Gradient for Stability E and F (K/m)	0.02, 0.035	0.02, 0.035	
Minimum $?_y$ of New puffs (m)	0.01	0.01	
Minimum $?_z$ of New Puffs (m)	0.01	0.01	
Minimum Turbulence $?_v$ (m/s)	0.50	0.50	
Minimum Turbulence $?_w$ (m/s)	0.016	0.016	
Minimum Wind Speed for Non-Calm Conditions (m/s)	1.0	0.1	
Maximum Mixing Height (m)	3000	2800	
Minimum Mixing Height (m)	20	20	

6.7.4 CALPUFF Limitations

CALPUFF is a highly parameterized Lagrangian puff model that has limitations and simplifications in its representation of each atmospheric process.

Transport is treated with these considerations:

The assumption of puff coherency becomes invalid in the complex terrain flow fields around the Wilderness. Puffs of emissions are advected by a single wind at puff center, even though the puff may have large horizontal and vertical extent. The complex terrain wind fields probably include significant variations in winds horizontally and vertically across the puff that are not considered by CALPUFF.

Once final rise from a stack is determined, the elevation of a puff center is not adjusted to a mean height when puffs mix through large depths. In reality, puffs do not necessarily travel with the mean flow over puff depth (particularly those emanating from low-level area sources). This may artificially lead to a buildup of mass due to weaker near-surface winds, and puffs may not be advected with the most realistic speed or direction.

It is possible for one receptor to simultaneously sample concentrations from near- surface puffs and from deeply mixed puffs aloft that move at different speeds and directions. This contradicts the fundamental principle that two columns of mass cannot impinge on a point from more than one direction.

While the puff splitting option to handle vertical shear is available in Modification 1 of CALPUFF, this was a recent addition. Documentation explaining the parameters controlling puff splitting were not included in the user's guide or in the code. While other model parameters are adjustable through the control file, the puff splitting parameters (except the flag to select this option) were set internally to fixed values without descriptions of their origin or what they are intended to simulate. A sensitivity test of plume transport with and without the puff splitting option (Appendix B.2) showed no difference between estimated concentrations, despite large shears in vertical winds. This may not be an inherent limitation of the CALPUFF model, as plume splitting parameters might be customized to specific applications when a protocol for such customization has been developed. Regardless of these findings, it was assumed that puffs from other sources may meet the criteria necessary to split puffs due to vertical shear, so the puff splitting option was selected for all production runs of each episode.

Dispersion is treated with the following considerations:

Except for the CTDM option, the CALPUFF dispersion options are not designed to simulate regional dispersion in complex terrain. For most options, puffs are dispersed uniformly. The effects of enhanced dispersion in portions of the puffs owing to complex-terrain-induced turbulence cannot be simulated.

The CALPUFF user's manual is unclear about the CTDM option. It suggests that the CTDM-based "simple CALPUFF" terrain adjustment option adjusts receptor elevations relative to puff centerline height, and that it calculates terrain-enhanced puff dispersion to account for slope strain. Investigation of the CALPUFF model code revealed that while the ISC (option 1) and the partial plume height correction (option 3) explicitly account for varying ground-level receptor elevations in complex terrain, the CTDM option does not. However, this effect in CTDM may be indirectly accounted for in the routine that adjusts puff dispersion coefficients. Options 1 and 3 were not tested owing to complexities of incorporating elevated receptors for sight path calculations. When the CTDM option was selected, CALPUFF required 16.5 times longer to run with elevated receptors, and 5 times longer without elevated receptors. Concentrations at Buffalo Pass were found to be all zero for the entirety of the simulation, suggesting an error in the computer code. Therefore, no terrain adjustment was specified for the detailed or everyday modeling. CALPUFF was applied in a flat-plane mode wherein terrain effects are realized solely via gridded wind inputs.

Chemical transformation is treated as follows:

The mechanism has no temperature dependence, which is an important factor in the Rocky Mountain region where there are wide variations in temperature.

SO_x transformation parameterization is based on box model simulations for conditions more representative of the eastern U.S. than the Rocky Mountains. Section 6.3 shows that under dry conditions, with reactive constituents typical of nonurban rather than urban areas, conversion of sulfur dioxide to sulfate is very slow (~0.1 percent per hour).

The largest chemical deficiency is the treatment of in-cloud (aqueous-phase) enhanced oxidation of SO_2 to sulfate. At 100% relative humidity (RH), the MESOPUFF-II aqueous-phase surrogate SO_2 oxidation rate is 3% per hour. Section 6.3 demonstrates that transformation rates are much larger than this when a plume passes through clouds or fogs.

Wet deposition is treated as follows:

CALPUFF uses a simple scavenging coefficient to simulate wet pollutant removal. The most uncertain component in the treatment of wet deposition is the interpolation of observed daily precipitation rates to the grid as hourly rates, despite the numerous precipitation measurement locations identified in Section 2. Precipitation is highly variable, both spatially and temporally, in the study region.

Mass is removed from the entirety of each puff based on hourly precipitation rates at the cell containing the puff centerpoint (puffs may span as much as 50 km or more), even though the convective precipitation in the Wilderness during the summer is spotty.

Dry deposition is treated as follows:

CALPUFF uses a highly-developed resistance dry deposition module that is limited by the lack of sufficiently detailed data as input.

Mass is removed from the entirety of each puff based on surface and micrometeorological conditions within the cell containing the puff centerpoint (puffs may span as much as 50 km or more).

CALPUFF tests (Appendix B.2) show that the model works best for direct or nearly-direct source-receptor transport of primary species with well-characterized emission rates. It is also accurate in noncomplex terrain. CALPUFF performance is questionable during periods of spotty and varying precipitation patterns, when and where significant vertical shears develop, when and where there are significant impacts from area sources due to simple puff treatment, for species arising from uncertain source emissions (dust, SOA, fires), and for NO_x and nitrate equilibrium and chemistry of overlapping puffs. CALPUFF breaks down when horizontally and vertically expansive puffs are advected by winds at the puff centerpoint that are not adjusted vertically, when surface-based relative humidity does not represent humidity at puff elevation for deeply mixed puffs, and when sulfate production is dominated by aqueous chemistry.

6.7.5 Comparison of Modeled Concentrations with Measurements

CALMET/CALPUFF model performance evaluation results are provided in Appendix B.2. Several of the limitations discussed above degrade the comparison of modeled and measured particle concentrations and light extinction. Table 6.7.3 summarizes the episode- and site-averaged model bias for each period modeled and for each modeled species. Average bias is defined as the percent difference between the CALPUFF and measured six-hour $PM_{2.5}$ concentrations averaged across the six MZVS aerosol measurement sites and averaged over the duration each modeling period. Even with the model limitations cited above, the average CALPUFF-estimated $PM_{2.5}$ levels were close to what was observed during the 09/17/95–09/21/95 and 10/07/95–10/19/95 periods. However, the modeling system systematically underestimated $PM_{2.5}$ concentrations for the 08/07/95–08/09/95 and 08/21/95–08/27/95 periods.

Table 6.7.3
Summary of Statistical Comparisons
between Measured and CALPUFF-Predicted Species Concentrations[1]

Episode	Total $PM_{2.5}$	Sulfate	Nitrate	Primary $PM_{2.5}$	Elemental Carbon	Organic Aerosol
Sep 17-21	+21	+16	+112	+12	-62	-17
Aug 7-9	-71	-71	-11	-79	-87	-75
Oct 7-19	-6	+21	+69	-46	-70	-21
Aug 21-27	-63	-59	+75	-62	-88	-77

[1] Reported is the mean bias (%) among all sites and among all days for each of four intensive modeling episodes, calculated as percent difference between average observed and average estimated PM concentrations.

There are several potential reasons for the poor performance of the modeling system for the two August episodes, including the influence of super-regional transport of pollutants from outside of the regional modeling domain. The modeling system tends to overestimate ammonium nitrate and to underestimate elemental carbon concentrations. It does not accurately estimate noncarbonaceous primary $PM_{2.5}$. Non-carbonaceous primary $PM_{2.5}$ is dominated by fugitive dust emissions that are highly uncertain. Measured values are frequently due to local emissions that are not included in the inventory and are not resolved by CALPUFF modeling. For the September and October episodes, the modeling system tended to overestimate sulfate concentrations at Buffalo Pass near the Wilderness.

For each modeling period, Table 6.7.4 compares CALPUFF $PM_{2.5}$ mass budgets averaged over all sites and days with corresponding measured mass budgets. Although the absolute concentrations calculated by CALMET/CALPUFF do not compare well with the measured values, the relative concentrations compare reasonably well. Both the modeled and measured results agree that 20-40% of the $PM_{2.5}$ is due to sulfate and that a majority (30-50%) of the modeled and measured $PM_{2.5}$ is due to organic aerosols. The model tends to overestimate ammonium nitrate and to underestimate elemental carbon concentrations. Although the model exhibits some skill in estimating the relative contribution of the $PM_{2.5}$ chemical components, this does not necessarily mean that the model estimates accurate source

attribution to $PM_{2.5}$. This is especially true for the two August episodes, when a portion of the measured $PM_{2.5}$ concentrations may derive from long-range transport of pollutants from upwind of the regional modeling domain.

Table 6.7.4
Average Relative Contribution (%) of Estimated and Observed PM Components to Total $PM_{2.5}$ (Mass Budgets) for the Four Intensive Modeling Episodes

	Sulfate	Nitrate	Primary $PM_{2.5}$	Elemental Carbon	Organic Aerosol	Total $PM_{2.5}$ (ug/m^3)
September 17-21						
Measured	34	6	7	10	44	3.50
Estimated	39	13	8	4	36	4.23
August 7-9						
Measured	23	5	13	9	50	6.63
Estimated	24	17	10	4	45	1.84
October 7-19						
Measured	26	7	17	12	39	2.82
Estimated	36	14	11	4	36	2.66
August 21-27						
Measured	31	3	9	10	47	4.87
Estimated	38	15	10	3	33	1.79

The CALMET/CALPUFF modeling system overestimates measured sulfate and ammonium nitrate levels at receptors in the vicinity of the Wilderness, indicating that the model may overstate the $PM_{2.5}$ impacts due to the two generating stations in the Yampa Valley. More confidence can be placed in the relative contributions of sources to different chemical components than on the absolute CALMET/CALPUFF source contribution estimates.

6.7.6 Source Contributions to $PM_{2.5}$ and Extinction

As discussed in Section 6.3 above and Section 6.9 below, the conversion of SO_2 to sulfates is a nonlinear process, such that reductions of SO_2 emissions may not result in corresponding reductions in particulate sulfate. Nonlinearities are also associated with NO_x/ozone and nitrate/ammonia equilibria. For the analyses that follow, CALPUFF was run independently for each source region, and nonlinearities associated with secondary particulate formation from SO_2 and NO_x combined from different sources are

not treated. By associating the various sources with levels of secondary particulate species, and then to extinction, the following analyses assume that the SO_2/sulfate and NO_x/nitrate relationships are linear. This may overstate the effects of emissions reductions on secondary $PM_{2.5}$ and resulting extinction estimates.

Table 6.7.5 and Figure 6.7.1 display the modeled six-hour source contributions to total $PM_{2.5}$ and extinction at three Wilderness receptors during the 09/17/95–09/21/95 period. Source contributions are presented for each unit of the Hayden (Units 1 and 2) and Craig (Units 1, 2, and 3) stations, the remainder of the sources in the mesoscale domain referred to as Yampa Valley, the remainder of Colorado, for the non-Colorado sources in the regional domain, and for fires. More detailed source apportionment, including separate apportionments for Steamboat Springs, Denver, and Salt Lake City, are provided in Appendix B.2.

The contributions from the Hayden and Craig stations to the estimated $PM_{2.5}$ concentrations at Buffalo Pass vary from 1% (morning of 09/21/95) to 51% (afternoon of 09/18/95). In general, the Hayden station contribution to the total $PM_{2.5}$ concentration is approximately three times the contribution from the Craig station. Despite the fact that Hayden Unit 2 has higher SO_2 emission rates than Hayden Unit 1, Hayden Unit 1 has higher estimated $PM_{2.5}$ impacts at Buffalo Pass than Hayden Unit 2.

This is likely due to the lower plume height from Hayden Unit 1 that affects its transport toward the Wilderness. The lower plume might be channeled more eastward within Yampa Valley flows, while higher plumes are transported toward the north or northeast. The lower plume will also produce higher ground-level concentrations before it is uniformly mixed. The model estimates two significant periods during which the Hayden and Craig stations have larger than average contributions to the total $PM_{2.5}$: the afternoon of 09/18/95 (51%); and the afternoon of 09/19/95 (49%). Note that on the afternoon of 09/21/95, Hayden Unit 1 has a significant contribution (19%), but the other units from the Hayden and Craig stations do not.

For most periods, the source regions that contribute the most to $PM_{2.5}$ at Buffalo Pass are outside of the Yampa Valley, either within or outside of Colorado. Emissions from fires are also significant contributors on some days, with the model suggesting relative contributions to the total $PM_{2.5}$ of ~30% during some periods (09/20/95).

The relative CALMET/CALPUFF source contributions to light extinction at Buffalo Pass during the 09/17/95–09/21/95 period are similar to the relative contributions to $PM_{2.5}$ concentrations, except that clean air Rayleigh scattering of 10 Mm^{-1} is included, thereby lowering the contribution from all source categories. A nominal value of 10 Mm^{-1} is used for clean air scattering rather than the 8.4 Mm^{-1} cited for Buffalo Pass in Section 3 to simplify processing and analyses. The maximum contribution to extinction at Buffalo Pass from the Hayden and Craig stations during this episode is 46% on the afternoon of 09/18/95, with 32% contributed by Hayden Units 1 and 2 and 12% contributed by Craig Units 1 and 2.

The modeled source contributions for Gilpin Creek (Tables 6.7.5c,d) and Mad Creek (Tables 6.7.5e,f) are similar to those for Buffalo Pass. The contributions of emissions from the Hayden and Craig stations to $PM_{2.5}$ and extinction in the Wilderness decreases with increasing northerly distance from Buffalo Pass.

Table 6.7.5a
CALPUFF Estimated Source Contribution to Total $PM_{2.5}$ Concentrations (u g/m^3) at Buffalo Pass for the September 17-21, 1995 Episode

		Hayden Generating station				Craig Generating station											
	Total $PM_{2.5}$	Unit #1		Unit #2		Unit #1		Unit #2		Unit #3		Remainder Yampa Valley		Colorado w/o Yampa Valley		Non-Colorado		Fires	
Date	ug/m3	ug/m3	(%)	ug/m3	(%)	ug/m3	(%)	ug/m3	(%)	ug/m3	(%)	ug/m3	(%)	ug/m3	(%)	ug/m3	(%)	ug/m3	(%)
Sep. 17 am	5.67	0.23	4	0.23	4	0.08	1	0.09	2	0.05	1	0.33	6	3.47	61	1.02	18	0.17	3
Sep. 17 pm	4.56	0.49	11	0.47	10	0.09	2	0.09	2	0.05	1	0.38	8	1.87	41	0.79	17	0.34	8
Sep. 18 am	5.49	0.44	8	0.30	6	0.14	3	0.15	3	0.08	2	0.49	9	2.19	40	0.96	18	0.71	13
Sep. 18 pm	3.77	0.72	19	0.64	17	0.24	6	0.25	7	0.09	2	0.19	5	0.59	16	0.78	21	0.28	8
Sep. 19 am	2.00	0.20	10	0.15	8	0.05	3	0.05	2	0.01	1	0.26	13	0.49	25	0.69	35	0.09	5
Sep. 19 pm	3.07	0.70	23	0.46	15	0.10	3	0.17	6	0.07	2	0.29	9	0.31	10	0.75	25	0.21	7
Sep. 20 am	6.06	0.31	5	0.34	6	0.13	2	0.13	2	0.04	1	0.44	7	0.68	11	2.17	36	1.81	30
Sep. 20 pm	3.91	0.12	3	0.05	1	0.00	0	0.01	0	0.00	0	0.21	5	0.24	6	2.37	61	0.93	24
Sep. 21 am	2.95	0.02	1	0.00	0	0.00	0	0.00	0	0.00	0	0.49	17	0.24	8	1.94	66	0.26	9
Sep. 21 pm	2.46	0.47	19	0.05	2	0.00	0	0.00	0	0.00	0	0.28	11	0.23	10	1.30	53	0.11	5

Table 6.7.5b
CALPUFF Estimated Source Contribution to Total Extinction (Mm^{-1}) at Buffalo Pass for the September 17-21, 1995 Episode
(total extinction includes a nominal value of 10 Mm^{-1} for Rayleigh scattering)

		Hayden Generating station				Craig Generating station											
	Total bext	Unit #1		Unit #2		Unit #1		Unit #2		Unit #3		Remainder Yampa Valley		Colorado w/o Yampa Valley		Non-Colorado		Fires	
Date	Mm^{-1}	Mm^{-1}	(%)	Mm^{-1}	(%)	Mm^{-1}	(%)	Mm^{-1}	(%)	Mm^{-1}	(%)	Mm^{-1}	(%)	Mm^{-1}	(%)	Mm^{-1}	(%)	Mm^{-1}	(%)
Sep. 17 am	25.79	0.48	2	0.48	2	0.16	1	0.18	1	0.11	0	1.05	4	10.09	39	2.62	10	0.61	2
Sep. 17 pm	22.20	1.02	5	0.98	4	0.18	1	0.19	1	0.09	0	1.20	5	5.36	24	1.96	9	1.21	5
Sep. 18 am	82.78	6.87	8	4.70	6	2.14	3	2.37	3	1.26	2	5.68	7	27.32	33	13.60	16	8.84	11
Sep. 18 pm	64.19	11.09	17	9.84	15	3.72	6	3.83	6	1.43	2	2.14	3	7.49	12	11.18	17	3.48	5
Sep. 19 am	29.14	2.08	7	1.60	6	0.55	2	0.51	2	0.16	1	2.22	8	4.31	15	6.91	24	0.81	3
Sep. 19 pm	22.04	2.68	12	1.74	8	0.39	2	0.66	3	0.28	1	1.14	5	1.29	6	2.92	13	0.95	4

Sep. 20 am	90.93	4.87	5	5.19	6	2.05	2	2.06	2	0.65	1	5.02	6	8.08	9	30.98	34	22.02	24
Sep. 20 pm	63.55	1.78	3	0.71	1	0.07	0	0.10	0	0.02	0	2.22	3	2.87	5	34.53	54	11.23	18
Sep. 21 am	32.10	0.16	1	0.03	0	0.00	0	0.00	0	0.00	0	3.36	10	1.63	5	15.00	47	1.90	6
Sep. 21 pm	24.53	2.85	12	0.33	1	0.01	0	0.03	0	0.00	0	1.55	6	1.35	6	7.74	32	0.67	3

Table 6.7.5c
CALPUFF Estimated Source Contribution to Total $PM_{2.5}$ Concentrations (u g/m^3) at Gilpin Creek for the September 17-21, 1995 Episode

		Hayden Generating station				Craig Generating station											
	Total $PM_{2.5}$	Unit #1		Unit #2		Unit #1		Unit #2		Unit #3		Remainder Yampa Valley		Colorado w/o Yampa Valley		Non-Colorado		Fires	
Date	ug/m3	ug/m3	(%)	ug/m3	(%)	ug/m3	(%)	ug/m3	(%)	ug/m3	(%)	ug/m3	(%)	ug/m3	(%)	ug/m3	(%)	ug/m3	(%)
Sep. 17 am	5.14	0.23	5	0.23	5	0.08	2	0.09	2	0.05	1	0.30	6	2.74	53	1.23	24	0.18	4
Sep. 17 pm	4.50	0.42	9	0.35	8	0.14	3	0.14	3	0.06	1	0.39	9	1.62	36	0.97	22	0.42	9
Sep. 18 am	5.27	0.44	8	0.38	7	0.12	2	0.13	2	0.05	1	0.46	9	1.82	35	1.07	20	0.80	15
Sep. 18 pm	3.66	0.52	14	0.42	12	0.28	8	0.27	7	0.14	4	0.16	4	0.53	14	1.02	28	0.32	9
Sep. 19 am	1.51	0.10	7	0.09	6	0.03	2	0.03	2	0.01	0	0.17	11	0.30	20	0.71	47	0.07	5
Sep. 19 pm	2.35	0.38	16	0.27	12	0.06	3	0.07	3	0.03	2	0.16	7	0.26	11	0.91	39	0.21	9
Sep. 20 am	4.86	0.04	1	0.05	1	0.02	0	0.02	0	0.00	0	0.34	7	0.46	9	2.35	48	1.57	32
Sep. 20 pm	3.49	0.03	1	0.01	0	0.00	0	0.00	0	0.00	0	0.13	4	0.17	5	2.59	74	0.56	16
Sep. 21 am	2.23	0.00	0	0.00	0	0.00	0	0.00	0	0.00	0	0.29	13	0.13	6	1.64	74	0.17	8
Sep. 21 pm	1.94	0.14	7	0.00	0	0.00	0	0.00	0	0.00	0	0.17	9	0.23	12	1.31	68	0.09	5

Table 6.7.5d
CALPUFF Estimated Source Contribution to Total Extinction (Mm^{-1}) at Gilpin Creek for the September 17-21, 1995 Episode
(total extinction includes a nominal value of 10 Mm^{-1} for Rayleigh scattering)

		Hayden Generating station				Craig Generating station											
	Total bext	Unit #1		Unit #2		Unit #1		Unit #2		Unit #3		Remainder Yampa Valley		Colorado w/o Yampa Valley		Non-Colorado		Fires	
Date	Mm^{-1}	Mm^{-1}	(%)	Mm^{-1}	(%)	Mm^{-1}	(%)	Mm^{-1}	(%)	Mm^{-1}	(%)	Mm^{-1}	(%)	Mm^{-1}	(%)	Mm^{-1}	(%)	Mm^{-1}	(%)
Sep. 17 am	24.43	0.49	2	0.49	2	0.17	1	0.19	1	0.10	0	0.95	4	8.18	34	3.22	13	0.62	3
Sep. 17 pm	21.30	0.78	4	0.65	3	0.25	1	0.27	1	0.11	1	1.17	5	4.42	21	2.23	11	1.42	7
Sep. 18 am	57.02	4.37	8	3.79	7	1.17	2	1.29	2	0.52	1	3.65	6	15.38	27	9.96	18	6.88	12
Sep. 18 pm	34.93	3.67	11	2.95	9	1.97	6	1.89	5	1.02	3	1.00	3	3.40	10	6.90	20	2.12	6
Sep. 19 am	18.40	0.56	3	0.49	3	0.18	1	0.17	1	0.04	0	0.93	5	1.65	9	3.97	22	0.41	2
Sep. 19 pm	16.97	1.02	6	0.73	4	0.17	1	0.19	1	0.09	1	0.52	3	0.83	5	2.61	15	0.81	5

Sep. 20 am	56.45	0.42	1	0.56	1	0.21	0	0.23	0	0.05	0	3.01	5	4.01	7	23.75	42	14.22	25
Sep. 20 pm	27.92	0.13	1	0.06	0	0.01	0	0.01	0	0.00	0	0.67	2	0.88	3	13.17	47	3.00	11
Sep. 21 am	20.38	0.02	0	0.00	0	0.00	0	0.00	0	0.00	0	1.34	7	0.59	3	7.56	37	0.87	4
Sep. 21 pm	15.69	0.37	2	0.01	0	0.00	0	0.00	0	0.00	0	0.57	4	0.71	5	3.72	24	0.31	2

Table 6.7.5e
CALPUFF Estimated Source Contribution to Total $PM_{2.5}$ Concentrations (u g/m^3) at Mad Creek for the September 17-21, 1995 Episode

		Hayden Generating station				Craig Generating station											
	Total $PM_{2.5}$	Unit #1		Unit #2		Unit #1		Unit #2		Unit #3		Remainder Yampa Valley		Colorado w/o Yampa Valley		Non-Colorado		Fires	
Date	ug/m3	ug/m3	(%)	ug/m3	(%)	ug/m3	(%)	ug/m3	(%)	ug/m3	(%)	ug/m3	(%)	ug/m3	(%)	ug/m3	(%)	ug/m3	(%)
Sep. 17 am	5.55	0.26	5	0.30	5	0.08	1	0.09	2	0.05	1	0.37	7	3.08	56	1.10	20	0.22	4
Sep. 17 pm	4.80	0.57	12	0.42	9	0.17	4	0.17	4	0.07	1	0.44	9	1.66	35	0.84	18	0.46	10
Sep. 18 am	5.84	0.71	12	0.47	8	0.17	3	0.18	3	0.08	1	0.54	9	1.86	32	0.99	17	0.85	15
Sep. 18 pm	3.41	0.50	15	0.47	14	0.24	7	0.24	7	0.10	3	0.17	5	0.52	15	0.85	25	0.31	9
Sep. 19 am	1.93	0.17	9	0.12	7	0.05	2	0.04	2	0.01	1	0.25	13	0.41	21	0.78	40	0.10	5
Sep. 19 pm	2.97	0.55	19	0.36	12	0.09	3	0.12	4	0.05	2	0.29	10	0.29	10	0.87	29	0.34	12
Sep. 20 am	6.21	0.24	4	0.23	4	0.08	1	0.09	1	0.03	0	0.46	7	0.60	10	2.34	38	2.15	35
Sep. 20 pm	3.97	0.04	1	0.01	0	0.00	0	0.00	0	0.00	0	0.17	4	0.21	5	2.64	67	0.90	23
Sep. 21 am	2.79	0.04	2	0.00	0	0.00	0	0.00	0	0.00	0	0.44	16	0.17	6	1.91	68	0.22	8
Sep. 21 pm	2.19	0.33	15	0.03	2	0.00	0	0.00	0	0.00	0	0.24	11	0.20	9	1.29	59	0.10	4

Table 6.7.5f
CALPUFF Estimated Source Contribution to Total Extinction (Mm^{-1}) at Mad Creek for the September 17-21, 1995 Episode
(total extinction includes a nominal value of 10 Mm^{-1} for Rayleigh scattering)

		Hayden Generating station				Craig Generating station											
	Total bext	Unit #1		Unit #2		Unit #1		Unit #2		Unit #3		Remainder Yampa Valley		Colorado w/o Yampa Valley		Non-Colorado		Fires	
Date	Mm^{-1}	Mm^{-1}	(%)	Mm^{-1}	(%)	Mm^{-1}	(%)	Mm^{-1}	(%)	Mm^{-1}	(%)	Mm^{-1}	(%)	Mm^{-1}	(%)	Mm^{-1}	(%)	Mm^{-1}	(%)
Sep. 17 am	24.72	0.50	2	0.58	2	0.15	1	0.18	1	0.11	0	1.12	5	8.64	35	2.69	11	0.76	3
Sep. 17 pm	22.20	1.11	5	0.81	4	0.33	2	0.33	2	0.14	1	1.34	6	4.59	21	1.98	9	1.58	7
Sep. 18 am	41.04	3.82	9	2.49	6	0.94	2	0.96	2	0.46	1	2.78	7	9.63	24	5.25	13	4.72	12
Sep. 18 pm	26.54	2.43	9	2.25	9	1.16	4	1.17	4	0.48	2	0.82	3	2.49	9	4.11	16	1.61	6
Sep. 19 am	18.13	0.67	4	0.50	3	0.18	1	0.17	1	0.06	0	1.08	6	1.76	10	3.23	18	0.48	3
Sep. 19 pm	18.05	1.32	7	0.84	5	0.22	1	0.28	2	0.12	1	0.92	5	0.90	5	2.23	12	1.23	7

Sep. 20 am	70.85	2.62	4	2.51	4	0.86	1	0.95	1	0.31	0	4.00	6	5.36	8	24.24	34	20.00	28
Sep. 20 pm	37.79	0.27	1	0.09	0	0.01	0	0.01	0	0.00	0	1.06	3	1.37	4	18.81	50	6.15	16
Sep. 21 am	26.54	0.26	1	0.03	0	0.00	0	0.00	0	0.00	0	2.49	9	0.99	4	11.43	43	1.34	5
Sep. 21 pm	17.73	1.09	6	0.11	1	0.00	0	0.01	0	0.00	0	0.91	5	0.75	4	4.45	25	0.40	2

Table 6.7.6a

CALPUFF Estimated Source Contribution to Total $PM_{2.5}$ Concentrations (u g/m^3) at Buffalo Pass for the August 7-9, 1995 Episode

		Hayden Generating station				Craig Generating station											
	Total $PM_{2.5}$	Unit #1		Unit #2		Unit #1		Unit #2		Unit #3		Remainder Yampa Valley		Colorado w/o Yampa Valley		Non-Colorado		Fires	
Date	ug/m3	ug/m3	(%)	ug/m3	(%)	ug/m3	(%)	ug/m3	(%)	ug/m3	(%)	ug/m3	(%)	ug/m3	(%)	ug/m3	(%)	ug/m3	(%)
Aug. 7 am	2.99	0.06	2	0.04	1	0.00	0	0.01	0	0.00	0	0.29	10	2.23	75	0.24	8	0.12	4
Aug. 7 pm	0.76	0.01	1	0.00	1	0.00	0	0.00	0	0.00	0	0.07	9	0.60	79	0.03	4	0.05	6
Aug. 8 am	0.54	0.01	2	0.01	2	0.00	0	0.00	0	0.00	0	0.15	27	0.34	62	0.03	6	0.00	1
Aug. 8 pm	0.59	0.03	6	0.03	4	0.01	1	0.01	2	0.01	1	0.15	25	0.10	18	0.12	21	0.13	23
Aug. 9 am	1.65	0.01	1	0.00	0	0.00	0	0.00	0	0.00	0	0.40	24	0.31	19	0.87	53	0.05	3
Aug. 9 pm	1.56	0.31	20	0.17	11	0.05	4	0.07	5	0.04	2	0.21	13	0.20	13	0.46	29	0.05	3

Table 6.7.6b

CALPUFF Estimated Source Contribution to Total Extinction (Mm^{-1}) at Buffalo Pass for the August 7-9, 1995 Episode

(total extinction includes a nominal value of 10 Mm^{-1} for Rayleigh scattering)

		Hayden Generating station				Craig Generating station											
	Total bext	Unit #1		Unit #2		Unit #1		Unit #2		Unit #3		Remainder Yampa Valley		Colorado w/o Yampa Valley		Non-Colorado		Fires	
Date	Mm^{-1}	Mm^{-1}	(%)	Mm^{-1}	(%)	Mm^{-1}	(%)	Mm^{-1}	(%)	Mm^{-1}	(%)	Mm^{-1}	(%)	Mm^{-1}	(%)	Mm^{-1}	(%)	Mm^{-1}	(%)
Aug. 7 am	18.53	0.11	1	0.08	0	0.01	0	0.02	0	0.01	0	0.89	5	6.35	34	0.66	4	0.40	2
Aug. 7 pm	12.21	0.01	0	0.01	0	0.00	0	0.00	0	0.00	0	0.21	2	1.72	14	0.10	1	0.16	1
Aug. 8 am	11.78	0.02	0	0.03	0	0.00	0	0.00	0	0.00	0	0.50	4	1.12	10	0.11	1	0.01	0

Aug.	8 pm	11.79	0.08	1	0.06	1	0.01	0	0.03	0	0.01	0	0.47	4	0.33	3	0.34	3	0.47	4
Aug.	9 am	14.67	0.02	0	0.00	0	0.00	0	0.00	0	0.01	0	1.20	8	0.93	6	2.33	16	0.18	1
Aug.	9 pm	13.79	0.59	4	0.33	2	0.10	1	0.14	1	0.07	1	0.64	5	0.62	5	1.14	8	0.16	1

Table 6.7.6c

CALPUFF Estimated Source Contribution to Total $PM_{2.5}$ Concentrations ($\mu g/m^3$) at Gilpin Creek for the August 7-9, 1995 Episode

		Hayden Generating station				Craig Generating station											
	Total $PM_{2.5}$	Unit #1		Unit #2		Unit #1		Unit #2		Unit #3		Remainder Yampa Valley		Colorado w/o Yampa Valley		Non-Colorado		Fires	
Date	ug/m3	ug/m3	(%)	ug/m3	(%)	ug/m3	(%)	ug/m3	(%)	ug/m3	(%)	ug/m3	(%)	ug/m3	(%)	ug/m3	(%)	ug/m3	(%)
Aug. 7 am	2.99	0.08	3	0.06	2	0.01	0	0.01	1	0.00	0	0.22	7	2.09	70	0.35	12	0.18	6
Aug. 7 pm	0.95	0.09	9	0.05	5	0.00	0	0.01	1	0.00	0	0.08	9	0.61	64	0.04	4	0.07	7
Aug. 8 am	0.55	0.02	4	0.02	3	0.00	0	0.02	4	0.02	3	0.13	23	0.29	52	0.05	9	0.00	1
Aug. 8 pm	0.44	0.00	0	0.00	0	0.00	0	0.00	1	0.00	1	0.13	29	0.07	17	0.14	31	0.10	22
Aug. 9 am	1.44	0.00	0	0.00	0	0.00	0	0.00	0	0.00	0	0.24	17	0.22	16	0.92	64	0.05	4
Aug. 9 pm	1.03	0.08	8	0.08	8	0.02	2	0.03	3	0.02	2	0.14	14	0.14	14	0.48	47	0.04	4

Table 6.7.6d

CALPUFF Estimated Source Contribution to Total Extinction (Mm^{-1}) at Gilpin Creek for the August 7-9, 1995 Episode

(total extinction includes a nominal value of 10 Mm^{-1} for Rayleigh scattering)

		Hayden Generating station				Craig Generating station											
	Total bext	Unit #1		Unit #2		Unit #1		Unit #2		Unit #3		Remainder Yampa Valley		Colorado w/o Yampa Valley		Non-Colorado		Fires	
Date	Mm^{-1}	Mm^{-1}	(%)	Mm^{-1}	(%)	Mm^{-1}	(%)	Mm^{-1}	(%)	Mm^{-1}	(%)	Mm^{-1}	(%)	Mm^{-1}	(%)	Mm^{-1}	(%)	Mm^{-1}	(%)
Aug. 7 am	18.36	0.16	1	0.12	1	0.01	0	0.03	0	0.01	0	0.67	4	5.86	32	0.92	5	0.59	3
Aug. 7 pm	12.55	0.17	1	0.09	1	0.01	0	0.01	0	0.01	0	0.25	2	1.67	13	0.12	1	0.22	2
Aug. 8 am	11.64	0.05	0	0.04	0	0.00	0	0.05	0	0.04	0	0.40	3	0.90	8	0.15	1	0.02	0
Aug. 8 pm	11.32	0.00	0	0.00	0	0.00	0	0.01	0	0.00	0	0.39	3	0.22	2	0.36	3	0.33	3
Aug. 9 am	14.10	0.00	0	0.00	0	0.00	0	0.00	0	0.00	0	0.73	5	0.67	5	2.51	18	0.18	1
Aug. 9 pm	12.55	0.15	1	0.14	1	0.04	0	0.05	0	0.03	0	0.42	3	0.42	3	1.17	9	0.12	1

Table 6.7.6e

CALPUFF Estimated Source Contribution to Total $PM_{2.5}$ Concentrations (u g/m^3) at Mad Creek for the August 7-9, 1995 Episode

		Hayden Generating station				Craig Generating station											
	Total $PM_{2.5}$	Unit #1		Unit #2		Unit #1		Unit #2		Unit #3		Remainder Yampa Valley		Colorado w/o Yampa Valley		Non-Colorado		Fires	
Date	ug/m3	ug/m3	(%)	ug/m3	(%)	ug/m3	(%)	ug/m3	(%)	ug/m3	(%)	ug/m3	(%)	ug/m3	(%)	ug/m3	(%)	ug/m3	(%)
Aug. 7 am	2.91	0.08	3	0.06	2	0.00	0	0.01	0	0.00	0	0.37	13	1.98	68	0.27	9	0.14	5
Aug. 7 pm	0.92	0.11	13	0.09	9	0.00	0	0.00	0	0.00	0	0.09	9	0.54	59	0.04	4	0.05	6
Aug. 8 am	0.75	0.08	10	0.06	8	0.00	1	0.01	1	0.00	1	0.25	33	0.31	41	0.04	5	0.00	1
Aug. 8 pm	0.54	0.00	0	0.00	0	0.00	1	0.01	2	0.01	1	0.13	25	0.08	16	0.16	29	0.15	27
Aug. 9 am	1.67	0.01	0	0.01	0	0.00	0	0.00	0	0.00	0	0.43	26	0.23	14	0.94	56	0.06	3
Aug. 9 pm	1.44	0.22	15	0.16	11	0.05	4	0.07	5	0.04	3	0.21	14	0.16	11	0.49	34	0.05	3

Table 6.7.6f

CALPUFF Estimated Source Contribution to Total Extinction (Mm^{-1}) at Mad Creek for the August 7-9, 1995 Episode

(total extinction includes a nominal value of 10 Mm^{-1} for Rayleigh scattering)

		Hayden Generating station				Craig Generating station											
	Total bext	Unit #1		Unit #2		Unit #1		Unit #2		Unit #3		Remainder Yampa Valley		Colorado w/o Yampa Valley		Non-Colorado		Fires	
Date	Mm^{-1}	Mm^{-1}	(%)	Mm^{-1}	(%)	Mm^{-1}	(%)	Mm^{-1}	(%)	Mm^{-1}	(%)	Mm^{-1}	(%)	Mm^{-1}	(%)	Mm^{-1}	(%)	Mm^{-1}	(%)
Aug. 7 am	18.12	0.15	1	0.11	1	0.01	0	0.02	0	0.01	0	1.12	6	5.55	31	0.71	4	0.45	3
Aug. 7 pm	12.40	0.21	2	0.16	1	0.00	0	0.00	0	0.00	0	0.26	2	1.49	12	0.11	1	0.17	1
Aug. 8 am	12.20	0.16	1	0.12	1	0.01	0	0.02	0	0.01	0	0.78	6	0.98	8	0.12	1	0.01	0
Aug. 8 pm	11.57	0.00	0	0.00	0	0.01	0	0.02	0	0.01	0	0.40	3	0.25	2	0.39	3	0.49	4
Aug. 9 am	14.68	0.01	0	0.01	0	0.00	0	0.00	0	0.00	0	1.29	9	0.69	5	2.48	17	0.18	1
Aug. 9 pm	13.34	0.39	3	0.28	2	0.09	1	0.12	1	0.07	1	0.62	5	0.46	4	1.16	9	0.16	1

As noted previously, CALMET/CALPUFF performance for the 08/07/95–08/09/95 period was poor, with the model underestimating the observed concentrations and extinctions throughout the monitoring network. Interpretation of modeled source contributions is tempered by this uncertainty. Table 6.7.6 and Figure 6.7.2 display the source contributions to concentrations and extinctions for 08/07/95–08/09/95. CALPUFF estimates that emissions from the Hayden and Craig stations make minor contributions (<10%) to $PM_{2.5}$ and extinction at Buffalo Pass during most of this period. On the afternoons of 08/08/95 and 08/09/95, however, the two generating stations contributed 14% and 42% to $PM_{2.5}$, respectively. Although these contributions are large relative to other sources, the absolute concentrations of $PM_{2.5}$ are low. Sources within Colorado (including the non-Hayden/Craig Yampa Valley sources) contribute the majority (> 50%) of the $PM_{2.5}$ during most of the period, and almost all at the beginning of the episode. Non-Colorado sources contribute a significant amount by the end of the episode. The source contribution to extinction at Buffalo Pass (Table 6.7.6b) cannot be interpreted since the underestimation of $PM_{2.5}$ results in extinction values close those of clean air.

The 08/07/95–08/09/95 CALPUFF source contributions at Gilpin Creek and Mad Creek are similar to those at Buffalo Pass (Table 6.7.6c-f). Again, the relative contributions of the Hayden and Craig stations decrease with distance north of Buffalo Pass. For example, on the afternoon of 08/09/95, the model estimates that the generating stations contribute 42% of $PM_{2.5}$ at the most southerly Buffalo Pass receptor, 23% at the more northerly Gilpin Creek site, and 38% at the Mad Creek receptor between the two.

CALMET/CALPUFF source contributions for the 10/07/95–10/19/95 period (two episodes) are summarized in Table 6.7.7 and Figure 6.7.3. As shown in Section 5.3, at the start of this period, Hayden Unit 1 was operating at a low level or not at all, so it had a negligible impact on $PM_{2.5}$ concentrations at Buffalo Pass. Craig Unit 3 was also shut down for much of this period until 10/13/95. For most of the six-hour aerosol measurement periods, the Hayden and Craig stations made minor (< 10%) contributions to $PM_{2.5}$ and extinction at the Wilderness receptors.

On 10/13/95, however, CALMET/CALPUFF estimates that the two generating stations contributed a large or major portion of the $PM_{2.5}$ (32% in morning and 55% in afternoon) at Buffalo Pass. Generating station contributions to extinction for 10/13/95 are 18% in the morning and only 21% in the afternoon. The fraction of extinction is less than the contribution to $PM_{2.5}$ owing to the presence of clean air scattering in the extinction budget.

Sources from outside of Colorado and in Colorado outside of Yampa Valley were estimated to be the dominant contributors to $PM_{2.5}$ and light extinction at Buffalo Pass during these October episodes. Fires are not a large contributor to $PM_{2.5}$ for most of this period. However, the 10/19/95 Chavez Mountain view of Hayden shows a smoke plume from a prescribed burn within the Yampa Valley, resulting in an obvious layered haze. The results for Gilpin Creek and Mad Creek are similar to those for Buffalo Pass. Again, the contributions from Yampa Valley generating stations decreases with distance north from Buffalo Pass. An exception is found on the afternoon of 10/13/95, during which the contributions from

Hayden Units 1 and 2 are larger at Gilpin Creek than at Buffalo Pass. The reverse is true for the Craig station units.

Table 6.7.7a

CALPUFF Estimated Source Contribution to Total $PM_{2.5}$ Concentrations (u g/m^3) at Buffalo Pass for the October 7-19, 1995 Episode

		Hayden Generating station				Craig Generating station											
	Total	Unit #1		Unit #2		Unit #1		Unit #2		Unit #3		Remainder Yampa Valley		Colorado w/o Yampa Valley		Non-Colorado	
Date	$PM_{2.5}$ ug/m3	ug/m3	(%)	ug/m3	(%)	ug/m3	(%)	ug/m3	(%)	ug/m3	(%)	ug/m3	(%)	ug/m3	(%)	ug/m3	(%)
Oct. 7 am	1.81	0.02	1	0.02	1	0.01	1	0.01	1	0.00	0	0.20	11	1.29	72	0.25	14
Oct. 7 pm	1.76	0.02	1	0.22	12	0.08	4	0.08	5	0.00	0	0.29	17	0.87	49	0.21	12
Oct. 8 am	4.26	0.01	0	0.06	1	0.00	0	0.00	0	0.00	0	0.37	9	1.47	34	2.35	55
Oct. 8 pm	3.11	0.01	0	0.57	18	0.10	3	0.07	2	0.00	0	0.27	9	0.89	29	1.20	39
Oct. 9 am	5.32	0.01	0	0.07	1	0.07	1	0.06	1	0.00	0	0.39	7	3.27	61	1.45	27
Oct. 9 pm	3.57	0.01	0	0.32	9	0.20	6	0.16	5	0.00	0	0.42	12	1.31	37	1.15	32
Oct. 10 am	3.81	0.00	0	0.20	5	0.15	4	0.01	0	0.00	0	0.36	9	1.08	28	2.01	53
Oct. 10 pm	3.30	0.00	0	0.38	12	0.42	13	0.03	1	0.00	0	0.35	11	0.68	21	1.43	43
Oct. 11 am	3.34	0.00	0	0.08	2	0.04	1	0.02	1	0.00	0	0.25	7	1.43	43	1.53	46
Oct. 11 pm	1.66	0.00	0	0.01	1	0.00	0	0.00	0	0.00	0	0.16	10	0.68	41	0.81	49
Oct. 12 am	1.47	0.03	2	0.02	1	0.00	0	0.00	0	0.00	0	0.18	12	0.88	60	0.37	25
Oct. 12 pm	1.18	0.11	9	0.07	6	0.05	5	0.05	5	0.00	0	0.13	11	0.34	28	0.43	37
Oct. 13 am	3.01	0.47	16	0.27	9	0.12	4	0.09	3	0.00	0	0.38	13	0.24	8	1.44	48
Oct. 13 pm	3.10	0.56	18	0.42	13	0.39	13	0.33	11	0.00	0	0.30	10	0.13	4	0.98	32
Oct. 14 am	2.16	0.01	0	0.01	1	0.00	0	0.00	0	0.00	0	0.38	17	0.55	25	1.22	56
Oct. 14 pm	2.23	0.32	14	0.24	11	0.06	3	0.06	3	0.01	0	0.32	14	0.38	17	0.85	38
Oct. 15 am	3.14	0.20	6	0.11	4	0.03	1	0.03	1	0.01	0	0.37	12	1.16	37	1.24	40
Oct. 15 pm	2.68	0.29	11	0.31	12	0.04	2	0.04	2	0.01	1	0.34	12	0.78	29	0.86	32
Oct. 16 am	3.33	0.07	2	0.02	1	0.01	0	0.00	0	0.00	0	0.29	9	1.67	50	1.26	38
Oct. 16 pm	2.75	0.31	11	0.16	6	0.05	2	0.05	2	0.02	1	0.41	15	0.72	26	0.96	35
Oct. 17 am	5.02	0.15	3	0.18	4	0.06	1	0.06	1	0.03	1	0.46	9	1.72	34	2.22	44
Oct. 17 pm	5.20	0.43	8	0.11	2	0.22	4	0.23	4	0.09	2	0.38	7	1.62	31	1.78	34
Oct. 18 am	4.79	0.06	1	0.00	0	0.00	0	0.00	0	0.00	0	0.36	8	2.51	52	1.75	37
Oct. 18 pm	3.09	0.12	4	0.00	0	0.03	1	0.03	1	0.01	0	0.30	10	0.69	22	1.67	54
Oct. 19 am	4.48	0.00	0	0.00	0	0.00	0	0.00	0	0.00	0	0.40	9	0.44	10	3.18	71
Oct. 19 pm	2.81	0.05	2	0.00	0	0.00	0	0.00	0	0.00	0	0.31	11	0.27	10	1.92	68

	Fires	
Date	ug/m3	(%)
Oct. 7 am	0.00	0
Oct. 7 pm	0.00	0
Oct. 8 am	0.00	0
Oct. 8 pm	0.00	0
Oct. 9 am	0.00	0
Oct. 9 pm	0.00	0
Oct. 10 am	0.00	0
Oct. 10 pm	0.00	0
Oct. 11 am	0.00	0
Oct. 11 pm	0.00	0
Oct. 12 am	0.00	0
Oct. 12 pm	0.00	0
Oct. 13 am	0.00	0
Oct. 13 pm	0.00	0
Oct. 14 am	0.00	0
Oct. 14 pm	0.00	0
Oct. 15 am	0.00	0
Oct. 15 pm	0.00	0
Oct. 16 am	0.00	0
Oct. 16 pm	0.05	2
Oct. 17 am	0.15	3
Oct. 17 pm	0.33	6
Oct. 18 am	0.09	2
Oct. 18 pm	0.24	8
Oct. 19 am	0.47	10
Oct. 19 pm	0.26	9

Table 6.7.7b

CALPUFF Estimated Source Contribution to Total Extinction (Mm^{-1}) at Buffalo Pass for the October 7-19, 1995 Episode

(total extinction includes a nominal value of 10 Mm^{-1} for Rayleigh scattering)

		Hayden Generating station				Craig Generating station													
	Total bext	Unit #1		Unit #2		Unit #1		Unit #2		Unit #3		Remainder Yampa Valley		Colorado w/o Yampa Valley		Non-Colorado		Fires	
Date	Mm^{-1}	Mm^{-1}	(%)	Mm^{-1}	(%)	Mm^{-1}	(%)	Mm^{-1}	(%)	Mm^{-1}	(%)	Mm^{-1}	(%)	Mm^{-1}	(%)	Mm^{-1}	(%)	Mm^{-1}	(%)
Oct. 7 am	15.53	0.04	0	0.03	0	0.03	0	0.03	0	0.00	0	0.66	4	4.08	26	0.66	4	0.00	0
Oct. 7 pm	14.93	0.04	0	0.49	3	0.17	1	0.18	1	0.00	0	0.92	6	2.60	17	0.55	4	0.00	0
Oct. 8 am	37.72	0.08	0	0.41	1	0.04	0	0.03	0	0.00	0	2.30	6	9.20	24	15.65	42	0.00	0
Oct. 8 pm	17.86	0.02	0	1.22	7	0.21	1	0.16	1	0.00	0	0.85	5	2.56	14	2.85	16	0.00	0
Oct. 9 am	26.18	0.02	0	0.17	1	0.18	1	0.13	1	0.00	0	1.30	5	10.31	39	4.07	16	0.00	0
Oct. 9 pm	19.52	0.01	0	0.69	4	0.45	2	0.35	2	0.00	0	1.31	7	3.84	20	2.87	15	0.00	0
Oct. 10 am	21.06	0.00	0	0.48	2	0.37	2	0.03	0	0.00	0	1.18	6	3.44	16	5.55	26	0.00	0
Oct. 10 pm	18.69	0.00	0	0.84	5	0.92	5	0.06	0	0.00	0	1.11	6	2.15	12	3.61	19	0.00	0
Oct. 11 am	18.99	0.00	0	0.15	1	0.07	0	0.04	0	0.00	0	0.75	4	4.22	22	3.75	20	0.00	0
Oct. 11 pm	14.38	0.00	0	0.02	0	0.01	0	0.00	0	0.00	0	0.49	3	1.99	14	1.85	13	0.00	0
Oct. 12 am	14.84	0.07	1	0.04	0	0.00	0	0.00	0	0.00	0	0.61	4	2.98	20	1.14	8	0.00	0
Oct. 12 pm	21.07	1.13	5	0.72	3	0.57	3	0.55	3	0.00	0	0.99	5	2.94	14	4.16	20	0.01	0
Oct. 13 am	22.95	1.99	9	1.12	5	0.50	2	0.40	2	0.00	0	1.66	7	1.07	5	6.21	27	0.00	0
Oct. 13 pm	17.89	1.32	7	0.96	5	0.92	5	0.78	4	0.00	0	0.95	5	0.43	2	2.54	14	0.00	0
Oct. 14 am	16.12	0.02	0	0.02	0	0.01	0	0.01	0	0.00	0	1.17	7	1.72	11	3.18	20	0.00	0
Oct. 14 pm	15.93	0.70	4	0.52	3	0.14	1	0.12	1	0.02	0	1.02	6	1.19	8	2.21	14	0.00	0
Oct. 15 am	18.59	0.42	2	0.23	1	0.06	0	0.06	0	0.01	0	1.14	6	3.47	19	3.18	17	0.00	0
Oct. 15 pm	16.93	0.60	4	0.62	4	0.08	1	0.08	1	0.03	0	1.03	6	2.35	14	2.14	13	0.01	0
Oct. 16 am	18.93	0.14	1	0.04	0	0.01	0	0.01	0	0.00	0	0.89	5	4.76	25	3.07	16	0.01	0
Oct. 16 pm	17.02	0.64	4	0.32	2	0.11	1	0.11	1	0.05	0	1.25	7	2.08	12	2.29	13	0.17	1
Oct. 17 am	25.01	0.37	2	0.44	2	0.14	1	0.14	1	0.07	0	1.53	6	5.49	22	6.29	25	0.54	2
Oct. 17 pm	24.14	0.93	4	0.22	1	0.48	2	0.49	2	0.19	1	1.23	5	4.87	20	4.57	19	1.15	5
Oct. 18 am	23.83	0.14	1	0.01	0	0.01	0	0.01	0	0.00	0	1.16	5	7.55	32	4.61	19	0.33	1
Oct. 18 pm	18.34	0.27	2	0.00	0	0.06	0	0.06	0	0.03	0	0.94	5	2.05	11	4.11	22	0.82	5
Oct. 19 am	23.82	0.00	0	0.00	0	0.00	0	0.00	0	0.00	0	1.35	6	1.45	6	9.32	39	1.70	7
Oct. 19 pm	17.14	0.11	1	0.00	0	0.00	0	0.00	0	0.00	0	0.91	5	0.77	5	4.52	26	0.83	5

Table 6.7.7c

CALPUFF Estimated Source Contribution to Total $PM_{2.5}$ Concentrations (u g/m^3) at Gilpin Creek for the October 7-19, 1995 Episode

		Hayden Generating station				Craig Generating station											
	Total	Unit #1		Unit #2		Unit #1		Unit #2		Unit #3		Remainder Yampa Valley		Colorado w/o Yampa Valley		Non-Colorado		Fires	
Date	$PM_{2.5}$ ug/m3	ug/m3	(%)	ug/m3	(%)	ug/m3	(%)	ug/m3	(%)	ug/m3	(%)	ug/m3	(%)	ug/m3	(%)	ug/m3	(%)	ug/m3	(%)
Oct. 7 am	1.76	0.02	1	0.01	1	0.01	1	0.01	1	0.00	0	0.21	12	1.16	66	0.34	19	0.00	0
Oct. 7 pm	1.64	0.01	1	0.19	11	0.09	5	0.09	6	0.00	0	0.21	13	0.78	47	0.28	17	0.00	0
Oct. 8 am	3.83	0.01	0	0.01	0	0.00	0	0.00	0	0.00	0	0.25	6	1.13	30	2.43	63	0.00	0
Oct. 8 pm	2.32	0.01	0	0.22	9	0.04	2	0.03	1	0.00	0	0.17	7	0.67	29	1.18	51	0.00	0
Oct. 9 am	4.53	0.01	0	0.06	1	0.07	2	0.06	1	0.00	0	0.41	9	2.45	54	1.47	33	0.00	0
Oct. 9 pm	2.95	0.00	0	0.17	6	0.16	6	0.14	5	0.00	0	0.30	10	1.04	35	1.14	39	0.00	0
Oct. 10 am	3.60	0.00	0	0.18	5	0.03	1	0.01	0	0.00	0	0.33	9	0.91	25	2.14	59	0.00	0
Oct. 10 pm	2.65	0.00	0	0.17	6	0.15	6	0.01	1	0.00	0	0.28	10	0.57	21	1.47	56	0.00	0
Oct. 11 am	3.39	0.00	0	0.11	3	0.05	2	0.04	1	0.00	0	0.27	8	1.36	40	1.56	46	0.00	0
Oct. 11 pm	1.88	0.00	0	0.14	7	0.04	2	0.03	2	0.00	0	0.18	9	0.65	34	0.85	45	0.00	0
Oct. 12 am	1.53	0.01	0	0.06	4	0.02	1	0.01	1	0.00	0	0.16	10	0.86	56	0.42	27	0.00	0
Oct. 12 pm	1.10	0.00	0	0.00	0	0.09	8	0.08	8	0.00	0	0.12	11	0.26	24	0.54	49	0.00	0
Oct. 13 am	2.60	0.30	12	0.17	7	0.01	0	0.01	0	0.00	0	0.28	11	0.17	7	1.66	64	0.00	0
Oct. 13 pm	2.78	0.61	22	0.46	16	0.09	3	0.07	3	0.00	0	0.19	7	0.08	3	1.28	46	0.00	0
Oct. 14 am	2.03	0.00	0	0.01	0	0.00	0	0.00	0	0.00	0	0.35	17	0.38	19	1.29	63	0.00	0
Oct. 14 pm	1.81	0.07	4	0.12	7	0.04	2	0.03	2	0.00	0	0.26	14	0.27	15	1.02	56	0.00	0
Oct. 15 am	3.38	0.27	8	0.16	5	0.04	1	0.04	1	0.01	0	0.42	12	1.00	30	1.44	43	0.00	0
Oct. 15 pm	2.27	0.11	5	0.12	5	0.03	1	0.03	1	0.01	1	0.30	13	0.67	30	0.99	44	0.00	0
Oct. 16 am	3.67	0.12	3	0.05	1	0.02	1	0.01	0	0.00	0	0.39	11	1.62	44	1.45	39	0.01	0
Oct. 16 pm	2.62	0.12	5	0.08	3	0.03	1	0.04	1	0.02	1	0.28	11	0.67	26	1.13	43	0.26	10
Oct. 17 am	5.13	0.11	2	0.13	3	0.04	1	0.04	1	0.02	0	0.47	9	1.56	30	2.54	50	0.21	4
Oct. 17 pm	4.51	0.19	4	0.08	2	0.10	2	0.10	2	0.05	1	0.26	6	1.50	33	2.00	44	0.23	5
Oct. 18 am	5.02	0.13	3	0.01	0	0.01	0	0.01	0	0.00	0	0.40	8	2.42	48	1.91	38	0.13	3
Oct. 18 pm	3.11	0.09	3	0.00	0	0.05	2	0.05	1	0.03	1	0.21	7	0.60	19	1.82	59	0.27	9
Oct. 19 am	3.76	0.00	0	0.00	0	0.00	0	0.00	0	0.00	0	0.22	6	0.31	8	3.04	81	0.19	5
Oct. 19 pm	2.35	0.00	0	0.00	0	0.00	0	0.00	0	0.00	0	0.17	7	0.16	7	1.85	79	0.16	7

Table 6.7.7d

CALPUFF Estimated Source Contribution to Total Extinction (Mm^{-1}) at Gilpin Creek for the October 7-19, 1995 Episode

(total extinction includes a nominal value of 10 Mm^{-1} for Rayleigh scattering)

		Hayden Generating station				Craig Generating station													
	Total bext	Unit #1		Unit #2		Unit #1		Unit #2		Unit #3		Remainder Yampa Valley		Colorado w/o Yampa Valley		Non-Colorado		Fires	
Date	Mm^{-1}	Mm^{-1}	(%)	Mm^{-1}	(%)	Mm^{-1}	(%)	Mm^{-1}	(%)	Mm^{-1}	(%)	Mm^{-1}	(%)	Mm^{-1}	(%)	Mm^{-1}	(%)	Mm^{-1}	(%)
Oct. 7 am	15.37	0.04	0	0.03	0	0.02	0	0.03	0	0.00	0	0.67	4	3.66	24	0.93	6	0.00	0
Oct. 7 pm	14.54	0.03	0	0.42	3	0.20	1	0.20	1	0.00	0	0.64	4	2.31	16	0.74	5	0.00	0
Oct. 8 am	34.98	0.07	0	0.04	0	0.02	0	0.02	0	0.00	0	1.55	4	7.06	20	16.22	46	0.00	0
Oct. 8 pm	15.95	0.02	0	0.46	3	0.09	1	0.07	0	0.00	0	0.54	3	1.93	12	2.85	18	0.00	0
Oct. 9 am	23.77	0.02	0	0.15	1	0.17	1	0.13	1	0.00	0	1.35	6	7.79	33	4.16	18	0.00	0
Oct. 9 pm	17.89	0.01	0	0.36	2	0.35	2	0.30	2	0.00	0	0.95	5	3.06	17	2.88	16	0.00	0
Oct. 10 am	20.42	0.00	0	0.44	2	0.07	0	0.02	0	0.00	0	1.08	5	2.88	14	5.93	29	0.00	0
Oct. 10 pm	17.09	0.00	0	0.36	2	0.33	2	0.03	0	0.00	0	0.86	5	1.78	10	3.72	22	0.00	0
Oct. 11 am	19.13	0.00	0	0.23	1	0.10	1	0.07	0	0.00	0	0.83	4	4.04	21	3.85	20	0.00	0
Oct. 11 pm	14.78	0.00	0	0.26	2	0.08	1	0.07	1	0.00	0	0.53	4	1.89	13	1.95	13	0.00	0
Oct. 12 am	14.96	0.01	0	0.16	1	0.04	0	0.04	0	0.00	0	0.53	4	2.90	19	1.27	9	0.00	0
Oct. 12 pm	20.23	0.00	0	0.00	0	0.94	5	0.86	4	0.00	0	0.91	5	2.26	11	5.25	26	0.00	0
Oct. 13 am	21.24	1.28	6	0.71	3	0.04	0	0.04	0	0.00	0	1.23	6	0.75	4	7.18	34	0.00	0
Oct. 13 pm	17.03	1.45	9	1.05	6	0.21	1	0.17	1	0.00	0	0.60	3	0.26	2	3.29	19	0.00	0
Oct. 14 am	15.77	0.01	0	0.01	0	0.00	0	0.00	0	0.00	0	1.10	7	1.22	8	3.43	22	0.00	0
Oct. 14 pm	14.92	0.16	1	0.25	2	0.08	1	0.07	1	0.00	0	0.82	5	0.86	6	2.66	18	0.00	0
Oct. 15 am	19.15	0.57	3	0.33	2	0.09	1	0.09	1	0.03	0	1.28	7	3.02	16	3.73	20	0.00	0
Oct. 15 pm	16.01	0.21	1	0.24	2	0.06	0	0.06	0	0.03	0	0.91	6	2.01	13	2.47	15	0.01	0
Oct. 16 am	19.78	0.24	1	0.10	1	0.03	0	0.02	0	0.00	0	1.19	6	4.60	23	3.56	18	0.02	0
Oct. 16 pm	16.90	0.26	2	0.15	1	0.06	0	0.08	1	0.05	0	0.85	5	1.92	11	2.68	16	0.86	5
Oct. 17 am	25.33	0.28	1	0.31	1	0.10	0	0.10	0	0.06	0	1.56	6	4.95	20	7.22	29	0.76	3
Oct. 17 pm	22.33	0.42	2	0.17	1	0.21	1	0.22	1	0.12	1	0.82	4	4.47	20	5.11	23	0.80	4
Oct. 18 am	24.40	0.29	1	0.02	0	0.02	0	0.02	0	0.01	0	1.26	5	7.29	30	5.04	21	0.46	2
Oct. 18 pm	18.31	0.19	1	0.00	0	0.10	1	0.10	1	0.06	0	0.66	4	1.78	10	4.48	25	0.93	5
Oct. 19 am	21.38	0.00	0	0.00	0	0.00	0	0.00	0	0.00	0	0.76	4	1.00	5	8.96	42	0.66	3
Oct. 19 pm	15.90	0.00	0	0.00	0	0.00	0	0.00	0	0.00	0	0.52	3	0.47	3	4.39	28	0.52	3

Table 6.7.7e

CALPUFF Estimated Source Contribution to Total $PM_{2.5}$ Concentrations (u g/m^3) at Mad Creek for the October 7-19, 1995 Episode

		Hayden Generating station				Craig Generating station											
	Total	Unit #1		Unit #2		Unit #1		Unit #2		Unit #3		Remainder Yampa Valley		Colorado w/o Yampa Valley		Non-Colorado	
Date	$PM_{2.5}$ ug/m3	ug/m3	(%)	ug/m3	(%)	ug/m3	(%)	ug/m3	(%)	ug/m3	(%)	ug/m3	(%)	ug/m3	(%)	ug/m3	(%)
Oct. 7 am	1.66	0.01	1	0.02	1	0.01	1	0.01	1	0.00	0	0.22	13	1.13	68	0.25	15
Oct. 7 pm	1.69	0.01	1	0.20	12	0.06	4	0.07	4	0.00	0	0.35	21	0.76	45	0.23	14
Oct. 8 am	4.06	0.01	0	0.05	1	0.00	0	0.00	0	0.00	0	0.35	9	1.16	29	2.48	61
Oct. 8 pm	3.17	0.01	0	0.83	26	0.14	4	0.10	3	0.00	0	0.22	7	0.69	22	1.18	37
Oct. 9 am	4.89	0.01	0	0.08	2	0.07	2	0.05	1	0.00	0	0.44	9	2.72	56	1.52	31
Oct. 9 pm	3.36	0.00	0	0.30	9	0.21	6	0.18	5	0.00	0	0.36	11	1.10	33	1.20	36
Oct. 10 am	3.70	0.00	0	0.19	5	0.11	3	0.01	0	0.00	0	0.41	11	0.88	24	2.10	57
Oct. 10 pm	2.90	0.00	0	0.23	8	0.32	11	0.03	1	0.00	0	0.31	11	0.55	19	1.46	50
Oct. 11 am	3.21	0.00	0	0.08	2	0.03	1	0.02	1	0.00	0	0.27	8	1.22	38	1.59	50
Oct. 11 pm	1.71	0.00	0	0.07	4	0.00	0	0.00	0	0.00	0	0.19	11	0.61	36	0.83	49
Oct. 12 am	1.66	0.05	3	0.04	2	0.04	2	0.03	2	0.00	0	0.31	19	0.80	48	0.39	23
Oct. 12 pm	1.33	0.18	14	0.10	7	0.07	5	0.07	5	0.00	0	0.15	11	0.29	22	0.47	36
Oct. 13 am	3.52	0.65	19	0.56	16	0.09	2	0.07	2	0.00	0	0.43	12	0.19	5	1.54	44
Oct. 13 pm	3.02	0.50	17	0.37	12	0.29	10	0.26	9	0.00	0	0.30	10	0.11	4	1.17	39
Oct. 14 am	2.10	0.00	0	0.01	0	0.00	0	0.00	0	0.00	0	0.37	18	0.45	21	1.26	60
Oct. 14 pm	2.59	0.44	17	0.43	17	0.11	4	0.10	4	0.02	1	0.31	12	0.29	11	0.88	34
Oct. 15 am	3.07	0.20	6	0.12	4	0.03	1	0.03	1	0.01	0	0.39	13	1.00	33	1.31	43
Oct. 15 pm	2.39	0.16	7	0.24	10	0.04	2	0.04	2	0.02	1	0.31	13	0.66	28	0.91	38
Oct. 16 am	3.31	0.07	2	0.05	2	0.01	0	0.00	0	0.00	0	0.35	10	1.47	45	1.35	41
Oct. 16 pm	2.62	0.19	7	0.09	4	0.06	3	0.06	2	0.03	1	0.36	14	0.63	24	1.06	41
Oct. 17 am	4.87	0.20	4	0.15	3	0.06	1	0.06	1	0.03	1	0.48	10	1.41	29	2.32	48
Oct. 17 pm	4.87	0.28	6	0.08	2	0.17	4	0.17	4	0.07	2	0.31	6	1.34	28	1.87	38
Oct. 18 am	4.68	0.06	1	0.00	0	0.00	0	0.00	0	0.00	0	0.45	10	2.18	47	1.87	40
Oct. 18 pm	3.44	0.11	3	0.00	0	0.03	1	0.03	1	0.01	0	0.25	7	0.60	18	1.77	51
Oct. 19 am	4.41	0.00	0	0.00	0	0.00	0	0.00	0	0.00	0	0.37	8	0.33	8	3.18	72
Oct. 19 pm	2.65	0.00	0	0.00	0	0.00	0	0.00	0	0.00	0	0.26	10	0.18	7	1.92	73

	Fires	
Date	ug/m3	(%)
Oct. 7 am	0.00	0
Oct. 7 pm	0.00	0
Oct. 8 am	0.00	0
Oct. 8 pm	0.00	0
Oct. 9 am	0.00	0
Oct. 9 pm	0.00	0
Oct. 10 am	0.00	0
Oct. 10 pm	0.00	0
Oct. 11 am	0.00	0
Oct. 11 pm	0.00	0
Oct. 12 am	0.00	0
Oct. 12 pm	0.00	0
Oct. 13 am	0.00	0
Oct. 13 pm	0.00	0
Oct. 14 am	0.00	0
Oct. 14 pm	0.00	0
Oct. 15 am	0.00	0
Oct. 15 pm	0.00	0
Oct. 16 am	0.01	0
Oct. 16 pm	0.13	5
Oct. 17 am	0.16	3
Oct. 17 pm	0.57	12
Oct. 18 am	0.10	2
Oct. 18 pm	0.63	18
Oct. 19 am	0.53	12
Oct. 19 pm	0.29	11

Table 6.7.7f

CALPUFF Estimated Source Contribution to Total Extinction (Mm^{-1}) at Mad Creek for the October 7-19, 1995 Episode

(total extinction includes a nominal value of 10 Mm^{-1} for Rayleigh scattering)

		Hayden Generating station				Craig Generating station											
	Total bext	Unit #1		Unit #2		Unit #1		Unit #2		Unit #3		Remainder Yampa Valley		Colorado w/o Yampa Valley		Non-Colorado		Fires	
Date	Mm^{-1}	Mm^{-1}	(%)	Mm^{-1}	(%)	Mm^{-1}	(%)	Mm^{-1}	(%)	Mm^{-1}	(%)	Mm^{-1}	(%)	Mm^{-1}	(%)	Mm^{-1}	(%)	Mm^{-1}	(%)
Oct. 7 am	14.96	0.03	0	0.04	0	0.02	0	0.03	0	0.00	0	0.68	5	3.49	23	0.67	5	0.00	0
Oct. 7 pm	14.34	0.03	0	0.38	3	0.12	1	0.13	1	0.00	0	1.02	7	2.10	15	0.56	4	0.00	0
Oct. 8 am	23.31	0.03	0	0.16	1	0.01	0	0.01	0	0.00	0	1.25	5	4.00	17	7.85	34	0.00	0
Oct. 8 pm	17.17	0.02	0	1.56	9	0.26	2	0.20	1	0.00	0	0.66	4	1.88	11	2.58	15	0.00	0
Oct. 9 am	23.55	0.02	0	0.16	1	0.15	1	0.11	1	0.00	0	1.36	6	7.93	34	3.83	16	0.00	0
Oct. 9 pm	18.21	0.01	0	0.56	3	0.41	2	0.35	2	0.00	0	1.08	6	3.03	17	2.75	15	0.00	0
Oct. 10 am	19.71	0.00	0	0.39	2	0.23	1	0.02	0	0.00	0	1.26	6	2.58	13	5.22	27	0.00	0
Oct. 10 pm	17.23	0.00	0	0.45	3	0.64	4	0.06	0	0.00	0	0.94	5	1.67	10	3.47	20	0.00	0
Oct. 11 am	18.46	0.00	0	0.15	1	0.06	0	0.05	0	0.00	0	0.80	4	3.56	19	3.83	21	0.00	0
Oct. 11 pm	14.23	0.00	0	0.12	1	0.01	0	0.01	0	0.00	0	0.55	4	1.73	12	1.80	13	0.00	0
Oct. 12 am	15.15	0.13	1	0.09	1	0.09	1	0.08	1	0.00	0	1.00	7	2.63	17	1.13	7	0.00	0
Oct. 12 pm	15.61	0.75	5	0.39	3	0.29	2	0.28	2	0.00	0	0.60	4	1.27	8	2.02	13	0.00	0
Oct. 13 am	20.37	1.73	9	1.47	7	0.23	1	0.18	1	0.00	0	1.46	7	0.63	3	4.67	23	0.00	0
Oct. 13 pm	16.61	1.00	6	0.71	4	0.57	3	0.52	3	0.00	0	0.89	5	0.32	2	2.61	16	0.00	0
Oct. 14 am	15.62	0.01	0	0.02	0	0.00	0	0.00	0	0.00	0	1.12	7	1.36	9	3.12	20	0.00	0
Oct. 14 pm	16.03	0.84	5	0.82	5	0.20	1	0.19	1	0.03	0	0.95	6	0.88	6	2.12	13	0.00	0
Oct. 15 am	18.04	0.39	2	0.24	1	0.05	0	0.05	0	0.02	0	1.16	6	2.90	16	3.22	18	0.00	0
Oct. 15 pm	15.90	0.29	2	0.43	3	0.08	1	0.08	1	0.04	0	0.93	6	1.90	12	2.14	14	0.01	0
Oct. 16 am	18.62	0.13	1	0.10	1	0.01	0	0.01	0	0.00	0	1.04	6	4.10	22	3.21	17	0.02	0
Oct. 16 pm	16.34	0.36	2	0.17	1	0.12	1	0.12	1	0.05	0	1.05	6	1.75	11	2.33	14	0.41	3
Oct. 17 am	23.23	0.43	2	0.31	1	0.13	1	0.13	1	0.06	0	1.50	6	4.18	18	5.94	26	0.54	2
Oct. 17 pm	22.46	0.53	2	0.16	1	0.32	1	0.33	2	0.14	1	0.93	4	3.78	17	4.37	20	1.90	9
Oct. 18 am	22.63	0.12	1	0.01	0	0.01	0	0.01	0	0.00	0	1.38	6	6.22	28	4.55	20	0.33	2
Oct. 18 pm	18.85	0.20	1	0.00	0	0.05	0	0.06	0	0.03	0	0.76	4	1.70	9	3.96	21	2.08	11
Oct. 19 am	21.81	0.00	0	0.00	0	0.00	0	0.00	0	0.00	0	1.12	5	0.98	5	7.97	37	1.75	8
Oct. 19 pm	16.32	0.00	0	0.00	0	0.00	0	0.00	0	0.00	0	0.74	5	0.49	3	4.22	26	0.87	5

Table 6.7.8a

CALPUFF Estimated Source Contribution to Total $PM_{2.5}$ Concentrations (ug/m^3) at Buffalo Pass for the August 21-27, 1995 Episode

		Hayden Generating station				Craig Generating station											
	Total	Unit #1		Unit #2		Unit #1		Unit #2		Unit #3		Remainder Yampa Valley		Colorado w/o Yampa Valley		Non-Colorado		Fires	
Date	$PM_{2.5}$ ug/m3	ug/m3	(%)	ug/m3	(%)	ug/m3	(%)	ug/m3	(%)	ug/m3	(%)	ug/m3	(%)	ug/m3	(%)	ug/m3	(%)	ug/m3	(%)
Aug. 21 am	2.07	0.12	6	0.02	1	0.01	0	0.01	0	0.00	0	0.29	14	1.47	71	0.15	7	0.00	0
Aug. 21 pm	1.24	0.23	18	0.20	16	0.02	2	0.01	1	0.01	1	0.17	14	0.54	44	0.05	5	0.00	0
Aug. 22 am	1.08	0.01	1	0.00	0	0.00	0	0.00	0	0.00	0	0.23	21	0.77	71	0.07	6	0.01	1
Aug. 22 pm	0.72	0.01	1	0.03	4	0.00	0	0.00	0	0.00	0	0.21	29	0.42	59	0.05	7	0.00	1
Aug. 23 am	1.07	0.00	0	0.01	1	0.00	0	0.00	0	0.00	0	0.31	28	0.64	60	0.10	9	0.00	0
Aug. 23 pm	0.47	0.01	2	0.02	4	0.00	0	0.00	0	0.00	0	0.13	28	0.28	59	0.03	6	0.00	0
Aug. 24 am	1.23	0.08	6	0.00	0	0.01	1	0.00	0	0.00	0	0.29	24	0.80	65	0.05	4	0.00	0
Aug. 24 pm	1.08	0.27	25	0.20	18	0.01	1	0.03	2	0.01	1	0.23	22	0.28	26	0.05	5	0.00	0
Aug. 25 am	1.58	0.04	3	0.03	2	0.02	1	0.04	2	0.01	0	0.31	20	0.89	57	0.23	15	0.00	0
Aug. 25 pm	1.02	0.10	10	0.10	10	0.02	2	0.04	3	0.01	1	0.24	24	0.39	38	0.13	12	0.00	0
Aug. 26 am	2.60	0.36	14	0.22	9	0.08	3	0.10	4	0.05	2	0.36	14	1.11	43	0.31	12	0.00	0
Aug. 26 pm	1.76	0.20	12	0.20	11	0.06	4	0.08	5	0.03	2	0.27	15	0.75	43	0.15	9	0.00	0
Aug. 27 am	4.10	0.21	5	0.16	4	0.07	2	0.07	2	0.04	1	0.34	8	3.00	73	0.22	5	0.00	0
Aug. 27 pm	3.08	0.31	10	0.30	10	0.10	3	0.09	3	0.06	2	0.26	8	1.84	60	0.12	4	0.00	0

Table 6.7.8b

CALPUFF Estimated Source Contribution to Total Extinction (Mm^{-1}) at Buffalo Pass for the August 21-27, 1995 Episode

(total extinction includes a nominal value of 10 Mm^{-1} for Rayleigh scattering)

		Hayden Generating station				Craig Generating station											
	Total	Unit #1		Unit #2		Unit #1		Unit #2		Unit #3		Remainder Yampa Valley		Colorado w/o Yampa Valley		Non-Colorado		Fires	
Date	bext Mm^{-1}	Mm^{-1}	(%)	Mm^{-1}	(%)	Mm^{-1}	(%)	Mm^{-1}	(%)	Mm^{-1}	(%)	Mm^{-1}	(%)	Mm^{-1}	(%)	Mm^{-1}	(%)	Mm^{-1}	(%)
Aug. 21 am	21.52	0.73	3	0.11	1	0.03	0	0.05	0	0.02	0	1.60	7	8.15	38	0.83	4	0.01	0
Aug. 21 pm	14.30	0.72	5	0.63	4	0.06	0	0.02	0	0.03	0	0.66	5	1.97	14	0.20	1	0.01	0
Aug. 22 am	16.19	0.05	0	0.01	0	0.00	0	0.01	0	0.00	0	1.32	8	4.38	27	0.38	2	0.04	0
Aug. 22 pm	12.78	0.02	0	0.09	1	0.00	0	0.00	0	0.00	0	0.85	7	1.61	13	0.19	2	0.02	0
Aug. 23 am	15.55	0.02	0	0.07	1	0.00	0	0.00	0	0.00	0	1.58	10	3.33	21	0.52	3	0.03	0
Aug. 23 pm	12.64	0.07	1	0.10	1	0.00	0	0.00	0	0.00	0	0.74	6	1.56	12	0.16	1	0.01	0
Aug. 24 am	23.41	1.01	4	0.06	0	0.08	0	0.03	0	0.05	0	3.05	13	8.60	37	0.54	2	0.01	0
Aug. 24 pm	14.49	1.10	8	0.78	5	0.04	0	0.10	1	0.03	0	1.01	7	1.22	8	0.22	2	0.00	0
Aug. 25 am	16.04	0.15	1	0.12	1	0.06	0	0.13	1	0.02	0	1.23	8	3.45	22	0.88	6	0.00	0
Aug. 25 pm	13.05	0.24	2	0.23	2	0.05	0	0.08	1	0.02	0	0.81	6	1.24	10	0.37	3	0.00	0

Aug. 26 am	17.35	0.82	5	0.51	3	0.19	1	0.24	1	0.12	1	1.16	7	3.43	20	0.88	5	0.00	0	
Aug. 26 pm	14.70	0.42	3	0.41	3	0.13	1	0.16	1	0.07	1	0.88	6	2.24	15	0.40	3	0.00	0	
Aug. 27 am	22.61	0.53	2	0.39	2	0.17	1	0.17	1	0.11	1	1.17	5	9.41	42	0.68	3	0.00	0	
Aug. 27 pm	19.08	0.77	4	0.74	4	0.25	1	0.23	1	0.16	1	0.90	5	5.67	30	0.37	2	0.00	0	

Table 6.7.8c

CALPUFF Estimated Source Contribution to total $PM_{2.5}$ Concentrations ($\mu g/m^3$) at Gilpin Creek for the August 21-27, 1995 Episode

		Hayden Generating station				Craig Generating station					Remainder Yampa Valley		Colorado w/o Yampa Valley		Non-Colorado		Fires	
Date	Total $PM_{2.5}$ ug/m3	Unit #1 ug/m3	(%)	Unit #2 ug/m3	(%)	Unit #1 ug/m3	(%)	Unit #2 ug/m3	(%)	Unit #3 ug/m3	(%)	ug/m3	(%)	ug/m3	(%)	ug/m3	(%)	ug/m3	(%)
Aug. 21 am	2.24	0.22	10	0.03	1	0.01	0	0.01	0	0.00	0	0.28	12	1.46	65	0.23	10	0.00	0
Aug. 21 pm	1.17	0.20	18	0.14	12	0.04	3	0.02	1	0.02	2	0.15	12	0.51	44	0.09	8	0.00	0
Aug. 22 am	1.09	0.02	2	0.01	1	0.00	0	0.00	0	0.00	0	0.20	18	0.74	68	0.11	10	0.01	1
Aug. 22 pm	0.71	0.02	3	0.04	6	0.00	0	0.00	0	0.00	1	0.17	23	0.39	55	0.08	12	0.00	1
Aug. 23 am	0.98	0.01	1	0.00	0	0.00	0	0.00	0	0.00	0	0.25	26	0.56	57	0.15	16	0.00	1
Aug. 23 pm	0.79	0.14	18	0.18	23	0.01	1	0.01	1	0.01	1	0.14	18	0.25	32	0.04	5	0.00	0
Aug. 24 am	1.25	0.06	5	0.03	2	0.00	0	0.01	1	0.00	0	0.29	23	0.77	62	0.09	7	0.00	0
Aug. 24 pm	0.80	0.13	16	0.12	16	0.01	1	0.01	1	0.00	1	0.18	23	0.25	31	0.09	11	0.00	0
Aug. 25 am	1.47	0.04	3	0.03	2	0.02	1	0.03	2	0.01	1	0.22	15	0.73	50	0.38	26	0.00	0
Aug. 25 pm	0.91	0.08	9	0.07	8	0.02	2	0.03	3	0.01	1	0.17	19	0.32	35	0.21	23	0.00	0
Aug. 26 am	2.69	0.40	15	0.28	10	0.10	4	0.13	5	0.06	2	0.32	12	0.95	35	0.46	17	0.00	0
Aug. 26 pm	1.73	0.23	13	0.22	13	0.07	4	0.09	5	0.03	2	0.22	13	0.66	38	0.21	12	0.00	0
Aug. 27 am	3.82	0.23	6	0.21	6	0.07	2	0.08	2	0.04	1	0.33	9	2.53	66	0.33	9	0.00	0
Aug. 27 pm	3.34	0.47	14	0.50	15	0.10	3	0.10	3	0.06	2	0.26	8	1.68	50	0.17	5	0.00	0

Table 6.7.8d

CALPUFF Estimated Source Contribution to Total Extinction (Mm^{-1}) at Gilpin Creek for the August 21-27, 1995 Episode

(total extinction includes a nominal value of 10 Mm^{-1} for Rayleigh scattering)

		Hayden Generating station				Craig Generating station					Remainder Yampa Valley		Colorado w/o Yampa Valley		Non-Colorado		Fires	
Date	Total bext Mm^{-1}	Unit #1 Mm^{-1}	(%)	Unit #2 Mm^{-1}	(%)	Unit #1 Mm^{-1}	(%)	Unit #2 Mm^{-1}	(%)	Unit #3 Mm^{-1}	(%)	Mm^{-1}	(%)	Mm^{-1}	(%)	Mm^{-1}	(%)	Mm^{-1}	(%)
Aug. 21 am	17.57	0.64	4	0.09	1	0.02	0	0.03	0	0.01	0	0.99	6	5.01	29	0.77	4	0.01	0
Aug. 21 pm	13.16	0.46	4	0.32	2	0.08	1	0.04	0	0.04	0	0.46	4	1.50	11	0.25	2	0.01	0
Aug. 22 am	13.89	0.07	1	0.02	0	0.00	0	0.00	0	0.01	0	0.74	5	2.62	19	0.41	3	0.03	0
Aug. 22 pm	12.16	0.05	0	0.09	1	0.00	0	0.00	0	0.01	0	0.54	4	1.18	10	0.26	2	0.02	0
Aug. 23 am	13.53	0.02	0	0.00	0	0.00	0	0.00	0	0.00	0	0.94	7	2.00	15	0.55	4	0.02	0
Aug. 23 pm	12.44	0.38	3	0.48	4	0.02	0	0.02	0	0.02	0	0.51	4	0.86	7	0.14	1	0.01	0
Aug. 24 am	15.16	0.23	2	0.11	1	0.01	0	0.03	0	0.01	0	1.20	8	3.18	21	0.38	3	0.00	0
Aug. 24 pm	12.99	0.45	4	0.42	3	0.03	0	0.04	0	0.02	0	0.72	6	0.97	8	0.34	3	0.00	0
Aug. 25 am	15.91	0.16	1	0.12	1	0.07	0	0.12	1	0.03	0	0.90	6	2.97	19	1.53	10	0.00	0

Aug. 25 pm	12.49	0.17	1	0.15	1	0.04	0	0.06	1	0.02	0	0.54	4	0.96	8	0.56	4	0.00	0
Aug. 26 am	17.67	0.94	5	0.66	4	0.23	1	0.30	2	0.14	1	1.06	6	2.99	17	1.34	8	0.00	0
Aug. 26 pm	14.27	0.43	3	0.41	3	0.13	1	0.17	1	0.07	1	0.66	5	1.88	13	0.52	4	0.00	0
Aug. 27 am	21.53	0.56	3	0.51	2	0.17	1	0.19	1	0.11	1	1.10	5	7.86	37	1.03	5	0.00	0
Aug. 27 pm	19.14	1.09	6	1.14	6	0.24	1	0.24	1	0.15	1	0.86	4	4.91	26	0.50	3	0.00	0

Table 6.7.8e

CALPUFF Estimated Source Contribution to Total $PM_{2.5}$ Concentrations ($\mu g/m^3$) at Mad Creek for the August 21-27, 1995 Episode

		Hayden Generating station				Craig Generating station													
	Total $PM_{2.5}$	Unit #1		Unit #2		Unit #1		Unit #2		Unit #3		Remainder Yampa Valley		Colorado w/o Yampa Valley		Non-Colorado		Fires	
Date	ug/m3	ug/m3	(%)	ug/m3	(%)	ug/m3	(%)	ug/m3	(%)	ug/m3	(%)	ug/m3	(%)	ug/m3	(%)	ug/m3	(%)	ug/m3	(%)
Aug. 21 am	1.99	0.16	8	0.03	1	0.00	0	0.01	0	0.00	0	0.33	17	1.29	65	0.17	8	0.00	0
Aug. 21 pm	1.60	0.40	25	0.38	24	0.05	3	0.02	1	0.03	2	0.17	11	0.49	31	0.06	4	0.00	0
Aug. 22 am	1.03	0.01	1	0.01	1	0.00	0	0.00	0	0.00	0	0.26	25	0.67	65	0.07	7	0.01	1
Aug. 22 pm	0.79	0.02	2	0.14	18	0.00	0	0.00	0	0.00	0	0.21	26	0.37	47	0.05	7	0.00	1
Aug. 23 am	1.05	0.03	3	0.05	5	0.00	0	0.00	0	0.00	0	0.32	30	0.54	51	0.11	10	0.00	1
Aug. 23 pm	0.75	0.17	22	0.14	19	0.00	0	0.00	0	0.00	0	0.17	23	0.23	31	0.03	4	0.00	0
Aug. 24 am	1.12	0.03	3	0.01	1	0.00	0	0.00	0	0.00	0	0.32	29	0.69	62	0.05	5	0.00	0
Aug. 24 pm	1.34	0.36	27	0.38	28	0.03	2	0.03	2	0.01	1	0.24	17	0.25	18	0.06	5	0.00	0
Aug. 25 am	1.50	0.06	4	0.04	3	0.02	1	0.03	2	0.01	1	0.33	22	0.75	50	0.27	18	0.00	0
Aug. 25 pm	1.10	0.16	15	0.13	12	0.03	3	0.04	3	0.02	2	0.25	22	0.34	31	0.14	13	0.00	0
Aug. 26 am	2.51	0.38	15	0.24	10	0.09	3	0.12	5	0.05	2	0.38	15	0.91	36	0.34	14	0.00	0
Aug. 26 pm	1.77	0.27	15	0.25	14	0.06	4	0.08	5	0.03	2	0.28	16	0.62	35	0.17	9	0.00	0
Aug. 27 am	3.81	0.23	6	0.19	5	0.08	2	0.08	2	0.05	1	0.38	10	2.57	68	0.24	6	0.00	0
Aug. 27 pm	3.75	0.78	21	0.67	18	0.10	3	0.11	3	0.06	2	0.29	8	1.61	43	0.13	4	0.00	0

Table 6.7.8f

CALPUFF Estimated Source Contribution to total Extinction (Mm^{-1}) at Mad Creek for the August 21-27, 1995 Episode

(total extinction includes a nominal value of 10 Mm^{-1} for Rayleigh scattering)

		Hayden Generating station				Craig Generating station													
	Total bext	Unit #1		Unit #2		Unit #1		Unit #2		Unit #3		Remainder Yampa Valley		Colorado w/o Yampa Valley		Non-Colorado		Fires	
Date	Mm^{-1}	Mm^{-1}	(%)	Mm^{-1}	(%)	Mm^{-1}	(%)	Mm^{-1}	(%)	Mm^{-1}	(%)	Mm^{-1}	(%)	Mm^{-1}	(%)	Mm^{-1}	(%)	Mm^{-1}	(%)
Aug. 21 am	16.42	0.42	3	0.07	0	0.01	0	0.02	0	0.01	0	1.16	7	4.19	26	0.52	3	0.01	0
Aug. 21 pm	14.17	0.90	6	0.84	6	0.12	1	0.04	0	0.06	0	0.57	4	1.45	10	0.18	1	0.01	0
Aug. 22 am	13.65	0.04	0	0.03	0	0.00	0	0.00	0	0.00	0	0.93	7	2.35	17	0.27	2	0.03	0
Aug. 22 pm	12.33	0.04	0	0.31	3	0.00	0	0.00	0	0.00	0	0.68	6	1.11	9	0.16	1	0.02	0
Aug. 23 am	13.45	0.08	1	0.12	1	0.00	0	0.00	0	0.00	0	1.11	8	1.76	13	0.36	3	0.02	0
Aug. 23 pm	12.63	0.52	4	0.44	4	0.00	0	0.00	0	0.01	0	0.67	5	0.86	7	0.11	1	0.01	0
Aug. 24 am	14.26	0.11	1	0.03	0	0.00	0	0.01	0	0.00	0	1.26	9	2.62	18	0.21	2	0.00	0
Aug. 24 pm	14.16	1.01	7	1.06	8	0.07	1	0.07	1	0.03	0	0.84	6	0.87	6	0.21	2	0.00	0

Aug. 25 am	15.17	0.18	1	0.12	1	0.05	0	0.10	1	0.02	0	1.17	8	2.62	17	0.91	6	0.00	0
Aug. 25 pm	12.96	0.33	3	0.26	2	0.06	1	0.08	1	0.04	0	0.78	6	1.02	8	0.38	3	0.00	0
Aug. 26 am	17.13	0.89	5	0.56	3	0.20	1	0.27	2	0.13	1	1.23	7	2.86	17	0.99	6	0.00	0
Aug. 26 pm	14.35	0.50	4	0.46	3	0.12	1	0.16	1	0.06	0	0.87	6	1.78	12	0.40	3	0.00	0
Aug. 27 am	21.04	0.53	3	0.43	2	0.17	1	0.17	1	0.10	1	1.23	6	7.69	37	0.71	3	0.00	0
Aug. 27 pm	19.28	1.61	8	1.38	7	0.22	1	0.22	1	0.14	1	0.92	5	4.45	23	0.35	2	0.00	0

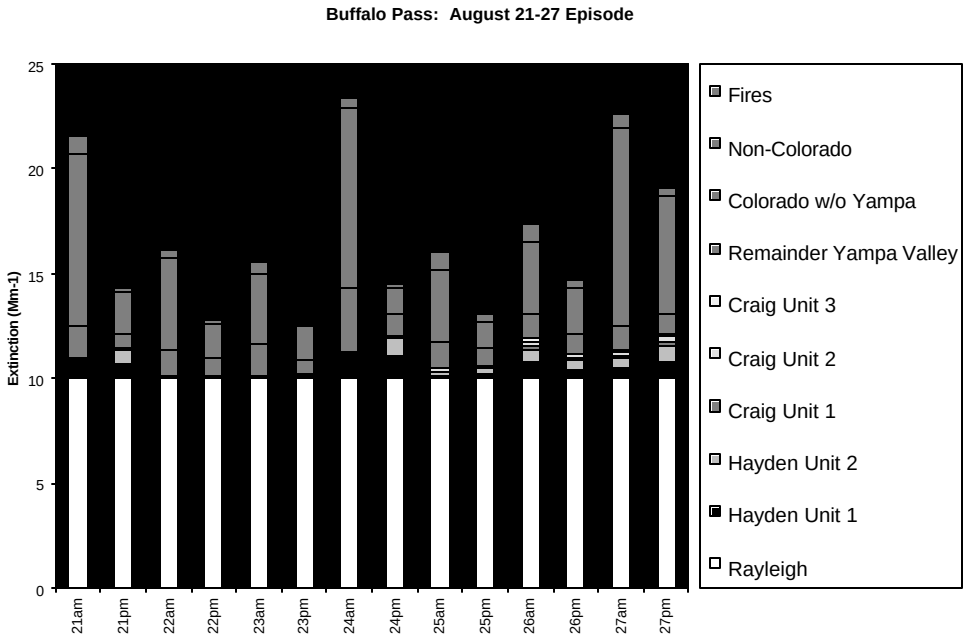

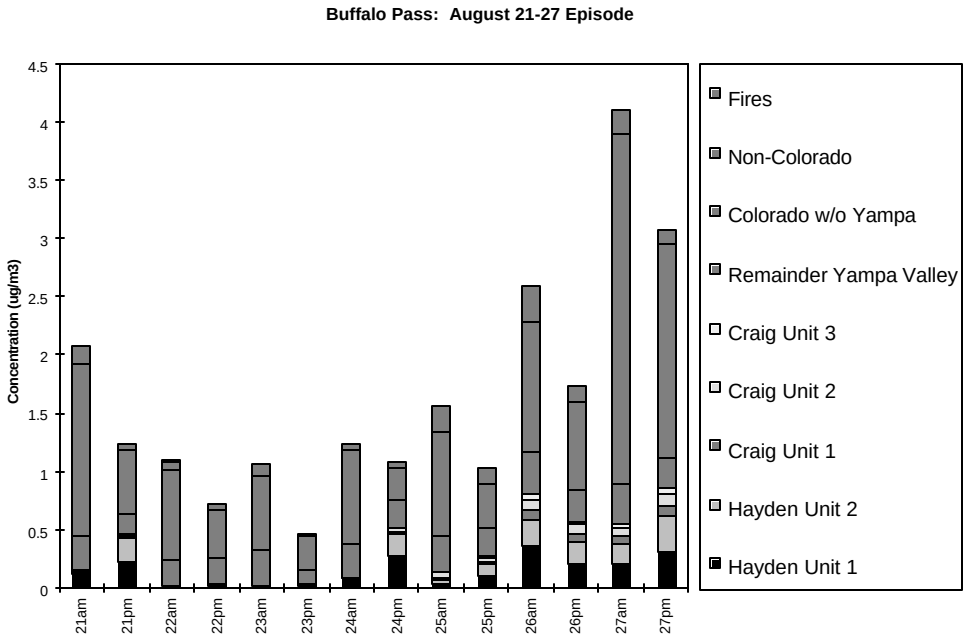

Figure 6.7.4a Source contribution to CALPUFF estimated six-hour average $PM_{2.5}$ concentrations and total extinction for the August 21-27, 1995 episode. Buffalo Pass.

Gilpin Creek: August 21-27 Episode

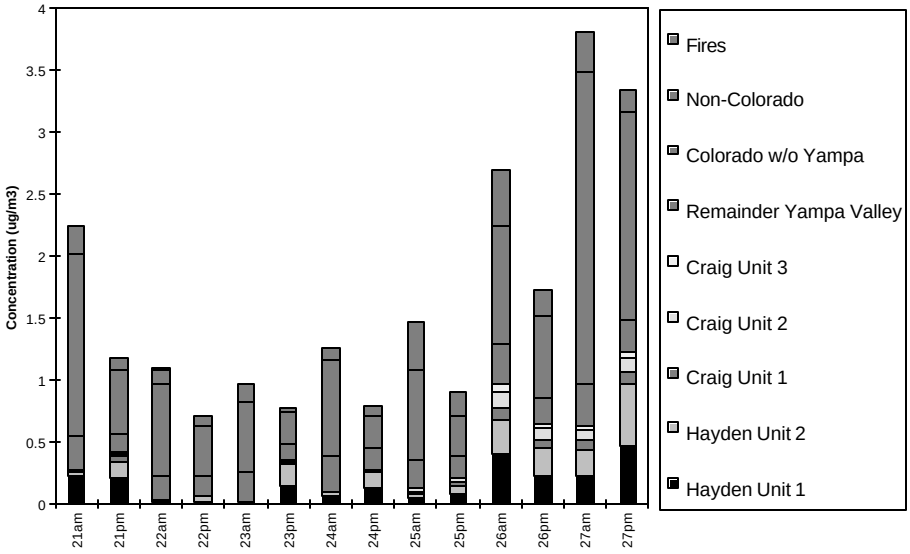

Gilpin Creek: August 21-27 Episode

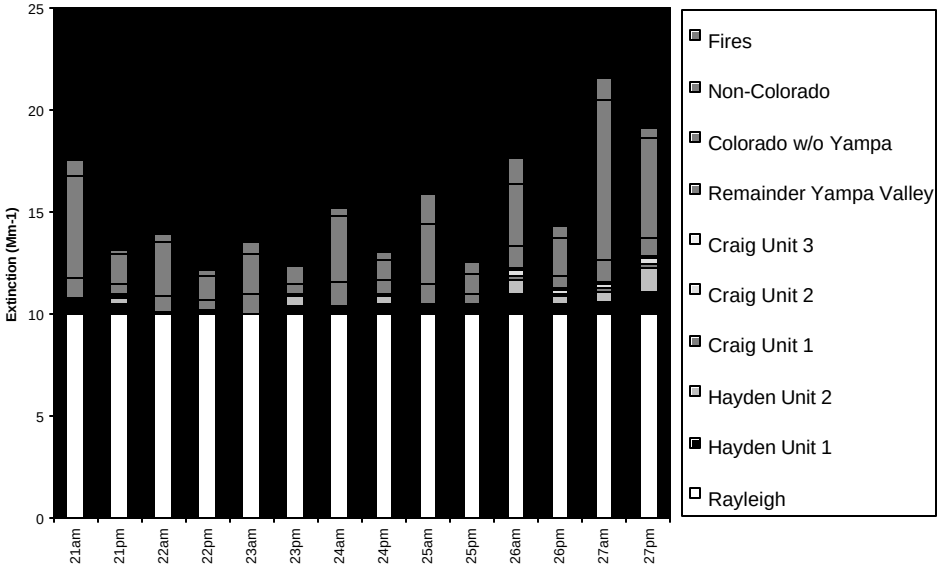

Figure 6.7.4b Source contribution to CALPUFF estimated six-hour average $PM_{2.5}$ concentrations and total extinction for the August 21-27 episode. Gilpin Creek.

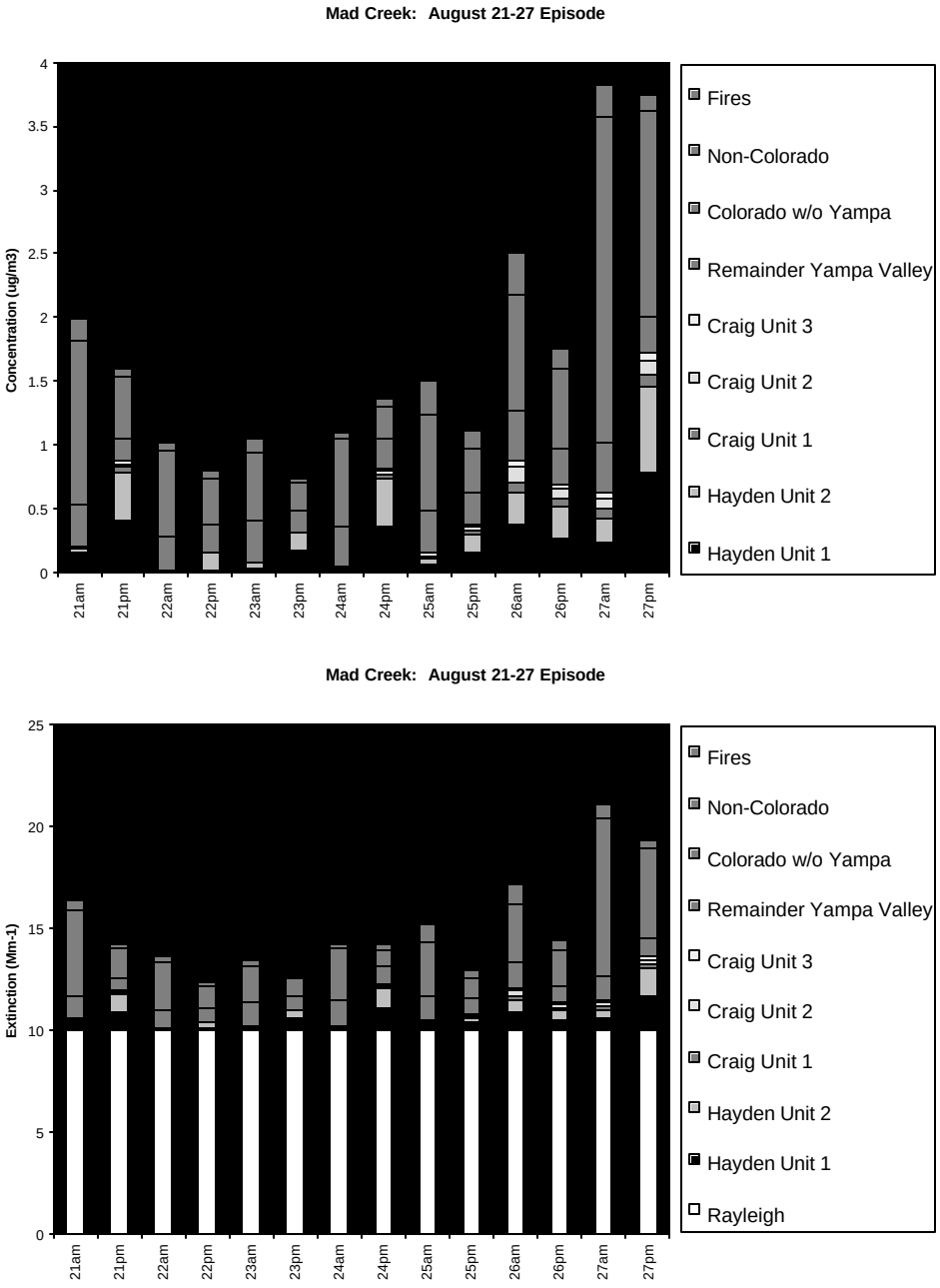

Figure 6.7.4c Source contribution to CALPUFF estimated six-hour average $PM_{2.5}$ concentrations and total extinction for the August 21-27, 1995 episode.

Mad Creek CALMET/CALPUFF source contributions for the 08/21/95–08/27/95 period are presented in Table 6.7.8 and Figure 6.7.4. These results underestimate measured concentrations and extinctions, and the above-stated cautions apply to their interpretation. Total light extinction is dominated by clean air scattering in these results. Contributions from the Craig station to $PM_{2.5}$ are minor (< 10%) at Buffalo Pass. The Hayden station contributions are frequently significant and large contributors to $PM_{2.5}$ at Buffalo Pass, achieving 43% on the afternoon of 08/24/95.

For most six-hour segments during this episode, CALMET/CALPUFF estimates that non-Yampa-Valley Colorado sources are the major (> 50%) contributors to $PM_{2.5}$ at Buffalo Pass. While certain sources are estimated to contribute much to the $PM_{2.5}$ in a relative sense, they make no significant contribution to extinction during this episode owing to the large fraction of extinction accounted for by clean air. Results at the Gilpin Creek and Mad Creek receptors are similar to what was seen at Buffalo Pass. Unlike the other episodes, there are more frequent occurrences of larger impacts at the northern receptor (Gilpin Creek) than at the southern receptor (Buffalo Pass).

6.7.7 Analysis of Estimated Contributions Along Sight Paths

In these analyses of source contribution to extinction along ten sight paths, only the contributions from Hayden Units 1 and 2 and Craig Units 1 and 2 are reported. Source contributions for Craig Unit 3 are not examined in accordance with the Memorandum of Understanding (Blumenthal *et al.*, 1995).

Table 6.7.9 presents hourly average estimated extinction (Mm^{-1}) and Deciview (dv) along ten sight paths emanating from various landmarks within the Wilderness for each day of the 09/17/95–09/21/95 episode. Indicated for each day is: 1) the daylight hour (MST) with the maximum total extinction along a particular sight path ("Max b_{ext}"); and 2) the daylight hour in which the model estimated the maximum contribution to extinction along the sight path due to the combined emissions from Hayden Units 1 and 2 and Craig Units 1 and 2 ("Max PP"). Given for each of these two types of entries is the total integrated extinction (with the nominal value for Rayleigh scattering of 10 Mm^{-1}), the total Hayden and Craig Units 1 and 2 contribution to sight-path extinction, and a breakdown of each unit's extinction contribution. The MZVS Technical Steering Committee agreed that the contribution of Hayden and Craig Units 1 and 2 to sight path extinction would be determined only for those sight path segments within the boundaries of the Mt. Zirkel Wilderness. For the six sight paths fully within the Wilderness, contributions from these sources were calculated for the entire sight path length, whereas for the four sight paths extending beyond the borders of the Mt. Zirkel Wilderness, the contributions of these sources to total extinction were determined for just those 10-20 km segments contained within the Wilderness boundaries. The process to estimate mean extinction along each sight path is documented in Appendix B.2.

The first six sight paths have both sight path endpoints within the Wilderness, whereas the last four sight paths start within the Wilderness and extend outside the boundaries to the north, east, south, and west (see Figure 6.8.3). Species concentrations were sampled at "elevated receptors" on grid coordinates that extended along each sight path. The mean distance between sight path

Table 6.7.8a

CALPUFF Estimated Source Contribution to Total $PM_{2.5}$ Concentrations (u g/m^3) at Buffalo Pass for the August 21-27, 1995 Episode

		Hayden Generating station				Craig Generating station							
Date	Total $PM_{2.5}$ ug/m3	Non-Colorado Fires ug/m3 (%)	Unit #1 ug/m3 (%)	Unit #2 ug/m3 (%)	Unit #1 ug/m3 (%)	Unit #2 ug/m3 (%)	Unit #3 ug/m3 (%)	Colorado w/o Yampa Valley ug/m3 (%)	Remainder Yampa Valley ug/m3 (%)
Aug. 21 am	2.07	0.12 6	0.02 1	0.01 0	0.01 0	0.00 0	0.29 14	1.47 71	0.15 7	0.00 0
Aug. 21 pm	1.24	0.23 18	0.20 16	0.02 2	0.01 1	0.01 1	0.17 14	0.54 44	0.05 5	0.00 0
Aug. 22 am	1.08	0.01 1	0.00 0	0.00 0	0.00 0	0.00 0	0.23 21	0.77 71	0.07 6	0.01 1
Aug. 22 pm	0.72	0.01 1	0.03 4	0.00 0	0.00 0	0.00 0	0.21 29	0.42 59	0.05 7	0.00 1
Aug. 23 am	1.07	0.00 0	0.01 1	0.00 0	0.00 0	0.00 0	0.31 28	0.64 60	0.10 9	0.00 0
Aug. 23 pm	0.47	0.01 2	0.02 4	0.00 0	0.00 0	0.00 0	0.13 28	0.28 59	0.03 6	0.00 0
Aug. 24 am	1.23	0.08 6	0.00 0	0.01 1	0.00 0	0.00 0	0.29 24	0.80 65	0.05 4	0.00 0
Aug. 24 pm	1.08	0.27 25	0.20 18	0.01 1	0.03 2	0.01 1	0.23 22	0.28 26	0.05 5	0.00 0
Aug. 25 am	1.58	0.04 3	0.03 2	0.02 1	0.04 2	0.01 0	0.31 20	0.89 57	0.23 15	0.00 0
Aug. 25 pm	1.02	0.10 10	0.10 10	0.02 2	0.04 3	0.01 1	0.24 24	0.39 38	0.13 12	0.00 0
Aug. 26 am	2.60	0.36 14	0.22 9	0.08 3	0.10 4	0.05 2	0.36 14	1.11 43	0.31 12	0.00 0
Aug. 26 pm	1.76	0.20 12	0.20 11	0.06 4	0.08 5	0.03 2	0.27 15	0.75 43	0.15 9	0.00 0
Aug. 27 am	4.10	0.21 5	0.16 4	0.07 2	0.07 2	0.04 1	0.34 8	3.00 73	0.22 5	0.00 0
Aug. 27 pm	3.08	0.31 10	0.30 10	0.10 3	0.09 3	0.06 2	0.26 8	1.84 60	0.12 4	0.00 0

Table 6.7.8b

CALPUFF Estimated Source Contribution to Total Extinction (Mm^{-1}) at Buffalo Pass for the August 21-27, 1995 Episode

(total extinction includes a nominal value of 10 Mm^{-1} for Rayleigh scattering)

		Hayden Generating station				Craig Generating station									
				Unit #1		Unit #2		Unit #1		Unit #2		Unit #3			
Date	Total Colorado w/o Yampa Valley Mm^{-1}	(%)	Non-bext Colorado Mm^{-1}	(%)	Fires Mm^{-1}	(%)	Mm^{-1}	(%)	Mm^{-1}	(%)	Mm^{-1}	(%)	Mm^{-1}	(%)	Remainder Yampa Valley Mm^{-1}	(%)
Aug. 21 am	21.52		0.73	3	0.11	1	0.03	0	0.05	0	0.02	0	1.60	7		
8.15	38	0.83	4	0.01	0											
Aug. 21 pm	14.30		0.72	5	0.63	4	0.06	0	0.02	0	0.03	0	0.66	5		
1.97	14	0.20	1	0.01	0											
Aug. 22 am	16.19		0.05	0	0.01	0	0.00	0	0.01	0	0.00	0	1.32	8		
4.38	27	0.38	2	0.04	0											
Aug. 22 pm	12.78		0.02	0	0.09	1	0.00	0	0.00	0	0.00	0	0.85	7		
1.61	13	0.19	2	0.02	0											
Aug. 23 am	15.55		0.02	0	0.07	1	0.00	0	0.00	0	0.00	0	1.58	10		
3.33	21	0.52	3	0.03	0											
Aug. 23 pm	12.64		0.07	1	0.10	1	0.00	0	0.00	0	0.00	0	0.74	6		
1.56	12	0.16	1	0.01	0											
Aug. 24 am	23.41		1.01	4	0.06	0	0.08	0	0.03	0	0.05	0	3.05	13		
8.60	37	0.54	2	0.01	0											
Aug. 24 pm	14.49		1.10	8	0.78	5	0.04	0	0.10	1	0.03	0	1.01	7		
1.22	8	0.22	2	0.00	0											
Aug. 25 am	16.04		0.15	1	0.12	1	0.06	0	0.13	1	0.02	0	1.23	8		
3.45	22	0.88	6	0.00	0											
Aug. 25 pm	13.05		0.24	2	0.23	2	0.05	0	0.08	1	0.02	0	0.81	6		
1.24	10	0.37	3	0.00	0											
Aug. 26 am	17.35		0.82	5	0.51	3	0.19	1	0.24	1	0.12	1	1.16	7		
3.43	20	0.88	5	0.00	0											
Aug. 26 pm	14.70		0.42	3	0.41	3	0.13	1	0.16	1	0.07	1	0.88	6		
2.24	15	0.40	3	0.00	0											
Aug. 27 am	22.61		0.53	2	0.39	2	0.17	1	0.17	1	0.11	1	1.17	5		
9.41	42	0.68	3	0.00	0											
Aug. 27 pm	19.08		0.77	4	0.74	4	0.25	1	0.23	1	0.16	1	0.90	5		
5.67	30	0.37	2	0.00	0											

Table 6.7.8c

CALPUFF Estimated Source Contribution to total $PM_{2.5}$ Concentrations (u g/m^3) at Gilpin Creek for the August 21-27, 1995 Episode

		Hayden Generating station			Craig Generating station					Remainder	
	Total $PM_{2.5}$	Unit #1	Unit #2		Unit #1	Unit #2	Unit #3			Colorado w/o Yampa Valley	
Date	Non-Colorado Fires ug/m3	ug/m3 (%)	ug/m3 (%)		ug/m3 (%)	ug/m3 (%)	ug/m3 (%)			ug/m3 (%)	
Aug. 21 am	2.24	0.22	10	0.03	1	0.01	0	0.01	0	0.00	0	0.28	12	1.46	65	0.23	10	0.00	0
Aug. 21 pm	1.17	0.20	18	0.14	12	0.04	3	0.02	1	0.02	2	0.15	12	0.51	44	0.09	8	0.00	0
Aug. 22 am	1.09	0.02	2	0.01	1	0.00	0	0.00	0	0.00	0	0.20	18	0.74	68	0.11	10	0.01	1
Aug. 22 pm	0.71	0.02	3	0.04	6	0.00	0	0.00	0	0.00	1	0.17	23	0.39	55	0.08	12	0.00	1
Aug. 23 am	0.98	0.01	1	0.00	0	0.00	0	0.00	0	0.00	0	0.25	26	0.56	57	0.15	16	0.00	1
Aug. 23 pm	0.79	0.14	18	0.18	23	0.01	1	0.01	1	0.01	1	0.14	18	0.25	32	0.04	5	0.00	0
Aug. 24 am	1.25	0.06	5	0.03	2	0.00	0	0.01	1	0.00	0	0.29	23	0.77	62	0.09	7	0.00	0
Aug. 24 pm	0.80	0.13	16	0.12	16	0.01	1	0.01	1	0.00	1	0.18	23	0.25	31	0.09	11	0.00	0
Aug. 25 am	1.47	0.04	3	0.03	2	0.02	1	0.03	2	0.01	1	0.22	15	0.73	50	0.38	26	0.00	0
Aug. 25 pm	0.91	0.08	9	0.07	8	0.02	2	0.03	3	0.01	1	0.17	19	0.32	35	0.21	23	0.00	0
Aug. 26 am	2.69	0.40	15	0.28	10	0.10	4	0.13	5	0.06	2	0.32	12	0.95	35	0.46	17	0.00	0
Aug. 26 pm	1.73	0.23	13	0.22	13	0.07	4	0.09	5	0.03	2	0.22	13	0.66	38	0.21	12	0.00	0
Aug. 27 am	3.82	0.23	6	0.21	6	0.07	2	0.08	2	0.04	1	0.33	9	2.53	66	0.33	9	0.00	0
Aug. 27 pm	3.34	0.47	14	0.50	15	0.10	3	0.10	3	0.06	2	0.26	8	1.68	50	0.17	5	0.00	0

Table 6.7.8d

CALPUFF Estimated Source Contribution to Total Extinction (Mm^{-1}) at Gilpin Creek for the August 21-27, 1995 Episode

(total extinction includes a nominal value of 10 Mm^{-1} for Rayleigh scattering)

			Hayden Generating station				Craig Generating station							
Date	Total Non-Colorado Mm-1	(%)	Unit #1 Mm-1	(%)	Unit #2 Mm-1	(%)	Unit #1 Mm-1	(%)	Unit #2 Mm-1	(%)	Unit #3 Mm-1	(%)	Remainder Mm-1	(%)
Aug. 21 am	17.57		0.64	4	0.09	1	0.02	0	0.03	0	0.01	0	0.99	6
5.01	29	0.77	4	0.01	0									
Aug. 21 pm	13.16		0.46	4	0.32	2	0.08	1	0.04	0	0.04	0	0.46	4
1.50	11	0.25	2	0.01	0									
Aug. 22 am	13.89		0.07	1	0.02	0	0.00	0	0.00	0	0.01	0	0.74	5
2.62	19	0.41	3	0.03	0									
Aug. 22 pm	12.16		0.05	0	0.09	1	0.00	0	0.00	0	0.01	0	0.54	4
1.18	10	0.26	2	0.02	0									
Aug. 23 am	13.53		0.02	0	0.00	0	0.00	0	0.00	0	0.00	0	0.94	7
2.00	15	0.55	4	0.02	0									
Aug. 23 pm	12.44		0.38	3	0.48	4	0.02	0	0.02	0	0.02	0	0.51	4
0.86	7	0.14	1	0.01	0									
Aug. 24 am	15.16		0.23	2	0.11	1	0.01	0	0.03	0	0.01	0	1.20	8
3.18	21	0.38	3	0.00	0									
Aug. 24 pm	12.99		0.45	4	0.42	3	0.03	0	0.04	0	0.02	0	0.72	6
0.97	8	0.34	3	0.00	0									
Aug. 25 am	15.91		0.16	1	0.12	1	0.07	0	0.12	1	0.03	0	0.90	6
2.97	19	1.53	10	0.00	0									
Aug. 25 pm	12.49		0.17	1	0.15	1	0.04	0	0.06	1	0.02	0	0.54	4
0.96	8	0.56	4	0.00	0									
Aug. 26 am	17.67		0.94	5	0.66	4	0.23	1	0.30	2	0.14	1	1.06	6
2.99	17	1.34	8	0.00	0									
Aug. 26 pm	14.27		0.43	3	0.41	3	0.13	1	0.17	1	0.07	1	0.66	5
1.88	13	0.52	4	0.00	0									
Aug. 27 am	21.53		0.56	3	0.51	2	0.17	1	0.19	1	0.11	1	1.10	5
7.86	37	1.03	5	0.00	0									
Aug. 27 pm	19.14		1.09	6	1.14	6	0.24	1	0.24	1	0.15	1	0.86	4
4.91	26	0.50	3	0.00	0									

Table 6.7.8e

CALPUFF Estimated Source Contribution to Total $PM_{2.5}$ Concentrations (u g/m^3) at Mad Creek for the August 21-27, 1995 Episode

		Hayden Generating station				Craig Generating station						Remainder	
	Total $PM_{2.5}$	Unit #1		Unit #2		Unit #1		Unit #2		Unit #3		Colorado w/o Yampa Valley	
Date	Non-Colorado Fires ug/m3	ug/m3	(%)	ug/m3	(%)	ug/m3	(%)	ug/m3	(%)	ug/m3	(%)	ug/m3	(%)
Aug. 21 am	1.99	0.16	8	0.03	1	0.00	0	0.01	0	0.00	0	0.33	17
1.29	65	0.17	8	0.00	0								
Aug. 21 pm	1.60	0.40	25	0.38	24	0.05	3	0.02	1	0.03	2	0.17	11
0.49	31	0.06	4	0.00	0								
Aug. 22 am	1.03	0.01	1	0.01	1	0.00	0	0.00	0	0.00	0	0.26	25
0.67	65	0.07	7	0.01	1								
Aug. 22 pm	0.79	0.02	2	0.14	18	0.00	0	0.00	0	0.00	0	0.21	26
0.37	47	0.05	7	0.00	1								
Aug. 23 am	1.05	0.03	3	0.05	5	0.00	0	0.00	0	0.00	0	0.32	30
0.54	51	0.11	10	0.00	1								
Aug. 23 pm	0.75	0.17	22	0.14	19	0.00	0	0.00	0	0.00	0	0.17	23
0.23	31	0.03	4	0.00	0								
Aug. 24 am	1.12	0.03	3	0.01	1	0.00	0	0.00	0	0.00	0	0.32	29
0.69	62	0.05	5	0.00	0								
Aug. 24 pm	1.34	0.36	27	0.38	28	0.03	2	0.03	2	0.01	1	0.24	17
0.25	18	0.06	5	0.00	0								
Aug. 25 am	1.50	0.06	4	0.04	3	0.02	1	0.03	2	0.01	1	0.33	22
0.75	50	0.27	18	0.00	0								
Aug. 25 pm	1.10	0.16	15	0.13	12	0.03	3	0.04	3	0.02	2	0.25	22
0.34	31	0.14	13	0.00	0								
Aug. 26 am	2.51	0.38	15	0.24	10	0.09	3	0.12	5	0.05	2	0.38	15
0.91	36	0.34	14	0.00	0								
Aug. 26 pm	1.77	0.27	15	0.25	14	0.06	4	0.08	5	0.03	2	0.28	16
0.62	35	0.17	9	0.00	0								
Aug. 27 am	3.81	0.23	6	0.19	5	0.08	2	0.08	2	0.05	1	0.38	10
2.57	68	0.24	6	0.00	0								
Aug. 27 pm	3.75	0.78	21	0.67	18	0.10	3	0.11	3	0.06	2	0.29	8
1.61	43	0.13	4	0.00	0								

Table 6.7.8f

CALPUFF Estimated Source Contribution to total Extinction (Mm^{-1}) at Mad Creek for the August 21-27, 1995 Episode

(total extinction includes a nominal value of 10 Mm^{-1} for Rayleigh scattering)

		Hayden Generating station				Craig Generating station									
Date	Total Colorado w/o Yampa Valley Mm^{-1}	Total Non-bext Colorado Mm^{-1}	(%)	Fires Unit #1 Mm^{-1}	(%)	Unit #2 Mm^{-1}	(%)	Unit #1 Mm^{-1}	(%)	Unit #2 Mm^{-1}	(%)	Unit #3 Mm^{-1}	(%)	Remainder Yampa Valley Mm^{-1}	(%)
Aug. 21 am	16.42	0.42	3	0.07	0	0.01	0	0.02	0	0.01	0	1.16	7	4.19	26
Aug. 21 pm	14.17	0.90	6	0.84	6	0.12	1	0.04	0	0.06	0	0.57	4	1.45	10
Aug. 22 am	13.65	0.04	0	0.03	0	0.00	0	0.00	0	0.00	0	0.93	7	2.35	17
Aug. 22 pm	12.33	0.04	0	0.31	3	0.00	0	0.00	0	0.00	0	0.68	6	1.11	9
Aug. 23 am	13.45	0.08	1	0.12	1	0.00	0	0.00	0	0.00	0	1.11	8	1.76	13
Aug. 23 pm	12.63	0.52	4	0.44	4	0.00	0	0.00	0	0.01	0	0.67	5	0.86	7
Aug. 24 am	14.26	0.11	1	0.03	0	0.00	0	0.01	0	0.00	0	1.26	9	2.62	18
Aug. 24 pm	14.16	1.01	7	1.06	8	0.07	1	0.07	1	0.03	0	0.84	6	0.87	6
Aug. 25 am	15.17	0.18	1	0.12	1	0.05	0	0.10	1	0.02	0	1.17	8	2.62	17
Aug. 25 pm	12.96	0.33	3	0.26	2	0.06	1	0.08	1	0.04	0	0.78	6	1.02	8
Aug. 26 am	17.13	0.89	5	0.56	3	0.20	1	0.27	2	0.13	1	1.23	7	2.86	17
Aug. 26 pm	14.35	0.50	4	0.46	3	0.12	1	0.16	1	0.06	0	0.87	6	1.78	12
Aug. 27 am	21.04	0.53	3	0.43	2	0.17	1	0.17	1	0.10	1	1.23	6	7.69	37
Aug. 27 pm	19.28	1.61	8	1.38	7	0.22	1	0.22	1	0.14	1	0.92	5	4.45	23
		0.35	2	0.00	0										

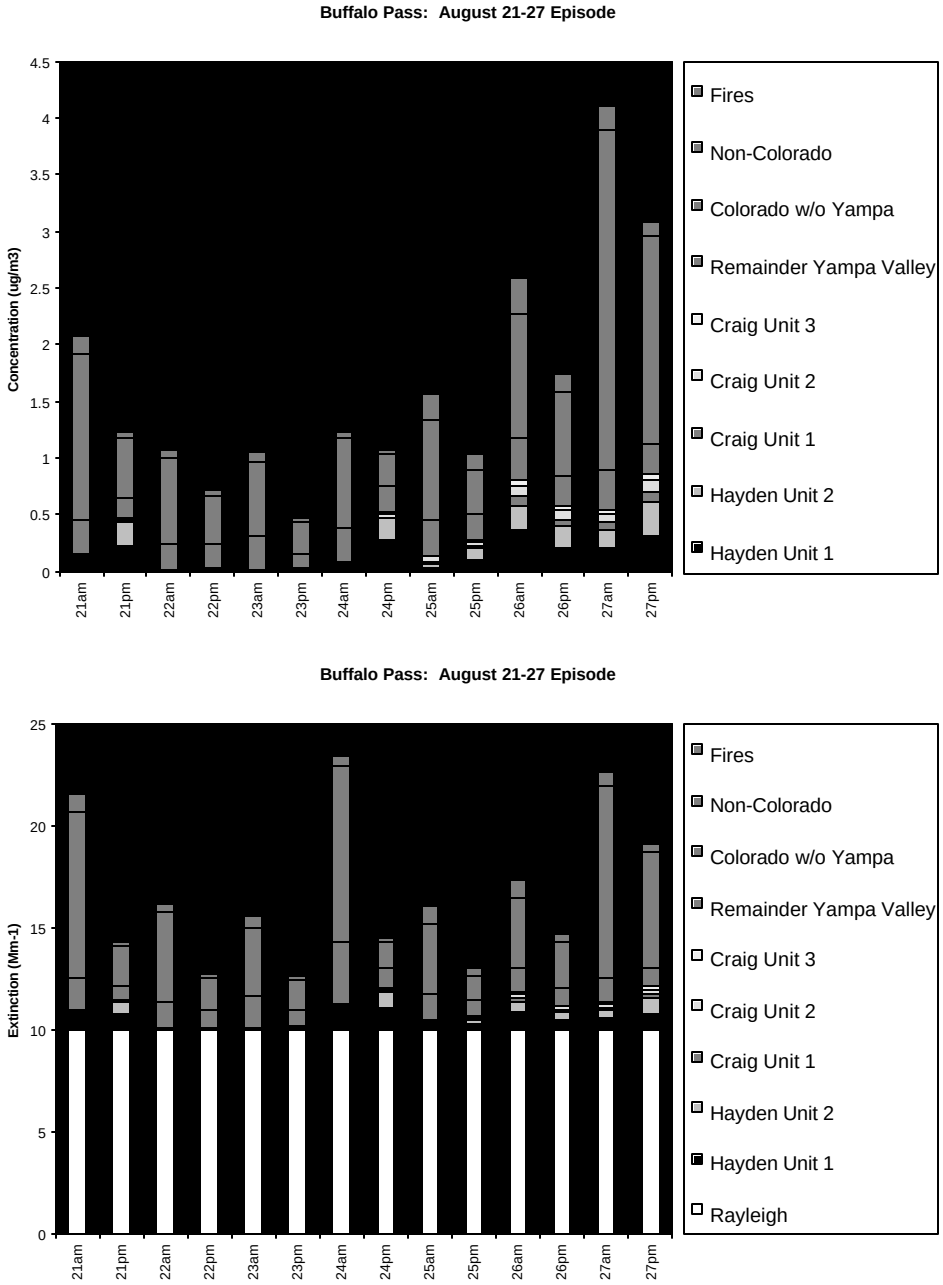

Figure 6.7.4a Source contribution to CALPUFF estimated six-hour average $PM_{2.5}$ concentrations and total extinction for the August 21-27, 1995 episode. Buffalo Pass.

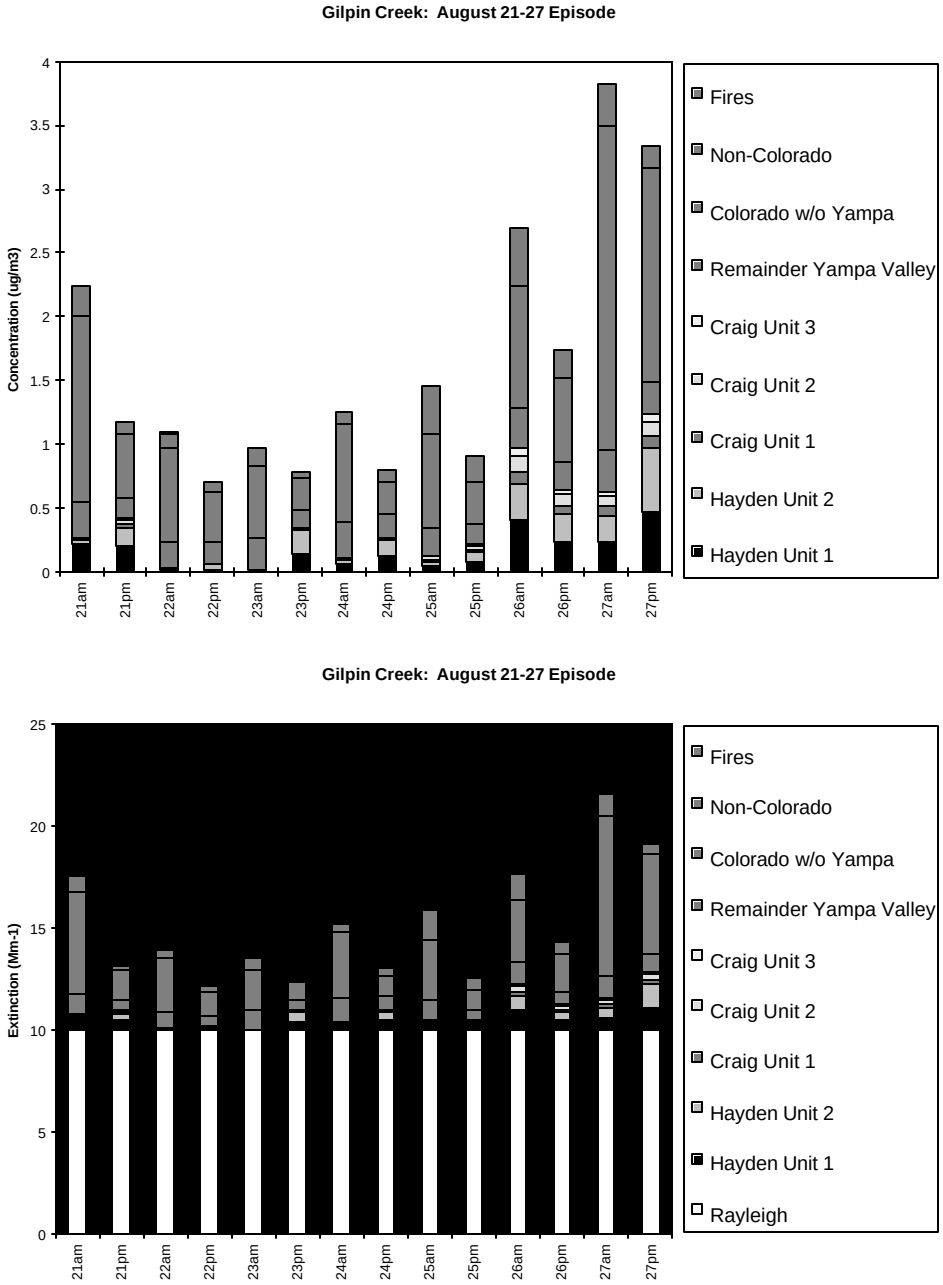

Figure 6.7.4b Source contribution to CALPUFF estimated six-hour average $PM_{2.5}$ concentrations and total extinction for the August 21-27 episode. Gilpin Creek.

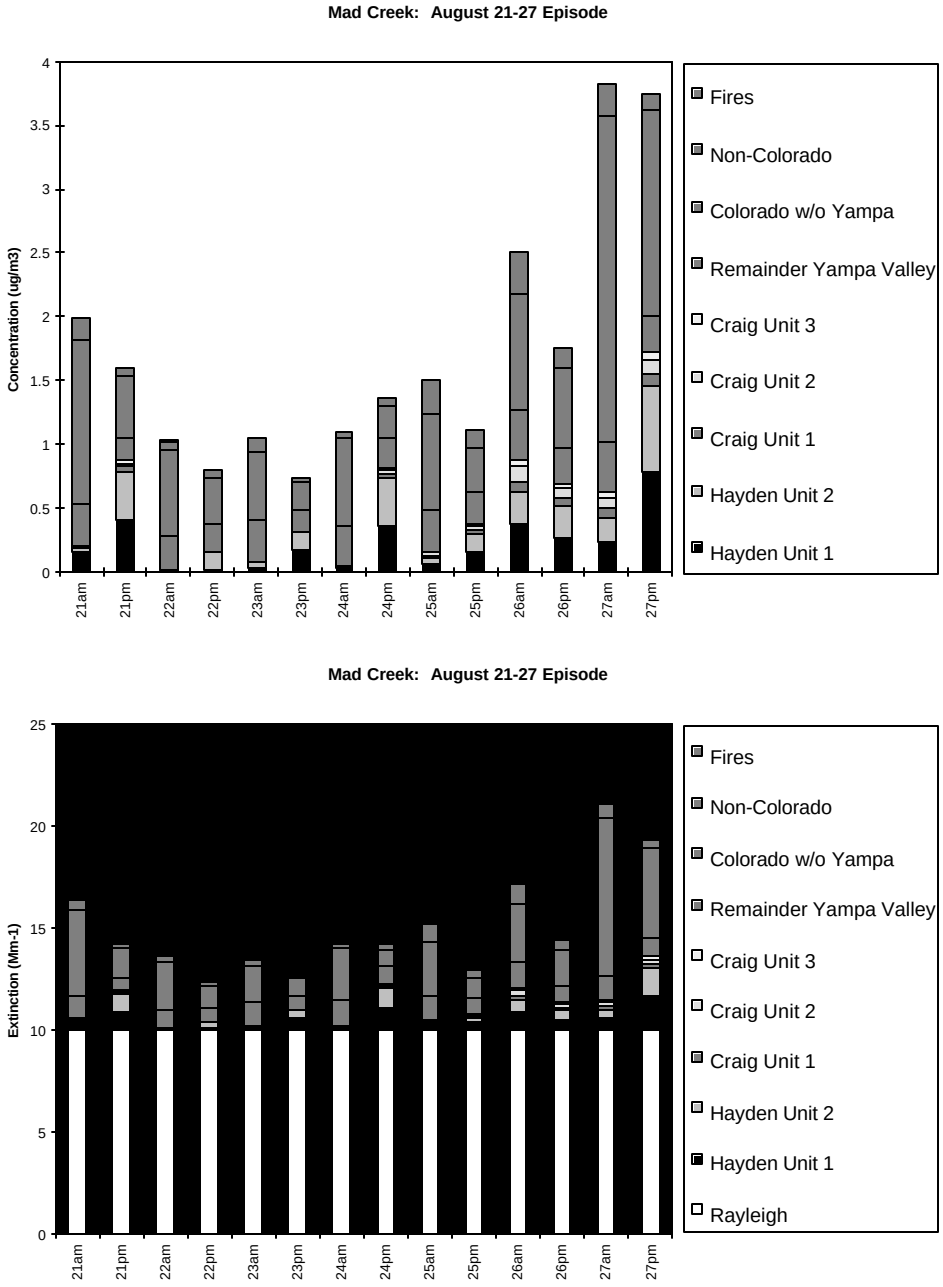

Figure 6.7.4c Source contribution to CALPUFF estimated six-hour average $PM_{2.5}$ concentrations and total extinction for the August 21-27, 1995 episode. Mad Creek.

receptors was ~10 km. For those short sight paths within Wilderness (~10 km or less), only concentrations from the two endpoint receptors were used to obtain the mean extinction along the segment. For the longer sight paths, extinction was calculated for each receptor, and the average extinction along the entire path was determined from a weighted average of the distance between receptors.

Table 6.7.9
Hourly Average Estimated Extinction (Mm^{-1}) and Deciview (dv) along 10 Sight Paths for the September 17-21, 1995 Episode

Indicated for each day is (1) the daylight hour with the maximum total extinction along a particular sight path ("Max bext"), and (2) the daylight hour in which the model estimated the maximum contribution to extinction along the path segments within the MZWA due to the combined emissions from Hayden Units 1&2 and Craig Units 1&2 ("Max PP"). Given for each of these two types of entries is the total integrated extinction (with the nominal value for Rayleigh scattering of 10 Mm^{-1}), the total Hayden and Craig Units 1&2 contribution to sight-path extinction, and a breakdown of each unit's extinction contribution (Mm^{-1} only).

View 1: Davis Pk - Mt Zirkel

	Date	Hour	Total Path Mm^{-1}	Total Path dv	PP Contrib Mm^{-1}	PP Contrib dv	Craig1 Mm^{-1}	Craig2 Mm^{-1}	Hyden1 Mm^{-1}	Hyden2 Mm^{-1}
Max bext	95/ 9/17	7	16.80	2.25	0.55	0.14	0.09	0.09	0.18	0.20
Max PP	95/ 9/17	17	16.47	2.17	1.05	0.29	0.15	0.16	0.41	0.33
Max bext	95/ 9/18	7	40.26	6.05	3.65	0.41	0.44	0.48	1.39	1.34
Max PP	95/ 9/18	14	23.63	3.73	4.40	0.89	0.94	0.85	1.36	1.25
Max bext	95/ 9/19	7	20.33	3.08	1.84	0.41	0.26	0.26	0.81	0.51
Max PP	95/ 9/19	7	20.33	3.08	1.84	0.41	0.26	0.26	0.81	0.51
Max bext	95/ 9/20	6	43.39	6.37	0.33	0.03	0.11	0.07	0.07	0.08
Max PP	95/ 9/20	8	39.15	5.93	0.53	0.06	0.15	0.14	0.06	0.17
Max bext	95/ 9/21	6	17.39	2.40	0.00	0.00	0.00	0.00	0.00	0.00
Max PP	95/ 9/21	13	12.59	1.00	0.16	0.06	0.00	0.00	0.16	0.00

View 2: Davis Pk - Little Agnes Pk

	Date	Hour	Total Path Mm^{-1}	Total Path dv	PP Contrib Mm^{-1}	PP Contrib dv	Craig1 Mm^{-1}	Craig2 Mm^{-1}	Hyden1 Mm^{-1}	Hyden2 Mm^{-1}
Max bext	95/ 9/17	17	16.45	2.16	1.02	0.28	0.15	0.16	0.39	0.33
Max PP	95/ 9/17	17	16.45	2.16	1.02	0.28	0.15	0.16	0.39	0.33
Max bext	95/ 9/18	6	38.74	5.88	3.42	0.40	0.43	0.45	1.30	1.23
Max PP	95/ 9/18	14	23.58	3.73	4.38	0.89	0.99	0.89	1.30	1.21
Max bext	95/ 9/19	7	19.98	3.01	1.81	0.41	0.27	0.26	0.79	0.50
Max PP	95/ 9/19	7	19.98	3.01	1.81	0.41	0.27	0.26	0.79	0.50
Max bext	95/ 9/20	6	39.48	5.96	0.42	0.05	0.15	0.10	0.07	0.10

Max PP	95/ 9/20	8	36.14	5.58	0.57	0.07	0.17	0.15	0.05	0.20
Max bext	95/ 9/21	6	17.21	2.36	0.00	0.00	0.00	0.00	0.00	0.00
Max PP	95/ 9/21	13	12.58	1.00	0.19	0.07	0.00	0.00	0.18	0.00

View 3: Mt Zirkel - The Dome

	Date	Hour	Total Path Mm^{-1}	Total Path dv	PP Contrib Mm^{-1}	PP Contrib dv	Craig1 Mm^{-1}	Craig2 Mm^{-1}	Hyden1 Mm^{-1}	Hyden2 Mm^{-1}
Max bext	95/ 9/17	17	16.18	2.09	1.12	0.31	0.17	0.18	0.42	0.35
Max PP	95/ 9/17	17	16.18	2.09	1.12	0.31	0.17	0.18	0.42	0.35
Max bext	95/ 9/18	6	34.58	5.39	3.56	0.47	0.61	0.62	1.13	1.21
Max PP	95/ 9/18	14	23.27	3.67	4.82	1.01	0.93	0.87	1.52	1.49
Max bext	95/ 9/19	7	19.05	2.80	2.12	0.51	0.32	0.31	0.83	0.65
Max PP	95/ 9/19	7	19.05	2.80	2.12	0.51	0.32	0.31	0.83	0.65
Max bext	95/ 9/20	6	36.37	5.61	0.85	0.10	0.43	0.21	0.07	0.13
Max PP	95/ 9/20	8	33.94	5.31	0.94	0.12	0.35	0.25	0.08	0.27
Max bext	95/ 9/21	6	17.22	2.36	0.00	0.00	0.00	0.00	0.00	0.00
Max PP	95/ 9/21	13	13.25	1.22	0.69	0.23	0.00	0.00	0.65	0.00

View 4: Mt Zirkel - Mt Ethel

	Date	Hour	Total Path Mm^{-1}	Total Path dv	PP Contrib Mm^{-1}	PP Contrib dv	Craig1 Mm^{-1}	Craig2 Mm^{-1}	Hyden1 Mm^{-1}	Hyden2 Mm^{-1}
Max bext	95/ 9/17	17	16.30	2.12	1.09	0.30	0.17	0.18	0.42	0.33
Max PP	95/ 9/17	17	16.30	2.12	1.09	0.30	0.17	0.18	0.42	0.33
Max bext	95/ 9/18	6	35.66	5.52	3.41	0.44	0.46	0.49	1.22	1.23
Max PP	95/ 9/18	14	24.00	3.80	5.18	1.06	0.94	0.89	1.67	1.68
Max bext	95/ 9/19	6	19.88	2.98	2.44	0.57	0.35	0.34	1.06	0.69
Max PP	95/ 9/19	6	19.88	2.98	2.44	0.57	0.35	0.34	1.06	0.69
Max bext	95/ 9/20	6	38.91	5.90	0.96	0.11	0.42	0.26	0.08	0.21
Max PP	95/ 9/20	8	35.79	5.54	1.40	0.17	0.43	0.38	0.09	0.51
Max bext	95/ 9/21	6	18.13	2.58	0.01	0.00	0.00	0.00	0.00	0.00
Max PP	95/ 9/21	13	14.46	1.60	1.09	0.34	0.00	0.00	1.03	0.05

View 5: Mt Ethel - Continental Divide Trail

	Date	Hour	Total Path Mm^{-1}	Total Path dv	PP Contrib Mm^{-1}	PP Contrib dv	Craig1 Mm^{-1}	Craig2 Mm^{-1}	Hyden1 Mm^{-1}	Hyden2 Mm^{-1}
Max bext	95/ 9/17	7	17.69	2.48	0.41	0.10	0.05	0.06	0.15	0.15
Max PP	95/ 9/17	15	15.17	1.81	1.05	0.31	0.08	0.07	0.47	0.42
Max bext	95/ 9/18	7	43.13	6.35	3.27	0.34	0.37	0.41	1.31	1.18
Max PP	95/ 9/18	13	26.21	4.18	7.26	1.41	0.92	0.77	2.72	2.86
Max bext	95/ 9/19	6	23.70	3.75	3.25	0.64	0.40	0.39	1.59	0.87
Max PP	95/ 9/19	6	23.70	3.75	3.25	0.64	0.40	0.39	1.59	0.87
Max bext	95/ 9/20	6	50.36	7.02	1.31	0.11	0.50	0.31	0.10	0.40
Max PP	95/ 9/20	10	49.65	6.96	3.85	0.35	0.43	0.57	1.44	1.41
Max bext	95/ 9/21	7	21.30	3.28	0.01	0.00	0.00	0.00	0.01	0.00
Max PP	95/ 9/21	13	18.14	2.59	2.43	0.62	0.01	0.01	2.23	0.18

View 6: Davis Pk - Southern Ridge

	Date	Hour	Total Path Mm^{-1}	Total Path dv	PP Contrib Mm^{-1}	PP Contrib dv	Craig1 Mm^{-1}	Craig2 Mm^{-1}	Hyden1 Mm^{-1}	Hyden2 Mm^{-1}
Max bext	95/ 9/17	7	16.59	2.20	0.53	0.14	0.09	0.08	0.18	0.19
Max PP	95/ 9/17	17	16.48	2.17	1.00	0.27	0.16	0.18	0.36	0.30
Max bext	95/ 9/18	6	39.43	5.96	3.56	0.41	0.49	0.52	1.32	1.23
Max PP	95/ 9/18	8	36.83	5.66	4.31	0.54	0.57	0.60	1.52	1.62
Max bext	95/ 9/19	7	21.03	3.23	2.12	0.46	0.31	0.29	0.91	0.61
Max PP	95/ 9/19	7	21.03	3.23	2.12	0.46	0.31	0.29	0.91	0.61
Max bext	95/ 9/20	6	41.62	6.19	0.60	0.06	0.24	0.12	0.07	0.17
Max PP	95/ 9/20	8	40.01	6.02	0.95	0.10	0.23	0.19	0.14	0.40

Max bext	95/ 9/21	6	18.98	2.78	0.00	0.00	0.00	0.00	0.00	0.00
Max PP	95/ 9/21	13	13.10	1.17	0.58	0.20	0.00	0.00	0.56	0.03

View 7: Mt Zirkel - Medicine Bow Pk

	Date	Hour	Total Path Mm^{-1}	Total Path dv	PP Contrib Mm^{-1}	PP Contrib dv	Craig1 Mm^{-1}	Craig2 Mm^{-1}	Hyden1 Mm^{-1}	Hyden2 Mm^{-1}
Max bext	95/ 9/17	17	14.40	1.58	0.15	0.05	0.02	0.02	0.06	0.05
Max PP	95/ 9/17	17	14.40	1.58	0.15	0.05	0.02	0.02	0.06	0.05
Max bext	95/ 9/18	7	19.50	2.90	0.48	0.11	0.06	0.06	0.17	0.18
Max PP	95/ 9/18	14	15.45	1.89	0.58	0.17	0.12	0.11	0.19	0.17
Max bext	95/ 9/19	6	12.94	1.12	0.25	0.08	0.04	0.04	0.11	0.07
Max PP	95/ 9/19	7	12.69	1.03	0.26	0.09	0.04	0.04	0.12	0.07
Max bext	95/ 9/20	6	18.81	2.74	0.06	0.01	0.02	0.01	0.01	0.01
Max PP	95/ 9/20	8	17.62	2.46	0.10	0.02	0.03	0.03	0.01	0.03
Max bext	95/ 9/21	9	12.86	1.09	0.00	0.00	0.00	0.00	0.00	0.00
Max PP	95/ 9/21	12	11.26	0.52	0.03	0.01	0.00	0.00	0.02	0.00

View 8: Mt Zirkel - Longs Pk

	Date	Hour	Total Path Mm^{-1}	Total Path dv	PP Contrib Mm^{-1}	PP Contrib dv	Craig1 Mm^{-1}	Craig2 Mm^{-1}	Hyden1 Mm^{-1}	Hyden2 Mm^{-1}
Max bext	95/ 9/17	17	13.46	1.29	0.08	0.03	0.01	0.01	0.03	0.02
Max PP	95/ 9/17	17	13.46	1.29	0.08	0.03	0.01	0.01	0.03	0.02
Max bext	95/ 9/18	17	20.80	3.18	0.19	0.04	0.04	0.04	0.05	0.05
Max PP	95/ 9/18	14	17.74	2.49	0.29	0.07	0.06	0.05	0.09	0.09
Max bext	95/ 9/19	6	12.51	0.97	0.12	0.04	0.02	0.02	0.06	0.03
Max PP	95/ 9/19	7	12.16	0.85	0.13	0.05	0.02	0.02	0.06	0.04
Max bext	95/ 9/20	17	18.57	2.69	0.00	0.00	0.00	0.00	0.00	0.00
Max PP	95/ 9/20	10	17.04	2.31	0.04	0.01	0.01	0.01	0.01	0.01
Max bext	95/ 9/21	6	13.42	1.28	0.00	0.00	0.00	0.00	0.00	0.00
Max PP	95/ 9/21	14	12.01	0.80	0.01	0.00	0.00	0.00	0.01	0.00

View 9: Davis Pk - Flat Tops

	Date	Hour	Total Path Mm^{-1}	Total Path dv	PP Contrib Mm^{-1}	PP Contrib dv	Craig1 Mm^{-1}	Craig2 Mm^{-1}	Hyden1 Mm^{-1}	Hyden2 Mm^{-1}
Max bext	95/ 9/17	17	14.50	1.61	0.10	0.03	0.02	0.02	0.04	0.03
Max PP	95/ 9/17	17	14.50	1.61	0.10	0.03	0.02	0.02	0.04	0.03
Max bext	95/ 9/18	6	23.28	3.67	0.39	0.07	0.04	0.05	0.16	0.14
Max PP	95/ 9/18	14	16.70	2.23	0.47	0.12	0.11	0.09	0.14	0.13
Max bext	95/ 9/19	6	14.72	1.68	0.18	0.05	0.03	0.03	0.08	0.05
Max PP	95/ 9/19	7	14.30	1.55	0.18	0.06	0.03	0.03	0.08	0.05
Max bext	95/ 9/20	6	20.77	3.17	0.03	0.01	0.01	0.00	0.01	0.01
Max PP	95/ 9/20	10	17.79	2.50	0.03	0.01	0.00	0.00	0.01	0.01
Max bext	95/ 9/21	6	14.81	1.71	0.00	0.00	0.00	0.00	0.00	0.00
Max PP	95/ 9/21	14	12.39	0.93	0.01	0.00	0.00	0.00	0.01	0.00

View 10: Mt Zirkel - Meaden Pk

	Date	Hour	Total Path Mm^{-1}	Total Path dv	PP Contrib Mm^{-1}	PP Contrib dv	Craig1 Mm^{-1}	Craig2 Mm^{-1}	Hyden1 Mm^{-1}	Hyden2 Mm^{-1}
Max bext	95/ 9/17	17	15.70	1.96	0.23	0.06	0.03	0.03	0.09	0.08
Max PP	95/ 9/17	17	15.70	1.96	0.23	0.06	0.03	0.03	0.09	0.08
Max bext	95/ 9/18	6	27.35	4.37	0.68	0.11	0.09	0.09	0.25	0.25
Max PP	95/ 9/18	14	22.57	3.54	0.88	0.17	0.18	0.17	0.28	0.26
Max bext	95/ 9/19	6	15.51	1.91	0.39	0.11	0.06	0.06	0.17	0.10
Max PP	95/ 9/19	7	15.42	1.88	0.39	0.11	0.06	0.05	0.17	0.11
Max bext	95/ 9/20	6	27.02	4.32	0.09	0.01	0.03	0.02	0.01	0.02
Max PP	95/ 9/20	8	25.63	4.09	0.14	0.02	0.04	0.04	0.01	0.05
Max bext	95/ 9/21	6	14.16	1.51	0.00	0.00	0.00	0.00	0.00	0.00
Max PP	95/ 9/21	13	12.43	0.94	0.05	0.02	0.00	0.00	0.05	0.00

For 09/17/95–09/21/95 (Table 6.7.9), base-case mean hourly extinction is estimated to range from ~12 to 50 Mm^{-1} among all sight paths. The estimated effects of emissions from Hayden and Craig Units 1 and 2 on sight path extinction range from 0 to 5 Mm^{-1} for sight paths within the Wilderness boundaries. For sight lines that extend outside of the boundaries, local generating station contributions were removed from the path segments within the boundaries only, leading to a contribution of only a few tenths of Mm^{-1}. In the latter case, the smaller contribution is due to the longer integration length and the minimal sight path distance between the Wilderness starting point and the Wilderness boundary.

Most of the time, the contributions from Craig Units 1 and 2 are about half the contributions from Hayden Units 1 and 2. Longer sight paths that extend outside the Wilderness boundaries are characterized by lower maximum hourly extinction than the sight paths within the boundaries. On 09/19/95, estimated contributions from the two generating stations on extinction along sight paths within the Wilderness were significant enough for some hours to exceed 1 dv. The maximum impact of the two generating stations on extinction along sight paths is always predicted to be less than 1 dv for the rest of the episode.

Tables 6.7.10 and 6.7.12 present sight path calculations for the 08/07/95–08/09/95, and 08/21/95–08/27/95 episodes. Results are markedly different from the September episode, in that base-case mean extinction along the same sight paths are low and just 1-5 Mm^{-1} above Rayleigh. This is consistent with the CALMET/CALPUFF underestimation of concentrations and extinctions at Wilderness receptors described above and in Appendix B.2. Maximum hourly average estimated impacts from Craig and Hayden Units 1 and 2 are smaller than 0.4 Mm^{-1} for the 08/07/95–08/09/95 episode, but as much as 2.5 Mm^{-1} (0.8 dv) for the 08/21/95–08/27/95 episode. Owing to the poor model performance for both of these August episodes, little can be said about the contributions of the two Yampa Valley generating stations to visibility degradation along sight paths emanating from the Wilderness for these periods.

Maximum hourly extinction along the sight paths for the 10/07/95–10/19/95 period (Table 6.7.11) are in the 11-16 Mm^{-1} range for sight paths within the Wilderness and in the 11-13 Mm^{-1} range for sight paths that extend out of the Wilderness. The maximum contribution to extinction from emissions from the two Yampa Valley generating stations along sight paths within the Wilderness is 2.13 Mm^{-1} (0.6 dv), with contributions closer to 0.2 Mm^{-1} being more typical. For sight paths that extend outside of the Wilderness, the contribution of the two Yampa Valley generating stations to average extinction along the portion of the sight path the Wilderness boundaries is always less than 0.2 Mm^{-1}.

6.8Changes in Perceived Haze

This section reports the results of calculations of contrast and the deciview haze index, dv, that have the objective of indicating whether or not the changes in light extinction calculated in Section 6.7 may be visually perceptible. Calculations were performed for

several sight paths. The changes that were calculated in both contrast and deciview would occur if the contributions to extinction from the Hayden station and Yampa Project (Craig Units 1 and 2) were removed from

---

Table 6.7.10
Hourly Average Estimated Extinction (Mm^{-1}) and Deciview (dv) along 10 Sight Paths
for the August 7-9, 1995 Episode

Indicated for each day is (1) the daylight hour with the maximum total extinction along a particular sight path ("Max bext"), and (2) the daylight hour in which the model estimated the maximum contribution to extinction along the path segments within the MZWA due to the combined emissions from Hayden Units 1&2 and Craig Units 1&2 ("Max PP"). Given for each of these two types of entries is the total integrated extinction (with the nominal value for Rayleigh scattering of 10 Mm^{-1}), the total Hayden and Craig Units 1&2 contribution to sight-path extinction, and a breakdown of each unit's extinction contribution (Mm^{-1} only).

View 1: Davis Pk - Mt Zirkel

	Date	Hour	Total Path Mm^{-1}	Total Path dv	PP Contrib Mm^{-1}	PP Contrib dv	Craig1 Mm^{-1}	Craig2 Mm^{-1}	Hyden1 Mm^{-1}	Hyden2 Mm^{-1}
Max bext	95/ 8/ 7	6	15.32	1.85	0.14	0.04	0.01	0.02	0.06	0.05
Max PP	95/ 8/ 7	6	15.32	1.85	0.14	0.04	0.01	0.02	0.06	0.05
Max bext	95/ 8/ 8	14	10.64	0.27	0.00	0.00	0.00	0.00	0.00	0.00
Max PP	95/ 8/ 8	10	10.34	0.15	0.08	0.03	0.00	0.02	0.05	0.02
Max bext	95/ 8/ 9	6	11.90	0.76	0.00	0.00	0.00	0.00	0.00	0.00
Max PP	95/ 8/ 9	17	11.13	0.46	0.25	0.10	0.03	0.04	0.09	0.08

View 2: Davis Pk - Little Agnes Pk

	Date	Hour	Total Path Mm^{-1}	Total Path dv	PP Contrib Mm^{-1}	PP Contrib dv	Craig1 Mm^{-1}	Craig2 Mm^{-1}	Hyden1 Mm^{-1}	Hyden2 Mm^{-1}
Max bext	95/ 8/ 7	6	14.96	1.75	0.13	0.04	0.01	0.02	0.06	0.05
Max PP	95/ 8/ 7	6	14.96	1.75	0.13	0.04	0.01	0.02	0.06	0.05
Max bext	95/ 8/ 8	14	10.63	0.27	0.00	0.00	0.00	0.00	0.00	0.00
Max PP	95/ 8/ 8	10	10.34	0.15	0.07	0.03	0.00	0.02	0.04	0.01
Max bext	95/ 8/ 9	6	11.76	0.70	0.00	0.00	0.00	0.00	0.00	0.00

Max PP	95/ 8/ 9	17	11.14	0.47	0.26	0.10	0.03	0.04	0.10	0.09

View 3: Mt Zirkel - The Dome

	Date	Hour	Total Path Mm^{-1}	dv	PP Contrib Mm^{-1}	dv	Craig1 Mm^{-1}	Craig2 Mm^{-1}	Hyden1 Mm^{-1}	Hyden2 Mm^{-1}
Max bext	95/ 8/ 7	6	13.87	1.42	0.12	0.04	0.01	0.01	0.05	0.04
Max PP	95/ 8/ 7	13	11.20	0.49	0.13	0.05	0.00	0.00	0.06	0.06
Max bext	95/ 8/ 8	15	10.65	0.27	0.00	0.00	0.00	0.00	0.00	0.00
Max PP	95/ 8/ 8	10	10.40	0.17	0.15	0.06	0.00	0.00	0.08	0.07
Max bext	95/ 8/ 9	6	11.31	0.53	0.01	0.00	0.00	0.00	0.00	0.00
Max PP	95/ 8/ 9	17	11.25	0.51	0.32	0.13	0.04	0.05	0.12	0.11

View 4: Mt Zirkel - Mt Ethel

	Date	Hour	Total Path Mm^{-1}	dv	PP Contrib Mm^{-1}	dv	Craig1 Mm^{-1}	Craig2 Mm^{-1}	Hyden1 Mm^{-1}	Hyden2 Mm^{-1}
Max bext	95/ 8/ 7	6	14.35	1.57	0.12	0.04	0.01	0.01	0.05	0.04
Max PP	95/ 8/ 7	13	11.22	0.50	0.13	0.05	0.00	0.00	0.07	0.06
Max bext	95/ 8/ 8	15	10.70	0.29	0.00	0.00	0.00	0.00	0.00	0.00
Max PP	95/ 8/ 8	11	10.41	0.17	0.12	0.05	0.00	0.04	0.05	0.04
Max bext	95/ 8/ 9	6	11.53	0.62	0.00	0.00	0.00	0.00	0.00	0.00
Max PP	95/ 8/ 9	17	11.30	0.53	0.34	0.13	0.04	0.05	0.13	0.11

View 5: Mt Ethel - Continental Divide Trail

	Date	Hour	Total Path Mm^{-1}	Total Path dv	PP Contrib Mm^{-1}	PP Contrib dv	Craig1 Mm^{-1}	Craig2 Mm^{-1}	Hyden1 Mm^{-1}	Hyden2 Mm^{-1}
Max bext	95/ 8/ 7	6	15.20	1.82	0.10	0.03	0.01	0.01	0.05	0.04
Max PP	95/ 8/ 7	12	11.35	0.55	0.14	0.05	0.00	0.00	0.08	0.06
Max bext	95/ 8/ 8	14	11.02	0.42	0.00	0.00	0.00	0.00	0.00	0.00
Max PP	95/ 8/ 8	12	10.71	0.30	0.22	0.09	0.04	0.07	0.07	0.04
Max bext	95/ 8/ 9	6	12.34	0.91	0.00	0.00	0.00	0.00	0.00	0.00
Max PP	95/ 8/ 9	17	11.67	0.67	0.51	0.19	0.06	0.08	0.21	0.15

View 6: Davis Pk - Southern Ridge

	Date	Hour	Total Path Mm^{-1}	Total Path dv	PP Contrib Mm^{-1}	PP Contrib dv	Craig1 Mm^{-1}	Craig2 Mm^{-1}	Hyden1 Mm^{-1}	Hyden2 Mm^{-1}
Max bext	95/ 8/ 7	6	14.66	1.66	0.11	0.03	0.01	0.01	0.05	0.04
Max PP	95/ 8/ 7	11	11.44	0.58	0.13	0.05	0.00	0.00	0.06	0.06
Max bext	95/ 8/ 8	14	10.74	0.31	0.00	0.00	0.00	0.00	0.00	0.00
Max PP	95/ 8/ 8	10	10.41	0.17	0.13	0.05	0.00	0.01	0.08	0.05
Max bext	95/ 8/ 9	6	11.87	0.74	0.00	0.00	0.00	0.00	0.00	0.00
Max PP	95/ 8/ 9	17	11.35	0.55	0.37	0.14	0.04	0.06	0.14	0.12

View 7: Mt Zirkel - Medicine Bow Pk

	Date	Hour	Total Path Mm^{-1}	Total Path dv	PP Contrib Mm^{-1}	PP Contrib dv	Craig1 Mm^{-1}	Craig2 Mm^{-1}	Hyden1 Mm^{-1}	Hyden2 Mm^{-1}
Max bext	95/ 8/ 7	6	11.74	0.70	0.02	0.01	0.00	0.00	0.01	0.01
Max PP	95/ 8/ 7	11	11.25	0.51	0.02	0.01	0.00	0.00	0.01	0.01
Max bext	95/ 8/ 8	17	10.33	0.14	0.00	0.00	0.00	0.00	0.00	0.00
Max PP	95/ 8/ 8	11	10.24	0.10	0.01	0.00	0.00	0.01	0.00	0.00
Max bext	95/ 8/ 9	17	10.69	0.29	0.04	0.02	0.00	0.01	0.01	0.01
Max PP	95/ 8/ 9	17	10.69	0.29	0.04	0.02	0.00	0.01	0.01	0.01

View 8: Mt Zirkel - Longs Pk

	Date	Hour	Total Path Mm^{-1}	Total Path dv	PP Contrib Mm^{-1}	PP Contrib dv	Craig1 Mm^{-1}	Craig2 Mm^{-1}	Hyden1 Mm^{-1}	Hyden2 Mm^{-1}
Max bext	95/ 8/ 7	8	11.65	0.66	0.00	0.00	0.00	0.00	0.00	0.00
Max PP	95/ 8/ 7	17	10.68	0.29	0.01	0.00	0.00	0.00	0.00	0.00
Max bext	95/ 8/ 8	17	10.38	0.16	0.00	0.00	0.00	0.00	0.00	0.00
Max PP	95/ 8/ 8	12	10.24	0.10	0.01	0.00	0.00	0.00	0.00	0.00
Max bext	95/ 8/ 9	17	11.15	0.47	0.02	0.01	0.00	0.00	0.01	0.01
Max PP	95/ 8/ 9	17	11.15	0.47	0.02	0.01	0.00	0.00	0.01	0.01

View 9: Davis Pk - Flat Tops

	Date	Hour	Total Path Mm^{-1}	Total Path dv	PP Contrib Mm^{-1}	PP Contrib dv	Craig1 Mm^{-1}	Craig2 Mm^{-1}	Hyden1 Mm^{-1}	Hyden2 Mm^{-1}
Max bext	95/ 8/ 7	6	11.48	0.60	0.02	0.01	0.00	0.00	0.01	0.01
Max PP	95/ 8/ 7	7	11.37	0.56	0.02	0.01	0.00	0.00	0.01	0.00
Max bext	95/ 8/ 8	13	10.61	0.26	0.00	0.00	0.00	0.00	0.00	0.00
Max PP	95/ 8/ 8	10	10.27	0.12	0.01	0.00	0.00	0.00	0.01	0.00
Max bext	95/ 8/ 9	17	11.19	0.49	0.02	0.01	0.00	0.00	0.01	0.01
Max PP	95/ 8/ 9	17	11.19	0.49	0.02	0.01	0.00	0.00	0.01	0.01

View 10: Mt Zirkel - Meaden Pk

	Date	Hour	Total Path Mm^{-1}	Total Path dv	PP Contrib Mm^{-1}	PP Contrib dv	Craig1 Mm^{-1}	Craig2 Mm^{-1}	Hyden1 Mm^{-1}	Hyden2 Mm^{-1}
Max bext	95/ 8/ 7	6	12.18	0.86	0.03	0.01	0.00	0.00	0.01	0.01
Max PP	95/ 8/ 7	6	12.18	0.86	0.03	0.01	0.00	0.00	0.01	0.01
Max bext	95/ 8/ 8	14	10.48	0.20	0.00	0.00	0.00	0.00	0.00	0.00
Max PP	95/ 8/ 8	11	10.38	0.16	0.02	0.01	0.00	0.01	0.00	0.00
Max bext	95/ 8/ 9	17	11.18	0.48	0.06	0.02	0.01	0.01	0.02	0.02
Max PP	95/ 8/ 9	17	11.18	0.48	0.06	0.02	0.01	0.01	0.02	0.02

Table 6.7.11
Hourly Average Estimated Extinction (Mm^{-1}) and Deciview (dv) along 10 Sight Paths for the October 7-19, 1995 Episode

Indicated for each day is (1) the daylight hour with the maximum total extinction along a particular sight path ("Max bext"), and (2) the daylight hour in which the model estimated the maximum contribution to extinction along the path segments within the MZWA due to the combined emissions from Hayden Units 1&2 and Craig Units 1&2 ("Max PP"). Given for each of these two types of entries is the total integrated extinction (with the nominal value for Rayleigh scattering of 10 Mm^{-1}), the total Hayden and Craig Units 1&2 contribution to sight-path extinction, and a breakdown of each unit's extinction contribution (Mm^{-1} only).

View 1: Davis Pk - Mt Zirkel

	Date	Hour	Total Path Mm^{-1}	Total Path dv	PP Contrib Mm^{-1}	PP Contrib dv	Craig1 Mm^{-1}	Craig2 Mm^{-1}	Hyden1 Mm^{-1}	Hyden2 Mm^{-1}
Max bext	95/10/ 7	8	12.46	0.96	0.06	0.02	0.01	0.01	0.02	0.01
Max PP	95/10/ 7	14	11.56	0.63	0.45	0.17	0.17	0.15	0.01	0.12
Max bext	95/10/ 8	8	16.96	2.29	0.05	0.01	0.01	0.01	0.02	0.01
Max PP	95/10/ 8	17	11.81	0.72	0.16	0.06	0.02	0.02	0.00	0.11
Max bext	95/10/ 9	8	14.92	1.74	0.12	0.04	0.04	0.03	0.01	0.04
Max PP	95/10/ 9	14	12.39	0.93	0.27	0.10	0.09	0.07	0.00	0.11
Max bext	95/10/10	7	13.54	1.32	0.02	0.01	0.00	0.00	0.00	0.02
Max PP	95/10/10	17	12.18	0.86	0.14	0.05	0.08	0.01	0.00	0.05
Max bext	95/10/11	7	13.37	1.26	0.12	0.04	0.03	0.02	0.00	0.07
Max PP	95/10/11	15	11.50	0.61	0.19	0.07	0.01	0.01	0.00	0.18
Max bext	95/10/12	17	14.95	1.75	0.00	0.00	0.00	0.00	0.00	0.00
Max PP	95/10/12	9	12.09	0.82	0.66	0.24	0.18	0.17	0.01	0.31
Max bext	95/10/13	6	13.61	1.34	0.00	0.00	0.00	0.00	0.00	0.00
Max PP	95/10/13	13	11.51	0.61	0.58	0.22	0.02	0.01	0.22	0.34
Max bext	95/10/14	7	12.27	0.89	0.00	0.00	0.00	0.00	0.00	0.00
Max PP	95/10/14	17	11.74	0.70	0.32	0.12	0.05	0.04	0.09	0.13
Max bext	95/10/15	8	12.91	1.11	0.20	0.07	0.02	0.02	0.08	0.07
Max PP	95/10/15	6	11.97	0.78	0.23	0.08	0.02	0.03	0.10	0.09
Max bext	95/10/16	7	13.59	1.33	0.09	0.03	0.01	0.00	0.06	0.02
Max PP	95/10/16	15	12.53	0.98	0.14	0.05	0.01	0.01	0.06	0.07
Max bext	95/10/17	8	15.56	1.92	0.07	0.02	0.01	0.01	0.02	0.03
Max PP	95/10/17	17	14.32	1.56	0.09	0.03	0.02	0.02	0.03	0.01
Max bext	95/10/18	7	15.63	1.94	0.09	0.03	0.01	0.01	0.07	0.01
Max PP	95/10/18	6	14.93	1.74	0.11	0.03	0.01	0.01	0.08	0.01

Max bext	95/10/19	7	14.06	1.48	0.00	0.00	0.00	0.00	0.00	0.00
Max PP	95/10/19	17	12.09	0.82	0.00	0.00	0.00	0.00	0.00	0.00

View 2: Davis Pk - Little Agnes Pk

	Date	Hour	Total Path Mm^{-1}	Total Path dv	PP Contrib Mm^{-1}	PP Contrib dv	Craig1 Mm^{-1}	Craig2 Mm^{-1}	Hyden1 Mm^{-1}	Hyden2 Mm^{-1}
Max bext	95/10/ 7	8	12.32	0.91	0.06	0.02	0.01	0.01	0.02	0.01
Max PP	95/10/ 7	14	11.54	0.62	0.45	0.17	0.18	0.17	0.01	0.10
Max bext	95/10/ 8	8	16.77	2.25	0.05	0.01	0.01	0.01	0.02	0.01
Max PP	95/10/ 8	17	11.77	0.71	0.15	0.06	0.03	0.02	0.00	0.11
Max bext	95/10/ 9	8	14.76	1.69	0.12	0.04	0.04	0.03	0.01	0.04
Max PP	95/10/ 9	14	12.37	0.92	0.27	0.10	0.09	0.08	0.00	0.11
Max bext	95/10/10	7	13.33	1.25	0.02	0.01	0.00	0.00	0.00	0.02
Max PP	95/10/10	17	12.15	0.85	0.14	0.05	0.07	0.01	0.00	0.05
Max bext	95/10/11	7	13.19	1.20	0.12	0.04	0.03	0.02	0.00	0.06
Max PP	95/10/11	15	11.48	0.60	0.18	0.07	0.01	0.01	0.00	0.17
Max bext	95/10/12	17	14.88	1.73	0.00	0.00	0.00	0.00	0.00	0.00
Max PP	95/10/12	9	12.08	0.82	0.67	0.25	0.20	0.19	0.01	0.27
Max bext	95/10/13	8	13.42	1.28	0.00	0.00	0.00	0.00	0.00	0.00
Max PP	95/10/13	13	11.49	0.60	0.57	0.22	0.01	0.01	0.22	0.32
Max bext	95/10/14	8	12.19	0.86	0.01	0.00	0.00	0.00	0.00	0.00
Max PP	95/10/14	17	11.73	0.69	0.33	0.12	0.05	0.05	0.09	0.10

Max bext	95/10/15	8	12.81	1.08	0.19	0.06	0.02	0.02	0.08	0.07
Max PP	95/10/15	6	11.95	0.77	0.24	0.09	0.02	0.03	0.10	0.09
Max bext	95/10/16	8	13.44	1.28	0.08	0.03	0.00	0.00	0.05	0.02
Max PP	95/10/16	15	12.56	0.99	0.15	0.05	0.01	0.01	0.06	0.07
Max bext	95/10/17	7	14.96	1.75	0.06	0.02	0.01	0.01	0.02	0.03
Max PP	95/10/17	15	13.73	1.38	0.09	0.03	0.02	0.02	0.03	0.02
Max bext	95/10/18	7	15.30	1.85	0.09	0.03	0.01	0.01	0.07	0.01
Max PP	95/10/18	6	14.76	1.69	0.10	0.03	0.01	0.01	0.07	0.01
Max bext	95/10/19	7	13.91	1.43	0.00	0.00	0.00	0.00	0.00	0.00
Max PP	95/10/19	17	12.08	0.82	0.00	0.00	0.00	0.00	0.00	0.00

View 3: Mt Zirkel - The Dome

	Date	Hour	Total Path Mm^{-1}	dv	PP Contrib Mm^{-1}	dv	Craig1 Mm^{-1}	Craig2 Mm^{-1}	Hyden1 Mm^{-1}	Hyden2 Mm^{-1}
Max bext	95/10/ 7	8	11.90	0.76	0.06	0.02	0.01	0.02	0.02	0.01
Max PP	95/10/ 7	15	11.61	0.65	0.50	0.19	0.16	0.17	0.01	0.15
Max bext	95/10/ 8	8	16.55	2.19	0.05	0.01	0.01	0.01	0.02	0.01
Max PP	95/10/ 8	17	11.99	0.79	0.32	0.12	0.05	0.03	0.01	0.23
Max bext	95/10/ 9	9	14.53	1.62	0.10	0.03	0.03	0.03	0.01	0.03
Max PP	95/10/ 9	15	12.34	0.91	0.31	0.11	0.10	0.09	0.00	0.11
Max bext	95/10/10	7	12.70	1.04	0.03	0.01	0.01	0.00	0.00	0.02
Max PP	95/10/10	17	12.23	0.87	0.18	0.06	0.09	0.01	0.00	0.07
Max bext	95/10/11	8	12.74	1.05	0.07	0.02	0.02	0.01	0.00	0.04
Max PP	95/10/11	15	11.48	0.60	0.21	0.08	0.00	0.00	0.00	0.21
Max bext	95/10/12	17	14.50	1.61	0.00	0.00	0.00	0.00	0.00	0.00
Max PP	95/10/12	13	12.42	0.94	1.38	0.51	0.73	0.63	0.01	0.00
Max bext	95/10/13	8	12.70	1.04	0.09	0.03	0.00	0.00	0.06	0.02
Max PP	95/10/13	13	11.72	0.69	0.82	0.32	0.05	0.04	0.27	0.47
Max bext	95/10/14	9	11.94	0.77	0.02	0.01	0.00	0.00	0.01	0.01
Max PP	95/10/14	17	11.71	0.69	0.41	0.15	0.06	0.05	0.12	0.18
Max bext	95/10/15	9	12.41	0.94	0.20	0.07	0.02	0.02	0.10	0.07
Max PP	95/10/15	6	11.86	0.74	0.25	0.09	0.02	0.03	0.11	0.09
Max bext	95/10/16	8	12.82	1.08	0.06	0.02	0.00	0.00	0.04	0.01
Max PP	95/10/16	14	11.84	0.73	0.14	0.05	0.04	0.04	0.04	0.02
Max bext	95/10/17	17	14.69	1.67	0.11	0.03	0.03	0.03	0.04	0.02
Max PP	95/10/17	14	13.99	1.46	0.16	0.05	0.04	0.04	0.05	0.03
Max bext	95/10/18	6	14.17	1.51	0.06	0.02	0.01	0.01	0.04	0.01
Max PP	95/10/18	6	14.17	1.51	0.06	0.02	0.01	0.01	0.04	0.01
Max bext	95/10/19	7	13.43	1.28	0.00	0.00	0.00	0.00	0.00	0.00
Max PP	95/10/19	17	12.12	0.84	0.00	0.00	0.00	0.00	0.00	0.00

View 4: Mt Zirkel - Mt Ethel

	Date	Hour	Total Path Mm^{-1}	Total Path dv	PP Contrib Mm^{-1}	PP Contrib dv	Craig1 Mm^{-1}	Craig2 Mm^{-1}	Hyden1 Mm^{-1}	Hyden2 Mm^{-1}
Max bext	95/10/ 7	8	12.20	0.86	0.06	0.02	0.01	0.02	0.02	0.01
Max PP	95/10/ 7	15	11.63	0.66	0.50	0.19	0.16	0.16	0.01	0.18
Max bext	95/10/ 8	8	17.02	2.31	0.05	0.01	0.01	0.01	0.02	0.01
Max PP	95/10/ 8	17	12.07	0.82	0.35	0.13	0.05	0.03	0.01	0.26
Max bext	95/10/ 9	8	14.97	1.75	0.12	0.03	0.04	0.03	0.01	0.04
Max PP	95/10/ 9	15	12.42	0.94	0.34	0.12	0.11	0.10	0.00	0.13
Max bext	95/10/10	7	13.20	1.21	0.06	0.02	0.01	0.00	0.00	0.05
Max PP	95/10/10	17	12.29	0.90	0.20	0.07	0.10	0.01	0.00	0.08
Max bext	95/10/11	8	12.96	1.13	0.08	0.03	0.02	0.01	0.00	0.04
Max PP	95/10/11	15	11.46	0.59	0.17	0.06	0.00	0.00	0.00	0.16
Max bext	95/10/12	17	14.76	1.69	0.00	0.00	0.00	0.00	0.00	0.00
Max PP	95/10/12	13	12.65	1.02	1.60	0.59	0.63	0.55	0.29	0.13
Max bext	95/10/13	8	13.35	1.25	0.15	0.05	0.00	0.00	0.11	0.05
Max PP	95/10/13	13	11.81	0.72	0.88	0.34	0.06	0.05	0.28	0.49
Max bext	95/10/14	8	12.14	0.84	0.02	0.01	0.00	0.00	0.01	0.01
Max PP	95/10/14	17	11.73	0.69	0.42	0.16	0.06	0.05	0.13	0.19
Max bext	95/10/15	8	12.65	1.02	0.18	0.06	0.02	0.02	0.08	0.07
Max PP	95/10/15	16	11.93	0.77	0.24	0.09	0.04	0.04	0.05	0.12
Max bext	95/10/16	8	13.19	1.20	0.06	0.02	0.00	0.00	0.04	0.01
Max PP	95/10/16	14	11.86	0.74	0.15	0.06	0.04	0.04	0.04	0.02
Max bext	95/10/17	17	14.90	1.73	0.13	0.04	0.03	0.03	0.05	0.02
Max PP	95/10/17	14	14.14	1.50	0.19	0.06	0.05	0.04	0.07	0.04
Max bext	95/10/18	7	14.68	1.67	0.06	0.02	0.01	0.01	0.04	0.01
Max PP	95/10/18	14	12.67	1.03	0.06	0.02	0.02	0.02	0.02	0.00
Max bext	95/10/19	7	14.00	1.46	0.00	0.00	0.00	0.00	0.00	0.00
Max PP	95/10/19	17	12.17	0.85	0.00	0.00	0.00	0.00	0.00	0.00

View 5: Mt Ethel - Continental Divide Trail

	Date	Hour	Total Path Mm^{-1}	Total Path dv	PP Contrib Mm^{-1}	PP Contrib dv	Craig1 Mm^{-1}	Craig2 Mm^{-1}	Hyden1 Mm^{-1}	Hyden2 Mm^{-1}
Max bext	95/10/ 7	7	12.95	1.12	0.05	0.02	0.01	0.02	0.02	0.01
Max PP	95/10/ 7	15	11.71	0.69	0.51	0.19	0.12	0.12	0.01	0.26
Max bext	95/10/ 8	7	18.97	2.78	0.05	0.01	0.01	0.01	0.03	0.01
Max PP	95/10/ 8	16	12.28	0.89	0.50	0.18	0.05	0.03	0.01	0.41
Max bext	95/10/ 9	7	16.22	2.10	0.12	0.03	0.04	0.03	0.01	0.05

Max PP	95/10/ 9	15	12.73	1.05	0.45	0.16	0.13	0.12	0.01	0.20
Max bext	95/10/10	7	14.30	1.55	0.07	0.02	0.01	0.00	0.00	0.05
Max PP	95/10/10	17	12.58	1.00	0.33	0.12	0.16	0.02	0.00	0.15
Max bext	95/10/11	7	13.54	1.32	0.08	0.03	0.02	0.01	0.00	0.05
Max PP	95/10/11	6	12.84	1.09	0.09	0.03	0.02	0.01	0.00	0.06
Max bext	95/10/12	15	16.50	2.17	2.13	0.60	0.89	0.91	0.22	0.11
Max PP	95/10/12	15	16.50	2.17	2.13	0.60	0.89	0.91	0.22	0.11
Max bext	95/10/13	6	14.57	1.63	0.23	0.07	0.00	0.00	0.20	0.04
Max PP	95/10/13	13	12.08	0.82	1.00	0.38	0.15	0.11	0.27	0.46
Max bext	95/10/14	7	12.83	1.08	0.01	0.00	0.00	0.00	0.00	0.00
Max PP	95/10/14	17	11.98	0.78	0.59	0.22	0.07	0.06	0.21	0.25
Max bext	95/10/15	7	13.23	1.22	0.16	0.05	0.01	0.01	0.07	0.06
Max PP	95/10/15	17	12.30	0.90	0.40	0.14	0.03	0.03	0.14	0.20
Max bext	95/10/16	7	13.65	1.35	0.05	0.02	0.00	0.00	0.03	0.01
Max PP	95/10/16	13	12.13	0.84	0.35	0.13	0.04	0.02	0.18	0.10
Max bext	95/10/17	7	16.04	2.05	0.17	0.05	0.02	0.02	0.05	0.08
Max PP	95/10/17	14	14.99	1.76	0.44	0.13	0.11	0.10	0.17	0.06
Max bext	95/10/18	7	15.55	1.92	0.04	0.01	0.00	0.00	0.04	0.00
Max PP	95/10/18	14	12.62	1.01	0.09	0.03	0.02	0.02	0.05	0.00
Max bext	95/10/19	7	17.07	2.32	0.00	0.00	0.00	0.00	0.00	0.00
Max PP	95/10/19	17	12.55	0.99	0.01	0.00	0.00	0.00	0.01	0.00

View 6: Davis Pk - Southern Ridge

	Date	Hour	Total Path Mm^{-1}	Total Path dv	PP Contrib Mm^{-1}	PP Contrib dv	Craig1 Mm^{-1}	Craig2 Mm^{-1}	Hyden1 Mm^{-1}	Hyden2 Mm^{-1}
Max bext	95/10/ 7	7	12.37	0.92	0.07	0.02	0.01	0.02	0.02	0.01
Max PP	95/10/ 7	14	11.47	0.60	0.41	0.16	0.12	0.12	0.01	0.16
Max bext	95/10/ 8	7	16.04	2.05	0.04	0.01	0.01	0.01	0.02	0.01
Max PP	95/10/ 8	16	11.81	0.72	0.28	0.10	0.04	0.03	0.01	0.21
Max bext	95/10/ 9	8	14.49	1.61	0.11	0.03	0.03	0.03	0.01	0.03
Max PP	95/10/ 9	14	12.50	0.97	0.35	0.12	0.11	0.10	0.00	0.13
Max bext	95/10/10	7	13.27	1.23	0.03	0.01	0.00	0.00	0.00	0.02
Max PP	95/10/10	17	12.24	0.88	0.19	0.07	0.10	0.02	0.00	0.08
Max bext	95/10/11	7	13.07	1.16	0.09	0.03	0.02	0.02	0.00	0.05
Max PP	95/10/11	15	11.44	0.58	0.17	0.07	0.00	0.00	0.00	0.16
Max bext	95/10/12	17	13.88	1.42	0.00	0.00	0.00	0.00	0.00	0.00
Max PP	95/10/12	13	11.69	0.68	0.75	0.29	0.34	0.30	0.07	0.05
Max bext	95/10/13	6	12.81	1.08	0.01	0.00	0.00	0.00	0.01	0.00
Max PP	95/10/13	13	11.68	0.67	0.75	0.29	0.05	0.04	0.26	0.40
Max bext	95/10/14	7	12.20	0.86	0.01	0.00	0.00	0.00	0.00	0.00

Max PP	95/10/14	17	11.72	0.69	0.41	0.15	0.05	0.05	0.13	0.18
Max bext	95/10/15	7	12.70	1.04	0.21	0.07	0.02	0.02	0.09	0.08
Max PP	95/10/15	6	11.95	0.77	0.23	0.08	0.02	0.02	0.10	0.08
Max bext	95/10/16	7	13.22	1.21	0.06	0.02	0.00	0.00	0.04	0.02
Max PP	95/10/16	15	12.57	0.99	0.13	0.05	0.01	0.00	0.06	0.06
Max bext	95/10/17	7	14.78	1.70	0.09	0.03	0.01	0.01	0.03	0.04
Max PP	95/10/17	14	14.09	1.49	0.16	0.05	0.04	0.04	0.06	0.03
Max bext	95/10/18	7	14.76	1.69	0.06	0.02	0.00	0.01	0.04	0.01
Max PP	95/10/18	6	14.34	1.57	0.07	0.02	0.01	0.01	0.05	0.01
Max bext	95/10/19	7	14.11	1.50	0.00	0.00	0.00	0.00	0.00	0.00
Max PP	95/10/19	17	12.19	0.86	0.00	0.00	0.00	0.00	0.00	0.00

View 7: Mt Zirkel - Medicine Bow Pk

	Date	Hour	Total Path Mm^{-1}	Total Path dv	PP Contrib Mm^{-1}	PP Contrib dv	Craig1 Mm^{-1}	Craig2 Mm^{-1}	Hyden1 Mm^{-1}	Hyden2 Mm^{-1}
Max bext	95/10/ 7	15	11.19	0.49	0.07	0.03	0.02	0.03	0.00	0.02
Max PP	95/10/ 7	15	11.19	0.49	0.07	0.03	0.02	0.03	0.00	0.02
Max bext	95/10/ 8	10	12.10	0.83	0.01	0.00	0.00	0.00	0.00	0.00
Max PP	95/10/ 8	17	11.53	0.62	0.02	0.01	0.00	0.00	0.00	0.02
Max bext	95/10/ 9	12	12.08	0.82	0.02	0.01	0.01	0.00	0.00	0.01
Max PP	95/10/ 9	15	11.74	0.70	0.04	0.01	0.01	0.01	0.00	0.01
Max bext	95/10/10	10	11.29	0.53	0.01	0.00	0.00	0.00	0.00	0.01
Max PP	95/10/10	17	11.24	0.51	0.02	0.01	0.01	0.00	0.00	0.01
Max bext	95/10/11	11	11.58	0.64	0.01	0.00	0.00	0.00	0.00	0.00
Max PP	95/10/11	17	11.27	0.52	0.03	0.01	0.01	0.01	0.00	0.00
Max bext	95/10/12	15	12.14	0.84	0.00	0.00	0.00	0.00	0.00	0.00
Max PP	95/10/12	13	10.65	0.27	0.09	0.04	0.05	0.04	0.00	0.00
Max bext	95/10/13	17	11.05	0.43	0.01	0.00	0.00	0.00	0.00	0.00
Max PP	95/10/13	13	10.86	0.36	0.10	0.04	0.00	0.00	0.03	0.05
Max bext	95/10/14	17	11.10	0.45	0.04	0.02	0.01	0.01	0.01	0.02
Max PP	95/10/14	17	11.10	0.45	0.04	0.02	0.01	0.01	0.01	0.02
Max bext	95/10/15	17	11.37	0.56	0.03	0.01	0.00	0.00	0.01	0.01
Max PP	95/10/15	17	11.37	0.56	0.03	0.01	0.00	0.00	0.01	0.01
Max bext	95/10/16	6	11.62	0.65	0.01	0.00	0.00	0.00	0.01	0.00
Max PP	95/10/16	15	11.45	0.59	0.02	0.01	0.00	0.00	0.01	0.01
Max bext	95/10/17	13	12.02	0.80	0.01	0.00	0.00	0.00	0.00	0.00
Max PP	95/10/17	15	11.93	0.77	0.02	0.01	0.00	0.00	0.00	0.00
Max bext	95/10/18	6	11.86	0.74	0.01	0.00	0.00	0.00	0.01	0.00
Max PP	95/10/18	15	11.56	0.63	0.01	0.00	0.00	0.00	0.00	0.00
Max bext	95/10/19	6	11.42	0.58	0.00	0.00	0.00	0.00	0.00	0.00

Max PP	95/10/19	17	11.16	0.48	0.00	0.00	0.00	0.00	0.00	0.00

View 8: Mt Zirkel - Longs Pk

	Date	Hour	Total Path Mm^{-1}	Total Path dv	PP Contrib Mm^{-1}	PP Contrib dv	Craig1 Mm^{-1}	Craig2 Mm^{-1}	Hyden1 Mm^{-1}	Hyden2 Mm^{-1}
Max bext	95/10/ 7	17	11.81	0.72	0.00	0.00	0.00	0.00	0.00	0.00
Max PP	95/10/ 7	14	11.51	0.61	0.04	0.02	0.01	0.01	0.00	0.01
Max bext	95/10/ 8	17	12.66	1.02	0.01	0.00	0.00	0.00	0.00	0.01
Max PP	95/10/ 8	17	12.66	1.02	0.01	0.00	0.00	0.00	0.00	0.01
Max bext	95/10/ 9	13	12.53	0.98	0.02	0.01	0.00	0.00	0.00	0.00
Max PP	95/10/ 9	14	12.31	0.90	0.02	0.01	0.01	0.00	0.00	0.01
Max bext	95/10/10	6	11.51	0.61	0.00	0.00	0.00	0.00	0.00	0.00
Max PP	95/10/10	17	11.49	0.60	0.01	0.00	0.01	0.00	0.00	0.00
Max bext	95/10/11	12	11.60	0.64	0.00	0.00	0.00	0.00	0.00	0.00
Max PP	95/10/11	15	11.48	0.60	0.02	0.01	0.00	0.00	0.00	0.01
Max bext	95/10/12	16	12.59	1.00	0.00	0.00	0.00	0.00	0.00	0.00
Max PP	95/10/12	13	10.81	0.34	0.05	0.02	0.02	0.02	0.00	0.00
Max bext	95/10/13	17	11.29	0.53	0.00	0.00	0.00	0.00	0.00	0.00
Max PP	95/10/13	13	11.06	0.44	0.05	0.02	0.00	0.00	0.02	0.03
Max bext	95/10/14	17	11.28	0.52	0.02	0.01	0.00	0.00	0.01	0.01
Max PP	95/10/14	17	11.28	0.52	0.02	0.01	0.00	0.00	0.01	0.01
Max bext	95/10/15	17	11.76	0.70	0.01	0.00	0.00	0.00	0.00	0.00
Max PP	95/10/15	17	11.76	0.70	0.01	0.00	0.00	0.00	0.00	0.00
Max bext	95/10/16	6	11.53	0.62	0.00	0.00	0.00	0.00	0.00	0.00
Max PP	95/10/16	16	11.45	0.59	0.01	0.00	0.00	0.00	0.00	0.00
Max bext	95/10/17	16	12.31	0.90	0.01	0.00	0.00	0.00	0.00	0.00
Max PP	95/10/17	16	12.31	0.90	0.01	0.00	0.00	0.00	0.00	0.00
Max bext	95/10/18	13	11.81	0.72	0.00	0.00	0.00	0.00	0.00	0.00
Max PP	95/10/18	15	11.63	0.66	0.01	0.00	0.00	0.00	0.00	0.00
Max bext	95/10/19	15	11.58	0.64	0.00	0.00	0.00	0.00	0.00	0.00
Max PP	95/10/19	17	11.19	0.49	0.00	0.00	0.00	0.00	0.00	0.00

View 9: Davis Pk - Flat Tops

	Date	Hour	Total Path Mm^{-1}	Total Path dv	PP Contrib Mm^{-1}	PP Contrib dv	Craig1 Mm^{-1}	Craig2 Mm^{-1}	Hyden1 Mm^{-1}	Hyden2 Mm^{-1}
Max bext	95/10/ 7	17	11.09	0.45	0.01	0.00	0.00	0.00	0.00	0.00
Max PP	95/10/ 7	15	11.04	0.43	0.04	0.02	0.01	0.02	0.00	0.01
Max bext	95/10/ 8	6	12.79	1.07	0.01	0.00	0.00	0.00	0.00	0.00
Max PP	95/10/ 8	17	11.69	0.68	0.02	0.01	0.00	0.00	0.00	0.01

Max bext	95/10/ 9	12	12.17	0.85	0.02	0.01	0.01	0.01	0.00	0.01
Max PP	95/10/ 9	14	11.93	0.77	0.03	0.01	0.01	0.01	0.00	0.01
Max bext	95/10/10	17	11.68	0.67	0.01	0.00	0.01	0.00	0.00	0.00
Max PP	95/10/10	17	11.68	0.67	0.01	0.00	0.01	0.00	0.00	0.00
Max bext	95/10/11	11	11.45	0.59	0.01	0.00	0.00	0.00	0.00	0.00
Max PP	95/10/11	9	11.27	0.52	0.02	0.01	0.00	0.00	0.00	0.01
Max bext	95/10/12	17	11.81	0.72	0.00	0.00	0.00	0.00	0.00	0.00
Max PP	95/10/12	9	10.72	0.30	0.07	0.03	0.02	0.02	0.00	0.03
Max bext	95/10/13	10	11.52	0.61	0.03	0.01	0.00	0.00	0.02	0.01
Max PP	95/10/13	13	11.21	0.50	0.05	0.02	0.00	0.00	0.02	0.03
Max bext	95/10/14	17	11.45	0.59	0.03	0.01	0.01	0.00	0.01	0.01
Max PP	95/10/14	17	11.45	0.59	0.03	0.01	0.01	0.00	0.01	0.01
Max bext	95/10/15	17	11.58	0.64	0.02	0.01	0.00	0.00	0.01	0.01
Max PP	95/10/15	13	11.27	0.52	0.02	0.01	0.00	0.00	0.01	0.01
Max bext	95/10/16	6	11.68	0.67	0.01	0.00	0.00	0.00	0.01	0.00
Max PP	95/10/16	15	11.52	0.61	0.02	0.01	0.00	0.00	0.01	0.01
Max bext	95/10/17	6	12.37	0.92	0.00	0.00	0.00	0.00	0.00	0.00
Max PP	95/10/17	17	12.13	0.84	0.01	0.00	0.00	0.00	0.00	0.00
Max bext	95/10/18	6	11.96	0.78	0.02	0.01	0.00	0.00	0.01	0.00
Max PP	95/10/18	6	11.96	0.78	0.02	0.01	0.00	0.00	0.01	0.00
Max bext	95/10/19	17	11.94	0.77	0.00	0.00	0.00	0.00	0.00	0.00
Max PP	95/10/19	17	11.94	0.77	0.00	0.00	0.00	0.00	0.00	0.00

View 10: Mt Zirkel - Meaden Pk

	Date	Hour	Total Path Mm^{-1}	dv	PP Contrib Mm^{-1}	dv	Craig1 Mm^{-1}	Craig2 Mm^{-1}	Hyden1 Mm^{-1}	Hyden2 Mm^{-1}
Max bext	95/10/ 7	6	11.45	0.59	0.01	0.00	0.00	0.00	0.01	0.00
Max PP	95/10/ 7	14	11.29	0.53	0.10	0.04	0.03	0.03	0.00	0.03
Max bext	95/10/ 8	6	13.42	1.28	0.01	0.00	0.00	0.00	0.00	0.00
Max PP	95/10/ 8	17	11.61	0.65	0.04	0.01	0.01	0.00	0.00	0.03
Max bext	95/10/ 9	11	12.72	1.04	0.02	0.01	0.01	0.01	0.00	0.01
Max PP	95/10/ 9	15	11.87	0.74	0.05	0.02	0.02	0.02	0.00	0.02
Max bext	95/10/10	6	12.00	0.79	0.01	0.00	0.00	0.00	0.00	0.00
Max PP	95/10/10	17	11.84	0.73	0.03	0.01	0.02	0.00	0.00	0.01
Max bext	95/10/11	6	11.89	0.75	0.02	0.01	0.01	0.00	0.00	0.01
Max PP	95/10/11	15	11.27	0.52	0.05	0.02	0.00	0.00	0.00	0.04
Max bext	95/10/12	17	12.11	0.83	0.00	0.00	0.00	0.00	0.00	0.00
Max PP	95/10/12	13	10.91	0.38	0.14	0.06	0.07	0.06	0.00	0.00
Max bext	95/10/13	10	11.63	0.66	0.10	0.04	0.00	0.00	0.06	0.03
Max PP	95/10/13	13	11.29	0.53	0.14	0.05	0.00	0.00	0.05	0.08

Max bext	95/10/14	17	11.56	0.63	0.06	0.02	0.01	0.01	0.02	0.03
Max PP	95/10/14	17	11.56	0.63	0.06	0.02	0.01	0.01	0.02	0.03
Max bext	95/10/15	17	11.80	0.72	0.03	0.01	0.01	0.01	0.01	0.01
Max PP	95/10/15	6	11.73	0.69	0.05	0.02	0.00	0.01	0.02	0.02
Max bext	95/10/16	6	12.12	0.84	0.01	0.00	0.00	0.00	0.01	0.00
Max PP	95/10/16	15	11.97	0.78	0.02	0.01	0.00	0.00	0.01	0.01
Max bext	95/10/17	17	13.19	1.20	0.02	0.01	0.00	0.00	0.01	0.00
Max PP	95/10/17	14	13.09	1.17	0.03	0.01	0.00	0.00	0.01	0.01
Max bext	95/10/18	6	12.80	1.07	0.02	0.01	0.00	0.00	0.01	0.00
Max PP	95/10/18	6	12.80	1.07	0.02	0.01	0.00	0.00	0.01	0.00
Max bext	95/10/19	9	12.07	0.82	0.00	0.00	0.00	0.00	0.00	0.00
Max PP	95/10/19	17	11.96	0.78	0.00	0.00	0.00	0.00	0.00	0.00

Table 6.7.12
Hourly Average Estimated Extinction (Mm^{-1}) and Deciview (dv) along 10 Sight Paths for the August 21-27, 1995 Episode

Indicated for each day is (1) the daylight hour with the maximum total extinction along a particular sight path ("Max bext"), and (2) the daylight hour in which the model estimated the maximum contribution to extinction along the path segments within the MZWA due to the combined emissions from Hayden Units 1&2 and Craig Units 1&2 ("Max PP"). Given for each of these two types of entries is the total integrated extinction (with the nominal value for Rayleigh scattering of 10 Mm^{-1}), the total Hayden and Craig Units 1&2 contribution to sight-path extinction, and a breakdown of each unit's extinction contribution (Mm^{-1} only).

View 1: Davis Pk - Mt Zirkel

			Total Path		PP Contrib		Craig1	Craig2	Hyden1	Hyden2
	Date	Hour	Mm^{-1}	dv	Mm^{-1}	dv	Mm^{-1}	Mm^{-1}	Mm^{-1}	Mm^{-1}
Max bext	95/ 8/21	6	15.67	1.95	1.16	0.33	0.02	0.02	1.00	0.12
Max PP	95/ 8/21	6	15.67	1.95	1.16	0.33	0.02	0.02	1.00	0.12
Max bext	95/ 8/22	6	11.81	0.72	0.09	0.03	0.00	0.00	0.07	0.02
Max PP	95/ 8/22	6	11.81	0.72	0.09	0.03	0.00	0.00	0.07	0.02
Max bext	95/ 8/23	6	12.01	0.80	0.05	0.02	0.00	0.00	0.05	0.00
Max PP	95/ 8/23	16	11.11	0.46	0.63	0.25	0.03	0.04	0.31	0.25
Max bext	95/ 8/24	6	12.95	1.12	0.92	0.32	0.12	0.19	0.44	0.16

Max PP	95/ 8/24	6	12.95	1.12	0.92	0.32	0.12	0.19	0.44	0.16
Max bext	95/ 8/25	6	14.58	1.64	0.69	0.21	0.15	0.21	0.17	0.15
Max PP	95/ 8/25	6	14.58	1.64	0.69	0.21	0.15	0.21	0.17	0.15
Max bext	95/ 8/26	6	15.05	1.78	2.13	0.66	0.29	0.41	0.84	0.59
Max PP	95/ 8/26	6	15.05	1.78	2.13	0.66	0.29	0.41	0.84	0.59
Max bext	95/ 8/27	6	15.90	2.01	0.97	0.27	0.15	0.15	0.36	0.32
Max PP	95/ 8/27	17	14.70	1.67	2.02	0.64	0.14	0.15	0.89	0.83

View 2: Davis Pk - Little Agnes Pk

	Date	Hour	Total Path Mm^{-1}	Total Path dv	PP Contrib Mm^{-1}	PP Contrib dv	Craig1 Mm^{-1}	Craig2 Mm^{-1}	Hyden1 Mm^{-1}	Hyden2 Mm^{-1}
Max bext	95/ 8/21	6	15.24	1.83	1.11	0.33	0.02	0.02	0.97	0.11
Max PP	95/ 8/21	6	15.24	1.83	1.11	0.33	0.02	0.02	0.97	0.11
Max bext	95/ 8/22	6	11.69	0.68	0.09	0.03	0.00	0.00	0.07	0.02
Max PP	95/ 8/22	6	11.69	0.68	0.09	0.03	0.00	0.00	0.07	0.02
Max bext	95/ 8/23	6	11.85	0.74	0.05	0.02	0.00	0.00	0.05	0.00
Max PP	95/ 8/23	16	11.12	0.46	0.65	0.26	0.04	0.04	0.33	0.25
Max bext	95/ 8/24	6	12.83	1.08	0.96	0.34	0.12	0.20	0.48	0.16
Max PP	95/ 8/24	6	12.83	1.08	0.96	0.34	0.12	0.20	0.48	0.16
Max bext	95/ 8/25	6	14.37	1.57	0.75	0.23	0.16	0.24	0.19	0.16
Max PP	95/ 8/25	6	14.37	1.57	0.75	0.23	0.16	0.24	0.19	0.16
Max bext	95/ 8/26	6	15.00	1.76	2.20	0.69	0.31	0.43	0.84	0.62
Max PP	95/ 8/26	6	15.00	1.76	2.20	0.69	0.31	0.43	0.84	0.62
Max bext	95/ 8/27	6	15.69	1.96	1.02	0.29	0.16	0.15	0.37	0.33
Max PP	95/ 8/27	17	14.83	1.71	2.19	0.69	0.15	0.16	1.01	0.88

View 3: Mt Zirkel - The Dome

	Date	Hour	Total Path Mm^{-1}	Total Path dv	PP Contrib Mm^{-1}	PP Contrib dv	Craig1 Mm^{-1}	Craig2 Mm^{-1}	Hyden1 Mm^{-1}	Hyden2 Mm^{-1}
Max bext	95/ 8/21	6	13.77	1.39	0.91	0.30	0.02	0.02	0.78	0.09
Max PP	95/ 8/21	6	13.77	1.39	0.91	0.30	0.02	0.02	0.78	0.09
Max bext	95/ 8/22	6	11.24	0.51	0.04	0.02	0.00	0.00	0.03	0.01
Max PP	95/ 8/22	17	10.71	0.30	0.07	0.03	0.00	0.00	0.02	0.05
Max bext	95/ 8/23	6	11.33	0.54	0.02	0.01	0.00	0.00	0.02	0.00
Max PP	95/ 8/23	13	11.19	0.49	0.63	0.25	0.00	0.00	0.27	0.36
Max bext	95/ 8/24	6	11.98	0.78	0.70	0.26	0.10	0.15	0.36	0.10
Max PP	95/ 8/24	6	11.98	0.78	0.70	0.26	0.10	0.15	0.36	0.10
Max bext	95/ 8/25	6	13.98	1.46	1.17	0.38	0.24	0.39	0.25	0.29
Max PP	95/ 8/25	6	13.98	1.46	1.17	0.38	0.24	0.39	0.25	0.29
Max bext	95/ 8/26	6	14.76	1.69	2.42	0.78	0.37	0.51	0.89	0.66
Max PP	95/ 8/26	6	14.76	1.69	2.42	0.78	0.37	0.51	0.89	0.66
Max bext	95/ 8/27	6	15.39	1.87	1.10	0.32	0.18	0.16	0.40	0.37
Max PP	95/ 8/27	17	14.93	1.74	2.30	0.73	0.13	0.13	1.08	0.95

View 4: Mt Zirkel - Mt Ethel

	Date	Hour	Total Path Mm^{-1}	Total Path dv	PP Contrib Mm^{-1}	PP Contrib dv	Craig1 Mm^{-1}	Craig2 Mm^{-1}	Hyden1 Mm^{-1}	Hyden2 Mm^{-1}
Max bext	95/ 8/21	6	15.94	2.02	1.15	0.33	0.02	0.03	0.99	0.11
Max PP	95/ 8/21	17	12.04	0.81	1.17	0.44	0.10	0.03	0.61	0.42
Max bext	95/ 8/22	6	12.35	0.92	0.07	0.02	0.00	0.00	0.05	0.01
Max PP	95/ 8/22	17	10.83	0.35	0.08	0.03	0.00	0.00	0.02	0.06
Max bext	95/ 8/23	13	12.09	0.82	1.18	0.45	0.00	0.00	0.54	0.63
Max PP	95/ 8/23	13	12.09	0.82	1.18	0.45	0.00	0.00	0.54	0.63
Max bext	95/ 8/24	6	13.03	1.15	0.65	0.22	0.09	0.14	0.33	0.10
Max PP	95/ 8/24	6	13.03	1.15	0.65	0.22	0.09	0.14	0.33	0.10
Max bext	95/ 8/25	6	13.71	1.37	0.98	0.32	0.20	0.32	0.22	0.25
Max PP	95/ 8/25	6	13.71	1.37	0.98	0.32	0.20	0.32	0.22	0.25
Max bext	95/ 8/26	6	14.69	1.67	2.26	0.73	0.34	0.47	0.86	0.61
Max PP	95/ 8/26	6	14.69	1.67	2.26	0.73	0.34	0.47	0.86	0.61
Max bext	95/ 8/27	6	15.62	1.94	1.01	0.29	0.16	0.15	0.37	0.33
Max PP	95/ 8/27	17	15.06	1.78	2.27	0.71	0.14	0.14	1.05	0.94

View 5: Mt Ethel - Continental Divide Trail

	Date	Hour	Total Path Mm^{-1}	Total Path dv	PP Contrib Mm^{-1}	PP Contrib dv	Craig1 Mm^{-1}	Craig2 Mm^{-1}	Hyden1 Mm^{-1}	Hyden2 Mm^{-1}
Max bext	95/ 8/21	6	21.95	3.41	1.48	0.30	0.03	0.05	1.28	0.12

Max PP	95/ 8/21	17	12.90	1.11	1.71	0.62	0.12	0.04	0.94	0.60
Max bext	95/ 8/22	6	15.83	1.99	0.09	0.02	0.00	0.01	0.07	0.01
Max PP	95/ 8/22	17	11.24	0.51	0.13	0.05	0.00	0.00	0.02	0.10
Max bext	95/ 8/23	13	14.16	1.51	2.13	0.71	0.00	0.00	1.15	0.98
Max PP	95/ 8/23	13	14.16	1.51	2.13	0.71	0.00	0.00	1.15	0.98
Max bext	95/ 8/24	7	16.50	2.17	0.21	0.06	0.00	0.03	0.12	0.06
Max PP	95/ 8/24	17	12.06	0.81	1.15	0.44	0.04	0.06	0.59	0.46
Max bext	95/ 8/25	7	12.82	1.08	0.20	0.07	0.03	0.06	0.06	0.05
Max PP	95/ 8/25	6	12.57	0.99	0.33	0.12	0.06	0.09	0.10	0.08
Max bext	95/ 8/26	6	13.74	1.38	1.28	0.42	0.15	0.21	0.61	0.31
Max PP	95/ 8/26	6	13.74	1.38	1.28	0.42	0.15	0.21	0.61	0.31
Max bext	95/ 8/27	7	15.71	1.96	0.46	0.13	0.06	0.06	0.19	0.14
Max PP	95/ 8/27	17	15.12	1.80	1.95	0.60	0.15	0.15	0.92	0.73

View 6: Davis Pk - Southern Ridge

	Date	Hour	Total Path Mm^{-1}	Total Path dv	PP Contrib Mm^{-1}	PP Contrib dv	Craig1 Mm^{-1}	Craig2 Mm^{-1}	Hyden1 Mm^{-1}	Hyden2 Mm^{-1}
Max bext	95/ 8/21	6	14.69	1.67	0.87	0.27	0.01	0.02	0.76	0.08
Max PP	95/ 8/21	6	14.69	1.67	0.87	0.27	0.01	0.02	0.76	0.08
Max bext	95/ 8/22	6	11.89	0.75	0.06	0.02	0.00	0.00	0.04	0.01
Max PP	95/ 8/22	16	10.75	0.31	0.09	0.04	0.00	0.00	0.02	0.07
Max bext	95/ 8/23	13	12.03	0.80	1.31	0.50	0.00	0.00	0.77	0.53
Max PP	95/ 8/23	13	12.03	0.80	1.31	0.50	0.00	0.00	0.77	0.53
Max bext	95/ 8/24	6	12.41	0.94	0.56	0.20	0.07	0.11	0.30	0.09
Max PP	95/ 8/24	6	12.41	0.94	0.56	0.20	0.07	0.11	0.30	0.09
Max bext	95/ 8/25	6	14.33	1.56	0.82	0.26	0.15	0.27	0.22	0.19
Max PP	95/ 8/25	6	14.33	1.56	0.82	0.26	0.15	0.27	0.22	0.19
Max bext	95/ 8/26	6	14.71	1.68	2.06	0.66	0.29	0.40	0.82	0.56
Max PP	95/ 8/26	6	14.71	1.68	2.06	0.66	0.29	0.40	0.82	0.56
Max bext	95/ 8/27	6	15.58	1.93	0.97	0.28	0.15	0.14	0.36	0.31
Max PP	95/ 8/27	17	14.98	1.76	2.46	0.78	0.14	0.15	1.24	0.93

View 7: Mt Zirkel - Medicine Bow Pk

	Date	Hour	Total Path Mm^{-1}	Total Path dv	PP Contrib Mm^{-1}	PP Contrib dv	Craig1 Mm^{-1}	Craig2 Mm^{-1}	Hyden1 Mm^{-1}	Hyden2 Mm^{-1}
Max bext	95/ 8/21	6	11.95	0.77	0.14	0.05	0.00	0.00	0.12	0.02
Max PP	95/ 8/21	6	11.95	0.77	0.14	0.05	0.00	0.00	0.12	0.02
Max bext	95/ 8/22	6	10.90	0.37	0.01	0.00	0.00	0.00	0.01	0.00
Max PP	95/ 8/22	16	10.70	0.29	0.01	0.00	0.00	0.00	0.00	0.00
Max bext	95/ 8/23	15	10.96	0.40	0.06	0.02	0.00	0.00	0.02	0.03
Max PP	95/ 8/23	16	10.81	0.34	0.06	0.02	0.00	0.00	0.03	0.02
Max bext	95/ 8/24	6	12.13	0.84	0.13	0.05	0.02	0.03	0.06	0.02
Max PP	95/ 8/24	6	12.13	0.84	0.13	0.05	0.02	0.03	0.06	0.02

	Date	Hour	Total Path Mm^{-1}	Total Path dv	PP Contrib Mm^{-1}	PP Contrib dv	Craig1 Mm^{-1}	Craig2 Mm^{-1}	Hyden1 Mm^{-1}	Hyden2 Mm^{-1}
Max bext	95/ 8/25	6	11.99	0.79	0.11	0.04	0.02	0.03	0.02	0.02
Max PP	95/ 8/25	6	11.99	0.79	0.11	0.04	0.02	0.03	0.02	0.02
Max bext	95/ 8/26	6	14.02	1.47	0.30	0.09	0.04	0.06	0.11	0.08
Max PP	95/ 8/26	6	14.02	1.47	0.30	0.09	0.04	0.06	0.11	0.08
Max bext	95/ 8/27	6	16.22	2.10	0.13	0.03	0.02	0.02	0.05	0.04
Max PP	95/ 8/27	17	13.36	1.26	0.27	0.09	0.02	0.02	0.12	0.11

View 8: Mt Zirkel - Longs Pk

	Date	Hour	Total Path Mm^{-1}	Total Path dv	PP Contrib Mm^{-1}	PP Contrib dv	Craig1 Mm^{-1}	Craig2 Mm^{-1}	Hyden1 Mm^{-1}	Hyden2 Mm^{-1}
Max bext	95/ 8/21	17	11.25	0.51	0.04	0.02	0.00	0.00	0.02	0.02
Max PP	95/ 8/21	6	10.88	0.37	0.07	0.03	0.00	0.00	0.06	0.01
Max bext	95/ 8/22	17	11.12	0.46	0.00	0.00	0.00	0.00	0.00	0.00
Max PP	95/ 8/22	7	10.31	0.13	0.01	0.00	0.00	0.00	0.00	0.00
Max bext	95/ 8/23	13	10.89	0.37	0.02	0.01	0.00	0.00	0.00	0.01
Max PP	95/ 8/23	16	10.60	0.25	0.03	0.01	0.00	0.00	0.01	0.01
Max bext	95/ 8/24	17	13.53	1.31	0.01	0.00	0.00	0.00	0.01	0.01
Max PP	95/ 8/24	6	10.35	0.15	0.07	0.03	0.01	0.01	0.03	0.01
Max bext	95/ 8/25	6	12.77	1.06	0.05	0.02	0.01	0.02	0.01	0.01
Max PP	95/ 8/25	6	12.77	1.06	0.05	0.02	0.01	0.02	0.01	0.01
Max bext	95/ 8/26	6	11.80	0.72	0.15	0.06	0.02	0.03	0.06	0.04
Max PP	95/ 8/26	6	11.80	0.72	0.15	0.06	0.02	0.03	0.06	0.04
Max bext	95/ 8/27	6	13.43	1.28	0.06	0.02	0.01	0.01	0.02	0.02
Max PP	95/ 8/27	17	13.24	1.22	0.14	0.05	0.01	0.01	0.06	0.06

View 9: Davis Pk - Flat Tops

	Date	Hour	Total Path Mm^{-1}	Total Path dv	PP Contrib Mm^{-1}	PP Contrib dv	Craig1 Mm^{-1}	Craig2 Mm^{-1}	Hyden1 Mm^{-1}	Hyden2 Mm^{-1}
Max bext	95/ 8/21	6	11.35	0.55	0.14	0.05	0.00	0.00	0.11	0.01
Max PP	95/ 8/21	6	11.35	0.55	0.14	0.05	0.00	0.00	0.11	0.01
Max bext	95/ 8/22	17	10.64	0.27	0.01	0.00	0.00	0.00	0.00	0.00
Max PP	95/ 8/22	17	10.64	0.27	0.01	0.00	0.00	0.00	0.00	0.00
Max bext	95/ 8/23	13	11.83	0.73	0.01	0.00	0.00	0.00	0.00	0.01
Max PP	95/ 8/23	16	10.52	0.22	0.09	0.04	0.01	0.01	0.05	0.03
Max bext	95/ 8/24	15	11.49	0.60	0.03	0.01	0.00	0.00	0.01	0.01
Max PP	95/ 8/24	6	10.71	0.30	0.10	0.04	0.01	0.02	0.04	0.02
Max bext	95/ 8/25	6	12.12	0.84	0.06	0.02	0.01	0.02	0.02	0.01
Max PP	95/ 8/25	6	12.12	0.84	0.06	0.02	0.01	0.02	0.02	0.01
Max bext	95/ 8/26	6	12.18	0.86	0.21	0.08	0.03	0.04	0.09	0.06
Max PP	95/ 8/26	6	12.18	0.86	0.21	0.08	0.03	0.04	0.09	0.06
Max bext	95/ 8/27	17	13.17	1.20	0.22	0.07	0.02	0.02	0.09	0.09
Max PP	95/ 8/27	17	13.17	1.20	0.22	0.07	0.02	0.02	0.09	0.09

View 10: Mt Zirkel - Meaden Pk

	Date	Hour	Total Path Mm^{-1}	Total Path dv	PP Contrib Mm^{-1}	PP Contrib dv	Craig1 Mm^{-1}	Craig2 Mm^{-1}	Hyden1 Mm^{-1}	Hyden2 Mm^{-1}
Max bext	95/ 8/21	6	12.02	0.80	0.22	0.08	0.00	0.00	0.18	0.02
Max PP	95/ 8/21	6	12.02	0.80	0.22	0.08	0.00	0.00	0.18	0.02
Max bext	95/ 8/22	9	10.85	0.35	0.00	0.00	0.00	0.00	0.00	0.00
Max PP	95/ 8/22	17	10.76	0.32	0.01	0.00	0.00	0.00	0.00	0.01
Max bext	95/ 8/23	14	11.48	0.60	0.07	0.03	0.00	0.00	0.02	0.05
Max PP	95/ 8/23	15	11.13	0.46	0.09	0.04	0.00	0.00	0.03	0.05
Max bext	95/ 8/24	13	11.09	0.45	0.05	0.02	0.00	0.00	0.03	0.01
Max PP	95/ 8/24	6	11.09	0.45	0.19	0.08	0.03	0.04	0.09	0.03
Max bext	95/ 8/25	6	12.95	1.12	0.16	0.05	0.03	0.05	0.04	0.04
Max PP	95/ 8/25	6	12.95	1.12	0.16	0.05	0.03	0.05	0.04	0.04
Max bext	95/ 8/26	6	13.43	1.28	0.45	0.15	0.06	0.09	0.17	0.12
Max PP	95/ 8/26	6	13.43	1.28	0.45	0.15	0.06	0.09	0.17	0.12
Max bext	95/ 8/27	17	15.15	1.80	0.40	0.12	0.03	0.03	0.18	0.17
Max PP	95/ 8/27	17	15.15	1.80	0.40	0.12	0.03	0.03	0.18	0.17

the sight path segments within the Wilderness. If both ends of the sight path were within the Wilderness boundaries, the whole path was assumed to be in the Wilderness.

It is current custom to perform optical measurements of the effects of air quality on visibility using only light with a wavelength range in the green part of the spectrum. Also, theoretical calculations are typically performed only for this wavelength. The main reason for this is that the eye is most sensitive to green light, and much less sensitive to red or blue light. In practice, making measurements and performing calculations only at green wavelengths has produced results in reasonable agreement with visibility observations. In accordance with current practice, the analyses in this section consider only green light. The integrating nephelometer measurements were made at a wavelength of 550 nm, so that wavelength is used in these analyses.

6.8.1 Conclusions about Perceived Haze

The following results were obtained from calculations of apparent contrasts, contrast transmittances, and dv values based on the light extinction calculated by the CALMET/ CALPUFF model (see Section 6.7):

The largest changes in the apparent contrasts of ridges against the horizon sky caused by omitting the effects of various combinations of emissions were as follows: 0.066 due to omitting the Hayden station and the Yampa Project, 0.039 due to the Hayden station, and 0.027 due to the Yampa Project.

The largest changes in contrast transmittances for features on the surfaces of the targets caused by omitting the effects of various combinations of emissions were as follows: 0.092 due to omitting the Hayden station and the Yampa Project, 0.068 due to the Hayden station, and 0.032 due to the Yampa Project.

These calculated contrast changes are large enough to be perceived if they were displayed in a split-screen image, but it is not known if they are large enough to be perceived by an observer in the MZWA comparing observations made at different times.

The maximum values of the calculated changes in contrasts and contrast transmittances due to changes in generating station emissions were very nearly the same for clear skies and completely overcast skies.

There were large differences in the calculated apparent contrasts and contrast transmittances for different sight paths in the MZWA and for different times of day. These differences were primarily caused by differences in the amount of light reflected from the target, which depends on its reflectance and orientation to the sun.

For most sight paths on clear days, diurnal changes in illumination caused changes in apparent contrasts and contrast transmittances that were far greater than any changes due to changes in the generating station emissions.

Values of the deciview haze index changed by as much as 3.2 units when the effects of the emissions of both the Hayden station and the Yampa Project were omitted. When only the effects of the Hayden station emissions were omitted , the largest change in dv was 2.4 units, and the largest change from omitting the effects Yampa Project emissions was approximately 1.1 units. A 1 unit change in dv corresponds to a 10% change in b_{ext}.

The time-lapse videos were reviewed for the times the integrating nephelometers at Buffalo Pass indicated that haze pulses were associated with SO_2 pulses. Most observers of these videos could see haze pulses in the views from Storm Peak on the afternoons of 08/23/95 and 09/18/95 that corresponded in time to the haze pulses observed by the nephelometers at Buffalo Pass. On 08/23/95, the haze pulses could also be seen in the time-lapse views from Chavez Peak.

The time lapse videos show only one case of a layered haze or well-defined plume attributed to either the Hayden station or the Yampa Project that approached the location of the MZWA. This event occurred on 01/03/95 and was caused by greater-than-normal emissions of primary particles (fly ash). All haze events associated with the formation of secondary particles (sulfate and associated water) that could be detected in the time-lapse videos showed a haze that was mixed to the ground and did not have apparent edges or top. Therefore, it is more appropriate to describe the haze pulses identified in Section 6.6 as uniform haze rather than layered haze.

6.8.2 Contrast Calculations

The ability of humans to perceive objects depends on the contrast of the objects against their background. If an object has no contrast, i.e., has the same color and brightness as the surrounding background, it is imperceptible. An object can be visually detected if either the luminance contrast or color contrast exceeds the perception threshold. In natural settings, such as in the Mt.Zirkel Wilderness, it is rare that a natural feature can be perceived only because of its color contrast. Typically, the perceptibility of an object is determined by its luminance contrast.

The luminance of an object is a measure of its apparent brightness to a human observer, and its theoretical calculation requires information about the intensity of light at all wavelengths. Restricting the analyses to green light allows the use of radiance, which is a measure of the amount of energy transmitted by the light. The analyses in this report calculate radiance contrast, C, for green light. If an object (target) of radiance, I, is viewed against a background of radiance, I_b, the radiance contrast is

$$C = (I - I_b) / I_b \qquad (6.8.1)$$

If an object is brighter than its background, its contrast is positive, and if it is darker, its contrast is negative. The apparent contrast is the contrast determined at the location of the observer.

Calculations were also done to determine the contrast transmittance for features on the surface of the target. This is the fraction of the contrast measured at the target that is transmitted through the atmosphere to the observer. This contrast transmittance determines whether or not features on the surface of the target can be perceived by the observer. If the contrast transmittance is very low, the target appears as a silhouette with no surface features. If the

contrast transmittance is very high, then the rocks, gullies, patches of trees, etc. on the target are clearly visible.

It is a property of human vision that the threshold contrast for the perception of an object is relatively constant over a wide range of illumination and viewing conditions. For vision through the atmosphere, a threshold contrast of 2% is most often used. It is customarily assumed an object is perceptible if it is 2% lighter or darker than its surrounding background. This threshold is often used to determine whether a ridge can be perceived against the horizon sky, or whether one ridge can be perceived against the backdrop of another ridge. In actual fact, the threshold contrast depends on the viewing conditions (e.g., the angle subtended by the object being viewed), and can vary from less than 1% to more than 20%. In the Mt. Zirkel Wilderness Area, a threshold contrast of 2% is appropriate for estimating whether or not a ridge can be seen against its background.

Hourly values of the apparent contrast of a target (i.e., a ridge or mountain peak) against the horizon sky and the contrast transmittance for features on the face of the target were calculated from hourly values of the average light extinction reported in Section 6.7. The highest hourly b_{ext} values from these model calculations for each episode day are tabulated in Tables 6.7.9 through 6.7.12. These tables also show data for the hour each day with the highest modeled contribution of the four units of the Hayden station and Yampa Project to b_{ext}. Contrast calculations were performed with and without the contribution of these units to b_{ext} for all sight paths within the Wilderness and all hours in the 09/17/95–09/21/95 period and the 10/07/95–10/19/95 period using data from Tables 6.7.9 and 6.7.11, respectively. These two episodes were selected because they include both the greatest increments in b_{ext} attributed to all four units as well as the largest increments attributed to only the two units of the Yampa Project.

The methods and equations used for the contrast calculations are presented in Appendix B.7. The sight paths for which calculations were done are shown in Figure 6.8.1, the locations of the endpoints for these sight paths are listed in Table 6.8.1, and the lengths and headings of the sight paths appear in Table 6.8.2. The properties of the targets are listed in Table 6.8.3. Calculations were performed for both cloud-free and uniformly overcast skies. The major limitation of the calculation methods is that approximate equations were used to calculate the source function (also known as the equilibrium radiance) and the radiance of the horizon sky. Even with these limitations, the calculated results provide useful information about contrasts and contrast transmittances for sight paths in and near the Mt. Zirkel Wilderness.

Figure 6.8.1 Sight paths in the Mt. Zirkel Wilderness Area for which contrast calculations were performed.

Selected results from the contrast calculations for the 09/17/95–09/21/95 period are presented in Figures 6.8.2 through 6.8.7. The first figure of each pair shows results calculated for a clear sky and the second figure results for a uniformly overcast sky. The top panel in each figure shows the hourly values of b_{ext} calculated by the CALMET/CALPUFF model. The solid curve shows the results obtained for all sources and the dotted curve the results for all sources

except the four stacks of the Hayden station and the Yampa Project. The value of the light absorption coefficient b_{abs} was also included in the results and used in the calculations. Typically, b_{abs} accounted for 1% to 4% of the extinction.

Table 6.8.1
Location of Sight Path End Points

Site Name	Latitude (degree)	Longitude (degree)
Davis Peak	40.921	106.7
Mt. Zirkel	40.831	106.662
Little Agnes Peak	40.827	106.715
The Dome	40.686	106.705
Mt. Ethel	40.648	106.68
Continental Divide Trail	40.558	106.698
Southern Ridge	40.611	106.779
Intervening Ridge	40.921	106.700

Table 6.8.2
Sight Path Length and Azimuth

View	Observer From	To Target	Sight Path Length (km)	Sight Path Azimuth Angle (Observer to Target) (degrees)
1	Davis Peak	Mt. Zirkel	10.5	163.3
	Mt. Zirkel	Davis Peak	10.5	343.3
2	Davis Peak	Little Agnes Peak	10.5	188.0
	Little Agnes Peak	Davis Peak	10.5	8.0
3	Mt. Zirkel	The Dome	16.5	193.8
	The Dome	Mt. Zirkel	16.5	13.8
4	Mt. Zirkel	Mt. Ethel	20.4	185.4
	Mt. Ethel	Mt. Zirkel	20.4	5.4
5	Mt. Ethel	Continental Divide Trail	10.1	189.8
	Continental Divide Trail	Mt. Ethel (cliffs)	10.1	9.8
	Continental Divide Trail	Mt. Ethel (shoulder)	10.1	9.8
6	Davis Peak	Southern Ridge	35.1	192.1
	Southern Ridge	Davis Peak	35.1	12.1
7	Davis Peak	Intervening Ridge	29.3	192.3
	Intervening Ridge	Davis Peak	29.3	12.3

Table 6.8.3
Orientation and Reflectance of the Targets

View	Observer From	To Target	Zenith Angle of Normal to Target (degrees)	Azimuth Angle of Normal to Target (degrees)	Target Surface Reflectance
1	Davis Peak	Mt. Zirkel	50	280	0.25
	Mt. Zirkel	Davis Peak	30	180	0.45
2	Davis Peak	Little Agnes Peak	45	0	0.25
	Little Agnes Peak	Davis Peak	30	180	0.45
3	Mt. Zirkel	The Dome	60	20	0.25
	The Dome	Mt. Zirkel	45	170	0.25
4	Mt. Zirkel	Mt. Ethel	20	300	0.45
	Mt. Ethel	Mt. Zirkel	45	170	0.25
5	Mt. Ethel	Continental Divide Trail	20	0	0.25
	Continental Divide Trail	Mt. Ethel (cliffs)	80	160	0.50
	Continental Divide Trail	Mt. Ethel (shoulder)	20	200	0.45
6	Davis Peak	Southern Ridge	70	0	0.20
	Southern Ridge	Davis Peak	30	180	0.45
7	Davis Peak	Intervening Ridge	70	0	0.20
	Intervening Ridge	Davis Peak	30	180	0.45

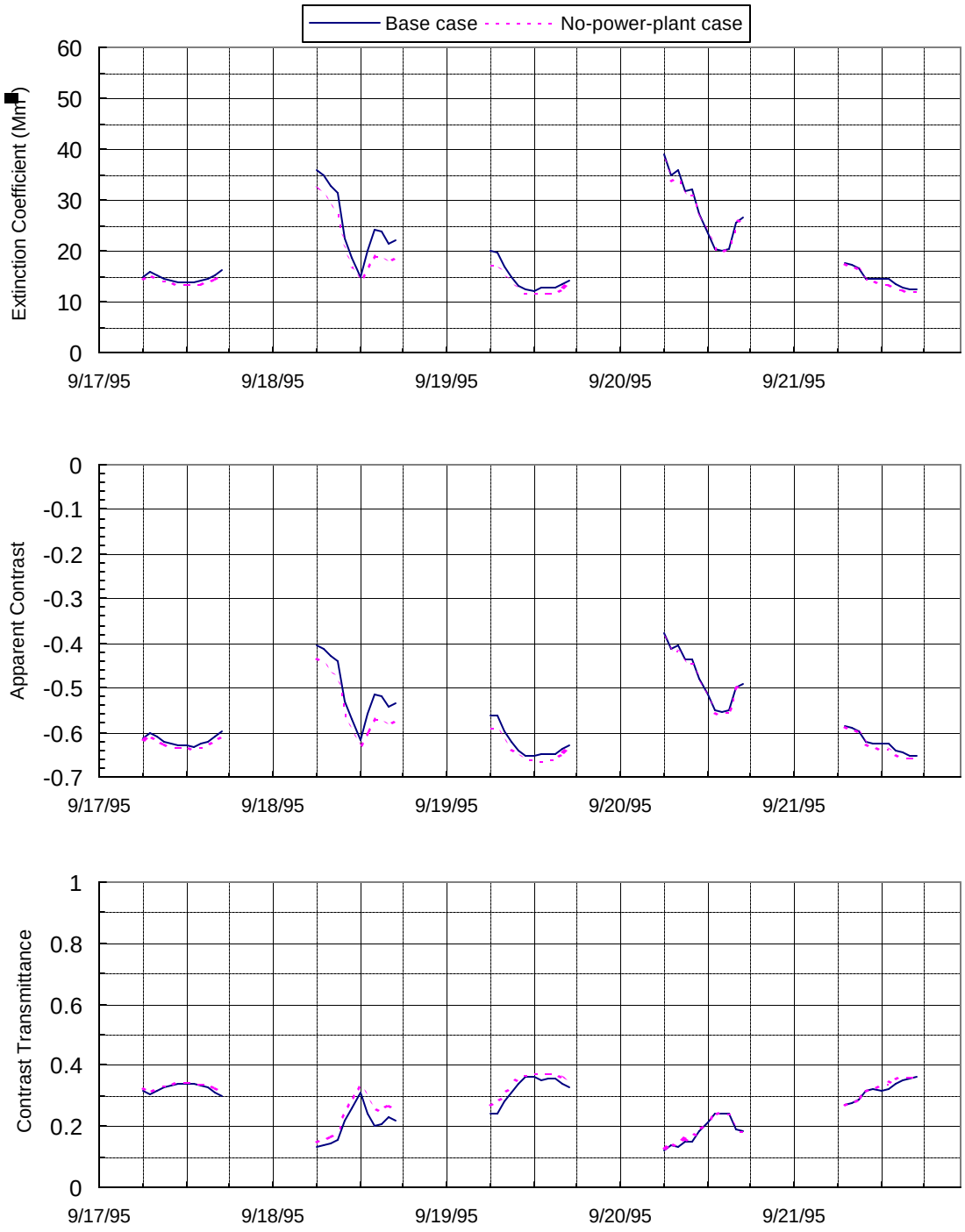

Figure 6.8.3 Contrasts and contrast transmittances for a uniformly overcast sky for View 4 from Mt. Ethel to Mt. Zirkel.

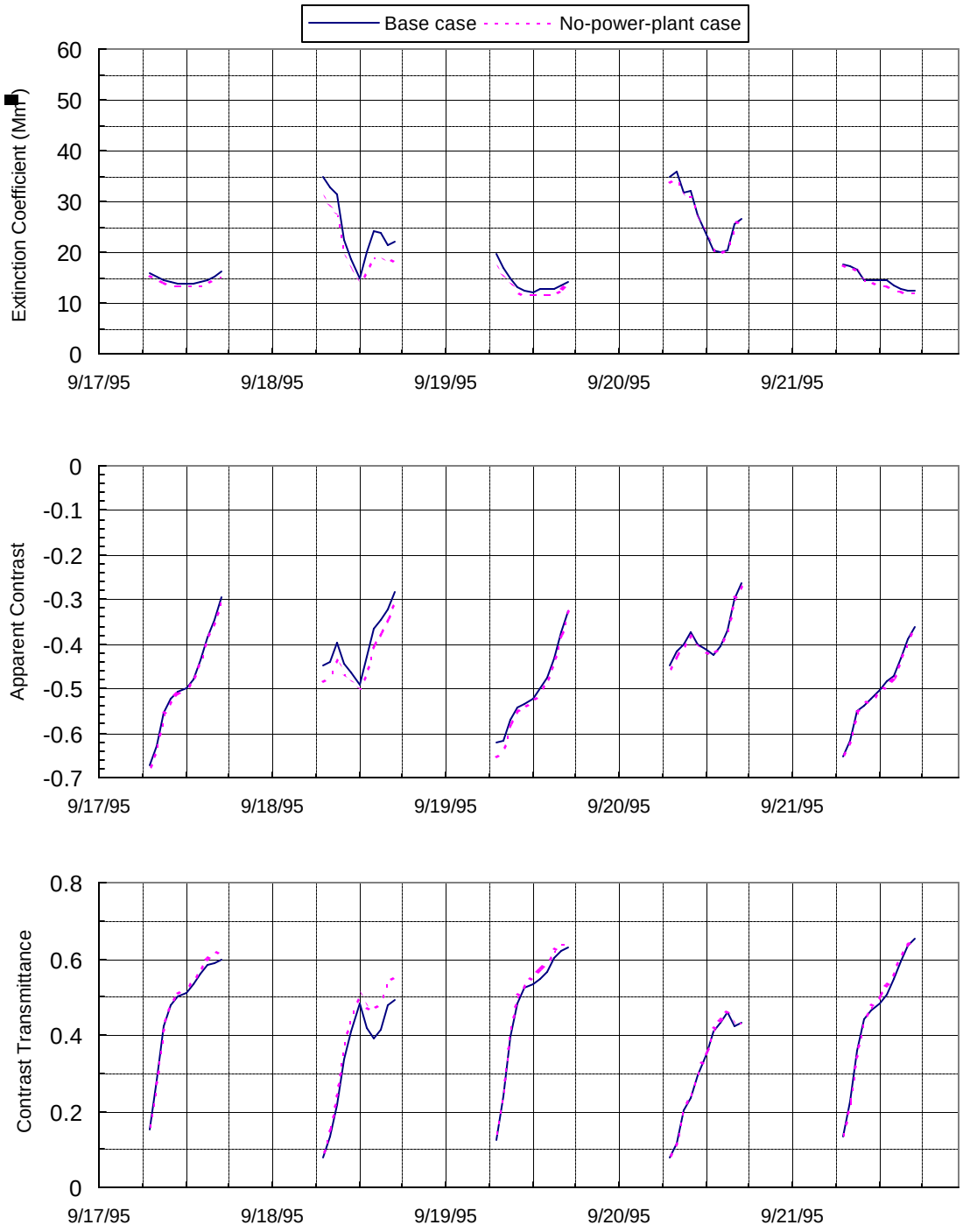

Figure 6.8.4 Contrasts and contrast transmittances for a clear sky for View 4 from Mt. Zirkel to Mt. Ethel.

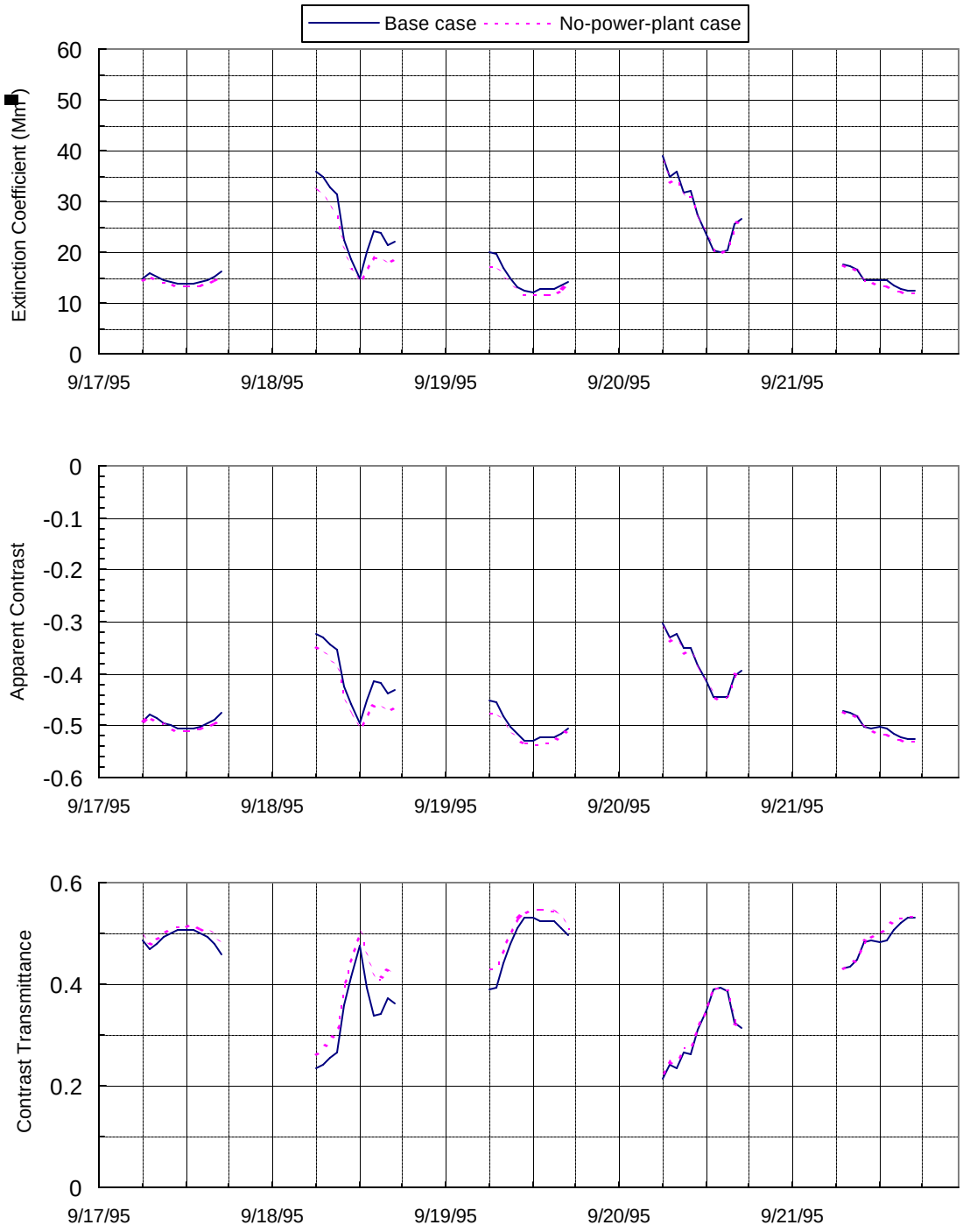

Figure 6.8.5 Contrasts and contrast transmittances for a uniformly overcast sky for View 4 from Mt. Zirkel to Mt. Ethel.

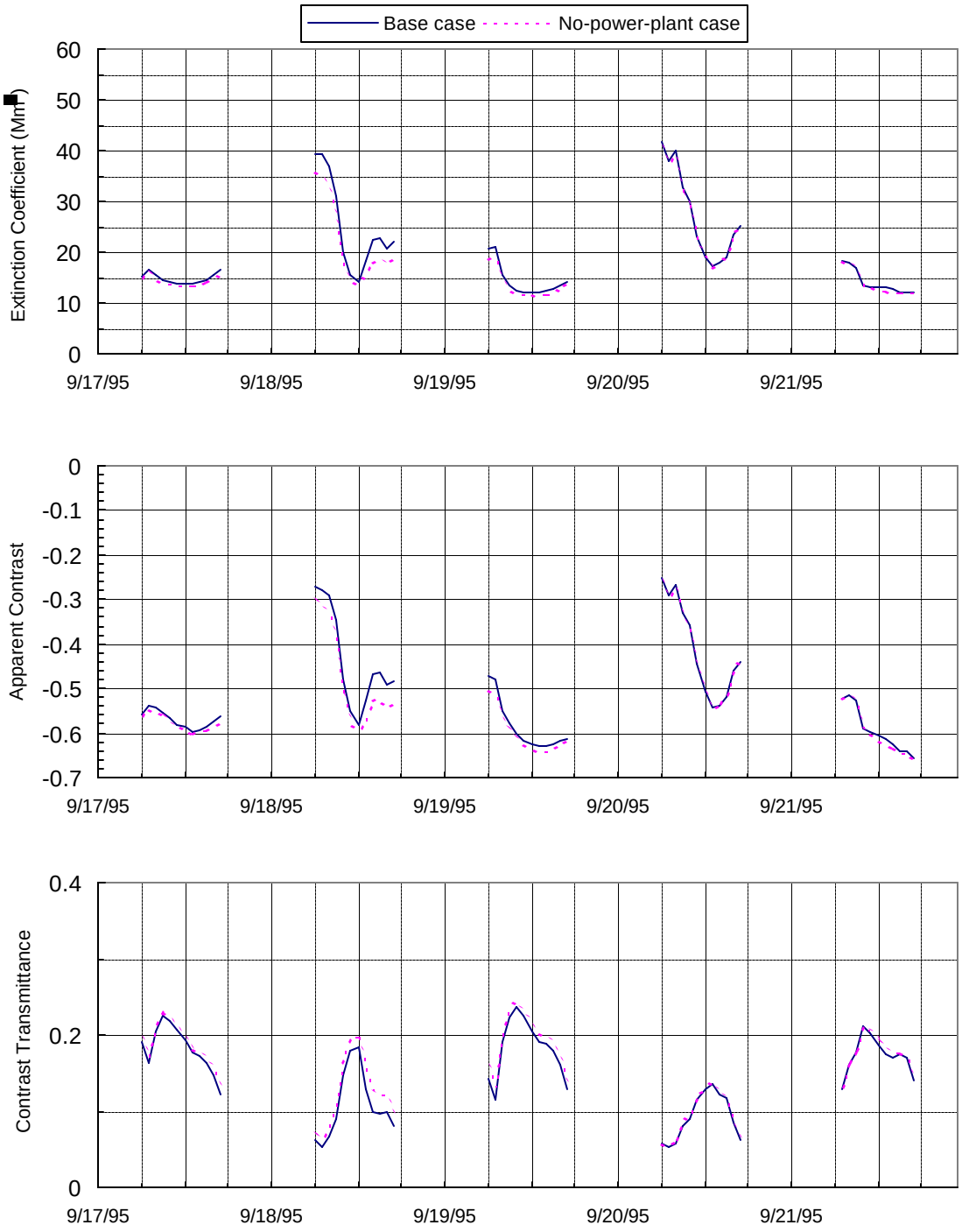

Figure 6.8.6 Contrasts and contrast transmittances for a clear sky for View 6 from Davis Peak to Intervening Ridge.

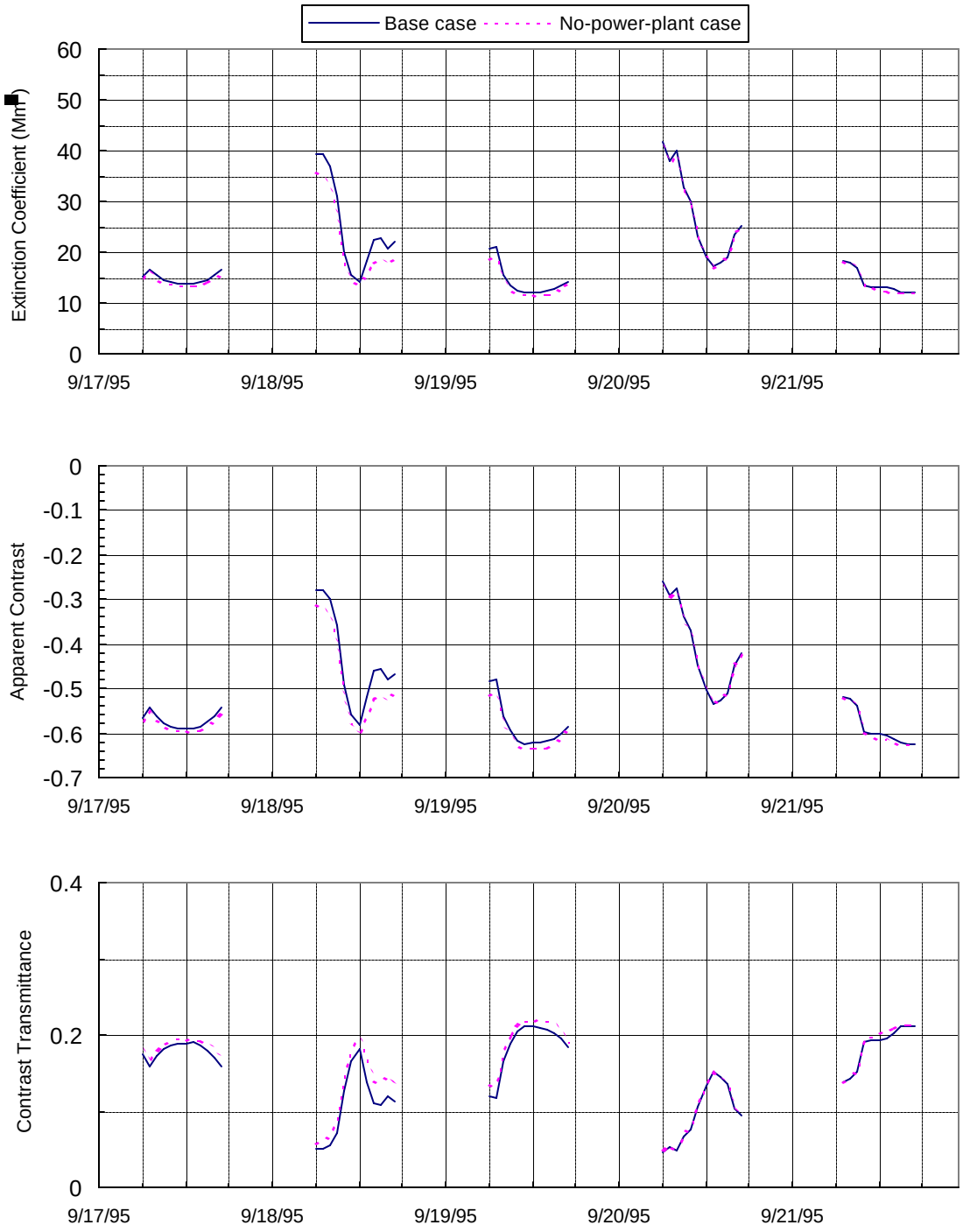

Figure 6.8.7 Contrasts and contrast transmittances for a uniformly overcast sky for View 6 from Davis Peak to Intervening Ridge.

The second panel shows the apparent contrast C of the target against the sky. This is the contrast defined in Equation 6.8.1 measured at the location of the observer. The third panel shows the contrast transmittance for features on the face of the target, such as rocks, gullies, patches of trees, etc. The contrast transmittance is the fraction of the contrast measured at the

target that is transmitted through the atmosphere to the observer. This contrast transmittance is controlled by the competition between the transmitted radiance and path radiance. When the target is bright (e.g., light-colored rocks in strong sunlight), the transmitted radiance is large and the contrast transmittance is good. When the target is dark (e.g., the shaded side of the mountain), the transmitted radiance is small and the contrast transmittance is much less good. A simplified discussion of these effects appears in Richards (1990).

Figures 6.8.2 and 6.8.3 show contrasts for a south-facing target. The clear-sky data in Figure 6.8.2 show that the target is most brightly illuminated during midday and is darker in the early morning and late afternoon. The contrast transmittance for features on the face of the target is largest when they are brightly illuminated. Changes in the apparent contrast and contrast transmittance due to changing illumination are much larger than those due to changes in b_{ext}. Figure 6.8.3 shows results for a uniformly overcast sky. Since the illumination is uniform throughout the day, variations in the apparent contrast and contrast transmittance are caused by variations in b_{ext}. The calculated contrast values do not depend on the darkness of the uniform cloud layer, because changes in the illumination affect the transmitted radiance and path radiance equally.

Figures 6.8.4 through 6.8.7 show contrasts for north-facing targets. In Figure 6.8.4 the target is oriented so it receives more sunlight in the afternoon than in the morning. For overcast skies, the apparent contrast is closer to zero and the contrast transmittance is greater for Mt. Ethel in Figure 6.8.5 than for Mt. Zirkel in Figure 6.8.3 because the rocks on Mt. Zirkel are darker and reflect less light.

Figures 6.8.6 and 6.8.7 are for the view from Davis Peak to the Intervening Ridge. This is a ridge that blocks the view of nearly all of the Southern Ridge from Davis Peak. The Intervening Ridge is a dark, north-facing distant target, and thus is suitable for use in contrast teleradiometry. In these calculations, which assume ideal viewing conditions, the calculated contrasts track the value of b_{ext} very well. Plots were prepared for the sight path from Davis Peak to the Southern Ridge, and they are almost identical to those in Figures 6.8.6 and 6.8.7.

The results in Figures 6.8.2 through 6.8.7 show that the values and diurnal patterns of contrasts and contrast transmittances are quite different from one sight path to the next. The variations caused by the illumination of the target are much larger than the variations caused by including or omitting the effects of the emissions from the Hayden station and the Yampa Project. In many cases, the contrasts change more in a few minutes due to the illumination changes than they are changed by including or omitting the effects of the generating station emissions.

Table 6.8.4 shows the results from contrast calculations for cases with either a maximum b_{ext} attributed to one or both of the generating stations as well as the case with the maximum dv (i.e., maximum percent change in b_{ext}, attributed to the Yampa Project). Most sight paths in this table are

toward the south, because views toward shaded targets are more sensitive to changes in b_{ext}. The data show that for these sight paths, changes in contrasts resulting from changes in b_{ext} are essentially the same for the clear sky cases as for the overcast sky cases. The Yampa Project is singled out for separate consideration in this table because it is farther from the Wilderness, and, therefore, its effects are smaller than for the Hayden station. It is desired to evaluate the separate effects of the generating station with the smaller effects.

Table 6.8.4 Tabulation of Calculated Contrasts and Contrast Transmittances for Selected Maximum Values of the Change in b_{ext}

Figures 6.8.8 through 6.8.10 show the largest calculated changes in contrasts and contrast transmittances due to three changes in the emissions used in the CALMET/CALPUFF modeling described in Section 6.7: 1) omitting the emissions of the Hayden station and Yampa Project; 2) omitting the emissions of the Hayden station; and 3) omitting the emissions of the Yampa Project. As shown in Table 6.8.4, the differences are the value for the base case (all emissions included) minus the value for the decreased emissions. Contrast transmittances are always positive numbers, and always become smaller as the emissions increase. Therefore, the differences in contrast transmittances are always negative. The apparent contrasts are usually negative numbers, and become closer to zero as the emissions increase. Therefore, the differences in apparent contrasts are usually, but not always positive.

Figures 6.8.8 through 6.8.10 show only the largest (most positive) values for the change in apparent contrast. The smallest (most negative) values are not shown because their magnitude never exceed 0.007. Figures 6.8.8 through 6.8.10 also show the most negative values for the change in contrast transmittance. The contrast calculations were performed for all sight paths that begin and end in the Wilderness and for all hours in the 09/17/95–09/21/95 and 10/07/95–10/19/95 episodes. A total of 3,029 calculations were done for each of the clear sky and overcast cases for each value of the emissions. The calculated contrasts and contrast transmittances were sorted separately to prepare the plots.

The results for clear (cloud-free) and uniformly overcast skies are quite similar. They show that contrast changes due to the Hayden station are larger than for the Yampa Project. They also indicate that the changes for the Yampa Project are large enough in a few cases out of more than 3,000 that the contrast changes could be seen in a split-screen display. All of the cases in which the change in the Yampa Project emissions caused a change in a calculated contrast or contrast transmittance greater than 0.02 occurred on the afternoons of 09/18/95 or 10/12/95. It is not known if the modeled contrast changes resulting from the change in the Yampa Project emissions are large enough to be seen in the Wilderness.

The data in Tables 6.7.9 through 6.7.12 show that the changes in b_{ext} in sight paths that end outside the Wilderness boundaries resulting from the elimination of the effects of the Hayden station and the Yampa Project within the boundaries is always very small. The largest percent change in b_{ext} is 3.9%. This is less than the 10% change in b_{ext} that is often, but not exclusively, used as a threshold for the perception of a change in a uniform, regional haze.

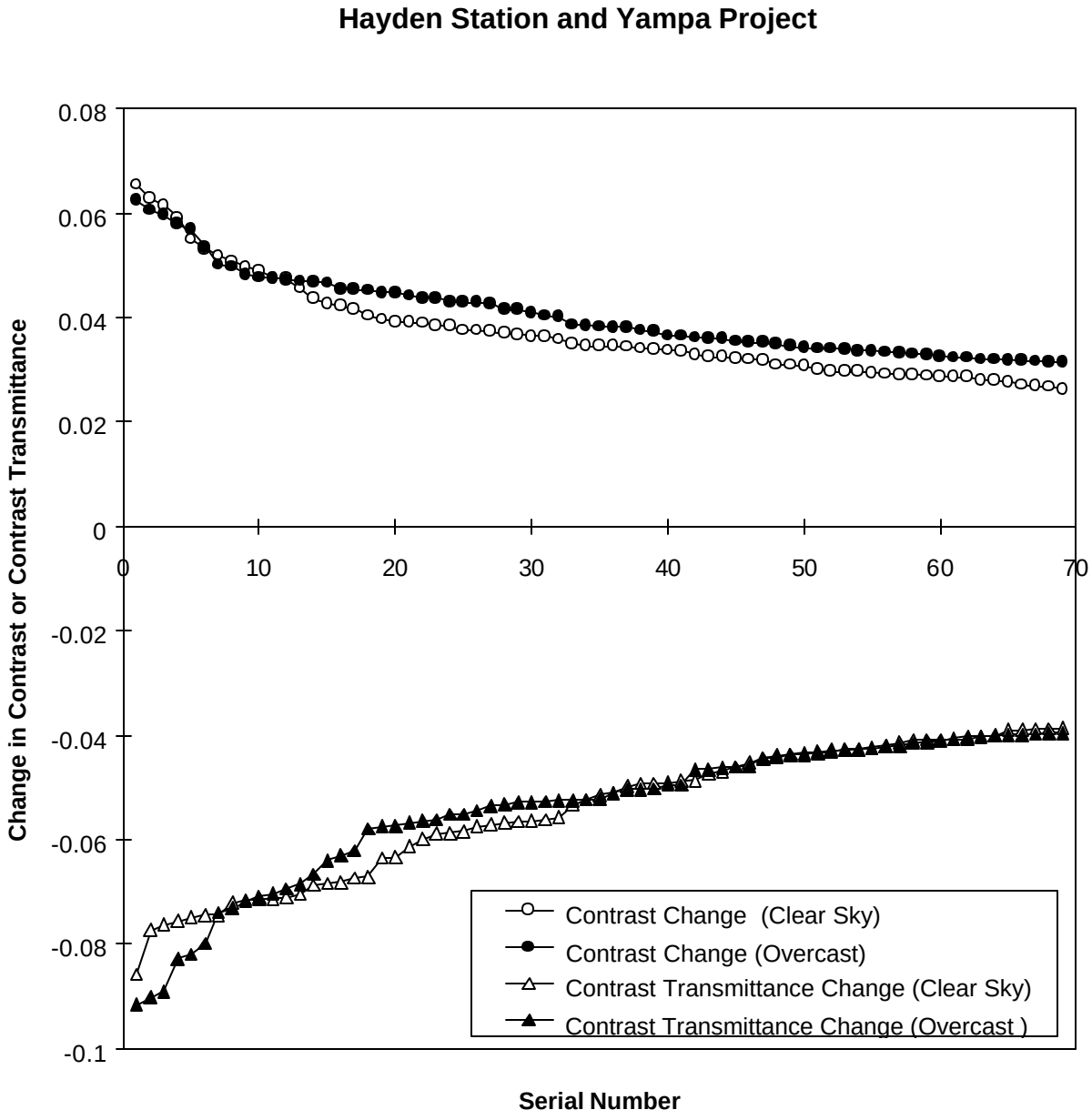

Figure 6.8.8 Largest changes in calculated contrasts and contrast transmittances resulting from removing the emissions of the Hayden Station and Yampa Project from the CALMET/CALPUFF model inputs.

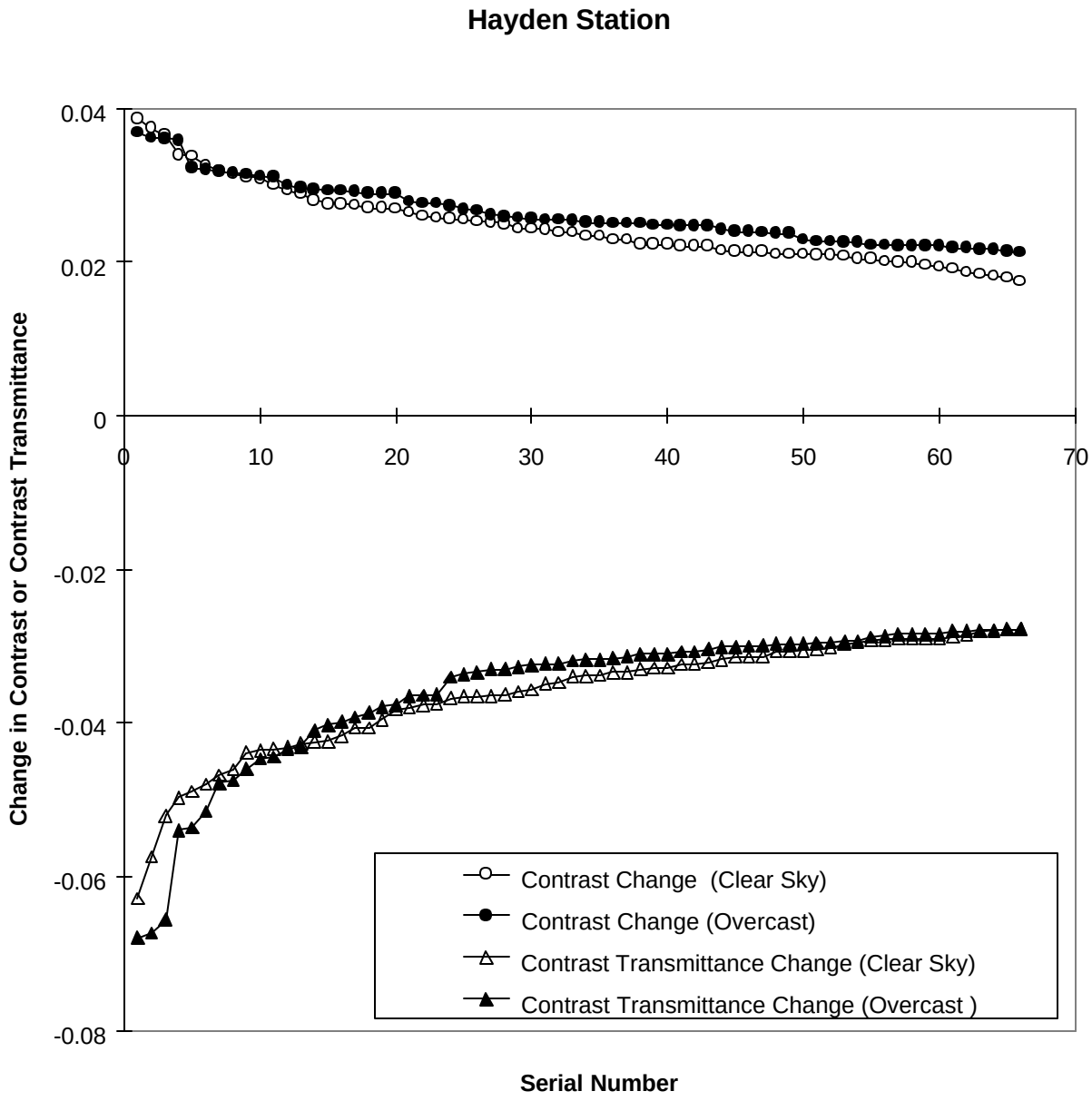

Figure 6.8.9 Largest changes in calculated contrasts and contrast transmittances resulting from removing the emissions of the Hayden Station from the CALMET/CALPUFF model inputs.

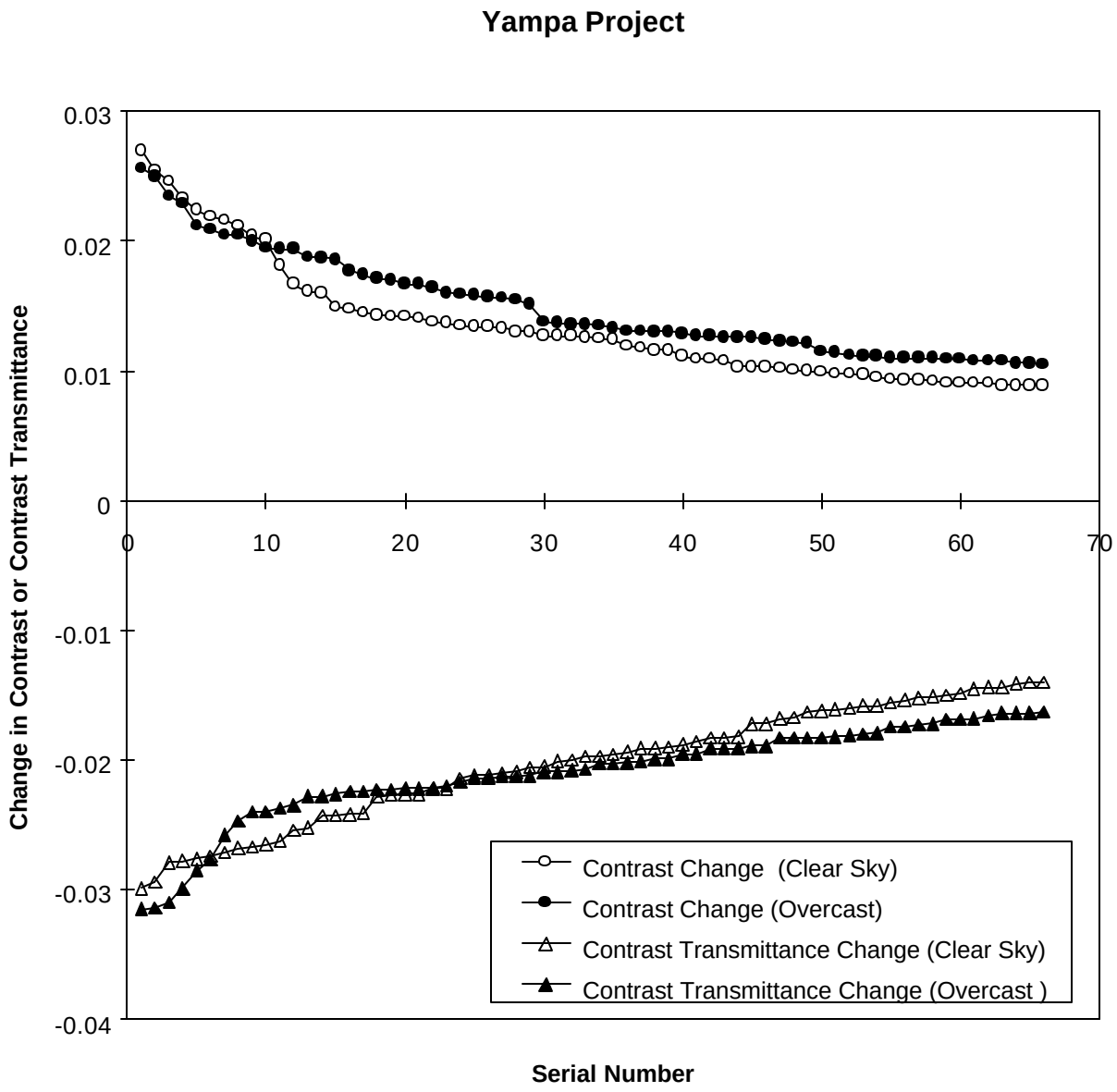

Figure 6.8.10 Largest changes in calculated contrasts and contrast transmittances resulting from removing the emissions of the Yampa Project from the CALMET/CALPUFF model inputs.

The time lapse videos show only one case of a layered haze or well-defined plume attributed to either the Hayden station or the Yampa Project that approached the Wilderness. This event occurred on 01/03/95 and was caused by greater-than-normal emissions of primary particles (fly ash). All haze events associated with the formation of secondary particles (sulfate and associated water) that could be detected in the time-lapse videos showed a haze that was mixed to the ground and did not have

apparent edges or top. Therefore, it is more appropriate to describe the haze pulses identified in Section 6.6 as uniform haze rather than layered haze.

6.8.3 Deciview Haze Index Calculations

The deciview haze index, dv, was proposed by Pitchford and Malm (1994) to provide an indicator of haze that is scaled to correspond to the properties of human vision. It is calculated from the light-extinction coefficient, b_{ext}, for green light by the equation

$$dv=10 \ln_e(b_{ext}/10 \text{ Mm}^{-1}) \quad (6.8.2)$$

This index has a value of zero when $b_{ext} = 10 \text{ Mm}^{-1}$, which is approximately the value of b_{ext} for particle-free air at sea level The value of the deciview haze index increases by one unit for each 10% increase in b_{ext}. The logarithmic scaling is similar to that of the decimal scale, which is also related to human perception.

Pitchford and Malm (1994) also derive the change in dv corresponding to a just-noticeable change in the intensity of a haze that has a uniform appearance. They concluded that for scenes containing elements at every distance, a 1-dv change is a small but perceptible scenic change under many circumstances.

The deciview haze index was applied to the CALMET/CALPUFF model results reported in Section 6.7 by calculating the value of dv corresponding to the b_{ext} values with and without the effects of the emissions of the Hayden station and the Yampa Project. The results are shown in Table 6.8.5 for the 09/17/95–09/21/95 and Table 6.8.6 for the 10/07/95–10/19/95 periods. The View column in these tables identifies the sight paths by the numbers in the first columns of Tables 6.8.2 and 6.8.3. The largest effects of the generating station emissions occurred during these two episodes, so similar calculations were not performed for the 08/07/95–08/09/95 and 08/21/95–08/27/95 periods.

The "base b_{ext}" column presents the modeled light extinction with all emissions included. The next two columns indicate the decrease in b_{ext} calculated when the emissions from either the Yampa Project or the Hayden station were omitted. The "base dv" column was calculated from "base b_{ext}" using Equation 6.8.2. The dv values (not shown) were also calculated from the b_{ext} values with either the Yampa Project or Hayden station emissions omitted. The difference between these values and the "base dv" values are shown in the last two columns of Tables 6.8.5 and 6.8.6. These data give the separate effects of each of the generating stations on the modeled dv value. The data in these tables have been sorted in decreasing order of Yampa Project dv values so no high values due to that source are overlooked. Only the highest 56 values are shown (the complete Table 6.8.6 has 1,560 rows of data).

There are several cases where a dv change exceeding one unit is attributed to the Hayden station during a given hour for a given sight path, but only two cases for the Yampa Project (in Table 6.8.6). In both of these cases, the dv change is only marginally larger than one unit.

The derivation presented by Pitchford and Malm (1994) assumes the availability of sensitive scenic targets at every distance. They further show that the most sensitive distance for the perception of apparently uniform haze is approximately equal to the visual range. In the Mt. Zirkel Wilderness, the visual range is typically larger than 100 km, but the longest sight path

Table 6.8.5
Largest Deciview Haze Index Values Calculated from the CALMET/CALPUFF Model Results for 09/17/95-09/21/95

Date	Hour	View	Base b_{ext} (Mm^{-1})	Yampa Project b_{ext} (Mm^{-1})	Hayden Station b_{ext} (Mm^{-1})	Base dv	Yampa Project dv	Hayden Station dv
09/18/95	15	3	23.1	1.95	2.57	8.37	0.88	1.18
09/18/95	15	4	23.71	1.95	2.9	8.63	0.86	1.30
09/18/95	15	6	22.57	1.82	2.26	8.14	0.84	1.06
09/18/95	14	5	26.72	2.15	4.61	9.83	0.84	1.89
09/18/95	15	2	23.38	1.88	2.1	8.49	0.84	0.94
09/18/95	14	2	23.58	1.88	2.51	8.58	0.83	1.13
09/18/95	15	1	23.41	1.82	2.21	8.51	0.81	0.99
09/18/95	14	3	23.27	1.8	3.01	8.45	0.81	1.39
09/18/95	14	4	24	1.83	3.35	8.75	0.79	1.50
09/18/95	15	5	25.6	1.94	3.97	9.40	0.79	1.69
09/18/95	14	1	23.63	1.79	2.61	8.60	0.79	1.17
09/18/95	16	5	25.26	1.9	3.69	9.27	0.78	1.58
09/18/95	14	6	22.31	1.66	2.56	8.02	0.77	1.22
09/18/95	17	5	25.24	1.78	3.34	9.26	0.73	1.42
09/18/95	16	4	21.32	1.49	2.25	7.57	0.72	1.12
09/18/95	16	6	20.82	1.43	1.85	7.33	0.71	0.93
09/18/95	16	3	20.02	1.36	1.81	6.94	0.70	0.95
09/18/95	17	4	22.18	1.49	2.15	7.97	0.70	1.02
09/18/95	17	3	21.19	1.38	1.79	7.51	0.67	0.88
09/18/95	13	5	26.21	1.69	5.58	9.64	0.67	2.39
09/18/95	17	6	21.85	1.4	1.77	7.82	0.66	0.84
09/18/95	16	2	20.22	1.24	1.48	7.04	0.63	0.76
09/18/95	16	1	20.24	1.21	1.55	7.05	0.62	0.80
09/18/95	17	2	21.39	1.23	1.45	7.60	0.59	0.70
09/18/95	17	1	21.41	1.22	1.52	7.61	0.59	0.74
09/18/95	13	4	19.92	0.97	2.58	6.89	0.50	1.39
09/18/95	11	5	28.16	1.36	3.34	10.35	0.50	1.26
09/18/95	13	2	18.58	0.85	1.74	6.20	0.47	0.98
09/18/95	13	3	18.35	0.83	2.02	6.07	0.46	1.17
09/18/95	13	6	18.23	0.82	1.9	6.00	0.46	1.10
09/18/95	13	1	18.62	0.83	1.76	6.22	0.46	0.99
09/18/95	9	3	30.04	1.28	2.88	11.00	0.44	1.01
09/18/95	8	3	31.75	1.34	2.73	11.55	0.43	0.90
09/18/95	7	3	33.47	1.33	2.53	12.08	0.41	0.79

09/18/95	10	5	29.12	1.09	3.18	10.69	0.38	1.16
09/18/95	11	4	18.72	0.68	1.51	6.27	0.37	0.84
09/18/95	6	3	34.58	1.23	2.34	12.41	0.36	0.70
09/19/95	6	4	19.88	0.69	1.75	6.87	0.35	0.92
09/18/95	9	4	31.43	1.08	3.02	11.45	0.35	1.01
09/19/95	7	4	19.74	0.66	1.73	6.80	0.34	0.92
09/19/95	6	3	18.85	0.63	1.43	6.34	0.34	0.79
09/19/95	6	5	23.7	0.79	2.46	8.63	0.34	1.10
09/19/95	7	3	19.05	0.63	1.48	6.44	0.34	0.81
09/18/95	10	4	22.51	0.73	2.29	8.11	0.33	1.07
09/18/95	9	6	30.85	1	2.95	11.27	0.33	1.01
09/18/95	8	4	32.8	1.06	2.85	11.88	0.33	0.91
09/18/95	9	2	33.31	1.07	3.05	12.03	0.33	0.96
09/18/95	8	6	36.83	1.17	3.14	13.04	0.32	0.89
09/18/95	10	3	20.31	0.64	1.95	7.09	0.32	1.01
09/18/95	9	1	33.78	1.03	3.1	12.17	0.31	0.96
09/19/95	7	5	22.37	0.67	2.11	8.05	0.30	0.99
09/19/95	6	6	20.57	0.61	1.47	7.21	0.30	0.74
09/18/95	10	6	20.05	0.59	1.76	6.96	0.30	0.92
09/19/95	8	5	21.43	0.63	2.11	7.62	0.30	1.04
09/18/95	8	2	35.66	1.02	2.87	12.71	0.29	0.84
09/19/95	7	6	21.03	0.6	1.52	7.43	0.29	0.75

Table 6.8.6
Largest Deciview Haze Index Values Calculated from the CALMET/CALPUFF Model Results for 10/07/95-10/19/95

Date	Hour	View	Base b_{ext} (Mm^{-1})	Yampa Project b_{ext} (Mm^{-1})	Hayden Station b_{ext} (Mm^{-1})	Base dv	Yampa Project dv	Hayden Station dv
10/12/95	13	3	12.42	1.36	0.01	2.17	1.16	0.01
10/12/95	15	5	16.5	1.8	0.33	5.01	1.16	0.20
10/12/95	13	4	12.65	1.18	0.42	2.35	0.98	0.34
10/12/95	14	5	13.42	1.04	0.99	2.94	0.81	0.77
10/12/95	12	4	13.08	0.96	0.56	2.68	0.76	0.44
10/12/95	14	4	12.21	0.82	0.04	2.00	0.70	0.03
10/12/95	12	3	12.7	0.83	0.32	2.39	0.68	0.26
10/12/95	11	5	13.38	0.75	0.82	2.91	0.58	0.63
10/12/95	13	6	11.69	0.64	0.12	1.56	0.56	0.10
10/12/95	14	3	11.9	0.55	0	1.74	0.47	0.00
10/12/95	11	4	12.5	0.55	0.12	2.23	0.45	0.10
10/12/95	12	6	11.99	0.41	0.25	1.81	0.35	0.21
10/12/95	9	2	12.08	0.39	0.28	1.89	0.33	0.23

10/12/95	11	3	12.19	0.38	0.01	1.98	0.32	0.01
10/07/95	16	5	11.88	0.37	0.06	1.72	0.32	0.05
10/12/95	13	1	11.35	0.35	0	1.27	0.31	0.00
10/07/95	14	2	11.54	0.35	0.11	1.43	0.31	0.10
10/12/95	9	1	12.09	0.35	0.32	1.90	0.29	0.27
10/07/95	15	1	11.57	0.33	0.11	1.46	0.29	0.10
10/07/95	15	3	11.61	0.33	0.16	1.49	0.29	0.14
10/07/95	14	1	11.56	0.32	0.13	1.45	0.28	0.11
10/07/95	15	4	11.63	0.32	0.19	1.51	0.28	0.16
10/07/95	15	2	11.55	0.31	0.1	1.44	0.27	0.09
10/07/95	15	6	11.51	0.27	0.11	1.41	0.24	0.10
10/12/95	13	2	11.24	0.26	0	1.17	0.23	0.00
10/13/95	14	5	11.96	0.27	0.6	1.79	0.23	0.51
10/13/95	13	5	12.08	0.26	0.73	1.89	0.22	0.62
10/12/95	14	6	11.46	0.24	0.02	1.36	0.21	0.02
10/07/95	14	6	11.47	0.24	0.17	1.37	0.21	0.15
10/07/95	15	5	11.71	0.24	0.27	1.58	0.21	0.23
10/12/95	11	6	11.88	0.24	0.07	1.72	0.20	0.06
10/07/95	14	3	11.53	0.23	0.21	1.42	0.20	0.18
10/09/95	15	5	12.73	0.25	0.21	2.41	0.20	0.17
10/13/95	12	5	12.05	0.23	0.66	1.86	0.19	0.56
10/12/95	12	5	12.86	0.24	1.05	2.52	0.19	0.85
10/09/95	14	5	12.9	0.23	0.2	2.55	0.18	0.16
10/07/95	16	4	11.54	0.2	0.06	1.43	0.17	0.05
10/09/95	15	4	12.42	0.21	0.13	2.17	0.17	0.11
10/09/95	14	6	12.5	0.21	0.13	2.23	0.17	0.10
10/12/95	10	3	11.32	0.19	0	1.24	0.17	0.00
10/12/95	10	4	11.36	0.19	0.01	1.28	0.17	0.01
10/07/95	14	4	11.51	0.19	0.22	1.41	0.17	0.19
10/09/95	15	3	12.34	0.19	0.11	2.10	0.16	0.09
10/12/95	9	6	11.78	0.18	0.22	1.64	0.15	0.19
10/09/95	14	3	12.49	0.19	0.11	2.22	0.15	0.09
10/09/95	14	4	12.56	0.19	0.12	2.28	0.15	0.10
10/12/95	15	4	14.25	0.21	0	3.54	0.15	0.00
10/13/95	15	5	11.57	0.17	0.3	1.46	0.15	0.26
10/13/95	11	5	11.85	0.17	0.47	1.70	0.14	0.40
10/10/95	17	5	12.58	0.18	0.15	2.30	0.14	0.12
10/17/95	14	5	14.99	0.21	0.23	4.05	0.14	0.15
10/13/95	16	5	11.44	0.16	0.14	1.35	0.14	0.12
10/13/95	17	5	11.49	0.16	0.05	1.39	0.14	0.04
10/09/95	15	6	12.26	0.17	0.11	2.04	0.14	0.09
10/17/95	15	5	15.28	0.21	0.17	4.24	0.14	0.11
10/09/95	14	2	12.37	0.17	0.11	2.13	0.14	0.09

identified within the Wilderness boundaries has a length of 35 km. Therefore, scenes within the MZWA do not satisfy the assumptions used in Pitchford and Malm (1994).

To permit the application of the dv parameter to haze analyses in the Wilderness, the derivation reported in Appendix B.6 was applied. This derivation uses the data and equations presented in Pitchford and Malm (1994) to determine the effect of the length, r, of the longest

available sight path in a scene on the threshold for the perception of regional haze. It was found that using a threshold change in b_{ext} of 0.39/r is equivalent to using a threshold of 1 dv for scenes that contain elements at a distance approximately equal to the visual range. Since the longest sight path identified in the Wilderness has a length of 35 km, this relation indicates that a change in b_{ext} of 11 Mm^{-1} within the Wilderness is equivalent to a change of 1 dv in scenes that contain elements at a distance approximately equal to the visual range. At locations where all available sight paths within the Wilderness are shorter than 35 km, the equivalent change in b_{ext} can be calculated from the relation, 0.39/r.

Though Pitchford and Malm (1994) indicate that, under most circumstances, a 1-dv change could be easily noticed by the casual observer, some researchers believe that observers can detect changes in extinction of less than 2%. A 2% change in extinction corresponds to a change of 0.2 dv. Use of this threshold for scenes that have elements at every distance corresponds to using a change in b_{ext} of 2 Mm^{-1} in a 35 km sight path. If only shorter sight paths are available, the equivalent change in b_{ext} becomes 0.08/r.

During the planning of this study, a threshold change of 1 dv was cited by government representatives as being appropriate for use in these analysis. Discussions with representatives of Federal Land Managers has also indicated some acceptance of this threshold. Subsequent review of published literature did not yield evidence of documented alternatives to the Pitchford and Malm (1994) recommended values for the threshold dv change. Therefore, the 1-dv change is used as a reference value for these analyses. The calculated results are presented in such a way that other thresholds can be easily applied.

Tables 6.8.5 and 6.8.6 indicate that the modeled changes in b_{ext} are always smaller than the 11 Mm^{-1} reference value. Therefore, this analysis indicates that the changes in b_{ext} calculated in Section 6.7 cause visual effects that are smaller than those that would result from a 1-dv change in a scene that contains elements at the most sensitive distance.

The analysis in Section 6.6 identified haze pulses measured at Buffalo Pass that caused changes in b_{ext} in excess of 11 Mm^{-1}. Therefore, experimental measurements detected haze pulses of larger magnitude than were calculated by the CALMET/CALPUFF modeling reported in Section 6.7.

6.8.4 Perception Thresholds

There is reasonable experimental evidence that the threshold for the perception of a ridge against its background is approximately 2%, or that 1-deciview changes in haze cause perceptible changes in the appearance of a scene when the scene contains objects at the most sensitive distance and the scenes are compared side-by-side in split-screen images. There is less experimental data, and less scientific agreement, about the change in contrast in a scene that can be perceived when one view is compared to another at different times. For example, at one moment in time, a ridge could have a contrast of –40% against the horizon sky, indicating it is 40% darker than the sky. How much must that contrast change over a period of time for an observer to perceive that there has been a change in contrast? If the haze increased so the contrast was reduced to –35% an hour later, what fraction of the human observers would notice that change? How much contrast change is required for most observers

to notice the change? The answers to these questions are not well established. For most sight paths, the change in contrast or contrast transmittance due to generating station contributions is small compared to the changes that occur in short time periods due to changes in the position of the sun.

Direct observation has made moot the question of whether the modeled changes in b_{ext} cause perceptible changes in contrasts. The TSI nephelometer observed a change in fine-particle scattering of 19 Mm^{-1} and the OPTEC nephelometer observed a change of total scattering of approximately 36 Mm^{-1} during the September 18 event. These changes are much larger than the 7.3 Mm^{-1} change calculated by the CALMET/CALPUFF models. As indicated in Sections 5.6 and 6.8.6 below, a haze pulse was perceptible in the time-lapse videos taken from Storm Peak during this event.

6.8.5 Observations of Video Images

Time-lapse video images were viewed for the days of the haze pulses identified in Section 5.6. Haze pulses were visible in the video images on two of these days. On other days, the haze pulses were either imperceptible for all observers (sometimes because of the weather conditions) or indistinct enough that observers differed on the existence and timing of a haze pulse.

The haze pulse most clearly recorded in the video images occurred on the afternoon of 08/23/95. This pulse was especially visible because the atmosphere became clearer than normal at the end of the pulse. The second perceptible haze pulse occurred on the afternoon of 09/18/95. Additional information on these haze pulses is summarized in a summary video, part of the MZVS data base, that shows selected haze events recorded during this study.

6.9 Changes in Nitrate Concentrations

The SCAPE (Kim *et al.*, 1993a, 1993b) mechanism, using the Pitzer (Pitzer and Kim, 1974; Pitzer, 1991) method for calculating activity coefficients, was applied to determine how much particulate ammonium nitrate concentrations might change in response to changes in total ammonia and ammonium sulfate concentrations. Increases in ammonia gas and ammonia currently associated with sulfate might shift nitrate equilibrium from the gaseous to the particulate phase. These changes might result from increases in ammonia emissions (e.g., larger fertilizer applications, a larger number of cattle) or from reductions in sulfur dioxide emissions that would provide less sulfuric acid to react with existing ammonia.

The results for SCAPE calculations are presented in Table 6.9.1 for the Juniper Mountain (JUNZ), Buffalo Pass (BUFZ), and Hayden VOR (VORZ) sites where six-hour morning and afternoon concentrations of total nitrate, total ammonia, and nitric acid were measured. The JUNZ measurements were incomplete for many samples, so conclusions are drawn primarily from the BUFZ and the VORZ tests. As shown in Sections 3 and 4, Juniper

Table 6.9.1 Effects of Changes to Ammonia and Sulfate Concentrations on Particulate Ammonium Nitrate

Mountain measurements were often similar to those found at Buffalo Pass, so conclusions are not greatly affected by this deficiency.

Results of these simulations in Table 6.9.1 are divided into four sections after the measured concentrations are listed. The first "Base Model" calculations were made using measured concentrations of ammonia, ammonium, nitric acid, chloride, particulate nitrate, and sulfate as inputs to SCAPE. The second "High Ammonia Model" repeated SCAPE calculations with total ammonia concentrations double those that were measured. The third and fourth "Low Sulfate Model" and "Zero Sulfate Model" recalculated the ammonium nitrate equilibrium with the measured sulfate concentrations halved and set equal to zero, respectively. The purpose of these changes from ambient data are: 1) to determine the extent to which ammonium nitrate is ammonia limited (doubling the ammonia); and 2) to determine whether or not ammonium nitrate particles will increase when additional ammonia is freed from reduced ammonium sulfate.

For each of these modeled cases, the "Total" column reports the sum of ammonium, nitrate, and sulfate concentrations in the particle phase. The "Water" column reports the SCAPE-calculated liquid water content associated with this mixture for the average temperature and relative humidity corresponding to the sample, and the "Amm. Nitrate" column reports the SCAPE-calculated particulate ammonium nitrate that would be expected under the modeled conditions. Deviations from the base case show what the effects of emissions changes might be on these three variables, all of which affect light scattering.

Table 6.9.1 reports the results for only 38% of all the samples available with nitric acid, ammonium, and other chemical measurements, including 1 of 14 available samples for JUNZ, 25 of 47 for BUFZ, and 18 of 54 for VORZ. SCAPE results are not reported in Table 6.9.1 for cases in which: 1) particulate ammonium nitrate for all of the four cases were zero; 2) calculated ionic strengths exceeded 30, beyond the capability of the Pitzer method to accurately estimate activity coefficients; or 3) SCAPE did not return results owing to numerical instabilities.

Table 6.9.1 shows that particulate nitrate should occur only in the presence of liquid water. For the base case, the minimum liquid water concentration associated with nitrate was 0.29 ug/m^3 at the Buffalo Pass site on the morning of 02/23/95. Particulate nitrate is not generally found in the absence of liquid water owing to the relatively low gas phase pressures for nitric acid and ammonia; they are, generally, not high enough to produce solid phase ammonium nitrate. Solid phase ammonium nitrate occurred in only two of the cases given in Table 6.9.1: 1) the zero-sulfate case for BUFZ, 10/09/95, 0600 MST; and 2) the high-ammonia case for VORZ, 02/24/95. 0600 MST. In the former case, all the nitrate was solid phase, as there was no liquid water present. In the latter case, 0.71 ug/m^3 were present in the solid phase. In the presence of liquid water, nitrate enters the particulate phase though the dissociation of liquid-phase HNO_3 into H^+ and NO_3^-. The nitrate that enters the liquid phase is determined by the gas-phase pressures of nitric acid and ammonia and the amount of liquid water. Ammonia tends to neutralize the drop and allows more nitric acid to dissociate. Liquid water provides the volume for dissociation.

Total particulate concentrations estimated by the base case are somewhat less than measured concentrations because the calculated ammonium nitrate is often less than the measured ammonium nitrate. The fact that six-hour averages are used as inputs to SCAPE and that these averages do not reflect the total history experienced by the measured particles may account for some of this discrepancy. SCAPE may also underestimate the liquid water content. Tang (1980) shows that liquid water can be associated with ammonium sulfate at relative humidities as low as ~30% when relative humidity decreases from values exceeding 80%. Table 6.9.2 gives mass averages over the cases of Table 6.9.1 plus those with zero nitrate excluded from Table 6.9.1. Table 6.9.2 shows that, on average, model agreement with measurements increases as RH increases.

When ammonia is doubled, particulate nitrate concentrations increase proportionately more over the base case concentrations for low humidities than they do for high relative humidities. This is because at high relative humidities, the liquid water concentrations are, in general, higher and most or all of the available nitrate is already in the liquid phase (e.g., BUFZ, 09/18/95, 0600 MST). For example, for the cases given in Table 6.9.1, for RH < 90% the mean liquid water concentration is 1.9 ug/m^3 and the mean particulate nitrate concentration increases from 0.12 ug/m^3 for the base case to 0.35 ug/m^3 for the high ammonia case, a factor of 3; for RH 90% the mean liquid water concentration is 730 ug/m^3 and the mean particulate nitrate concentration increases from 0.28 ug/m^3 for the base case to 0.42 ug/m^3 for the high ammonia case, a factor of 1.5. The absolute change in the mean particulate nitrate concentration falls from 0.23 ug/m^3 for RH < 90% to 0.14 ug/m^3 for RH greater than 90%.

When the sulfate concentration is halved, there is no effect on ammonium nitrate without the presence of liquid water. SCAPE-calculated nitrate concentrations are close to those of the base case and below those of the high ammonia case. The reduction of sulfate increases the availability of ammonia in the gas phase, which drives more nitrate to the liquid phase. On the other hand, sulfate reduction also reduces the solute content of the drops, thereby reducing the liquid water concentration available for liquid phase nitrate.

The same observations result from the zero sulfate calculations, except for the sample at the Buffalo Pass site on 10/09/95 at 0600 MST. For this sample, SCAPE calculated solid-phase ammonium nitrate and zero liquid water concentration. This is our only example of particulate nitrate in the absence of liquid water. On average, model nitrate concentrations attain concentrations similar to that of the high ammonia case.

The SCAPE modeling of ammonium nitrate equilibrium shows the following:

Liquid water is necessary for the formation of ammonium nitrate. Only two model calculations yield solid ammonium nitrate; all other calculations produce ammonium nitrate only as ions in the liquid phase. For the cases considered in Table 6.9.1, for RH < 75% the mean ammonium nitrate produced in the base case is 0.09 ug/m^3; for RH greater than 75% it is 0.17 ug/m^3.

Doubling the ammonia concentration produces larger particulate nitrate concentration increases for lower liquid water contents. This, however, is offset by the smaller amounts of particle nitrate contained in the smaller amounts of liquid water, with the result that, on average, the increase in particle nitrate is limited to less than 0.1 ug/m^3, as shown in Table 6.9.2. Therefore, increasing ammonia does not effectively increase ammonium nitrate concentrations to significant levels.

Reducing sulfate concentrations frees up ammonia for potential reaction with nitric acid to form particulate ammonium nitrate, but sulfate reductions also reduce the liquid water available for reactions. These phenomena counteract each other, yielding no significant (> 0.1 ug/m^3) increases in particulate nitrate with decreases in sulfate concentration.

Table 6.9.2
Measured vs. Modeled Particulate Mass Averages

Site	RH (%)	Total Particulate Mass	Average (ug/m^3)	Nitrate Particulate Mass	Average (ug/m^3)
Buffalo Pass	67.5	Measured[a]	1.28	Measured[b]	0.23
		Base Model[c]	1.19	Base Model[c]	0.10
		High Ammonia Model[d]	1.19	High Ammonia Model[d]	0.17
		Low Sulfate Model[e]	1.31	Low Sulfate Model[e]	0.12
		Zero Sulfate Model[f]	0.72	Zero Sulfate Model[f]	0.18
Juniper Mountain	38.5	Measured[a]	1	Measured[b]	0.22
		Base Model[c]	0.73	Base Model[c]	0.00
		High Ammonia Model[d]	0.84	High Ammonia Model[d]	0.00
		Low Sulfate Model[e]	0.42	Low Sulfate Model[e]	0.00
		Zero Sulfate Model[f]	0	Zero Sulfate Model[f]	0.00
Hayden VOR	46.5	Measured[a]	1.66	Measured[b]	0.25
		Base Model[c]	1.57	Base Model[c]	0.03
		High Ammonia Model[d]	1.67	High Ammonia Model[d]	0.10
		Low Sulfate Model[e]	0.84	Low Sulfate Model[e]	0.03
		Zero Sulfate Model[f]	0.14	Zero Sulfate Model[f]	0.14

[a] Sum of measured $PM_{2.5}$ ammonium, nitrate, and sulfate.

[b] Model ammonium nitrate.

[c] Base case calculations were done with measured concentrations of gaseous ammonia and nitric acid, and $PM_{2.5}$ ammonium, chloride, nitrate, and sulfate specific to each sample used as inputs to SCAPE.

[d] High ammonia calculations were base case with ammonia concentrations doubled.

[e] Low sulfate calculations were base case with sulfate concentrations halved.

[f] Zero sulfate calculations were base case with sulfate concentrations set to zero.

7.0 MODEL RECONCILIATION AND STUDY FINDINGS

The material presented in the previous six sections is lengthy and detailed. Nevertheless, most of the measurements, data analyses, and modeling results are consistent with a basic description of visibility impairment and its causes in and near the Mt. Zirkel Wilderness. This basic description is expressed in this section as a simple, conceptual model of emissions, meteorology, particle concentrations, light extinction, and the perception of that extinction. Quantitative estimates were made of source contributions to suspended particles that cause light extinction by the CALMET/CALPUFF plume chemistry model and the Chemical Mass Balance receptor model, and an attempt is made to reconcile differences between them. Finally, MZVS findings for each of the seven study objectives are summarized.

7.1 Conceptual Model

The Mt. Zirkel Wilderness Area (MZWA) straddles the Continental Divide in the Routt Mountain Range in Northwest Colorado. The Wilderness lies to the northeast and above the Yampa River Drainage Basin (Yampa Valley), which extends to the west ~165 km along the course of the Yampa River. The Yampa Valley lies within Routt and Moffat Counties and contains the major population centers of Steamboat Springs (pop. ~7,500), Hayden (pop. ~1,600), and Craig (pop. ~8,500), Colorado. The permanent population of the Yampa Valley approaches 27,100, which is substantially augmented during winter by skiers and during summer by outdoor enthusiasts. The major economic interests in the Yampa Valley include tourism, cattle ranching, coal mining, and electric power generation.

Two coal-fired generating stations are located within the Yampa Valley. The Hayden station, in Hayden, CO, is ~30 km west of the closest Wilderness boundary, and consists of one 184-megawatt generating unit and one 262-megawatt generating unit with separate stacks preceded by hot-side electrostatic precipitators to remove primary particles. The Craig station, ~60 km west of the closest Wilderness boundary near Craig, CO, consists of three generating units – two 428-megawatt generators (Craig Units 1 and 2, also known as the Yampa Project) equipped with electrostatic precipitators and wet limestone scrubbers that remove sulfur dioxide with ~67% efficiency, and one 408-megawatt generator (Craig Unit 3) equipped with a dry sulfur dioxide scrubber with ~85% efficiency and a baghouse that removes particles from the flue-gas stream.

Visibility is impaired when light is reflected from an object and transmitted through the atmosphere is attenuated by being scattered and absorbed by gases and particles. The presence of particle-free atmospheric gases, such as oxygen and nitrogen, would limit horizontal visual range to ~400 km, if such a sight path were possible, and it would obscure many of the attributes of a view at less than half this distance. Particles with sizes comparable to the wavelength of light cause the greatest light scattering. Light is absorbed by nitrogen dioxide (NO_2) gas, but such absorption is negligible in pristine environments such as the Wilderness. Black carbonaceous particles and nontransparent dust absorb light. Sunlight illuminating the view path is also scattered toward the observer, and this air light increases

with distance from the target while the light reflected from the target decreases due to scattering and absorption.

In pristine areas, air pollution sources contribute directly-emitted particles that cause extinction, as well as invisible gases that might convert to particles that affect visibility after aging and combining with other gases and particles in the atmosphere.

Prescribed burns and wildfires cause visible plumes containing primary particles within and outside of the Yampa Valley. The most visible plumes within the Yampa Valley are those from the Hayden and Craig generating stations. The most noticeable of these are steam emissions from cooling towers that rapidly evaporate upon dilution with ambient air. Primary particles that are not captured by the electrostatic precipitators are the main cause of visible emissions from stacks. These primary particle plumes become more visible when precipitators malfunction. The majority of pollutant emissions from generating stations consist of SO_2 and nitric oxide that can be detected instrumentally but not visually.

Emissions from motor vehicles and residential burning can accumulate at night and during the morning near the floor of the Yampa Valley, to be mixed above the surface when the morning sun heats the surface layer. The time and nature of this coupling determines how these pollutants are transported to the Wilderness.

For a multi-state region including large parts of Colorado, Utah, and Wyoming, emissions from sources in the Yampa Valley are minor. During the summer, ~6% of the sulfur dioxide, ~5% of the oxides of nitrogen, ~3% of the primary $PM_{2.5}$, ~3% of the elemental carbon, ~1% of the primary organic carbon, and ~8% of the ammonia emissions in the region are from an area that includes the Yampa Valley.

Light extinction in the Wilderness is among the lowest measured in U.S. Class I areas. Winter is the clearest season and summer the haziest. The average light extinction in the Wilderness, including scattering by particle-free air, is approximately half that in the Grand Canyon. Most hazes in the Wilderness area are regional, with light extinction comparable at locations that are separated by more than 150 km. Contributions from nearby sources are measurable and perceptible on occasion, and are superimposed on the contributions from a mixture of source emissions from inside and outside the region.

Haze in the Yampa Valley typically appears uniform visually, vertically, and horizontally. Surface layers are sometimes perceptible, especially during morning when a surface temperature inversion is present. Elevated layers are noticeable when noncontinuous emissions (e.g., from fires) occur or when generating stations malfunction. Although appearing visually uniform, light extinction in the Yampa Valley is often much higher than that measured in the Wilderness and surrounding areas.

The largest and most frequent contributors to light extinction in the Wilderness are particle-free air (Rayleigh scattering), motor vehicle exhaust and secondary organics (formed from heavy gaseous hydrocarbons), vegetative burning, and regional secondary ammonium sulfate. These contributors are for the most part of regional origins, resulting from a mixture

of emissions from source areas that are hundreds of kilometers distant from the Wilderness. Residential coal combustion and hot springs are minor contributors to ammonium sulfate.

Liquid water is a major component of particles that cause extinction when relative humidities exceed 80%. The visibility-reducing effects of water-soluble particles such as ammonium sulfate and ammonium nitrate are enhanced when humidities exceed 80%. SO_2 and oxides of nitrogen (NO_x), along with ammonia (NH_3), can change into particulate ammonium sulfate and ammonium nitrate that contribute to light extinction. These transformation rates are highly variable, but they can be expected to be slow in clear air and rapid when plumes encounter fogs or clouds.

Significant, though not major, contributions to light extinction in the Wilderness from local power generating stations occur occasionally. These contributions are always superimposed on contributions to extinction from other sources. In the absence of relative humidities larger than 80% (an indicator for passage of plumes through fog or clouds), the Yampa Valley generating station plumes seldom cause perceptible increases in light scattering in the Wilderness, although they regularly arrive in the Wilderness. After passage through fogs or clouds, sufficient transformation of SO_2 to sulfate can take place in generating station plumes to cause perceptible changes in light scattering in the Wilderness.

Yampa Valley generating station plumes are usually confined below 400 m (1,300 ft) above ground level and flow to the west (down the Valley) at night and in the early morning. At midday, they mix aloft and couple with the upper level winds, which typically transport the plumes to the east, toward the southern end of the Wilderness. The generating station plumes tend to arrive in the Wilderness in pulses with typical durations of less than one to a few hours at any location.

The largest perceptible effects of the Yampa Valley generating stations on visibility in the Wilderness occur when the emissions accumulate in fogs or low clouds in the early morning or interact with higher clouds after mixing aloft and are subsequently transported to the Wilderness in the afternoon. Pulses of haze attributable to generating station emissions can be seen from the Wilderness on some occasions under these conditions. When they arrive under these conditions, the hazes appear well mixed vertically, rather than as a layer or plume.

Under nonroutine operating conditions, primary particle emissions from the Yampa Valley generating station stacks can cause perceptible, layered hazes with durations of several hours. These are not due to SO_2 emissions. On one occasion during the MZVS, a clearly-defined, coherent plume from the Hayden generating station could be seen in a west-facing video view from a camera on Storm Peak (which is south of the Wilderness boundary). The plume was moving toward Storm Peak at nearly the same elevation as the camera. The extent to which the plume reached or rose over the Continental Divide could not be determined because it could not be seen in views to the north. However, it is clear that the potential existed for the plume to reach the Storm Peak area. This was the only occasion when a clearly-defined, coherent generating station plume was documented coming close to the Wilderness.

High relative humidity and SO_2 concentrations greater than about 1-2 ppb indicate when generating station emissions might cause visible effects. Plumes arrived in the Wilderness at these concentrations during conditions when relative humidity was greater than 80% on approximately 3% - 8% of the daylight hours during the year. For 1995, the highest incidence (10% - 16%) of these conditions was in May (which was the wettest May on record) and the lowest (0.5% - 2%) in August. During many of these hours, however, views were obscured by weather.

Plumes from the Hayden and Craig Stations arrive in the Wilderness together most of the time. SO_2 concentrations arriving in the Wilderness from the Hayden station are three to four times higher than concentrations from the Craig station. This difference is caused by larger dispersion and dilution of Craig station emissions, due to its greater distance from the Wilderness boundary, and SO_2 emission rates during the periods studied that were approximately half the emissions from the Hayden station. On rare occasions, however, for some portions of the Wilderness, the emissions from the two generating stations can arrive separately, and Craig emissions can cause more light extinction than Hayden emissions.

Yampa Valley generating stations have their largest effects on extinction over periods of one or two hours. The effects along a sight path within the Wilderness or looking outside of the Wilderness are lower than those measured at the southern boundary, near Buffalo Pass, because this site is often near the location of the maximum extinction, while the sight paths cover a larger area. The total generating station contribution to extinction might be occasionally perceptible if images with and without the contribution were viewed side-by-side in a split screen image. It is likely that the Hayden contribution would be perceptible on its own on a few occasions. It is not certain that the Yampa Project contribution would be perceptible.

When only generating station contributions to extinction within the Wilderness boundaries are considered, views that extend outside the Wilderness are less sensitive to the removal of generating station emissions than sight paths with both endpoints in the Wilderness, due to the small proportions of the long sight paths that were within the Wilderness.

7.2 Model Reconciliation

The conceptual model presented in Section 7.1 embodies the essential features of the causes of haze found in and near the Mt. Zirkel Wilderness. Simulating this conceptual model with mathematical computer codes, applied to relatively sparse data, is a further challenge. Each of the models applied in the MZVS made assumptions from which there were certainly deviations during the study period. Appendix B delineates these assumptions and examines the effects of deviations from some, but not all, of them.

Both the CALMET/CALPUFF meteorological and plume chemistry models and the Chemical Mass Balance receptor model were applied to 47 of the same six-hour periods and four twelve-hour periods of Buffalo Pass data to estimate contributions to light extinction and $PM_{2.5}$ mass concentrations. Other data analyses and receptor modeling of source

contributions to extinction were also applied to data from these periods. This provides a good opportunity to compare results. Such a comparison is given in Table 7.2.1 for absolute contributions to $PM_{2.5}$, in Table 7.2.2 for relative contributions to $PM_{2.5}$, and Table 7.2.3 as average contributions for all of the modeled periods.

It is evident from these tables that the agreement between the CMB and CALMET/CALPUFF (CC) models for comparable source categories of Yampa Valley coal-fired generating stations, fires, and other $PM_{2.5}$ is not very good. While the CMB often reproduced the measured $PM_{2.5}$ within measurement uncertainty, as expected since the percent mass explained is one of the major performance parameters of this model, the CC model often underestimated $PM_{2.5}$ concentrations. On average (Table 7.2.3), the CMB model estimated local coal-fired generating station contributions to $PM_{2.5}$ to be ~33% of those calculated by the CC model, while the CMB model's fire contribution was six times that of the CC model. Average contributions from other sources were ~50% larger than those estimated by the CC model, but were nearly the same on a percentage basis.

Tables 7.2.1 and 7.2.2 show that these discrepancies are much larger on a sample by sample basis. The CC results show negligible impact from fires for the 08/21/95–08/26/95 and 10/07/95–10/15/95 periods, even though Appendix B.1 shows that fires did occur in the multi-state region on some days during these periods, and these fire emissions were included in the CC modeling. The 08/24/95 sample stands out with a very high $PM_{2.5}$ at Buffalo Pass, much of which was attributed to fires that may have been very close to the measurement site (e.g. campfires) and were not recorded in the inventory. The CMB also estimates a 2.79 $\mu g/m^3$ contribution to $PM_{2.5}$ on the morning of 10/08/95, even though no fires were reported immediately prior to or during that period. This could be due to an undocumented source, or an inadequacy of the CMB model.

Table 7.2.1 Comparison of CMB- and CALMET/CALPUFF-Estimated Source Contributions to $PM_{2.5}$ (individual periods)

Table 7.2.2 Comparison of CMB- and CALMET/CALPUFF-Estimated Source Contributions as Percentages of $PM_{2.5}$

Some of these events with elevated light extinction occurred during dry conditions (e.g., 08/08/95, 10/19/95) and others occurred under high humidity (e.g., 08/23/95, 09/18/95, 09/19/95, 10/12/95). Buffalo Pass SO_2 concentrations of about 2 ppb or more were estimated by the everyday modeling, the plume chemistry model, and measurements for all of these events except 10/12/95 and 10/19/95. For 10/12/95, a value of about 2 ppb was estimated by the plume model, but only about 0.5 ppb was measured. These days were examined to assess the source contributions to extinction in the Wilderness. They include the days of the highest estimated generating station contributions to extinction during the summer and fall.

For the dry periods of 08/08/95 and 10/19/95, data analyses, plume modeling, and receptor modeling agree that the Yampa Valley generating stations were negligible contributors to extinction in the Wilderness. These events were dominated by fires, motor vehicle emissions or secondary organic aerosol, and secondary sulfate transported from

Table 7.2.3

Comparison of CMB- and CALMET/CALPUFF-Estimated Source Contributions to $PM_{2.5}$ (average of 08/07/95-08/09/95, 08/21/95-08/27/95, 09/17/95-09/21/95, and 10/07/95-10/19/95)

		Measured Mass ($\mu g/m^3$)	Calculated Mass ($\mu g/m^3$)	Coal-Fired Generating Station ($\mu g/m^3$)	Vegetative Burning ($\mu g/m^3$)	Other Mass ($\mu g/m^3$)	Coal-Fired Generating Station (%)	Vegetative Burning (%)	Other Mass (%)
CMB	average	4.47	4.55	0.16	0.93	3.46	4.92	17.82	77.26
	σ	3.36	3.46	0.22	1.37	2.37	7.18	11.13	13.80
CALMET/CALPUFF	average	4.47	2.94	0.47	0.14	2.33	16.73	3.31	79.92
	σ	3.36	2.05	0.49	0.32	1.75	15.14	6.42	16.19
CMB-CALMET/CALPUFF	average	4.47	1.61	-0.31	0.79	1.13	-11.81	14.51	-2.66
	σ	3.36	4.57	0.41	1.43	3.39	12.64	12.12	18.81

outside the local region. For example, receptor modeling indicates that for the 08/08/95 afternoon sample at Buffalo Pass (with measured light extinction of 36 ± 6 Mm^{-1}), 23 ± 7% of the extinction derived from clean-air scattering, 20 ± 1% was contributed by fires, 29 ± 29% came from motor vehicle exhaust or secondary organics (note the large uncertainty estimate), 0.6 ± 0.3% was attributable to local coal-fired generating stations; 13 ± 2% was from regional ammonium sulfate, 1.7 ± 0.8% was from secondary ammonium nitrate; and 13 ± 1% was from suspended dust. The suspended dust contribution was real, but was probably very local and did not affect concentrations along long sight paths.

For 08/23/95, trajectory analyses, correlation between SO_2 and particle scattering (b_{sp}), and video images indicated a possible significant contribution to extinction at Buffalo Pass from the Yampa Valley generating stations. Regional background conditions, high values of aerosol light absorption, and the chemistry of the filter samples, however, indicated that geological material, regional sulfate, fires, and motor vehicles or secondary organics were the dominant contributors to extinction for the six-hour afternoon period. The CC plume model substantially underestimated the extinction because it did not adequately account for regional transport. The CMB receptor model attributed only 3.5 ± 1.7% of the 37 ± 7 Mm^{-1} measured extinction to the Yampa Valley generating stations. It should be noted, however, that the models were applied for six-hour samples and will underestimate the contribution of the generating stations to extinction for shorter time periods. From the high correlation between SO_2 and b_{sp} seen for this event, it is likely that the generating station contribution to extinction was higher than estimated by the models, but for a short portion of the six-hour averaging interval. A corresponding correlation between light absorption and b_{sp} indicates that other sources than the generating stations also contributed to the event.

The afternoons of 09/18/95 and 09/19/95 were the times of the largest documented contributions of Yampa Valley generating stations to light extinction in the Wilderness. For these afternoons, light scattering at Buffalo Pass peaked at about 60 Mm^{-1} and 25 Mm^{-1}, respectively, and the plume-model extinction estimates (for a six-hour period) agreed with the peak values.

For 09/18/95 and 09/19/95, the percentage contributions to afternoon six-hour-average extinction estimated by the CC plume chemistry model for the Yampa Valley generating stations were 46% for 09/18/95 and 26% for 09/19/95. The modeled component contributions for these days were, respectively: clean air, 15% and 44%; fires, 6% & 4%; non-Yampa-Valley sources, 31% and 19%; Hayden, 32% and 20%; Craig Units 1 & 2, 12% and 5%; Craig Unit 3, 2% and 1%; and other Yampa Valley sources, 4% and 6%. The CMB receptor model found the following contributions, respectively: clean air, 17 ± 4% and 38 ± 10%; fires, 15 ± 1% and 17 ± 1%; vehicle exhaust and secondary organics, 13 ± 20% and 24 ± 25%; suspended dust, 2 ± 0.4%; background ammonium sulfate, 33 ± 7% and 10 ± 4%; secondary ammonium nitrate, 7 ± 2% and 2 ± 1%; and Yampa Valley generating stations, 14 ± 7% and 7 ± 3%.

For the afternoons of 09/18/95 and 09/19/95, CMB receptor model results differed from CC plume model results. Observations of the magnitude of the changes in b_{sp}

coincident with changes in SO_2 from 1200 to 1500 MST on 09/18/95 and from 1400 through 1600 MST on 09/19/95 were closer to the six-hour average plume model results than to the corresponding receptor model results. The plume model may more closely represent the peak light extinction values seen for these days. Table 7.2.1 compares the source contributions to $PM_{2.5}$ at Buffalo Pass estimated by the CALMET/CALPUFF and CMB modeling.

The same event (09/18/95) also included the highest one-hour relative contribution to extinction estimated for Craig Units 1 and 2 (the Yampa Project) and Hayden station along any modeled sight path. This contribution was 27% of total extinction, with 21% due to Hayden station and 6% to the Yampa Project. This is equivalent to a 38% increase in the light extinction that would have occurred without the generating station emissions. The average modeled extinction was 26 Mm^{-1} along the sight path, compared to about ~60 Mm^{-1} modeled and measured at the southern Wilderness boundary. The equivalent deciview changes along the same sight path due to Hayden and Yampa Project were 2.39 dv and 0.67 dv, respectively.

There are large uncertainties in the quantitative results of both the CMB and CC apportionments of $PM_{2.5}$. These uncertainties are amplified when contributions are translated into units of extinction, because chemical-specific extinction efficiencies are very sensitive to changes in particle size for the distributions with modes <0.3 μm found during the MZVS. They are also inaccurate for very high humidities where particle growth is very sensitive to small changes in RH. None of these uncertainties is so large, however, that they contradict the conceptual model. The significant contributors to perceptible haze are significant or large according to both the CMB and CC particle apportionment models and their adjunct extinction and contrast models. Though the magnitudes and frequencies of these contributions can be disputed, the fact that they occur and are perceptible cannot.

7.3 Summary of Mt. Zirkel Visibility Study Findings

Though these findings are specific for the 1995 MZVS period, and the specific magnitudes and frequencies apply only to that year, they are expected to be generally valid for prior and subsequent years providing there are no major changes in emissions and meteorology. Some of the findings listed in this section have already been highlighted as elements of the conceptual model.

7.3.1 Measurements

The measurement network was adequate to detect occurrences of visibility impairment and to assess their causes. The major types of visibility impairment were encountered – including regional haze from transport of secondary aerosol, fire emissions, and other particulate matter; local haze from fires, local ground-level emissions, and secondary sulfates from generating station emissions; and surface and elevated haze layers from fires and generating station primary emissions.

The measurement year and the intensive operating periods were reasonably representative of the conditions encountered in other years, except that May was

exceptionally stormy. No more than 6% of the days during the study showed major deviations from long-term averages for temperatures, cloud-cover, or rainfall. However, May was the wettest on record for the upper Yampa Valley. The observables measured were sufficient to detect the presence or absence of major source contributions, including continental dust, vehicle exhaust, vegetative burning, and primary and secondary coal-fired generating station emissions.

7.3.2 Frequency, Character, and Intensity of Haze

Light extinction in the Wilderness was among the lowest measured in U.S. Class I areas. Winter is the clearest season and summer the haziest. In winter, the median light extinction at Buffalo Pass (next to the southern boundary of the Wilderness) for days not affected by weather was 11 Mm^{-1}, only 30% above that of clean air. In summer, the median was 16 Mm^{-1}. For comparison, these values are about half those measured at the Grand Canyon. High mountain views were obscured by weather for either all morning or all afternoon periods on about 25% to 50% of winter and spring days, about 5% of summer days, and 10% to 20% of fall days.

Haze in the Yampa Valley typically appeared uniform visually, vertically, and horizontally. Surface layers were sometimes perceptible, especially during morning. Layers were noticeable when noncontinuous emissions occurred, especially fires. Although appearing visually uniform, light extinction in the Yampa Valley was often much higher than that measured in the Wilderness and surrounding areas.

Most hazes were regional, with light extinction comparable at locations separated by more than 150 km. On some days, however, contributions to extinction from nearby sources were measurable and perceptible, and these contributions were superimposed on the contributions from a mixture of emissions from inside and outside the region.

7.3.3 Components of Light Extinction

Clean-air scattering was a large or major component of light extinction in the Wilderness for the most daylight hours not affected by weather. Particle light absorption (caused primarily by soot) constituted less than 20% of extinction for most cases, but contributed nearly 50% of extinction during some events. Except during the spring, particle light absorption at Buffalo Pass was almost always less than 15% of total extinction. In spring, it was about 25% of total extinction.

In winter and spring at Gilpin Creek (a lower-elevation, more-northerly site next to the Wilderness), light absorption was often one-third of total extinction but much less in other seasons. The high level at Gilpin Creek may be due to local wood or vegetative burning in the Elk River Valley below the site.

With the exception of the Gilpin Creek site in winter and spring, fine-particle light scattering was the major contributor to extinction that exceeded 20 Mm^{-1}. Coarse particle

scattering in the Wilderness was negligible, as evidenced by comparable light scattering measurements from nephelometers with and without $PM_{2.5}$ inlets.

7.3.4 Chemical Components of Light Extinction

When light extinction exceeded 20 Mm^{-1}, organic carbon and ammonium sulfate each commonly contributed more than 10% of extinction, and together often exceeded 50% of extinction, at all measurement locations for those six-hour and twelve-hour $PM_{2.5}$ samples submitted to chemical analysis. The proportions of their contributions varied from case to case.

$PM_{2.5}$ ammonium nitrate contributed less than 10% of extinction for almost all samples that were chemically analyzed at all sites. Ammonium nitrate was estimated to contribute more than 10% of six-hour average extinction on only two occasions at Buffalo Pass. Elemental carbon was a significant contributor in some events (especially at Gilpin Creek), but it was seldom a majority component of extinction.

Extinction from $PM_{2.5}$ dust seldom contributed more than 10% of extinction. Nine out of 64 aerosol samples at Buffalo Pass showed $PM_{2.5}$ dust contributions that slightly exceeded 10% of extinction, substantially higher and more frequent than dust contributions at other sites in the MZVS. Frequent heavy-duty truck traffic along an unpaved road near the Buffalo Pass site (a result of nearby reservoir construction) may have affected dust contributions, and probably do not appreciably affect extinction along sight paths.

Liquid water was a large component of particles that caused extinction when relative humidities exceeded 80%. The visibility-reducing effects of water-soluble particles such as ammonium sulfate and ammonium nitrate were enhanced at these humidities because the particles absorbed water and acted as nucleation sites for the formation of droplets. The conversion of gaseous SO_2 and oxides of nitrogen was also enhanced when they were absorbed in water drops.

Average sulfate concentrations ranged from 0.81 $\mu g/m^3$ at the Buffalo Pass site to 1.09 $\mu g/m^3$ at the Hayden VOR site. Maximum sulfate concentrations ranged from 1.8 $\mu g/m^3$ at Juniper Mountain to 4.5 $\mu g/m^3$ at Hayden Waste Water, with maxima of 2.1 $\mu g/m^3$ at Buffalo Pass and 1.9 $\mu g/m^3$ at Gilpin Creek. Though Buffalo Pass did not experience the highest sulfate concentrations in the network, it did experience higher contributions of sulfate to extinction because it recorded the highest relative humidities. The highest sulfate contributions to extinction often occurred when sulfate concentrations were below average, but relative humidity exceeded 95% and large nephelometer readings showed Buffalo Pass to be enveloped in a cloud or fog.

7.3.5 Yampa Valley Plume Behavior

In the absence of overriding synoptic influences, Yampa Valley generating station plumes were usually confined below about 400 m (1,300 ft) above ground level and drained down the Valley at night and in the early morning. During midday, they mixed aloft and

coupled with the upper level winds that typically transported the plumes toward the southern end of the Wilderness.

Both measurements and everyday plume modeling showed that SO_2 arrived at Buffalo Pass in pulses with typical durations of less than one to a few hours. SO_2 is a colorless gas that causes negligible light extinction. SO_2 pulses rarely lasted more than six hours, and SO_2 concentrations were negligible (i.e., below 0.2 ppbv) between pulses. The calculated magnitude and frequency of SO_2 pulses was in qualitative agreement with the measurements. The agreement between the timing of the modeled and measured pulses was often good and sometimes excellent.

Cumulative frequency distributions of SO_2 concentrations calculated by everyday plume modeling showed them to be largest at the southern end of the Wilderness, near Buffalo Pass. SO_2 levels decreased uniformly with distance north in the Wilderness. Detailed modeling with multiple source emissions showed the same results. This is consistent with the prevailing daytime winds. High-altitude receptor sites near the southern end of Wilderness, such as Buffalo Pass, provide an upper limit for the concentrations of emissions from Yampa Valley generating stations in the Wilderness.

The highest modeled SO_2 concentrations were at Mad Creek, a low-elevation receptor site in a canyon in the southwest corner of the Wilderness. The distance to Yampa Valley generating stations is at a minimum in this corner of the Wilderness.

Model results indicated that the emissions from the Hayden and Craig stations arrived in the Wilderness together most of the time. Emissions from only one of these stations rarely arrived at the Wilderness in significant amounts without being accompanied by emissions from the other station.

Trajectory analyses for episodes indicated that Yampa Valley generating station emissions can be transported directly to Buffalo Pass during midday in 2 to 5 hours, but emissions that are emitted into the early morning drainage flows could take 6 to 11 hours to arrive. Craig station emissions typically took 1 to 2 hours longer in transit than Hayden station emissions.

The modeled percentage contribution of each generating station unit to SO_2 concentrations in the Wilderness was approximately the same for all locations in the Wilderness, both for all hours and for only those hours with SO_2 concentrations greater than 2 ppbv. The approximate percentage contributions were: Hayden Unit 1, 40 to 45%; Hayden Unit 2, 35 to 40%; Craig Unit 1, 6 to 8%; Craig Unit 2, 7 to 9%; and Craig Unit 3, 3 to 4%.

The calculated plume rise for Hayden Unit 2 was greater than for Unit 1, causing more dilution before the emissions reach ground level.

In the absence of relative humidities greater than 80% (a possible surrogate for passage through fog or clouds), the Yampa Valley generating station plumes rarely cause perceptible increases in light scattering in the Wilderness.

After passage through fogs or clouds, sufficient transformation of SO_2 to sulfate can take place to cause perceptible changes in light scattering in the Wilderness. On at least two days (09/18/95 and 08/23/95), increases in haze of one to a few hours duration that coincided with the arrival of SO_2 attributed to the Yampa Valley generating stations were noticeable on video views of the Wilderness and detectable by the nephelometers at Buffalo Pass.

The largest perceptible effects of the Yampa Valley generating stations on visibility in the Wilderness (including the two events noted above) occurred when the emissions accumulated in fogs or low clouds in the early morning or were mixed into higher clouds after mixing aloft and were subsequently transported to the Wilderness in the afternoon. The interaction of the emissions with fogs or clouds allowed wet conversion of SO_2 to sulfate.

Various analyses suggest that high relative humidity and SO_2 concentrations greater than about 1-2 ppb may be a reasonable surrogate for conditions when generating station emissions might have visible effects. Trajectory model results for each study day and measured relative humidity at Buffalo Pass suggest that the plumes arrived in the Wilderness at these concentrations during conditions when relative humidity was greater than 80% on 3% - 8% of the daylight hours during the year, with the highest incidence (10% - 16%) in May (which was the wettest May on record) and the lowest (0.5% - 2%) in August. During many of these hours, views would have been obscured by weather.

The addition of ammonia to the Hayden plumes has a negligible effect on transformation rates or the formation of ammonium nitrate.

Under nonroutine operating conditions, primary particle emissions from generating station stacks caused perceptible, layered hazes with durations of several hours. These were not due to SO_2 emissions. For example on 01/03/95, a clearly defined, coherent plume from the Hayden station could be seen in a west-facing video view from a camera on Storm Peak (which is south of Buffalo Pass). The plume moved toward Storm Peak at nearly the same elevation as the camera. The extent to which the plume reached or rose over the Continental Divide could not be determined because it could not be seen in views to the north. However, it is clear that the potential existed for the plume to reach the Storm Peak area. This was the only time the time-lapse videos showed that a layered haze or well-defined plume attributed to one of the Yampa Valley generating stations reached the vicinity of the Wilderness Area.

Haze events associated with the formation of secondary particles (sulfate and associated water) that could be detected in the time-lapse videos showed a haze that was mixed to the ground and did not have apparent edges or top. Therefore, haze pulses identified from nephelometer measurements of light scattering at elevated locations were considered to be uniform haze rather than layered haze.

Chemical compositions of primary particle emissions were sufficient to separate coal-fired generating stations from other contributors, but not from each other. Abundances of sulfur-32 and sulfur-34 measured in source samples were sufficient to distinguish coal-fired generating station, motor vehicle exhaust, and geothermal hot springs from one another. The abundance of these isotopes in coal-fired generating station emissions were too variable, and

too similar to those in background air, to improve the resolution between Yampa Valley generating station and regional sulfate contributions.

Craig Unit 3 emissions contain no selenium, and its profile is too similar to geological material to be distinguished from that contributor.

7.3.6 Source Contributions to Light Extinction

For primary particles in the $PM_{2.5}$ size fraction, a multi-state (major parts of Colorado, Wyoming, and Utah) emissions inventory showed that motor vehicles accounted for ~46% of primary $PM_{2.5}$, with summer emissions distributed among vehicle exhaust, paved road dust, and unpaved road dust. Another 21% of $PM_{2.5}$ in the summer was emitted from natural dust sources, while 11% was emitted from agricultural tilling. During the winter months, residential wood and coal combustion were significant $PM_{2.5}$ sources, constituting 11% of the emissions.

Residential coal combustion and geothermal hot springs were minor contributors to ammonium sulfate. Emissions surveys showed them to constitute less than 1% of sulfur emissions in northwestern Colorado and a multi-state region. Coal combustion, mostly in power generation stations, was the largest sulfur emitter in the Yampa Valley and in a multi-state region. Yampa Valley SO_2 emissions were estimated to be ~6% of all SO_2 emissions in the multi-state region.

Sulfur-32 and sulfur-34 isotopic abundances in emissions from Yampa Valley coal-fired generating stations, motor vehicle exhaust, and geothermal hot springs differed sufficiently to allow contributions to sulfur from any two of these sources to be distinguished from each other. Isotopic abundances in sulfur emissions from Yampa Valley coal-fired generating stations and sulfur in background air were too similar, within measured variability, to allow their separation into separate categories. This is possibly due to the dominance of coal-burning as the major SO_2 emitter in the region.

Motor vehicle exhaust and fires (residential, wildfires, and prescribed burning) were the major contributors to the highest organic carbon concentrations. Secondary organic carbon could not be separately resolved and is most probably apportioned as vehicle exhaust by receptor models.

The contributions to extinction of Craig Units 1 and 2 (the Yampa Project) and Hayden station were calculated using the plume chemistry model for a variety of sight paths. The changes in light extinction and contrast that would occur along the sight paths from eliminating those emissions from the Hayden station and Yampa Project that were within the Wilderness boundaries were modeled. The highest one-hour percentage contribution estimated for these generating units along any modeled sight path on any day was 27% of total extinction (b_{ext}) on 09/18/95, with 21% due to Hayden station and 6% to the Yampa Project. This is equivalent to a 38% increase in the extinction that would have occurred without the generating station emissions. For this sight path (from Mt. Ethel to the Continental Divide Trail), the average modeled b_{ext} was 26 Mm^{-1}, compared to about

60 Mm^{-1} at Buffalo Pass. The equivalent deciview changes along the same sight path due to the Hayden station and Yampa Project were 2.39 dv and 0.67 dv, respectively. Sight-path extinction and generating-station percentages would be lower than for Buffalo Pass, because the Buffalo Pass site is generally near the location of the maximum extinction, while the sight paths cover a larger area.

Contrast calculations for 09/18/95 for the above sight path indicated that the total generating station contribution to extinction might be perceptible if images with and without the contribution were viewed side-by-side.

Changes in b_{ext}, measured and modeled, correspond with observed and perceptible changes in contrasts. The OPTEC nephelometer at Buffalo Pass measured a change of total scattering of approximately 36 Mm^{-1} from 1100 to 1300 MST during the 09/18/95 event, accompanied by a 2.1 ppb increase in SO_2. This light scattering change is much larger than the 7.3 Mm^{-1} maximum change along a sight path due to Hayden and Yampa Project emissions calculated by the plume chemistry model. It is also large compared to commonly discussed perception thresholds. In addition, an obvious haze pulse was perceptible in the time-lapse videos taken from Storm Peak during this event. Given the relative contributions of Hayden Station and the Yampa Project to this event, it is likely that the Hayden Station contribution would have been perceptible in the absence of the Yampa Project contribution. It cannot be determined that the Yampa Project contribution would have been perceptible on its own.

For the 10/12/95 event, the afternoon extinction at Buffalo Pass estimated by the plume model was about 21 Mm^{-1}. This is similar to the extinction measured at the site in midday while clouds were not present. Most of this extinction was attributed to clean-air scattering and a mixture of regional sources. Receptor modeling estimated the significant and large contributors to be clean-air scattering, suspended dust, motor vehicle or secondary organics, fires, and regional sulfate. The Yampa Valley generating station contributions were estimated to be about 14% by the plume model and less than 1% by the receptor model. For the same day, the average extinction calculated by the plume model for the sight paths varied from 12 to 16.5 Mm^{-1}.

10/12/95 is of interest because the maximum deciview change due to the Yampa Project was estimated to occur on that day. On most days, the contribution of Hayden station was about three times that of the Yampa Project. On this day, 9% of the 14% at Buffalo Pass was attributed to Hayden station and 5% to Yampa Project by the plume chemistry model. For the Mt. Ethel to the Continental Divide Trail View, a b_{ext} of 16.5 Mm^{-1} was estimated with about 13% of this attributed to Hayden station and the Yampa Project combined. For this view, the contribution of the Yampa Project was estimated by the plume model to exceed that of Hayden station. Unit 2 at Hayden station had been shut down for maintenance from 10/07/95 through 10/11/95, just prior to this event. The 13% was attributed as 0.33 Mm^{-1} or 2% to Hayden station and 1.8 Mm^{-1} or 11% to the Yampa Project, or alternatively, 0.2 dv to Hayden station and 1.16 dv to the Yampa Project. For this view, the Yampa Project contribution exceeded 1 dv. This value has been discussed as a change that can be noticed by casual observers. This applies, however, for views over distances close to the visual range of

the objects observed. For short views such as those within the Wilderness, it is unlikely that the above 1.8 Mm^{-1} b_{ext} change corresponding to the 1.16 dv change would be perceptible by most observers.

For the periods modeled above, there were large differences in the calculated apparent contrast and contrast transmittance for different sight paths in the Wilderness. These differences were primarily caused by differences in the brightness of the target, which depend on its reflectance and orientation to the sun. For most sight paths, diurnal changes in illumination caused changes in the calculated apparent contrast and contrast transmittance that were far greater than any changes due to changes in the emissions.

Values of the deciview haze index changed by as much as 3.2 units when the effects of the emissions of both the Hayden station and the Yampa Project were omitted. When only the effects of the Hayden station emissions were omitted, the largest change in dv was 2.4 units, and the largest change from omitting the effects of Yampa Project emissions was 1.16 units. A one-unit change in dv corresponds to a 10% change in b_{ext}.

For all episodes and views modeled, the largest change in apparent contrast of ridges against the horizon sky caused by omitting the effects of both the Hayden station and Yampa Project emissions was 0.066 units. The largest change in contrast transmittance for features on the surfaces of the targets was 0.092 units. For Hayden station alone, the comparable largest changes for contrast and contrast transmittance were 0.039 and 0.068 units, respectively. For the Yampa Project alone, the comparable largest changes for contrast and contrast transmittance were 0.027 and 0.032 units, respectively.

These calculated contrast changes are large enough to be perceived if they were displayed in a split-screen image, but it is not known if they are large enough to be perceived by an observer in the Wilderness comparing observations made at different times. Of more than 3,000 cases of days/hours/sight-paths modeled, several dozens of cases for Hayden station exceeded 2% contrast, while only 10 cases (2 days) exceeded this value for the Yampa Project (see Section 6.8).

The maximum values of the calculated changes in contrast and contrast transmittance due to changes in generating station emissions were very nearly the same for clear skies and for completely overcast skies.

Yampa Valley generating station contributions are always superimposed on contributions to extinction from other sources. For more than 90% of the daylight hours, their contribution to visibility impairment in the Wilderness was probably negligible. However, during the August-October period, when fine-particle light scattering was measured, approximately twelve events were identified with measurable increases in light scattering accompanying SO_2 pulses. Haze pulses were observed in the time-lapse videos during two of these events (08/23/95 and 09/18/95). In both, the light extinction increased from ~20 to ~60 Mm^{-1} over a few hours. In the remaining cases, either the camera views were obscured by weather or changes in haze could not be distinguished in the videos. For

the two events noted, the generating station plumes passed through clouds or fog, and ammonium sulfate was a large contributor to the extinction.

Increasing ammonia does not effectively increase ammonium nitrate concentrations to significant levels. An aerosol evolution and equilibrium model demonstrated that doubling ammonia concentrations increased particulate nitrate concentrations only when liquid water contents were low. This increase was offset by the small amounts of particle nitrate contained in the smaller amounts of liquid water, with the result that, on average, the increase in particle nitrate was less than 0.1 $\mu g/m^3$.

Increases in particulate nitrate did not exceed 0.1 $\mu g/m^3$ with decreases in sulfate concentrations. Reducing sulfate concentrations frees up ammonia for potential reaction with nitric acid to form particulate ammonium nitrate, but sulfate reductions also reduce the liquid water available for reactions. These phenomena counteract each other.

7.3.7 Limitations of Model Results

Aside from local generating station emissions that were directly measured, emission rate estimates were only qualitatively accurate in space and time, and may differ from reality by up to an order of magnitude for specific visibility events. This is especially true of fires that are episodic and may have regional, as well as local, influences.

Chemical-specific extinction efficiencies were very sensitive to changes in particle size for the distributions with modes <0.3 μm found during the MZVS. They were also inaccurate for very high humidities (>95%), but views were often obscured by weather under these conditions.

Chemical Mass Balance modeling did not distinguish between separate generating station contributions. Both dry- and wet-aged profiles provided adequate fits to the data. The profile used to apportion contributions from Yampa Valley generating stations was selected for a sample based on evidence of plume processing by fogs and clouds, even though a profile that did not undergo such processing would explain the measurements equally well. Lacking measurements of specific organic compounds, the motor vehicle source contributions probably explain secondary organic aerosol contributions as well as those from directly emitted exhaust. Uncertainties for motor vehicle contributions were high, often exceeding the source contribution estimate.

Since modeled hourly SO_2 concentrations from the Hayden and Craig generating stations showed reasonable agreement with the measured SO_2 concentrations, everyday plume modeling results should be reliable for drawing conclusions related to the frequency of occurrence and locations of SO_2 emissions from the two generating stations and their relative contributions to SO_2.

CALMET/CALPUFF plume chemistry modeling often underestimated measured $PM_{2.5}$ and extinction. This is probably due to sources contributions from outside the emissions domain, inaccurate emissions estimates for intermittent sources during episodes,

and inadequate mechanisms for determining aqueous-phase conversions of SO_2 to sulfate that are the cause of most events with perceptible visibility impairments.

Results obtained from CALMET/CALPUFF, CMB, and continuous measurements are qualitatively comparable in terms of timing and magnitude of nearby generating station contributions, but they show substantial quantitative differences. Results are most comparable for dry situations when local generating station contributions to ammonium sulfate were low. They were in greatest disagreement for those cases where transformations in fogs and clouds occurred.

Most relations used in the contrast calculations were accurate, but the diffuse skylight flux and horizon sky radiance were calculated from simplified relations of uncertain accuracy. The effect of these simplifications on the calculated contrasts has not been determined.

8.0 REFERENCES

Air Resource Specialists (1994a). Classification of 35mm Slides Associated with the Mt. Zirkel Wilderness Area, Colorado Visibility Monitoring Program, 1990 through 1994 Monitoring Seasons. Air Resource Specialists Inc., Fort Collins, CO. August 1, 1994.

Air Resource Specialists (1994b). Nephelometer Data Reduction and Validation (IMPROVE Protocol). Technical Instruction 4400-5010. Air Resource Specialists Inc., Fort Collins, CO. March 1995.

Air Resource Specialists (1995a). Mt. Zirkel Reasonable Attribution Study of Visibility Impairment Data Transmittal Report Series – Time-Lapse Video and 35mm Slide Scene Monitoring Data Transmittal Report for the Period December 14, 1994, through March 31, 1995. Air Resource Specialists Inc., Fort Collins, CO. June 30, 1995.

Air Resource Specialists (1995b). Mt. Zirkel Reasonable Attribution Study of Visibility Impairment Data Transmittal Report Series – Revised Time-Lapse Video and 35mm Slide Scene Monitoring Data Transmittal Report for the Period April 1 through June 30, 1995. Air Resource Specialists Inc., Fort Collins, CO. Revised February 2, 1996.

Air Resource Specialists (1995c). Mt. Zirkel Reasonable Attribution Study of Visibility Impairment Data Transmittal Report Series – Time-Lapse Video and 35mm Slide Scene Monitoring Data Transmittal Report for the Period July 1 through September 30, 1995. Air Resource Specialists Inc., Fort Collins, CO. December 28, 1995.

Air Resource Specialists (1995d). Mt. Zirkel Reasonable Attribution Study of Visibility Impairment Data Transmittal Report Series – Time-Lapse Video and 35mm Slide Scene Monitoring Data Transmittal Report for the Period October 1 through November 30, 1995. Air Resource Specialists Inc., Fort Collins, CO. February 15, 1996.

Albert, D.J., and P.K. Hopke (1981). A Determination of the Sources of Airborne Particles Collected during the Regional Air Pollution Study. *Atmos. Environ.* **15**(5):675-687.

Allwine, K. and C. Whiteman (1985). MESLAR: A Mesoscale Air Quality Model for Complex Terrain: Volume 1--Overview, Technical Description and User's Guide. Prepared by Pacific Northwest Laboratory, Richland, WA.

Andersen, S.R. (1995a). Mt. Zirkel Visibility Study Network Performance Audit Report - 1995 Winter Intensive Study. Prepared for Technical Steering Committee, Colorado Dept. of Public Health and Environment, Air Pollution Control Division, Denver, CO. June 1995.

Andersen, S.R. (1995b). Mt. Zirkel Visibility Study Network Performance Audit Report - 1995 Summer Intensive Study. Prepared for Technical Steering Committee, Colorado Dept. of Public Health and Environment, Air Pollution Control Division, Denver, CO. September 1995.

Annegarn, H.J., G.M. Braga Marcazzan, E. Cereda, M. Marchinonni, and A. Zucchiatti (1992). Source Profiles by Unique Ratios (SPUR) Analysis: Determination of Source Profiles from Receptor-Site Streaker Samples. *Atmos. Environ.* **26**(2):333-343.

Atkinson, R., A. Lloyd, and L. Winges (1982). An Updated chemical Mechanism for Hydrocarbon/NO_x/SO_x Photo Oxidation Suitable for Inclusion in Atmospheric Simulation Models. *Atmos. Environ.* **16**:1341.

Bavelas, P. (1995). Personal communication with Mr. Paul Bavelas of The Energy House (801-261-3210) and Mr. Marty Wolf of Radian International. August 11, 1995.

Bennett, P. (1995). Personal communication between Ms. Patricia Bennett of Colorado West Board of Realtors (970-824-8226) and Mr. Marty Wolf of Radian International. July 20, 1995.

Berkson, J. (1950). Are There Two Regressions? *J. Am. Statist. Assoc.,* **45**:164-180.

Bevington, P.R. (1969). Data Reduction and Error Analysis for the Physical Sciences. McGraw Hill, New York, NY.

Blumenthal, D.L. (1995). Mt. Zirkel Wilderness Area Reasonable Attribution Study of Visibility Impairment – Program Management Plan. Working Draft No. 3.1, STI Document No. STI-95031-1528-WD3.1. Prepared for Technical Steering Committee, Colorado Department of Public Health and Environment, Denver, CO, by Sonoma Technology Inc., Santa Rosa, CA. September 1995.

Bodhaine, B.A. (1979). Measurement of the Rayleigh Scattering Properties of Some Gases with a Nephelometer. *Appl. Opt.* **18**:121-125.

Bohren, C.F., and D.R. Huffman (1983). Absorption and Scattering of Light by Small Particles. John Wiley & Sons, New York.

Brown, D. (1995). Personal communication between Ms. DeLaine Brown of Moffat County Cooperative Extension (970-824-6673) and Mr. Marty Wolf of Radian International. November 16, 1995..

Bucholtz, A. (1995). Rayleigh-Scattering Calculations for the Terrestrial Atmosphere. *Appl. Opt.* **34**:2765-2773.

Cappa, J.A., and H.T. Hemborg (1995). 1992-1993 Low-Temperature Geothermal Assessment Program, Colorado. Open File Report 95-1. Colorado Geological Survey, Division of Minerals and Geology, Department of Natural Resources, Denver, CO.

Carson., D. (1973). The Development of a Dry, Inversion-Capped, Convectively Unstable Boundary Layer. *Quart J. Roy. Meteor. Soc.*, **99**:450-467.

Chagnon, D., T.B. McKee, and N.J. Doesken (1993). Annual Snowpack Patterns across the Rockies: Long-Term Trends and Associated 500-mb Synoptic Patterns. *Monthly Weather Review*, **121**(3): 633-647.

Chan, T., and M. Lippmann (1977). Particle Collection Efficiencies of Sampling Cyclones: An Empirical Theory. *Environ. Sci. Technol.*, **11**(4):377-386.

Chow, J.C., J.G. Watson, D.H. Lowenthal, Z. Lu, C.A. Frazier, L.C. Pritchett, and B.A. Hinsvark (1992). San Joaquin Valley Air Quality Study (SJVAQS)/Atmospheric Utility Signatures - Predictions and Experiment (AUSPEX), Monitoring and Analysis for Aerosols and Visibility, Volume III: Aerosol Measurements and Data Bases, Final Report. DRI Document #8743.3F, prepared for Pacific Gas and Electric Co., San Francisco, CA, by the Desert Research Institute, Reno, NV.

Chow, J.C., J.G. Watson, D.H. Lowenthal, C.A. Frazier, B.A. Hinsvark, L.C. Pritchett, and G.R. Neuroth (1992). Wintertime PM_{10} and $PM_{2.5}$ Mass and Chemical Compositions in Tucson, Arizona. In *Transactions: PM_{10} Standards and Non-Traditional Particulate Source Controls*, J.C. Chow and D.M. Ono, eds. Air and Waste Management Assoc., pp. 231-243.

Chow, J.C., J.G. Watson, D.H. Lowenthal, P. Solomon, K. Magliano, S. Ziman, and L.W. Richards (1993). PM_{10} and $PM_{2.5}$ Compositions in California's San Joaquin Valley. *Aerosol Sci. Technol.*, **18**:105-128.

Chow, J.C., J.G. Watson, J.L. Bowen, A.W. Gertler, C.A. Frazier, K.K. Fung, and L. Ashbaugh (1993). A Sampling System for Reactive Species in the Western U.S. In *Sampling and Analysis of Airborne Pollutants*, E. Winegar, ed. American Chemical Society, Washington, DC, pp. 209-228.

Chow, J.C., J.G. Watson, L.C. Pritchett, W.R. Pierson, C.A. Frazier, and R.G. Purcell (1993). The DRI Thermal/Optical Reflectance Carbon Analysis System: Description, Evaluation and Applications in U.S. Air Quality Studies. *Atmos. Enviro*n., **27A**:1185-1201.

Chow, J.C., E.M. Fujita, J.G. Watson, Z. Lu, D.R. Lawson, and L.L. Ashbaugh (1994). Evaluation of Filter-Based Aerosol Measurements During the 1987 Southern California Air Quality Study. *Environ. Mon. Assess*., **30**:49-80.

Chow, J.C., J.G. Watson, E.M. Fujita, Z. Lu, D.R. Lawson, and L.L. Ashbaugh (1994). Temporal and Spatial Variations of $PM_{2.5}$ and PM_{10} Aerosol in the Southern California Air Quality Study. *Atmos. Environ.*, **28**(12):2061-2080.

Chow, J.C., J.G. Watson, J.E. Houck, L.C. Pritchett, C.F. Rogers, C.A. Frazier, R.T. Egami, and B.M. Ball (1994). A Laboratory Resuspension Chamber to Measure Fugitive

Dust Size Distributions and Chemical Compositions. *Atmos. Environ.,* **28**(21):3463-3481.

Chow, J.C., J.G. Watson, P.A. Solomon, R.H. Thuillier, K.L. Magliano, S.D. Zinman, D.L. Blumenthal, L.W. Richards (1994). Planning for SJVAQS/AUSPEX Particulate Matter and Visibility Sampling. In *Planning and Managing Air Quality Modeling and Measurement Studies: A Perspective Through SJVAQS/AUSPEX*, P.A. Solomon, ed. Lewis Publishers, Chelsea, MI, pp. 171-216.

Chow, J.C. (1995). Critical Review: Measurement Methods to Determine Compliance with Ambient Air Quality Standards for Suspended Particles. *J. Air & Waste Management Assoc.* **45**:320-382.

Chow, J.C., D. Fairley, J.G. Watson, R. DeMandel, E.M. Fujita, D.H. Lowenthal, Z. Lu, C.A. Frazier, G. Long, and J. Cordova (1995). Source Apportionment of Wintertime PM_{10} at San Jose, California. *J. Environ. Engineering* **21**(5):378-387.

Chow, J.C., J.G. Watson, Z. Lu, D.H. Lowenthal, C.A. Frazier, P.A. Solomon, R.H. Thuillier, and K. Magliano (1996). Descriptive Analysis of $PM_{2.5}$ and PM_{10} at Regionally Representative Locations During SJVAQS/AUSPEX. *Atmos. Environ.*, **30**:2079-2112.

Chow, J.C., J.G. Watson, D.H. Lowenthal, and R.J. Countess (1996). Sources and Chemistry of PM_{10} Aerosol in Santa Barbara County, California. *Atmos. Environ.* **30**(9):1489-1499.

Clark, A.D., K.J. Noone, J. Heintzenberg, S.G. Warren, and D.S. Scott (1987). Aerosol Light Absorption Measurement Techniques: Analysis and Intercomparisons. *Atmos. Environ.* **21**(6):1455-1465.

Collins, W.G., and L.S. Gandin (1989). The Hydrostatic Checking of Radiosonde Heights and Temperatures. Part II. Report prepared for the National Weather Service by NOAA, Boulder, CO, NMC Office Note 351, 31 pp.

- Cowherd (1995) B1-2

Currie, L.A., R.W. Gerlach, C.W. Lewis, W.D. Balfour, J.A. Cooper, S.L. Dattner, R.T. DeCesar, G.E. Gordon, S.L. Heisler, P.K. Hopke, J.J. Shah, G.D. Thurston, and H.J. Williamson (1984). Interlaboratory Comparison of Source Apportionment Procedures: Results for Simulated Data Sets. *Atmos. Environ*., **18**:1517.

Daisey, J.M., and T.J. Kneip (1981). Atmospheric Particulate Organic Matter: Multivariate Models for Identifying Sources and Estimating their Contributions to the Ambient Aerosol. In *Atmospheric Aerosol-Source/Air Quality Relationship*, E.S. Macias and P.K. Hopke, eds. American Chemical Society, Washington, DC, pp. 197-221.

Daisey, J.M. (1985). A New Approach to the Identification of Sources of Airborne Mutagens and Carcinogens: Receptor Source Apportionment Modeling. *Environ. Int.* **11**:285-291.

DeCesar, R.T., S.A. Edgerton, M.A.K. Khalil, and R.A. Rasmussen (1985). Sensitivity Analysis of Mass Balance Receptor modeling: Methyl Chloride as an Indicator of Wood Smoke. *Chemosphere* **14**(10):1495-1501.

Dickson, C.L., and G.P. Sturm Jr. (1994). Diesel Fuel Oils, 1994. National Institute for Petroleum and Energy Research, Bartlesville, Oklahoma. December 1994.

Dickson, R.J., and W.R. Oliver (1991). Emissions Models for Regional Air Quality Studies. *Environ. Sci. & Technol.* **25**(9):1533-1535.

Dickson, R.J., W.R. Oliver, E.L. Dickson, and V.M. Sadeghi (1995). Development of an Emissions Inventory for Assessing Visual Air Quality in the Western United States. Report prepared for the Emissions Subcommittee of the Grand Canyon Visibility Transport Commission, Project VARED, and the Electric Power Research Institute, by Radian Corporation, Sacramento, CA.

Dixon, J.K. (1940). The Absorption Coefficient of Nitrogen Dioxide in the Visible Spectrum. *J. Chem. Phys*., **8**:157.

Doesken, N.J. (1996). Evaluation of Meteorological Conditions in Northwest Colorado during the December 1994 through November 1995 Period and Comparison with Historical Conditions for that Area. Report prepared by Air Resource Specialists, Fort Collins, CO. March 1996.

Douglas, S., and R. Kessler (1988). User's Guide to the Diagnostic Wind Field Model (Version 1.0). Systems Applications, Inc., San Rafael, CA.

Douglas, S., R. Kessler, and E. Carr (1990). User's Guide for the Urban Airshed Model, Version III: User's Manual for the Diagnostic Wind Model. Prepared for the U.S. Environmental Protection agency, EPA-450/4-90-007C, by Systems Applications, Inc., San Rafael, CA.

Dye, T.S., C.G Lindsey., Roberts P.T., and J.A. Anderson (1994). Evaluation of Mixing Depths Derived from 915 MHz Radar Profiler Reflectivities during Recent Air Quality Studies. In *Preprints of the Third International Symposium on Tropospheric Profiling: Needs and Technologies, Hamburg, Germany, August 30-September 2*, pp. 120-122.

Dye, T.S., C.G. Lindsey and J.A Anderson. (1995). Estimates of Mixing Depths from "Boundary Layer" Profilers. In *Preprints of the 9th Symposium on Meteorological Observations and Instrumentation, Charlotte, NC, March 27-31*, STI-94212-1451.

Dzubay, T.G., R.K. Stevens, W.D. Balfour, H.J. Williamson, J.A. Cooper, J.E. Core, R.T. DeCesar, E.R. Crutcher, S.L. Dattner, B.L. Davis, S.L. Heisler, J.J. Shah, P.K Hopke and D.L. Johnson (1984). Interlaboratory Comparison of Receptor Model Results for Houston Aerosol. *Atmos. Environ.* **18**:1555-1566

- Dzubay *et al.* (1988) B3-1

E. H. Pechan & Associates (1994). Development of the OPPE Particulate Programs Implementation Evaluation System. Report prepared for the Office of Policy, Planning, and Evaluation/Office of Policy Analysis, U.S. EPA, Washington, D.C.

Eatough, D.J., N. Aghdaie, M. Cottam, T. Gammon, L.D. Hansen, E.A. Lewis, and R.J. Farber (1990). Loss of Semi-Volatile Organic Compounds from Particles During Sampling on Filters. In *Transactions, Visibility and Fine Particles*, C.V. Mathai, ed. Air & Waste Management Association, Pittsburgh, PA, pp. 146-156.

Edlen, B. (1953). The Dispersion of Standard Air. *J. Opt. Soc. Am*. **43**:339.

Eldred, R.A., and T.A. Cahill (1994). Trends in Elemental Concentrations of Fine Particulates at Remote Sites in the United States of America. *Atmos. Environ.* **28**(5):1005-1022.

Ely, D., C. Campbell, L. Svoboda, S. McCaffrey, D. Haddow, and K. Wolfe (1993). Certifying Visibility Impairment in the Mt. Zirkel Wilderness Area, Technical Background Document, prepared by the Colorado Department of Health/Air Pollution Control Division.

Forrest, J., and L. Newman (1973). Sampling and Analysis of Atmospheric Sulfur Compounds for Isotope Ratio Studies. *Atmos. Environ.* **7**:561-573.

Friedlander, S.K (1973). Chemical Element Balances and Identification of Air Pollution Sources. *Environ. Sci. & Technol.* **7**(3):235-240.

Fujita, E.M., J.G. Watson, J.C. Chow, and Z. Lu (1994). Validation of the Chemical Mass Balance Receptor Model Applied to Hydrocarbon Source Apportionment in the Southern California Air Quality Study. *Environ. Sci. & Technol.* **28**(9):1633-1649.

Fujita, E.M., J.G. Watson, J.C. Chow, and K.L. Magliano (1995). Receptor Model and Emissions Inventory Source Apportionments of Nonmethane Organic Gases in California's San Joaquin Valley and San Francisco Bay Area. *Atmos. Environ.* **29**(21):3019-3035.

Gartrell, G., Jr., and S.K. Friedlander (1975). Relating Particulate Pollution to Sources: The 1972 California Aerosol Characterization Study. *Atmos. Environ.* **9**:279-299.

Gordon, G.E., W.H. Zoller, G.S. Kowalczyk, and S.W. Rheingrover (1981). Composition of Source Components needed for Aerosol Receptor Models. In *Atmospheric Aerosol-*

Source/Air Quality Relationships, E.S. Macias and P.K. Hopke, eds. American Chemical Society, Washington, DC, pp. 51-74.

Gundel, L.A., W.H. Benner, and A.D.A. Hansen (1994). Chemical Composition of Fog Water and Interstitial Aerosol in Berkeley, California. *Atmos. Environ.* **28**(16):2715-2725, 1994.

Hackley, K.C., and T.F. Anderson (1986). Sulfur Isotopic Variations in Low-Sulfur Coals from the Rocky Mountain Region. *Geochimica et Cosmochimica Acta* **50**:1703-1713.

Hanel, G. (1976). The Properties of Atmospheric Aerosol Particles as Functions of Relative Humidity at Thermodynamic Equilibrium with the Surrounding Moist Air. *Adv. Geophys.* **19**:73-88.

Hanel, G., and M. Lehmann (1981). Equilibrium Size of Aerosol Particles and Relative Humidity: New Experimental Data from Various Aerosol Types and their Treatment for Cloud Physics Application. *Contrib. Atmos. Phys.* **54**:57-71.

Haney, J.L., N.K. Lolk, T.C. Myers, M.C. Causley, C.K. Steiner, L. Gardner, G.Z. Whitten, S.G. Douglas, C.S. Burton, P.T. Roberts, T.S. Dye, M.E. Korc, C.G. Lindsey, H.H. Main, and S.E. Ray (1995). Gulf of Mexico Air Quality Study – Volume I: Summary of Data Analysis and Modeling – Final Report. Prepared for U.S. Dept. of the Interior, Minerals Management Service, Gulf of Mexico OCS Region, New Orleans, LA, by Systems Applications International, San Rafael, CA, and Sonoma Technology Inc., Santa Rosa, CA, under OCS Study MMS-95-0038 (SYSAPP-95/013d). August 1995.

Henry, R.C. (1984). Fundamental Limitations of Factor Analysis Receptor Models. In *Aerosols: Science, Technology, and Industrial Applications of Airborne Particles,* B.Y.H. Liu, D.Y.H. Pui, and H.J. Fissan, eds. New York: Elsevier Press. 359 p.

Henry, R.C. (1987). Psychophysics, Visibility, and Perceived Atmospheric Transparency. *Atmos. Envirn.* **21**:159-64.

Henry, R.C. (1992). Dealing with Near Collinearity in Chemical Mass Balance Receptor Models. *Atmos. Environ.* **26**A(5):933-938.

Hidy, G.M. (1985). Jekyll Island Meeting Report: George Hidy Reports on the Acquisition of Reliable Atmospheric Data. *Environ. Sci. Technol.,* **19**(11):1032-1033.

Hildemann, L.M., G.R. Markowski, and G.R. Cass (1991). Chemical Composition of Emissions from Urban Sources of Fine Organic Aerosol. *Environ. Sci. Technol*., **25**(4):744-759.

Holzworth, G.C. (1972). Mixing Heights, Windspeeds and Potential for Urban Air Pollution Throughout the Contiguous United States. AP-101. U.S. Environmental Protection Agency, Research Triangle Park, NC.

Holtslag, A. and A. van Ulden (1983)Simple Estimates of Nighttime Surface Fluxes from Routine Weather Data. KNMI Scientific Report, W.R. 82-4

Hopke, P.K., G.E. Gordon, W.H. Zoller, and E.S. Gladney (1976). Comparisons of Source Identification Techniques for Trace Elements in Ambient Air Particulates. In *Proceedings of the American Chemical Society 172nd National Meeting, San Francisco, CA.*

Horvath, H. (1993). Atmospheric Light Absorption - A Review. *Atmos. Environ.*, **27A**(3):293-317.

Horvath, H. (1993). Comparison of Measurement of Aerosol Optical Aborption by Filter Collection and a Transmissometric Method. *Atmos. Environ.*, **27A**(3):319-325.

Javitz, H.S., and J.G. Watson (1988). Feasibility Study of Receptor Modeling for Apportioning Utility Contributions to Air Constituents, Deposition Quality and Light Extinction. Report prepared by SRI International, Menlo Park, CA, for the Electric Power Research Institute, Palo Alto, CA.

Kendall, M.G. (1951). Regressions, Structure and Functional Relationship, Part I. *Biometrika,* **38**:11-25; also Part II, *Biometrika,* **39**:96-108.

Kendra, M. (1995). Personal conversation with Mr. Mark Kendra, Colorado Department of Public Health and Environment, Air Pollution Control Division, Denver, CO. May 31, 1995.

Kim, Y.P., J.H. Seinfeld, and P. Saxena (1993a). Atmospheric Gas-Aerosol Equilibrium I: Thermodynamic Model. *Aerosol Sci. & Technol.* **19**(2)157-181.

Kim, Y.P., J.H. Seinfeld, and P. Saxena (1993b). Atmospheric Gas-Aerosol Equilibrium II: Analysis of Common Approximations and Activity Coefficient Calculation Methods. *Aerosol Sci. & Technol.* **19**(2):182-198.

King, D.E. (1977). Methods and Standards of Environmental Measurement. National Bureau of Standards, Washington, DC.

Koschmieder, H. (1924). Theorie der Horizontalen Sichtweite. *Beitr. Phys. Freien Atmos.*, **12**(33-53):171-181.

Kowalczyk, G.S., G.E. Gordon, and S.W. Rheingrover (1982). Identification of Atmospheric Particulate Sources in Washington, DC, using Chemical Element Balances. *Environ. Sci. & Technol.* **16**:79-90.

Latimer, D.A. (1994). Assessment of Meteorological Data Available for the Yampa River Valley to Support Plume and Haze Modeling of the Hayden and Craig Power Plants, Final Report. Prepared for the U.S. Environmental Protection Agency, Region VIII, Air, Radiation and Toxics Division, by Sonoma Technology Inc., Santa Rosa, CA.

Leone J.A., and J.H. Seinfeld (1985). Comparative Analysis of Chemical Reaction Mechanisms for Photochemical Smog. *Atmos. Environ.* **19**(3).

Lewis, P. (1995). Letter from Mr. Paul Lewis (Tri-State Generation and Transmission Association, Inc.) to Mr. Marty Wolf (Radian International). August 18, 1995.

Lewis, C.W. and R.U. Stevens (1985). Hybird Receptor Model for Secondary Sulfate From an SO_2 Point Source. *Atmos. Environ.,* **19**:917.

Lewis, C.W., R.E. Baumgardner, R.K. Stevens (1986). Receptor Modeling Study of Denver Winter Haze. *Environ. Sci. Technol.,* **20**:1126-1136.

Li, C.K., and R.M. Kamens (1992). The Use of Polycyclic Aromatic Hydrocarbons as Source Signatures in Receptor Modeling. *Atmos. Environ.* **27**A(4)523-532.

Liousse, C., H. Cachier, and S.G. Jennings (1993). Optical and Thermal Measurements of Black Carbon Aerosol Content in Different Environments: Variation of the Specific Attenuation Cross-Section, Sigma (σ). *Atmos. Environ.* **27A**(8):1203-1211.

Liu, M.and M.Yocke (1980). Siting of Wind Turbine Generators in Complex Terrain. *J. Energy,* **4**(10):16.

Livo, K. (1995). Personal communication between Mr. Kim Livo of Colorado Air Pollution Control Division and Mr. Marty Wolf of Radian International. August 30, 1995.

Love, D. (1995). Personal communication between Ms. Dorothy Love of Steamboat Springs Board of Realtors (970-879-4663) and Mr. Marty Wolf of Radian International. July 13, 1995.

Lowe, D.C., U. Schmidt, D.H. Ehhalt, C.G.B. Frischkorn, and H.W. Nürnberg (1981). Determination of Formaldehyde in Clean Air. *Environ. Sci. Technol.* **15**(7):819-823.

Lowenthal, D.H., R.C. Hanumara, K.A. Rahn, and L.A. Currie (1987). Effects of Systematic Error, Estimates and Uncertainties in Chemical Mass Balance Apportionments: Quail Roost II Revisited. *Atmos. Environ.* **21**(3):501-510.

Lowenthal, D.H., and K.A. Rahn (1987). Application of the Factor-Analysis Receptor Model to Simulated Urban- and Regional-Scale Data Sets. *Atmos. Environ.* **21**:2005-2013.

Lowenthal, D.H., and K.A. Rahn (1988a). Tests of Regional Elemental Tracers of Pollution Aerosols: Sensitivity of Signatures and Apportionments to Variations in Operating Parameters. *Atmos. Environ.* **22**:420-426.

Lowenthal, D.H., and K.A. Rahn (1988b). Reproducibility of Regional Apportionments of Pollution Aerosol in the Northeastern United States. *Atmos. Environ.,* **22**:1829-1833.

Lowenthal, D.H., J.C. Chow, J.G. Watson, G.R. Neuroth, R.B. Robbins, B.P. Shafritz, and R.J. Countess (1992). The Effects of Collinearity on the Ability to Determine Aerosol Contributions from Diesel- and Gasoline-Powered Vehicles using the Chemical Mass Balance Model. *Atmos. Environ.* **26**A(13):2341-2351.

Lowenthal, D.H., B. Zielinska, J.C. Chow, J.G. Watson, M. Gautam, D.H. Ferguson, G.R. Neuroth, K.D. Stevens (1994). Characterization of Heavy-Duty Diesel Vehicle Emissions. *Atmos. Environ.*, **28**(4):731-743.

Lowenthal, D.H., C.F. Rogers, P. Saxena, J.G. Watson, and J.C. Chow (1995). Sensitivity of Estimated Light Extinction Coefficients to Model Assumptions and Measurement Errors. *Atmos. Environ.* **29**:751-766.

Lurmann, F. (1996). Personal communication., Sonoma Technology Inc., Santa Rosa, CA.

Madansky, A. (1959). The Fitting of Straight Lines When Both Variables are Subject to Error. *J. Am. Statist Assoc.*, **54:**173-205.

Malm, W.C. (1979). Visibility: A Physical Perspective. Presented at Workshop on Visibility Values, Fort Collins, CO.

Malm, W.C., E.G. Walther, K. O'Dell, and M. Kleine (1981). Visibility in the Southwestern United States from Summer 1978 to Spring 1979. *Atmos. Environ.*, **15**(10/11):2031-2042.

Malm, W.C., A. Pitchford, R. Tree, E. Walther, M. Pearson, and S. Archer (1981). The Visual Air Quality Predicted by Conventional and Scanning Teleradiometers and an Integrating Nephelometer. *Atmos. Environ.*, **15**:2547.

Malm, W.C., K. Kelly, J.V. Molenar, and T. Daniel (1981). Human Perception of Visual Air Quality (Uniform Haze). *Atmos. Environ.*, **15**:1875-1890.

Malm, W.C., K. Gebhard, T.A. Cahill, R.A. Eldred, R. Pielke, R. Stocker, J.G. Watson, and D.A. Latimer (1989). The Winter Haze Intensive Tracer Experiment (WHITEX). Report prepared by National Park Service, Fort Collins, CO.

Masek, T. (1995). Personal communication between Mr. Tom Masek of Chippewa Traders (801-972-4488) and Mr. Marty Wolf of Radian International. August 11, 1995.

Maul, P. (1980). Atmospheric Trasport of Sulfur Compound Polutants. Prepared by Central Electricity Generating Bureau MID/SSD/80/0026/R, Nottingham, England.

McArdle, N.C., and P.S. Liss (1995). Short Communication: Isotopes and Atmospheric Sulphur. *Atmos. Environ.* **29**(18):2553-2556.

McDow, S.R., and J.J. Huntzicker (1990). Vapor Adsorption Artifact in the Sampling of Organic Aerosol: Face Velocity Effects. *Atmos. Environ.*, **24A**:2563-2572.

Mercer, G.S. (1995). Nephelometer Data Reporting (IMPROVE Protocol). Technical Instruction 4500-5000. Air Resource Specialists Inc., Fort Collins, CO. March 1995.

Mie, G. (1908). Beitrage zur optik truber medien, speziell kolloidaler metallosungen. *Ann. Physik* **25**:377-445.

Miller, M., S.K. Friedlander, and G.M. Hidy (1972). A Chemical Element Balance for the Pasadena Aerosol. *J. Colloid Interface Sci.* **39**(1):165-176.

Morandi, M., J.M. Daisey, and P.J. Lioy (1987). Development of a Modified Factor Analysis/Multiple Regression Model to Apportion Suspended Particulate Matter in a Complex Urban Airshed. *Atmos. Environ.* **21**(3).

Morris, R., R. Kessler, S. Douglas, and K. Styles (1987). The Rocky Mountain Acid Deposition Model Assessment Project. Evaluation of Mesoscale Acid Deposition Models for Use in Complex Terrain. Prepared by Systems Applications, Inc., San Rafael, CA.

Morris, R., T. Myers, and J. Haney (1990). User's Guide for the Urban Airshed Model, Version I: User's Manual for UAM (CB-IV). Prepared for the U.S. Environmental Protection Agency, EPA-450/4-90-007A, by Systems Applications, Inc., San Rafael, CA.

Morris, R. and C. Emery (1995). Modeling Protocol for the CALMET/CALPUFF Modeling of the Effects of Emissions on Visibility-Related Air Quality in the Mount Zirkel Wilderness Area, Preliminary Draft Report. Prepared for the Technical Steering Committee, Mount Zirkel Visibility Study, by ENVIRON International Corp., Novato, CA.

Mucklow, C.J. (1995). Personal communication between Mr. C.J. Mucklow of Routt County Cooperative Extension (970-879-0825) and Mr. Marty Wolf of Radian International. November 16, 1995.

Newman, L., J. Forrest, and B. Manowitz (1975). The Application of an Isotopic Ratio Technique to a Study of the Atmospheric Oxidation of Sulphur Dioxide in the Plume from a Coal-Fired Power Plant. *Atmos. Environ.* **9**:959-968.

O'Brien, J. (1970). A Note on the Vertical Structure of the Eddy Exchange Coefficient in the Planetary Boundary Layer. *J. Atmos. Sci.*, **27**:1213-1215.

Orgill, M.M (1981). Atmospheric Studies in Complex Terrain (ASCOT) – A Planning Guide for Future Studies. Pacific Northwest Laboratory, Richland, WA. PNL-3656; ASCOT/80/4.

Pandis, S.N., R.A. Harley, G.R. Cass, and J.H. Seinfeld (1992). Secondary Organic Aerosol Formation and Transport. *Atmos. Environ.* **26**A(13):2269-2282.

Pandis, S.N., A.S. Wexler, and J.H. Seinfeld (1993). Secondary Organic Aerosol Formation and Transport: Predicting the Ambient Secondary Organic Aerosol Size Distribution. *Atmos. Environ.* **27**A(15):2403-2416.

Penndorf, R. (1957). Tables of the Refractive Index for Standard Air and the Rayleigh Scattering Coefficient for the Spectral Region Between 0.2 and 20 μm and their Application to Atmospheric Optics. *Optic. Soc. Am. J.* **47**:176-182.

Pietrick, D (1995). Facsimile transmission from Mr. Dave Pietrick (Public Service Company of Colorado) to Mr. Marty Wolf (Radian International). August 26, 1995.

Pitzer, K.S. (1991). In Activity Coefficients in Electrolyte Solutions, 2nd Ed. (K.S. Pitzer, ed.). CRC Press, Boca Raton, FL, pp. 75-153.

Pitzer, K.S., and J. Kim (1974). *J. Am. Chem. Soc.* **96**:5701-5707.

Pratsinis, S.E., M.D. Zeldin, and E.C. Ellis (1988). Source Resolution of the Fine Carbonaceous Aerosol by Principal Component-Stepwise Regression Analysis. *Environ. Sci. & Technol.* **22**(2):212-216.

Pratsinis, S.E. (1989). Receptor Models for Ambient Carbonaceous Aerosols. *Aerosol Sci. Technol.* **10:**258-266.

Reddy, P.J. (1995). Technical Support Document for the Colorado State Implementation Plan for PM_{10}: Steamboat Springs Element. Woodburning Emissions Inventory for the Steamboat Springs Metropolitan Area, Air Pollution Control Division, Colorado Department of Health, Denver, CO. March, 1995.

Richards, L.W. (1990). Effect of the Atmosphere on Visibility. In *Transactions, Visibility and Fine Particles*, C.V. Mathai, ed. Air & Waste Management Association, Pittsburgh, PA, p. 261.

Robinson, N.F., and M.R. Whitbeck (1985). A Flexible Nonempirical Model for Cloud Chamber Studies. *J. Air Pollution Control Assoc.* **35**:746-748.

Roscoe, B.A., P.K. Hopke, S.L. Dattner, and J.M. Jenks (1982). The Use of Principal Component Factor Analysis to Interpret Particulate Compositional Data Sets. *J. Air Pollution Control Assoc.* **32**:637-642.

Ruby, M.G., and A.P. Waggoner (1981). Intercomparison of Integrating Nephelometer Measurements. *Environ. Sci. Technol*., **15**:109-113.

Sadeghi, V.M. *et al.* (1991). Technical Assistance for the Development of the Denver Brown Cloud II Ammonia Inventory. Prepared for the Colorado Department of Health by Radian Corporation. April 1991.

Sakry, S. (1995). Facsimile transmission from Mr. Steve Sakry of Colorado Department of Agricultural Statistics (800-392-3202) to Mr. Marty Wolf (Radian International), August 11, 1995.

Seigneur, C. (1987). Computer Simulation of Air Pollution Chemistry. *Environ. Software* **2**(3).

Seigneur, C., and P. Saxena (1988). A Theoretical Investigation of Sulfate Formation in Clouds. *Atmos. Environ.* **22**(1).

Sloane, C.S. (1984). Optical Properties of Aerosols of Mixed Composition. *Atmos. Environ.* **18**:871-878.

Sloane, C.S. (1986). Effect of Composition on Aerosol Light Scattering Efficiencies. *Atmos. Environ.* **20**:1025-1037.

Sloane, C.S., J.G. Watson, J.C. Chow, L.C. Pritchett, and L.W. Richards (1991). Size-Segregated Fine Particle Measurements by Chemical Species and Their Impact on Visibility Impairment in Denver. *Atmos. Environ.*, **25A**:1013-1024.

Solomon, P.A., T. Fall, L. Salmon, G.R. Cass, H.A. Gray, and A. Davison (1989). chemical Characteristics of PM_{10} Aerosol collected in the Los Angeles Area. *JAPCA*, **39**:154-163.

Stockwell, W.R., and J.G. Calvert (1983). The Mechanism of NO3 and HONO Formation in the Nighttime Chemistry of the Urban Atmosphere. *J. Geophysical Research* **88**(C11).

Tang, H., E.A. Lewis, D.J. Eatough, R.M. Burton, and R.J. Farber (1994). Determination of the Particle Size Distribution and Chemical Composition of Semi-Volatile Organic Compounds in Atmospheric Fine Particles with a Diffusion Denuder System. Atmos. Environ. **28**(5):939-950.

Thurston, G.D., and J.D. Spengler (1985). A Quantitative Assessment of Source Contributions to Inhalable Particulate Matter Pollution in Metropolitan Boston. *Atmos. Environ.* **19**(1):9-25.

Tree, D. (1995). Personal communication between David Tree of _____ and Air Resource Specialists, Fort Collins, CO.

Trijonis, J.C., W.C. Malm, M. Pitchford, W.H. White, R. Charlson, and R. Husar (1990). Visibility: Existing and Historical Conditions-Causes and Effects. Natl. Acid Precip. Assess. Program Rep. 24. Washington, D.C.: U.S. Govt. Printing Office.

Turk, J.T., D.H. Campbell, and N.E. Spahr (1993). Use of Chemistry and Stable Sulfur Isotopes to Determine Sources of Trends in Sulfate of Colorado Lakes. *Water, Air, and Soil Pollution* **67**:415-431.

Turner, D.B. (1994). Workbook of Atmospheric Dispersion Estimates: An Introduction to Dispersion Modeling, 2nd Ed. CRC Press.

Turpin, B.J., J.J. Huntzicker, and S.V. Hering (1994). Investigation of Organic Aerosol Sampling Artifacts in the Los Angeles Basin. *Atmos. Environ.* **28**:3061-3071.

U.S. Environmental Protection Agency (1980). Visibility Protection for Federal Class I Areas. 45 Fed. Reg. 80084. December 2, 1980..

U.S. Environmental Protection Agency (1981). Procedures for Emission Inventory Preparation. Volume III: Area Sources. Document No. EPA-450/4-81-026c. U.S. EPA, OAQPS, Research Triangle Park, NC.

U.S. Environmental Protection Agency (1987). On-Site Meteorological Program Guidance for Regulatory Modeling Applications. Report prepared by the Office of Air and Radiation, Office of Air Quality Planning and Standards, U.S. Environmental Protection Agency, Research Triangle Park, NC, EPA-450/4-87-013, June.

U.S. Environmental Protection Agency (1989). Quality Assurance Handbook for Air Pollution Measurement Systems Volume IV - Meteorological Measurements. Report prepared by Office of Research and Development, Atmospheric Research and Exposure Assessment Laboratory, Document #EPA/600/4-90-003, Research Triangle Park, NC.

U.S. Environmental Protection Agency (1993). Interagency Workgroup on Air Quality Modeling (IWAQM). Phase I Report: Interim Recommendation for Modeling Long Range Transport and Impacts on Regional Visibility. Report prepared by Office of Air Quality Planning and Standards, U.S. Environmental Protection Agency, Research Triangle Park, NC, EPA-454/R-93-015.

U.S. Environmental Protection Agency (1993). Guideline on Air Quality Models (revised), Including Supplements A and B. U.S. Environmental Protection Agency, Research Triangle Park, NC, (See also 40 CFR Part 51 Appendix W), EPA-450/2-78-027R.

U.S. Environmental Protection Agency (1994). National Air Pollutant Emission Trends, Procedures. Document 1900-1993 (EPA-454/R-95-002). U.S.EPA, Research Triangle Park, NC.

U.S. Environmental Protection Agency (1995). A User's Guide for the CALMET Meteorological Model. Document No. EPA-454/B-95-002. U.S. Environmental Protection Agency, Emissions, Monitoring, and Analysis Division, Research Triangle Park, NC, March 1995.

U.S. Environmental Protection Agency (1995). A User's Guide for the CALPUFF Dispersion Model. Document No. EPA-454/B-95-006. U.S. Environmental Protection Agency, Office of Air Quality Planning and Standards, Research Triangle Park, NC, July 1995.

Watson, J.G. (1979). Chemical Element Balance Receptor Model Methodology for Assessing the Sources of Fine and Total Particulate Matter. University Microfilms International, Ann Arbor, MI.

Watson, J.G., J.C. Chow, J.J. Shah, and T.G. Pace (1983). The effect of Sampling Inlets on the PM_{10} and PM_{15} to TSP Ratios. *J. Air Pollut. Control Assoc.* **33**:114-119.

Watson, J.G., J.A. Cooper, and J.J. Huntzicker (1984). The Effective Variance Weighting for Least Squares Calculations Applied to the Mass Balance Receptor Model. *Atmos. Environ.*, **18**(7):1347-1355.

Watson, J.G., J.C. Chow, L.W. Richards, S.R. Anderson, J.E. Houck, and D.L. Dietrich (1988). The 1987-88 Metro Denver Brown Cloud Air Pollution Study, Volume II: Measurements. Document #8810.1F2, prepared for Greater Denver Chamber of Commerce, Denver, CO, by the Desert Research Institute, Reno, NV.

Watson, J.G., P.J. Lioy, and P.K. Mueller (1989). The Measurement Process: Precision, Accuracy, and Validity. In *Air Sampling Instruments for Evaluation of Atmospheric Contaminants*, S.V. Hering, ed. American Conference of Governmental Industrial Hygienists, Cincinnati, OH, 7th Ed., pp. 51-57.

Watson, J.G., J.C. Chow, L.W. Richards, D.L. Haase, C. McDade, D.L. Dietrich, D. Moon, L. Chinkin, and C. Sloane (1990). The 1989-90 Phoenix PM_{10} Study, Volume I: Program Plan. DRI Document #8931.2F, prepared for Arizona Department of Environmental Quality, Phoenix, AZ, by the Desert Research Institute, Reno, NV, 29 January 1990.

Watson, J.G., J.C. Chow, L.W. Richards, D.L. Haase, C. McDade, D.L. Dietrich, D. Moon, and C. Sloane (1991). The 1989-90 Phoenix Urban Haze Study, Volume II: The Apportionment of Light Extinction to Sources. Final Report. Prepared for the Arizona Department of Environmental Quality, Phoenix, AZ, by the Desert Research Institute, Reno, NV.

Watson, J.G., and J.C. Chow (1994). Ammonium Nitrate, Nitric Acid, and Ammonia Equilibrium in Wintertime Phoenix, Arizona. *J. Air & Waste Management Assoc.* b:405-412.

Watson, J.G., J.C. Chow, D.H. Lowenthal, L.C. Pritchett, C.A. Frazier, G.R. Neuroth, and R. Robbins (1994). Differences in the Carbon Composition of Source Profiles for Diesel- and Gasoline-Powered Vehicles. *Atmos. Environ.*, **28**(15):2493-2505.

Watson, J.G., J.C. Chow, F. Lurmann, and S. Musarra (1994). Ammonium Nitrate, Nitric Acid, and Ammonia Equilibrium in Wintertime Phoenix, AZ. *Air & Waste*, **44:**261-268.

Watson, J.G., J.C. Chow, Z. Lu, E.M. Fujita, D.H. Lowenthal, D.R. Lawson, and L.L. Ashbaugh (1994). Chemical Mass Balance Source Apportionment of PM_{10} during the Southern California Air Quality Study. *Aerosol. Sci. & Technol.* **21**:1-36.

Watson, J.G., M. Green, T.E. Hoffer, D.R. Lawson, D.J. Eatough, R.J. Farber, W.C. Malm, C.E. McDade, and M. Pitchford (1994). Project MOHAVE Data Analysis Plan. Document #93-MP-4.10, presented at 86th Annual Meeting & Exhibition, Denver, CO. Air & Waste Management Association, Pittsburgh, PA.

Watson, J.G., J.C. Chow, C.F. Cahill, F. Divita, Jr., D. Freeman, J.A. Gillies, D. Blumenthal, L.W. Richards, L. Chinken, C. Lindsey, J. Prouty, D. Dietrich, D. Cobb, J. Houck, R.J. Dickson, S. Andersen (1995). Mt. Zirkel Wilderness Arrea Reasonable Attribution Study of Visibility Impairment - Volume I - Technical Reasonable Attribution Study Plan - Working Draft Version 2. Prepared for Technical Steering Committee, Colorado Dept. of Public Health and Environment, Air Pollution Control Division, Denver, CO. August 1995.

Weber, B.L., and D.B. Wuertz (1991). Quality Control Algorithm for Profiler Measurements of Winds and Temperatures. NOAA Technical Memorandum ERL WPL-212, NOAA Environmental Research Laboratories, Boulder, CO, 32 pp.

Weber, B.L., D.B. Wuertz, D.C. Welsh, and R. McPeek (1993). Quality Controls for Profiler Measurement of Winds and RASS Temperatures. *J. Atmos. Ocean. Technol.* **10**:452-464.

White, W.H. (1986). On the Theoretical and Empirical Basis for Apportioning Extinction by Aerosols: A Critical Review. *Atmos. Environ.* **20**:1659-1672.

World Meteorological Organization (1971) Measurement of Upper Wind. Guide to Meteorological Instrument and Observing Practices. Third edition, XII.I-XII.11. Prepared by World Meteorological Organization.

Zeldin, M.D., B.M. Kim, R. Lewis, and J.C. Marlia (1990). PM_{10} Source Apportionment for the South Coast Air Basin. Technical Report V-F. South Coast Air Quality Management District, Diamond Bar, CA.

Zhang, Z.Q., B.J. Turpin, P.H. McMurry, S.V. Hering, and M.R. Stolzenburg (1994). Mie Theory Evaluation of Species Contributions to Wintertime Visibility Reduction in the Grand Canyon. *J. Air Waste Manage. Assoc.* **44**:153-162.

Zopf, M. (1995). Personal communication between Mr. Mike Zopf of Routt County Department of Health and Mr. Marty Wolf of Radian International. July 26, 1995.